

Sustainable Textiles: Production, Processing,
Manufacturing & Chemistry

Subramanian Senthilkannan Muthu
Ali Khadir *Editors*

Textile Wastewater Treatment

Sustainable Bio-nano Materials and
Macromolecules, Volume 1

 Springer

Sustainable Textiles: Production, Processing, Manufacturing & Chemistry

Series Editor

Subramanian Senthilkannan Muthu, Head of Sustainability, SgT and API,
Kowloon, Hong Kong

This series aims to address all issues related to sustainability through the lifecycles of textiles from manufacturing to consumer behavior through sustainable disposal. Potential topics include but are not limited to: Environmental Footprints of Textile manufacturing; Environmental Life Cycle Assessment of Textile production; Environmental impact models of Textiles and Clothing Supply Chain; Clothing Supply Chain Sustainability; Carbon, energy and water footprints of textile products and in the clothing manufacturing chain; Functional life and reusability of textile products; Biodegradable textile products and the assessment of biodegradability; Waste management in textile industry; Pollution abatement in textile sector; Recycled textile materials and the evaluation of recycling; Consumer behavior in Sustainable Textiles; Eco-design in Clothing & Apparels; Sustainable polymers & fibers in Textiles; Sustainable waste water treatments in Textile manufacturing; Sustainable Textile Chemicals in Textile manufacturing. Innovative fibres, processes, methods and technologies for Sustainable textiles; Development of sustainable, eco-friendly textile products and processes; Environmental standards for textile industry; Modelling of environmental impacts of textile products; Green Chemistry, clean technology and their applications to textiles and clothing sector; Eco-production of Apparels, Energy and Water Efficient textiles. Sustainable Smart textiles & polymers, Sustainable Nano fibers and Textiles; Sustainable Innovations in Textile Chemistry & Manufacturing; Circular Economy, Advances in Sustainable Textiles Manufacturing; Sustainable Luxury & Craftmanship; Zero Waste Textiles.

Subramanian Senthilkannan Muthu · Ali Khadir
Editors

Textile Wastewater Treatment

Sustainable Bio-nano Materials
and Macromolecules, Volume 1

 Springer

Editors

Subramanian Senthilkannan Muthu
SgT Group and API
Hong Kong, Kowloon, Hong Kong

Ali Khadir
Western University
London, ON, Canada

ISSN 2662-7108

ISSN 2662-7116 (electronic)

Sustainable Textiles: Production, Processing, Manufacturing & Chemistry

ISBN 978-981-19-2831-4

ISBN 978-981-19-2832-1 (eBook)

<https://doi.org/10.1007/978-981-19-2832-1>

© The Editor(s) (if applicable) and The Author(s), under exclusive license to Springer Nature Singapore Pte Ltd. 2022, corrected publication 2022

This work is subject to copyright. All rights are solely and exclusively licensed by the Publisher, whether the whole or part of the material is concerned, specifically the rights of translation, reprinting, reuse of illustrations, recitation, broadcasting, reproduction on microfilms or in any other physical way, and transmission or information storage and retrieval, electronic adaptation, computer software, or by similar or dissimilar methodology now known or hereafter developed.

The use of general descriptive names, registered names, trademarks, service marks, etc. in this publication does not imply, even in the absence of a specific statement, that such names are exempt from the relevant protective laws and regulations and therefore free for general use.

The publisher, the authors, and the editors are safe to assume that the advice and information in this book are believed to be true and accurate at the date of publication. Neither the publisher nor the authors or the editors give a warranty, expressed or implied, with respect to the material contained herein or for any errors or omissions that may have been made. The publisher remains neutral with regard to jurisdictional claims in published maps and institutional affiliations.

This Springer imprint is published by the registered company Springer Nature Singapore Pte Ltd. The registered company address is: 152 Beach Road, #21-01/04 Gateway East, Singapore 189721, Singapore

Contents

Textile Industry: Pollution Health Risks and Toxicity	1
Tasneem Sarwar and Sardar Khan	
Applications of Chitosan- and Chitin-Based Biomaterials in Cationic Dye Removal	29
Asitha T. Cooray, Kavindya Weerasinghe, and Samantha Ranaweera	
Chitosan-Based Composite Beads for Removal of Anionic Dyes	47
Joydeep Dutta	
Application of Lignin-Based Biomaterials in Textile Wastewater	75
Md. Din Islam, M. K. Mohammad Ziaul Hyder, Md. Masudur Rhaman, and Sajjad Husain Mir	
Application of Cellulose-Based Biomaterials in Textile Wastewater	101
Fatma Abdelghaffar	
Cellulose Nanocrystal as a New Promising Candidate in Textile Wastewater Treatment	121
Swarnalatha Venkatanarasimhan, D. Gangadharan, and Thilagavathy Palanisamy	
Carbon Materials for Dye Removal from Wastewater	141
Sarita Rai, Anindita De, Mridula Guin, and N. B. Singh	
Polysaccharide-Composites Materials as Adsorbents for Organic Dyes	185
Paulo V. O. Toledo and Denise F. S. Petri	
Application of Agricultural Wastes for Cationic Dyes Removal from Wastewater	239
Abdullahi Haruna Birniwa, Abdulsalam Salisu Abubakar, Habibun Nabi Muhammad Ekramul Mahmud, Shamsul Rahman Mohamed Kutty, Ahmad Hussaini Jagaba, Shehu Sa'ad Abdullahi, and Zakariyya Uba Zango	

Application of Aromatic-Based Synthetic Macromolecules in Textile Wastewater	275
Jumina, Yehezkiel Steven Kurniawan, and Anggit Fitria	
Synthesis of Hydroxyapatite Nanoparticle from Papermill Sludge	311
A. Geethakarthis	
Adsorptive Removal of Reactive Blue Dye by Cucumber Peel Adsorbent: Isotherm, Kinetics and Mass Transfer Studies	329
Gajendiran Vasu and Selvaraju Sivamani	
Application of Dried Fungus in Textile Wastewater	349
Ariani Dwi Astuti and Yonik Meilawati Yustiani	
Application of Waste Utilization in Textile Dye Removal	371
Arti Malviya and Dipika Jaspal	
Correction to: Chitosan-Based Composite Beads for Removal of Anionic Dyes	C1
Joydeep Dutta	

About the Editors

Dr. Subramanian Senthilkannan Muthu currently works for SgT Group as Head of Sustainability and is based out of Hong Kong. He earned his Ph.D. from The Hong Kong Polytechnic University and is a renowned expert in the areas of Environmental Sustainability in Textiles and Clothing Supply Chain, Product Life Cycle Assessment (LCA) and Product Carbon Footprint Assessment (PCF) in various industrial sectors. He has five years of industrial experience in textile manufacturing, research and development and textile testing and over a decade experience in life cycle assessment (LCA) and carbon and ecological footprints assessment of various consumer products. He has published more than 100 research publications, written numerous book chapters and authored/edited over 100 books in the areas of Carbon Footprint, Recycling, Environmental Assessment and Environmental Sustainability.

Ali Khadir is an environmental engineer and a member of the Young Researcher and Elite Club, Islamic Azad University of Shahre Rey Branch, Tehran, Iran. He has published several articles and book chapters in reputed international publishers. He also has been the reviewer of journals and international conferences. His research interests center on emerging pollutants, dyes and pharmaceuticals in aquatic media, advanced water and wastewater remediation techniques and technology.

Textile Industry: Pollution Health Risks and Toxicity



Tasneem Sarwar and Sardar Khan

1 Introduction

Being the oldest industry, the roots of the textile industry trace back to scraps found in a cave of Egypt at about 5000 B.C. [110]. The textile industry is comprised of making yarns and threads from either natural or synthetic fibres through the process of weaving and knitting, resulting in fabrics. The final step is the dyeing and finishing of yarn or threads and sometimes the fabrics are dyed [40]. The textile sector includes different characteristics which determine the textile sectors' sub-division into subsectors due to traits, length of the manufacturing process, and variety of technical process, such sector can also be divided into several ways, which depends on the production process and final products achievement [122]. Hence, the textile industry is subdivided into many fragments depending on various traits of the subsectors.

The textile industry is a key driver of the economy for every country, which not only fulfils the needs of individuals but also raises the quality and standard of living along with unemployment reduction [46]. Being the second-largest cloth exporter after China, Bangladesh not only makes 80% of total annual export, i.e., \$24 billion, but also contributes to 45% of industrial employment and 5% to the total national income. Also, Indian textile sector studies revealed the contributing role of the textile sector by providing 14% of total industrial production, 3% of GDP, and a source of employment while providing jobs to more than 35 million individuals [37]. In Pakistan, textile accounts for 60% income of export income, a source of employment for 38% of the total labour force, and fourth-largest exporter of cotton [154]. So, no

T. Sarwar · S. Khan (✉)

Department of Environmental Sciences, University of Peshawar, Peshawar 25120, Pakistan

e-mail: sardar.khan2008@yahoo.com

S. Khan

Kohat University of Science and Technology, Kohat, Pakistan

Table 1 Top 10 textile-producing countries

No.	Country	2020 outputs in global shares (%)
1	China	52.2
2	India	6.9
3	United States	5.3
4	Pakistan	3.6
5	Brazil	2.4
6	Indonesia	2.4
7	Turkey	1.9
8	South Korea	1.8
9	Thailand	1.1
10	Mexico	0.9

Source [168]

industry can compete with textile to bring foreign reserves and generate employment for individuals.

China leads the world in exporting textiles to other countries globally. Therefore, China was considered in the top list of textile exporters in 2016 with a net value of 106 billion US dollars. The 28 countries of the European Union were ranked second after China with a net value of 65 billion USD, while other countries like Turkey, India, and USA were ensuing with net values of 11, 16, and 13 billion USD [150]. In 2016, China and 28 countries of the EU were considered among the top two exporters of cloth followed by other countries like Bangladesh, Vietnam, India, Hong Kong, and Turkey. In 2016, the values of textile exports and apparel exports were 284 billion USD and 443 billion USD demonstrated by the World Trade Statistical Review (Table 1).

2 Textile Industry Processes

2.1 Yarn Manufacturing

The manufacturing processes in the textile sector include yarn preparation, which is obtained from natural plants and animals. The mechanical processes are involved in yarn preparation like fibre blae opening, blending, mixing, clearing, drawing, roving, and finally spinning [66]. Further detailed processes of such production are described via material processing and technical control. The important and useful topics in the textile are staple-yarn technology, rolling-drafting, ring spinning, advancements in fibre production technologies, air open-end rotor spinning, and jet spinning [90]. The yarn-producing technology is considered as an important study in the preparation of yarn containing different processes [92].

2.2 Fabric Manufacturing

Three different techniques like weaving, non-weaving, and knitting are used to produce fabrics via fibre/yarn interlacing. The plain and simple weaves, such as tabby or plain, and satin and the fancy weaves, such as pile, jacquard, dobby, and gauze, are the most common forms of woven fabric manufactured [162]. The second most common form of cloth is knitted fabric, which is used after woven fabric. Knitted fabric has different properties like fitting the body shape and allowing for ease of movement, which remain an especially pleasant sports fabric structure, leisure wear, and undergarments. Woven textiles include warp and weft kinds, as well as raschel and tricot [162].

Interlaced fabric designs such as net, lace, and braid are also valuable. Non-woven fabric usage is continuously increasing in the market. The interlaced-fabrics textiles are finding intriguing applications in industrial and residential settings. Non-woven textiles include felting and bonding compounds. Laminating methods are also becoming more important, and new progress involves needle weaving and sewing-knitting [162].

An ecological approach to make fabrics from raw bottles is also an environment-friendly process [124]. Fabric producers are encouraged by the ease and low cost of producing recycled polyester yarn. Chopped and grounded plastic bottles into little bits that soften and melt as they pass through a series of tiny holes, resulting in thin strands. The thin strands produced are then currently used in the woven and knit industries to make fabric [124]. Strong recommendations should be made in order to use environment-friendly processes to mitigate the textile wastes.

2.3 Product Planning

Production planning is a difficult aspect of any industrial business. Textile planning is complex due to the variety of fibres, counts, yarn, spinning systems, processes of preparation, and final products. All of these issues, when paired with the customer's needs for accurately completed orders and quick delivery dates, hinder the production planning process. Furthermore, since severe international rivalry has influenced the market, competent planning for production in the textile sector has become increasingly important [121].

The fibres are removed from other components such as capsule fragments, leaves, twigs, and soil and also from the seeds in the first phase of the methods outlined in a set of spinning drums and moving carding bars fitted with metal combing teeth comb the fibres in a carding machine. Consequently, the product formed is a soft homogenous fibre band. The silver has been holding between the parallel fibres as a result of friction among parallel fibres, which in turn provides rigidity in further manufacturing processes. Basically, the spinning process is responsible for transforming a loose fibre bundle into a real yarn. The twisting of the pack of similar fibres provides the yarn

its toughness. The most widely used spun techniques in the industry are open-end spinning, ring spinning, and air jet spinning [105].

Knitting, the most popular way of interloping and producing textile goods, necessitates a reasonably fine, smooth, and robust yarn with high elastic recovery characteristics. The outdone system has been shown to be particularly appropriate for spinning yarns used for knitted garments, socks, and outerwear, while the combed cotton system has proven to be highly appropriate for spinning yarns used for undergarments, sports, and socks. The production of innovative fibres and texturing methods have been especially advantageous to the knitting business, resulting in a tight relationship between the two sectors [105]. Weft and warp techniques are used to synthesise yarns in knitting processes. The distinction between weft and warp knitting stems from the movement of the needles during manufacturing and how the yarn is supplied. Weft knitting is a one-fibre method, which implies that the stitches are constructed using only one fibre. The needles are manipulated independently, whereas the warp knitting needles are moved concurrently. As a result, all needles require the fibre material simultaneously [149].

Braiding is a fabric-making technique that takes at least three yarns. The braid is produced by alternately interweaving the strands according to a certain algorithm. Braids are “real or large bodies with a regular thread density and a closed product surface, whose braid bobbin yarns are intertwined slantwise towards the product edge”. A woven fabric, on the other hand, has threads that are interwoven perpendicular to the product edge and can have a biaxial or triaxial structure [42].

Lastly, finishing is a modification that is applied to a cloth to alter its look, handling—touch, or durability. The intention of finishing is that the fabric will be more appropriate for its intended use and involves any common treatment given to clean and iron fabrics. Finishing also creates exclusive variations of fabrics by using chemical treatments, dyeing, printing, and other techniques to make the fabric attractive and appealing. Finishing is divided into two processes: chemical and mechanical. Chemical finishing refers to treatments that modify the performance of a textile fabric and in which the chemical is the primary component of the change. Mechanical finishing refers to mechanical devices that physically change the cloth. The finish processes assist to improve the appearance and look of the fabric; provide diversity in fabrics through dyeing and printing; improve the fabric texture; make the fabric more usable; increase the draping ability of lightweight fabrics; and make the fabric appropriate for an end purpose [105].

2.4 Processes Responsible for Environmental Pollution Especially for Dyes

The pollution generated by textile effluents has become a major problem since it endangers both human health and the environment [132]. The dyeing process is connected with an environmental issue since washing coloured cloth and discharging

dye wastewater may release 10–50% of different chemicals related to dyestuff into the environment. The inefficient dyeing and finishing process might result in the discharge of 200,000 tonnes of wasted dyestuff into the environment globally [28].

Textiles are offered varied functions through the finishing procedures. Formaldehyde is widely used as a glueing agent, softener, and cross-linking resin. Because of the release of formaldehyde, such textile goods can cause eye irritation, skin itching, and allergies [82]. Perfluoroalkyl chains with eight or more fluorinated carbons are utilised to provide resistance to oil stain and also water repellence in textile products [138]. Perfluorooctanoic acid and perfluoro octane sulphonate form a long chain, which degrades and produces harmful impacts for all living species [76]. Many finishing compounds used to provide flame retardancy, like polybrominated diphenyl ethers, have been proven to be extremely hazardous to people [134].

Water is used at each stage like wet finishing, transferring chemicals to textiles, and washing materials before going on to the next phase. Aside from these textile operations, water is consumed during boiler, cooling water, steam drying, and cleaning [165]. A medium-sized textile industry manufacturing roughly 8000 kg of cloth per day spends around 1.6 million litres on water. One-fifth of this amount is spent on dyeing, while the other half is spent on printing. Depending on the colour used in the dyeing, 30–50 l of water are consumed per kilogramme of cloth. Approximately 60 l of water are used per kilogramme of yarn during the dyeing process. The wastewater produced during the dyeing process accounts for approximately one-fifth of the total effluent. Water is also necessary to attain the requisite fastness values and to clean the equipment. The quantity of water used to make fabric for a couch cover is around 500 gallons [73]. Approximately two hundred thousand kilos of water are polluted during traditional dyeing and finishing procedures of 1000 kg of cloth, and a large amount of steam and hot water is required for energy during these phases [153]. A cotton shirt requires around 2500–3000 l of water to manufacture [56].

3 Environmental Pollution and Textile Industries

Many environmental issues are raised by textile waste [17]. Numerous studies were carried out to identify the environmental consequences of the business and mitigate its harmful effects.

3.1 Water Pollution

The textile business is global in scope, generating over \$1 trillion in revenue, accounting for 7% of entire global exports, and employing approximately 35 million people worldwide [36]. Despite unquestionable significance, the industrial sector is one of the most polluting in the world, using large amounts of chemicals and fuels [14]. The massive consumption of drinking water is in different activities of

its production chain, including washing, bleaching, and dyeing [65]. The ineffective dyeing and finishing processes might result in the discharge of 200,000 tonnes of wasted dyestuff into the environment globally [28]. 1.6 million litres of water are consumed to produce 8000 kg of clothes in a medium-sized textile mill. About 30–50 l of water are in each kilogramme of cloth production [73].

The textile sector is responsible for a wide range of environmental effects [108]. Particulate matter and dust, oxides of nitrogen and sulphur, and volatile organic compounds are among the pollutants released into the atmosphere. The major solid waste consists of fragments of textile fabrics and yarns, as well as wasted packaging. The textile sludge, on the other hand, exposes issues linked to excess quantities and undesirable composition, frequently exhibiting large loads of organic matter, micronutrients, heavy metal cations, and pathogenic microorganisms [14].

3.2 Soil Pollution

The effluent from the textile industry pollutes the land. The topsoil is the most significant medium for growing plants, shrubs, and crops, among other things. The quality of crops is determined by the condition of the soil. As a result, as the quality of the soil deteriorates due to contaminated industrial effluent, so do the quantity and quality of crops. It has also been observed that the lower areas are becoming more contaminated than the upper regions. Such contamination is attributed due to the position of the lower ground [72]. The solid wastes dispose into the underground water through porous soils and also contaminate land [155, 81].

3.3 Textile Aerial Pollution

Carbon dioxide, aerosol fumes and gases, toxic gases, smoke, and dust are all examples of air pollutants. The majority of textile mill processes emit pollutants into the atmosphere. Gaseous emissions have been recognised as the textile industry's second most serious pollution concern [72]. The primary source of air pollution in the textile sector is during the finishing phases when various procedures are used to coat the textiles. Lubricating oils, plasticisers, paints, and water repellent chemicals are examples of coating materials. Organic substances such as oils, waxes, or solvents, acid vapour, odours, and boiler exhausts are examples of coating materials [96]. Cleaning and production modifications produce sludge in the tanks containing process chemicals, which may contain hazardous compounds and metals [104].

Table 2 Dye pollution data reported from different countries

Dye conc. (mg/l)	Countries	References
100	China	[158]
3.9	Kenya	[173]
100–2000	China	[181]
50	India	[145]
100	Bangladesh	[77]
200	Turkey	[33]

3.4 Dye Pollution

Dyes are solvable organic chemicals, particularly those categorised as reactive, direct, basic, and acidic [95]. Dyes have a very high dissolution property in water, making it difficult to remove them using traditional techniques [59]. The capacity of dyes to transmit colour to a particular substrate is one of its characteristics due to the occurrence of chromographic groups in molecular structure [137]. Nevertheless, the ability to fix colour to the material is associated with auxotrophic groups, which are polar in nature and may bind to polar groups of textile fibres [174].

Textile dyes' colour may not only contribute to aesthetic harm to the aquatic environment [135], but also hinders light permeation through water [59], resulting in a drop-in photosynthesis rate [71] and (DO) dissolved oxygen levels, impacting the whole aquatic biota [59]. Textile dyes are also toxic, mutagenic, and carcinogenic agents [84]. The dyes act as important environmental pollutants as shown in Table 2 and transverse whole food chains, giving biomagnification [131], which in turn makes the prey more contaminated as compared to organisms at a higher level [111]. So, the azo-dyes due to their non-binding capacity to clothes contaminate water, which requires attention because such contaminated water is then used for irrigation and other purposes in poor countries [127]. Lastly, the microbes in the soil and germination and growth of plants are greatly influenced by the utilisation of azo chemicals [71, 127].

4 Health Risks

4.1 Air Pollution and Health Risks

The majority of operations in the wet processing industry emit air pollution shown in Table 3. Gaseous air has been recognised as the second most significant pollution concern for the dyeing and printing sectors. Air pollution is caused by the release of several gases such as Nitrogen dioxide (NO₂), Carbon dioxide (CO₂), Sulphur dioxide (SO₂), and others [163]. SO₂ is the causing agent of irritation in the respiratory system and bronchitis, while CO₂ inhibits oxygen into body cells causing

Table 3 The gases emission into the atmosphere and their health risks

Pollutant	Amount	Health risks	References
CO ₂	500–5000 ppm	Psychomotor abnormalities, complications in the cardiovascular and respiratory system	[99]
SO ₂	75 ppb	Effects on airway epithelial cell function, amplification of allergic irritation, and a possible increase in neurogenic inflammation due to chemical nuisance properties	[128]
NO ₂	4700 ug/m ³	Bronchoconstriction	[167]
	–	Respiratory infection	[123]
	–	Increase mortality	[7]
Arsenic	0.5 ug/kg	Leucomelanosis, melanosis, and keratosis	[126]
		High blood pressure, obstetric problems, diabetes mellitus, neurological disorders, and respiratory system diseases	[4]
Cadmium	3 ug/kg	Damage to kidney, liver, skeletal muscles, and cardiovascular system	[87]
		Steroidogenesis, menstrual cycle disorders, delay in puberty and menarche, miscarriages, premature births, and reduced birth weight	[157]
Chromium	100 ppb	Carcinogenic	[152]
		Nausea, headache, or even oral cavity cancer as well as genetic damage	[45]

unconsciousness [102]. The production of artificial fibres is the result of greenhouse gases emissions because of the energy requirement [12].

The amount of greenhouse gases was 2.69–8.6 kg CO₂ eq/kg fibre [164]. Higher results were stated, i.e., 35.7-kg CO₂ eq/kg fibre. It is estimated that the cytotoxic capability of acrylic fibre production is linked to the emission of As, Cd, zinc (Zn), and Cr into both air and water [12]. One kilogramme of acrylic fibre produces approximately 0.013-kg SO₂ equivalent. For every kilogramme of acrylic fibre produced, 0.007 kg of NO₂ is discharged into the closest disposal canal via effluent discharge. The carcinogenic risk of acrylic fibre is owing to the emission of As, Cd, Zn, and Cr into both air and water during the production process [179].

4.2 Land Pollution and Health Risks

The effluent from the textile industry contaminates the land. The soil is the most significant medium for growing plants, shrubs, and crops, among other things. The quality of crops is determined by the condition of the soil. As a result, as the quality of the soil deteriorates by contaminated industrial effluent, so do the quantity and quality of crops. It has also been observed that the lower areas are becoming more

contaminated than the upper regions [72]. In landfills, the solid waste decomposes to create methane (CH_4), a powerful greenhouse gas. This ameliorates climate change by causing the ozone layer to deplete. The ecosystem suffers as a result of inappropriate disposal of biodegradable garbage, often known as unlawful dumping. Leaching is the process by which solid waste enters the pores in the soil and pollutes groundwater, thereby contaminating the land [148, 155].

Textile industry sewage mostly comprises alkali, residual colours, starches, soluble salts, cellulose primarily calcium and sodium, silicate, oil, and other pollutants. Due to a lack of economically feasible treatment methods, the industrial effluent created by these rapidly growing textile and dyeing plants is typically dumped untreated onto the ground surface. Consequently, such processes result in contamination of soil level along with groundwater and the possibility of pollution of other biophysical resources along the discharged region. It has been demonstrated that textile industry wastewater has a direct influence on the physicochemical characteristics of soil [98].

4.3 Water Pollution and Health Risks

Textiles consume and pollute water more and ranked 2nd after agriculture portrayed in Table 4 [112]. Direct effluents from textiles into water bodies are the main source of water pollution [14]. Such discharge of effluents is 80% of total wastes produced by the textile industries [172]. In making a single cotton shirt, it is estimated that 2500–3000 l of water is used [151]. A case study was conducted to better understand how a conventional finishing factory operates and what may be accomplished via modernisation [156]. Without paying attention to the toxics in effluents, the waste from the textile is disposed into the water. Such wastewater contains high (BOD) Biological Oxygen Demand, (COD) Chemical Oxygen Demand, high (SS) total suspended solids, grease and oil, sulphides, sulphates, phosphates, Cr, copper (Co), and/or the salts of other heavy metals [160].

Improper or apparently processed wastewaters contain varying levels of heavy metals such as As, lead (Pb), nickel (Ni), Cd, Co, Mercury (Hg), Zn, and Cr, which have the potential to harm crops grown under such irrigation condition [139, 143]. The contamination of heavy metals is a growing issue in our seas, lakes, and rivers. Heavy metal deposition in fish, oysters, sediments, and other aquatic ecosystem components has been observed globally [144]. These hazardous heavy metals that enter the aquatic environment are adsorbed on top of particulate matter, despite the fact that they can form free metal ions and soluble complexes that are readily available [144].

Table 4 Water pollution due to textile and health risks

Pollutant	Short-term effects	Long-term effects	References
Zinc	–	Support cancer development	[23, 75]
		Involved in the pathogenesis of Alzheimer's disease	[171]
		Age-related degenerative diseases	[103]
		Influence Type I and Type II diabetes	[130]
	Cramps in the stomach, vomiting, and nausea may occur. Ingesting high levels of Zn may cause anaemia, pancreas damage, and drop in levels of high-density lipoprotein cholesterol in the body	–	[11]
	Inhalation exposure to Zn for up to 3 days caused severe damage to liver and lung tissues	–	[169]
Mercury	–	Increased cardiovascular health effects	[129]
		Atherosclerosis disease and acute coronary insufficiency	[166]
		Mercuric chloride (HgCl ₂) and methylmercury (CH ₃ Hg) are cancerous to humans; these can damage the human nervous system; high levels of exposure can permanently damage the kidney, brain, and foetuses; and effects on the brain may result in irritability, shyness, tremors, changes in eye sight or hearing loss, and memory problems	[101]
	Short-term exposure to high levels of metallic mercury vapours may cause lung damage, nausea, diarrhoea, vomiting, increased blood pressure or heart rate, skin diseases, and eyes diseases		[101]
Sulphates	Insufficient evidence about the toxicity of Sulphates to humans	–	[175]
	Increase in stool volume, moisture, and reduced intestinal transit time if exposure exceeds more than 500 mg/l		[41]

(continued)

Table 4 (continued)

Pollutant	Short-term effects	Long-term effects	References
		Not found yet	[29]
Sulphides	Severe mitochondrial swelling in support cells and olfactory neurons, thus resulting in olfactory epithelial necrosis and sloughing	–	[16]
	Hyperpnea, Unconsciousness, apnea, and death	–	[114]
	Neurological disorders such as headaches, dizziness, loss of balance, lack of concentration, recent and long-term memory loss, mood swings, irritability, excitement, and sleep disturbances. Behaviour changes such as anger, depression, tension, confusion, anxiety, fatigue, and vigour. The respiratory symptoms may include apnea, cough, noncardiogenic pulmonary edema, and cyanosis. Eye irritations like conjunctivitis, lacrimation, and photophobia and skin symptoms include itching, dryness, and redness	–	[170]
		Damage to the nervous system, status epilepticus, bronchospasms, and delayed respiratory failure	[141]
		Neuronal olfactory damage, sense of smell is disturbed, and rhinitis	[39]
Phosphates	Hypocalcaemia and related signs including tetany, hypotension, and tachycardia, deposition of calcium phosphate crystals in various tissues, including often fatal cardiovascular calcification	–	[125]
		Cancer, affects the metabolism of Vitamin D, effect the nervous systems, adverse reproductive outcomes, as well as adversative mental development in infants	[64]

(continued)

Table 4 (continued)

Pollutant	Short-term effects	Long-term effects	References
Copper	Short-term effects from ingestion of high levels of Co can cause gastrointestinal distress with symptoms such as nausea, vomiting, and pain in abdomen. Also, liver toxicity was seen in doses high enough that resulted in death. High levels of exposure to Co can cause damage to red blood cells, possibly resulting in anaemia	–	[97]
		Carcinogenic, damage to liver and kidney	[97]
Nickle	–	Decreased body weight, heart and liver diseases, and irritation of the skin	[107]
	–	Lung, nose, larynx and prostate cancer, Sickness and dizziness, Asthma and chronic bronchitis, Allergic reactions, and pneumonitis	[97]

4.4 Dye Pollution

Dyes are present in varying concentrations in effluents when released containing numerous processes. The dye content in the discharged wastewater ranges from 20 to 200 ppm [54]. The aquatic life is largely influenced by the release of toxics into water producing mutagenic and carcinogenic effects [30]. The 4-aminobiphenyl induces chromosomal instability and damage to DNA along with other serious complications [25, 93]. Similarly, gastrointestinal issues are caused by sunset yellow dye, while quinoline yellow dye, which is used in the pharmaceutical sector, can induce itching, sneezing, and hyperactivity in youngsters when consumed [31]. Headache, vomiting, ulcer, nausea, and other cardiac complications are attributed to exposure to methylene blue dyes [83]. Hence, dyes can alter the rate of photosynthetic activity in phytoplankton, which in turn is responsible for global warming [78].

Dye concentrations in textile effluent have been recorded in a variety of ranges. The ranges include the dye level in textile effluent is 10–50 mg/l [89]. The reactive dyes in cotton mills are allegedly discharged in concentrations of 60 mg/l [140] and 100–200 mg/l [55]. An extremely high concentration of reactive dyes has been reported, i.e., 7000 mg/l [86]. About 20–50 mg/l of dye concentration has been reported in samples collected from 14 Ramadhan Textiles in Iraq [2]. Moreover, the dye Acid orange-10 concentration was 45 mg/l [146], while 10–250 mg/l of dye concentration was found in disposals from houses [53].

4.5 *Dye Classification and Health Effects*

Dyes, metals, and other toxins are mixed with the effluents emitted by textile producers. Natural and synthetic dyes are the two types of colourants. Synthetic dyes are cheaply manufactured, come in a variety of colours, and are distinguished by their fastness, making them more commonly utilised as compared to natural dyes [85]. Synthetic dyes are categorised into various groups according to their chemical structure, i.e., azo, sulphur anthraquinone, phthalocyanine, and triarylmethane, and according to their mode of application, i.e., reactive, direct, disperse, basic, and vat dyeing [120]. The production of dyes is approximately 70 million tonnes, and 10 thousand dyes are used in textile processes throughout the world [22].

Different toxics are present in the textile effluents containing a high load of salts, alkalis, binders, dispersants, volatile organic compounds, surfactants, chlorobenzenes, reducing agents, dioxin, phthalates, phenols, pentachlorophenol, detergents, and heavy metals [63, 68, 180]. The yearly disposal of about 0.4–0.5 million tonnes containing dyes and compounds flow into water bodies, creating pollution, health issues shown in Table 5, and other environmental difficulties [15].

Natural dyes like Indigoid dyes, Anthraquinone dyes, Naphthoquinone dyes, Benzoquinone dyes, Flavonoid dyes, Carotenoid dyes, and Tannin-based dyes are classified on the basis of chemical structures of dyes [133]. Natural dyes are extracted from plants, animals, minerals, and microorganisms [93]. Some of the examples include blue colour dye obtained from indigo plants, red colour dye from madder and morinda, and yellow from various plants like turmeric barberry and marigold. Dyes obtained from animals include red colour dye from insects and Tyrian purple obtained from sea molluscs [133]. The textile standard has suggested that synthetic dyes be used within acceptable limits and that natural resources not be depleted for dye extraction. So, because the extraction of natural dyes utilising natural resources is not a sustainable choice when the entire globe is suffering the detrimental effects of climate change, synthetic dyes are favoured over natural colours [26, 108].

4.6 *Colouring Agents*

Textile colourants give colour to a textile item as a result of physical entrapment or chemical binding inside or around the textile substance, generally with a high degree of permanence. The textile material can take various forms, including fibre, yarn, fabric, garment, and so on. Textile colourants are available in liquid and solid forms, such as powders, granules, solutions, and dispersions. In some cases, precursors are applied to textile materials in order to create the colourant in situ within the cloth [159]. To colour textile items, both dyes and pigments are used [182]. Dyes are present in solution either at any stage during its application, while pigments are insoluble. The process by which dyes stay within a cloth is determined by the type of colourant used. Intermolecular forces work between dye and fibre following

Table 5 Dyes and their harmful effects

Dye classification	Health effects	References
Congo red	Carcinogenic	[177]
Triphenylmethane dyes	Carcinogenic to microbial and mammalian cells, mutagenic to rodents, and cause abnormalities in the reproductive system of fish and rabbits	[24]
Brilliant Cresyl Blue	Harmful impacts on humans and microorganisms	[3]
Rhodamine 6G	Causes human health issues such as irritation to the skin, eyes, and respiratory tracks. Ingestion via drinking water may cause subcutaneous tissue-borne sarcoma, a highly carcinogenic disease	[74]
Rhodamine B	Irritation to skin, eyes, and respiratory tract. It is a chronic neurotoxin and is carcinogenic to humans and animals	[51, 136]
Phenol red	Carcinogenic and toxic that stops the growth of renal epithelial cells irritation in skin, eyes, and respiratory tract. It has been testified that phenol red is mutagenic and is lethal to muscle fibres	[1]
Methylene Blue	Though it is a little toxic due to its effects like cyanosis, vomiting, heartbeat increase, quadriplegia, shock, jaundice, and tissue necrosis in humans	[88]
Crystal violet dye	Mutagenic and poisoning agent. It acts as a potent mutagenic and carcinogen and is responsible for tumour growth in some fish	[113]
Malachite green	It is a great threat to human health and the potential teratogenic, carcinogenic, and mutagenic	[43]
Azure B	Intercalate with the helical structure of DNA	[57]
Disperse Red 1	Increase the frequency of micro nuclei	[48]
	Formation of DNA adducts	[27]
	Mutagenic effects	[67]
Disperse Orange 1	DNA damage and cytotoxic effects	[49]
Sudan-I dye	Enzymatically altered into carcinogenic aromatic amines through the action of the intestinal flora	[117]
Basic Red 9	Breaks down into carcinogenic aromatic amines under anaerobic conditions and their disposal in water bodies has the potential for allergic dermatitis, skin irritation, mutations, and also cancer itself	[147]
	Local sarcomas and tumours in the liver and bladder	[118]
Crystal violet dye	Mitotic poisoning, which is associated with abnormal accumulation of metaphases	[100]
	Damage to chromosome	[111]
	Carcinogenic cause	[13]

(continued)

Table 5 (continued)

Dye classification	Health effects	References
	Chemical cystitis in humans, irritation of the skin and digestive tract, and respiratory and failure of the renal system	[100]

adsorption onto and/or dissolution inside the polymer. The formation of covalent bonds between the dye and the fibre and entrapment of colourant particles within the textile by deposition of an insoluble form of the dye may all contribute to retention [182].

4.6.1 Types of Colouring Agents

Natural Colourants

All textile colourants were derived directly from natural sources, such as insects, plants, and shellfish before the production of picric acid as a yellow dye for silk [34, 182]. In the 1920s, natural colourants were gradually supplanted by synthetic dyes and pigments, which provided a broader and brighter colour range as well as better economy and convenience. While, a recent surge in interest in natural textile colourants due to notions of renewable supply and minimal environmental effect due to non-suitability for industrial usage, have a restricted colour range, and exhibit only modest degrees of fastness at best. Furthermore, natural dyes sometimes need the application of a fixative, known as a mordant, to achieve adequate permanence; conventional metallic mordants are harmful to the environment. Textile colours derived from natural sources, such as Indigo, may now be produced more effectively by chemical synthesis [69].

Synthetic Colourants

A large proportion of textile colourants are chemically synthesised on an industrial scale [61]. Every year, about a million tonnes are generated globally. Since the first commercially effective synthetic textile dye, Mauveine, was produced in the late 1850s, tens of thousands of colourants have been sold [8, 182]. A more methodical approach to textile colourant research, however, spearheaded mostly by the German dye industry, resulted in a greater knowledge of both colour and chemistry structure connections. At the turn of the century, Germany produced 85% of the world's synthetic dyes, with the remaining 10% produced in the United Kingdom, France, and Switzerland. After some decades, manufacturing is centred in Asia, notably China and India, due to lower cost bases. Textile colourants have a multibillion-dollar global market [9]. The clothing sector consumes the most dyes and organic pigments. Some of the most popular textile dyes are quite commodities, produced

in large quantities of over 1000 tonnes per year for delivery at a few dollars per kilogramme or even less.

5 Other Aspects of Textile Industries

5.1 *Microplastics*

Microplastic is the form of a plastic polymer having a particle size of less than 5 mm [6]. Microplastic can be derived from either primary or secondary sources. Also, the European Chemicals Agency (ECHA) is more specific in its proposed definition:

“‘Microplastic’ means particles containing solid polymer, to which additives or other substances may have been added, and where $\geq 1\%$ w/w of particles have:

- (i) all dimensions $0.1 \mu\text{m} \leq x \leq 5 \text{ mm}$, or
- (ii) for fibres, a length of $0.3 \mu\text{m} \leq x \leq 15 \text{ mm}$ and length to diameter ratio of >3 ” [32].

Since their origin, primary microplastics have a micrometre size, such as microplastic fibre generated from fabric washing [109] and cosmetic goods (facial cleanser) labelled as “microbeads” or “microexfoliates” [47]. Secondary microplastics are formed as a result of physiochemical and biochemical mechanisms in the environment that degrade bigger plastic trash [19].

5.1.1 Production of Microplastics from Textile Industries

Many research on the release of microplastics from textiles have concentrated on home washing as a source of fibres entering waterways. Shedding is affected by the qualities of the textile item, such as fibre material, yarn size, fabric structure, fabric weight, and fabric finishing [21]. Polyester fleece, for instance, has been shown in several tests to have greater fibre counts, i.e., $>7000 \text{ fibres/m}^{-2}/\text{l}^{-1}$ as compared to other forms of polyester textiles [5]. Variability in washing equipment and settings, as well as detergents, can also affect the number of fibres released from a garment or item, with both dryers and washers causing textile fibre shedding. Several researchers have discovered that tumble drying increases fibre release by 3.5 times as compared to washing polyester fleece items [116]. Further possible sources of textile-derived microplastics in the environment include ropes and netting fragmentation and the breakdown of carelessly disposed non-woven hygiene items [21].

5.1.2 Process of Microplastic Formation

The rising global manufacturing of synthetic fibres poses a threat that microplastics produced by synthetic textiles will continue to pollute our ecosystem in near future [60]. Fibres are frequently identified as the major ingredient of microplastics discovered in wastewater treatment facilities [80, 106], as well as in a wide range of environmental samples [35, 50]. According to a recent modelling research, fibres from textiles substantially contribute to microplastic emissions into freshwater [79]. As a result, these microplastics are released into the environment, which in turn are present in effluents or trapped by the sludge.

Several inferences about the release processes, however, may still be drawn. Because the washing studies looked at different textiles using different experimental setups and analytical methods, the amount of microplastics released per wash reported varied, ranging from 0.012 mg/g [116] to 3.3 mg/g [142] and from 23 MPF/g [116] to 1273 MPF/g [44]. It is estimated that the release of microplastics from textiles is heavily influenced by the types of textiles and their treatment procedures [20]. Hence, materials utilised in several research ranged from complete garments [18, 58] to textile pieces [44], to double folded and stitched edges [62], and to scissor-cut edges (Table 6).

6 Conclusion

This study focused on the wastes generated by textile industries and their negative influences on humans and the environment. Dyeing may be either natural or artificial, which has serious environmental health issues. About, 200,000 dyes are disposed into our environment every year. Also, colourants are either primary or secondary and have negative effects on the environment in the form of health complications to humans. Different types of microplastics can also have serious effects on the environment and humans.

Table 6 Types of microplastics and their impacts on human health

Types of microplastic	Concentration	Health effects	References
Polystyrene	Short-term exposure (170 mg/m ³) long-term exposure (85 mg/m ³)	Possibly penetrate into the outer cell membrane, intracellular oxygen species endocytosis internalisation, cytotoxicity, oxidative stress, genotoxicity, and even cause damage to DNA	[119, 178]
	–	Low toxicity on cell capability, oxidative stress and membrane reliability and fluidity, disrupt mitochondrial membrane potential and plasma membrane inhibition, Adenosine triphosphate binding cassette	[176]
	–	Cytotoxic effects, oxidative stress, inflammatory reactions, and disruption of the epithelial layer	[38]
Polypropylene	10 mg/day		[161]
		Asthma, pneumothorax, alveolitis, chronic bronchitis, and pneumonia	[115]
		Cytotoxicity, hypersensitivity, disruptive immune responses, and acute responses such as haemolysis	[70]
		Some degree of cytotoxicity at high dosages, low degree of induction of proinflammatory cytokines, and enhanced histamine release from various cells	[70]
Polyethylene	–	No obvious toxic effect, still some nanoparticles are internalised into endo-lysosomal compartments, which bears a high propensity to cross the intestinal barrier	[94]

(continued)

Table 6 (continued)

Types of microplastic	Concentration	Health effects	References
		Intestinal damage	[91]
		Variations in plasma levels of various metabolic enzymes and immune markers, combined with Cadmium polyethylene can enhance the toxicity of Cadmium	[10]
Polycarbonate	–	Bisphenol-A, a by-product of polycarbonate, is a known endocrine disruptor that may cause colon cancer	[52]

References

1. Abdullah NA, Othaman R, Abdullah I, Nazwa J, Baharum A (2012) Studies on the adsorption of phenol red dye using silica-filled ENR/PVC beads. *J Emerg Trends Eng Appl Sci* 3(5):845–850. <https://doi.org/10.10520/EJC131545>
2. Abid MF, Zablouk MA, Abid-Alameer AM (2012) Experimental study of dye removal from industrial wastewater by membrane technologies of reverse osmosis and nanofiltration. *Iran J Env Health Sci Eng* 9(1):1–9. <https://doi.org/10.1186/1735-2746-9-17>
3. Afkhami A, Saber-Tehrani M, Bagheri H (2010) Modified maghemite nanoparticles as an efficient adsorbent for removing some cationic dyes from aqueous solution. *Desalination* 263(1–3):240–248. <https://doi.org/10.1016/j.desal.2010.06.065>
4. Ahmed MK, Shaheen N, Islam MS, Habibullah-Al-Mamun M, Islam S, Islam MM, Kundu GK, Bhattacharjee L (2016) A comprehensive assessment of arsenic in commonly consumed foodstuffs to evaluate the potential health risk in Bangladesh. *Sci Total Environ* 544:125–133. <https://doi.org/10.1016/j.scitotenv.2015.11.133>
5. Almroth BMC, Åström L, Roslund S, Petersson H, Johansson M, Persson N-K (2018) Quantifying shedding of synthetic fibers from textiles; a source of microplastics released into the environment. *Environ Sci Pollut Res* 25(2):1191–1199. <https://doi.org/10.1007/s11356-017-0528-7>
6. Arthur C, Baker JE, Bamford HA (2009) Proceedings of the international research workshop on the occurrence, effects, and fate of microplastic Marine Debris. University of Washington Tacoma, Tacoma, WA, USA, 9–11 Sept 2008
7. Atkinson RW, Butland BK, Anderson HR, Maynard RL (2018) Long-term concentrations of nitrogen dioxide and mortality: a meta-analysis of cohort studies. *Epidemiology (Cambridge, MA)* 29(4):460. <https://doi.org/10.1097/EDE.0000000000000847>
8. Baldwin T, Shore J (1990) In: Shore J (ed) *Colorants and auxiliaries*, vol 2, pp 338–339
9. Bamfield P (2010) *Chromic phenomena: technological applications of colour chemistry*. Royal Society of Chemistry
10. Banaee M, Soltanian S, Sureda A, Gholamhosseini A, Haghi BN, Akhlaghi M, Derikvandy A (2019) Evaluation of single and combined effects of cadmium and micro-plastic particles on biochemical and immunological parameters of common carp (*Cyprinus carpio*). *Chemosphere* 236:124335
11. Belay K, Abisa Z (2015) Developing a method for trace metal analysis in spices using spectroscopic techniques: a review. *Int J Chem Nat Sci* 3:195–199
12. Beton A, Dias D, Farrant L, Gibon T, Le Guern Y, Desaxce M, Kougoulis J et al (2014) Environmental improvement potential of textiles (IMPRO-textiles). European Commission

13. Bharagava RN, Mani S, Mulla SI, Saratale GD (2018) Degradation and decolorization potential of a ligninolytic enzyme producing *Aeromonas hydrophila* for crystal violet dye and its phytotoxicity evaluation. *Ecotoxicol Environ Saf* 156:166–175. <https://doi.org/10.1016/j.ecoenv.2018.03.012>
14. Bhatia S, Devraj S (2017) Pollution control in textile industry. WPI Publishing
15. Bhavsar S, Dudhagara P, Tank S (2018) R software package based statistical optimization of process components to simultaneously enhance the bacterial growth, laccase production and textile dye decolorization with cytotoxicity study. *PloS One* 13(5):e0195795
16. Brenneisen KA, Meleason DF, Sar M, Marshall MW, James RA, Gross EA, Martin JT, Dorman DC (2002) Olfactory mucosal necrosis in male CD rats following acute inhalation exposure to hydrogen sulfide: reversibility and the possible role of regional metabolism. *Toxicol Pathol* 30(2):200–208. <https://doi.org/10.1080/019262302753559533>
17. Briga-Sa A, Nascimento D, Teixeira N, Pinto J, Caldeira F, Varum H, Paiva A (2013) Textile waste as an alternative thermal insulation building material solution. *Constr Build Mater* 38:155–160. <https://doi.org/10.1016/j.conbuildmat.2012.08.037>
18. Browne MA, Crump P, Niven SJ, Teuten E, Tonkin A, Galloway T, Thompson R (2011) Accumulation of microplastic on shorelines worldwide: sources and sinks. *Environ Sci Technol* 45(21):9175–9179. <https://doi.org/10.1021/es201811s>
19. Browne MA, Niven SJ, Galloway TS, Rowland SJ, Thompson RC (2013) Microplastic moves pollutants and additives to worms, reducing functions linked to health and biodiversity. *Curr Biol* 23(23):2388–2392. <https://doi.org/10.1016/j.cub.2013.10.012>
20. Cai Y, Mitrano DM, Heuberger M, Hufenus R, Nowack B (2020) The origin of microplastic fiber in polyester textiles: the textile production process matters. *J Clean Prod* 267:121970. <https://doi.org/10.1016/j.jclepro.2020.121970>
21. Cesa FS, Turra A, Baruaque-Ramos J (2017) Synthetic fibers as microplastics in the marine environment: a review from textile perspective with a focus on domestic washings. *Sci Total Environ* 598:1116–1129. <https://doi.org/10.1016/j.scitotenv.2017.04.172>
22. Chandanshive V, Kadam S, Rane N, Jeon B-H, Jadhav J, Govindwar S (2020) In situ textile wastewater treatment in high rate transpiration system furrows planted with aquatic macrophytes and floating phytobeds. *Chemosphere* 252:126513. <https://doi.org/10.1016/j.chemosphere.2020.126513>
23. Chasapis CT, Spyroulias GA (2009) RING finger E3 ubiquitin ligases: structure and drug discovery. *Curr Pharm Des* 15(31):3716–3731. <https://doi.org/10.2174/138161209789271825>
24. Chen C-H, Chang C-F, Liu S-M (2010) Partial degradation mechanisms of malachite green and methyl violet B by *Shewanella decolorationis* NTOU1 under anaerobic conditions. *J Hazard Mater* 177(1–3):281–289. <https://doi.org/10.1016/j.jhazmat.2009.12.030>
25. Chen K-C, Wu J-Y, Liou D-J, Hwang S-CJ (2003) Decolorization of the textile dyes by newly isolated bacterial strains. *J Biotechnol* 101(1):57–68. [https://doi.org/10.1016/S0168-1656\(02\)00303-6](https://doi.org/10.1016/S0168-1656(02)00303-6)
26. Chengalroyen M, Dabbs E (2013) The microbial degradation of azo dyes: minireview. *World J Microbiol Biotechnol* 29(3):389–399. <https://doi.org/10.1007/s11274-012-1198-8>
27. Chequer FMD, Lizier TM, de Felício R, Zanoni MVB, Deboni HM, Lopes NP, Marcos R, de Oliveira DP (2011) Analyses of the genotoxic and mutagenic potential of the products formed after the biotransformation of the azo dye Disperse Red 1. *Toxicol In Vitro* 25(8):2054–2063. <https://doi.org/10.1016/j.tiv.2011.05.033>
28. Chequer FD, De Oliveira GR, Ferraz EA, Cardoso JC, Zanoni MB, de Oliveira DP (2013) Textile dyes: dyeing process and environmental impact. In: *Eco-friendly textile dyeing and finishing*, vol 6(6), pp 151–176
29. Chou C (2003) Hydrogen sulfide: human health aspects. World Health Organization
30. Chowdhury S, Saha P (2010) Sea shell powder as a new adsorbent to remove Basic Green 4 (Malachite Green) from aqueous solutions: equilibrium, kinetic and thermodynamic studies. *Chem Eng J* 164(1):168–177. <https://doi.org/10.1016/j.cej.2010.08.050>

31. Chung K-T (2016) Azo dyes and human health: a review. *J Environ Sci Health C* 34(4):233–261. <https://doi.org/10.1080/10590501.2016.1236602>
32. Committee for Risk Assessment and Committee for Socio-economic Analysis (2020) Opinion on an Annex XV dossier proposing restrictions on intentionally-added microplastics. <https://echa.europa.eu/documents/10162/5a730193-cb17-2972-b595-93084c4f39c8>. Accessed on 30 July 2020
33. Dauda MY, Erkert EA (2020) Investigation of reactive Blue 19 biodegradation and byproducts toxicity assessment using crude laccase extract from *Trametes versicolor*. *J Hazard Mater* 393:121555. <https://doi.org/10.1016/j.jhazmat.2019.121555>
34. De Graaff JH (2004) The colourful past. Origins, chemistry and identification of natural dyestuffs, pp 234–235
35. Desforges J-PW, Galbraith M, Dangerfield N, Ross PS (2014) Widespread distribution of microplastics in subsurface seawater in the NE Pacific Ocean. *Mar Pollut Bull* 79(1–2):94–99. <https://doi.org/10.1016/j.marpolbul.2013.12.035>
36. Desore A, Narula SA (2018) An overview on corporate response towards sustainability issues in textile industry. *Environ Dev Sustain* 20(4):1439–1459. <https://doi.org/10.1007/s10668-017-9949-1>
37. Dharmaraj A, Sivakumar S (2013) Direct and indirect effects of independents variables on return on the total assets of composite cotton sector—an analytical study in Indian textile companies. *Bonfring Int J Ind Eng Manag Sci* 3(1):24–26
38. Dong CD, Chen CW, Chen YC, Chen HH, Lee JS, Lin CH (2020) Polystyrene microplastic particles: In vitro pulmonary toxicity assessment. *J Hazard Mater* 385:121575
39. Dorman DC, Struve MF, Gross EA, Brenneman KA (2004) Respiratory tract toxicity of inhaled hydrogen sulfide in Fischer-344 rats, Sprague-Dawley rats, and B6C3F1 mice following subchronic (90-day) exposure. *Toxicol Appl Pharmacol* 198(1):29–39. <https://doi.org/10.1016/j.taap.2004.03.010>
40. EPA E (1997) Office of compliance sector notebook project: profile of the textile industry. EPA310R97009, Washington
41. EPA E (2002) Drinking water advisory: consumer acceptability advice and health effects analysis on sulfate (draft). USA
42. Eichhoff J, Hehl A, Jockenhoewel S, Gries T (2013) Textile fabrication technologies for embedding electronic functions into fibres, yarns and fabrics. In: *Multidisciplinary know-how for smart-textiles developers*. Woodhead Publishing, pp 191–226
43. FAO (2009) Food and Agriculture Organization of the United Nations and World Health Organization. Evaluation of certain veterinary drug residues in food. *World Health Organ Tech Rep Ser* 1–134
44. De Falco F, Gullo MP, Gentile G, Di Pace E, Cocca M, Gelabert L, Brouta-Agnésa M, Rovira A, Escudero R, Villalba R, Mossotti R, Montarsolo A, Gavignano S, Tonin C, Villalba R (2018) Evaluation of microplastic release caused by textile washing processes of synthetic fabrics. *Environ Pollut* 236:916–925. <https://doi.org/10.1016/j.envpol.2017.10.057>
45. Fallahzadeh RA, Khosravi R, Dehdashti B, Ghahramani E, Omid F, Adli A, Miri M (2018) Spatial distribution variation and probabilistic risk assessment of exposure to chromium in ground water supplies; a case study in the east of Iran. *Food Chem Toxicol* 115:260–266. <https://doi.org/10.1016/j.fct.2018.03.019>
46. Fedajev A, Nikolić R, Urošević S (2010) The importance of textile industry in the economy of Serbia. *Tekst Ind* 58(2):25–32
47. Fendall LS, Sewell MA (2009) Contributing to marine pollution by washing your face: microplastics in facial cleansers. *Mar Pollut Bull* 58(8):1225–1228. <https://doi.org/10.1016/j.marpolbul.2009.04.025>
48. Fernandes FH, Bustos-Obregon E, Salvadori DMF (2015) Disperse Red 1 (textile dye) induces cytotoxic and genotoxic effects in mouse germ cells. *Reprod Toxicol* 53:75–81. <https://doi.org/10.1016/j.reprotox.2015.04.002>
49. Ferraz ER, Grando MD, Oliveira DP (2011) The azo dye disperse orange 1 induces DNA damage and cytotoxic effects but does not cause ecotoxic effects in *Daphnia similis* and *Vibrio fischeri*. *J Hazard Mater* 192(2):628–633. <https://doi.org/10.1016/j.jhazmat.2011.05.063>

50. Frias J, Gago J, Otero V, Sobral P (2016) Microplastics in coastal sediments from Southern Portuguese shelf waters. *Mar Environ Res* 114:24–30. <https://doi.org/10.1016/j.marenvres.2015.12.006>
51. Fu F, Wang Q (2011) Removal of heavy metal ions from wastewaters: a review. *J Environ Manage* 92(3):407–418. <https://doi.org/10.1016/j.jenvman.2010.11.011>
52. Gao H, Yang B-J, Li N, Feng L-M, Shi X-Y, Zhao W-H, Liu S-J (2015) Bisphenol A and hormone-associated cancers: current progress and perspectives. *Medicine* 94(1). <https://doi.org/10.1097/MD.0000000000000211>
53. Ghaly A, Ananthashankar R, Alhattab M, Ramakrishnan V (2014) Production, characterization and treatment of textile effluents: a critical review. *J Chem Eng Process Technol* 5(1):1–19. <https://doi.org/10.4172/2157-7048.1000182>
54. Gita S, Shukla S, Saharan N, Prakash C, Deshmukhe G (2019) Toxic Effects of selected textile dyes on elemental composition, photosynthetic pigments, protein content and growth of a freshwater chlorophycean alga *Chlorella vulgaris*. *Bull Environ Contam Toxicol* 102(6):795–801. <https://doi.org/10.1007/s00128-019-02599-w>
55. Gähr F, Hermanutz F, Oppermann W (1994) Ozonation—an important technique to comply with new German laws for textile wastewater treatment. *Water Sci Technol* 30(3):255
56. Güleriyüz Ö (2011) Textile sector and future in Turkey in global developments. M.Sc. thesis. Isparta, Turkey
57. Haq I, Raj A (2018) Biodegradation of Azure-B dye by *Serratia liquefaciens* and its validation by phytotoxicity, genotoxicity and cytotoxicity studies. *Chemosphere* 196:58–68. <https://doi.org/10.1016/j.chemosphere.2017.12.153>
58. Hartline NL, Bruce NJ, Karba SN, Ruff EO, Sonar SU, Holden PA (2016) Microfiber masses recovered from conventional machine washing of new or aged garments. *Environ Sci Technol* 50(21):11532–11538. <https://doi.org/10.1021/acs.est.6b03045>
59. Hassan MM, Carr CM (2018) A critical review on recent advancements of the removal of reactive dyes from dyehouse effluent by ion-exchange adsorbents. *Chemosphere* 209:201–219. <https://doi.org/10.1016/j.chemosphere.2018.06.043>
60. Henry B, Laitala K, Klepp IG (2019) Microfibres from apparel and home textiles: prospects for including microplastics in environmental sustainability assessment. *Sci Total Environ* 652:483–494. <https://doi.org/10.1016/j.scitotenv.2018.10.166>
61. Herbst W, Hunger K (1997) *Industrial Organic Pigments*, 2nd completely revised edn. Wiley-VCH, Weinheim
62. Hernandez E, Nowack B, Mitrano DM (2017) Polyester textiles as a source of microplastics from households: a mechanistic study to understand microfiber release during washing. *Environ Sci Technol* 51(12):7036–7046. <https://doi.org/10.1021/acs.est.7b01750>
63. Herrera-González AM, Caldera-Villalobos M, Peláez-Cid A-A (2019) Adsorption of textile dyes using an activated carbon and crosslinked polyvinyl phosphonic acid composite. *J Environ Manage* 234:237–244. <https://doi.org/10.1016/j.jenvman.2019.01.012>
64. Von der Heyden C, New M (2004) Groundwater pollution on the Zambian Copperbelt: deciphering the source and the risk. *Sci Total Environ* 327(1–3):17–30. <https://doi.org/10.1016/j.scitotenv.2003.08.028>
65. Hossain L, Sarker SK, Khan MS (2018) Evaluation of present and future wastewater impacts of textile dyeing industries in Bangladesh. *Environ Dev* 26:23–33
66. Hossain I (2011) Textile knowledge. Available from: <https://textileknowledge.files.wordpress.com/2011/10/flow-chart-for-combedyarn1.jpg>. Accessed: 8 June 2011
67. Hsu C-H, Stedeford T (2010) Cancer risk assessment: chemical carcinogenesis, hazard evaluation, and risk quantification. Wiley
68. Hubadillah SK, Othman MHD, Tai ZS, Jamalludin MR, Yusuf NK, Ahmad A, Rahman MA, Jaafar J, Kadir SHSA, Harun Z (2020) Novel hydroxyapatite-based bio-ceramic hollow fiber membrane derived from waste cow bone for textile wastewater treatment. *Chem Eng J* 379:122396. <https://doi.org/10.1016/j.cej.2019.122396>
69. Hunger K (2007) *Industrial dyes: chemistry, properties, applications*

70. Hwang J, Choi D, Han S, Choi J, Hong J (2019) An assessment of the toxicity of polypropylene microplastics in human derived cells. *Sci Total Environ* 684:657–669. <https://doi.org/10.1016/j.scitotenv.2019.05.071>
71. Imran M, Crowley DE, Khalid A, Hussain S, Mumtaz MW, Arshad M (2015) Microbial biotechnology for decolorization of textile wastewaters. *Rev Environ Sci Bio/Technol* 14(1):73–92. <https://doi.org/10.1007/s11157-014-9344-4>
72. Intiazuddin S, Tiki S, Chemicals A (2018) Impact of textile wastewater pollution on the environment. *Pak Text J* 10:38–39
73. Jaganathan V, Cherurveetil P, Chellasamy A, Premapriya M (2014) Environmental pollution risk analysis and management in textile industry: a preventive mechanism. *Eur Sci J*, 480–486. <https://doi.org/10.1.1.685.6416&rep=rep1&type=pdf#page=522>
74. Jain R, Mathur M, Sikarwar S, Mittal A (2007) Removal of the hazardous dye rhodamine B through photocatalytic and adsorption treatments. *J Environ Manage* 85(4):956–964. <https://doi.org/10.1016/j.jenvman.2006.11.002>
75. John E, Laskow TC, Buchser WJ, Pitt BR, Basse PH, Butterfield LH, Kalinski P, Lotze MT (2010) Zinc in innate and adaptive tumor immunity. *J Transl Med* 8(1):1–16. <https://doi.org/10.1186/1479-5876-8-118>
76. Kant R (2012) Textile dyeing industry an environmental hazard. *Nat Sci* 4(1):22–26. <https://doi.org/10.4236/ns.2012.41004>
77. Karim ME, Dhar K, Hossain MT (2018) Decolorization of textile reactive dyes by bacterial monoculture and consortium screened from textile dyeing effluent. *J Genet Eng Biotechnol* 16(2):375–380. <https://doi.org/10.1016/j.jgeb.2018.02.005>
78. Katheresan V, Kansedo J, Lau SY (2018) Efficiency of various recent wastewater dye removal methods: a review. *J Environ Chem Eng* 6(4):4676–4697. <https://doi.org/10.1016/j.jece.2018.06.060>
79. Kawecki D, Nowack B (2019) Polymer-specific modeling of the environmental emissions of seven commodity plastics as macro- and microplastics. *Environ Sci Technol* 53(16):9664–9676. <https://doi.org/10.1021/acs.est.9b02900>
80. Kay P, Hiscoe R, Moberley I, Bajic L, McKenna N (2018) Wastewater treatment plants as a source of microplastics in river catchments. *Environ Sci Pollut Res* 25(20):20264–20267. <https://doi.org/10.1007/s11356-018-2070-7>
81. Keith-Roach MJ (2008) The speciation, stability, solubility and biodegradation of organic co-contaminant radionuclide complexes: a review. *Sci Total Environ* 396(1):1–11
82. Khandare RV, Govindwar SP (2015) Phytoremediation of textile dyes and effluents: current scenario and future prospects. *Biotechnol Adv* 33(8):1697–1714. <https://doi.org/10.1016/j.biotechadv.2015.09.003>
83. Khandare RV, Govindwar SP (2016) Microbial degradation mechanism of textile dye and its metabolic pathway for environmental safety. *Environ Waste Manag*, 399–439
84. Khatri J, Nidheesh P, Singh TA, Kumar MS (2018) Advanced oxidation processes based on zero-valent aluminium for treating textile wastewater. *Chem Eng J* 348:67–73. <https://doi.org/10.1016/j.cej.2018.04.074>
85. Khehra MS, Saini HS, Sharma DK, Chadha BS, Chimni SS (2006) Biodegradation of azo dye CI Acid Red 88 by an anoxic–aerobic sequential bioreactor. *Dyes Pigm* 70(1):1–7. <https://doi.org/10.1016/j.dyepig.2004.12.021>
86. Koprivanac N, Bosanac G, Grabaric Z, Papic S (1993) Treatment of wastewaters from dye industry. *Environ Technol* 14(4):385–390. <https://doi.org/10.1080/0959339309385304>
87. Kumar S, Sharma A (2019) Cadmium toxicity: effects on human reproduction and fertility. *Rev Environ Health* 34(4):327–338. <https://doi.org/10.1515/reveh-2019-0016/html>
88. Kushwaha AK, Gupta N, Chattopadhyaya M (2014) Removal of cationic methylene blue and malachite green dyes from aqueous solution by waste materials of *Daucus carota*. *J Saudi Chem Soc* 18(3):200–207. <https://doi.org/10.1016/j.jscs.2011.06.011>
89. Laing I (1991) The impact of effluent regulations on the dyeing industry. *Rev Prog Color Relat Top* 21(1):56–71. <https://doi.org/10.1111/j.1478-4408.1991.tb00081.x>

90. Lawrence CA (2003) *Fundamentals of Spun Yarn technology*, 1st edn., CRC Press, UK, p 552. ISBN 9781566768214
91. Lei L, Wu S, Lu S, Liu M, Song Y, Fu Z, He D (2018) Microplastic particles cause intestinal damage and other adverse effects in zebrafish *Danio rerio* and nematode *Caenorhabditis elegans*. *Sci Total Environ* 619:1–8
92. Lord PR (2003) *Handbook of Yarn Production*, 1st edn. Woodhead Publishing, UK, p 504 (2003). ISBN 9781855736962
93. Lyon (2010) Some aromatic amines, organic dyes and related exposures. IARC Monographs on the Evaluation of Carcinogenic Risks to Humans
94. Magri D, Sanchez-Moreno P, Caputo G, Gatto F, Veronesi M, Bardi G, Fragouli D (2018) Laser ablation as a versatile tool to mimic polyethylene terephthalate nanoplastic pollutants: characterization and toxicology assessment. *ACS Nano* 12(8):7690–7700
95. Mahapatra N (2016) *Textile dyes*. Woodhead Publishing India Pvt. New Delhi. CRC Press, Boca Raton
96. Mahmoud A, Ghaly A, Brooks M (2007) Removal of dye from textile wastewater using plant oils under different pH and temperature conditions. *Am J Environ Sci* 3(4):205–218. <https://doi.org/10.3844/ajessp.2007>
97. Mahurpawar M (2015) Effects of heavy metals on human health. *Int J Res Granthaalayah* 3(9SE):1–7. <https://doi.org/10.29121/granthaalayah.v3.i9SE.2015.3282>
98. Malik SN, Ghosh PC, Vaidya AN, Waindeskar V, Das S, Mudliar SN (2017) Comparison of coagulation, ozone and ferrate treatment processes for color, COD and toxicity removal from complex textile wastewater. *Water Sci Technol* 76(5):1001–1010
99. Mallongi A, Indra R, Arief MKM, Satrianegara MF (2020) Environmental pollution and health problems due to forest fires with CO₂ parameters. *Med Leg Update* 20(3):888–892
100. Mani S, Bharagava RN (2016) Exposure to crystal violet, its toxic, genotoxic and carcinogenic effects on environment and its degradation and detoxification for environmental safety. *Rev Environ Contam Toxicol* 237:71–104. https://doi.org/10.1007/978-3-319-23573-8_4
101. Martin S, Griswold W (2009) Human health effects of heavy metals. *Environ Sci Technol Briefs Citizens* 15:1–6. <https://doi.org/10.1.1.399.9831&rep=rep1&type=pdf>
102. Mia R, Selim M, Shamim A, Chowdhury M, Sultana S, Armin M, Hossain M, Akter R, Dey S, Naznin H (2019) Review on various types of pollution problem in textile dyeing and printing industries of Bangladesh and recommendation for mitigation. *J Text Eng Fashion Technol* 5(4):220–226
103. Mocchegiani E, Costarelli L, Giacconi R, Piacenza F, Basso A, Malavolta M (2011) Zinc, metallothioneins and immunosenescence: effect of zinc supply as nutrigenomic approach. *Biogerontology* 12(5):455–465. <https://doi.org/10.1007/s10522-011-9337-4>
104. Modak (1991) Environmental aspects of the textile industry: a technical guide. Prepared for United Nations Environment Programme Industry and Environment Office. <http://www.miga.org/documents/Textiles.pdf>
105. Morón FP (1994) Operaciones fundamentales en la hilatura de fibras textiles. Hespérides
106. Murphy F, Ewins C, Carbonnier F, Quinn B (2016) Wastewater treatment works (WwTW) as a source of microplastics in the aquatic environment. *Environ Sci Technol* 50(11):5800–5808. <https://doi.org/10.1021/acs.est.5b05416>
107. Mushtaq N, Singh DV, Bhat RA, Dervash MA, bin Hameed O (2020) Freshwater contamination: sources and hazards to aquatic biota. In: *Fresh water pollution dynamics and remediation*. Springer, pp 27–50
108. Muthu SS (2014) *Roadmap to sustainable textiles and clothing: eco-friendly raw materials, technologies, and processing methods*. Springer
109. Napper IE, Thompson RC (2016) Release of synthetic microplastic plastic fibres from domestic washing machines: effects of fabric type and washing conditions. *Mar Pollut Bull* 112(1–2):39–45. <https://doi.org/10.1016/j.marpollbul.2016.09.025>
110. Neefus JD (1982) *Textile industrial processes*. In: Cralley LV, Cralley LJ (eds) *Industrial hygiene aspects of plant operations, volume 1, process flows*. MacMillan Publishing Co., Inc., New York, NY

111. Newman MC (2015) *Fundamentals of ecotoxicology: the science of pollution*. CRC Press, Boca Raton
112. Oecotextiles (2012) Textile industry poses environmental hazards. Available at http://www.oecotextiles.com/PDF/textile_industry_hazards.pdf, accessed. Accessed 1 Dec 12
113. Parshetti G, Parshetti S, Telke A, Kalyani D, Doong R, Govindwar SP (2011) Biodegradation of crystal violet by *Agrobacterium radiobacter*. *J Environ Sci* 23(8):1384–1393. [https://doi.org/10.1016/S1001-0742\(10\)60547-5](https://doi.org/10.1016/S1001-0742(10)60547-5)
114. Pearson RJ, Wilson T, Wang R (2006) Endogenous hydrogen sulfide and the cardiovascular system—what’s the smell all about? *Clin Invest Med* 29(3):146
115. Pimentel JC, Avila R, Lourenço AG (1975) Respiratory disease caused by synthetic fibres: a new occupational disease. *Thorax* 30(2):204–219. <https://doi.org/10.1136/thx.30.2.204>
116. Pirc U, Vidmar M, Mozer A, Kržan A (2016) Emissions of microplastic fibers from microfiber fleece during domestic washing. *Environ Sci Pollut Res* 23(21):22206–22211. <https://doi.org/10.1007/s11356-016-7703-0>
117. Piątkowska M, Jedziniak P, Olejnik M, Żmudzki J, Posylniak A (2018) Absence of evidence or evidence of absence? a transfer and depletion study of Sudan I in eggs. *Food Chem* 239:598–602. <https://doi.org/10.1016/j.foodchem.2017.06.156>
118. Pohanish RP (2017) *Sittig’s handbook of toxic and hazardous chemicals and carcinogens*. William Andrew
119. Poma A, Vecchiotti G, Colafarina S, Zarivi O, Aloisi M, Arrizza L, Chichiricò G, Di Carlo P (2019) In vitro genotoxicity of polystyrene nanoparticles on the human fibroblast Hs27 cell line. *Nanomaterials* 9(9):1299. <https://doi.org/10.3390/nano9091299>
120. Popli S, Patel UD (2015) Destruction of azo dyes by anaerobic–aerobic sequential biological treatment: a review. *Int J Environ Sci Technol* 12(1):405–420. <https://doi.org/10.1007/s13762-014-0499-x>
121. Pérez JB, Arrieta AG, Encinas AH, Dios AQ (2016) Textile engineering and case based reasoning. Paper presented at the distributed computing and artificial intelligence, 13th international conference
122. Pérez JJ-B, Arrieta AG, Encinas AH, Dios MAQ (2017) Manufacturing processes in the textile industry. Expert systems for fabrics production. *ADCAIJ Adv Distrib Comput Artif Intell J* 6(4):15–23
123. Pönkä A (1990) Absenteeism and respiratory disease among children and adults in Helsinki in relation to low-level air pollution and temperature. *Environ Res* 52(1):34–46. [https://doi.org/10.1016/S0013-9351\(05\)80149-5](https://doi.org/10.1016/S0013-9351(05)80149-5)
124. Rasel S, Sarkar J (2019) Manufacturing of fabric by recycling plastic bottles: an ecological approach part 2: manufacturing process
125. Razzaque MS (2011) Phosphate toxicity: new insights into an old problem. *Clin Sci* 120(3):91–97. <https://doi.org/10.1042/CS20100377>
126. Rehman U, Khan S, Muhammad S (2020) Ingestion of arsenic-contaminated drinking water leads to health risk and traces in human biomarkers (hair, nails, blood, and urine), Pakistan. *Exposure Health* 12(2):243–254. <https://doi.org/10.1007/s12403-019-00308-w>
127. Rehman K, Shahzad T, Sahar A, Hussain S, Mahmood F, Siddique MH, Siddique MA, Rashid MI (2018) Effect of reactive black 5 azo dye on soil processes related to C and N cycling. *PeerJ* 6:e4802. <https://doi.org/10.7717/peerj.4802>
128. Reno AL, Brooks EG, Ameredes BT (2015) Mechanisms of heightened airway sensitivity and responses to inhaled SO₂ in asthmatics. *Environ Health Insights (EHI)* 9:S15671. <https://doi.org/10.4137/EHI.S15671>
129. Roman HA, Walsh TL, Coull BA, Dewailly É, Guallar E, Hattis D, Mariën K, Schwartz J, Stern AH, Virtanen JK, Virtanen JK (2011) Evaluation of the cardiovascular effects of methylmercury exposures: current evidence supports development of a dose–response function for regulatory benefits analysis. *Environ Health Perspect* 119(5):607–614. <https://doi.org/10.1289/ehp.1003012>
130. Rutter GA (2010) Think zinc: new roles for zinc in the control of insulin secretion. *Islets* 2(1):49–50. <https://doi.org/10.4161/isl.2.1.10259>

131. Sandhya S (2010) Biodegradation of azo dyes under anaerobic condition: role of azoreductase. In: Biodegradation of azo dyes, pp 39–57. <https://doi.org/10.1007/978-2009-43>
132. Sarker BC, Baten MA, Eqram M, Haque U, Das AK, Hossain A, Hasan MZ (2015) Heavy metals concentration in textile and garments industries' wastewater of Bhaluka industrial area, Mymensingh, Bangladesh. *Curr World Environ* 10(1):61. <https://doi.org/10.12944/CWE.10.1.07>
133. Saxena S, Raja A (2014) Natural dyes: sources, chemistry, application and sustainability issues roadmap to sustainable textiles and clothing. Springer, pp 37–80
134. Saxena S, Raja A, Arputharaj A (2017) Challenges in sustainable wet processing of textiles textiles and clothing sustainability. Springer, pp 43–79
135. Setiadi T, Andriani Y, Erlania M (2006) Treatment of textile wastewater by a combination of anaerobic and aerobic processes: a denim processing plant case. *Southeast Asian Water Environ J*. <https://doi.org/10.2166/9781780402987>
136. Shakir K, Elkafrawy AF, Ghoneimy HF, Beheir SGE, Refaat M (2010) Removal of rhodamine B (a basic dye) and thoron (an acidic dye) from dilute aqueous solutions and wastewater simulants by ion flotation. *Water Res* 44(5):1449–1461. <https://doi.org/10.1016/j.watres.2009.10.029>
137. Shamey R, Zhao X (2014) Modelling, simulation and control of the dyeing process. Elsevier
138. Sharma S (2012) Energy management in textile industry. *Int J Power Syst Oper Energy Manage ISSN (PRINT)* 2(1):2
139. Sharma RK, Agrawal M, Marshall FM (2004) Effects of waste water irrigation on heavy metal accumulation in soil and plants. Paper presented at a National Seminar, Bangalore University, Bangalore, Abstract no. 7, p 8
140. Shelley T (1994) Dye pollution clean-up by synthetic mineral. *Int Dyer* 79:26–31
141. Shivanthan MC, Perera H, Jayasinghe S, Karunanayake P, Chang T, Ruwanpathirana S, Jayasinghe N, De Silva Y, Jayaweera Bandara D (2013) Hydrogen sulphide inhalational toxicity at a petroleum refinery in Sri Lanka: a case series of seven survivors following an industrial accident and a brief review of medical literature. *J Occup Med Toxicol* 8(1):1–5. <https://doi.org/10.1186/1745-6673-8-9>
142. Sillanpää M, Sainio P (2017) Release of polyester and cotton fibers from textiles in machine washings. *Environ Sci Pollut Res* 24(23):19313–19321. <https://doi.org/10.1007/s11356-017-9621-1>
143. Singare P, Lokhande R, Naik K (2010) A case study of some lakes located at and around thane city of Maharashtra, India, with special reference to physico-chemical properties and heavy metal content of lake water. *Interdiscip Environ Rev* 11(1):90–107. <https://doi.org/10.1504/IER.2010.034608>
144. Singare PU, Lokhande RS, Pathak PP (2010) Soil pollution along Kalwa Bridge at Thane Creek of Maharashtra, India. *J Environ Protect* 1(02):121. <https://doi.org/10.4236/jep.2010.12016>
145. Sinha S, Singh R, Chaurasia AK, Nigam S (2016) Self-sustainable *Chlorella pyrenoidosa* strain NCIM 2738 based photobioreactor for removal of Direct Red-31 dye along with other industrial pollutants to improve the water-quality. *J Hazard Mater* 306:386–394. <https://doi.org/10.1016/j.jhazmat.2015.12.011>
146. Sivakumar D (2014) Role of Lemna minor Lin. in treating the textile industry wastewater. *Int J Environ Ecol Geol Mining Eng* 8:55–59
147. Sivarajasekar N, Baskar R (2014) Adsorption of basic red 9 on activated waste *Gossypium hirsutum* seeds: process modeling, analysis and optimization using statistical design. *J Ind Eng Chem* 20(5):2699–2709. <https://doi.org/10.1016/j.jiec.2013.10.058>
148. Slater K (2003) Environmental impact of textiles: production, processes and protection, vol 27. Woodhead Publishing
149. Spencer DJ (2001) Knitting technology: a comprehensive handbook and practical guide, vol 16. CRC press

150. Statista (2016) Textile data of different countries. <https://www.statista.com/search/?q=Textile+data+globally&qKat=newSearchFilter&sortMethod=idrelevance&isRegionPref=1&statistics=1&accuracy=and&isoregion=0&isocountrySearch=&category=0&interval=0&archive=1>
151. Ströhle J, Beninger AG (2008) Protecting the environment through waste water recycling and heat recovery in textile finishing. Benninger AG Uzwil, Switzerland
152. Sugiyama M, Tsuzuki K, Lin X, Costa M (1992) Potentiation of sodium chromate (VI)-induced chromosomal aberrations and mutation by vitamin B2 in Chinese hamster V79 cells. *Mutat Res Lett* 283(3):211–214. [https://doi.org/10.1016/0165-7992\(92\)90109-U](https://doi.org/10.1016/0165-7992(92)90109-U)
153. Suzuki D, Dressel H (2002) Good news for a change: hope for a troubled planet. Stoddart Toronto
154. Tanveer MA, Zafar S (2012) The stagnant performance of textile industry in Pakistan. *Eur J Sci Res* 77(3):362–372
155. Tanvir SI, Mahmood T (2014) Solid waste for knit fabric: quantification and ratio analysis. *J Environ Earth Sci* 4(12):68–80
156. Textile World (2008) Water and energy-saving solutions. TW special report. Mar/Apr 2008. http://www.textileworld.com/Issues/2008/March-April/Dyeing_Printing_and_Finishing/Water-And_Energy-Saving_Solutions
157. Thompson J, Bannigan J (2008) Cadmium: toxic effects on the reproductive system and the embryo. *Reprod Toxicol* 25(3):304–315. <https://doi.org/10.1016/j.reprotox.2008.02.001>
158. Tian F, Guo G, Zhang C, Yang F, Hu Z, Liu C, Wang S-W (2019) Isolation, cloning and characterization of an azoreductase and the effect of salinity on its expression in a halophilic bacterium. *Int J Biol Macromol* 123:1062–1069. <https://doi.org/10.1016/j.ijbiomac.2018.11.175>
159. Towns A (2013) Colorant, textile. In: Luo R (eds) *Encyclopedia of color science and technology*. Springer, New York, NY. https://doi.org/10.1007/978-3-642-27581-8_161_10
160. Tüfekci N, Sivri N, Toroz İ (2007) Pollutants of textile industry wastewater and assessment of its discharge limits by water quality standards. *Turk J Fish Aquat Sci* 7(2)
161. USEPA (2017) US EPA Office of Research and Development (USEPA), 2017 US EPA Office of Research and Development (USEPA). In: *Exposure factors handbook (Chapter 5) (Update)*. Soil and Dust Ingestion. Accessed 22 Mar 2019
162. Uddin F (2019) Introductory chapter: textile manufacturing processes textile manufacturing processes. IntechOpen
163. Vallero D (2014) *Fundamentals of air pollution*. Academic Press
164. Van der Velden NM, Patel MK, Vogtländer JG (2014) LCA benchmarking study on textiles made of cotton, polyester, nylon, acryl, or elastane. *Int J Life Cycle Assess* 19(2):331–356
165. Vietnam Cleaner Production Centre (2000) Mini-guide to cleaner production. VNCCPC, Vietnam, pp 1–24
166. Virtanen JK, Voutilainen S, Rissanen TH, Mursu J, Tuomainen T-P, Korhonen MJ, Salonen JT (2005) Mercury, fish oils, and risk of acute coronary events and cardiovascular disease, coronary heart disease, and all-cause mortality in men in eastern Finland. *Arterioscler Thromb Vasc Biol* 25(1):228–233. <https://doi.org/10.1161/01.ATV.0000150040.20950.61>
167. WHO (1997) World health organization: nitrogen oxides - environmental health criteria 188
168. WTO (2020) World Trade Report 2020: government policies to promote innovation in the digital age. WTO, Geneva. <https://doi.org/10.30875/60123dd4-en>
169. Wang ZL (2008) Splendid one-dimensional nanostructures of zinc oxide: a new nanomaterial family for nanotechnology. *ACS Nano* 2(10):1987–1992
170. Wang R (2012) Physiological implications of hydrogen sulfide: a whiff exploration that blossomed. *Physiol Rev* 92(2):791–896. <https://doi.org/10.1152/physrev.00017.2011>
171. Wang L, Wang L, Ding W, Zhang F (2010) Acute toxicity of ferric oxide and zinc oxide nanoparticles in rats. *J Nanosci Nanotechnol* 10(12):8617–8624. <https://doi.org/10.1166/jnn.2010.2483>
172. Wang D (2016) Environmental protection in clothing industry. Paper presented at the sustainable development: proceedings of the 2015 international conference on sustainable development (ICSD2015)

173. Wanyonyi WC, Onyari JM, Shiundu PM, Mula FJ (2019) Effective biotransformation of reactive black 5 dye using crude protease from *Bacillus cereus* strain KM201428. *Energy Proc* 157:815–824. <https://doi.org/10.1016/j.egypro.2018.11.247>
174. Wardman RH (2017) *An introduction to textile coloration: principles and practice*. Wiley
175. World Health Organization (2004) *Sulfate in drinking-water-background document for development of WHO guidelines for drinking-water quality*
176. Wu B, Wu X, Liu S, Wang Z, Chen L (2019) Size-dependent effects of polystyrene microplastics on cytotoxicity and efflux pump inhibition in human Caco-2 cells. *Chemosphere* 221:333–341
177. Xia H, Chen L, Fang Y (2013) Highly efficient removal of Congo red from wastewater by nano-cao. *Sep Sci Technol* 48(17):2681–2687. <https://doi.org/10.1080/01496395.2013.805340>
178. Xu M, Halimu G, Zhang Q, Song Y, Fu X, Li Y, Li Y, Zhang H (2019) Internalization and toxicity: a preliminary study of effects of nanoplastic particles on human lung epithelial cell. *Sci Total Environ* 694:133794. <https://doi.org/10.1016/j.scitotenv.2019.133794>
179. Yacout DM, Abd El-Kawi M, Hassouna M (2016) Cradle to gate environmental impact assessment of acrylic fiber manufacturing. *Int J Life Cycle Assess* 21(3):326–336. <https://doi.org/10.1007/s11367-015-1023-3>
180. Yuan Y, Ning X-A, Zhang Y, Lai X, Li D, He Z, Chen X (2020) Chlorobenzene levels, component distribution, and ambient severity in wastewater from five textile dyeing wastewater treatment plants. *Ecotoxicol Environ Saf* 193:110257. <https://doi.org/10.1016/j.ecoenv.2020.110257>
181. Zhuang M, Sanganyado E, Zhang X, Xu L, Zhu J, Liu W, Song H (2020) Azo dye degrading bacteria tolerant to extreme conditions inhabit nearshore ecosystems: optimization and degradation pathways. *J Environ Manage* 261:110222. <https://doi.org/10.1016/j.jenvman.2020.110222>
182. Zollinger H (2003) *Color chemistry: syntheses, properties, and applications of organic dyes and pigments*. Wiley

Applications of Chitosan- and Chitin-Based Biomaterials in Cationic Dye Removal



Asitha T. Cooray , Kavindya Weerasinghe , and Samantha Ranaweera 

1 Introduction

Industrial development is one of the major drivers of prosperity and eradication of poverty through the creation of employment and a source of income [75]. It is also a major contributor to environmental pollution, and its unsustainable industrial growth has severe negative impacts on the environment and natural resources. Textile, apparel, and related industries, such as yarn, dye, and pigment industries, have grown into a multibillion-dollar industry, and it is considered as an important industrial segment in China, India, Bangladesh, Turkey, and Vietnam [26, 51, 78]. One of the major environmental impacts of the textile industries is the water pollution by dye-contaminated industrial wastewater.

The pollution of natural waters by dye-contaminated industrial effluents is well documented and has been recognized as a severe environmental, ecological, and health hazard [31, 50, 63]. It has been estimated that up to 15% of the dye mass is lost during the dyeing process, and approximately 2×10^5 tons of dyes are annually discharged worldwide [58, 74]. It is not easy to investigate the long-term fate of dyes discharged into the environment due to many reasons. Most importantly, there are more than 3000 dyes alone used in the textile industry with a broad range of chemical structures and properties [58]. Most of the dyes are marketed with trade names and

A. T. Cooray (✉) · K. Weerasinghe
Department of Chemistry, Faculty of Applied Sciences, University of Sri Jayewardenepura,
Nugegoda, Sri Lanka
e-mail: atcooray@sjp.ac.lk

A. T. Cooray
Instrument Centre, Faculty of Applied Sciences, University of Sri Jayewardenepura, Nugegoda,
Sri Lanka

S. Ranaweera
Department of Chemistry, Faculty of Science, University of Ruhuna, Matara, Sri Lanka

often, their chemical compositions are undisclosed. The type and quantities of dyes used by the textile industries may change in the short term (daily basis) or long term (monthly or annual) upon the request of the customers. In addition, dyes may be present at trace levels in the environment, and identification and quantification of dyes, and their degradation products is a challenging task. As a result, it is not easy to follow the dyes discarded to the environment to investigate their fate and degradation products even from a single textile manufacturer [31].

2 Cationic Dyes

Dyes have been classified according to their chemical structure and methods of application. The dyes have been classified into three broad categories as azo, anthraquinone, and phthalocyanines dyes based on their structure. In addition, dyes also have been categorized as acid, metal-complex, direct, basic, reactive, vat, and sulfur dyes based on the methods of application [49].

Cationic dyes also known as basic dyes are characterized by the positive charge in the molecule and are often available as hydrochloride and $ZnCl_2$ complexes [65]. The positive charge-bearing atom in the dye molecule is usually N, O, S, or P atoms and the charge-balancing counter ion is either a low molecular weight organic or inorganic acid. The positive charge can be localized on a particular atom or can be delocalized across the dye molecule. The cationic dyes with a delocalized charge are characterized by their high color strength and are classified with methine dyes [29]. The charge-bearing atom in a localized charge dye is isolated from the chromophore of the dye by a non-conjugate functional group and therefore, charge is not a component of the chromophore [29]. Cationic dyes are widely used in the textile industry for the coloration of silk, nylon, wool, and nylon and acrylic-nylon blended fibers. In addition, they are also used in food, cosmetics, paper, leathers, ink, and plastic industries [29, 50].

2.1 *Harmful Effects of Cationic Dyes*

Cationic dyes have a wide variety of chemical structures with various types of substituted aromatic groups as shown in Fig. 1. Because of their stable and complex structures, these dyes are difficult to break down and remove completely from chemical, physical, and biological treatment technologies [19, 65]. In addition, the wastewater treatment processes may also produce toxic and carcinogenic by-products at trace levels during the treatment process [19]. The use of dye-contaminated water even with low dye concentrations can lead to adverse health effects including eye and skin irritations, respiratory tract-related issues, and various types of cancer [13, 33]. Because of their resistance to photochemical and biological degradation, they can accumulate in the farmlands, natural environment, and soil and sediments [13, 35].

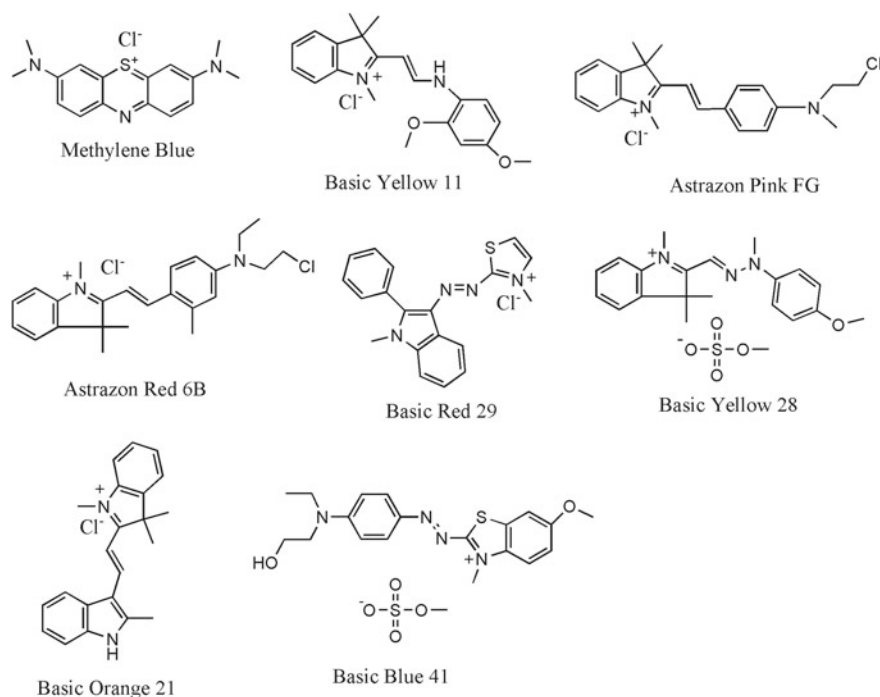


Fig. 1 The structures of some cationic dyes used in industry

Furthermore, dyes can alter the color of natural waters affecting light penetration through the water column. The reduced light penetration negatively affects photosynthesis and photosynthesis-driven oxygen cycle [33, 61]. The reduced dissolved oxygen concentrations are lethal to many aquatic life forms, and also affect the solubility of minerals, redox speciation of metals like Fe and Mn, and adsorption and release of metal ions, organic pollutants, and phosphate adsorbed onto iron- and manganese-(oxy)hydroxides and clay [16, 64, 69]. Apart from that, dyes affect chemical oxygen demand (COD), and biological oxygen demand (BOD), total nitrogen (TN), total phosphorous (TP) concentrations, and total dissolved solid (TDS) content of natural waters [33, 5].

2.2 Current Removal Methods of Cationic Dyes

Because of their extensive use, and well-known harmful effects of dye-contaminated water on humans and the natural environment, significant efforts have been made to develop lab- and industrial-scale technologies to remove cationic dyes from industrial effluents. Some of the most commonly used techniques are chemical oxidation, electrochemical coagulation, membrane separation, chemical coagulation, adsorption,

aerobic and anaerobic microbial degradation, ozonation, photocatalytic degradation, and enzyme-based and nanomaterial-based removal [9, 11, 13, 22, 25, 27, 30, 67, 70, 81, 82, 85, 87]. Each of the dye removal methods has its own advantages and disadvantages; however, none of the methods is capable of eliminating or degrading the dyes completely from effluents. Some of the most desired characteristics of treatment methods include low cost, ease of operation, higher efficiency, selectivity, and non-generation of toxic by-products and sludge [22, 33].

3 Chitin and Chitosan

Chitin is the second most abundant natural polysaccharide and bio-waste material after cellulose in nature, and it is one of the major structural components of the exoskeleton of animals, particularly in crustacea, mollusks, insects, and also in cell walls of certain fungi [18, 46, 60]. Chitin is a polysaccharide with glucosamine units having hydroxyl and amide functional groups that is structurally similar to cellulose except that the hydroxyl group of cellulose at the C-2 position is replaced by an acetamide group. Similar to cellulose, chitin exists in three polymorphic forms as α , β , and γ [40]. On the other hand, chitosan is a linear polymer produced by the alkaline deacetylation of chitin (although the degree of N-deacetylation is almost never complete), where the primary amine groups ($-\text{NH}_2$) are produced by the hydrolysis of amide groups in chitin [41, 59, 68]. The structures of chitin and chitosan are shown in Fig. 2.

Among a variety of methods used to produce chitin, chemical and biological processes are primarily used for the processing of chitin. Chemical extraction involves the demineralization, deproteinization, and decolorization steps based on acidic and alkali treatments. Biological treatment is an alternative method involving enzymatic demineralization, deproteinization, and decolorization stages which eliminate several drawbacks of chemical methods [23, 59, 68].

Chitosan is prepared by chemical or biological deacetylation of chitin, where the acetamide groups are replaced by $-\text{NH}_2$ groups and thereby changing the molecular weight of the polymer. The conventional thermo chemical production of chitosan involves alkaline deacetylation, and the degree of deacetylation depends

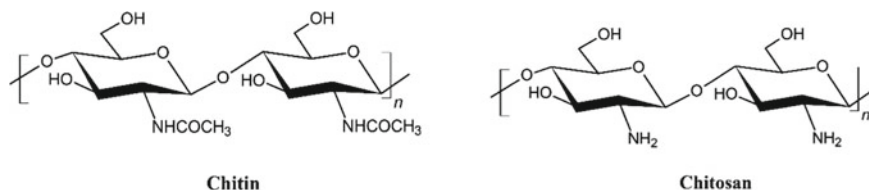


Fig. 2 Chemical structures of chitin and chitosan

on NaOH/KOH concentration, temperature, and heating time in the deacetylation process. Recently, enzymatic, or microbiological fermentation processes have popularized as economic and environmentally friendly pathways utilizing enzymatic reactions (mainly chitin deacetylase) or fermentation with enzyme-producing microorganisms, respectively [59, 84, 68].

In general, both chitin and chitosan are copolymers of glucosamine and N-acetylglucosamine units with variable molecular weights, whereas chitosan is mostly glucosamine with $\geq 60\%$ amine groups. However, a sharp nomenclature border has not been defined between chitin and chitosan on the basis of the degree of N-deacetylation. Chitin is insoluble in water, organic solvents, dilute alkalis, and acids. Chitosan dissolves in aqueous acids even though it is insoluble in water [23, 59, 68].

Moreover, both chitin and chitosan are highly amenable to chemical modifications through their reactive functional groups. Therefore, these polymers are usually chemically modified to obtain improved derivatives and overcome the limitations in their applications due to several reasons such as low solubility, acid instability, and limited selectivity. According to the literature, chitin is subjected to chemical reactions mainly etherification, grafting, and acylation reactions [23]. In chitosan, modifications have been done using metal templates, forming composites, functional group substitutions, and crosslinking to produce various chitosan derivatives.

Early research studies have shown that chitin, chitosan, and their derivatives possess a unique set of valuable characteristics such as biodegradability, environmentally friendliness, bio-renewability, biocompatibility, nontoxicity, and superior adsorption properties. Therefore, these versatile properties allow them to be easily processed into beads, membranes, hydrogel, films, nanofibers, and many other forms [2, 59, 68]. Thus, they can be suggested as functional materials widely used for a broad range of applications in agriculture, textile industry, bioplastics, nanocomposites, fuel cells, pharmaceuticals, and industrial food processing. The lack of toxicity together with its rapid biodegradability has made these polymers suitable for several environmental applications primarily in wastewater treatment.

3.1 Importance of Chitosan- and Chitin-Based Biomaterials for Dye Removal

As previously mentioned, in addition to being natural and biodegradable, chitosan- and chitin-based biomaterials offer several advantages as adsorbents for dye removal. Mainly, these polymers are low-cost materials obtained from natural resources. Moreover, they possess high adsorption capacities, higher selectivity, and high rate of adsorption toward dyes. In addition, their versatile nature reflects the ability to develop novel derivatives based on the type of dye to be adsorbed. Therefore, chitosan- and chitin-based biomaterials have been shown to be utilized widely in dye removal as proven by the growing number of research articles published in recent years.

3.2 *Different Types of Chitosan/Chitin-Based Biomaterials for Dye Removal*

The versatile chemical and biological properties of chitin and chitosan allow them to be easily processed into different forms like flakes, powder, gel, beads, membranes, films, micro- and nano-particles, etc. [2]. Generally, physical modification expands chitosan polymer chains, reduces the crystalline state of the polymer, and increases the access to more sorption sites allowing the diffusion of larger dye molecules [3]. On the other hand, chemical modifications result in new derivatives with improved properties controlling the hydrophobic, cationic, and anionic nature of the polymer, without changing the basic structure. An insight into the most common modifications and different forms that can be applied to chitin and chitosan polymers is given in this section.

With regard to dye removal, the most common chemical modifications carried out with chitin and chitosan biopolymers can be categorized as etherification, acylation, sulfation, crosslinking, graft polymerization, etc. Hydroxyl functional groups in chitin and hydroxyl, and amino functional groups in chitosan can be modified through different reactions to obtain derivatives with specific adsorbent properties for the removal of dyes.

In grafting reactions, different functional groups are grafted onto chitin/chitosan via the covalent bonding of a molecule onto the polymer backbone. The possibility of grafting synthetic polymers to chitin/chitosan (graft copolymerization) has also been explored in recent literature as a method of introducing side chains. Modification of the polymer leads to the formation of new derivatives consisting of natural and synthetic polymers. According to the literature, different functional groups like amino, carboxyl, sulfur, and alkyl groups have been used for grafting reactions related to dye removal [76].

To overcome the dissolution tendency of chitin and chitosan, polymer chains can be crosslinked and thereby improve the chemical stability of polymer at different pH. The crosslinking introduces intermolecular bridges and links between macromolecules attributing enhanced resistance to structural changes under hydrated conditions. The most common crosslinkers used for modifications in dye removal are glutaraldehyde, epichlorohydrin, ethylene glycol diglycidyl ether, etc. [76, 84].

The most common etherified derivatives used in dye adsorption are the derivatives of carboxymethyl chitin and chitosan. The O- and N-carboxymethylation reaction occurs with monochloroacetic acid in the presence of NaOH which introduces carboxyl groups into the polymer [86]. Introduction of carboxymethyl groups into the polymer results in the formation of anionic derivatives. While carboxymethylation in chitin mostly proceeds via a more reactive C-6 position, in chitosan, both hydroxyl and amino groups are preferred for the introduction of carboxymethyl groups [42].

Despite the fact that chitin and chitosan do not generally exist in gel form, but as fibrous forms in nature, synthesized gels of chitin and chitosan have shown great potential use in the field of dye removal. Chitosan based physical gels are easy to prepare by exploiting different types of physical interactions between

polymer networks such as hydrogen bonds, electrostatic, and hydrophobic interactions. Tripolyphosphates are considered as a common ionic crosslinker used in the gelation process. On the other hand, covalently crosslinked gels are synthesized with covalent bonds forming crosslinkers. In one type, the polymer is entangled with itself in covalent bonding forming a gel. In some cases, chitin or chitosan is covalently crosslinked with a different polymeric chain and in another type, a nonreactive polymer is trapped in the crosslinked polymer network. Hydrogels are three dimensional polymeric networks that have gained much importance in dye removal and are composed of the polymer backbone, water, and a crosslinking agent [57]. Aerogels which exhibit unique properties such as large surface area, high porosity, and low density are produced from wet gels using an appropriate drying technology [21, 83].

With the aim of developing dye adsorption properties of chitin and chitosan, composites have been synthesized that exhibit combinations of properties that could not be obtained by individual materials. Different substances including both natural and synthetic fillers have been used to form composites with chitin and chitosan such as montmorillonite, bentonite, activated clay, and polyurethane [55].

Surface impregnation is a way of improving the adsorption capacity of chitin/chitosan adsorbents using surfactants such as sodium dodecyl sulfate (SDS), cetyltrimethyl ammonium bromide (CTAB), and triton X-100 (TX-100). Surfactants can increase the electrostatic interactions by forming a chemical bond with hydrophilic groups of surfactant and polymer. In addition, hydrophobic interactions can also occur between the polymer backbone and the hydrophobic part of the surfactant [76]. Altogether, these interactions will facilitate dye adsorption by forming compatible bonding between the dye molecules and the adsorbent.

Chitin and chitosan can be converted to various nanomaterials with special properties for use in dye removal. Commonly prepared chitin- and chitosan-based nanomaterials include nanofibers, nano-whiskers, and nanocomposites [23]. Nanofibers are crystalline in nature having high mechanical properties. Rod-like nanosized structures are termed as nano-whiskers, and they possess high surface area, high adsorption ability, biodegradability, and nontoxicity. Nanocomposites based on chitin and chitosan also have been widely employed in recent literature in the dye adsorption applications subjecting to different modifications using carboxylation, amination, incorporation of magnetic particles, hydroxyapatites, etc. [23, 56].

3.3 Recent Studies on Cationic Dye Removal Using Chitin- and Chitosan-Based Biomaterials

The modification of chitin and chitosan is important to improve the adsorption capacity and broaden the applications for the removal of dyes with greater efficiency. The physicochemical properties of the bio-sorbents are altered by the modifications and in turn, their adsorption capacity is achieved to meet the specific requirements depending on the nature of the dye. This section will highlight some of both modified

and unmodified forms of chitin and chitosan that have been studied so far for cationic dye removal.

Utilization of chitosan beads for the removal of cationic dye, Malachite Green by varying the temperature, was investigated [4]. The monolayer adsorption capacities were found to be 93.55 mg/g and 74.83 mg/g at 303 K and 313 K, respectively. Moreover, beyond pH 8, the dye adsorption remained constant. In another experiment, the removal of cationic dye, Crystal Violet, was studied using deacetylated chitin (chitosan) varying the degree of deacetylation. Different isotherm models were used to study the adsorption behavior [47]. The adsorption of Methyl Red was investigated using chitin and chitosan in both single-component systems and cationic dye-cation multicomponent systems with Cu(II). Considering multicomponent systems, the total adsorption efficiency of Cu(II)-methyl red on chitosan (46.4%) was higher than that of Cu(II)-methyl red on chitin (41.0%) [1]. In another study by the same authors, simultaneous adsorption of Cu(II) and Crystal Violet in a multicomponent system was carried out with chitin and chitosan. Binary system with chitosan demonstrated synergistic effects on adsorption behavior, while the system with chitin showed both antagonistic and synergistic interactions with respect to single component systems [24].

Crosslinked O-carboxymethyl chitosan was synthesized with different degrees of substitution, and the removal of Crystal Violet dye from aqueous solutions was examined. Crosslinking was done with glutaraldehyde and the results showed an increase in adsorption capacity from 28.49 to 239.54 mg/g by modified chitosan [66]. Adsorption performance of N,O-carboxymethyl chitosan for the removal of cationic dye, Methylene Blue from aqueous solutions, was studied and also the effect of degree of substitution and several other factors on adsorption were examined. The maximum monolayer adsorption capacity was found to be 351 mg/g and according to the results, the adsorption capacity of the chitosan derivative increased with the increase in the degree of substitution [80].

The adsorption using a chitosan-based adsorbent for the removal of Basic Blue 3 was studied. The adsorbent was prepared by chemical grafting of sulfonate groups onto chitosan by the reaction with 4-formyl-1,3-benzene sodium disulfonate. Depending on the presence of sulfonate groups, a maximum adsorption capacity of 166.5 mg/g was obtained [12].

A xanthate-modified magnetic chitosan was synthesized to be used as an adsorbent for the removal of cationic azo dyes, Methylene Blue, and Safranin O. A significant improvement in adsorption was observed with a maximum adsorption capacity of 197.8 mg/g and 169.8 mg/g for Methylene Blue and Safranin O, respectively [72].

Chitin grafted with poly (acrylic acid) has been synthesized for the adsorption of Malachite Green. A prominent adsorption capacity of 285.7 mg/g was observed for the cationic dye [28]. Chitosan modified by grafting ethyl acrylate was prepared and used for the removal of two cationic dyes, Basic Blue 41, and Basic Red 18 from colored solutions. The authors suggest that the removal of dyes was found to be increased after the modification, and the maximum adsorption capacities were obtained as 217.39 mg/g and 158.73 mg/g for Basic Blue 41 and Basic Red 18,

respectively [62]. Chitosan derivatives grafted with poly (acrylic acid) and poly (acrylamide) were synthesized and evaluated as bio-sorbents for the removal of Remacryl Red TGL dye. The adsorption performance was found to be significantly increased by grafting. Based on Langmuir analysis, maximum adsorption capacities of 0.479, 0.727, and 1.068 mmol/L (204.22, 309.82, and 510.74 mg/g) were obtained for the three derivatives of chitosan [7, 44]. The efficacy of enzymatic grafting of four phenol derivatives [4-hydroxybenzoic acid (BA), 3,4-dihydroxybenzoic acid (DBA), 3,4-dihydroxyphenyl-acetic acid (PA), and hydrocaffeic acid (CA)] on to the chitosan for the removal of cationic dyes, Crystal Violet and Bismarck Brown Y, has been examined [9]. For both dyes, maximum adsorption capacities were in the order of chitosan-CA > chitosan-PA > chitosan-DBA > chitosan > BA.

A study reported the chitin hydrogel prepared by crosslinking with epichlorohydrin as a low-cost alternative adsorbent for Malachite Green removal from aqueous solutions. As the authors suggest, a high uptake capacity of dye was observed due to the microporous structure and large surface area of chitin hydrogel in addition to the affinity of the dye [71]. To investigate the adsorption of cationic dye, Methylene Blue, chitosan hydrogel beads were prepared by anionic surfactant gelation. The maximum adsorption capacity (226.24 mg/g) obtained was higher compared to the chitosan hydrogel beads formed by conventional alkali gelation [10]. A novel bio-aerogel was prepared from bifunctional nanocellulose and carboxymethylated chitosan through a Schiff base reaction. The ability of the aerogel in adsorption of dyes was tested with cationic dye, Methylene Blue. The maximum adsorption capacity of the aerogel was 785 mg/g, which is significantly higher than reported reusable adsorbents synthesized from biopolymers [83]. In another experiment, a novel 3D graphene oxide-chitosan gel was prepared to investigate the efficiency of Methylene Blue and Methyl Violet adsorption. Porous biopolymer gel was found to be efficiently removing cationic dyes and displayed significantly high adsorption capacities as 1100 mg/g and 1350 mg/g for Methylene Blue and Methyl Violet, respectively [14].

A study was reported to investigate the adsorption of Methylene Blue onto a composite of chitosan and activated clay. The composite was prepared by physical modification of chitosan beads followed by embedding activated clay particles into them. The absorption of dye onto composite was compared with that of chitosan beads and activated clay [8]. A new magnetic chitosan/active charcoal (CTN/AC-Fe₃O₄) composite has been prepared by in situ co-precipitation method and its adsorption efficiency was tested with Methylene Blue dye. The effect of several parameters on dye removal was investigated, and maximum adsorption capacity was found to be 500 mg/g with a removal percentage of more than 90% at 318 K [37]. In another work, the mesoporous crosslinked chitosan-activated charcoal composite was prepared to be used as a bio-sorbent for the removal of Thionine dye. The composite has been synthesized by coalescing chitosan with activated charcoal followed by crosslinking with epichlorohydrin. According to the experimental data, the maximum adsorption capacity for thionine dye was 60.9 mg/g at 303 K [32]. For the removal of Malachite Green from aqueous solutions, a composite of crosslinked chitosan-coated bentonite beads has been examined, and the effect of several physiochemical

parameters was also investigated. The maximum adsorption capacity was found to be 435.0 mg/g [79]. Chitosan-intercalated montmorillonite composite was synthesized through modification of sodium montmorillonite by intercalation of chitosan [53]. The adsorption capacity of the composite was investigated in comparison with sodium montmorillonite and chitosan using three cationic dyes (Basic Blue 9, Basic Blue 66, and Basic Yellow 1). Accordingly, enhanced adsorption of all three dyes was observed for the composite compared to starting materials, indicating 92–99 wt% of dye removal. As the authors suggest, this increase resulted mainly from the synergistic effect of broadened pores and electrostatic interaction between intercalated chitosan and the dyes.

H₂SO₄ crosslinked magnetic chitosan nanocomposite beads have been prepared using nanosized Fe₃O₄ crystallite and H₂SO₄ [54]. The efficiency of adsorbate was tested with Methylene Blue. According to the results, modification of chitosan increased dye removal, reaching a maximum adsorption capacity of 20.408 mg/g. For the removal of Crystal Violet, chitin nano-whiskers were prepared by acid hydrolysis. A maximum adsorption capacity of 59.52 mg/g was obtained. As the authors suggest, improved adsorption was observed due to the increase in average pore size, rod-like shape, and nanometric size of the adsorbent [17]. A nano-adsorbent, magnetic β -cyclodextrin-chitosan/graphene oxide, was synthesized for the Methylene Blue adsorption. Nanocomposite resulted in the combined features of both β -cyclodextrin-chitosan and graphene oxide exhibiting fast adsorption rates for the dye because of the high surface area of graphene oxide, hydrophobicity of β -cyclodextrin, and the abundant functional groups of chitosan. A maximum adsorption capacity of 84.32 mg/g was obtained for the synthesized nanocomposite [20].

The use of ultrasonic surface-modified chitin for the removal of Methylene Blue was investigated [15]. The adsorbent has presented properties such as higher surface area, higher porosity, lower crystallinity, and a more rugged surface. At pH 10, the dye removal percentage was about 85% while the maximum adsorption capacity was found to be 26.69 mg/g at 298 K.

4 Major Limitations

Chitin- and chitosan-based treatment methods are based on sorption which merely phase-separate the dye from industrial effluents onto a semi-solid or solid adsorbent. Unlike chemical and biological methods, sorption-based physical methods can efficiently remove dyes from effluents; however, do not mineralize the adsorbed dyes [6, 36, 39]. As a result, a separate waste disposal method is required to safely dispose of the dye-containing sludge. In that sense, all the physical treatment methods, including chitin- and chitosan-based methods, cannot be considered as effective treatment methods that guarantee total mineralization of the contaminants. Furthermore, effective desorption methods have to be developed to regenerate the adsorbent for further use [6, 36, 39]. In most of the reported literature, adsorption capacity and stability of the adsorbents over a broad pH range have been investigated; however, experimental

data related to efficiency of desorption, operational cost, total number of effective sorption/desorption cycles, and selectivity toward specific dyes are harder to find. As a result, the industrial suitability of most of the developed adsorbents remains uncertain.

There are some other limitations specific to chitin- and chitosan-based adsorbents. Chitin is a non-toxic, readily available biomaterial; however, it is not water-soluble due to its highly crystalline structure. As a result, structural modifications are always required to make it a versatile adsorbent [59, 68, 77]. Even though some of the chitin- and chitosan-based adsorbents have higher adsorbent capacities, it is not uncommon to find relatively low adsorbent capacities (<100 mg/g) for the removal of cationic dyes making them un-attractive from industrial use [32, 34, 45, 73]. In addition, most of the reported literature have not tested the reusability of the adsorbents which is essential in real-world applications. Only a very few have tested the reusability of the material using more than 25 cycles [43]. Most of the chitin- and chitosan-based adsorbents are pH-sensitive. The operational pH of most of these adsorbents is often limited to near neutral to basic pH, and the dye removal efficiency dramatically reduces in the acidic pH range [38, 43, 48, 52, 65].

5 Future Prospective

Chitosan and chitin available as flakes and powders have very low adsorption capacities and therefore, the development of nano-dispersions, nanocomposites, and hydrogel beads is essential to improve their capacity. In addition, the selectivity of the adsorbents plays an important role in industrial applications. Almost all the current studies have used pure dye solutions to evaluate the performance; however, real-world applications require the adsorbents to selectively remove the targeted dyes from industrial effluents. The selectivity of the adsorbents can be achieved by introducing specific functional groups onto the polymer backbone. In addition, studies related to real-world applications of chitin- and chitosan-based material to remove cationic dyes from industrial effluents are needed to show the real strength of these materials. Whenever it is possible, these methods should be coupled with aerobic and anaerobic biological methods to achieve the complete mineralization of the dye contaminants.

6 Conclusions

Chitin- and chitosan-based materials developed for the removal of cationic dyes have shown encouraging results which highlight them as one of the most cost-effective, environmentally benign, non-toxic, and effective materials available for industrial effluent treatment. These adsorbents are available in a wide variety of physical forms in the range of macro- and nanocomposite materials, nano-dispersions, hydrogel

beads, and intercalations. They are very effective in the basic pH range, and the cationic dye removal efficiency gradually decreases with decreasing pH. Some of the chitin- and chitosan-based materials have adsorption capacities well over 200 mg/g with good reusability making them good candidates for industrial wastewater treatment applications. One of the major disadvantages is that sorption-based treatment methods using chitin-chitosan-based materials can perform only a phase separation of the dye. Some of the chemical and biological treatment methods used in the industry can achieve complete mineralization of the dyes which is more advantageous than just physical separation of the dyes from effluents.

Acknowledgements The authors would like to thank the Department of Chemistry, Faculty of Applied Sciences, University of Sri Jayewardenepura, and Department of Chemistry, Faculty of Science, University of Ruhuna, Matara, Sri Lanka, for their support.

References

1. Açikel YS, Göze B (2017) Removal of Methyl Red, a cationic dye, Acid Blue 113, an anionic dye, from wastewaters using chitin and chitosan: influence of copper ions. *Desalin Water Treat* 73:289–300
2. Anitha A, Sowmya S, Sudheesh Kumar PT, Deepthi S, Chennazhi KP, Ehrlich H, Tsurkan M, Jayakumar R (2014) Chitin and chitosan in selected biomedical applications. *Prog Polym Sci* 39(9):1644–1667. <https://doi.org/10.1016/j.progpolymsci.2014.02.008>
3. Azlan K, Wan Saime WN, Lai Ken L (2009) Chitosan and chemically modified chitosan beads for acid dyes sorption. *J Environ Sci* 21(3):296–302. [https://doi.org/10.1016/S1001-0742\(08\)62267-6](https://doi.org/10.1016/S1001-0742(08)62267-6)
4. Bekçi Z, Özveri C, Seki Y, Yurdaoç K (2008) Sorption of malachite green on chitosan bead. *J Hazard Mater* 154(1–3):254–261. <https://doi.org/10.1016/j.jhazmat.2007.10.021>
5. Berradi M, Hsissou R, Khudhair M, Assouag M, Cherkaoui O, El Bachiri A, El Harfi A (2019) Textile finishing dyes and their impact on aquatic environs. *Heliyon* 5(11):e02711. <https://doi.org/10.1016/j.heliyon.2019.e02711>
6. Bhatia D, Sharma NR, Singh J, Kanwar RS (2017) Biological methods for textile dye removal from wastewater: a review. *Crit Rev Environ Sci Technol* 47(19):1836–1876. <https://doi.org/10.1080/10643389.2017.1393263>
7. Bhatnagar A, Sillanpää M (2009) Applications of chitin-and chitosan-derivatives for the detoxification of water and wastewater—a short review. *Adv Coll Interface Sci* 152(1–2):26–38. <https://doi.org/10.1016/j.cis.2009.09.003>
8. Chang M-Y, Juang R-S (2004) Adsorption of tannic acid, humic acid, and dyes from water using the composite of chitosan and activated clay. *J Colloid Interface Sci* 278(1):18–25. <https://doi.org/10.1016/j.jcis.2004.05.029>
9. Chao A-C, Shyu S-S, Lin Y-C, Mi F-L (2004) Enzymatic grafting of carboxyl groups on to chitosan—to confer on chitosan the property of a cationic dye adsorbent. *Biores Technol* 91(2):157–162. [https://doi.org/10.1016/S0960-8524\(03\)00171-8](https://doi.org/10.1016/S0960-8524(03)00171-8)
10. Chatterjee S, Chatterjee T, Lim S-R, Woo SH (2011) Adsorption of a cationic dye, methylene blue, on to chitosan hydrogel beads generated by anionic surfactant gelation. *Environ Technol* 32(13):1503–1514. <https://doi.org/10.1080/09593330.2010.543157>
11. Chu TPM, Nguyen NT, Vu TL, Dao TH, Dinh LC, Nguyen HL, Hoang TH, Le TS, Pham TD (2019) Synthesis, characterization, and modification of alumina nanoparticles for cationic dye removal. *Materials* 12(3):450. <https://doi.org/10.3390/ma12030450>

12. Crini G, Gimbert F, Robert C, Martel B, Adam O, Morin-Crini N, De Giorgi F, Badot P-M (2008) The removal of Basic Blue 3 from aqueous solutions by chitosan-based adsorbent: batch studies. *J Hazard Mater* 153(1–2):96–106. <https://doi.org/10.1016/j.jhazmat.2007.08.025>
13. Dalal C, Garg AK, Sonkar SK (2021) Carboxylic acid-terminated carbon nanoflakes for selective adsorption of water-soluble cationic dyes. *ACS Appl Nano Mater*. <https://doi.org/10.1021/acsnm.1c01148>
14. Deng J, Lei B, He A, Zhang X, Ma L, Li S, Zhao C (2013) Toward 3D graphene oxide gels based adsorbents for high-efficient water treatment via the promotion of biopolymers. *J Hazard Mater* 263:467–478. <https://doi.org/10.1016/j.jhazmat.2013.09.065>
15. Dotto GL, Santos JMN, Rodrigues IL, Rosa R, Pavan FA, Lima EC (2015) Adsorption of methylene blue by ultrasonic surface modified chitin. *J Colloid Interface Sci* 446:133–140. <https://doi.org/10.1016/j.jcis.2015.01.046>
16. Doubek JP, Campbell KL, Doubek KM, Hamre KD, Lofton ME, McClure RP, Ward NK, Carey CC (2018) The effects of hypolimnetic anoxia on the diel vertical migration of freshwater crustacean zooplankton. *Ecosphere* 9(7):e02332
17. Druzian SP, Zanatta NP, Côrtes LN, Streit AFM, Dotto GL (2019) Preparation of chitin nanowhiskers and its application for crystal violet dye removal from wastewaters. *Environ Sci Pollut Res* 26(28):28548–28557. <https://doi.org/10.1007/s11356-018-3547-0>
18. El-Sayed EM, Tamer TM, Omer AM, Mohy Eldin MS (2016) Development of novel chitosan schiff base derivatives for cationic dye removal: methyl orange model. *Desalin Water Treat* 57(47):22632–22645. <https://doi.org/10.1080/19443994.2015.1136694>
19. Eren E, Afsin B (2008) Investigation of a basic dye adsorption from aqueous solution onto raw and pre-treated bentonite surfaces. *Dyes Pigm* 76(1):220–225. <https://doi.org/10.1016/j.dyepig.2006.08.019>
20. Fan L, Luo C, Sun M, Qiu H, Li X (2013) Synthesis of magnetic β -cyclodextrin-chitosan/graphene oxide as nanoadsorbent and its application in dye adsorption and removal. *Colloids Surf, B* 103:601–607. <https://doi.org/10.1016/j.colsurfb.2012.11.023>
21. García-González CA, Alnaief M, Smirnova I (2011) Polysaccharide-based aerogels—promising biodegradable carriers for drug delivery systems. *Carbohydr Polym* 86(4):1425–1438. <https://doi.org/10.1016/j.carbpol.2011.06.066>
22. Ge F, Ye H, Li M-M, Zhao B-X (2012) Efficient removal of cationic dyes from aqueous solution by polymer-modified magnetic nanoparticles. *Chem Eng J* 198–199:11–17. <https://doi.org/10.1016/j.cej.2012.05.074>
23. Gopi S, Thomas S, Pius A (2020) Handbook of chitin and chitosan Volume 1 Preparation and properties
24. Goze B, Evirgen OA, Acikel YS (2016) Investigation of antagonistic and synergistic interactions on simultaneous adsorption of crystal violet and Cu(II) using chitin and chitosan. *Desalin Water Treat* 57(9):4059–4072. <https://doi.org/10.1080/19443994.2014.989914>
25. Hameed BH (2009) Removal of cationic dye from aqueous solution using jackfruit peel as non-conventional low-cost adsorbent. *J Hazard Mater* 162(1):344–350. <https://doi.org/10.1016/j.jhazmat.2008.05.045>
26. Holkar CR, Jadhav AJ, Pinjari DV, Mahamuni NM, Pandit AB (2016) A critical review on textile wastewater treatments: possible approaches. *J Environ Manage* 182:351–366. <https://doi.org/10.1016/j.jenvman.2016.07.090>
27. Hosseini SA, e Asl SD, Vossoughi M, Simchi A, Sadrzadeh M (2021) Green electrospun membranes based on chitosan/amino-functionalized nanoclay composite fibers for cationic dye removal: synthesis and kinetic studies. *ACS Omega* 6(16):10816–10827. <https://doi.org/10.1021/acsomega.1c00480>
28. Huang C-M, Chen L-C, Yang H-C, Li M-H, Pan T-C (2012) Preparation of acrylic acid-modified chitin improved by an experimental design and its application in absorbing toxic organic compounds. *J Hazard Mater* 241:190–196. <https://doi.org/10.1016/j.jhazmat.2012.09.032>
29. Hunger K (2007) Industrial dyes: chemistry, properties, applications
30. Idohou EA, Fatombi JK, Ossen SA, Agani I, Neumeyer D, Verelst M, Mauricot R, Aminou T (2020) Preparation of activated carbon/chitosan/Carica papaya seeds composite for efficient

- adsorption of cationic dye from aqueous solution. *Surf Interfaces* 21:100741. <https://doi.org/10.1016/j.surf.2020.100741>
31. Ito T, Adachi Y, Yamanashi Y, Shimada Y (2016) Long-term natural remediation process in textile dye-polluted river sediment driven by bacterial community changes. *Water Res* 100:458–465. <https://doi.org/10.1016/j.watres.2016.05.050>
 32. Jawad AH, Abdulhameed AS, Mastuli MS (2020) Mesoporous crosslinked chitosan-activated charcoal composite for the removal of thionine cationic dye: comprehensive adsorption and mechanism study. *J Polym Environ* 28(3):1095–1105. <https://doi.org/10.1007/s10924-020-01671-5>
 33. Jawad AH, Abdulhameed AS, Surip SN, Sabar S (2020) *Int J Environ Anal Chem*, 1–15. <https://doi.org/10.1080/03067319.2020.1807966>
 34. Jawad AH, Norrahma SSA, Hameed BH, Ismail K (2019) Chitosan-glyoxal film as a superior adsorbent for two structurally different reactive and acid dyes: adsorption and mechanism study. *Int J Biol Macromol* 135:569–581. <https://doi.org/10.1016/j.ijbiomac.2019.05.127>
 35. Jayanthi V, Geetha R, Rajendran R, Prabhavathi P, Karthik Sundaram S, Dinesh Kumar S, Santhanam P (2014) Phytoremediation of dye contaminated soil by *Leucaena leucocephala* (subabul) seed and growth assessment of *Vigna radiata* in the remediated soil. *Saudi J Biol Sci* 21(4):324–333. <https://doi.org/10.1016/j.sjbs.2013.12.001>
 36. Kandelbauer A, Guebitz GM (2005) Bioremediation for the decolorization of textile dyes—a review. *Environ Chem*, 269–288. https://doi.org/10.1007/3-540-26531-7_26
 37. Karaer H, Kaya I (2016) Synthesis, characterization of magnetic chitosan/active charcoal composite and using at the adsorption of methylene blue and reactive blue4. *Microporous Mesoporous Mater* 232:26–38. <https://doi.org/10.1016/j.micromeso.2016.06.006>
 38. Kazemi J, Javanbakht V (2020) Alginate beads impregnated with magnetic Chitosan@Zeolite nanocomposite for cationic methylene blue dye removal from aqueous solution. *Int J Biol Macromol* 154:1426–1437. <https://doi.org/10.1016/j.ijbiomac.2019.11.024>
 39. Khan R, Bhawana P, Fulekar MH (2013) Microbial decolorization and degradation of synthetic dyes: a review. *Rev Environ Sci Bio/Technol* 12(1):75–97. <https://doi.org/10.1007/s11157-012-9287-6>
 40. Khoushab F, Yamabhai M (2010) Chitin research revisited. *Mar Drugs* 8(7):1988–2012. <https://doi.org/10.3390/md8071988>
 41. Kumar, MNVR (2000) A review of chitin and chitosan applications. *React Funct Polym* 46(1):1–27. [https://doi.org/10.1016/S1381-5148\(00\)00038-9](https://doi.org/10.1016/S1381-5148(00)00038-9)
 42. Kurita K (2001) Controlled functionalization of the polysaccharide chitin. *Prog Polym Sci* 26(9):1921–1971. [https://doi.org/10.1016/S0079-6700\(01\)00007-7](https://doi.org/10.1016/S0079-6700(01)00007-7)
 43. Kyzas GZ, Siafaka PI, Pavlidou EG, Chrissafis KJ, Bikiaris DN (2015) Synthesis and adsorption application of succinyl-grafted chitosan for the simultaneous removal of zinc and cationic dye from binary hazardous mixtures. *Chem Eng J* 259:438–448. <https://doi.org/10.1016/j.cej.2014.08.019>
 44. Lazaridis NK, Kyzas GZ, Vassiliou AA, Bikiaris DN (2007) Chitosan derivatives as biosorbents for basic dyes. *Langmuir* 23(14):7634–7643. <https://doi.org/10.1021/la700423j>
 45. León O, Muñoz-Bonilla A, Soto D, Pérez D, Rangel M, Colina M, Fernández-García M (2018) Removal of anionic and cationic dyes with bioadsorbent oxidized chitosans. *Carbohydr Polym* 194:375–383. <https://doi.org/10.1016/j.carbpol.2018.04.072>
 46. Lewandowska K, Sionkowska A, Kaczmarek B, Furtos G (2014) Characterization of chitosan composites with various clays. *Int J Biol Macromol* 65:534–541. <https://doi.org/10.1016/j.ijbiomac.2014.01.069>
 47. Ling SLY, Yee CY, Eng HS (2011) Removal of a cationic dye using deacetylated chitin (chitosan). *J Appl Sci* 11(7):1445–1448
 48. Ma H, Kong A, Ji Y, He B, Song Y, Li J (2019) Ultrahigh adsorption capacities for anionic and cationic dyes from wastewater using only chitosan. *J Clean Prod* 214:89–94. <https://doi.org/10.1016/j.jclepro.2018.12.217>
 49. Mahapatra NN (2016) *Textile dyes*. CRC Press

50. Mathur N, Bhatnagar P, Nagar P, Bijarnia MK (2005) Mutagenicity assessment of effluents from textile/dye industries of Sanganer, Jaipur (India): a case study. *Ecotoxicol Environ Saf* 61(1):105–113. <https://doi.org/10.1016/j.ecoenv.2004.08.003>
51. Mia R, Selim M, Shamim A, Chowdhury M, Sultana S, Armin M, Hossain M, Akter R, Dey S, Naznin H (2019) Review on various types of pollution problem in textile dyeing & printing industries of Bangladesh and recommendation for mitigation. *J Text Eng Fashion Technol* 5(4):220–226
52. Minisy IM, Salahuddin NA, Ayad MM (2019) Chitosan/polyaniline hybrid for the removal of cationic and anionic dyes from aqueous solutions. *J Appl Polym Sci* 136(6):47056. <https://doi.org/10.1002/app.47056>
53. Monvisade P, Siriphannon P (2009) Chitosan intercalated montmorillonite: preparation, characterization and cationic dye adsorption. *Appl Clay Sci* 42(3–4):427–431. <https://doi.org/10.1016/j.clay.2008.04.013>
54. Mustafa I (2019) Methylene blue removal from water using H₂SO₄ crosslinked magnetic chitosan nanocomposite beads. *Microchem J* 144:397–402. <https://doi.org/10.1016/j.microc.2018.09.032>
55. Ngah WSW, Teong LC, Megat Hanafiah MAK (2011) Adsorption of dyes and heavy metal ions by chitosan composites: a review. *Carbohydr Polym* 83(4):1446–1456. <https://doi.org/10.1016/j.carbpol.2010.11.004>
56. Olivera S, Muralidhara HB, Venkatesh K, Guna VK, Gopalakrishna K, Kumar Y (2016) Potential applications of cellulose and chitosan nanoparticles/composites in wastewater treatment: a review. *Carbohydr Polym* 153:600–618. <https://doi.org/10.1016/j.carbpol.2016.08.017>
57. Peppas NA, Bures P, Leobandung WS, Ichikawa H (2000) Hydrogels in pharmaceutical formulations. *Eur J Pharm Biopharm* 50(1):27–46. [https://doi.org/10.1016/S0939-6411\(00\)00090-4](https://doi.org/10.1016/S0939-6411(00)00090-4)
58. Piaskowski K, Świdarska-Dąbrowska R, Zarzycki PK (2018) Dye removal from water and wastewater using various physical, chemical, and biological processes. *J AOAC Int* 101(5):1371–1384. <https://doi.org/10.5740/jaoacint.18-0051>
59. Rinaudo M (2006) Chitin and chitosan: properties and applications. *Prog Polym Sci* 31(7):603–632. <https://doi.org/10.1016/j.progpolymsci.2006.06.001>
60. Roberts GAF (1992) Chitin chemistry: Macmillan International Higher Education
61. Roy DC, Biswas SK, Saha AK, Sikdar B, Rahman M, Roy AK, Prodhan ZH, Tang S-S (2018) Biodegradation of Crystal Violet dye by bacteria isolated from textile industry effluents. *PeerJ* 6:e5015. <https://doi.org/10.7717/peerj.5015>
62. Sadeghi-Kiakhani M, Arami M, Gharanjig K (2013) Preparation of chitosan-ethyl acrylate as a biopolymer adsorbent for basic dyes removal from colored solutions. *J Environ Chem Eng* 1(3):406–415. <https://doi.org/10.1016/j.jece.2013.06.001>
63. Sakamoto M, Ahmed T, Begum S, Huq H (2019) Water pollution and the textile industry in Bangladesh: flawed corporate practices or restrictive opportunities? *Sustainability* 11(7):1951. <https://doi.org/10.3390/su11071951>
64. Sakata M (1985) Diagenetic remobilization of manganese, iron, copper and lead in anoxic sediment of a freshwater pond. *Water Res* 19(8):1033–1038. [https://doi.org/10.1016/0043-1354\(85\)90373-2](https://doi.org/10.1016/0043-1354(85)90373-2)
65. Salleh MAM, Mohd DK, Mahmoud WA, Karim WA, Idris A (2011) Cationic and anionic dye adsorption by agricultural solid wastes: a comprehensive review. *Desalination* 280(1–3):1–13. <https://doi.org/10.1016/j.desal.2011.07.019>
66. Sarkar K, Debnath M, Kundu PP (2012) Recyclable crosslinked O-carboxymethyl chitosan for removal of cationic dye from aqueous solutions. *Hydrol Curr Res* 3(138):2. <https://doi.org/10.4172/2157-7587.1000138>
67. Sharma P, Das MR (2013) Removal of a cationic dye from aqueous solution using graphene oxide nanosheets: investigation of adsorption parameters. *J Chem Eng Data* 58(1):151–158. <https://doi.org/10.1021/je301020n>
68. Sivashankari PR, Prabakaran M (2017) 5—Deacetylation modification techniques of chitin and chitosan. In: Amber Jennings J, Bumgardner JD (eds) Chitosan based biomaterials, vol 1. Woodhead Publishing, pp 117–133

69. Small K, Keller Kopf R, Watts RJ, Howitt J (2014) Hypoxia, blackwater and fish kills: experimental lethal oxygen thresholds in juvenile predatory lowland river fishes. *PLoS ONE* 9(4):e94524. <https://doi.org/10.1371/journal.pone.0094524>
70. Tahir SS, Rauf N (2006) Removal of a cationic dye from aqueous solutions by adsorption onto bentonite clay. *Chemosphere* 63(11):1842–1848. <https://doi.org/10.1016/j.chemosphere.2005.10.033>
71. Tang H, Zhou W, Zhang L (2012) Adsorption isotherms and kinetics studies of malachite green on chitin hydrogels. *J Hazard Mater* 209:218–225. <https://doi.org/10.1016/j.jhazmat.2012.01.010>
72. Tanhaei B, Ayati A, Sillanpää M (2019) Magnetic xanthate modified chitosan as an emerging adsorbent for cationic azo dyes removal: kinetic, thermodynamic and isothermal studies. *Int J Biol Macromol* 121:1126–1134. <https://doi.org/10.1016/j.ijbiomac.2018.10.137>
73. Tapan Kumar S (2010) Adsorption of methyl orange onto chitosan from aqueous solution. *J Water Res Protect*. <https://doi.org/10.4236/jwarp.2010.210107>
74. Tkaczyk A, Mitrowska K, Posyniak A (2020) Synthetic organic dyes as contaminants of the aquatic environment and their implications for ecosystems: a review. *Sci Total Environ* 717:137222. <https://doi.org/10.1016/j.scitotenv.2020.137222>
75. Upadhyaya S, Kepplinger D (2014) How industrial development matters to the well-being of the population: some statistical evidence. UNIDO, Vienna
76. Vakili M, Rafatullah M, Salamatinia B, Abdullah AZ, Ibrahim MH, Tan KB, Gholami Z, Amouzgar P (2014) Application of chitosan and its derivatives as adsorbents for dye removal from water and wastewater: a review. *Carbohydr Polym* 113:115–130. <https://doi.org/10.1016/j.carbpol.2014.07.007>
77. Varlamov VP, Il'ina AV, Shagdarova BT, Lunkov AP, Mysyakina IS (2020) Chitin/chitosan and its derivatives: fundamental problems and practical approaches. *Biochemistry (Moscow)* 85(1):154–176. <https://doi.org/10.1134/S0006297920140084>
78. Vu HT, Pham LC (2016) A dynamic approach to assess international competitiveness of Vietnam's garment and textile industry. *Springerplus* 5(1):1–13
79. Wan Ngah WS, Md Ariff NF, Hashim A, Hanafiah MAKM (2010) Malachite green adsorption onto chitosan coated bentonite beads: isotherms, kinetics and mechanism. *CLEAN–Soil, Air, Water* 38(4):394–400. <https://doi.org/10.1002/clen.200900251>
80. Wang L, Li Q, Wang A (2010) Adsorption of cationic dye on N, O-carboxymethyl-chitosan from aqueous solutions: equilibrium, kinetics, and adsorption mechanism. *Polym Bull* 65(9):961–975. <https://doi.org/10.1007/s00289-010-0363-1>
81. Wang Z, Zhang J-H, Jiang J-J, Wang H-P, Wei Z-W, Zhu X, Pan M, Su C-Y (2018) A stable metal cluster-metalloporphyrin MOF with high capacity for cationic dye removal. *J Mater Chem A* 6(36):17698–17705. <https://doi.org/10.1039/C8TA06249H>
82. Wu J-S, Liu C-H, Chu KH, Suen S-Y (2008) Removal of cationic dye methyl violet 2B from water by cation exchange membranes. *J Membr Sci* 309(1–2):239–245. <https://doi.org/10.1016/j.memsci.2007.10.035>
83. Yang H, Sheikhi A, Van De Ven TGM (2016) Reusable green aerogels from cross-linked hairy nanocrystalline cellulose and modified chitosan for dye removal. *Langmuir* 32(45):11771–11779. <https://doi.org/10.1021/acs.langmuir.6b03084>
84. Yong SK, Shrivastava M, Srivastava P, Kunhikrishnan A, Bolan N (2015) Environmental applications of chitosan and its derivatives. *Rev Environ Contam Toxicol* 233:1–43. https://doi.org/10.1007/978-3-319-10479-9_1
85. Yun J, Wang Y, Liu Z, Li Y, Yang H, Xu Z-L (2020) High efficient dye removal with hydrolyzed ethanalamine-Polyacrylonitrile UF membrane: rejection of anionic dye and selective adsorption of cationic dye. *Chemosphere* 259:127390. <https://doi.org/10.1016/j.chemosphere.2020.127390>

86. Zargar V, Asghari M, Dashti A (2015) A review on chitin and chitosan polymers: structure, chemistry, solubility, derivatives, and applications. *ChemBioEng Rev* 2(3):204–226. <https://doi.org/10.1002/cben.201400025>
87. Zereshti S, Daraei P, Shokri A (2018) Application of edible paraffin oil for cationic dye removal from water using emulsion liquid membrane. *J Hazard Mater* 356:1–8. <https://doi.org/10.1016/j.jhazmat.2018.05.037>

Chitosan-Based Composite Beads for Removal of Anionic Dyes



Joydeep Dutta

1 Introduction

The contamination of water bodies is one of the astoundingly challenged agendas worldwide, as it causes undesirable consequences for living life forms [1]. Dyes and pigments are the challenging pollutants of the water system. Dyes are used in food, rubber, paper, cosmetic, pharmaceutical, automotive, and textile industries [2, 3], and the leftovers gain access to the water environment and act as pollutants. The approximate annual production of dyes for industrial use is about 1.6 million tons [4]. Industries involved in the dyeing process often throw out spent water treated or untreated, which takes up in the environment. According to a report, 10–25% of textile dyes are lost during the dyeing process (10–25%) and are directly discharged as aqueous effluents (2–20%) in different environmental components [5]. These dyes in lakes and rivers decrease dissolved oxygen concentration, causing anoxic conditions causing discomfort to aquatic organisms [6]. These dyes persist in the environment due to their high stability to light, temperature, water, detergents, chemicals, soap, and other parameters such as bleach and perspiration [7]. Dyes can be mutagenic, carcinogenic, teratogenic and genotoxic. It generates dysfunction of the kidneys, digestive system, brain, and skin and decreases food intake capacity, growth, and fertility rates in mammalian cells [8] (Fig. 1). This prompts a quick action to remove such harmful dye from the water matrices to improve the quality standards.

Efforts are in progress from earlier days for casting off those waste from the water environment, which can be analyzed from the understanding that people have started

The original version of this chapter was revised: Cited Figures and Tables have been placed in correction chapter 15 along with captions. The correction to this chapter is available at https://doi.org/10.1007/978-981-19-2832-1_15

J. Dutta (✉)

Department of Zoology, Lovely Professional University, Phagwara, Punjab 144411, India
e-mail: joydeep.dutta@lpu.co.in

© The Author(s), under exclusive license to Springer Nature Singapore Pte Ltd. 2022, corrected publication 2022

S. S. Muthu and A. Khadir (eds.), *Textile Wastewater Treatment*, Sustainable Textiles: Production, Processing, Manufacturing & Chemistry, https://doi.org/10.1007/978-981-19-2832-1_3

using various techniques to purify water bodies (Fig. 2). A more comprehensive range of physical, chemical, and biological methods have been employed to treat dyeing wastewater, but still, a vast gap exists. Techniques like reverse osmosis [9], membrane filtration [10], bacterial action [11, 12], integrated chemical–biological degradation [13], precipitation [14], sonochemical degradation [15], electrochemical destruction [16, 17], ozonation [18], coagulation [19], nano membrane filtration [20], ion exchange [21], and each of these mentioned technologies have their own technical and economic limitations for real-life application.

2 Adsorption: The Future Technology

From its inception date, adsorption is being used to remove solutes from water and gases from the atmosphere. Adsorption nowadays is contributing to a better and viable technology for water purification and is gaining prominence in the field of research and real-existence applications [22] (Fig. 3). It also shows a promising research activity in recent years. It has gained its importance in treating wastewaters, groundwater, and industrial effluents, including the production of drinking water [23]. Adsorption is a function of the concentration of materials, i.e. adsorbate (pollutants) on the surface of solid bodies (adsorbent). Surface forces are involved in the adsorption of the pollutant over adsorbents. The principle behind the adsorption is the binding of contaminants over highly porous adsorbate. Adsorption offers many advantages; however, it depends upon many factors and limits its usability to remove various pollutants (Table 1). The ongoing research is to focus on the development of effective adsorbents. Studies have mainly used multiple materials with their modification and composition to frame advanced adsorbents, effectively separating complex pollutants in a wide range of physical and chemical environments.

The quantity of adsorbate defines a promising adsorbent that can concentrate on its surface, usually calculated from the adsorption isotherms. An adsorbent with a high surface area is taken as a better choice, and the time taken for adsorption should be as small as possible so that it can be used to remove dye wastes in lesser time [22]. The adsorption isotherms are the relationship between the quantity of adsorbate per unit of adsorbent and its equilibrium solution concentration. Several equations or models like the Freundlich and Langmuir equations are available. The Langmuir model calculates the number of molecules adsorbed onto a solid surface in a monolayer fashion onto a homogeneous surface with little interaction between adjacent adsorbed molecules. At the same time, Freundlich assumes that the adsorption sites are heterogeneous surfaces, and there is multilayer adsorption on the adsorbate. Pseudo-first-order and second-order kinetic models are applied to determine the best fit kinetic model for evaluating the adsorbents and further development [24].

2.1 Adsorbents

Many wastewaters contain toxic contaminants, which are undesirable (Fig. 1). Therefore, technologies are required and need to be developed to improve water quality. These challenges require better and cost-effective removal technologies. Adsorption is an upcoming and promising system in which there is an interaction between adsorbents and adsorbates. The adsorbent is a substance that will adsorb other molecules on its surface, thereby promoting separation. A promising adsorbent is highly porous and has a large surface area with more specific adsorption sites. The pore size of the adsorbent is classified as recommended by the International Union of Pure and Applied Chemistry (IUPAC) (d is the pore diameter), micropores $d < 2$ nm, mesopores $2 < d < 50$ nm and macropores $d > 50$ nm [25]. Other essential attributes for an adsorbent are capacity for adsorption, selective adsorption, kinetics, renewability, compatibility for adsorption function, and low-cost of preparation based on which selection of suitable adsorbent could be achieved [26] (Fig. 4).

Characteristics of a suitable adsorbent depend on its capacity to separate molecules from the medium because it is directly related to the amount of adsorbent required and the cost of the function. The capacity of the adsorbent also depends upon other parameters like temperature, pH, the number of adsorbates etc. Adsorbents can be developed, however; it is based on experimentation. Some of the most challenging separation and purification problems require new adsorbents or designed adsorbents [27]. Adsorbents could be natural, synthetic, biomass, industrial waste, and agricultural waste. For the commercialization of adsorbents, kinetic studies are a must that give the idea of adsorption capacity and the speed of adsorption. Batch studies are conducted to optimize the conditions by varying the parameters like initial contaminant concentration, temperature, pH, the dosage of adsorbent, and particle for large scale applications. The two most widely used models are the pseudo-first-order and the pseudo-second-order model, which can study the dye adsorption kinetics and quantify the extent of uptake in adsorption kinetics.

2.2 Types of Adsorbents

The capacity of adsorption of adsorbates defines the characteristics of adsorbents. Dyes that are stable in the aquatic environment need to be removed by using the adsorbents. A promising adsorbent can remove the dyes from the water within less time or can achieve equilibrium in a short time. Many approaches have been made to frame an effective and low-cost adsorbent, and still, the studies are going on. Some of the adsorbents reported are non-conventional low-cost adsorbents, including natural materials, biosorbents, waste materials from industry and agriculture, marine materials, and mineral materials.

2.2.1 Agricultural Waste as Adsorbent

Agricultural waste substances are typically ample and proven to be eco-friendly and monetary sources of precursors or adsorbent substances (Table 2). It has been said that numerous agricultural wastes may be without problems transformed into value-introduced products. Wastes had been recycled and utilized in the elimination of various forms of pollution from effluent. The primary additives of agricultural waste substances encompass hemicelluloses, lignin, lipids, simple sugars, proteins, hydrocarbons, and starch, which are adsorbent substances for dye adsorption. Agricultural waste may be used directly or with minimal modifications to increase the capacity and reduce the production cost [28]. The direct use of agricultural waste as adsorbent is procurement, washing, and making it into the desired particle size. At the same time, the other format is to pretreat the waste before use to enhance the functional groups over the adsorbent, thus increasing the capacity of adsorption [24] (Fig. 5).

2.2.2 Industrial By-products for Adsorption

Industrial waste is produced during industrial activity. It includes material that is taken as useless during a manufacturing operation. Industrial by-products are considered unusable waste and cause central disposal and dumping problems. Types of industrial waste include dirt and gravel, masonry and concrete, scrap metal, oil, solvents, chemicals, scrap lumber, and semi-solid, or liquid form. Most nations have established enactment to manage modern waste; however, severity and consistency systems shift. Thus, it is essential to use such industrial waste to make it a meaningful resource. Due to the low-cost, industrial waste has been used to prepare adsorbents. Waste like fly ash contains a high percentage of silica and alumina [29]. Fly ash is used as a low-cost adsorbent for the treatment of wastewater and removal of reactive and acid dyes removal (Reactive Red 23—2.102 mg g⁻¹, Reactive Blue 171—1.860 mg g⁻¹, Acid Black 1—10.331 mg g⁻¹, and Acid Blue 193—10,937 mg g⁻¹) [30]. In an experiment, it was shown that Raw coal fly ash reached adsorption equilibrium within 50 min of the batch reaction of all the dyes (Acid blue 193, Acid Black 1, Reactive blue 4, and Reactive blue 171) and followed Second-order kinetic models [31]. The treated and untreated raw coal fly ash showed better Acid Red 1 dye adsorption with a maximum value of 103.09 mg g⁻¹ and followed pseudo-second-order kinetics [32].

Red mud is an industrial waste generated during bauxite processing into alumina and is composed of solid and metallic oxides like iron oxides (red colour). The mud is basic, with a pH ranging from 10 to 13 [33]. Red mud also contains components like silica, unleached residual aluminium compounds, and titanium oxide [34]. Red mud removed Congo Red from the water, and the equilibrium was attained at 90 min of the batch adsorption study [35]. The adsorption of Congo Red in a batch adsorption study shows removal efficiency of red mud is 4.05 mg g⁻¹ [36]. Alkaline white mud has been investigated to remove the dye acid blue 80 from the water matrices and found that the dye removal efficiency reached up to 95% [14]. Blast furnace slag is the by-product of the steel industry and is also used as an adsorbent. Treated blast

furnace slag efficiently removed acid red 138 and acid green 27 with a maximum capacity of 208.3 mg g⁻¹ and 265.2 mg g⁻¹, respectively [37].

2.2.3 Natural Clay Materials

Natural materials are readily available, low-cost, biodegradable substitutes made from natural resources to remove organic contaminants and used as effective adsorbents. Clay is a significant component of the earth's crust containing aluminosilicates [38]. Due to their lamellar structure, clays have a high adsorption capacity and the possibility to adsorb ions and polar organic molecules. Clays have a difference in mineralogy, size, and large surface area up to 800 m²g⁻¹ [39]. Therefore, clay and clay minerals are regarded as adsorbents in modified or unmodified forms. Natural clays have negative charges on their surface and can adsorb positively charged dyes but induce low adsorption for anionic dyes. However, surface-modified clays have shown enhanced adsorption capacity of anionic dyes. There are different types of pure clays which provide an opportunity for investigation of adsorption behaviour. Other types of clays which are being tested for adsorption of dyes are bentonite, zeolite, montmorillonite, smectite, palygorskite, attapulgite, kaolinite, vermiculite, sepiolite, clinoptilolites, illite, etc. (Fig. 6). Natural clays are a mixture of different types of weathered minerals and exhibit efficient adsorption capacities. Natural clays have shown efficient adsorption of Reactive Red 120 [40], Congo Red [41], Remazol brilliant blue R [42], Alizarin red S [43], Reactive Orange 84 and Reactive Blue 160 from wastewater [44]. Kaolinite plays a significant role in the adsorption of anionic dye, but its efficiency reduces when mixed with illite and smectite. Palygorskite shows the lowest efficiency in adsorption even though the clay is highly porous, having a high specific surface. Thus, these clays in combination do not enhance the adsorption of RR 120 dye because of the nature of the characters and the cover charges [45]. The adsorption process of alizarin S increased with the enhancement of initial dye concentration, adsorbent dosage, and contact time but decreased with the enhancement of solution pH [30, 43, 46]. However, some experiments suggested that adsorption is endothermic [47], or exothermic [40, 41, 48]. The experimental data is well fitted with both the Langmuir and the Freundlich models. The kinetics also followed the pseudo-second-order reaction model [30]. Natural or unmodified clays have high adsorption efficiency of dyes from water matrices in experimental conditions (Fig. 6).

2.2.4 Biological Adsorbents

Fungi and bacteria are used for the adsorption of dyes from water and are called bioadsorbents (Table 3). Bioadsorbents provide a wide range of effective characteristics for the adsorption of dyes, even in a complex environment (Fig. 7). Microorganisms can be used live or dead (especially fungi), and microbial treatment of coloured water involved aerobic, anaerobic, and combination methods [22, 49]. Microbial biomass

is used for the decolourization of water [50]. Certain dyes have a particular affinity for binding with microbial species, thus, microbes could be used as an effective tool for dye adsorption. The use of NaCl is to enhance the bath dye exhaustion, but this does not hamper the adsorption of dye onto *S. cerevisiae* as Cl ions do not compete with the sulfonate group of AR14 [51]. The advantage of using microbial biomass is reducing toxic dyes in water matrices at a low level involving low-cost with live or dead organisms. However, sometimes adsorption is slow, dependent on the pH of the medium, and the presence of functional groups, salt or other ions may occur in competition for adsorption or clog the column [49].

The use of peat as an adsorbent has gained attention over the past thirty years to treat wastewater. Peat is widely available and studied as an adsorbent for dyes. Peat is complex soil material with organic matter in various stages of decomposition, usually of a dark brown colour, and is classified into four groups: moss peat, herbaceous peat, woody peat, and sedimentary peat [49]. The major constituents of peat are lignin, cellulose, fulvic, and humic acid, which provide a polar character. Peat is comparable to silica and alumina, both in cost and adsorption capacity. Peat is polar, and it is known to adsorb dyes like Basic blue 3, Basic Yellow 21, Basic Red 22, Basic Magenta and Basic Brilliant Green, Basic Blue 69 and Acid Blue 25, and other acid dyes & basic dyes [49, 52].

2.2.5 Chitin and Chitosan: As a Modern Choice of Adsorbent

Chitin is a white hard inelastic, semitransparent, nitrogenous polysaccharide compound with low reactivity and insoluble to many organic solvents. It is a by-product of the fishery industry (Fig. 7). It is the naturally occurring mucopolysaccharide and is the main component in the shell of insects, crustacean shrimps, crabs, and lobsters. It is also found in the shell wall of fungi and the exoskeleton of fungi molluscs and fish [53, 54]. Chitin is commercially available as a by-product of food processing from crustaceans (Crab, Crayfish) [49]. The annual worldwide production is estimated at approximately 1010–1012 tons [55]. Chitin contains 2-acetamido-2-deoxy- β -D-glucose through α β (1–4) linkage. Chitin is a white, rigid, inelastic, nitrogenous polysaccharide. It is a waste product second only to cellulose in terms of abundance in nature and the primary source of surface pollution in coastal areas [56]. The applications of chitin are in wastewater treatment, food industry, agriculture, pulp and paper industry, cosmetics and toiletries and biomedical applications [57]. One of the essential uses of chitin is dye separation from water matrices because of hydroxyl and amino groups favouring adsorption and desorption [58]. Acid Blue 25 and Acid Blue 158 show a strong affinity towards chitin, and dyes can even penetrate the internal pore structure [59]. It has been used successfully for the removal of reactive dyes [58, 60, 61], Acid Blue 25, Acid Blue 158, Mordant Yellow 5, and Direct Red 84 [59], indigo carmine [62], malachite green [63] and acid dye [64]. This adsorption is because of electrostatic attraction between the dye molecule and the anion group of the chitin. However, the degree of crosslinking may reduce the positive charges over the adsorbent, thus, the higher the cross-linking the lesser would be the

adsorption [58]. Due to its low surface area, porosity, and high crystallinity, chitin is generally modified by different chemical modification techniques to introduce various functional groups to improve its adsorption capacity [65]. Ultrasonic modification of chitin gives a 25 times higher surface than raw chitin, resulting in increased adsorption of methylene blue upto 26.69 mg g^{-1} [66]. Such modification of chitin was achieved for the separation of dyes and wastewater minimization (Table 7). In an experiment, it was observed that modification of chitin through ultrasonication gives methylene blue (positively charged) more chance for interaction with N-acetyl and hydroxyl groups of modified chitins [67]. Cyclodextrin-linked chitosan was used for decontamination of waters containing textile dyes [65]. Research reported that mixed modification of the surface of chitin yielded better sorption of methylene blue. The texture of chitin was changed with acid treatment followed by ultrasonication [68]. Adsorption of malachite green, methyl violet, and paraquat from water is enhanced by Chitin grafted with poly (acrylic acid) which shows its multifunctional uses of modified chitin [69]. The introduction of monochloroacetic acid in isopropanol adds the carboxyl group into chitin's structure prompting the arrangement of anionic derivatives that can be useful in the adsorption of pollutants from the environmental system [70]. Even though chitin is used for the adsorption of different dye molecules, its low surface area, porosity, and high crystallinity lose its adsorptive efficiency. The use of various chemical surface modification techniques increases the efficiency of chitin for the adsorption of dye from the water environment. Surface modification improves the adsorption efficiency by enhancing the charged interaction between the adsorbent and the dye molecules.

Chitosan is the derivative of chitin, similar in solubility limitations as chitin despite being soluble in diluted acid solutions [70]. Chitosan is a deacetylated product of chitin (Fig. 7) and consists of β -(1 \rightarrow 4)-2-amino-2-deoxy-D-glucose units and a lower percentage of β -(1 \rightarrow 4)-2-acetamido-D-glucose by treatment with alkali [71, 72]. During deacetylation (influenced by temperature, time, and the concentration of NaOH used), the acetyl groups of chitins are hydrolyzed to give free amine groups. It states that the more the amino groups more is the adsorption capacity of chitosan [73]. Because of hydrogen bonds, chitosan is insoluble in water, alkaline solutions, and organic solvents but is soluble in acidic solutions due to the protonation of its amine groups; thus, chitosan has a high affinity to adsorb heavy metals and dyes [73]. $-\text{NH}_2$ and $-\text{OH}$ contribute primarily to adsorption interfaces between chitosan and adsorbate molecules [72, 74]. Chitosan contains carbon, hydrogen, oxygen, and additional nitrogen (6.89%) [75], therefore making it one of the most important organic compounds used for adsorption of heavy metals, dyes, and pharmaceuticals [76], phenol & pesticides [75] (Table 5). Chitosan is hydrophobic, biocompatible, biodegradable, and non-toxic [77], thus, making it an effective adsorbent material for the removal of wastewater pollutants. However, drawbacks like solubility in acid, low mechanical strength, and low surface area hinder adsorption efficiency, prompting the modification of chitosan [73].

3 Use of Chitosan Beads as Adsorbents

Chitosan is a versatile carbohydrate polymer, and presence of $-\text{NH}_2$ and $-\text{OH}$ contributes primarily to adsorption interfaces between adsorbent and adsorbate. It has good adsorption capacity and flocculating ability; therefore, it finds a place to treat organically polluted wastewaters. Cross-linked chitosan was used for the adsorption of dyes and oil. Adsorption of residue oil from palm oil mill effluent (POME) using chitosan powder and flake has been investigated. The powder form of chitosan exhibited a greater adsorption rate than the flake type and could adsorb 99% residual oil from POME. The equilibria data fitted very well with the Freundlich isotherm and second-order kinetic model signifying chemisorption between residue oil and chitosan [78]. Powder and flake forms of chitosan are extensively used for removal of residual oil [79], heavy metals [80–82], biodiesel [83] and petroleum spills [84]. However, the technical disadvantage of using chitosan in powder and flakes is because of low adsorption capacity due to crystallized structure [85], it also poses difficulty as it reduces water transparency and reduces water chances of recovery from the water environment. Secondly, chitosan-flakes have low adsorption capacity, surface area, hydrophilicity, non-porosity, and mass transfer resistance [86]. Therefore, the chitosan is designed in beads that can be immobilized, have higher loading capacity, increased porosity & surface area, expanded polymer chains, decreased crystallinity, and more sorption in internal sites [85] and can be recovered for recycling. And the use of beads had gained its importance for separation technology which can be viewed in the form of published works based on Pubmed database screening (using the terms “chitosan” in combination with “beads” or “adsorption”): (i) 1992–2000-11 papers; (ii) 2001–2010-71 papers; (iii) 2011–2020-195 papers, and (iv) 2021-to date-21 papers (Fig. 8).

Chitosan beads are three-dimensional that swell in water but maintain their structural integrity (Fig. 9). Recent development has shown that the use of beads has increased because of their excellent biocompatibility and easy preparation. In recent years, it has also gained its importance as a bioadsorbent because of rich amino and hydroxyl groups and, therefore, in separation technology and wastewater treatment. Considering the importance and usability, chitosan beads are synthesized. However, the amino groups of chitosan hydrogel beads generally get protonated at lower pH and thus get less stable and more soluble in a highly acidic environment [75]. Because of its limited capacity crosslinking, blending, and grafting have been developed to improve the physicochemical properties, such as mechanical strength, colloidal stability, and efficiency of chitosan beads at lower pH for better adsorption. Most of the crosslinkers used to modify chitosan beads are- epichlorohydrin, ethylene glycol diglycidyl ether, glyoxal, formaldehyde, isocyanates, and glutaraldehyde [87]. The target of crosslinkers is $-\text{NH}_2$ and $-\text{OH}$ on the chitosan beads, epichlorohydrin target $-\text{OH}$ and ethylene glycol diglycidyl ether, and glutaraldehyde target $-\text{NH}_2$ [85].

Crosslinker acts as a bridge improving the mechanical strength and chemical stability. On the other hand, free amino groups are attacked by cross-linkers, which may reduce the ligand density or induce denaturation and aggregation, ultimately

reducing the adsorption capacity of chitosan beads for wastewater treatment applications [85]. To minimise this effect an effort for maintaining the degree of crosslinking other alternative chemical modification like composite bead formation is practised to improve the adsorption capacity.

4 Chitosan Composite Beads for Adsorption of Anionic Dyes

Recently chitosan has gained its importance in the field of wastewater decontamination technology through adsorption. Therefore, numerous researches have been carried out regarding chitosan as an adsorbent for wastewater treatment, either inorganic (metals, ions, etc.) or organic (dyes, phenolic and pharmaceutical compounds, herbicides, pesticides, drugs, etc.) [88]. However, the drawback with chitosan is its sensitivity to pH, which can either form gel or dissolve depending upon the system's pH value [89]. On the other hand, cross-linking reagents stabilize chitosan in acidic solutions and enhance its mechanical properties [89]. Nevertheless, cross-linking also reduces adsorption capacity as these molecules attack free amino groups on chitosan.

Nowadays, chitosan composites have been developed and are extensively investigated for the adsorption of dyes from wastewater. Different kinds of substances have been used to form a composite with chitosan (Table 6), and the composites have shown a better adsorption capacity and resistance to acidic environment [90], high rigidity, low specific gravity, and higher resistance to corrosion and oxidation [91]. Figure 10 shows the general process of composite bead preparation. The Pubmed database shows the importance of the development of chitosan beads for adsorption studies (using the terms “chitosan” in combination with “beads” “composite” or “adsorption”): (i) 2003–2010-13 papers; (iii) 2011–2020-105 articles, and (iv) 2021-to date-10 reports. Furthermore, free amino groups on chitosan greatly enhance the adsorption capacity of anionic dyes even at low pH due to electrostatic attraction between anionic dyes and protonated sites on the chitosan. Thus, chitosan composites have gained attention as an alternative method to conventional wastewater treatment technology for the adsorption of dyes.

4.1 Chitosan/Montmorillonite Composites

Clay minerals have been used to form chitosan composites, and among them is montmorillonite which is abundant and low-cost. Montmorillonite has a high cation exchange capacity and a large specific area accommodating bulky molecules such as chitosan. Montmorillonite has a low affinity for anionic dyes; therefore, modification with polymers changes its chemical property and improves its affinity for

anionic dyes [91]. Montmorillonite has a tetrahedral and octahedral layer, and the substitution of Al_3+ for Si_4+ for the tetrahedral layer and Mg_2+ for Al_3+ for the octahedral layer results in the negatively charged surface of montmorillonite, making it a good choice for adsorption [90]. In a hybrid system, an increase in the molar ratio of chitosan to montmorillonite causes increased adsorption due to balancing the initial negative charges of montmorillonite with chitosan. Two different adsorption mechanisms are stated in the study- electrostatic attraction and chemisorption depending upon the pH of the medium. Adsorption of anionic dyes at lower pH favours electrostatic attraction between the amine group in chitosan and the anionic dyes. Still, competitive interest occurs between the dye and the $-OH$ groups for the active groups at higher pH [92]. Apart from electrostatic attraction, hydrogen bonding also plays a vital role in adsorption. Removal of anionic dye from water results from hydrogen bonding between $-Cl$, $-N$, and $-O$ containing functional groups. Diamond Fast Brown KE and H atoms from $=NH$, and $-OH$ groups prepared two different weight ratios of chitosan-montmorillonite composites [93]. The adsorption kinetics of anionic dyes on chitosan-montmorillonite composite better follows the pseudo-second-order model suggesting that adsorption was influenced by the structure of the composite. The Langmuir isotherm indicated monolayer adsorption of dye Congo red (54.52 mg g^{-1}) [92], and Diamond Fast Brown KE (403.23 mg g^{-1}) [93]. The other anionic dyes adsorbed by chitosan-montmorillonite composite are Bezactive Orange V-3R [94], Congo Red [95], Methyl orange [96, 97], which follows pseudo-second-order kinetic model and Langmuir isotherm confirming structural benefit towards adsorption and monolayer formation around the adsorbent.

4.2 Chitosan/Bentonite Composites

Clay, such as bentonite available naturally and bears unique physiochemical properties and thus acts as low-cost adsorbents because of its ability to exchange cations. It consists of two tetrahedral silica sheets and one octahedral alumina sheet sandwiched in silica sheets. It is mainly composed of montmorillonite with SiO_2 , Al_2O_3 , CaO , MgO , Fe_2O_3 , Na_2O , and K_2O [90]. Bentonite has net negative charges on its layer due to aluminium or ferric cations in the tetrahedral sheets, and aluminium ions by magnesium or ferrous cations in the octahedral sheets, sodium or calcium ions are commonly present in the interlayer region [98].

Chitosan/ bentonite composite was prepared, which shows a heterogenous structure with better mechanical strength confirmed by tensile strength and elongation values and is better than pure chitosan film, ensuring the insertion of bentonite. The X-ray studies show that the composite surface has N (from chitosan) & Al (from bentonite) and Si being concentrated in some regions proving its heterogeneity. The EDS data shows that the composite surface has the combination of C, N, and O (of chitosan) and Si, Al, Mg and Na (of bentonite). The possible adsorption of anionic dyes because of the functional groups from chitosan and bentonite is confirmed by FTIR data [99]. The adsorption of Amaranth red was favoured at pH 2 because of

the protonation of chitosan amino groups and Si–O groups from bentonite facilitating adsorption. The pseudo-second-order model best described the adsorption of amaranth red. This showed that the rate-limiting step was due to chemical adsorption. As much as 362.1 mg g^{-1} of amaranth red could be adsorbed as determined by the Langmuir model [99]. The pH plays a vital role in the adsorption process. As the pH of the medium is lowered, the surface of the adsorbent becomes positive, which promotes the adsorption of anionic dyes like tartrazine [90]. However, the ratio of chitosan/bentonite also derives the adsorption efficiency (224.8 mg g^{-1}) of the anionic dyes onto the composites. In an experiment, it was found that the maximum removal efficiency of methyl orange was observed at the ratio of 2/2 of composite chitosan/ bentonite. This high removal may be due to interlayer spacing because of the intercalation of chitosan in bentonite [100].

A cross-linking agent can stabilize the chitosan in an acidic solution so that the chitosan can become insoluble. After crosslinking with glutaraldehyde, [101], epichlorohydrin [102, 103] chitosan and bentonite composite enhance the removal of Amido Black 10B, because of intercalation of cross-linked chitosan in bentonite increasing the basal spacing of bentonite. Secondly, the stability of the beads was improved due to the treatment of chitosan with a cross-linker, and the adsorption was optimal at pH 2 with a best fit pseudo-second-order kinetic model. The Langmuir model well described the adsorption isotherm, and the maximum adsorption capacity was 323.6 mg g^{-1} [101] and 990.1 mg g^{-1} [102, 103]. The high adsorption capacity was attributed to the strong electrostatic interaction and the valence forces through the sharing or exchange of electrons between dye molecules and this composite. The desorption studies proved that the cross-linked chitosan/bentonite composite beads were efficient (98%—removal efficiency of Amido Black 10B) even after 5th regeneration, thus highlighting the importance of reusability [102, 103].

Cross-linked chitosan/bentonite composite beads, when further treated with HCl, result in bentonite activation and the protonation of crosslinking chitosan. The resultant enhanced cross-linked chitosan/bentonite composite exhibited a higher adsorption capacity of methyl orange. During treatment, an increase in HCl concentration showed the maximum removal of methyl orange. The following mechanism was attributed to enhanced removal capacity (i) activation of bentonite and the protonation of crosslinking chitosan bringing more electropositivity facilitating anionic dye removal, (ii) acid treatment increases the basal spacing of bentonite and dredges the inner passage. The kinetic data followed the pseudo-second-order equation and was determined by the Langmuir model with a maximum adsorption capacity of 36.8 mg g^{-1} [102, 103].

4.3 Chitosan/Polyurethane Composites

Polyurethanes (PU) are multipurpose materials due to their comfort, cost benefits, energy savings and potential environmental reliability. PU is used in upholstered furniture, as insulators, roofs and appliances, medical devices and footwear, coatings,

adhesives, sealants and elastomers used on floors and automotive interiors [104]. PU have a high surface area, and open porous structures thus have high usage in immobilization of adsorbent and turn in treatment of waste water. In addition, this porous structure of polyurethane foams gives exceptional water-purifying abilities. The composite of PU/Chitosan is formed due to hydrogen bond interaction. The addition of chitosan to PU causes additional $-OH$ and $-NH_2$ adsorption sites and caused higher porosity [105] and showed a semi-crystalline structure with several functional groups [106].

PU/Chitosan composite has smooth surfaces with well-developed open cell structures, which provide the accessibility of Acid Violet 48 in aqueous solutions to the chitosan adsorbent [107]. On the other hand, the PU/humic acid-chitosan composite shows that the structure is much rougher and more porous, favouring the higher adsorption capacity of the Methyl orange dye [108]. The dye adsorption followed pseudo-second-order kinetics and at lower pH, favouring chemisorption between the amine group of chitosan and the sulfonic group of Acid Violet 48. The adsorption onto PU/Chitosan composite followed Langmuir isotherm equilibrium with maximum adsorption of Acid Violet 48 (30 mg g^{-1}) [107] and Reactive blue dye 198 (86.43 mg g^{-1}) [109]. The monolayer sorption over the solid surface with homogeneous sites confirms no further adsorption on the composites. The interesting fact of the composite is that the PU matrices provide a skeleton framework in which the chitosan as adsorbent is well dispersed and immobilized. The efficiency of the composite is pronounced by the fact that the composites can be reused without desorption or other coatings of chitosan for the removal of the Reactive blue 198 dye [109].

4.4 Chitosan/Kaolinite Composites

Kaolinites contain tetrahedral silica sheets bound to the octahedral aluminium oxide/hydroxide layer sheets by hydrogen bonds. It is known to adsorb ions by (i) ion exchange at the permanent negatively charged sites or (ii) through the formation of surface complexes [110]. Kaolinite has a long history of dye binding capabilities independently or when combined with other adsorbents. Kaolin has little affinity for anionic dyes, therefore, kaolin/chitosan composite is used to incorporate positively charged sites to enhance the adsorption characteristics of negatively charged dyes. Kaolinite/Chitosan composites have been used to frame the adsorbents in the form of beads. SEM studies show that the beads are smooth but discrete spherical particles confirming the combination of the organic modifying agent into the inorganic clay materials [111]. Kaolin/Chitosan composite beads have many pores and pleats on the surface, providing a good option for dyes to be adsorbed. The adsorption of methyl orange onto Kaolin/Chitosan composite beads shows better results at pH 2.9 because of increased electrostatic attraction between the beads and the dye [112]. Adsorption at lower pH (3.0 is again attributed to protonation of the amine group of chitosan molecule, however, the maximum adsorption occurred at pH 2.5 when the chitosan forms composite with kaolinite resists dissolution of chitosan at lower

pH [113]. The formation of Kaolin/Chitosan composite reduces the crystallinity of chitosan molecules and thus enhances the penetration of dye molecules. Adding kaolin to chitosan increases surface area and specific gravity, thus providing an ample opportunity for dye molecules to penetrate deep into the beads. An increase in % of kaolin in composite increases the Remazol Red dye removal efficiency of the beads [113]. The presence of free amine groups (in %) defines the adsorptive capacity of the composite. In an experiment, chitosan-glyoxal/kaolin composite beads were prepared. The characteristics state that 27.4% free amine groups were present, with 39.8 ($\text{m}^2 \text{g}^{-1}$) of surface and 6.2 nm as mean pore diameter. The higher surface area is attributed to kaolin particles scattered on the chitosan-glyoxal matrix. This higher surface area with suitable pore diameter and free amine groups makes the composite a better choice material for the adsorption of Remazol Brilliant Blue R [114].

4.5 Chitosan/Plant Materials Composites

Plant waste is lignocellulosic materials that contain lignin, cellulose and hemicellulose. Lignocellulosic materials have excellent structural properties with small molecular sizes. The different plant-based adsorbent has been prepared and reported for the removal of anionic dyes from wastewater. As adsorbents, plant wastes are available in large amounts and are less expensive as compared to other materials. Chitosan, because of its adsorption properties, has gained importance; however, its low hydrophilicity, surface area, high crystallinity, specific gravity, non-porosity, dissolution at low pH (Fig. 10) and mass transfer resistance. But when chitosan is crosslinked and/or mixed with other plant wastes or minerals improves its characteristics that help in significant adsorption of dyes from the water environment. Various plant materials were used in combination with chitosan for framing composite beads. These beads were then used for the removal of anionic dyes from wastewaters. The resultant beads showed heterogenous surface morphologies, which enables them to adsorb dye molecules. In combination with different ratios with plant materials, Chitosan behaved differently in the adsorption of dye molecules. It was observed that the plant materials due to lignin, hemicellulose and cellulose content provide mechanical support to the chitosan and thus prevent it from dissolution at low pH, which improves the adsorption efficiency of anionic dyes. Studies have shown that beads with chitosan in combination with raw or modified plant forms have proved to be an efficient system for adsorption of both anionic and cation molecules from the water environment. However, few studies have been quoted below to understand the composite beads and their efficiency in removing anionic dyes.

Chitosan combined with bamboo charcoal in a different ratio shows that the composite beads had improved porosity and surface area due to the presence of bamboo charcoal. It results in increased adsorption of Reactive Red 152; however, the increase in adsorption is due to the increased bamboo charcoal concentration in the composite beads. The micrographs study showed that the dye's adsorption onto

beads was homogenous due to electrostatic forces on chitosan molecules. The adsorption followed the Langmuir isotherm model with maximum adsorption of 87.5% at pH 4 [115]. The SEM study shows that composite beads' surface before adsorption was smooth, and after adsorption, the surface becomes irregular due to the presence of adsorbates [116] and [115]. Chitosan/Waste tea activated carbon composite beads were prepared and used for removal of Acid Blue 29. The adsorption of Acid Blue 29 by chitosan/waste tea activated carbon was spontaneous, endothermic, best described by the pseudo-second-order reaction model, and fit according to Langmuir and Freundlich isotherm at pH 2–4 [116]. As opposed to the smooth surface of the composite beads, the chitosan/coffee residue mixed beads have a scraggy character with a variety of cavities. After adsorption of Reactive Red 152, a substantial reduction of cavities on the surface of the beads could confirm the adsorption of the dye molecule. Maximum adsorption (99.14%) was recorded at pH 4 clearly states the electrostatic interaction between the dye molecule and the active sites.

Interestingly, the chitosan to coffee residue ratio of 60/40 was the best combination for the composite beads that could follow Langmuir isotherm with maximum adsorption of 4.27 mg g^{-1} states the efficiency of the adsorbent [117]. Chitosan/Oil palm ash zeolite was combined to form composite beads. The characteristics of the beads were non-uniform pores (mesoporous) with a surface area of $82.96 \text{ m}^2/\text{g}$. It was observed that as the percentage of chitosan was increased, Acid Blue 29 dye adsorption was also increased and is also dependent upon the temperature of the reaction. The adsorption followed the pseudo-second-order reaction and the Freundlich isotherm model [118]. The adsorption of dye on the composite bead shows that the accumulation of dye is in the form of layers. It was confirmed by the change in the colour of the beads after adsorption of the Acid Black 194 dye on chitosan/zeolite composite beads with maximum adsorption of 2140 mg g^{-1} . The surface morphology of beads had a more uniform particle size with the smooth entity. The adsorption of dye depends upon pH, initial dye concentration, competitive ions, and temperature [119].

5 Conclusion

Adsorption technology has expanded its status in the treatment of wastewater. Chitosan, because of its accessibility and its excellent adsorption properties, is used to treat sewage along with other naturally available molecules. However, if chitosan is used in powder and flakes, it further degrades the quality of water and is also not available for further reuse. And is also not capable of adsorption at low pH due to dissolution. Therefore, chitosan is framed in the form of beads and natural molecules to be recovered and reused. Chitosan is composited in beads with montmorillonite, bentonite, kaolinite, polyurethane and plant materials. Experiments have shown that the beads were subjected to adsorption of anionic dyes. These combinations have proved a better adsorbent for the removal of dyes from the water environment.

References

1. Mashkoor F, Nasar A (2020) Magsorbents: potential candidates in wastewater treatment technology—a review on the removal of methylene blue dye. *J Magn Magn Mater* 500:166408
2. Gong R, Zhu S, Zhang D, Chen J, Ni S, Guan R (2008) Adsorption behavior of cationic dyes on citric acid esterifying wheat straw: kinetic and thermodynamic profile. *Desalination* 230:220–228
3. Diqarternasi Y (2009) Removal of basic blue 3 and reactive orange 16 by adsorption onto quaternized sugar cane bagasse. *Malays J Anal Sci* 13(2):185–193
4. Banerjee S, Chattopadhyaya MC (2017) Adsorption characteristics for the removal of a toxic dye, tartrazine from aqueous solutions by a low cost agricultural by-product. *Arab J Chem* 10:S1629–S1638
5. Carmen Z, Daniela S (2012) Textile organic dyes-characteristics, polluting effects and separation/elimination procedures from industrial effluents—a critical overview. *IntechOpen*, pp. 55–86
6. Vijayaraghavan K, Yun YS (2008) Bacterial biosorbents and biosorption. *Biotechnol Adv* 26(3):266–291
7. Chequer FD, De Oliveira GR, Ferraz EA, Cardoso JC, Zanoni MB, de Oliveira DP (2013) Textile dyes: dyeing process and environmental impact. *Eco-Friendly Text Dyeing Finish* 6(6):151–176
8. Roy U, Manna S, Sengupta S, Das P, Datta S, Mukhopadhyay A, Bhowal A (2018) Dye removal using microbial biosorbents. *Green adsorbents for pollutant removal*. Springer, Cham, pp 253–280
9. Suksaroj C, Heran M, Allegre C, Persin F (2005) Treatment of textile plant effluent by nanofiltration and/or reverse osmosis for water reuse. *Desalination* 178(1–3):333–341
10. Kin C, Heran M, Allegre C, Persin F (2005) Treatment of textile plant effluent by nanofiltration and/or reverse osmosis for water reuse. *Desalination* 178(1–3):333–341
11. Kalyani DC, Patil PS, Jadhav JP, Govindwar SP (2008) Biodegradation of reactive textile dye Red BLI by an isolated bacterium *Pseudomonas* sp. SUK1. *Biores Technol* 99(11):4635–4641
12. Tony BD, Goyal D, Khanna S (2009) Decolorization of textile azo dyes by aerobic bacterial consortium. *Int Biodeterior Biodegradation* 63(4):462–469
13. Sudarjanto G, Keller-Lehmann B, Keller J (2006) Optimization of integrated chemical–biological degradation of a reactive azo dye using response surface methodology. *J Hazard Mater* 138(1):160–168
14. Zhu MX, Lee L, Wang HH, Wang Z (2007) Removal of an anionic dye by adsorption/precipitation processes using alkaline white mud. *J Hazard Mater* 149(3):735–741
15. Abbasi M, Asl NR (2008) Sonochemical degradation of Basic Blue 41 dye assisted by nanoTiO₂ and H₂O₂. *J Hazard Mater* 153(3):942–947
16. Ammar S, Abdelhedi R, Flox C, Arias C, Brillas E (2006) Electrochemical degradation of the dye indigo carmine at boron-doped diamond anode for wastewaters remediation. *Environ Chem Lett* 4(4):229–233
17. Fan L, Zhou Y, Yang W, Chen G, Yang F (2008) Electrochemical degradation of aqueous solution of Amaranth azo dye on ACF under potentiostatic model. *Dyes Pigment* 76(2):440–446
18. Srinivasan SV, Rema T, Chitra K, Balakameswari KS, Suthanthararajan R, Maheswari BU, Ravindranath E, Rajamani S (2009) Decolourisation of leather dye by ozonation. *Desalination* 235(1–3):88–92
19. Harrelkas F, Azizi A, Yaacoubi A, Benhammou A, Pons MN (2009) Treatment of textile dye effluents using coagulation–flocculation coupled with membrane processes or adsorption on powdered activated carbon. *Desalination* 235(1–3):330–339
20. Rashidi HR, Sulaiman MNM, Hashim NA, Hassan CRC, Ramli MR (2015) Synthetic reactive dye wastewater treatment by using nano-membrane filtration. *Desalin Water Treat* 55(1):86–95
21. Hassan MM, Carr CM (2018) A critical review on recent advancements of the removal of reactive dyes from dyehouse effluent by ion-exchange adsorbents. *Chemosphere* 209:201–219

22. Gupta VK, Suhas (2009) Application of low-cost adsorbents for dye removal—a review. *J Environ Manage* 90(8):2313–2342
23. Bonilla-Petriciolet A, Mendoza-Castillo DI, Reynel-Ávila HE (eds) (2017) Adsorption processes for water treatment and purification. Springer International Publishing, Berlin
24. Xu M, McKay G (2017) Removal of heavy metals, lead, cadmium, and zinc, using adsorption processes by cost-effective adsorbents. *Adsorption processes for water treatment and purification*. Springer, Cham, pp. 109–138
25. Sing KS (1985) Reporting physisorption data for gas/solid systems with special reference to the determination of surface area and porosity (Recommendations 1984). *Pure Appl Chem* 57(4):603–619
26. Knaebel KS (2011) Adsorbent selection. Accessed on 6(8)
27. Yang RT (2003) Adsorbents: fundamentals and applications. Wiley
28. Salleh MAM, Mahmoud DK, Karim WAWA, Idris A (2011) Cationic and anionic dye adsorption by agricultural solid wastes: a comprehensive review. *Desalination* 280(1–3):1–13
29. Bhatnagar A, Sillanpää M (2010) Utilization of agro-industrial and municipal waste materials as potential adsorbents for water treatment—a review. *Chem Eng J* 157:277–296
30. Sun D, Zhang X, Wu Y, Liu X (2010) Adsorption of anionic dyes from aqueous solution on fly ash. *J Hazard Mater* 181(1–3):335–342
31. Sun D, Zhang X, Wu Y, Liu T (2013) Kinetic mechanism of competitive adsorption of disperse dye and anionic dye on fly ash. *Int J Environ Sci Technol* 10(4):799–808
32. Hsu TC (2008) Adsorption of an acid dye onto coal fly ash. *Fuel* 87(13–14):3040–3045
33. Chandra S (1996) Waste materials used in concrete manufacturing. Elsevier
34. Ayres RU, Holmberg J, Andersson B (2001) Materials and the global environment: waste mining in the 21st century. *MRS Bull* 26(6):477–480
35. Tor A, Cengeloglu Y (2006) Removal of Congo red from aqueous solution by adsorption onto acid activated red mud. *J Hazard Mater* 138(2):409–415
36. Namasivayam C, Arasi DJSE (1997) Removal of congo red from wastewater by adsorption onto waste red mud. *Chemosphere* 34(2):401–417
37. Zhao D, Qiu Q, Wang Y, Huang M, Wu Y, Liu X, Jiang T (2016) Efficient removal of acid dye from aqueous solutions via adsorption using low-cost blast-furnace slag. *Desalin Water Treat* 57(58):28486–28495
38. Mysin BO, Wheeler K (2000) Alkali aluminosilicate-saturated aqueous fluids in the Earth's upper mantle. *Gochim Cosmochim Acta* 64(24):4243–4256
39. Kausar A, Iqbal M, Javed A, Aftab K, Bhatti HN, Nouren S (2018) Dyes adsorption using clay and modified clay: a review. *J Mol Liq* 256:395–407
40. Errais E, Duplay J, Darragi F, M'Rabet I, Aubert A, Huber F, Morvan G (2011) Efficient anionic dye adsorption on natural untreated clay: kinetic study and thermodynamic parameters. *Desalination* 275(1–3):74–81
41. Vimonses V, Jin B, Chow CW, Saint C (2009) Enhancing removal efficiency of anionic dye by combination and calcination of clay materials and calcium hydroxide. *J Hazard Mater* 171(1–3):941–947
42. Bhatt AS, Sakaria PL, Vasudevan M, Pawar RR, Sudheesh N, Bajaj HC, Mody HM (2012) Adsorption of an anionic dye from aqueous medium by organoclays: equilibrium modeling, kinetic and thermodynamic exploration. *RSC Adv* 2(23):8663–8671
43. Fu F, Gao Z, Gao L, Li D (2011) Effective adsorption of anionic dye, alizarin red S, from aqueous solutions on activated clay modified by iron oxide. *Ind Eng Chem Res* 50(16):9712–9717
44. Abidi N, Errais E, Duplay J, Berez A, Jrad A, Schäfer G, Ghazi M, Semhi K, Trabelsi-Ayadi M (2015) Treatment of dye-containing effluent by natural clay. *J Cleaner Prod* 86:432–440
45. Abidi N, Duplay J, Jada A, Baltenweck R, Errais E, Semhi K, Trabelsi-Ayadi M (2017) Toward the understanding of the treatment of textile industries' effluents by clay: adsorption of anionic dye on kaolinite. *Arab J Geosci* 10(16):1–14
46. Liu S, Ding Y, Li P, Diao K, Tan X, Lei F, Zhan Y, Li Q, Huang B, Huang Z (2014) Adsorption of the anionic dye Congo red from aqueous solution onto natural zeolites modified with N, N-dimethyl dehydrobiethylamine oxide. *Chem Eng J* 248:135–144

47. Omer OS, Hussein MA, Hussein BH, Mgaidi A (2018) Adsorption thermodynamics of cationic dyes (methylene blue and crystal violet) to a natural clay mineral from aqueous solution between 293.15 and 323.15 K. *Arab J Chem* 11(5):615–623
48. Tahir SS, Rauf N (2006) Removal of a cationic dye from aqueous solutions by adsorption onto bentonite clay. *Chemosphere* 63(11):1842–1848
49. Crini G (2006) Non-conventional low-cost adsorbents for dye removal: a review. *Biores Technol* 97(9):1061–1085
50. Won SW, Kim HJ, Choi SH, Chung BW, Kim KJ, Yun YS (2006) Performance, kinetics and equilibrium in biosorption of anionic dye Reactive Black 5 by the waste biomass of *Corynebacterium glutamicum* as a low-cost biosorbent. *Chem Eng J* 121(1):37–43
51. Farah JY, Elgendy N (2013) Performance, kinetics and equilibrium in biosorption of anionic dye Acid Red 14 by the waste biomass of *Saccharomyces cerevisiae* as a low-cost biosorbent. *Turk J Eng Environ Sci* 37(2):146–161
52. Sharma P, Kaur H, Sharma M, Sahore V (2011) A review on applicability of naturally available adsorbents for the removal of hazardous dyes from aqueous waste. *Environ Monit Assess* 183(1):151–195
53. Islam S, Bhuiyan MR, Islam MN (2017) Chitin and chitosan: structure, properties and applications in biomedical engineering. *J Polym Environ* 25(3):854–866
54. Yeul VS, Rayalu SS (2013) Unprecedented chitin and chitosan: a chemical overview. *J Polym Environ* 21(2):606–614
55. Gortari MC, Hours RA (2013) Biotechnological processes for chitin recovery out of crustacean waste: a mini-review. *Electron J Biotechnol* 16(3):1–18. Pontificia Universidad Católica de Valparaíso Valparaíso, Chile
56. Elsabee MZ, Morsi RE, Fathy M (2020) Chemical modifications of chitin and chitosan. *Encycl Mar Biotechnol* 2:885–963
57. Barikani M, Oliaei E, Seddiqi H, Honarkar H (2014) Preparation and application of chitin and its derivatives: a review. *Iran Polym J* 23(4):307–326
58. Annadurai G, Chellapandian M, Krishnan MRV (1999) Adsorption of reactive dye on chitin. *Environ Monit Assess* 59(1):111–119
59. Mckay GBHS, Blair HS, Gardner JR (1982) Adsorption of dyes on chitin. I. Equilibrium studies. *J Appl Polym Sci* 27(8):3043–3057
60. Akkaya G, Uzun I, Güzel F (2007) Kinetics of the adsorption of reactive dyes by chitin. *Dyes Pigm* 73(2):168–177
61. Filipkowska U, Klimiuk E, Grabowski S, Siedlecka E (2002) Adsorption of reactive dyes by modified chitin from aqueous solutions. *Pol J Environ Stud* 11(4):315–324
62. Prado AG, Torres JD, Faria EA, Dias SC (2004) Comparative adsorption studies of indigo carmine dye on chitin and chitosan. *J Colloid Interface Sci* 277(1):43–47
63. Tang H, Zhou W, Zhang L (2012) Adsorption isotherms and kinetics studies of malachite green on chitin hydrogels. *J Hazard Mater* 209:218–225
64. Annadurai G, Krishnan MRV (1997) Adsorption of acid dye from aqueous solution by chitin: equilibrium studies
65. Sashiwa H, Aiba SI (2004) Chemically modified chitin and chitosan as biomaterials. *Prog Polym Sci* 29(9):887–908
66. Dotto GL, Santos JMN, Rodrigues IL, Rosa R, Pavan FA, Lima EC (2015) Adsorption of methylene blue by ultrasonic surface modified chitin. *J Colloid Interface Sci* 446:133–140
67. Sellaoui L, Franco DSP, Dotto GL, Lima EC, Lamine AB (2017) Single and binary adsorption of cobalt and methylene blue on modified chitin: application of the Hill and exclusive extended Hill models. *J Mol Liq* 233:543–550
68. Ablouh EH, Jalal R, Rhazi M, Taourirte M (2020) Surface modification of α -chitin using an acidic treatment followed by ultrasonication: measurements of their sorption properties. *Int J Biol Macromol* 151:492–498
69. Huang CM, Chen LC, Yang HC, Li MH, Pan TC (2012) Preparation of acrylic acid-modified chitin improved by an experimental design and its application in absorbing toxic organic compounds. *J Hazard Mater* 241:190–196

70. Farinha I, Freitas F (2020) Chemically modified chitin, chitosan, and chitinous polymers as biomaterials. In: Thomas S, Pius A, Gopi S (eds) *Handbook of chitin and chitosan: Volume 3: chitin- and chitosan-based polymer materials for various applications*. Elsevier, pp 43–69
71. Chokradjaroen C, Theeramunkong S, Yui H, Saito N, Rujiravanit R (2018) Cytotoxicity against cancer cells of chitosan oligosaccharides prepared from chitosan powder degraded by electrical discharge plasma. *Carbohydr Polym* 201:20–30
72. Kyzas GZ, Bikiaris DN (2015) Recent modifications of chitosan for adsorption applications: a critical and systematic review. *Mar Drugs* 13(1):312–337
73. Vakili M, Rafatullah M, Salamatinia B, Abdullah AZ, Ibrahim MH, Tan KB, Gholami Z, Amouzgar P (2014) Application of chitosan and its derivatives as adsorbents for dye removal from water and wastewater: a review. *Carbohydr Polym* 113:115–130
74. Di Bello MP, Mergola L, Scorrano S, Del Sole R (2017) Towards a new strategy of a chitosan-based molecularly imprinted membrane for removal of 4-nitrophenol in real water samples. *Polym Int* 66(7):1055–1063
75. da Silva Alves DC, Healy B, Pinto LA, Cadaval TR, Breslin CB (2021) Recent developments in chitosan-based adsorbents for the removal of pollutants from aqueous environments. *Molecules* 26(3):594
76. Dutta J, Mala AA (2020) Removal of antibiotic from the water environment by the adsorption technologies: a review. *Water Sci Technol* 82(3):401–426
77. Nechita P (2017) Applications of chitosan in wastewater treatment. Biological activities and application of marine polysaccharides, p 209
78. Ahmad AL, Sumathi S, Hameed BH (2005) Adsorption of residue oil from palm oil mill effluent using powder and flake chitosan: equilibrium and kinetic studies. *Water Res* 39(12):2483–2494
79. Ahmad AL, Sumathi S, Hameed BH (2004) Chitosan: a natural biopolymer for the adsorption of residue oil from oily wastewater. *Adsorpt Sci Technol* 22(1):75–88
80. Mende M, Schwarz D, Steinbach C, Boldt R, Schwarz S (2016) Simultaneous adsorption of heavy metal ions and anions from aqueous solutions on chitosan—investigated by spectrophotometry and SEM-EDX analysis. *Colloids Surf, A* 510:275–282
81. Padilla-Rodríguez A, Hernández-Viezcás JA, Peralta-Videa JR, Gardea-Torresdey JL, Perales-Pérez O, Román-Velázquez FR (2015) Adsorption of arsenic (V) oxyanion from aqueous solutions by using protonated chitosan flakes. *Sep Sci Technol* 50(14):2099–2111
82. Rojas G, Silva J, Flores JA, Rodriguez A, Ly M, Maldonado H (2005) Adsorption of chromium onto cross-linked chitosan. *Sep Purif Technol* 44(1):31–36
83. Pitakpoolsil W, Hunsom M (2014) Treatment of biodiesel wastewater by adsorption with commercial chitosan flakes: parameter optimization and process kinetics. *J Environ Manage* 133:284–292
84. Barros FCDF, Vasconcellos LCG, Carvalho TV, Nascimento RFD (2014) Removal of petroleum spill in water by chitin and chitosan. *Orbital Electron J Chem* 6(1):70–74
85. Qu B, Luo Y (2020) Chitosan-based hydrogel beads: preparations, modifications and applications in food and agriculture sectors—a review. *Int J Biol Macromol* 152:437–448
86. Qamar SA, Ashiq M, Jahangeer M, Riasat A, Bilal M (2020) Chitosan-based hybrid materials as adsorbents for textile dyes—a review. *Case Stud Chem Environ Eng* 2:100021
87. Crini G, Badot PM (2008) Application of chitosan, a natural aminopolysaccharide, for dye removal from aqueous solutions by adsorption processes using batch studies: a review of recent literature. *Prog Polym Sci* 33(4):399–447
88. Kyzas GZ, Bikiaris DN, Mitropoulos AC (2017) Chitosan adsorbents for dye removal: a review. *Polym Int* 66(12):1800–1811
89. Chiou MS, Ho PY, Li HY (2004) Adsorption of anionic dyes in acid solutions using chemically cross-linked chitosan beads. *Dyes Pigment* 60(1):69–84
90. Ngah WW, Teong LC, Hanafiah MM (2011) Adsorption of dyes and heavy metal ions by chitosan composites: a review. *Carbohydr Polym* 83(4):1446–1456
91. Pereira FA, Sousa KS, Cavalcanti GR, França DB, Queiroga LN, Santos IM, Fonseca MG, Jaber M (2017) Green biosorbents based on chitosan-montmorillonite beads for anionic dye removal. *J Environ Chem Eng* 5(4):3309–3318

92. Wang L, Wang A (2007) Adsorption characteristics of Congo Red onto the chitosan/montmorillonite nanocomposite. *J Hazard Mater* 147(3):979–985
93. El-Defrawy MM, Kenawy IMM, Zaki E, El-tabey RM (2019) Adsorption of the anionic dye (Diamond Fast Brown KE) from textile wastewater onto chitosan/montmorillonite nanocomposites. *Egypt J Chem* 62(12):2183–2193
94. Nesic AR, Velickovic SJ, Antonovic DG (2012) Characterization of chitosan/montmorillonite membranes as adsorbents for Bezactiv Orange V-3R dye. *J Hazard Mater* 209:256–263
95. Zhang H, Ma J, Wang F, Chu Y, Yang L, Xia M (2020) Mechanism of carboxymethyl chitosan hybrid montmorillonite and adsorption of Pb(II) and Congo red by CMC-MMT organic-inorganic hybrid composite. *Int J Biol Macromol* 149:1161–1169
96. Joudi M, Nasserlah H, Hafdi H, Mouldar J, Hatimi B, Mhammedi ME, Bakasse M (2020) Synthesis of an efficient hydroxyapatite–chitosan–montmorillonite thin film for the adsorption of anionic and cationic dyes: adsorption isotherm, kinetic and thermodynamic study. *SN Appl Sci* 2:1–13
97. Umpuch C, Sakaew S (2013) Removal of methyl orange from aqueous solutions by adsorption using chitosan intercalated montmorillonite. *Songklanakarin J Sci Technol* 35(4)
98. Hu QH, Qiao SZ, Haghseresh F, Wilson MA, Lu GQ (2006) Adsorption study for removal of basic red dye using bentonite. *Ind Eng Chem Res* 45(2):733–738
99. Dotto GL, Rodrigues FK, Tanabe EH, Fröhlich R, Bertuol DA, Martins TR, Foletto EL (2016) Development of chitosan/bentonite hybrid composite to remove hazardous anionic and cationic dyes from colored effluents. *J Environ Chem Eng* 4(3):3230–3239
100. Huang R, Liu Q, Zhang L, Yang B (2015) Utilization of cross-linked chitosan/bentonite composite in the removal of methyl orange from aqueous solution. *Water Sci Technol* 71(2):174–182
101. Liu Q, Yang B, Zhang L, Huang R (2015) Adsorption of an anionic azo dye by cross-linked chitosan/bentonite composite. *Int J Biol Macromol* 72:1129–1135
102. Zhang L, Hu P, Wang J, Huang R (2016) Crosslinked quaternized chitosan/bentonite composite for the removal of Amino black 10B from aqueous solutions. *Int J Biol Macromol* 93:217–225
103. Zhang L, Liu Q, Hu P, Huang R (2016) Adsorptive removal of methyl orange using enhanced cross-linked chitosan/bentonite composite. *Desalin Water Treat* 57(36):17011–17022
104. Zia KM, Bhatti HN, Bhatti IA (2007) Methods for polyurethane and polyurethane composites, recycling and recovery: a review. *React Funct Polym* 67(8):675–692
105. Piotrowska-Kirschling A, Brzeska J (2020) The effect of chitosan on the chemical structure, morphology, and selected properties of polyurethane/chitosan composites. *Polymers* 12(5):1205
106. da Rosa Schio R, da Rosa BC, Gonçalves JO, Pinto LA, Mallmann ES, Dotto GL (2019) Synthesis of a bio-based polyurethane/chitosan composite foam using ricinoleic acid for the adsorption of Food Red 17 dye. *Int J Biol Macromol* 121:373–380
107. Lee HC, Jeong YG, Min BG, Lyoo WS, Lee SC (2009) Preparation and acid dye adsorption behavior of polyurethane/chitosan composite foams. *Fibers Polym* 10(5):636–642
108. Yang HC, Gong JL, Zeng GM, Zhang P, Zhang J, Liu HY, Huan SY (2017) Polyurethane foam membranes filled with humic acid-chitosan crosslinked gels for selective and simultaneous removal of dyes. *J Colloid Interface Sci* 505:67–78
109. Centenaro GSM, Facin BR, Valério A, de Souza AAU, da Silva A, de Oliveira JV, de Oliveira D (2017) Application of polyurethane foam chitosan-coated as a low-cost adsorbent in the effluent treatment. *J Water Process Eng* 20:201–206
110. Ziółkowska D, Shyichuk A, Karwasz I, Witkowska M (2009) Adsorption of cationic and anionic dyes onto commercial kaolin. *Adsorpt Sci Technol* 27(2):205–214
111. Biswas S, Rashid TU, Debnath T, Haque P, Rahman MM (2020) Application of chitosan-clay biocomposite beads for removal of heavy metal and dye from industrial effluent. *J Compos Sci* 4(1):16
112. Zhu HY, Jiang R, Xiao L (2010) Adsorption of an anionic azo dye by chitosan/kaolin/ γ -Fe₂O₃ composites. *Appl Clay Sci* 48(3):522–526

113. Dey SC, Moztahida M, Sarker M, Ashaduzzaman M, Shamsuddin SM (2019) pH-triggered interfacial interaction of kaolinite/chitosan nanocomposites with anionic azo dye. *J Compos Sci* 3(2):39
114. Jawad AH, Abdulhameed AS, Kashi E, Yaseen ZM, ALOthman ZA, Khan MR (2021) Cross-linked chitosan-glyoxal/kaolin clay composite: parametric optimization for color removal and COD reduction of remazol brilliant blue R dye. *J Polym Environ* 1–15
115. Nitayaphat W (2014) Utilization of chitosan/bamboo charcoal composite as reactive dye adsorbent. *Chiang Mai J Sci* 41(1):174–183
116. Auta M, Hameed BH (2013) Coalesced chitosan activated carbon composite for batch and fixed-bed adsorption of cationic and anionic dyes. *Colloids Surf, B* 105:199–206
117. Nitayaphat W (2017) Chitosan/coffee residue composite beads for removal of reactive dye. *Mater Today: Proc* 4(5):6274–6283
118. Khanday WA, Asif M, Hameed BH (2017) Cross-linked beads of activated oil palm ash zeolite/chitosan composite as a bio-adsorbent for the removal of methylene blue and acid blue 29 dyes. *Int J Biol Macromol* 95:895–902
119. Metin AU, Çiftçi H, Alver E (2013) Efficient removal of acidic dye using low-cost biocomposite beads. *Ind Eng Chem Res* 52(31):10569–10581
120. Abe FR, Machado AL, Soares AM, de Oliveira DP, Pestana JL (2019) Life history and behavior effects of synthetic and natural dyes on *Daphnia magna*. *Chemosphere* 236:124390
121. Abou El-Reash YG (2016) Magnetic chitosan modified with cysteine-glutaraldehyde as adsorbent for removal of heavy metals from water. *J Environ Chem Eng* 4(4):3835–3847
122. Adriano WS, Veredas V, Santana CC, Gonçalves LB (2005) Adsorption of amoxicillin on chitosan beads: kinetics, equilibrium and validation of finite bath models. *Biochem Eng J* 27(2):132–137
123. Ahmadzadeh S, Asadipour A, Yoosefian M, Dolatabadi M (2017) Improved electrocoagulation process using chitosan for efficient removal of cefazolin antibiotic from hospital wastewater through sweep flocculation and adsorption: kinetic and isotherm study. *Desalin Water Treat* 92:160–171
124. Akgül M (2014) Enhancement of the anionic dye adsorption capacity of clinoptilolite by Fe³⁺-grafting. *J Hazard Mater* 267:1–8
125. Akkaya G, Uzun İ, Güzel F (2009) Adsorption of some highly toxic dyestuffs from aqueous solution by chitin and its synthesized derivatives. *Desalination* 249(3):1115–1123
126. Aksu Z, Dönmez G (2003) A comparative study on the biosorption characteristics of some yeasts for Remazol Blue reactive dye. *Chemosphere* 50(8):1075–1083
127. Ali ME (2018) Synthesis and adsorption properties of chitosan-CDTA-GO nanocomposite for removal of hexavalent chromium from aqueous solutions. *Arab J Chem* 11(7):1107–1116
128. Alkan M, Demirbaş Ö, Doğan M (2007) Adsorption kinetics and thermodynamics of an anionic dye onto sepiolite. *Microporous Mesoporous Mater* 101(3):388–396
129. Alver E, Metin AU (2012) Anionic dye removal from aqueous solutions using modified zeolite: adsorption kinetics and isotherm studies. *Chem Eng J* 200:59–67
130. Arami M, Limaee NY, Mahmoodi NM, Tabrizi NS (2005) Removal of dyes from colored textile wastewater by orange peel adsorbent: equilibrium and kinetic studies. *J Colloid Interface Sci* 288(2):371–376
131. Ardejani FD, Badii K, Nimal NY, Shafaei SZ, Mirhabibi AR (2008) Adsorption of direct red 80 dyes from aqueous solution on to almond shells: effect of pH, initial concentration and shell type. *J Hazard Mater* 151:730–737
132. Ayari F, Manai G, Khelifi S, Trabelsi-Ayadi M (2019) Treatment of anionic dye aqueous solution using Ti, HDTMA and Al/Fe pillared bentonite. Essay to regenerate the adsorbent. *J Saudi Chem Soc* 23(3):294–306
133. Bahmani E, Koushkbaghi S, Darabi M, ZabihiSahebi A, Askari A, Irani M (2019) Fabrication of novel chitosan-g-PNVCL/ZIF-8 composite nanofibers for adsorption of Cr (VI), As (V) and phenol in a single and ternary systems. *Carbohydr Polym* 224:115148
134. Bayramoglu G, Yilmaz M (2018) Azo dye removal using free and immobilized fungal biomasses: isotherms, kinetics and thermodynamic studies. *Fibers Polym* 19(4):877–886

135. Bello K, Sarojini BK, Narayana B, Rao A, Byrappa K (2018) A study on adsorption behavior of newly synthesized banana pseudo-stem derived superabsorbent hydrogels for cationic and anionic dye removal from effluents. *Carbohydr Polym* 181:605–615
136. Bhatnagar A, Minocha AK (2006) Conventional and non-conventional adsorbents for removal of pollutants from water—a review
137. Binaeian E, Zadvarzi SB, Yuan D (2020) Anionic dye uptake via composite using chitosan-polyacrylamide hydrogel as matrix containing TiO₂ nanoparticles; comprehensive adsorption studies. *Int J Biol Macromol* 162:150–162
138. Cao JS, Lin JX, Fang F, Zhang MT, Hu ZR (2014) A new adsorbent by modifying walnut shell for the removal of anionic dye: kinetic and thermodynamic studies. *Biores Technol* 163:199–205
139. Cao YL, Pan ZH, Shi QX, Yu JY (2018) Modification of chitin with high adsorption capacity for methylene blue removal. *Int J Biol Macromol* 114:392–399
140. Chaari I, Fakhfakh E, Medhioub M, Jamoussi F (2019) Comparative study on adsorption of cationic and anionic dyes by smectite rich natural clays. *J Mol Struct* 1179:672–677
141. Chaari I, Moussi B, Jamoussi F (2015) Interactions of the dye, CI direct orange 34 with natural clay. *J Alloy Compd* 647:720–727
142. Chandra R, Bharagava RN, Yadav S, Mohan D (2009) Accumulation and distribution of toxic metals in wheat (*Triticum aestivum* L.) and Indian mustard (*Brassica campestris* L.) irrigated with distillery and tannery effluents. *J Hazard Mater* 162(2–3):1514–1521
143. Chang MY, Juang RS (2004) Adsorption of tannic acid, humic acid, and dyes from water using the composite of chitosan and activated clay. *J Colloid Interface Sci* 278(1):18–25
144. Chatterjee S, Chatterjee S, Chatterjee BP, Guha AK (2007) Adsorptive removal of congo red, a carcinogenic textile dye by chitosan hydrobeads: binding mechanism, equilibrium and kinetics. *Colloids Surf, A* 299(1–3):146–152
145. Chatterjee S, Chatterjee T, Woo SH (2011) Influence of the polyethyleneimine grafting on the adsorption capacity of chitosan beads for Reactive Black 5 from aqueous solutions. *Chem Eng J* 166(1):168–175
146. Chatterjee S, Kumar A, Basu S, Dutta S (2012) Application of response surface methodology for methylene blue dye removal from aqueous solution using low cost adsorbent. *Chem Eng J* 181:289–299
147. Chen Y, Hu J, Wang J (2012) Kinetics and thermodynamics of Cu(II) biosorption on to a novel magnetic chitosan composite bead. *Environ Technol* 33(20):2345–2351
148. Chiou MS, Li HY (2003) Adsorption behavior of reactive dye in aqueous solution on chemical cross-linked chitosan beads. *Chemosphere* 50(8):1095–1105
149. Cho DW, Jeon BH, Chon CM, Schwartz FW, Jeong Y, Song H (2015) Magnetic chitosan composite for adsorption of cationic and anionic dyes in aqueous solution. *J Ind Eng Chem* 28:60–66
150. Chung KT (2016) Azo dyes and human health: a review. *J Environ Sci Health C* 34(4):233–261
151. Çınar S, Kaynar ÜH, Aydemir T, Kaynar SÇ, Ayvacıklı M (2017) An efficient removal of RB5 from aqueous solution by adsorption onto nano-ZnO/Chitosan composite beads. *Int J Biol Macromol* 96:459–465
152. Consolin Filho N, Venancio EC, Barriquello MF, Hechenleitner AAW, Pineda EAG (2007) Methylene blue adsorption onto modified lignin from sugar cane bagasse. *Eclética Química* 32(4):63–70
153. Couillard D (1994) The use of peat in wastewater treatment. *Water Res* 28(6):1261–1274
154. Dehaghi SM, Rahmanifar B, Moradi AM, Azar PA (2014) Removal of permethrin pesticide from water by chitosan–zinc oxide nanoparticles composite as an adsorbent. *J Saudi Chem Soc* 18(4):348–355
155. Dolphen R, Sakkayawong N, Thiravetyan P, Nakbanpote W (2007) Adsorption of Reactive Red 141 from wastewater onto modified chitin. *J Hazard Mater* 145(1–2):250–255
156. Doltabadi M, Alidadi H, Davoudi M (2016) Comparative study of cationic and anionic dye removal from aqueous solutions using sawdust-based adsorbent. *Environ Prog Sustain Energy* 35(4):1078–1090

157. Dong W, Lu Y, Wang W, Zong L, Zhu Y, Kang Y, Wang A (2019) A new route to fabricate high-efficient porous silicate adsorbents by simultaneous inorganic-organic functionalization of low-grade palygorskite clay for removal of Congo red. *Microporous Mesoporous Mater* 277:267–276
158. El Harmoudi H, El Gaini L, Daoudi E, Rhazi M, Boughaleb Y, El Mhammedi MA, Migalska-Zalas A, Bakasse M (2014) Removal of 2, 4-D from aqueous solutions by adsorption processes using two biopolymers: chitin and chitosan and their optical properties. *Opt Mater* 36(9):1471–1477
159. Errais E, Duplay J, Elhabiri M, Khodja M, Ocampo R, Baltenweck-Guyot R, Darragi F (2012) Anionic RR120 dye adsorption onto raw clay: surface properties and adsorption mechanism. *Colloids Surf, A* 403:69–78
160. Ferrero F (2007) Dye removal by low cost adsorbents: hazelnut shells in comparison with wood sawdust. *J Hazard Mater* 142:144–152
161. Franco DSP, Piccin JS, Lima EC, Dotto GL (2015) Interpretations about methylene blue adsorption by surface modified chitin using the statistical physics treatment. *Adsorption* 21(8):557–564
162. Fu Y, Viraraghavan T (2000) Removal of a dye from an aqueous solution by the fungus *Aspergillus Niger*. *Water Qual Res J* 35(1):95–112
163. Gita S, Hussan A, Choudhury TG (2017) Impact of textile dyes waste on aquatic environments and its treatment. *Environ Ecol* 35(3C):2349–2353
164. Gita S, Shukla SP, Saharan N, Prakash C, Deshmukhe G (2019) Toxic effects of selected textile dyes on elemental composition, photosynthetic pigments, protein content and growth of a freshwater chlorophycean alga *Chlorella vulgaris*. *Bull Environ Contam Toxicol* 102(6):795–801
165. Gong R, Ding Y, Li M, Yang C, Liu H, Sun Y (2005) Utilization of powdered peanut hull as biosorbent for removal of anionic dyes from aqueous solution. *Dyes Pigm* 64(3):187–192
166. Guo DM, An QD, Xiao ZY, Zhai SR, Yang DJ (2018) Efficient removal of Pb(II), Cr(VI) and organic dyes by polydopamine modified chitosan aerogels. *Carbohydr Polym* 202:306–314
167. Gupta VK, Fakhri A, Agarwal S, Azad M (2017) Synthesis and characterization of Ag₂S decorated chitosan nanocomposites and chitosan nanofibers for removal of lincosamides antibiotic. *Int J Biol Macromol* 103:1–7
168. Hamad MT, Saied MS (2021) Kinetic studies of Congo red dye adsorption by immobilized *Aspergillus Niger* on alginate. *Appl Water Sci* 11(2):1–12
169. Hasan M, Ahmad AL, Hameed BH (2008) Adsorption of reactive dye onto cross-linked chitosan/oil palm ash composite beads. *Chem Eng J* 136(2–3):164–172
170. Hasyimah NAR, Furusawa G, Amirul AA (2020) Biosorption of a dye and heavy metals using dead cells of filamentous bacterium, *Aureispira* sp. CCB-QB1. *Int J Environ Sci Technol* 1–10
171. Hernández-Zamora M, Martínez-Jerónimo F (2019) Exposure to the azo dye Direct blue 15 produces toxic effects on microalgae, cladocerans, and zebrafish embryos. *Ecotoxicology* 28(8):890–902
172. Ho YS, McKay G (1998) Kinetic models for the sorption of dye from aqueous solution by wood. *Process Saf Environ Prot* 76:183–191
173. Hou F, Wang D, Ma X, Fan L, Ding T, Ye X, Liu D (2021) Enhanced adsorption of Congo red using chitin suspension after sonoenzymolysis. *Ultrason Sonochem* 70:105327
174. Hu TL (1992) Sorption of reactive dyes by *Aeromonas* biomass. *Water Sci Technol* 26(1–2):357–366
175. Hu TL (1996) Removal of reactive dyes from aqueous solution by different bacterial genera. *Water Sci Technol* 34(10):89–95
176. Huang Y, Wu H, Shao T, Zhao X, Peng H, Gong Y, Wan H (2018) Enhanced copper adsorption by DTPA-chitosan/alginate composite beads: mechanism and application in simulated electroplating wastewater. *Chem Eng J* 339:322–333
177. Hunger K (2003) Dyes, general survey. *Industrial dyes: chemistry, properties, applications*. Wiley Subscription Services, Inc., A Wiley Company, Frankfurt, pp 1–10

178. Imran M, Crowley DE, Khalid A, Hussain S, Mumtaz MW, Arshad M (2015) Microbial biotechnology for decolorization of textile wastewaters. *Rev Environ Sci Bio/Technol* 14(1):73–92
179. Jagruti B (2015) Evaluation of azo dye toxicity using some haematological and histopathological alterations in fish *Catla catla*. *Int J Biol Biomol Agric Food Biotechnol Eng* 9(5):415–418
180. Jain SN, Tamboli SR, Sutar DS, Jadhav SR, Marathe JV, Shaikh AA, Prajapati AA (2020) Batch and continuous studies for adsorption of anionic dye onto waste tea residue: kinetic, equilibrium, breakthrough and reusability studies. *J Clean Prod* 252:119778
181. Jaiswal M, Chauhan D, Sankaramkrishnan N (2012) Copper chitosan nanocomposite: synthesis, characterization, and application in removal of organophosphorous pesticide from agricultural runoff. *Environ Sci Pollut Res* 19(6):2055–2062
182. Jamali M, Akbari A (2021) Facile fabrication of magnetic chitosan hydrogel beads and modified by interfacial polymerization method and study of adsorption of cationic/anionic dyes from aqueous solution. *J Environ Chem Eng* 9(3):105175
183. Jawad AH, Abdulhameed AS, Reghioua A, Yaseen ZM (2020) Zwitterion composite chitosan-epichlorohydrin/zeolite for adsorption of methylene blue and reactive red 120 dyes. *Int J Biol Macromol* 163:756–765
184. Jintakosol T, Nitayaphat W (2016) Adsorption of silver (I) from aqueous solution using chitosan/montmorillonite composite beads. *Mater Res* 19(5):1114–1121
185. Juang RS, Tseng RL, Wu FC, Lee SH (1997) Adsorption behavior of reactive dyes from aqueous solutions on chitosan. *J Chem Technol Biotechnol Int Res Process, Environ Clean Technol* 70(4):391–399
186. Kabbout R, Taha S (2014) Biodecolorization of textile dye effluent by biosorption on fungal biomass materials. *Phys Procedia* 55:437–444
187. Khan S, Malik A (2018) Toxicity evaluation of textile effluents and role of native soil bacterium in biodegradation of a textile dye. *Environ Sci Pollut Res* 25(5):4446–4458
188. Kılıç NK, Nielsen JL, Yüce M, Dönmez G (2007) Characterization of a simple bacterial consortium for effective treatment of wastewaters with reactive dyes and Cr(VI). *Chemosphere* 67(4):826–831
189. Kim TH, Park C, Kim S (2005) Water recycling from desalination and purification process of reactive dye manufacturing industry by combined membrane filtration. *J Clean Prod* 13(8):779–786
190. Kittinaovarat S, Kansomwan P, Jiratumnukul N (2010) Chitosan/modified montmorillonite beads and adsorption Reactive Red 120. *Appl Clay Sci* 48(1–2):87–91
191. Klimiuk E, Filipkowska U, Wojtasz-Pajak A (2003) The effect of pH and chitin preparation on adsorption of reactive dyes. *Polish J Environ Stud* 12(5)
192. Kumar KV, Kumaran A (2005) Removal of methylene blue by mango seed kernel powder. *Biochem Eng J* 27(1):83–93
193. Kyzas GZ, Lazaridis NK (2009) Reactive and basic dyes removal by sorption onto chitosan derivatives. *J Colloid Interface Sci* 331(1):32–39
194. Le AT, Pung SY, Chiam SL, Josoh NBN, Koay TY, Lee JS, Mustar NB (2020) Photocatalytic performance of TiO₂ particles in degradation of various organic dyes under visible and UV light irradiation. In: AIP conference proceedings, vol 2267(1). AIP Publishing LLC, p 020017
195. Le TTN, Le VT, Dao MU, Nguyen QV, Vu TT, Nguyen MH, Tran DL, Le HS (2019) Preparation of magnetic graphene oxide/chitosan composite beads for effective removal of heavy metals and dyes from aqueous solutions. *Chem Eng Commun* 206(10):1337–1352
196. Li J, Jiang B, Liu Y, Qiu C, Hu J, Qian G, Guo W, Ngo HH (2017) Preparation and adsorption properties of magnetic chitosan composite adsorbent for Cu²⁺ removal. *J Cleaner Prod* 158:51–58
197. Li Y, Gao H, Wang C, Zhang X, Zhou H (2018) One-step fabrication of chitosan-Fe(OH)₃ beads for efficient adsorption of anionic dyes. *Int J Biol Macromol* 117:30–41
198. Li Z, Dotto GL, Bajahzar A, Sellaoui L, Belmabrouk H, Lamine AB, Bonilla-Petriciolet A (2019) Adsorption of indium(III) from aqueous solution on raw, ultrasound-and supercritical-modified chitin: experimental and theoretical analysis. *Chem Eng J* 373:1247–1253

199. Li Z, Liu Y, Zou S, Lu C, Bai H, Mu H, Duan J (2020) Removal and adsorption mechanism of tetracycline and cefotaxime contaminants in water by NiFe₂O₄-COF-chitosan-terephthalaldehyde nanocomposites film. *Chem Eng J* 382:123008
200. Li Z, Wang X, Zhang X, Yang Y, Duan J (2021) A high-efficiency and plane-enhanced chitosan film for cefotaxime adsorption compared with chitosan particles in water. *Chem Eng J* 413:127494
201. Lin Q, Wang K, Gao M, Bai Y, Chen L, Ma H (2017) Effectively removal of cationic and anionic dyes by pH-sensitive amphoteric adsorbent derived from agricultural waste-wheat straw. *J Taiwan Inst Chem Eng* 76:65–72
202. Liu J, Chen Y, Han T, Cheng M, Zhang W, Long J, Fu X (2019) A biomimetic SiO₂@chitosan composite as highly-efficient adsorbent for removing heavy metal ions in drinking water. *Chemosphere* 214:738–742
203. Ma J, Cui B, Dai J, Li D (2011) Mechanism of adsorption of anionic dye from aqueous solutions onto organobentonite. *J Hazard Mater* 186(2–3):1758–1765
204. Mala AA, Dutta J (2021) Studies on batch adsorption of gemifloxacin using hybrid beads from biomass. *Indian J Ecol* 48(1):116–122
205. Mani S, Bharagava RN (2016) Exposure to crystal violet, its toxic, genotoxic and carcinogenic effects on environment and its degradation and detoxification for environmental safety. *Rev Environ Contam Toxicol* 237:71–104
206. Marrakchi F, Hameed BH, Hummadi EH (2020) Mesoporous biohybrid epichlorohydrin crosslinked chitosan/carbon–clay adsorbent for effective cationic and anionic dyes adsorption. *Int J Biol Macromol* 163:1079–1086
207. Maurya NS, Mittal AK, Cornel P, Rother E (2006) Biosorption of dyes using dead macro fungi: effect of dye structure, ionic strength and pH. *Biores Technol* 97(3):512–521
208. Moawad H, El-Rahim WMA, Khalafallah M (2003) Evaluation of biotoxicity of textile dyes using two bioassays. *J Basic Microbiol Int J Biochem Physiol Genet Morphol Ecol Microorganisms* 43(3):218–229
209. Mokhtar A, Abdelkrim S, Djelad A, Sardi A, Boukoussa B, Sassi M, Bengueddach A (2020) Adsorption behavior of cationic and anionic dyes on magadiite-chitosan composite beads. *Carbohydr Polym* 229:115399
210. Morais LC, Freitas OM, Goncalves EP, Vasconcelos LT, Beca CG (1999) Reactive dyes removal from wastewaters by adsorption on eucalyptus bark: variables that define the process. *Water Res* 33(4):979–988
211. Namasivayam C, Kavitha D (2002) Removal of Congo red from water by adsorption on to activated carbon prepared from coir pith, an agricultural solid waste. *Dyes Pigm* 54:47–58
212. Nejjib A, Joelle D, Fadhila A, Sophie G, Malika TA (2015) Adsorption of anionic dye on natural and organophilic clays: effect of textile dyeing additives. *Desalin Water Treat* 54(6):1754–1769
213. Newman MC (2009) *Fundamentals of ecotoxicology*. CRC Press
214. Nirmalarani J, Janardhanan K (1988) Effect of south India Viscose factory effluent on seed germination seedling growth and chloroplast pigments content in five varieties of Maize (*Zea mays* L). *Madras Agric J* 75:41–47
215. Nitayaphat W, Jintakosol T (2015) Removal of silver (I) from aqueous solutions by chitosan/bamboo charcoal composite beads. *J Clean Prod* 87:850–855
216. Obeid L, Bée A, Talbot D, Jaafar SB, Dupuis V, Abramson S, Cabuil V, Welschbillig M (2013) Chitosan/maghemite composite: a magsorbent for the adsorption of methyl orange. *J Colloid Interface Sci* 410:52–58
217. Ofomaja AE, Ho YS (2007) Equilibrium sorption of anionic dye from aqueous solution by palm kernel fibre as sorbent. *Dyes Pigm* 74(1):60–66
218. Ong ST, Seou CK (2014) Removal of Reactive Black 5 from aqueous solution using chitosan beads: optimization by Plackett-Burman design and response surface analysis. *Desalin Water Treat* 52(40–42):7673–7684
219. Ouasif H, Yousfi S, Bouamrani ML, El Kouali M, Benmokhtar S, Talbi M (2013) Removal of a cationic dye from wastewater by adsorption onto natural adsorbents. *J Mater Environ Sci* 4(1):1–10

220. Oussalah A, Boukerroui A, Aichour A, Djellouli B (2019) Cationic and anionic dyes removal by low-cost hybrid alginate/natural bentonite composite beads: adsorption and reusability studies. *Int J Biol Macromol* 124:854–862
221. Ouyang A, Gong Q, Liang J (2015) Carbon nanotube–chitosan composite beads with radially aligned channels and nanotube-exposed walls for bilirubin adsorption. *Adv Eng Mater* 17(4):460–466
222. Peng Q, Liu M, Zheng J, Zhou C (2015) Adsorption of dyes in aqueous solutions by chitosan–halloysite nanotubes composite hydrogel beads. *Microporous Mesoporous Mater* 201:190–201
223. Periyaraman PM, Karan S, Ponnusamy SK, Vaidyanathan V, Vasanthakumar S, Dhanasekaran A, Subramanian S (2019) Adsorption of an anionic dye onto native and chemically modified agricultural waste. *Environ Eng Manage J (EEMJ)* 18(1)
224. Polman K, Breckenridge CR (1996) Biomass-mediated binding and recovery of textile dyes from waste effluents. *Text Chem Colorist* 28(4)
225. Ponnusami V, Vikram S, Srivastava SN (2008) Guava (*Psidium guajava*) leaf powder: novel adsorbent for removal of methylene blue from aqueous solutions. *J Hazard Mater* 152(1):276–286
226. Popuri SR, Vijaya Y, Boddu VM, Abburi K (2009) Adsorptive removal of copper and nickel ions from water using chitosan coated PVC beads. *Biores Technol* 100(1):194–199
227. Radoor S, Karayil J, Parameswaranpillai J, Siengchin S (2020) Adsorption study of anionic dye, Eriochrome black T from aqueous medium using polyvinyl alcohol/starch/ZSM-5 zeolite membrane. *J Polym Environ* 28(10):2631–2643
228. Raghuvanshi SP, Singh R, Kaushik CP, Raghav A (2004) Kinetics study of methylene blue dye bioadsorption on baggase. *Appl Ecol Environ Res* 2(2):35–43
229. Rangunathan I, Palanikumar L, Panneerselvam N (2007) Cytogenetic studies on the peripheral lymphocytes of occupationally exposed textile dye industry workers. *Med Biol* 14:43–46
230. Reddy MS, Sivaramakrishna L, Reddy AV (2012) The use of an agricultural waste material, Jujuba seeds for the removal of anionic dye (Congo red) from aqueous medium. *J Hazard Mater* 203:118–127
231. Rusmin R, Sarkar B, Liu Y, McClure S, Naidu R (2015) Structural evolution of chitosan–palygorskite composites and removal of aqueous lead by composite beads. *Appl Surf Sci* 353:363–375
232. Russo ME, Di Natale F, Prigione V, Tigini V, Marzocchella A, Varese GC (2010) Adsorption of acid dyes on fungal biomass: equilibrium and kinetics characterization. *Chem Eng J* 162(2):537–545
233. Saheed IO, Da OW, Suah FBM (2020) Chitosan modifications for adsorption of pollutants—a review. *J Hazard Mater*
234. Sandhya S (2010) Biodegradation of azo dyes under anaerobic condition: role of azoreductase. *Biodegradation of azo dyes*, pp 39–57
235. Saranraj P, Sumathi V, Reetha D, Stella D (2010) Decolourization and degradation of direct azo dyes and biodegradation of textile dye effluent by using bacteria isolated from textile dye effluent. *J. Ecobiotechnol* 2(7):7–11
236. Sarim KM, Kukreja K, Shah I, Choudhary CK (2019) Biosorption of direct textile dye Congo red by *Bacillus subtilis* HAU-KK01. *Bioremediat J* 23(3):185–195
237. Sarvajith M, Reddy GKK, Nancharaiah YV (2018) Textile dye biodecolourization and ammonium removal over nitrite in aerobic granular sludge sequencing batch reactors. *J Hazard Mater* 342:536–543
238. Selvaraj D, Leena R, Kamal DC (2015) Toxicological and histopathological impacts of textile dyeing industry effluent on a selected teleost fish *Poecilia reticulata*. *Asian J Pharmacol Toxicol* 3(10):26–30
239. Setiadi T, Andriani Y, Erlania M (2006) Treatment of textile wastewater by a combination of anaerobic and aerobic processes: a denim processing plant case. *Southeast Asian Water Environ* 1

240. Shankar A, Kongot M, Saini VK, Kumar A (2020) Removal of pentachlorophenol pesticide from aqueous solutions using modified chitosan. *Arab J Chem* 13(1):1821–1830
241. Shawkly HA, El-Aassar AHM, Abo-Zeid DE (2012) Chitosan/carbon nanotube composite beads: preparation, characterization, and cost evaluation for mercury removal from wastewater of some industrial cities in Egypt. *J Appl Polym Sci* 125(S1):E93–E101
242. Sikder MT, Tanaka S, Saito T, Kurasaki M (2014) Application of zerovalent iron impregnated chitosan-caboxymethyl- β -cyclodextrin composite beads as arsenic sorbent. *J Environ Chem Eng* 2(1):370–376
243. Silva MM, Oliveira MM, Avelino MC, Fonseca MG, Almeida RK, Silva Filho EC (2012) Adsorption of an industrial anionic dye by modified-KSF-montmorillonite: evaluation of the kinetic, thermodynamic and equilibrium data. *Chem Eng J* 203:259–268
244. Srivastava R, Rupainwar DC (2011) A comparative evaluation for adsorption of dye on neem bark and mango bark powder, Indian. *J Chem Technol* 18:67–75
245. Stavrinou A, Aggelopoulos CA, Tsakiroglou CD (2018) Exploring the adsorption mechanisms of cationic and anionic dyes onto agricultural waste peels of banana, cucumber and potato: adsorption kinetics and equilibrium isotherms as a tool. *J Environ Chem Eng* 6(6):6958–6970
246. Sugashini S, Sheriffa Begum KM (2013) Column adsorption studies for the removal of Cr(VI) ions by ethylamine modified chitosan carbonized rice husk composite beads with modelling and optimization. *J Chem*
247. Tay SY, Wong VL, Lim SS, Teo ILR (2020) Adsorption equilibrium, kinetics and thermodynamics studies of anionic methyl orange dye adsorption using chitosan-calcium chloride gel beads. *Chem Eng Commun* 1–19
248. Tirtom VN, Dinçer A, Becerik S, Aydemir T, Çelik A (2012) Comparative adsorption of Ni(II) and Cd(II) ions on epichlorohydrin crosslinked chitosan–clay composite beads in aqueous solution. *Chem Eng J* 197:379–386
249. Tran HV, Dai Tran L, Nguyen TN (2010) Preparation of chitosan/magnetite composite beads and their application for removal of Pb(II) and Ni(II) from aqueous solution. *Mater Sci Eng, C* 30(2):304–310
250. Vega-Negron AL, Alamo-Nole L, Perales-Perez O, Gonzalez-Mederos AM, Jusino-Olivencia C, Roman-Velazquez FR (2018) Simultaneous adsorption of cationic and anionic dyes by chitosan/cellulose beads for wastewaters treatment. *Int J Environ Res* 12(1):59–65
251. Wang N, Xiao W, Niu B, Duan W, Zhou L, Zheng Y (2019) Highly efficient adsorption of fluoroquinolone antibiotics using chitosan derived granular hydrogel with 3D structure. *J Mol Liq* 281:307–314
252. Wang XL, Guo DM, An QD, Xiao ZY, Zhai SR (2019) High-efficacy adsorption of Cr(VI) and anionic dyes onto β -cyclodextrin/chitosan/hexamethylenetetramine aerogel beads with task-specific, integrated components. *Int J Biol Macromol* 128:268–278
253. Wang Y, Yu J (1998) Adsorption and degradation of synthetic dyes on the mycelium of *Trametes versicolor*. *Water Sci Technol* 38(4–5):233–238
254. Wollin KM, Gorlitz BD (2004) Comparison of genotoxicity of textile dyestuffs in *Salmonella* mutagenicity assay, in vitro micronucleus assay, and single cell gel/comet assay. *J Environ Pathol Toxicol Oncol* 23(4)
255. Wong SY, Tan YP, Abdullah AH, Ong ST (2009a) Removal of Basic Blue 3 and Reactive Orange 16 by adsorption onto quarterized sugar cane bagasse. *Malays J Anal Sci* 13:185–193
256. Wong SY, Tan YP, Abdullah AH, Ong ST (2009b) The removal of basic and reactive dyes using quarterised sugar cane bagasse. *J Phys Sci* 20(1):59–74
257. Wong S, Abd Ghafar N, Ngadi N, Razmi FA, Inuwa IM, Mat R, Amin NAS (2020) Effective removal of anionic textile dyes using adsorbent synthesized from coffee waste. *Sci Rep* 10(1):1–13
258. Wu FC, Tseng RL, Juang RS (2000) Comparative adsorption of metal and dye on flake-and bead-types of chitosans prepared from fishery wastes. *J Hazard Mater* 73(1):63–75
259. Yazidi A, Sellaoui L, Badawi M, Dotto GL, Bonilla-Petriciolet A, Lamine AB, Erto A (2020) Ternary adsorption of cobalt, nickel and methylene blue on a modified chitin: phenomenological modeling and physical interpretation of the adsorption mechanism. *Int J Biol Macromol* 158:595–604

260. Yoshizuka K, Lou Z, Inoue K (2000) Silver-complexed chitosan microparticles for pesticide removal. *React Funct Polym* 44(1):47–54
261. Yu X, Wei C, Ke L, Hu Y, Xie X, Wu H (2010) Development of organovermiculite-based adsorbent for removing anionic dye from aqueous solution. *J Hazard Mater* 180(1–3):499–507
262. Zeroual Y, Kim BS, Kim CS, Blaghen M, Lee KM (2006) A comparative study on biosorption characteristics of certain fungi for bromophenol blue dye. *Appl Biochem Biotechnol* 134(1):51–60
263. Zhang L, Tang S, He F, Liu Y, Mao W, Guan Y (2019) Highly efficient and selective capture of heavy metals by poly (acrylic acid) grafted chitosan and biochar composite for wastewater treatment. *Chem Eng J* 378:122215
264. Zhang L, Xia W, Teng B, Liu X, Zhang W (2013) Zirconium cross-linked chitosan composite: preparation, characterization and application in adsorption of Cr(VI). *Chem Eng J* 229:1–8
265. Zhang W, Wang H, Hu X, Feng H, Xiong W, Guo W, Zhou J, Mosa A, Peng Y (2019) Multi-cavity triethylenetetramine-chitosan/alginate composite beads for enhanced Cr(VI) removal. *J Cleaner Prod* 231:733–745
266. Zhao S, Zhou F, Li L, Cao M, Zuo D, Liu H (2012) Removal of anionic dyes from aqueous solutions by adsorption of chitosan-based semi-IPN hydrogel composites. *Compos B Eng* 43(3):1570–1578
267. Zhao X, Wang X, Lou T (2021) Preparation of fibrous chitosan/sodium alginate composite foams for the adsorption of cationic and anionic dyes. *J Hazard Mater* 403:124054

Application of Lignin-Based Biomaterials in Textile Wastewater



Md. Din Islam, M. K. Mohammad Ziaul Hyder, Md. Masudur Rhaman, and Sajjad Husain Mir

1 Introduction

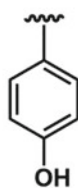
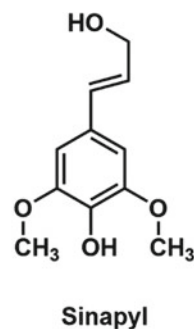
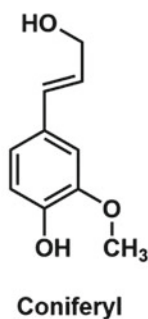
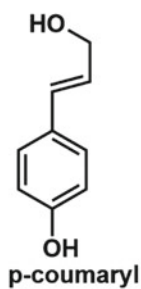
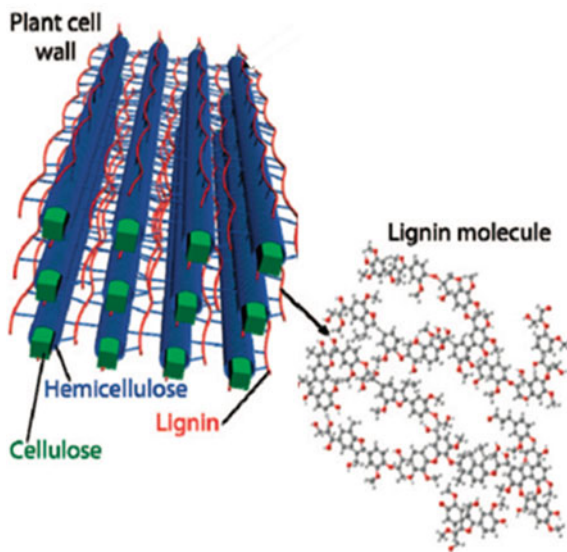
Lignin is the second most naturally abundant biopolymer after cellulose. It is treated as a non-commercialized waste product in paper, sugar, ethanol, and other bio-based industries. Globally, more than a hundred millions tons of lignin are produced in a year as a byproduct [13] where pulping process generates nearly fifty million tons [40]. Lignin contains higher amount of softwoods than hardwoods and grasses. The maximum quantity of lignin is found in leaning stems of conifers and compression wood on the lower side of leaning softwood stems. The largest concentration of lignin exists between middle lamella (adjacent cell walls) and the cell corners. Though the secondary wall contains only a lower amount of lignin concentration, the highest amount of lignin is found from the secondary wall due to the existence of the larger quantity of secondary wall in wood. Lignin is distributed in the cell wall along with cellulose and hemicelluloses [88]. In the cell walls, lignin occupies the area between hemicellulose and cellulose holding the lignocellulose matrix together (Fig. 1).

Lignin is a highly branched macromolecule yield with molecular masses between 1000 and 20,000 g mol^{-1} . Lignin is composed of three monolignol subunits known as coniferyl alcohol, para-coumaryl alcohol and sinapyl alcohol. The monolignols give three phenolic sub-structures known as syringyl (S), guaiacyl (G), and hydroxyphenyl (H) that bears hydroxyl, carboxyls, carbonyls and methoxy groups that acts as active sites for heavy metal ions adsorption [3, 73] (Fig. 2). Lignin is derived mainly from lignocellulosic biomass whose structure directly depends on the source and method

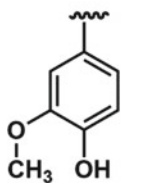
Md. D. Islam · M. K. Mohammad Ziaul Hyder (✉) · Md. Masudur Rhaman
Department of Chemistry, Chittagong University of Engineering & Technology, Chittogram,
Bangladesh
e-mail: ziaulhyder@cuet.ac.bd

S. H. Mir
School of Chemistry, Trinity College Dublin, Dublin 2, Ireland

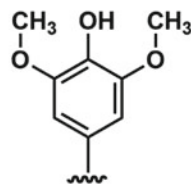
Fig. 1 Lignin distribution in cell wall. Reproduce with permission from [112]. Copyright@2010, American Chemical Society



p-hydroxyphenyl(H)



guaiacyl(G)



syringyl(S)

Fig. 2 Different lignin units

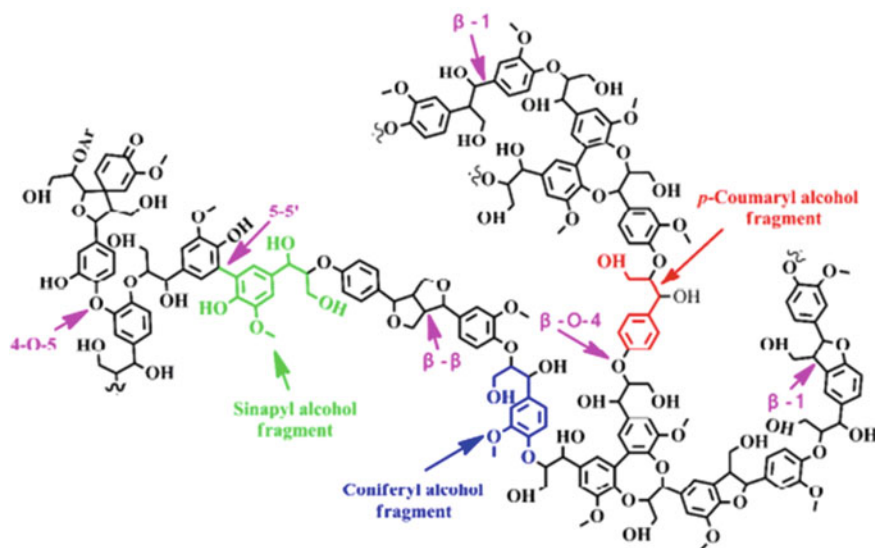


Fig. 3 Linkage in lignin structure. Reproduce with permission from [33]. Copyright©2018, American Chemical Society

of extraction. Lignin primarily consisted of guaiacyl units in softwoods which are connected with each other by ether bonds or carbon-carbon linkage. On the other hand, almost equal amounts of guaiacyl and syringyl units present in hardwoods. However, the grass lignin is composed of all three units.

There are common bondages among these units in a lignin structure, namely 5–5 biphenyl α -O-4' ether, β -5 phenyl coumaran, β -1' diphenyl, 4-O-5'diphenyl ether, and β - β' resinol. Figure 3 represents linkages between the lignin structures. The β -O-4 linkage represents almost half of the entire linkage in lignin structures. On the other hand, β - β' resinol, β -5 phenyl coumaran, β -1' diphenyl methane, α -O-4' ether, 4-O-5'diphenyl ether and 5-5 biphenyl account smaller portion of linkages in lignin [16, 90].

Pure lignin with three-dimensional polymer structures comprises different active groups such as aldehyde, phenol, methoxyl, carboxyl, hydroxyl groups. Many effective researches were carried out for efficient removal of dyes and heavy metals from wastewater with materials containing these functional groups [4]. The existence of these reactive functional groups in lignin influence the physico-chemical characteristics of lignin like functionality, reactivity and hydrophilicity. Lignin is an inexpensive and nontoxic as well as a biodegradable and biocompatible biomaterial and thus it can be applied for the decontamination of heavy metal and dyes from wastewater due to its origin and presence of various functional groups.

On the other hand, The effluents coming from various industries have to be treated to control environmental pollution which helps to build up a healthy environment

around us [15]. With the growth of human population, a significant number of industries are rising gradually such as textile industries, tanneries, fertilizers, paper, paint, electroplating, petroleum refining. These industries release their effluents into water or land that consist of high concentration of contaminants like heavy metals, toxic dyes, organic or inorganic ions, micropollutants, etc. [27, 50, 74]. This pollutant has high toxicity, carcinogenicity and non-degradability properties that are responsible for severe environmental concerns [27, 75].

The effluent coming from the textile industry contains contaminants like organic and inorganic dyes, heavy metals like chromium (Cr), lead (Pb), cadmium (Cd), mercury (Hg), copper (Cu). These pollutants in textile effluents have a negative effect on the environment and create serious health threats to aquatic life, animal and human beings [51]. It is reported that 60% of the consumption of the world's dye was used by the textile industries of which 10–15% of dye is released to the effluent. The growth of the textile industry is accompanied by the increase of wastewater containing synthetic dyes. The discharge of a huge amount of dye into water bodies causes severe environmental concerns [1, 100]. To save the environment from pollution, it is very significant to remove this toxic dye from the textile wastewater as much as possible before being released to the water bodies or landfills. Moreover, the heavy metals exist in textile effluent are toxic, carcinogenic and nonbiodegradable that causes a variety of diseases and disorders in living organism [5, 30, 44] and can create serious disorder in ecosystem including aquatic and terrestrial life [48, 89].

Techniques employed to treat the industrial effluent include biological processes, adsorption, coagulation, chemical oxidation processes and photocatalytic degradation, etc. [41, 54, 58]. The merits and demerits of these techniques are presented in Table 1.

Among these methods, adsorption technique has been shown to be a useful method due to its inexpensiveness, simple design and high adsorption capacity [47]. Nowadays, biomaterials generated from natural materials have gained much attention due to their low cost, simple preparation and high effectiveness for the removal of dyes and heavy metals [46, 66, 69, 84]. Especially lignin is an important constituent of renewable biomass which is the most abundant natural biopolymer after cellulose

Table 1 Techniques for wastewater treatment

Methods	Advantages	Disadvantages
Ion exchange	Wide applicability	Required regeneration or disposal
Oxidation	Rapid process	Cost effective and byproduct formation
Ozonation	Applicable in gaseous state	Short half-life
Coagulation	Economically feasible	High sludge production and large particle formation
Photochemical	No sludge production	Byproduct formation
Electrochemical process	Rapid process	Cost effective and byproduct formation
Biological process	Economically feasible	Technology should be established and commercialized

[19, 79, 99]. Moreover, lignin and lignin-based biomaterials contain several active functional groups which enable them to act as good bioadsorbent for the remediation of heavy metal ions, dyes, etc. A lot of research has been carried out for the decontamination of dyes and heavy metals from industrial wastewater using lignin and its derivatives as efficient bioadsorbents. Therefore, lignin-based biomaterials have occupied a significant area in the field of wastewater treatments [110].

2 Pure and Processed Lignin in Textile Wastewater

2.1 Pure Lignin in Wastewater Treatment

The use of pure lignin to adsorb dye from wastewater is still insufficient [33, 105]. Instead, the adsorption of dyes on lignin was largely investigated with processed lignin (Fig. 4), hybrid and composite lignin [21, 41, 73, 95, 102]. Guo et al. studied the adsorption of heavy metals on pure lignin. The affinity of metal ions to adsorbent was found in the order as $\text{Pb(II)} > \text{Cu(II)} > \text{Cd(II)} > \text{Zn(II)} > \text{Ni(II)}$ [41]. Mohan et al. used sole lignin in a study to remove Cu(II) from wastewater. In equilibrium, the amount of Cu(II) adsorbed by the biomaterials was estimated as 87.05 mg/g [72]. Quintana et al. applied pure lignin obtained from various lignin sources like cane bagasse, eucalyptus lignin for the remediation of Cd(II) . The lignin thus obtained was oxidized with aqueous H_2O_2 and applied for the Cd(II) removal from aqueous media [82].

The investigation of the remediation of malachite green dye on pure lignin was carried out by Lee et al. The remediation efficiency of malachite green on lignin was estimated as 31.2 mg/g and the adsorption of malachite green by lignin was closely related to the O–H and S–O bonds [55]. Pure lignin, as well as its industrial lignin was utilized for the remediation of methylene blue dye from wastewater [92]. The investigation reported with the remediation capacity of lignin adsorbent to methylene blue was 28 mg/g at pH 6. Similarly, the isolated bamboo lignin was applied for the adsorption of crystal violet dye from aqueous solution [9]. Similarly, lignin was applied for the adsorption of brilliant red HE-3B reactive dye from wastewater. Lignin was observed to be a promising bioadsorbent for the remediation of brilliant red HE-3B [93].

2.2 Kraft Lignin in Wastewater Treatment

Kraft lignin obtained by the sulfate process is estimated to be eighty-five percent of total world lignin production. In this process, about ninety to ninety-five percent of wood with lignin goes to aqueous solution of sodium hydroxide and sodium sulfide by dissolution. Firstly, lignin is dissolved at pH values 13–14 and temperatures

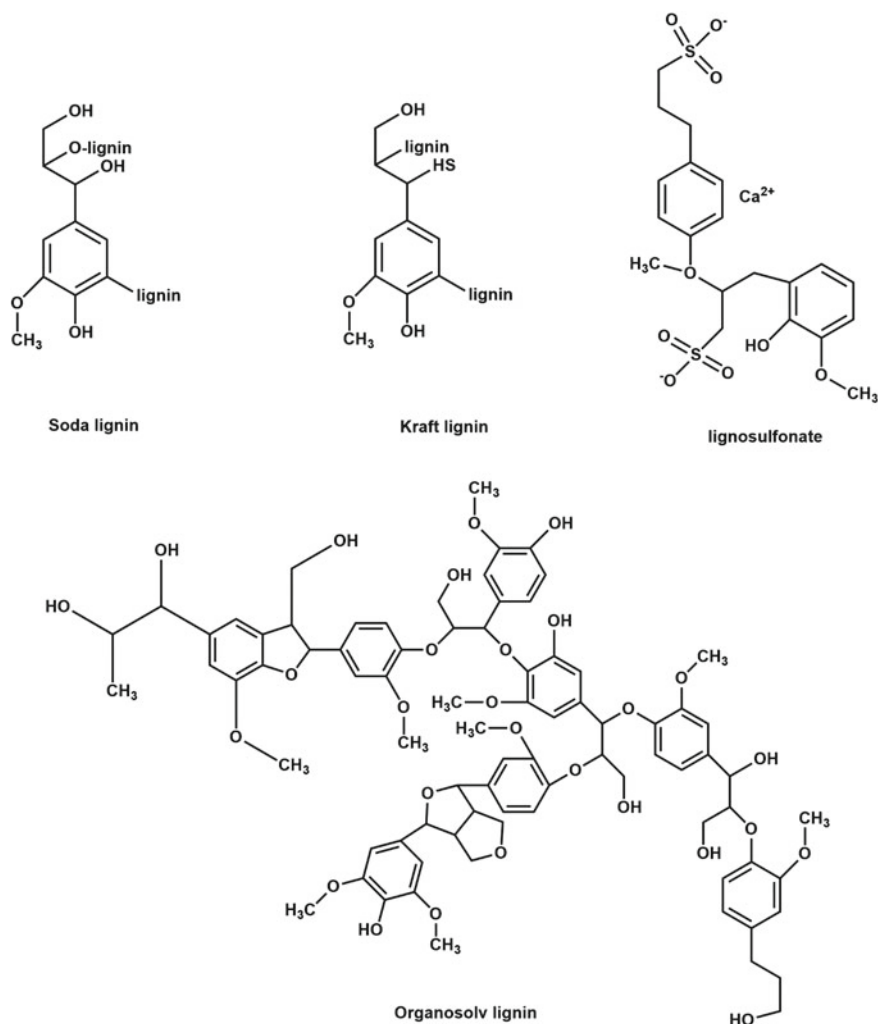


Fig. 4 Different types of processed lignin

around 170 °C to cleavage ether linkages raise the hydroxyl groups of phenol that ionizes within above pH ranges. Subsequently, lignin is isolated from the alkali solution by lowering pH in the ranges between 5 and 7.5. The mean molecular mass of the obtained kraft lignin is in between 1000 and 3000 Da. However, it can increase up to 15,000 Da [32, 62, 76, 97, 112]. In an adsorption study, kraft lignin has been applied for the remediation of Pb(II). In equilibrium, the adsorption amount of Pb(II) on kraft lignin was calculated 49.8 mg/g and the mechanism of the sorption process was expressed by “1-n cooperative” theory [18]. In another study, the remediation of Cu(II) from wastewater was studied using kraft lignin [42].

The adsorption of Cu(II) by the lignin biomaterials was reported to be observed in the following order: softwood kraft lignin > hardwood kraft lignin. The mechanism of the adsorption process was interpreted with ion-exchange interactions between metal ions and phenolic and carboxylic groups of lignin. Another investigation was carried out using kraft lignin collected from the pulp industry for the removal of Cr(VI), Cd(II), Cu(II) and Zn(II) from wastewater. The sorption capacity of kraft lignin toward different heavy metals was observed as Cr(VI) = Cd(II) > Cu(II) > Zn(II) [90].

Silica and kraft lignin were blended to prepare a bioadsorbent to remediate Cd(II) from aqueous media. They showed good adsorption efficiency of 84.66 mg/g to Cd(II) [52]. Mohan et al. studied the adsorption criteria of kraft lignin collected from the paper industry toward Cd(II) and Cu(II). In equilibrium, the adsorption amount of Cu(II) and Cd(II) onto adsorbent was reported to be 137.14 mg/g and 87.05 mg/g [72]. Fang et al. reported the high adsorption capacity toward Congo red dyes on magnetic kraft lignin adsorbent with a good reuse performance [28]. Budnyaket al. prepared a hybrid adsorbent from kraft lignin and silica and used for the removal of methylene blue dye from aqueous solution. It was reported that prepared lignin biomaterials showed higher adsorption capacity to methylene blue than pure lignin [15].

2.3 Alkaline Lignin in Wastewater Treatment

Alkaline lignin is attained by soda pulping process of grass, hardwoods, straw, bagasse, and flax. The lignin thus acquired is comparatively less modified than the other types of lignins. The biomass is digested with aqueous solution of sodium hydroxide at the temperature ranges between 140 to 170 °C. For the lower degradation of carbohydrates and proper dissolving of lignin in sodium hydroxide aqueous solution, anthraquinone catalyst is used in this process. The obtained lignin contains high amount of carboxylic acid so it is tough to isolate by filtration or centrifugation. Depending on carbon contents, the molecular masses of the soda lignin exist between 1000 and 3000 Da. The main advantages of this lignin are it is totally free of sulfur and can be a good potential to prepare high-end products [10, 112]. Alkali lignin contains high amount of carboxylic groups. Hence, it is expected to be efficient and effective adsorbent for toxic metals and dyes for the decontamination of textile effluent. In an experiment, biomaterials prepared from alkaline lignin with methylamine and formaldehyde were synthesized by Mannich-based reaction [35]. The batch adsorption experiment was done for the adsorption Pb(II). The adsorption efficiency observed by the bioadsorbent to Pb(II) was calculated as 79.9 mg/g. In a similar way, mercapto-functionalized alkali lignin was prepared to decontaminate Hg(II) from aqueous media [118]. The sorption efficiency of functional alkali lignin toward Hg(II) was calculated to be 101.2 mg/g. A bioadsorbent comprised of dithiocarbamate on alkaline lignin matrix was prepared by [36]. The bioadsorbent was efficiently applied for the removal of metallic ions from aqueous solution.

There are some dyes such as cationic turquoise GB, cationic red GTL, Safranin-O and cationic yellow X-5GL that are often used in textile purposes and are required to remediate in a proper technique. Azimvand et al. prepared lignin nanoadsorbents using alkali lignin for the effective removal of Safranin-O [11]. Similarly, alkaline hydrolysis of elephant grass was used to remove crystal violet dyes from wastewater. The bioadsorbent was found to be more than 90% in 30 min. Albadarin et al. investigated the remediation of Cr(VI) in wastewater using alkali lignin. In equilibrium, the sorption capacity of lignin was reported at 31.6 mg/g toward Cr(IV) [7]. Demirbas et al. studied the remediation of Cd(II) and Pb(II) utilizing alkaline lignins isolated from poplar and beech woods [22]. Todorcevic et al. used alkaline lignin obtained from wheat straw for the adsorption of Cu(II) and found the adsorption capacity of lignin toward Cu(II) 26 mg/g in aqueous solution [98]. Wu et al. [105] investigated the sorption of Cr(III) using alkali lignin collected from black liquor and 17.97 mg/g of Cr(III) was reported to be adsorbed [105].

2.4 Sulfonate Lignin in Wastewater Treatment

Lignosulfonates are produced by breaking the infinite lignin network during the sulfite process of wood pulping. In the sulfite pulping processes, sulfurous acid or a metal sulfite containing calcium, sodium, and magnesium is used with pulp to produce Lignosulfonates. The process is executed at temperatures 120–180 °C, with 1–5 h duration at a pH range 2–12. The process breaks α -ether (α -O-4') and β -ether (β -O-4') bondage of lignin. The lignosulfonates produced by using the sulfite treatment have a higher MW 1000 and 50,000 Da. [10, 32]. Lignosulfonates thus obtained have higher sulfur contents in the form of HSO_3^{3-} and SO_3^{2-} groups [74]. Lignosulfonate materials were applied as surfactants for pesticides, emulsifiers, drilling muds, binders for foundry and wood adhesives, oil recovery and concrete cure retarders and plasticizers. However, lignosulfonate may be used for heavy metals and dye removal from the effluent of textile wastewater due to the existence of active functional groups [12]. The hydrophilic nature of lignosulfonate makes it capable of use for dye and heavy metals removal in aqueous phase. Instead, hydrophobic property of lignosulfonates gives it an extra advantage to remove dye which is not soluble in aqueous media [87].

In a study, removal of methylene blue has been investigated with the help of sodium lignosulfonate [83]. The adsorption results displayed that nearly 100% of dye removal could be acquired at the dosage of sodium lignosulfonate 1.1 g and the investigation here manifests the potential application of inexpensive sodium lignosulfonate for textile wastewater treatment. Similarly, sodium lignosulfonates with three individual molecular masses were obtained by ultrafiltration method. The impact of prepared lignosulfonates on the dye's properties was studied. The purity, chroma, and guaiacyl contents in lignosulfonate and carboxyl, and sulfonic group and phenolic hydroxyls in lignosulfonate decrease with the increases of the molecular weight of lignosulfonates. The weakest reduction effect on dyestuffs was observed

with the molecular mass above 2.5 kDa [109]. Li et al. [59] synthesized porous lignin-based spheres by crosslinking lignosulfonate with epichlorohydrin and sodium alginate. The fabricated lignin-based microspheres displayed excellent adsorption efficiency of 95.6% toward Pb(II). In a separate study, 1-carboxypropylyed lignosulfonates and 5-carboxypentylyed lignosulfonates were prepared for the remediation of ethyl violet dye from a simulated solution. 1-carboxypropylyed lignosulfonates and 5-carboxypentylyed lignosulfonates displayed improved performance in removing dye than carboxyethylated lignosulfonate [12].

2.5 *Organosolv Lignin in Wastewater Treatment*

Organosolv lignin is a high-grade lignin containing many aliphatic and phenolic hydroxyl groups, which enable it as an excellent bioadsorbent for dye and heavy metals removal from wastewater. Organosolv lignin is obtained from biomass using organic solvents and delignifying agents. Generally, the solvents such as methanol, ethanol, formic acid, acetic acid are used with water at temperatures ranging from 170 to 190 °C. The efficacy of this process is improved by adding basic or acidic catalysts. The part of lignin and hemicellulose dissolve in the addition of mixtures of water and organic solvent. In this process, the lignin components are liberated from the lignocellulose through the breaking of α -O-4' and lignin-carbohydrate linkages. The dissolved lignin and hemicelluloses are recovered and separated by evaporation of the organic solvent or precipitation. The molecular weight of the obtained lignin exists in the range of 500–5000 Da [32, 68].

A bioadsorbent was prepared from organosolv lignin 2-hydrazinyl-2-oxoethyl]-trimethylazanium chloride and was used for the efficient decontamination of Cr(VI). The capacity of bioadsorbent to remove Cr (VI) was observed as 93.40%, 96.70%, 98.78% and 97.84% when the initial concentration was 10, 20, 50, 80 and 100 mg/L, respectively [101]. Similarly, using a microwave-assisted method a bioadsorbent was prepared from organosolv lignin and dithiocarbamate and was applied for the decontamination of Hg(II) from waste effluents [34]. In equilibrium, the adsorption amount of Hg(II) on bioadsorbent was estimated to be 210 mg/g which is observed to be almost three times more than that of pure lignin. In another investigation, organosolv and kraft lignin blended adsorbent were applied for the decontamination of Cu(II) from wastewater [42]. The order of the adsorption capacities by the used bioadsorbents was observed as softwood kraft lignin > hardwood kraft lignin > hardwood organosolv lignin > softwood organosolv lignin. Similarly, organosolv lignin was reported to use for the remediation of methylene blue in batch modes. The adsorption capability of methylene blue on bioadsorbent was estimated as 40.02 mg/g. In another study, organosolv lignin was used to study the adsorption performance of methylene blue from wastewater. The experimental result displayed that the amount of adsorption methylene blue on organosolv lignin was 40.02 mg/g in equilibrium and the adsorption process was pH-dependent [115].

3 Chemically Modified Lignin in Textile Wastewater

Pure lignins are less capable of removing heavy metals and dyes from contamination due to its heterogeneous macromolecular structure and low hydroxyl content [25, 68]. Therefore, the sorption capacity of pure lignins can be enhanced by the modification of pure lignin. Many reactive sites on lignin for heavy metals and dyes are created through modification. This modification is done by various chemical methods known as demethylation, methylation, hydrothermal depolymerization/liquefaction, and phenolation, etc. [8].

3.1 Lignin Modified with Oxygen-Containing Functional Groups

Lignin biopolymers generally have oxygen-containing hydroxyl and carboxyl functional groups in its structure. The number of oxygen-containing functional groups in lignin can be enhanced by oxidation reaction using some oxidants and co-oxidants. The increased numbers of functional groups improve the polyelectrolyte and hydrophilicity behavior of lignin and enhance the adsorption capacity toward heavy metals and dye from wastewater. Dizhbite et al. oxidized the organosolv lignin using polyoxometalate oxidant and O_2 or H_2O_2 cooxidants and increased the number of hydroxyl and carboxyl functional groups significantly into organosolv lignin without altering the lignin structure. The sorption capacity of modified lignin was improved threefold toward Cd(II) and twofold toward Pb(II) [23]. Tian studied the sorption capacity of synthesized dimethyl-acetoxy-(2-carboxymethyl ether)-lignin ammonium chloride toward Cu(II). The estimated amount of Cu(II) that was adsorbed on synthesized biomaterials was found as 399.0 mg/g and Freundlich model was reported as best fit for this adsorption process. Lignosulfonate resin was prepared by step-growth polymerization with glucose and lignosulfonate [60]. The Lignosulfonate resin adsorbed 194.5, 59.9, 48.8, 42.5 and 41.8 mg/g of Pb(II), Cu(II), Cd(II), Ni(II), and Cr(III), respectively. The highest adsorption capacity gained for Pb(II) as compared to other metals indicates the stronger bonding tendency toward Pb(II) due to the existence of carboxyl and phenol hydroxyl groups.

In a study, carboxymethylated formic lignin was reported to show adsorption efficiency of 67.7 and 107.7 mg/g for Cd(II) and Pb(II), respectively. Monolayer sorption mechanism was depicted as Langmuir isotherm model found to be best fit for this investigation [80]. Parajuli et al. studied the adsorption capacity of a lignin-based biomaterials prepared from lignin and catechol toward Cd (II), Pb (II) and Co(II). The incorporation of higher amounts of phenol hydroxyl groups onto modified lignin enhances the capacity of this bioadsorbent to adsorb high amounts of Pb(II), Cd (II) and Co(II). The sorption mechanism was explained to be a cation exchange interaction between heavy metals and the phenol hydroxyl functional groups [78]. Similarly, acetic acid lignin impregnated with various acidic hydroxyl groups was

reported to adsorb methylene blue from aqueous solution with a maximum sorption capacity of 63.3 mg/g. The sorption capacity of acetic acid lignin increased with the increment of pH [29]. In another study, sulfuric acid lignin was improved by increasing the amount of phenol hydroxyl functional group from 2.99 to 9.49 mmol/g just after phenolisation. The sorption capacity of sulfuric acid lignin after phenolation was carried out toward methylene blue. The remediation efficiency of methylene blue with the phenolated sulfuric acid lignin was enhanced to 99.6% [94].

3.2 Lignin Modified with Nitrogen-Containing Functional Groups in Wastewater Treatment

Modification of lignin with reactive components like the amino group gives the lignin improved properties for different applications. Amino groups can be introduced to lignin structure by many chemical methods. Chemically, many applicable methods can introduce amine groups into lignin. However, most of the amination of lignin is carried out by the simplest method of the Mannich reaction. In this method, primary, secondary and tertiary amino groups are incorporated into lignin structures where tertiary amino groups are dominating groups.

A Mannich base lignin adsorbent was prepared from lignin and methylamine [35]. The obtained lignin biomaterials showed approximately four folds higher sorption capacity toward Pb(II) than unmodified lignin. The monolayer sorption mechanism was suggested as the adsorption isotherm best fit the Langmuir isotherm model. Liu et al. prepared lignin biomaterials from alkali lignin and amine compound. The adsorbent showed adsorption capacity of 55.35 mg/g toward Cu(II) and 72.48 mg/g toward Pb(II) [64]. In another study, a bioadsorbent of enzyme hydrolyzed lignin was modified by the nitrogen and sulfur functional groups. The sorption capacity of modified lignin was estimated to be 180 mg/g toward Hg(II) [58].

3.3 Lignin Modified with Sulfur-Containing Functional Groups in Wastewater Treatment

Sulfur is a soft base and has an attraction to soft metal ions like Hg(II), Cd(II), Pb(II) and Cu(II). Generally, thiol, dithiocarbamate, xanthate and sulfonate functional groups exist in the lignin as sulfur-containing groups. Moreover, sulfomethylation and sulfonation reactions are used to incorporate sulfonate ($-\text{SO}_3^{3-}$) and methylene sulfonate ($-\text{CH}_2\text{SO}_3^{3-}$) in the lignin structure as shown in Fig. 5. The incorporation of more sulfur-containing function groups into lignin structure makes it more capable for advanced use in the design and adsorbing materials for dye and heavy metals from wastewater [36].

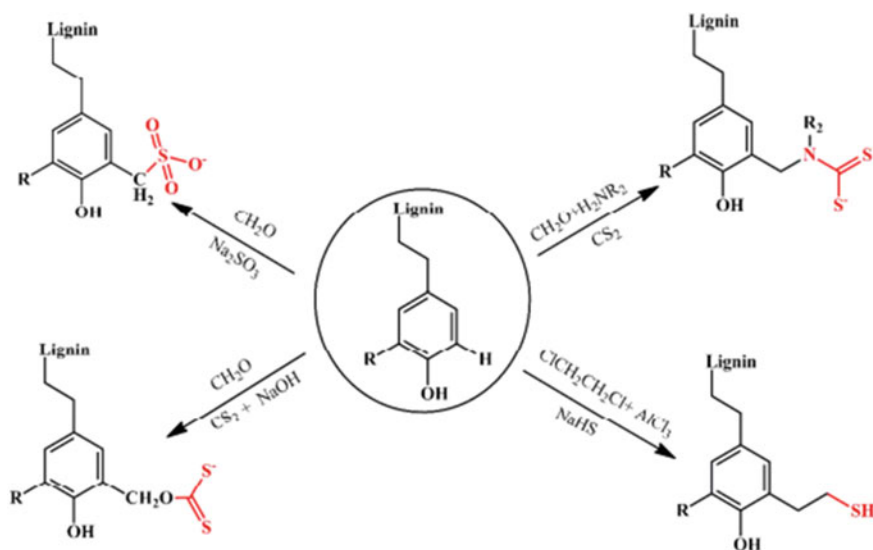


Fig. 5 Sulfonation of lignin structure. Reproduce with permission from [33]. Copyright@2018, American Chemical Society

Li et al. prepared a bioadsorbent by modification of lignin with dithiocarbamate moieties. The adsorbent has eleven times higher surface area ($22.3 \text{ m}^2/\text{g}$) and exhibits twelve times adsorption efficiency toward Pb(II) (188 mg/g) as compared to original lignin. The best-fitted Langmuir isotherm model of the adsorption study suggested the monolayer sorption of metal on the homogeneous surface of the adsorbent [58]. In another study, mesoporous lignin-based adsorbent was synthesized for the decontamination of Pb(II). The excellent sorption efficacy was marked toward Pb(II) (188 mg/g) by the prepared bioadsorbent [106].

4 Lignin-Based Hybrid Biomaterials in Textile Wastewater

Lignin-based hybrid biomaterials are now being used as viable bioadsorbents for the remediation of dyes and heavy metals from textile effluents. Lignin is a natural polymer and is available as an inexpensive byproduct of the pulp industry. Hence, the use of lignin to develop a material will minimise the cost and will help to synthesize environmentally friendly hybrid adsorbent. In a study, lignin-based sulfonated porous carbon bioadsorbent was found to show magnificent efficiency for the rapid removal of methylene blue. The adsorption capacity toward methylene blue increases rapidly from 234.19 to 621.52 mg/g with the change of pH from 2 to 11 [119]. Meng et al. studied the effective remediation of azo dye direct blue 1 by synthesized animated cosolvent-enhanced lignocellulosic fractionation with a sorption capacity

of 502.7 mg/g [69]. Budnyak et al. made electrostatic deposition of the oxidized kraft lignin onto the surface of aminosilicas to prepare hybrid materials for the remediation of crystal violet from textile wastewater (Fig. 6). The prepared hybrid biomaterials were found to absorb a high amount of textile dye (108–110 mg/g. Hence, the adsorbent showed high capacity toward the selected dye, which manifested it as a potential candidate for the decontamination of textile effluents [15].

Kriaa et al. fabricated Tunisian-activated lignin for adsorption of methylene blue dye. The maximum adsorption capacity were found 147 mg/g at pH 11 [53]. Similarly, lignin modified with 5-sulfosalicylic exhibited enhanced adsorption capacity toward methylene blue. This investigation revealed that the sorption capacities of methylene blue reached the maximum at 83.2 mg/g by the hybrid biomaterials [49]. In a study, chitosan-lifnosulfate hybrid adsorbent was prepared by crosslinking sulfonate group in lignosulfonate with the protonated amino group in chitosan [39]. The prepared bioadsorbent was applied for the effective remediation of Cr(VI), Congo red dye and Rhodamin B dye from wastewater. From adsorption isotherm and kinetic studies, the mechanism of adsorption was suggested for the electrostatic interaction between the anionic groups of Congo red and Cr(VI) with hydroxyl groups and protonated amino groups, respectively. Moreover, the electrostatic interaction between positively charged group of rhodamine B and sulfonate functional groups of the biomaterials exhibited a vital role in rhodamine B adsorption. Carboxy-methylating lignin with Al^{3+} and Mn^{2+} was reported in a study to remove procion blue MX-R textile dyes from

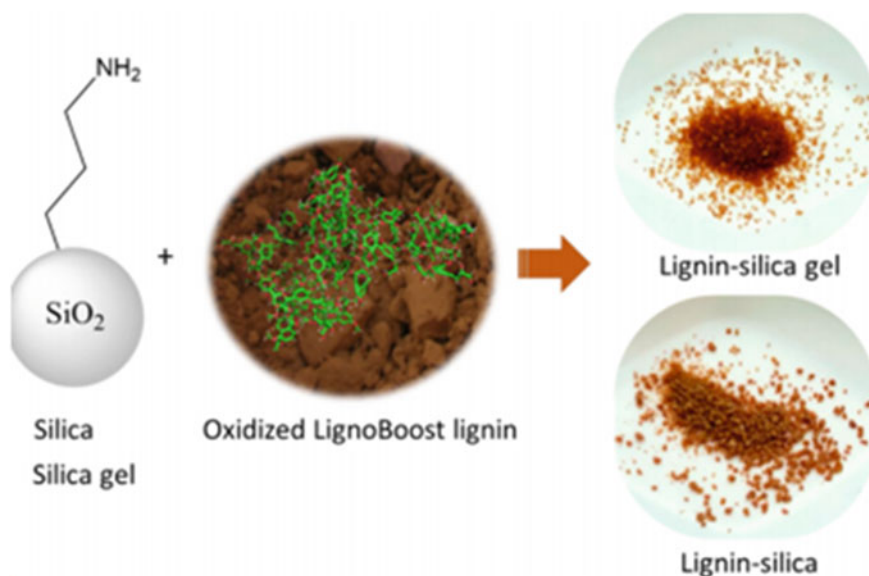


Fig. 6 Lignin-silica composites for synthetic dye adsorption. Further permissions related to the material excerpted should be directed to the ACS. Reproduce with permission from [15]. Copyright@2019, American Chemical Society

aqueous solution. The maximum sorption capacities found for carboxy-methylating lignin with Al^{3+} was 73.52 mg/g and for carboxy-methylating lignin with Mn^{2+} 55.16 mg/g. The sorption of procion blue MX-R on modified lignin best fit to the Langmuir model of adsorption [3]

In a study, lignin-derived hollow spheres were prepared and was used for the decontamination of Rhodamine B and methylene blue from effluents. The bioadsorbent were simply fabricated from maleic anhydride and organosolv lignin through self-assembly Fe_3O_4 nanoparticles (Fig. 7). The bioadsorbent exhibited adsorption capabilities of 31.23 mg/g toward methylene blue and 17.62 mg/g toward Rhodamine. The microspheres thus prepared manifested as a potential bioadsorbent with low cost and reusability for textile wastewater treatment [57]. Roy et al. used lignocellulosic-biomass jute fiber for remediation of azo dye from aqueous media. The maximum adsorption of azo dye in equilibrium for the biomaterials was found as 28.940 mg/g at pH 3.91 [86]. Activated carbons developed from various eucalyptus kraf lignin have been successfully employed for Congo red dye removal in aqueous phase. The adsorption capacity of the adsorbent was totally influenced by total amount of pore volumes of the activated carbons. In equilibrium, the adsorption data was fitted to both BET isotherms and Langmuir isotherms very well. The thermodynamic analysis indicated that the Congo red adsorption was endothermic in nature [20]. In another study,

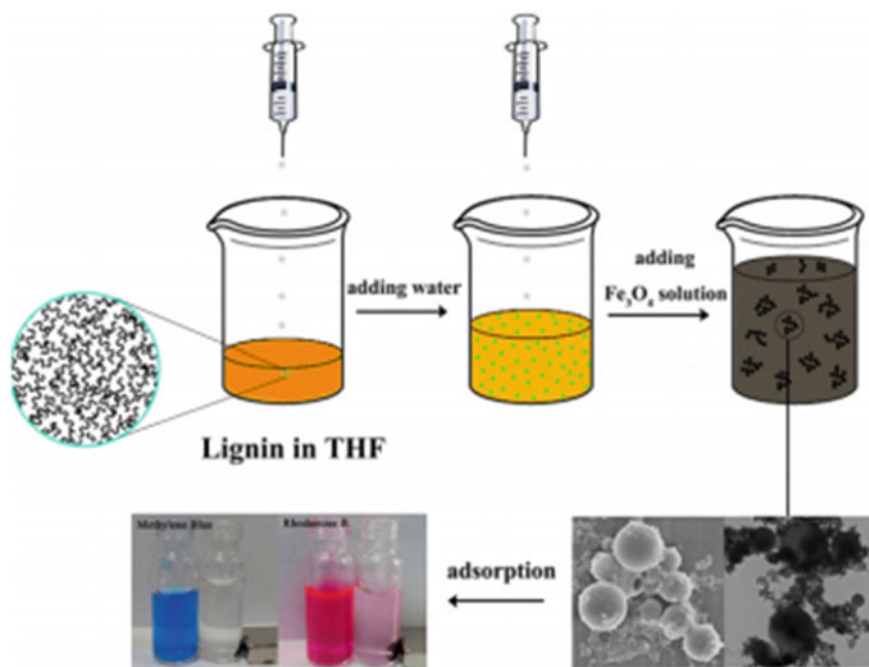


Fig. 7 Synthesis of magnetic lignin-based hollow microspheres for methylene blue dye adsorption. Reproduce with permission from [57]. Copyright©2016, American Chemical Society

lignin-chitosan biomaterials were prepared for effective remediation of methylene blue dye. The sorption of dye on adsorbent was occurred by the electrostatic attractions and chemical interactions between amino group of dye and hydroxyl groups of the adsorbent. The maximum adsorption capacity was estimated as 36.25 mg/g [6].

The chitin/lignin hybrid adsorbent was developed to adsorb anionic dye Direct Blue 71 from aqueous media. The sorption capacity was estimated to be 91% at pH range between 2.4 and 8.4. [103]. Budnyak et al. developed a hybrid lignin for the remediation of methylene blue dye. The hybrid lignin based on clean flow black exhibited sorption efficiency of 60 mg/g which was 30% more than the hybrid lignin obtained from ligno boost. Lignin hybrid biomaterials adsorbs 80–99% of the methyl blue in the pH range between 3 and 10 [15]. In another study, chitosan-alkali lignin composites material was reported for the remediation of Remazol Brilliant Blue R, anthraquinonic dye and Cr(VI). The chitosan-alkali lignin (50/50) hybrid adsorbent showed the remediation of maximum percentage of Remazol Brilliant Blue R, anthraquinonic dye, and Cr(VI) as compared to other composites, sole chitosan and sole alkali lignin. The mechanism of adsorption suggested the electrostatic interaction of anionic sulfonate and hydrogen chromate groups of dye and Cr(VI) and hydroxyl groups and protonated amino of the composite with as well as chemical interaction between carbonyl moiety of the dye and amino and hydroxyl functional groups of the biocomposite [73]. Hu et al. synthesized magnetic lignosulfonate bioadsorbent and the surface of the adsorbent was coated with an organic carbon. The study showed the highest adsorption efficiency of 198.24 and 192.51 mg/g for Congo red and titan yellow dye, respectively. The adsorption isotherm follows the Langmuir adsorption model [45].

5 Lignin-Based Polymer Composite Materials for Wastewater Treatment

Polymer composite research is now becoming a potential alternative to traditional adsorbent due to the requirements for materials with higher adsorption capacities of dyes, toxic metal and other toxic pollutants from industrial effluents. The polymers biocomposites are mainly categorized on the basis of sources and their structure [14, 70]. A large number of polymer composites were fabricated significantly for the remediation of wastewater [17, 65, 77]. Among them, the polymeric lignin biomaterials are playing an important role in the decontamination of various types of contaminants, such as dyes, metal ions, and other toxic contaminants from wastewater. Polymeric lignin biomaterials are explained as a unification of any polymers with lignin biopolymer to provide improved characteristics depending on the end use. A lignin biomaterial bears varieties of active functional groups and provides a bright prospect for diverse functionality for various applications [37]. Lignin could be straightly integrated onto another polymeric structure to work as a flame retardant [63], antioxidant [31], heavy metal adsorbent [67] and dye adsorbent [25, 111].

In a study, Gonzalez-Lopez et al. developed highly porous polymeric lignin composite from hardwood kraft lignin and low-density polyethylene to estimate the adsorption capacity toward methylene blue dye. The polymeric lignin composite showed the dye removal efficiency of 80% in a batch adsorption [38]. Similarly, Lignin-based hydrogel adsorbent was prepared by crosslinking the lignosulfonate with acrylamide (AM) and acryloyloxyethyl trimethylammonium chloride monomer. The bioadsorbent was then applied for the remediation of AR 73 dye. In equilibrium, maximum sorption capacity of the adsorbent is 409.84 mg/g toward AR 73 dye [104]. Similarly, the sorption study of methylene blue from wastewater was done on fabricated sulfonate lignin-based hydrogels [56]. The efficiency of adsorption was estimated to be 495 mg/g toward methylene blue for hydrogel bioadsorbent which is five folds more than the same for unmodified lignin. Tang et al. prepared lignin sulfonate-g-poly (acrylic acid-r-acrylamide) lignin and applied it to study the adsorption capacity, adsorption kinetics and isotherm for the removal of malachite green. The grafted biomaterials displayed a higher and higher percentage of adsorption toward malachite green than the un-grafted lignin [96].

In a study, dye dispersant was synthesized by 3-chloro-2-hydroxy propyl sodium sulfonic acid on alkali lignin. The dye dispersant containing the higher amount of sulfonic groups and lower amount of phenolic hydroxyl groups showed an ultra-weak reducing effect and well dispersion on azo dye [81]. Zhang et al. developed a high-performance absorbent for cationic dye Safranin T from lignin and polyvinyl alcohol polymer by electrospinning process. The capacity of adsorption was reported to be increased with increasing the initial dye pH [116]. In another study, lignosulfonate-g-acrylic acid hydrogels were prepared by grafting acrylic acid on the lignosulfonate structure. The introduction of a higher amount of carboxylic acid functional groups through the grafting process improved the adsorption efficiency of the hydrogel toward methylene blue (2013 mg/g) [111]. In a similar way, Domínguez-Robles prepared lignin-based hydrogels by crosslinking different technical lignins with poly (methyl vinyl ether co-maleic acid). The hydrogels were applied to remove methylene blue dye in aqueous media. The high sorption capacity of hydrogels was reported to be found from 440 to 840 mg/g toward methylene blue [26].

6 Lignin-Based Nanocomposite Materials for Wastewater Treatment

Lignin-based nanomaterials have been intensively investigated in a number of fields, such as, decontamination of wastewater, antioxidant, reinforced materials, nanomicrocarriers, membrane, drug delivery, etc. [43, 114]. The investigation on lignin-based nanocomposite has attained intense concentration for many applications. Moreover, for the unique properties of nanomaterials for their size distinctness,

many researchers have commenced to study on lignin at the nanoscale for potential applications in wide variety of fields [57, 85, 107, 108]. The more biodegradability of lignin nanocomposite than synthetic inorganic nanoparticles and the possibility to prepare aqueous nanoparticle dispersions of lignin nanoparticles enable it a prospective applicant in designing sustainable bionanocomposite [61]. Integration of nanoparticles in natural or synthetic polymers renders them as high valued materials since the novel materials with improved and new featured materials are thus obtained [71, 91]. Yu et al. prepared a high-performance modified lignin nano-adsorbent by the co-precipitation of ferric, ferrous, and permanganate with lignin. The adsorption efficiency of the nanocomposites for the methylene blue remediation from aqueous media was estimated (Fig. 8). The maximum adsorption of nano-adsorbent toward methylene blue estimated as 252.05 mg g^{-1} at 298 K indicated potential biomaterials for dye wastewater treatment [110]. de Araújo Padilha et al. studied the removal of methylene blue by lignin/ Fe_3O_4 nanoparticles adsorbent. Organosoluble lignin obtained from pretreated green coconut fiber was coated with Fe_3O_4 nanoparticles and subsequently β -glucosidase was immobilized on it to prepare the adsorbent. In adsorption experiments, high sorption capacity toward cibacron blue, methylene blue and remazol red was estimated as 112.36, 203.66 and 96.46 mg/g, respectively [24].

Azimvand et al. synthesized lignin nanoparticle-g-polyacrylic acid adsorbent for the remediation of Safranin-O from wastewater. They fabricated lignin nanoparticle-g-polyacrylic acid adsorbent through copolymerization reactions in presence of initiator as potassium persulfate. The maximum adsorption capacity was obtained

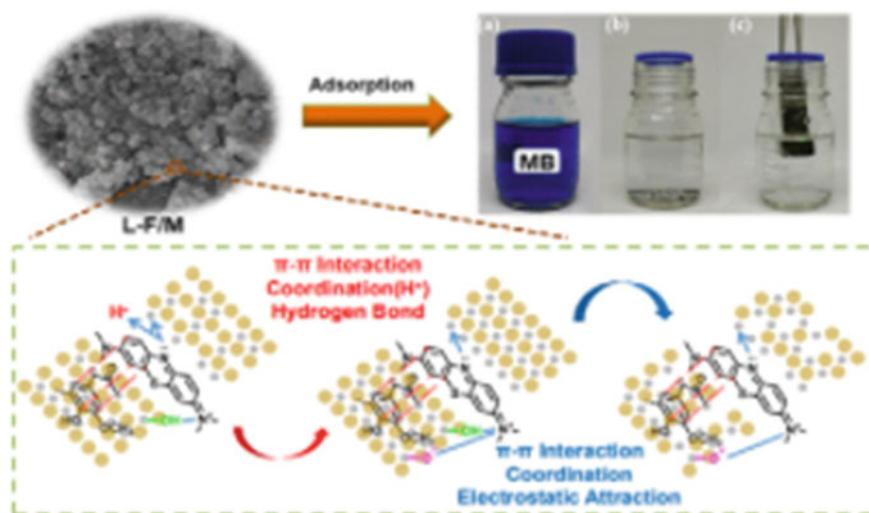


Fig. 8 Synthesis of a lignin-Fe/Mn binary oxide blend nanocomposite for methylene blue dye adsorption. Reproduce with permission from [110]. Further permissions related to the material excerpted should be directed to the ACS. Copyright@2021, American Chemical Society

at 99 mg/g and 138.88 mg/g toward safranin-O dye [11]. In another study, Chitosan/nano-lignin-based hollow spheres with the diameter of 138 ± 39 nm from the palm kernel. The highly efficient sorbent exhibited effective removal (~83%) of methylene blue dye under normal pH conditions. The adsorbent exhibited maximum adsorption capacity of 74.07 mg/g to methylene blue [91]. Similarly, Zhou prepared chitosan-decorated lignocellulose fiber by deposition–crosslinking to adsorb AR18 solution. Subsequently, chitosan-decorated lignocellulose was magnetized by easily blending it with magnetic nanoparticles very easily in an aqueous solution. The sorption capacity of the magnetized chitosan-decorated lignocellulose fiber was estimated to be 1184 mg/g [117].

In an investigation, MnO₂ nanodots modified lignin nanocomposite was reported for remediation of methylene blue dye sorption. The hierarchical spherical nanostructures with evenly dispersed MnO₂ nanodots were observed for this nanoadsorbent. In the case of adsorbent 80% of adsorption capacity was reached within 5 min at room temperature. [113]. In a similar way, the adsorption of brilliant black dye from contaminated wastewater was reported using chitosan-lignin-titania nanoadsorbent. The adsorbent was prepared from kraft lignin derived from paper and pulp black liquor, titania (TiO₂) and chitosan. The adsorbent exhibited a maximum sorption capacity of 15.8 mg/g [67]. In another study, novel lignosulfonate/amino-functionalized nanocomposite was prepared and applied for the remediation of methylene blue from wastewater. The adsorption study showed the incorporation of lignosulfonate to amino-functionalized nanocomposite improved the stability of the composite in water and enhanced its adsorption capacity of methylene blue. Hence, this novel nanoadsorbent can be effectively applied for the remediation of organic dyes from textile effluents [2].

7 Conclusion

This chapter gives a brief review on the importance of lignin-based biomaterials for the treatment of effluent from textile industries. The textile industry uses large quantities of potable water and consequently generates large amounts of wastewater. Hence, textile wastewater is not desirable to be released to the environment untreated. Different types of methods such as physical, chemical and biological methods have been applied to treat the textile effluent. Adsorption techniques have been proven as one of the viable methods for the decontamination of textile effluents. However, more developments are required to adopt these techniques for acquiring a more cost-effective and environmentally friendly process. Development of inexpensive and efficient bioadsorbents for removal of toxic dyes and heavy metals from contaminated water has been a topic of great interest. Lignin is a very influential bio-derived biomaterials. The existence of various functional groups in the backbone of lignin creates many chances to apply it for many applications and many researches have been carried out in this field. In this chapter, we highlighted the role of lignin and lignin-based biomaterials in the decontamination of textile effluents. The discussion

was categorized into types of lignin-based biomaterials used in the remediation of wastewater. Finally, it is concluded that lignin-based biomaterials being biodegradable, inexpensive and environmentally friendly have been proven to be the promising alternative for the remediation of textile effluents.

References

1. Abdelhamid HN, Zou X (2018) Template-free and room temperature synthesis of hierarchical porous zeolitic imidazolate framework nanoparticles and their dye and CO₂ sorption. *Green Chem* 20(5):1074–1084
2. Abboud M, Sahlabji T, Abu Haija M, El-Zahhar AA, Bondock S, Ismail I, Keshk S (2020) Synthesis and characterization of liginosulfonate/aminofunctionalized SBA-15 nanocomposite for the adsorption of methylene blue from wastewater. *New. J Chem* 44:2291–2302. <https://doi.org/10.1039/D0NJ00076K>
3. Adebayo MA, Prola LDT, Lima EC, Puchana-Rosero MJ, Cataluña R, Saucier C, Umpierrez CS, Vagheti JCP, da Silva LG, Ruggiero R (2014) Adsorption of Procion Blue MX-R dye from aqueous solutions by lignin chemically modified with aluminium and manganese. *J Hazard Mater* 268:43–50
4. Ahmad M, Rajapaksha AU, Lim JE, Zhang M, Bolan N, Mohan D, Vithan-age M, Lee SS, Ok YS (2014) Biochar as a sorbent for contaminant management in soil and water: a review. *Chemosphere* 99:19–33
5. Ahmed MJK, Ahmaruzzaman M (2016) A review on potential usage of industrial waste materials for binding heavy metal ions from aqueous solutions. *J Water Process Eng.* 10(April 2016):39–47. <https://doi.org/10.1016/j.jwpe.2016.01.014> (Internet)
6. Albadarin AB, Collins MN, Naushad M, Shirazian S, Walker G, Mangwandi C (2017) Activated lignin-chitosan extruded blends for efficient adsorption of methylene blue. *Chem Eng J [Internet]* 307:264–272. <https://doi.org/10.1016/j.cej.2016.08.089>
7. Albadarin AB, Al-Muhtaseb AH, Walker GM, Allen SJ, Ahmad MNM (2011) Retention of toxic chromium from aqueous phase by H₃PO₄-activated lignin: effect of salts and desorption studies. *Desalination* 274(1–3). <https://doi.org/10.1016/j.desal.2011.01.079>
8. Alonso MV, Oliet M, Pérez JM, Rodríguez F, Echeverría J (2004) Determination of curing kinetic parameters of lignin-phenol-formaldehyde resol resins by several dynamic differential scanning calorimetry methods. *Thermochim Acta* 419(1–2):161–167
9. Aniagor C, Menkiti M (2019) Synthesis, modification and use of lignified bamboo isolate for the renovation of crystal violet dye effluent. *Appl Water Sci* 9(4):77
10. Azadi P, Inderwildi OR, Farnood R, King DA (2013) Liquid fuels, hydrogen and chemicals from lignin: a critical review. *Renew Sustain Energy Rev [Internet]* 21:506–523. <https://doi.org/10.1016/j.rser.2012.12.022>
11. Azimvand J, Didehban K, Mirshokraie SA (2018) Safranin-O removal from aqueous solutions using lignin nanoparticle-g-polyacrylic acid adsorbent: synthesis, properties, and application. *Adsorpt Sci Technol* 36(7–8):1422–1440
12. Bahrpaima K, Fatehi P (2019) Preparation and coagulation performance of carboxypropylated and carboxypentylated liginosulfonates for dye removal. *Biomolecules* 9:383. <https://doi.org/10.3390/biom9080383>
13. Bajwa DS, Pourhashem G, Ullah AH, Bajwa SG (2019) A concise review of current lignin production, applications, products and their environment impact. *Ind Crops Prod* 139:111526. <https://doi.org/10.1016/j.indcrop.2019.111526>
14. Berber MR (2020) Current advances of polymer composites for water treatment and desalination. *J Chem.* Article ID 7608423. <https://doi.org/10.1155/2020/7608423>

15. Budnyak TM, Aminzadeh S, Pylypchuk IV, Sternik D, Tertykh VA, Lindström ME, Sevastyanova O (2018) Methylene blue dye sorption by hybrid materials from technical lignins. *J Environ Chem Eng* [Internet] 6(4):4997–5007. <https://doi.org/10.1016/j.jece.2018.07.041>
16. Cardoso NF, Lima EC, Royer B, Bach MV, Dotto GL, Pinto LAA, Calvete T (2012) Comparison of *Spirulina platensis* microalgae and commercial activated carbon as adsorbents for the removal of Reactive Red 120 dye from aqueous effluents. *J Hazard Mater* 241–242:146–153. <https://doi.org/10.1016/j.jhazmat.2012.09.026>
17. Chen D, Wang L, Ma M, Yang W (2016) Super-adsorbent material based on functional polymer particles with a multilevel porous structure”. *NPG Asia Mater* 8(8):301
18. Chen H, Qu X, Liu N, Wang S, Chen X, Liu S (2018) Study of the adsorption process of heavy metals cations on Kraft lignin. *Chem Eng Res Des* 139:248–258
19. Chikri R, Elhadiri N, Benchanaa M, El maguana Y (2020) Efficiency of sawdust as low-cost adsorbent for dyes removal. *J Chem.* 2020:1–17
20. Cotoruelo LM, Marqués MD, Díaz FJ (2010) Equilibrium and kinetic study of congo red adsorption onto lignin-based activated carbons. *Transp Porous Med* 83:573–590. <https://doi.org/10.1007/s11242-009-9460-8>
21. da Silva LG, Ruggiero R, Gontijo PM, Pinto RB, Royer B, Lima EC, Fernandes THM, Calvete T (2011) Adsorption of Brilliant Red 2BE dye from water solutions by a chemically modified sugarcane bagasse lignin. *Chem Eng J* 168:620–628
22. Demirbas A (2004) Adsorption of lead and cadmium ions in aqueous solutions onto modified lignin from alkali glycerol delignification. *J Hazard Mater* 109(1–3). <https://doi.org/10.1016/j.jhazmat.2004.04.002>
23. Dizhbite T, Jashina L, Dobelev G, Andersone A, Evtuguin D, Bikovens O, Telysheva G (2013) Polyoxometalate (POM)-aided modification of lignin from wheat straw biorefinery. *Holzforschung* 67(5). <https://doi.org/10.1515/hf-2012-0193>
24. de Araújo Padilha CE, da Costa Nogueira C, de Santana Souza DF, de Oliveira JA, dos Santos ES (2020) Organosolv lignin/Fe₃O₄ nanoparticles applied as a β -glucosidase immobilization support and adsorbent for textile dye removal. *Ind Crops Prod.* 146(December 2019):112167. <https://doi.org/10.1016/j.indcrop.2020.112167>
25. Demirbas A (2008) Heavy metal adsorption onto agro-based waste materials: a review. *J Hazard Mater* 157(2–3):220–229
26. Domínguez-Robles J, Peresin MS, Tamminen T, Rodríguez A, Larrañeta E, Jääskeläinen AS (2018) Lignin-based hydrogels with “super-swelling” capacities for dye removal. *Int J Biol Macromol.* 115:1249–1259. <https://doi.org/10.1016/j.ijbiomac.2018.04.044> (Internet)
27. Ertaş M, Acemioğlu B, Alma MH, Usta M (2010) Removal of methylene blue from aqueous solution using cotton stalk, cotton waste and cotton dust. *J Hazard Mater* 183(1–3):421–427
28. Fang L, Wu H, Shi Y, Tao Y, Yong Q (2021) Preparation of bignin-based magnetic adsorbent from kraft lignin for adsorbing the Congo Red. *Front Bioeng Biotechnol* 9:691528. <https://doi.org/10.3389/fbioe.2021.691528>
29. Feng Q, Cheng H, Chen F, Zhou X, Wang P, Xie Y (2016) Investigation of cationic dye adsorption from water onto acetic acid lignin. *J Wood Chem Technol* 36(3):173–181
30. Fu F, Wang Q (2011) Removal of heavy metal ions from wastewaters: a review. *J Environ Manage* [Internet] 92(3):407–418. <https://doi.org/10.1016/j.jenvman.2010.11.011>
31. Gadioli R, Waldman WR, De Paoli MA (2016) Lignin as a green primary antioxidant for polypropylene. *J Appl Polym Sci* 2016(133):43558
32. Galkin MV, Samec JSM (2016) Lignin valorization through catalytic lignocellulose fractionation: a fundamental platform for the future biorefinery. *Chemsuschem* 9(13):1544–1558
33. Ge Y, Li Z (2018) Application of lignin and its derivatives in adsorption of heavy metal ions in water: a review. *ACS Sustain Chem Eng* 6:7181–7192
34. Ge Y, Wu S, Qin L, Li Z (2016) Conversion of organosolv lignin into an efficient mercury ion adsorbent by a microwave-assisted method. *J Taiwan Inst Chem Eng* 63:500–505
35. Ge Y, Song Q, Li Z (2015) A Mannich base biosorbent derived from alkaline lignin for lead removal from aqueous solution. *J Ind Eng Chem* 23:228–234

36. Ge Y, Xiao D, Li Z, Cui X (2014) Dithiocarbamate functionalized lignin for efficient removal of metallic ions and the usage of the metal-loaded bio-sorbents as potential free radical scavengers. *J Mater Chem A* 2(7). <https://doi.org/10.1039/C3TA14333C>
37. Gillet S, Aguedo M, Petitjean L, Morais ARC, da CostaLopes AM, Łukasik RM, Anastas PT (2017) Lignin transformations for high value applications: towards targeted modifications using green chemistry. *Green Chem* 2017(19):4200–4233
38. González-López ME, Robledo-Ortiz JR, Rodrigue D, Pérez-Fonseca AA (2020) Highly porous lignin composites for dye removal in batch and continuous-flow systems. *Mater Lett* 263:70–73
39. Gu F, Geng J, Li M, Chang J, Cui Y (2019) Synthesis of chitosan-ignosulfonate composite as an adsorbent for dyes and metal ions removal from wastewater. *ACS Omega* 4(25):21421–21430
40. Gundekari S, Karmee SK (2021) Selective synthesis of cyclohexanol intermediates from lignin-based phenolics and diaryl ethers using hydrogen over supported metal catalysts: a critical review. *Catal Surv Asia* 25:1–26. <https://doi.org/10.1007/s10563-020-09315-3>
41. Guo X, Zhang S, Shan XQ (2008) Adsorption of metal ions on lignin. *J Hazard Mater* 151(1):134–142
42. Harmita H, Karthikeyan K, Pan X (2009) Copper and cadmium sorption onto kraft and organosolv lignins. *Bioresour Technol* 100(24):6183–6191
43. Henn A, Mattinen ML (2019) Chemo-enzymatically prepared lignin nanoparticles for value-added applications. *World J Microbiol Biotechnol* 35:125
44. Hokkanen S, Bhatnagar A, Sillanpää M (2016) A review on modification methods to cellulose-based adsorbents to improve adsorption capacity. *Water Res* 91:156–173
45. Hu L, Guang C, Liu Y, Su Z, Gong S, Yao Y, Wang Y (2020) Adsorption behavior of dyes from an aqueous solution onto composite magnetic lignin adsorbent. *Chemosphere* [Internet] 246:125757. <https://doi.org/10.1016/j.chemosphere.2019.125757>
46. Hyder MKMZ, Ochiai B (2018) Selective recovery of Au(III), Pd(II), and Ag(I) from printed circuit boards using cellulose filter paper grafted with polymer chains bearing thiocarbamate moieties. *Microsyst Technol* 24:683–690. <https://doi.org/10.1007/s00542-017-3277-0>
47. Hyder MKMZ, Ochiai B (2017) Synthesis of a selective scavenger for Ag(I), Pd(II), and Au(III) based on cellulose filter paper grafted with polymer chains bearing thiocarbamate moieties. *Chem Lett* 46:492–494. <https://doi.org/10.1246/cl.160983>
48. Islam MS, Ahmed MK, Raknuzzaman M, Habibullah -Al- Mamun M, Islam MK (2015) Heavy metal pollution in surface water and sediment: a preliminary assessment of an urban river in a developing country. *Ecol Indic.* 48:282–291. <https://doi.org/10.1016/j.ecolind.2014.08.016> (Internet)
49. Jin Y, Zeng C, Lü QF, Yu Y (2019) Efficient adsorption of methylene blue and lead ions in aqueous solutions by 5-sulfosalicylic acid modified lignin. *Int J Biol Macromol* [Internet] 123:50–58. <https://doi.org/10.1016/j.ijbiomac.2018.10.213>
50. Kadirvelu K, Thamaraiselvi K, Namasivayam C (2001) Removal of heavy metals from industrial wastewaters by adsorption onto activated carbon prepared from an agricultural solid waste. *Bioresour Technol* 76(1):63–65
51. Kishor R, Purchase D, Ferreira LFR, Mulla SI, Bilal M, Bharagava RN. (2020) Environmental and health hazards of textile industry wastewater pollutants and its treatment approaches
52. Klapiszewski Ł, Bartczak P, Wysokowski M, Jankowska M, Kabat K, Jesionowski T (2015) Silica conjugated with kraft lignin and its use as a novel “green” sorbent for hazardous metal ions removal. *Chem Eng J* 260:684–693
53. Kriaa A, Hamdi N, Srasra E (2011) Adsorption studies of methylene blue dye on Tunisian activated lignin. *Russ J Phys Chem A* 85(2):279–287
54. Lataye DH, Mishra IM, Mall ID (2009) Adsorption of α -picoline onto rice husk ash and granular activated carbon from aqueous solution: equilibrium and thermodynamic study. *Chem Eng J* 147(2–3):139–149
55. Lee SL, Park JH, Kim SH, Kang SW, Cho JS, Jeon JR, Lee YB, Seo DC. (2019) Sorption behavior of malachite green onto pristine lignin to evaluate the possibility as a dye adsorbent by lignin. *Appl Biol Chem* 62:37. <https://doi.org/10.1186/s13765-019-0444-2>

56. Li J, Li H, Yuan Z, Fang J, Chang L, Zhang H, Li C (2019) Role of sulfonation in lignin-based material for adsorption removal of cationic dyes. *Int J Biol Macromol* [Internet] 135:1171–1181. <https://doi.org/10.1016/j.ijbiomac.2019.06.024>
57. Li Y, Wu M, Wang B, Wu Y, Ma M, Zhang X (2016) Synthesis of magnetic lignin-based hollow microspheres: a highly adsorptive and reusable adsorbent derived from renewable resources. *ACS Sustain Chem Eng* 4(10):5523–5532
58. Li Z, Chen J, Ge Y (2017) Removal of lead ion and oil droplet from aqueous solution by lignin-grafted carbon nanotubes. *Chem Eng J* [Internet] 308:809–817. <https://doi.org/10.1016/j.cej.2016.09.126>
59. Li Z, Ge Y, Wan L (2015) Fabrication of a green porous lignin-based sphere for the removal of lead ions from aqueous media. *J Hazard Mater* 285:77–83
60. Liang FB, Song YL, Huang CP, Zhang J, Chen BH (2013) Adsorption of hexavalent chromium on a lignin-based resin: equilibrium, thermodynamics, and kinetics. *J Environ Chem Eng* [Internet] 1(4):1301–1308. <https://doi.org/10.1016/j.jece.2013.09.025>
61. Lievonen M, Valle-Delgado JJ, Mattinen ML, Hult EL, Lintinen K, Kostianen MA, Paananen A, Szilvay GR, Setälä H, Österberg M (2016) A simple process for lignin nanoparticle preparation. *Green Chem* 18(5):1416–1422
62. Liitiä TM, Maunu SL, Hortling B, Toikka M, Kilpeläinen I (2003) Analysis of technical lignins by two- and three-dimensional NMR spectroscopy. *J Agric Food Chem* 51(8):2136–2143
63. Liu L, Qian M, Song PA, Huang G, Yu Y, Fu S (2016) Fabrication of green lignin-based flame retardants for enhancing the thermal and fire retardancy properties of polypropylene/wood composites. *ACS Sustain Chem Eng* 4:2422–2431
64. Liu X, Zhu H, Qin C, Zhou J, Zhao JR, Wang S (2013) Adsorption of heavy metal ion from aqueous single metal solution by aminated epoxy-lignin. *BioResources* 8(2):2257–2269
65. Liu X, Ma R, Wang X (2019) Graphene oxide-based materials for efficient removal of heavy metal ions from aqueous solution: a review. *Environ Pollut* 252:62–73
66. Lü QF, Luo JJ, Lin TT, Zhang YZ (2014) Novel lignin-poly(N-methylaniline) composite sorbent for silver ion removal and recovery. *ACS Sustain Chem Eng* 2(3):465–471
67. Masilompane TM, Chaukura N, Mishra SB, Mishra AK (2018) Chitosan-lignin-titania nanocomposites for the removal of brilliant black dye from aqueous solution. *Int J Biol Macromol* [Internet] 120:1659–1666. <https://doi.org/10.1016/j.ijbiomac.2018.09.129>
68. Mendoza-Castillo DI, Rojas-Mayorga CK, García-Martínez IP, Pérez-Cruz MA, Hernández-Montoya V, Bonilla-Petriciolet A, Montes-Morán MA (2015) Removal of heavy metals and arsenic from aqueous solution using textile wastes from denim industry. *Int J Environ Sci Technol* 12(5):1657–1668
69. Meng X, Scheidemantle B, Li M, Wang YY, Zhao X, Toro-González M, Singh P, Pu Y, Wyman CE, Ozcan S et al (2020) Synthesis, characterization, and utilization of a lignin-based adsorbent for effective removal of azo dye from aqueous solution. *ACS Omega*
70. Mir SH, Rydzek G, Hasan PMZ, Danish EY, Aslam M, Khosla A (2021) Free standing porous composite films and membranes obtained through substrate-guided assembly. *Mater Lett* 288:129317
71. Mir SH, Ochiai B (2016) Development of hierarchical Polymer@Pd nanowire-network: synthesis and application as highly active recyclable catalyst and printable conductive ink. *ChemistryOpen*. 5(3):213–218
72. Mohan D, Pittman CU, Steele PH (2006) Single, binary and multi-component adsorption of copper and cadmium from aqueous solutions on Kraft lignin—a biosorbent. *J Colloid Interface Sci* 297(2):489–504
73. Nair V, Panigrahy A, Vinu R (2014) Development of novel chitosan-lignin composites for adsorption of dyes and metal ions from wastewater. *Chem Eng J* 254:491–502. <https://doi.org/10.1016/j.cej.2014.05.045>
74. Nasrullah A, Bhat AH, Sada Khan A, Ajab H (2017) Comprehensive approach on the structure, production, processing, and application of lignin. *Lignocellulosic Fibre Biomass-Based Compos Mater* 165–178. <https://doi.org/10.1016/b978-0-08-100959-8.00009-3>

75. Nasrullah A, Khan H, Khan AS, Man Z, Muhammad N, Khan MI, Abd El-Salam NM (2015) Potential biosorbent derived from *Calligonum polygonoides* for removal of methylene blue dye from aqueous solution. *Sci World J*
76. Pan X, Kadla JF, Ehara K, Gilkes N, Saddler JN (2006) Organosolv ethanol lignin from hybrid poplar as a radical scavenger: relationship between lignin structure, extraction conditions, and antioxidant activity. *J Agric Food Chem* 54(16):5806–5813
77. Pang H, Wu Y, Wang X, Hu B, Wang X (2019) Recent advances in composites of graphene and layered double hydroxides for water remediation: a review. *Chem Asian J* 14(15):2542–2552
78. Parajuli D, Inoue K, Ohto K, Oshima T, Murota A, Funaoka M, Makino K (2005) Adsorption of heavy metals on crosslinked lignocatechol: a modified lignin gel. *React Funct Polym* 62(2):129–139
79. Parvin S, Hossen A, Rahman W, Hossen I, Halim A, Biswas BK, Khan AS (2018) Uptake hazardous dye from wastewater using water hyacinth as bio-adsorbent. *Eur J Sustain Dev Res* 3(1):1–10
80. Peternele WS, Winkler-Hechenleitner AA, Gómez Pineda EA (1999) Adsorption of Cd(II) and Pb(II) onto functionalized formic lignin from sugar cane bagasse. *Bioresour Technol* 68(1):95–100
81. Qin Y, Lin X, Lu Y, Wu S, Yang D, Qiu X, Fang Y, Wang T (2018) Preparation of a low reducing effect sulfonated alkali lignin and application as dye dispersant. *Polymers (Basel)* 10(9):1–12
82. Quintana GC, Rocha GJM, Goncalves AR, Velasquez JA (2008) Evaluation of heavy metal removal by oxidised lignins in acid media from various sources. *BioResources* 3(4):11
83. Rahmawati L, Azis MM, Rochmadi R (2021) Methylene blue removal from waste water using sodium lignosulfonate and polyaluminium chloride: optimization with RSM. *AIP Conf Proc* 2349:020035. <https://doi.org/10.1063/5.0052016> Published Online: 24 June 2021
84. Rhaman MM, Karim MR, Hyder MKMZ, Ahmed Y, Nath RK (2020) Removal of chromium (VI) from effluent by a magnetic bioadsorbent based on jute stick powder and its adsorption isotherm, kinetics and regeneration study. *Water Air Soil Pollut.* <https://doi.org/10.1007/s11270-020-04544-8>
85. Richter AP, Bharti B, Armstrong HB, JBrown JS, Plemmons D, Paunov VN, Stoyanov SD, Velev OD (2016) Synthesis and characterization of biodegradable lignin nanoparticles with tunable surface properties. *Langmuir* 32(25):6468–6477
86. Roy A, Chakraborty S, Kundu SP, Adhikari B, Majumder SB (2012) Adsorption of anionic-azo dye from aqueous solution by lignocellulose- biomass jute fiber: equilibrium, kinetics, and thermodynamics study. *Ind Eng Chem Res* 51(37):12095–12106
87. Ruwoldt J (2020) A critical review of the physicochemical properties of lignosulfonates: chemical structure and behavior in aqueous solution, at surfaces. *Surfaces* 3:622–648. <https://doi.org/10.3390/surfaces3040042>
88. Sain MNY (2013) A new method for demethylation of lignin from woody biomass using biophysical methods. *J Chem Eng Process Technol* 04(09)
89. Scheuhammer A, Braune B, Chan HM, Frouin H, Krey A, Letcher R, Loseto L, Noël M, Ostertag S, Ross P, Wayland M (2015) Recent progress on our understanding of the biological effects of mercury in fish and wildlife in the Canadian Arctic. *Sci Total Environ* [Internet] 509–510:91–103. <https://doi.org/10.1016/j.scitotenv.2014.05.142>
90. Šćiban MB, Klačnja MT, Antov MG (2011) Study of the biosorption of different heavy metal ions onto Kraft lignin. *Ecol Eng* 37(12):2092–2095
91. Sohni S, Hashim R, Nidaullah H, Lamaming J, Sulaiman O (2019) Chitosan/nano-lignin based composite as a new sorbent for enhanced removal of dye pollution from aqueous solutions. *Int J Biol Macromol* 132:1304–1317
92. Suteu D, Zaharia C (2012) Application of lignin materials for dye removal by sorption processes. *Lignin: Properties and applications in biotechnology and bioenergy*; Nova Science Publishers: New York, pp 677–688
93. Suteu D, Malutan T, Bilba D (2010) Removal of reactive dye Brilliant Red HE-3B from aqueous solutions by industrial lignin: equilibrium and kinetics modeling. *Desalination* 255(1–3):84–90. <https://doi.org/10.1016/j.desal.2010.01.010>

94. Taleb F, Ammar M, Mosbah M, Salem R, Moussaoui Y (2020) Chemical modification of lignin derived from spent coffee grounds for methylene blue adsorption. *Sci Rep* 10:11048. <https://doi.org/10.1038/s41598-020-68047-6>
95. Tang Y, Hu T, Zeng Y, Zhou Q, Peng Y (2015) Effective adsorption of cationic dyes by lignin sulfonate polymer based on simple emulsion polymerization: isotherm and kinetic studies. *RSC Adv* [Internet] 5(5):3757–3766. <https://doi.org/10.1039/C4RA12229A>
96. Tang Y, Zeng Y, Hu T, Zhou Q, Peng Y (2016) Preparation of lignin sulfonate-based mesoporous materials for adsorbing malachite green from aqueous solution. *J Environ Chem Eng* [Internet] 4(3):2900–2910. <https://doi.org/10.1016/j.jece.2016.05.040>
97. Tejado A, Peña C, Labidi J, Echeverria JM, Mondragon I (2007) Physico-chemical characterization of lignins from different sources for use in phenol-formaldehyde resin synthesis. *Bioresour Technol* 98(8):1655–1663
98. Todorciuc T, Bulgariu L, Popa VI (2015) Adsorption of Cu(II) from aqueous solution on wheat straw lignin: equilibrium and kinetic studies. *Cell Chem Technol* 49(5–6):439–447
99. Verma RK (2021) Eradication of fatal textile industrial dyes by wastewater treatment. *Biointerface Res Appl Chem* 12(1):567–587
100. Wang S, Kong F, Fatehi P, Hou Q (2018) Cationic high molecular weight lignin polymer: a flocculant for the removal of anionic azo-dyes from simulated wastewater. *Molecules* 23(8)
101. Wang Z, Huang W, Bin P, Zhang X, Yang G (2019) Preparation of quaternary amine-grafted organosolv lignin biosorbent and its application in the treatment of hexavalent chromium polluted water. *Int J Biol Macromol* 126:1014–1022. <https://doi.org/10.1016/j.ijbiomac.2018.12.087>
102. Wang X, Jiang C, Hough B, Wang Y, Hao C, Wu J (2018) Carbon composite lignin-based adsorbents for the adsorption of dyes. *Chemosphere* 206:587–596
103. Wawrzekiewicz M, Bartzak P, Jesionowski T (2017) Enhanced removal of hazardous dye from aqueous solutions and real textile wastewater using bifunctional chitin/lignin biosorbent. *Int J Biol Macromol* [Internet]. 99:754–764. <https://doi.org/10.1016/j.ijbiomac.2017.03.023>
104. Wei S, Chen W, Tong Z, Jiang N, Zhu M (2021) Synthesis of a functional biomass lignin-based hydrogel with high swelling and adsorption capability towards Acid Red 73. *Environ Sci Pollut Res* 1–30
105. Wu Y, Zhang S, Guo X, Huang H (2008) Adsorption of chromium(III) on lignin. *Bioresour Technol* 99:7709–7715
106. Xu F, Zhu TT, Rao QQ, Shui SW, Li WW, He HB, Yao RS (2017) Fabrication of mesoporous lignin-based biosorbent from rice straw and its application for heavy-metal-ion removal. *J Environ Sci (China)*. 53:132–140. <https://doi.org/10.1016/j.jes.2016.03.026> (Internet)
107. Yang W, Fortunati E, Bertoglio F, Owczarek J, Bruni G, Kozanecki M, Kenny J, Torre L, Visai L, Puglia D (2018) Polyvinyl alcohol/chitosan hydrogels with enhanced antioxidant and antibacterial properties induced by lignin nanoparticles. *Carbohydr Polym* 181:275–284
108. Yang W, Fortunati E, Gao D, Balestra GM, Giovanale G, He X, Torre L, Kenny JM, Puglia D (2018) Valorization of acid isolated high yield lignin nanoparticles as innovative antioxidant/antimicrobial organic materials. *ACS Sustain Chem Eng* 6(3):3502–3514
109. Yang D, Li H, Qin Y, Zhong R, Bai M, Qiu X (2014) Structure and properties of sodium lignosulfonate with different molecular weight used as dye dispersant. *J Dispersion Sci Technol* 36(4):532–539. <https://doi.org/10.1080/01932691.2014.916221>
110. Yu H, Yang J, Shi P, Li M, Bian J (2021) Synthesis of a Lignin-Fe/Mn binary oxide blend nanocomposite and its adsorption capacity for methylene blue. *ACS Omega* 26(6):16837–16846. <https://doi.org/10.1021/acsomega.1c01405>
111. Yu C, Wang F, Zhang C, Fu S, Lucia LA (2016) The synthesis and absorption dynamics of a lignin-based hydrogel for remediation of cationic dye-contaminated effluent. *React Funct Polym* [Internet] 106:137–142. <https://doi.org/10.1016/j.reactfunctpolym.2016.07.016>
112. Zakzeski J, Bruijninx PCA, Jongerius AL, Weckhuysen BM (2010) The catalytic valorization of lignin for the production of renewable chemicals. *Chem Rev* 110(6):3552–3599
113. Zhai R, Hu J, Chen X, Xu Z, Wen Z, Jin M (2020) Facile synthesis of manganese oxide modified lignin nanocomposites from lignocellulosic biorefinery wastes for dye removal. *Bioresour Technol* [Internet] 315(May):123846. <https://doi.org/10.1016/j.biortech.2020.123846>

114. Zhang Z, Terrasson V, Guéniin E (2021) Lignin nanoparticles and their nanocomposites. *Nanomaterials* 11, 1336. <https://doi.org/10.3390/nano11051336>
115. Zhang S, Wang Z, Zhang Y, Pan H, Tao L (2016) Adsorption of Methylene Blue on Organosolv Lignin from Rice Straw. *Procedia Environ Sci* [Internet] 31:3–11. <https://doi.org/10.1016/j.proenv.2016.02.001>
116. Zhang W, Yang P, Li X, Zhu Z, Chen M, Zhou X (2019) Electrospun lignin-based composite nanofiber membrane as high-performance absorbent for water purification. *Int J Biol Macromol* [Internet] 141:747–755. <https://doi.org/10.1016/j.ijbiomac.2019.08.221>
117. Zhou CG, Gao Q, Wang S, Gong YS, Xia KS, Han B, Li M, Ling Y (2016) Remarkable performance of magnetized chitosan-decorated lignocellulose fiber towards biosorptive removal of acidic azo colorant from aqueous environment. *React Funct Polym* [Internet] 100:97–106. <https://doi.org/10.1016/j.reactfunctpolym.2015.11.010>
118. Zhou Y, Zhang J, Luo X, Lin X (2014) Adsorption of Hg(II) in aqueous solutions using mercapto-functionalized alkali lignin. *J Appl Polym Sci* 131(18):40749
119. Zhu S, Xu J, Kuang Y, Cheng Z, Wu Q, Xie J, Wang B, Gao W, Zeng J, Li J, Chen K (2021) Lignin-derived sulfonated porous carbon from cornstalk for efficient and selective removal of cationic dyes. *Ind Crops Prod* 159:113071. <https://doi.org/10.1016/j.indcrop.2020.113071>

Application of Cellulose-Based Biomaterials in Textile Wastewater



Fatma Abdelghaffar

1 Introduction

Over time, the rapid environmental contamination of limited water resources has become a high public health concern that must be addressed quickly as possible to conserve the earth and its residents for later generations [74]. Owing to the increased demand for industrial products, especially textiles products that make a massive amount of wastewater containing various effluents are released every year. The textiles industry faces significant waste management and environmental commitment challenges. Whereas, textile industries' pollutions (dyes, heavy metals, organic and inorganic salts) [19, 25, 72] are a globally great concern. Especially, dyes effluents, described as the largest class of synthetic colorants, which estimated about 10,000 different forms of synthetic dyes produced over 7×10^5 tons worldwide annually, and a potential hazard to aquatic organisms because the released dyes harm living organisms. The world faces the dangers of such effluent release resulting from industrial growth, posing significant environmental and ecological concerns [39, 61].

Habitually, traditional techniques, advanced oxidation processes, ion exchange, coagulation/flocculation, floatation, reverse osmosis, ultra-filtration, electro-precipitation, adsorption, and membrane separation, are essentially resorted to as convenient technologies to treat industrial wastewater. However, conventional wastewater techniques and purifying cannot lead to the coveted degree of purification to reach accurate or cost-effective elimination levels [13, 31, 82]. Generally, consideration should be given to developing green and eco-friendly wastewater treatment techniques containing fewer chemical reagents, photocatalysts, templates, and precursors with fewer production steps [74].

F. Abdelghaffar (✉)

Textile Research And Technology Institute, National Research Centre, P.O. 12622, Dokki, Giza, Egypt

e-mail: fatma-abdelghaffar@hotmail.com

Therefore, the scientists' awareness increased to use sustainable biomaterials, derived from the plentiful natural resources, to develop efficient and low-cost eco-friendly sorbents for wastewater treatment [102]. Among the sustainable renewable materials, the cellulose-based biomaterial has been a high-priority resource, that cellulose holds high adsorptive properties toward both harmful dyestuffs and heavy metal ions in contaminated water, indicating cellulose's potential as a bio-sorbent.

Biopolymer cellulose is the most available, renewable, sustainable biomaterials, extracted from a broad range of natural materials such as plants, bacteria, fungi, and algae. It is environmentally safe, toxic-free, and biodegradable, making it appealing to apply within biomaterials-based sectors such as cosmetic, food, pharmaceutical, biomedical, and packaging [2, 22, 24, 99]. Furthermore, cellulose-based biomaterials and their derivatives have exhibited, in the wastewater treatment field, high-efficient in removing both organic and inorganic contaminations using sorption, degradation, or coagulation/flocculation processes. This chapter addresses recent advancements, discoveries, and challenges for cellulose-based biomaterials derived from sustainable resources for exploitation in treating wastewater discharged from the textiles industries.

2 Hazards of Textiles Industrial Effluent

Global growing industrialization enhanced the amount of organic and inorganic environmental pollutants in soil and water. The textiles industry is one of the significant industries that consume over half of the world's dyes and organic pigments, and their consumption is expected to increase annually [13, 72]. Synthetic dyes are broadly applied in the textile dyeing process. The azo type, comprising reactive, disperse, and acid dyes, is the most prevalent class of synthetic dyes. Azo dyes account for 65% of all dye production globally [27].

During the textile-producing process, a large number of chemicals and dyestuffs are wasted, such as dyes and pigments, metals, oils, surfactants, detergents, chloride, and sulfate. These effluents are eliminated through discharge into the environment that contribute to water contamination and negatively affect the water quality. Moreover, the textile industries emit harmful gases, dust, volatile organic compounds, as well as other products. The dye in the water environment of rivers, channels, and drains prevents light penetration, reducing photosynthetic activity and oxygen concentration in water, creating an ecological imbalance and threaten aquatic lives and species [9, 14, 46, 68]. Moreover, dye-contamination wastewater can also reach deep soil layers, impacting groundwater safety and posing a critical health risk to humans and marine life [31] (Fig. 1). Textile effluent is also mutagenic, carcinogenic, and highly toxic to all life forms.

A direct approach to limiting effluent waste in textiles industries is using alternative biodegradable, non-toxic dyes and chemicals. However, wastewater treatment itself is numerous processing sectors. In recent decades, various techniques and innovations for effluent processing have been developed in accordance with the

industry type. These innovations focused on finding a cost-effective and safe way to handle wastewater. Today, biochemical, physicochemical, incorporated processing, and other technologies are the most effective processing technology for textile dyeing effluents.

3 Sustainable Biomaterial for Wastewater Treatment

Biomaterials are natural or synthetic materials that possess a group of properties, including biological, chemical, physical, and mechanical properties that make them appropriate for safe, efficient, and credible use, i.e., polymers, metals, ceramics, and composites materials. Biomaterials can also be developed, designed, and functioned for use within medical and biological systems and engineering biomedical devices to interact directly with living organisms [8, 69, 93, 94]. Sustainable biomaterials are an interrelation between biomaterials and renewable natural resources that offers us a promising future to implement pioneering sustainable development strategies in the coming years. Sustainable bio-polymers are polymeric organic compounds derived from renewable sources (plants, animals, or microorganisms) that comprise covalently linked mono parts to form larger molecules.

Affordable sustainable biopolymers like polysaccharides of varying structure, size, and molecular chains, including cellulose, starch, chitin/chitosan, pectin, gum, and alginate, possess prominent structural characteristics, biocompatibility, modification ease, nontoxicity, abundant availability, and promising potentials, making them a desirable competitor for industries wastewater treatment. Cellulose biopolymer: micro-cellulose, nanocellulose, composite, is a promising sustainable biomaterial for sorption, membrane filtration, and photocatalytic in wastewater treatment applications.

4 Cellulose-Based Biomaterial

Cellulose is non-toxic, biodegradable, renewable polymer biomaterial, naturally occurs on the earth. Cellulose polymer distributes widely in the cell walls of plants, marine organisms, and even microorganisms (i.e., bacteria, algae, fungi), which depend on cellulose and use it in its life cycle [3, 51, 65]. These involve wood fibers (softwoods and hardwoods), seed fiber (cotton), bark fibers (jute, hemp, ramie, flax), grasses (bamboo, bagasse), bacteria (*Acetobacter xylinum*), and algae (*Valonica ventricosa*) [27, 81] (Fig. 2).

Plant-derived cellulose also contains hemicellulose, lignin, pectin, and waxes, as well as cellulose, while bacteria-derived cellulose is free of these substances. However, the cost of bacteria-derived cellulose is comparatively high. Thus, for mass production, plant-derived cellulose is favored due to its lower cost. Cotton and

wood pulp are the most fundamental sources of cellulose for industrial processes [64].

Cellulose is the principal component of cardboard, paper, flax, jute, cotton, or other plant textiles fibers'. It is also used to manufacture cellulose derivatives, films, and fiber. In reality, although cellulose was the base to produce the first commercial polymers (cellophanes, celluloids), cellulose-based materials have not yet been wholly explored [26].

Cellulose has outstanding physicochemical and mechanical properties as a natural polymer, i.e., bio-degradation, high chemical resistance, good durability, high thermal stability, excellent strength, and good bio-compatibility, with a high degree of polymerization estimated at 10,000 for natural cellulose chains and 15,000 for original cotton cellulose. It also has natural drawbacks, i.e., weak antibacterial properties, poor dimensional stability, and lack of thermoplastics. Moreover, original cellulose is insoluble in water or soluble weakly in general organic solvents due to strong hydrogen links within molecules or among molecules, limits its application and processing [5, 42, 47].

4.1 Cellulose Structure

Search a molecular structure of cellulose is critical to understand cellulose's characteristic properties compared to other polysaccharides linked through the α -glycosidic bond [62, 73]. Anselme Payen, a French chemist, was the pioneer to discover and describe cellulose in a study published in 1839. The cellulose molecular formula was also defined, $C_6H_{10}O_5$, concomitantly using elemental analysis [10, 47, 49, 54]. Cellulose is a linear polysaccharide composed of repeating β -D-glucopyranose units linked to three reactive hydroxyl groups for each anhydroglucose unit (AGU), making it a high level of functionality (Fig. 3). Moreover, via substituting other chemical groups for these reactive OH groups, such as carboxymethyl, acetyl, methyl, and so on, different cellulose derivative compounds may be synthesized [28] (Fig. 2).

4.2 Microorganism-Derived Cellulose

Microbial-based cellulose denotes an extracellular polysaccharide created by several microorganisms including, fungi, algae (*Valonica ventricosa*), and various bacteria types involving Gram-negative bacteria (i.e., *Agrobacterium*, *Acetobacter Azotobacter*, *Alcaligenes*, *Pseudomonas*, *Rhizobium*, *Salmonella*), along with Gram-positive bacterial types (i.e., *Sarcina ventriculi*). Adrian J. Brown announced in 1886 the first cellulose report derived from bacteria, precisely *Acetobacter xylinum*, subsequently called bacteria cellulose and revealed to have a similar chemical structure as plant cellulose. Bacterial cellulose (BC) manifests different chemical and physical properties, including shapes, morphology, and applications due to the diverse species

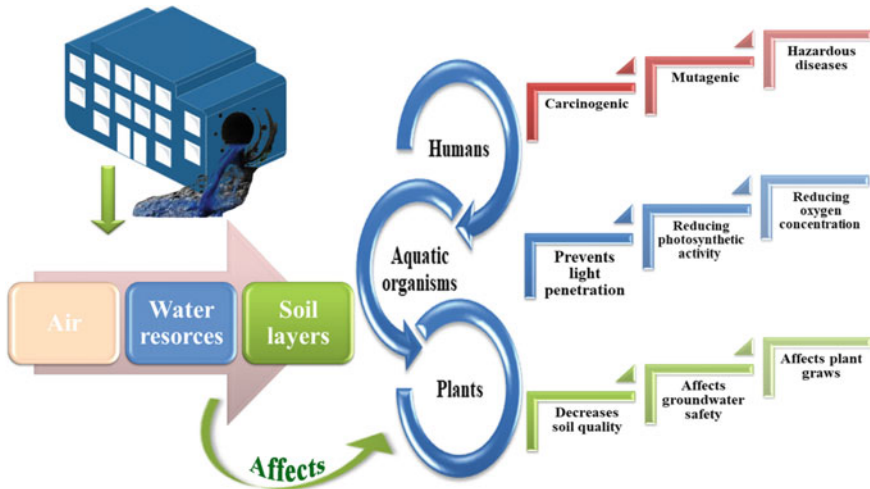


Fig. 1 The impact of textile industries effluent discharged into the environment

Fig. 2 Biomaterials sources for cellulose



of bacteria produced. It also varies from properties of plant cellulose in respect of purity, features, and macromolecular properties. BC has a high water sorption potential, high mechanical strength, high porosity, and a high aspect ratio in BC fibers [30, 52, 80, 88, 91].

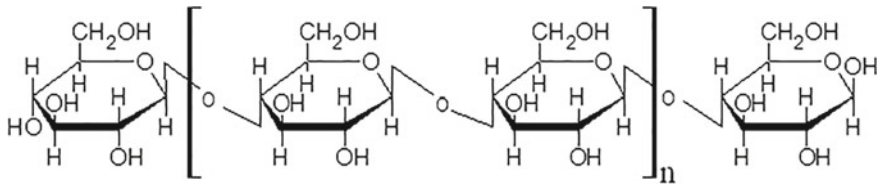


Fig. 3 Cellulose molecular structure

Bacterial-derived cellulose can be utilized as a sustainable polymer biomaterial, because of its excellent properties, in a variety of industrial and medical applications including, water treatment, adsorbent, filter membrane, food packing, cosmetics, artificial blood vessels, pharmaceutical industries, scaffolds for tissue engineering, transparent coating, battery separator, electric conductors or magnetic materials, and ethanol production [87, 91].

Principal hurdles for BC production and applications are the high nutrients cost and low productivity on an industrial level. A feasible strategy to avoid these hurdles is to take advantage of alternative low-cost, availability, and renewable carbon sources, thus reducing costly commercial nutrients use and low productivity [35, 57]. Biotechnological techniques enable scientists and researchers to isolate bacteria cellulose polymeric materials from sustainable natural sources such as industrial waste. The use of industrial waste to produce BC would also help with waste management, environmental clean-up, as well as lower waste disposal costs for industries. Among those industrial wastes is textile waste, consisting of natural fibers waste, as affordable carbon sources for bacterial cellulose production due to its rich cellulose contents.

Additionally, the BC can also be developed to remove metal ions and dyes from the textiles industry. Table 1 reviewed some publications that explored the application potential of BC as an adsorbent and membrane filtration for industrial wastewater filtration, as follows.

4.3 Agricultural Waste-Derived Cellulose

Every day, the world uses a wide range of agricultural materials to turn into various industrial products. After processing, agricultural materials generate a considerable volume of waste that often contains a high cellulose concentration [34]. Agricultural waste materials are lignocellulosic materials, composed of natural polymers mixture including cellulose, lignin, and hemicellulose [7]. The lignocellulosic material consists of organic components: oxygen (O), carbon (C), and hydrogen (H), in addition, a variety of inorganic elements, i.e., calcium (Ca), magnesium (Mg), potassium (K), sodium (Na), phosphorus (P), sulfur (S), chlorine (Cl), and nitrogen (N). Further, lignin comprises functional groups, containing alcohols, carboxylic acid, aldehydes, phenolic groups, ketones, and ether. Those organic and inorganic components collaborate to play a crucial roles in the sorption technique [60]. Besides,

Table 1 Microorganisms-derived cellulose

Microorganism	Pollution types	Process	Modification	Dye removal %	Time	References
<i>Acetobacter xylinum</i>	Metal ions (Cr ⁶⁺ , Cu ²⁺ , Pb ²⁺) Dye (Congo red)	Adsorption	Magnetic composites	–	–	[12]
<i>Acetobacter xylinum</i>	Dyes (Rhodamine B)	Adsorption	Nanocomposite	90%	180 min	[11]
<i>Acetobacter xylinum</i> NUST4.2	Dyes (Methylene blue) Antibiotics (tetracycline)	Adsorption	Composites	–	–	[29]
–	Dyes (Methylene Blue, Direct Orange S, Procion Red mx-5B, Stilbene Yellow)	Nano-filtration membrane	Nanofiber composite	–	–	[100]
<i>Acetobacter xylinum</i>	Metals ions (Cu(II), Pb(II))	Adsorption				[79]
<i>Bacillus paramycoides</i>	Dyes (Methylene Blue)	Nanofibrous membrane	Nanofibrous	93%	48 h	[97]
<i>Gluconacetobacter hansenii</i> NCIM 2529	Metal ions (Pb ²⁺ , Cd ²⁺ , Ni ²⁺) Dyes (Aniline blue)	Adsorption	–	80%	60 min	[59]
<i>Gluconacetobacter xylinus</i> (ATCC 10,245)	Metal ions (Cu ²⁺ , Cr ⁶⁺) Dyes (Active red X-3B)	Adsorption	–	Approaching to 100%	–	[50]
<i>Acetobacter xylinum</i> NUST4.2	Dyes (Rhodamine B, Methylene blue)	Membrane (photocatalyst degradation)	–	–	–	[96]

agricultural waste materials are plentiful, economical, eco-friendly, renewable, and compose an efficient alternative to acquiring high-value sorbents [89]. As a result, research and development are shifting toward using agricultural waste materials as bio-sorbents for various effluents. Table 2 exhibits cellulose-based agricultural waste application for wastewater treatment.

5 Application of Cellulose-Based Biomaterial in Wastewater Treatment

From an environmental standpoint, cellulose-based biomaterials are an excellent option for textile effluent treatment because it is a sustainable, biodegradable, and reusability materials with a diverse variety of resources. Furthermore, the presence of internal and external hydroxyl groups within cellulose promotes various cellulose modification methods for some different functionality by replacing some of these groups with various functional groups, such as $-\text{COOH}$, $-\text{NH}_2$, $-\text{CHO}$, and $-\text{SO}_3\text{H}$ [55].

Currently, cellulose production and development face several challenges, including higher rigidity, solubility, viscosity, stiffness, and inclination to crystallize or form fibrous structures. Cellulose and its derivatives are broadly contributed in a lot of industrial applications (e.g., cosmetic, medicine, pharmaceuticals, biomedicine, nanocomposites, barrier films, membranes, bioplastics, electronics, and supercapacitors).

Cellulose can be modified to promote its adsorption capacity to various types of pollutants. Modified cellulose includes chemical or physical alterations that enhance its adsorption properties, such as particle size and structure, increased surface area and adsorption sites, and homogeneous mesopores (amount and volume) [16, 75]. Several chemical modifications of cellulose, i.e., oxidation, esterification, etherification, grafting, halogenations, etc., have been executed to accomplish an efficient adsorption capability for organic and inorganic pollutants, as reported in the literature [90]. In addition, it can be chemically modified to form nanofibers, nanofibrils, nanocrystals, and crystallites. The cellulose combination with other materials has also been performed to create a composite or nanocomposite system [27]. The following explores the application of cellulose-based biomaterials and some of their fundamental modifications in textile wastewater treatment: cellulose-based activated carbon, bio-nano cellulose, cellulose-based gels, cellulose-based composite/nanocomposite, and cellulose-based photocatalytic.

Table 2 Agriculture waste-derived cellulose

Agriculture waste	Pollution types	Process	Modification	Adsorption capacity	References
<i>Juncus effusus</i>	C.I. Reactive Red 195 C.I. Reactive Blue	Adsorption	Magnetic cellulose	58.21 mg/g 86.06 mg/g	[101]
Sugarcane bagasse lettuce roots	Mn(II), Zn(II), Fe(II), Cu(II)	Adsorption	Chemical modified	–	[56]
Algerian olive cake waste	Acid blue 80	Adsorption	–	–	[86]
Sugarcane Bagasse	Methylene blue	Adsorption	Nanocellulose	35 mg/g	[41]
Sugarcane Bagasse	C.I. Reactive black 5 C.I. Acid orange 10	Adsorption	Cationization	–	[1]
Sugarcane Bagasse	Drimarine Yellow HF-3GL direct dye	Adsorption	Hybrid bionanocomposite	–	[44]
Sugarcane Bagasse	Rhodamine B direct dye	Adsorption	Composites	–	[43]
Corn stalk pith	Methylene blue	Adsorption	Malic acid-modified	328.46 mg/g	[66]
				566.27 mg/g	
				29.3 g/g	
	Crystal violet				

(continued)

Table 2 (continued)

Agriculture waste	Pollution types	Process	Modification	Adsorption capacity	References
Orange peel	Isopropyl alcohol Soybean oil			44.1 g/g	
	Lubricating oil			37.2 g/g	
	Diesel oil			33.8 g/g	
Orange peel	Methylene blue	Adsorption	-	256.4 mg/l	[23]
	Congo red			102.0 mg/g	
Banana peels	Methyl orange, Methylene blue,	Adsorption	-	-	[4]
	Methyl violet, Rhodamine B, Congo red, Amido black 10B				
Rice straw	CI Reactive Orange	Adsorption	Polyelectrolyte Layer-by-Layer assembly	-	[20]
	91, CI Acid Red 1, CI Reactive Yellow 145, CI Reactive Red 4, CI Reactive Red 195, CI Reactive Violet 5, CI Reactive Blue 19				
	Malachite green dye	Adsorption	Cross-linked graft copolymers	-	[48]
	Crystal violet dye			-	
Rice husk	Congo red dye			-	
	Ni(II), Cu(II)			112.74, 109.77 mg/g	
	Diamine Green B	Adsorption	Cationization	207.15 mg/g	[36]
Rice husk	Acid Black 24			268.88 mg/g	
	Congo red			580.09 mg/g	
<i>Eichhornia crassipes</i>	C.I. Acid Red 40	Adsorption	Coated	-	[19]
	C.I. Reactive Orange 91 C.I. Direct Red				

5.1 Cellulose-Based Activated Carbon

Activated carbons remain the most extensively prevalent sorbents in wastewater treatment worldwide, in the light of many properties that make it especially desirable for the purpose, including a high specific surface, an affinity for a wide range of compounds, and ease of regeneration. Despite its widespread use, the ultimate goal is to reduce activated carbon use due to its high expense [13, 15]. Fortunately, the commercially, costly, energy-consuming activated carbon can effectively be substituted with renewable alternatives and low-cost biosorbents from agriculture wastes [18].

An ideal biosorbent should meet the following criteria: availability, rapid sorption, high absorption potential, reusability, and low cost. Thus, preparing activated carbon based on sustainable biosources is one tool for producing low-cost and effective sorbents to remove various kinds of textile effluent from wastewater. As a result, scientists are looking at low-cost adsorbents as viable options for wastewater treatment.

Numerous agriculture wastes have been researched to prepare activated carbon for dye sorption. The adsorption of methylene blue and iodine from aqueous medium through activated carbon, developed from two cellulosic wastes, namely old cladodes and prickly pear seeds, were reviewed by Ouhammou et al. [63]. Whereas the adsorption of phenol, Acid Red 27 dye, and Cu^{2+} ions by activated carbon, derived from original cellulose, particularly coconut fibers and jute, were considered by Phan et al. [67].

On the other hand, Khamkeaw et al. generated activated carbon from bacterial cellulose via activating phosphoric acid through a carbonization temperature at 500 °C to remove methylene blue, resulting in a maximum sorption capability of 505.8 mg/g [45].

5.2 Bio-Nano Cellulose

Cellulose microfibrils and their nanofibers have recently acquired awareness; as a novel type of cellulose for numerous applications, owing to the fact that they are very fine natural polymeric has unique properties that are not possible to achieve with synthetic polymers [33]. To separate and modify cellulose fibrils from cellulose-based biomaterials, two stages are required:

1. Pretreatment, i.e., enzymatically or chemically, to make the following treatment reactions uniformity;
2. Separation of pretreated cellulose fibrils into microfibrils or crystals through enzyme hydrolysis, acid hydrolysis, or mechanical treatment [64].

Cellulose nanocrystallizations are generally sustainable nano-sized biomaterials that can be derived from the most abundant and renewable cellulose-rich sources,

such as plants or bacteria, and is one of the most prevalent techniques, and may be classified into the following categories:

- **Cellulose nanocrystals (CNC)** (less than 10 nm width and 25,500 nm length, produced through strong acid hydrolysis).
- **Cellulose nanofibrils (CNF)** (greater aspect rate than that of CNC, produced through high-pressure homogenizers moreover oxidation of TEMPO).
- **Hairy CNCs (HCNC)** (hairy neutral cellulose nanocrystals with stable sterile structure, produced through periodate oxidation) [53, 95].

Cellulose nanocrystallizations deliver a novel type of innovative and renewable nanoparticles, which can be merged and mixed with other micro- or nanomaterials to generate sustainable bio-sorbent. Numerous researches have been published about the nanocrystal cellulose application toward the removal of dyes. Tan et al. inspected the ability of commercial nanocrystalline cellulose (NCC) flakes to adsorb methylene blue. They also compared their adsorption capacity to other nanomaterials and discovered that NCC flakes are promising absorbent nanomaterials with a high adsorption potential of approximately 188.7 mg/g, which fits well with Langmuir Isotherm [83]. Jin et al. extracted nanocrystalline cellulose (NCC) from hardwood kraft pulp. Following, they grafted it with ethylenediamine to obtain ANCC. ANCC adsorption efficiency has been applied to absorb anionic dyes from aqueous solutions. The authors realized that the maximum adsorption capability of about 555.6 mg/g in acidic conditions [37]. Shanmugarajah and his colleagues isolated nanocrystalline cellulose (NCC) from oil palm waste. They demonstrate its high potential as a bio-sorbent for effective MB removal in aqueous solutions. The FTIR and ASTM results showed that the NCC was successfully isolated from EFB using a multistep method to effectively remove hemicellulose, lignin, dirt, and waxy substances. Following this, the remaining cellulose component was hydrolyzed to the cellulosic nanomaterial. The results from adsorption kinetic studies indicated that the sorption study follows pseudo-second-order kinetic model [78].

5.3 Cellulose-Based Gels

Hydrogels are hydrophilic polymers with a 3D network structure, composed of polymer chains cross-linked either chemically, physically, or by polymerization, and contain a significant amount of solvent or dispersant. Aerogels, ordinarily, are acquired via drying the building blocks material or the hydrogel, wherein an aqueous status is supplanted by air [38, 40].

Cellulose-based gels (hydrogels or aerogels) development has lately drawn a great deal of attention. Cellulose and its derivatives (e.g., nanocellulose), derived from agriculture waste, can be developed either chemically or physically to design high-performing cellulose-based absorbents hydrogels. Further, they could be incorporated with natural or synthetic polymers to design cellulose-based composite absorbents hydrogels. For example, Moharramia et al. applied cellulose nanocrystals

derived from agricultural waste to synthesize starch-based hydrogel nanocomposites, particularly for cationic dye adsorption. They considered the effects of nano-adsorbent dosage, pH, dye concentration, time, and temperature on the adsorption of crystal violet and methylene blue and found that the adsorption capacity was 2500.0 mg/g for crystal violet and 1428.6 mg/g for methylene blue [58].

Concerning the Cu (II) Ions sorption, carboxymethyl cellulose-based hydrogels were prepared using cellulose extracted from sugarcane bagasse. The fabrication of hydrogel was conducted under microwave-assisted irradiation that helped to enhance the reaction efficiency and decrease reaction time compared with a conventional method. This study reveals the promising potential of carboxymethyl cellulose-based hydrogels to be applied and reused in Cu (II) ions removal from contaminated water [6]. Another study used cellulose derived from rice straw for nanocellulose aerogels preparation to absorb Reactive Black 5. They incorporated the iron oxide nanoparticles in the composite matrix to prepare magnetic nanocomposite, which helps in the simple extraction of aerogel after adsorption of the dyes [17].

5.4 Cellulose-Based Catalyst or Photocatalyst

Cellulose-based biomaterials are excellent competitors for use as polymer support to increase semiconductor photodegradation efficiency. Cellulose has the potential to increase the stability and growth control of metal nanoparticles besides preserving their unique morphology. Under visible light or UV irradiation, numerous studies have conducted photocatalytic degradation utilizing cellulose-based metal oxide nanostructures within the forms of a membrane, thin film, filament, or nanocomposite materials. Comparing to individual components, cellulose/metal nanoparticles (ZnO, TiO₂, Fe₂O₃, graphene oxide, and AgNPs) nano-composites have been employed as photocatalysts to increase the degradation ratio of organic contaminants [21, 32, 77].

Rajagopal et al. extracted micro-cellulose (MC) from banana pseudostem to fabricate a composite, as a photocatalyst, with titanium dioxide (TiO₂) to degrade cationic and anionic dyes. The Langmuir–Hinshelwood kinetic model was used to examine the composite performance. The findings indicated that the composite is highly effective in degrading, removing 99% of Methylene blue (200 mg/L) dye in 150 min. Acid violet and Methyl violet dyes, on the other hand, took 6 and 7 h of reaction time to fully degrade [70].

Tavker et al. employed cellulose-based fruit waste to support molybdenum sulfide nanostructures. The cellulose-supported nanostructures photocatalytic performance was evaluated toward the Rhodamine B dye degradation, compared to bare MoS₂ nano-petals. The findings found that cellulose enhances the synthesized nanostructure photocatalytic efficiency for RB to 96% [85]. In another study, synthesized silver phosphate nanostructures supported by cellulose were isolated from different fruits. The photodegradation rate of Rhodamine B, using cellulose support nanostructures, was observed to be high compared to original materials [84]. Zhang et colleagues

checked bi-layered bacterial cellulose composite (CuS/BC) photocatalytic performance for wastewater purification, which exhibited degradation efficiency of 93.4% in 80 min for MB dye solution, indicating that the bi-layered BC bio foam can be used to purify dyeing wastewater. This work paves the stage for the future creation of multifunctional solar evaporators [98].

Furthermore, cellulose-based biomaterials can play a dual role in the production of silver nanoparticle photocatalysts by green synthesized the catalyst as well as increasing its photocatalytic activity. Wen et al. handled nano-tea cellulose (TTC nanofibers) to immobilize AgNPs to prepare the photocatalysts Ag-TTC-PVA composite film using a simple solvent casting process. The development of the photocatalytic film displayed a good potential of silver nanocomposite for Methyl orange dye photodegradation [92]. Another research assessed the green fabrication of AgNPs by *Ruellia tuberosa* leaf extract for photocatalytic degradation against crystal violet and Coomassie brilliant blue. According to the findings, the higher percentages of photocatalytic degradation of CV and CBB were determined to be 87% and 74%, respectively [76]. Furthermore, green algae (*Chlorella vulgaris*) were reported for the biosynthesis of AgNPs photocatalytic. AgNPs synthesized revealed 96.51% photocatalytic decolorization efficiency for methylene blue dye [71].

6 Future Outlook and Conclusions

Here, this chapter provides a fundamental overview of cellulose-based biomaterials application in textile wastewater purification is of great importance. Cellulose biomaterials, based on plants or microorganisms, are promising, low-cost, simple, available, and economic bioresources for wastewater treatment applications, including sorption, membrane filtration, and photocatalytic. Based on these findings, we discovered that using unmodified cellulose sorbents for textile effluent removal from wastewater was ineffective. However, various kinds of modification strategies have been described in earlier researches and appeared to increase the adsorption performance of bio-sorbents-based cellulose toward textile wastewater. Furthermore, several experiments onto the sorption of dyestuffs and metal ions onto bio-sorbents-based cellulose were performed in aqueous solutions and are dependent on a laboratory scale, according to the literature. These studies' abilities should not be overlooked. Thus, in order to be feasible and commercially viable, industrial waste adsorbents must be successfully implemented in actual industrial wastewater. As a final note, this chapter may inform researchers in future studies on textile wastewater treatment. The future features of this chapter are summarized as follows,

- It is expected that prospective studies will promote the development of low-cost, availability, and efficient bio-sorbents.
- A good design of bio-sorbents should be regarded for efficient textile effluent elimination in a large-scale wastewater treatment system.

- Despite Activated carbons' widespread use, it is a significant goal to substitute commercial activated carbon with an efficient sustainable renewable low-cost adsorbent.
- According to the literature, there have been some promising works on the creation and use of activated carbon derived from cellulose biomaterials to adsorb polluted. However, the effort is insufficient, and lack of systematic studies.
- It is predicted that research and development will result in industrially scalable techniques to fabricate sorbents from bacterial cellulose.

References

1. Abdelghaffar F, Abdelghaffar RA, Mahmoud SA, Youssef BM (2019) Modified sugarcane bagasse for the removal of anionic dyes from aqueous solution. *Pigm Resin Technol* 48:464–471. <https://doi.org/10.1108/PRT-01-2019-0003>
2. Abdelghaffar F, Mahmoud MG, Asker MS, Mohamed SS (2021) Facile green silver nanoparticles synthesis to promote the antibacterial activity of cellulosic fabric. *J Ind Eng Chem* 99:224–234. <https://doi.org/10.1016/j.jiec.2021.04.030>
3. Anand SC, Kennedy JF, Mirafat M, Rajendran S (2006) Medical textiles and biomaterials for healthcare: incorporating. In: Proceedings of MEDTEX03 international conference and exhibition on healthcare and medical textiles. Taylor & Francis, US
4. Annadurai G, Juang R-S, Lee D-J (2002) Use of cellulose-based wastes for adsorption of dyes from aqueous solutions. *J Hazard Mater* 92:263–274. [https://doi.org/10.1016/S0304-3894\(02\)00017-1](https://doi.org/10.1016/S0304-3894(02)00017-1)
5. Arca HC, Mosquera-Giraldo LI, Bi V, Xu D, Taylor LS, Edgar KJ (2018) Pharmaceutical applications of cellulose ethers and cellulose ether esters. *Biomacromol* 19:2351–2376. <https://doi.org/10.1021/acs.biomac.8b00517>
6. Baiya C, Nannuan L, Tassanapukdee Y, Chailapakul O, Songsrirote K (2019) The synthesis of carboxymethyl cellulose-based hydrogel from sugarcane bagasse using microwave-assisted irradiation for selective adsorption of Copper(II) ions. *Environ Prog Sustain Energy* 38:S157–S165. <https://doi.org/10.1002/ep.12950>
7. Bakar NA, Othman N, Yunus ZM, Altowayti WAH, Tahir M, Fitriani N, Mohd-Salleh SNA (2021) An insight review of lignocellulosic materials as activated carbon precursor for textile wastewater treatment. *Environ Technol Innov* 22:101445. <https://doi.org/10.1016/j.eti.2021.101445>
8. Biswal T, BadJena SK, Pradhan D (2020) Sustainable biomaterials and their applications: a short review. *Mater Today: Proc* 30:274–282. <https://doi.org/10.1016/j.matpr.2020.01.437>
9. Carneiro PA, Umbuzeiro GA, Oliveira DP, Zanoni MVB (2010) Assessment of water contamination caused by a mutagenic textile effluent/dyehouse effluent bearing disperse dyes. *J Hazard Mater* 174:694–699. <https://doi.org/10.1016/j.jhazmat.2009.09.106>
10. Chen P, Cho SY, Jin H-J (2010) Modification and applications of bacterial celluloses in polymer science. *Macromol Res* 18:309–320. <https://doi.org/10.1007/s13233-010-0404-5>
11. Chen S, Huang Y (2015) Bacterial cellulose nanofibers decorated with phthalocyanine: preparation, characterization and dye removal performance. *Mater Lett* 142:235–237. <https://doi.org/10.1016/j.matlet.2014.12.036>
12. Chen X, Cui J, Xu X, Sun B, Zhang L, Dong W, Chen C, Sun D (2020) Bacterial cellulose/attapulgitic magnetic composites as an efficient adsorbent for heavy metal ions and dye treatment. *Carbohydr Polym* 229:115512. <https://doi.org/10.1016/j.carbpol.2019.115512>
13. Chowdhury MF, Khandaker S, Sarker F, Islam A, Rahman MT, Awual MR (2020) Current treatment technologies and mechanisms for removal of indigo carmine dyes from wastewater: a review. *J Mol Liq* 318:114061. <https://doi.org/10.1016/j.molliq.2020.114061>

14. Crini G (2005) Recent developments in polysaccharide-based materials used as adsorbents in wastewater treatment. *Prog Polym Sci* 30:38–70. <https://doi.org/10.1016/j.progpolymsci.2004.11.002>
15. De Gisi S, Lofrano G, Grassi M, Notarnicola M (2016) Characteristics and adsorption capacities of low-cost sorbents for wastewater treatment: a review. *Sustain Mater Technol* 9:10–40. <https://doi.org/10.1016/j.susmat.2016.06.002>
16. Duri S, Tran CD (2013) Supramolecular composite materials from cellulose, chitosan, and cyclodextrin: facile preparation and their selective inclusion complex formation with endocrine disruptors. *Langmuir* 29:5037–5049. <https://doi.org/10.1021/la3050016>
17. El-Zawahry M, Hassabo A, Abdelghaffar F, Abdelghaffar R, Hakeim O (2021) Preparation and use of aqueous solutions magnetic chitosan/nanocellulose aerogels for the sorption of Reactive Black 5. *Biointerface Res Appl Chem* 11:12380–12402
18. El-Zawahry MM, Abdelghaffar F, Abdelghaffar RA, Hassabo AG (2016) Equilibrium and kinetic models on the adsorption of Reactive Black 5 from aqueous solution using Eichhornia crassipes/chitosan composite. *Carbohydr Polym* 136:507–515
19. El-Zawahry MM, Abdelghaffar F, Abdelghaffar RA, Mashaly HM (2016) Functionalization of the aquatic weed water hyacinth Eichhornia crassipes by using zinc oxide nanoparticles for removal of organic dyes effluent. *Fibers Polym* 17:186–193. <https://doi.org/10.1007/s12221-016-4818-3>
20. El Zawahry M, Hakeim O, Abdelghaffar F, El-Hawary N (2014) Modification of rice straw via polyelectrolyte layer-by-layer assembly for high performance dye adsorption. *Res J Chem Sci* 4:52–60
21. Fan J, Yu D, Wang W, Liu B (2019) The self-assembly and formation mechanism of regenerated cellulose films for photocatalytic degradation of C.I. Reactive Blue 19. *Cellulose* 26:3955–3972. <https://doi.org/10.1007/s10570-019-02350-y>
22. Gopi S, Balakrishnan P, Chandradhara D, Poovathankandy D, Thomas S (2019) General scenarios of cellulose and its use in the biomedical field. *Mater Today Chem* 13:59–78. <https://doi.org/10.1016/j.mtchem.2019.04.012>
23. Guiza S, Franck L, Bagané M (2018) Adsorption of dyes from aqueous solution under batch mode using cellulosic orange peel waste. *Desalin Water Treat* 113:262–269
24. Hakeim OA, Abdelghaffar F, Haroun AA (2019) UV-protection of cellulosic fabric prints using hyperbranched polyester-stabilized titania coating. *Prog Org Coat* 136:105295. <https://doi.org/10.1016/j.porgcoat.2019.105295>
25. Haroun AA, Abdelghaffar F, Hakeim OA (2021) Preparation of chitosan/hyperbranched polyester/cobalt composite for Acid Blue 277 dye adsorption. *Biointerface Res Appl Chem* 11:11653–11665
26. Havstad MR (2020) Chapter 5—Biodegradable plastics. In: Letcher TM (ed) *Plastic waste and recycling*. Academic Press, pp 97–129. <https://doi.org/10.1016/B978-0-12-817880-5.00005-0>
27. Hokkanen S, Bhatnagar A, Sillanpää M (2016) A review on modification methods to cellulose-based adsorbents to improve adsorption capacity. *Water Res* 91:156–173. <https://doi.org/10.1016/j.watres.2016.01.008>
28. Homem NC, Amorim MTP (2020) Synthesis of cellulose acetate using as raw material textile wastes. *Mater Today: Proc* 31:S315–S317. <https://doi.org/10.1016/j.matpr.2020.01.494>
29. Hu Y, Chen C, Yang L, Cui J, Hao Q, Sun D (2019) Handy purifier based on bacterial cellulose and Ca-montmorillonite composites for efficient removal of dyes and antibiotics. *Carbohydr Polym* 222:115017. <https://doi.org/10.1016/j.carbpol.2019.115017>
30. Hussain Z, Sajjad W, Khan T, Wahid F (2019) Production of bacterial cellulose from industrial wastes: a review. *Cellulose* 26:2895–2911. <https://doi.org/10.1007/s10570-019-02307-1>
31. Islam MA, Ali I, Karim SMA, Hossain Firoz MS, Chowdhury A-N, Morton DW, Angove MJ (2019) Removal of dye from polluted water using novel nano manganese oxide-based materials. *J Water Process Eng* 32:100911. <https://doi.org/10.1016/j.jwpe.2019.100911>
32. Ismail M, Akhtar K, Khan M, Kamal T, Khan MA, Asiri AM, Seo J, Khan SB (2019) Pollution, toxicity and carcinogenicity of organic dyes and their catalytic bio-remediation. *Curr Pharm Des* 25:3645–3663

33. Iwamoto S, Isogai A, Iwata T (2011) Structure and mechanical properties of wet-spun fibers made from natural cellulose nanofibers. *Biomacromol* 12:831–836. <https://doi.org/10.1021/bm101510r>
34. Jamshaid A, Hamid A, Muhammad N, Naseer A, Ghauri M, Iqbal J, Rafiq S, Shah NS (2017) Cellulose-based materials for the removal of heavy metals from wastewater—an overview. *ChemBioEng Rev* 4:240–256. <https://doi.org/10.1002/cben.201700002>
35. Jang WD, Hwang JH, Kim HU, Ryu JY, Lee SY (2017) Bacterial cellulose as an example product for sustainable production and consumption. *Microb Biotechnol* 10:1181
36. Jiang Z, Hu D (2019) Molecular mechanism of anionic dyes adsorption on cationized rice husk cellulose from agricultural wastes. *J Mol Liq* 276:105–114. <https://doi.org/10.1016/j.molliq.2018.11.153>
37. Jin L, Li W, Xu Q, Sun Q (2015) Amino-functionalized nanocrystalline cellulose as an adsorbent for anionic dyes. *Cellulose* 22:2443–2456. <https://doi.org/10.1007/s10570-015-0649-4>
38. Kabir SMF, Sikdar PP, Haque B, Bhuiyan MAR, Ali A, Islam MN (2018) Cellulose-based hydrogel materials: chemistry, properties and their prospective applications. *Prog Biomater* 7:153–174. <https://doi.org/10.1007/s40204-018-0095-0>
39. Kamel M, Mashaly H, Abdelghaffar F (2013) Photocatalyst decolorization of Reactive Orange 5 dye using MgO nano powder and H₂O₂ solution. *World Appl Sci J* 26:1053–1060
40. Kang H, Liu R, Huang Y (2016) Cellulose-based gels. *Macromol Chem Phys* 217:1322–1334. <https://doi.org/10.1002/macp.201500493>
41. Kardam A, Rajawat DS, Kanwar S, Madhubala (2017) Enhanced removal of cationic dye methylene blue from aqueous solution using nanocellulose prepared from agricultural waste sugarcane bagasse. Springer International Publishing, Cham, pp 29–36
42. Kargazadeh H, Mariano M, Gopakumar D, Ahmad I, Thomas S, Dufresne A, Huang J, Lin N (2018) Advances in cellulose nanomaterials. *Cellulose* 25:2151–2189. <https://doi.org/10.1007/s10570-018-1723-5>
43. Kausar A, Shahzad R, Asim S, BiBi S, Iqbal J, Muhammad N, Sillanpaa M, Din IU (2021) Experimental and theoretical studies of Rhodamine B direct dye sorption onto clay-cellulose composite. *J Mol Liq* 328:115165. <https://doi.org/10.1016/j.molliq.2020.115165>
44. Kausar A, Shahzad R, Iqbal J, Muhammad N, Ibrahim SM, Iqbal M (2020) Development of new organic-inorganic, hybrid bionanocomposite from cellulose and clay for enhanced removal of Drimarine Yellow HF-3GL dye. *Int J Biol Macromol* 149:1059–1071. <https://doi.org/10.1016/j.ijbiomac.2020.02.012>
45. Khamkeaw A, Jongsomjit B, Robison J, Phisalaphong M (2019) Activated carbon from bacterial cellulose as an effective adsorbent for removing dye from aqueous solution. *Sep Sci Technol* 54:2180–2193. <https://doi.org/10.1080/01496395.2018.1541906>
46. Khatri A, Peerzada MH, Mohsin M, White M (2015) A review on developments in dyeing cotton fabrics with reactive dyes for reducing effluent pollution. *J Clean Prod* 87:50–57. <https://doi.org/10.1016/j.jclepro.2014.09.017>
47. Klemm D, Heublein B, Fink H-P, Bohn A (2005) Cellulose: fascinating biopolymer and sustainable raw material. *Angew Chem Int Ed* 44:3358–3393. <https://doi.org/10.1002/anie.200460587>
48. Kumar R, Sharma RK, Singh AP (2018) Removal of organic dyes and metal ions by cross-linked graft copolymers of cellulose obtained from the agricultural residue. *J Environ Chem Eng* 6:6037–6048. <https://doi.org/10.1016/j.jece.2018.09.021>
49. Le Floch A, Jourdes M, Teissedre P-L (2015) Polysaccharides and lignin from oak wood used in cooperage: composition, interest, assays: a review. *Carbohydr Res* 417:94–102. <https://doi.org/10.1016/j.carres.2015.07.003>
50. Li D, Tian X, Wang Z, Guan Z, Li X, Qiao H, Ke H, Luo L, Wei Q (2020) Multifunctional adsorbent based on metal-organic framework modified bacterial cellulose/chitosan composite aerogel for high efficient removal of heavy metal ion and organic pollutant. *Chem Eng J* 383:123127. <https://doi.org/10.1016/j.cej.2019.123127>

51. Liu K, Du H, Zheng T, Liu H, Zhang M, Zhang R, Li H, Xie H, Zhang X, Ma M, Si C (2021) Recent advances in cellulose and its derivatives for oilfield applications. *Carbohydr Polym* 259:117740. <https://doi.org/10.1016/j.carbpol.2021.117740>
52. Liu W, Du H, Zhang M, Liu K, Liu H, Xie H, Zhang X, Si C (2020) Bacterial cellulose-based composite scaffolds for biomedical applications: a review. *ACS Sustain Chem Eng* 8:7536–7562. <https://doi.org/10.1021/acssuschemeng.0c00125>
53. Lizundia E, Puglia D, Nguyen T-D, Armentano I (2020) Cellulose nanocrystal based multi-functional nanohybrids. *Prog Mater Sci* 112:100668. <https://doi.org/10.1016/j.pmatsci.2020.100668>
54. Marchessault RH, Sundararajan PR (1983) 2—cellulose. In: Aspinall GO (ed) *The polysaccharides*. Academic Press, pp 11–95. <https://doi.org/10.1016/B978-0-12-065602-8.50007-8>
55. Mhd. Haniffa MAC, Ching YC, Illias HA, Munawar K, Ibrahim S, Nguyen DH, Chuah CH (2021) Cellulose supported promising magnetic sorbents for magnetic solid-phase extraction: a review. *Carbohydr Polym* 253:117245. <https://doi.org/10.1016/j.carbpol.2020.117245>
56. Milani PA, Debs KB, Labuto G, Carrilho ENVM (2018) Agricultural solid waste for sorption of metal ions: part I—characterization and use of lettuce roots and sugarcane bagasse for Cu(II), Fe(II), Zn(II), and Mn(II) sorption from aqueous medium. *Environ Sci Pollut Res* 25:35895–35905. <https://doi.org/10.1007/s11356-018-1615-0>
57. Moghazy RM, Labena A, Husien S, Mansor ES, Abdelhamid AE (2020) Neoteric approach for efficient eco-friendly dye removal and recovery using algal-polymer biosorbent sheets: characterization, factorial design, equilibrium and kinetics. *Int J Biol Macromol* 157:494–509. <https://doi.org/10.1016/j.ijbiomac.2020.04.165>
58. Moharrami P, Motamedi E (2020) Application of cellulose nanocrystals prepared from agricultural wastes for synthesis of starch-based hydrogel nanocomposites: efficient and selective nanoadsorbent for removal of cationic dyes from water. *Biores Technol* 313:123661. <https://doi.org/10.1016/j.biortech.2020.123661>
59. Mohite BV, Patil SV (2014) Bacterial cellulose of *Gluconoacetobacter hansenii* as a potential bioadsorption agent for its green environment applications. *J Biomater Sci Polym Ed* 25:2053–2065. <https://doi.org/10.1080/09205063.2014.970063>
60. Mpatani FM, Han R, Aryee AA, Kani AN, Li Z, Qu L (2021) Adsorption performance of modified agricultural waste materials for removal of emerging micro-contaminant bisphenol A: a comprehensive review. *Sci Total Environ* 780:146629. <https://doi.org/10.1016/j.scitotenv.2021.146629>
61. Nasrollahzadeh M, Sajjadi M, Irvani S, Varma RS (2021) Starch, cellulose, pectin, gum, alginate, chitin and chitosan derived (nano)materials for sustainable water treatment: a review. *Carbohydr Polym* 251:116986. <https://doi.org/10.1016/j.carbpol.2020.116986>
62. Oberlinter A, Likozar B, Novak U (2021) Hydrophobic functionalization reactions of structured cellulose nanomaterials: mechanisms, kinetics and in silico multi-scale models. *Carbohydr Polym* 259:117742. <https://doi.org/10.1016/j.carbpol.2021.117742>
63. Ouhammou M, Lahnine L, Mghazli S, Hidar N, Bouchdoug M, Jaouad A, Mandi L, Mahrouz M (2019) Valorisation of cellulose waste basic cactus to prepare activated carbon. *J Saudi Soc Agric Sci* 18:133–140. <https://doi.org/10.1016/j.jssas.2017.03.003>
64. Peng B, Yao Z, Wang X, Crombeen M, Sweeney DG, Tam KC (2020) Cellulose-based materials in wastewater treatment of petroleum industry. *Green Energy Environ* 5:37–49. <https://doi.org/10.1016/j.gee.2019.09.003>
65. Peng BL, Dhar N, Liu HL, Tam KC (2011) Chemistry and applications of nanocrystalline cellulose and its derivatives: a nanotechnology perspective. *Can J Chem Eng* 89:1191–1206. <https://doi.org/10.1002/cjce.20554>
66. Peng D, Cheng S, Li H, Guo X (2021) Effective multi-functional biosorbent derived from corn stalk pith for dyes and oils removal. *Chemosphere* 272:129963. <https://doi.org/10.1016/j.chemosphere.2021.129963>
67. Phan NH, Rio S, Faur C, Le Coq L, Le Cloirec P, Nguyen TH (2006) Production of fibrous activated carbons from natural cellulose (jute, coconut) fibers for water treatment applications. *Carbon* 44:2569–2577. <https://doi.org/10.1016/j.carbon.2006.05.048>

68. Prabha S, Kumar M, Kumar A, Das P, Ramanathan AL (2013) Impact assessment of textile effluent on groundwater quality in the vicinity of Tirupur industrial area, southern India. *Environ Earth Sci* 70:3015–3022. <https://doi.org/10.1007/s12665-013-2361-8>
69. Raghavendra GM, Varaprasad K, Jayaramudu T (2015) Chapter 2—Biomaterials: design, development and biomedical applications. In: Thomas S, Grohens Y, Ninan N (eds) *Nanotechnology applications for tissue engineering*. William Andrew Publishing, Oxford, pp 21–44. <https://doi.org/10.1016/B978-0-323-32889-0.00002-9>
70. Rajagopal S, Paramasivam B, Muniyasamy K (2020) Photocatalytic removal of cationic and anionic dyes in the textile wastewater by H₂O₂ assisted TiO₂ and micro-cellulose composites. *Sep Purif Technol* 252:117444. <https://doi.org/10.1016/j.seppur.2020.117444>
71. Rajkumar R, Ezhumalai G, Gnanadesigan M (2021) A green approach for the synthesis of silver nanoparticles by *Chlorella vulgaris* and its application in photocatalytic dye degradation activity. *Environ Technol Innov* 21:101282. <https://doi.org/10.1016/j.eti.2020.101282>
72. Raman CD, Kanmani S (2016) Textile dye degradation using nano zero valent iron: a review. *J Environ Manage* 177:341–355. <https://doi.org/10.1016/j.jenvman.2016.04.034>
73. Rojas OJ (2016) *Cellulose chemistry and properties: fibers, nanocelluloses and advanced materials*. Springer
74. Sajjadi M, Ahmadpoor F, Nasrollahzadeh M, Ghafari H (2021) Lignin-derived (nano)materials for environmental pollution remediation: current challenges and future perspectives. *Int J Biol Macromol* 178:394–423. <https://doi.org/10.1016/j.ijbiomac.2021.02.165>
75. Saurabh S, Garg S, Jana AK (2012) Synthesis of cellulose based polymers for sorption of azo dyes from aqueous solution. *J Environ Res Dev* 6:424–431
76. Seerangaraj V, Sathiyavimal S, Shankar SN, Nandagopal JGT, Balashanmugam P, Al-Misned FA, Shanmugavel M, Senthilkumar P, Pugazhendhi A (2021) Cytotoxic effects of silver nanoparticles on *Ruellia tuberosa*: photocatalytic degradation properties against crystal violet and coomassie brilliant blue. *J Environ Chem Eng* 9:105088. <https://doi.org/10.1016/j.jece.2021.105088>
77. Shak KPY, Pang YL, Mah SK (2018) Nanocellulose: recent advances and its prospects in environmental remediation. *Beilstein J Nanotechnol* 9:2479–2498
78. Shanmugarajah B, Chew IM, Mubarak NM, Choong TS, Yoo C, Tan K (2019) Valorization of palm oil agro-waste into cellulose biosorbents for highly effective textile effluent remediation. *J Clean Prod* 210:697–709. <https://doi.org/10.1016/j.jclepro.2018.10.342>
79. Shen W, Chen S, Shi S, Li X, Zhang X, Hu W, Wang H (2009) Adsorption of Cu(II) and Pb(II) onto diethylenetriamine-bacterial cellulose. *Carbohydr Polym* 75:110–114. <https://doi.org/10.1016/j.carbpol.2008.07.006>
80. Štefelová J, Slovák V, Siqueira G, Olsson RT, Tingaut P, Zimmermann T, Sehaqui H (2017) Drying and pyrolysis of cellulose nanofibers from wood, bacteria, and algae for char application in oil absorption and dye adsorption. *ACS Sustain Chem Eng* 5:2679–2692. <https://doi.org/10.1021/acssuschemeng.6b03027>
81. Suhas, Gupta VK, Carrott PJM, Singh R, Chaudhary M, Kushwaha S (2016) Cellulose: a review as natural, modified and activated carbon adsorbent. *Biores Technol* 216:1066–1076. <https://doi.org/10.1016/j.biortech.2016.05.106>
82. Taghipour S, Hosseini SM, Ataie-Ashtiani B (2019) Engineering nanomaterials for water and wastewater treatment: review of classifications, properties and applications. *New J Chem* 43:7902–7927
83. Tan KB, Reza AK, Abdullah AZ, Amini Horri B, Salamatinia B (2018) Development of self-assembled nanocrystalline cellulose as a promising practical adsorbent for methylene blue removal. *Carbohydr Polym* 199:92–101. <https://doi.org/10.1016/j.carbpol.2018.07.006>
84. Tavker N, Gaur UK, Sharma M (2020) Agro-waste extracted cellulose supported silver phosphate nanostructures as a green photocatalyst for improved photodegradation of RhB dye and industrial fertilizer effluents. *Nanoscale Adv* 2:2870–2884
85. Tavker N, Sharma M (2020) Designing of waste fruit peels extracted cellulose supported molybdenum sulfide nanostructures for photocatalytic degradation of RhB dye and industrial effluent. *J Environ Manage* 255:109906. <https://doi.org/10.1016/j.jenvman.2019.109906>

86. Toumi KH, Bergaoui M, Khalfaoui M, Benguerba Y, Erto A, Dotto GL, Amrane A, Nacef S, Ernst B (2018) Computational study of acid blue 80 dye adsorption on low cost agricultural Algerian olive cake waste: statistical mechanics and molecular dynamic simulations. *J Mol Liq* 271:40–50. <https://doi.org/10.1016/j.molliq.2018.08.115>
87. Ul-Islam M, Khan T, Park JK (2012) Water holding and release properties of bacterial cellulose obtained by in situ and ex situ modification. *Carbohyd Polym* 88:596–603. <https://doi.org/10.1016/j.carbpol.2012.01.006>
88. Uzyol HK, Saçan MT (2017) Bacterial cellulose production by *Komagataeibacter hansenii* using algae-based glucose. *Environ Sci Pollut Res* 24:11154–11162. <https://doi.org/10.1007/s11356-016-7049-7>
89. Ventura-Cruz S, Tecante A (2021) Nanocellulose and microcrystalline cellulose from agricultural waste: review on isolation and application as reinforcement in polymeric matrices. *Food Hydrocolloids* 118:106771. <https://doi.org/10.1016/j.foodhyd.2021.106771>
90. Wan Ngah WS, Hanafiah MAKM (2008) Removal of heavy metal ions from wastewater by chemically modified plant wastes as adsorbents: a review. *Biores Technol* 99:3935–3948. <https://doi.org/10.1016/j.biortech.2007.06.011>
91. Wang J, Tavakoli J, Tang Y (2019) Bacterial cellulose production, properties and applications with different culture methods—a review. *Carbohyd Polym* 219:63–76. <https://doi.org/10.1016/j.carbpol.2019.05.008>
92. Wen H, Hsu Y-I, Asoh T-A, Uyama H (2021) Poly(vinyl alcohol)-based composite film with Ag-immobilized TEMPO-oxidized nano-tea cellulose for improving photocatalytic performance. *J Mater Sci* 56:12224–12237. <https://doi.org/10.1007/s10853-021-06098-4>
93. Williams DF (1987) Tissue-biomaterial interactions. *J Mater Sci* 22:3421–3445. <https://doi.org/10.1007/BF01161439>
94. Xu C, Nasrollahzadeh M, Selva M, Issaabadi Z, Luque R (2019) Waste-to-wealth: biowaste valorization into valuable bio (nano) materials. *Chem Soc Rev* 48:4791–4822
95. Yan G, Chen B, Zeng X, Sun Y, Tang X, Lin L (2020) Recent advances on sustainable cellulosic materials for pharmaceutical carrier applications. *Carbohyd Polym* 244:116492. <https://doi.org/10.1016/j.carbpol.2020.116492>
96. Yang L, Chen C, Hu Y, Wei F, Cui J, Zhao Y, Xu X, Chen X, Sun D (2020) Three-dimensional bacterial cellulose/polydopamine/TiO₂ nanocomposite membrane with enhanced adsorption and photocatalytic degradation for dyes under ultraviolet-visible irradiation. *J Colloid Interface Sci* 562:21–28. <https://doi.org/10.1016/j.jcis.2019.12.013>
97. Zamel D, Hassanin AH, Ellethy R, Singer G, Abdelmoneim A (2019) Novel bacteria-immobilized cellulose acetate/poly(ethylene oxide) nanofibrous membrane for wastewater treatment. *Sci Rep* 9:18994. <https://doi.org/10.1038/s41598-019-55265-w>
98. Zhang D, Zhang M, Chen S, Liang Q, Sheng N, Han Z, Cai Y, Wang H (2021) Scalable, self-cleaning and self-floating bi-layered bacterial cellulose biofoam for efficient solar evaporator with photocatalytic purification. *Desalination* 500:114899. <https://doi.org/10.1016/j.desal.2020.114899>
99. Zhang Y-R, Chen J-T, Hao B, Wang R, Ma P-C (2020) Preparation of cellulose-coated cotton fabric and its application for the separation of emulsified oil in water. *Carbohyd Polym* 240:116318. <https://doi.org/10.1016/j.carbpol.2020.116318>
100. Zhijiang C, Ping X, Cong Z, Tingting Z, Jie G, Kongyin Z (2018) Preparation and characterization of a bi-layered nano-filtration membrane from a chitosan hydrogel and bacterial cellulose nanofiber for dye removal. *Cellulose* 25:5123–5137. <https://doi.org/10.1007/s10570-018-1914-0>
101. Zhou S, Xia L, Fu Z, Zhang C, Duan X, Zhang S, Wang Y, Ding C, Liu X, Xu W (2021) Purification of dye-contaminated ethanol-water mixture using magnetic cellulose powders derived from agricultural waste biomass. *Carbohyd Polym* 258:117690. <https://doi.org/10.1016/j.carbpol.2021.117690>
102. Zinge C, Kandasubramanian B (2020) Nanocellulose based biodegradable polymers. *Eur Polym J* 133:109758. <https://doi.org/10.1016/j.eurpolymj.2020.109758>

Cellulose Nanocrystal as a New Promising Candidate in Textile Wastewater Treatment



Swarnalatha Venkatanarasimhan, D. Gangadharan,
and Thilagavathy Palanisamy

1 Introduction

1.1 Textile Wastewater Treatment Processes

In the past few years, there is a massive increment in the manufacturing and utilization of textile products witnessed around the world because of the escalation in global population and quality of life [47]. Textile industry is the second largest industrial sector contributing to global water pollution. Around 72 toxic chemicals reach water bodies through the process of dyeing [32]. It is estimated that in the process of manufacturing 1 ton of textile products, approximately 200–300 tons of textile wastewater are generated [23]. Textile wastewater is rated as one of the most polluted waters on the earth, due to multiple adverse factors associated such as colour intensity, the presence of various toxic organic compounds, turbidity, excessive salinity, high biological oxygen demand, elevated chemical oxygen demand and drastic pH [7]. Various pollutants present in textile wastewater include but not restricted to dyestuffs, heavy metals, detergents, dissolved solids, oils and grease.

Hitherto, numerous physical, chemical and biological methods have been established and reported for the treatment of textile wastewater. Physical methods such as adsorption, and filtration, chemical methods like ozonation, ion-exchange,

S. Venkatanarasimhan (✉) · D. Gangadharan · T. Palanisamy
Department of Sciences, Amrita School of Engineering, Amrita Vishwa Vidyapeetham,
Coimbatore, India

e-mail: v_swarnalatha@cb.amrita.edu

D. Gangadharan

e-mail: d_gangadharan@cb.amrita.edu

T. Palanisamy

e-mail: p_thilagavathy@cb.amrita.edu

photo/electrochemical oxidation and coagulation and biological methods like activated sludge process, trickling filter and membrane bio reactor are the well-known processes currently adopted in textile wastewater treatment.

Amidst of hundreds of various new materials developed towards water treatment, cellulose nanocrystal-based materials have gained immense interest from researchers in the last few couple of years. The unique features of cellulose nanocrystals such as high surface area, eco-friendliness, biodegradability, ease of functionalization and mechanical strength render them the reputation as promising water purification materials. The purpose of this book chapter is to summarize and describe the latest research efforts made on the potential applications of cellulose nanocrystal-based materials in treating textile wastewater.

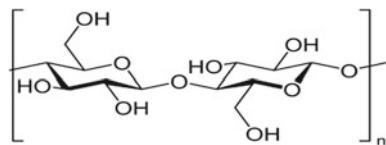
1.2 Introduction to Cellulose Nanocrystals

It is a noteworthy fact that cellulose being the most abundant polymer has an estimated global production of 90×10^9 metric tons per annum [38]. Derived from diverse sources such as trees, plants, bacteria, algae and fungi, cellulose in its simplest form is made up of several hundreds to thousands of D-glucose units connected via β -(1 \rightarrow 4) glycosidic linkages as shown in Fig. 1.

Even though cellulose is biodegradable and renewable, as a result of extensive hydrogen bonding and high crystallinity, it is insoluble in most of the common solvents. Nevertheless, the presence of multiple $-OH$ functional groups in cellulose helps in the formation of interactions and further functional modifications based on the requirements [49]. Owing to these attractive characteristics, cellulose and modified cellulose-based materials have occupied a huge space in the field of environmental remediation especially in the remediation of pollutants from textile wastewater. In most instances, modified cellulose-based materials are employed since natural cellulose has less adsorption capacity towards many pollutants.

From the latest research activities related to water purification, it is apparent that nanocellulose is acknowledged as a promising member of the cellulose family to be applied in various water treatment processes. A detailed review on the applicability of nanocellulose based materials in water purification has been already presented by several groups [6, 45, 54]. The term nanocellulose collectively represents both cellulose nanocrystals and cellulose nanofibers. Nanocellulose is biodegradable and it possesses distinctive properties over bulk cellulose such as high surface area, enhanced mechanical strength and liquid crystallinity. Moreover, nanocellulose is

Fig. 1 Chemical structure of cellulose



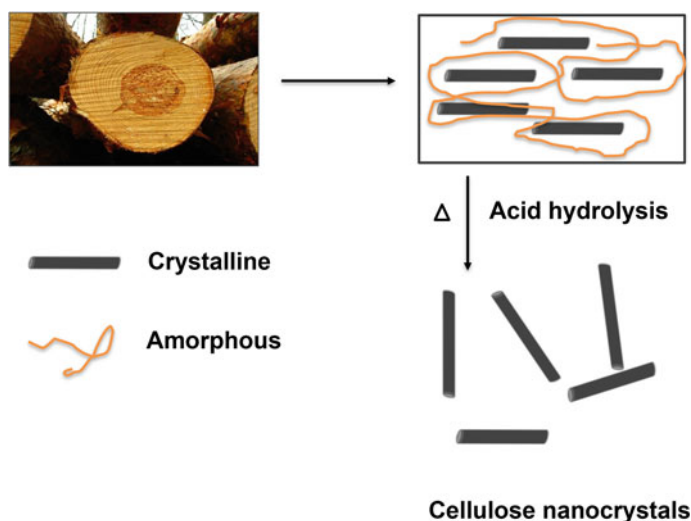


Fig. 2 Extraction of cellulose nanocrystals from cellulosic raw materials

sustainable and non-toxic in nature [2]. Cellulose nanocrystals (CNCs) are short rod-shaped whiskers possessing mainly crystalline regions whereas cellulose nanofibers are comparatively longer flexible fibers comprised of both amorphous and crystalline regions [50]. Cellulose nanocrystals can otherwise be known as cellulose nanowhiskers, cellulose nanorods or nanocrystalline cellulose. The targeted area for functional applications of CNCs majorly relies on their aspect ratios, which in turn are dependent on the sources chosen for preparing CNCs [35].

Cellulose is essentially semicrystalline, which is composed of both crystalline and amorphous regions of cellulose microfibril-reinforced matrices. In 1951, it was ascertained that a new class of nanomaterials called cellulose nanocrystals could be produced by selectively hydrolyzing less dense amorphous regions of cellulose using an acid as represented in Fig. 2 [42]. So far, acids such as sulphuric acid [21], hydrochloric acid [5], hydrobromic acid [44] and phosphoric acid [53] have been successfully demonstrated to produce CNCs on the acid hydrolysis of different cellulosic sources. Nonetheless, sulphuric acid is the widely used acid for this purpose as it produces CNCs with enhanced colloidal stability [52].

1.3 Cellulose Nanocrystals in Textile Water Treatment

Cellulose nanocrystals have captured environmental researcher's attention by reason of their salient features as listed earlier. CNC has been recently employed as a base material by environmental researchers in treating textile wastewater. The exhaustive usage of CNCs in removing common pollutants present in textile wastewater viz.

dyestuffs and metals is emphasized in the upcoming sections. Based upon the treatment mechanism while engaging CNC-based materials in treating textile wastewater, the next section is subdivided into four parts:

1. Textile wastewater treatment by adsorption
2. Textile wastewater treatment by photocatalysis
3. Textile wastewater treatment by membrane filtration
4. Textile wastewater treatment by coagulation–flocculation.

2 Textile Water Treatment by Adsorption

Adsorption is a surface phenomenon, where adsorbates are removed via the formation of some weak forces of interaction with the surface of adsorbents. Generally, adsorbents are selected based on factors like particle size, surface area, stability over a wide pH range, porosity, solubility, and surface charge. A wide range of adsorbents like carbon materials, biomaterials, inorganic materials, and polymers have been reported for textile water treatment. In this section, the discussion is mainly focused on the adsorption properties of cellulose nanocrystal-based adsorbents for textile wastewater treatment. By keeping the quantum of the literature reported on the adsorption-based textile water treatment in mind, only research articles and reviews published from the year 2015 have been integrated for the discussion. The removal of these pollutants from textile wastewater is mainly attributed to an enthalpy-driven binding approach accompanied by a favorable entropic contribution. The binding interactions are mainly due to the van der Waals forces of interaction, electrostatic interactions, hydrogen bonding and/or aromatic interactions [24]. These interactions bind the pollutants with cellulose thereby removing the pollutants from wastewater. The other aspect which makes cellulose as an excellent adsorbent is the ability to convert the –OH group in the cellulose backbone into any desired functional groups. Other properties such as surface area, porosity, biodegradability, and their capability to adsorb and desorb the contaminants make them a perfect candidate for adsorption.

Nanocrystalline cellulose synthesized from microcrystalline cellulose by ammonium persulfate treatment was examined for the adsorptive removal of methylene blue [13]. The synthesized nanocrystalline cellulose offered an adsorption capacity of 101 mg/g for methylene blue. The ensuing desorption trials carried out using acetonitrile and ethanol revealed 18% desorption and 90% desorption for acetonitrile and ethanol, respectively. Few of the research work reporting on the usage of native cellulose nanocrystals for the adsorptive removal of textile dyes have been listed in Table 1.

Table 1 Various cellulose nanocrystals-based materials reported for dye removal

S. No.	Material	Adsorption capacity	Dye removed	References
1	Nanocrystalline cellulose flakes	188.7 mg/g	Methylene blue	Tan et al. (2018)
2	Nanocellulose powder	0.17 mmol/g	Hydroxynaphthol blue	[40]
		0.1564 mmol/g	Congo red	
4	Cellulose nanocrystal	217.4 mg/g	Methylene blue	[58]
5	Cellulose nanocrystal	823 mg/g	Methylene blue	[30]

2.1 Surface Functionalization of Cellulose Nanocrystals

Functional modification of CNCs is often performed with the intention to accomplish a better dye adsorption capacity in comparison to that of the native cellulose nanocrystals. In some instances, CNCs flaunt low affinity for certain metal ions/dyes at their natural state, which necessitates the functionalization of CNCs prior to exercising them in water treatment processes. Often, surface functionalization of CNCs offers the additional advantage of selectivity in removal of dyes. The number of active adsorption sites for binding of contaminants also are found to increase after an apt functionalization.

2.1.1 Polydopamine Functionalized Cellulose Nanocrystals

Mohammed et al. reported the surface functionalization of CNC with polydopamine and melamine–formaldehyde for the selective separation of dyes from water [28]. Polydopamine functionalized CNC showed 100% uptake efficiency for methylene blue. Interestingly, with methylene blue–rhodamine B mixture and methylene blue–crystal violet mixture, the polydopamine functionalized CNC showed excellent selectivity towards the removal of methylene blue. When a combination of methylene blue and methyl orange was used, polydopamine functionalized cellulose nanocrystal removed methylene blue, and conversely, melamine–formaldehyde functionalized cellulose nanocrystal removed methyl orange from the solution (Fig. 3). The selectivity of dyes for the functional modification was ascribed to the binding interactions like electrostatic attraction, π - π stacking, and hydrogen bonding.

Similarly, polydopamine functionalized CNC reported by Wang et al. displayed an exceptionally large adsorption capacity of 2066.72 mg/g, when methylene blue was used as the dye [56]. The adsorbed dye was later effectively regenerated by using 0.1 M sulphuric acid whereas the adsorbent retained almost 90% of its adsorption capacity. In another work carried out by the same research team, the application of polydopamine functionalized CNCs in the adsorptive removal of chromium ions was

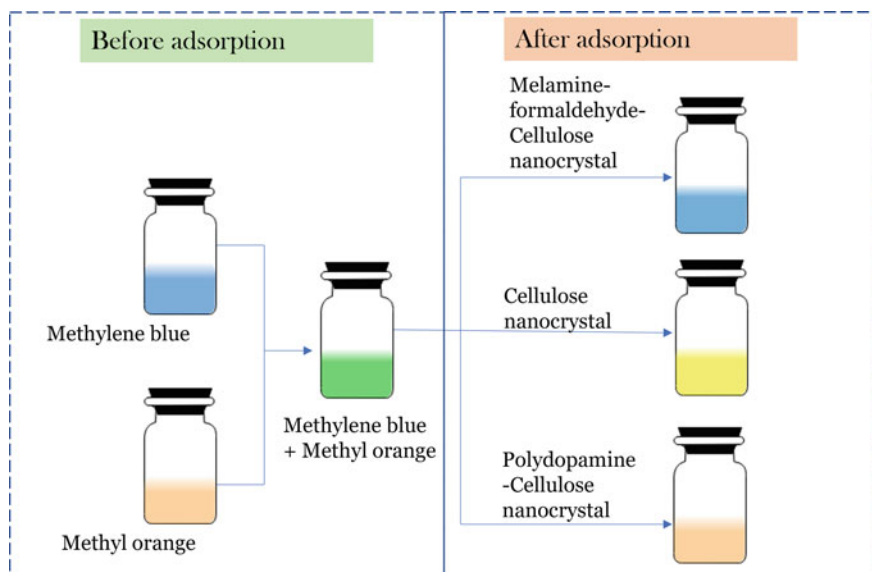


Fig. 3 Methyl orange and methylene blue before and after adsorption using functionalized cellulose nanocrystals (Redrawn from [28])

explored [8]. From the adsorption studies, chromium (VI) removal capacity of the material was found to be 205 mg/g at a pH of 3.

2.1.2 Carboxylated Cellulose Nanocrystals

Fan et al. developed carboxylated CNC using microcrystalline cellulose via an innovative one-step synthetic procedure [10]. Microcrystalline cellulose was treated with ferrous sulphate tetrahydrate and 30% hydrogen peroxide to produce carboxylated CNC and heated at 60 °C for variable durations. Then, the materials were subjected to freeze-drying to obtain carboxylated CNC. The carboxylated CNC sample heated for 6 h showed a maximum adsorption of 95.63% (110.21 mg/g) of methylene blue. Anionic carboxyl groups on the cellulose function as binding sites for the removal of the cationic dye blue via sharing or exchange of electrons, thus leading to an effective removal of methylene blue. Meanwhile, the heavy metal adsorption efficiency of the carboxylated CNC was analysed by conducting copper(II) ion removal studies. Analogous to the observation in the dye removal, the carboxylated CNC sample heated for 6 h was shown to exhibit the highest copper(II) adsorption capacity of 51.1 mg/g (82.3%).

Carboxylated CNCs and sulphated CNCs were derived from softwood pulp and hardwood pulp, respectively and their adsorption capacity of a toxic dye namely auramine O was analysed and compared [39]. Carboxylated CNCs were prepared through ammonium persulphate oxidation followed by lyophilization procedure,

whereas spray dried sulphated CNCs were synthesized via acid mediated hydrolysis of hardwood pulp. Between sulphated CNCs and carboxylated CNCs, sulphated CNCs exhibited a faster and better dye adsorption as compared to carboxylated CNCs. The maximum adsorption capacity of auramine O using sulphated CNCs was found to be much greater than those achieved by other adsorbents reported earlier.

2.1.3 Amino Functionalized Cellulose Nanocrystals

Amine functionalization is a prevalent choice made among different types of functionalization available for CNCs [18]. 250 mL of 0.4% nanocrystalline cellulose was treated with sodium periodate to produce dialdehyde nanocrystalline cellulose. 200 mL of 0.5% dialdehyde nanocrystalline cellulose was treated with ethylenediamine for 6 h at 30 °C. The resulting product was then reduced using sodium borohydride at room temperature. The resulting amine functionalized nanocrystalline cellulose was utilized for the removal of acid red GR. At a pH of 4.7, the material showed 67.3% dye uptake capacity, which reduced to 52.2% with the increase in the solution pH to 6.7. On rising the solution pH further to 9, the dye removal rate abruptly dropped to 31.3%. The availability of surface positive charges on amine groups at lower pH favored the removal of the anionic dye to a greater extent thereby indicating a decline in dye uptake with increasing pH.

In another work carried out, the nanocellulose was mixed with 50 mL of polyaniline and stirred for 10 h [16]. The resulting mixture was stirred at 2500 rpm and washed with water until the wash solution became clear. Then, the washed mixture was dried at ambient temperature. The polyaniline modified nanocellulose showed 47.06 and 48.92 mg/g adsorption for Cr(III) and Cr(VI) ions, respectively. Followed by the adsorption trials, the effective regeneration of the polyaniline modified cellulose was performed as well by using sodium hydroxide for 6 cycles. However, it is not clear whether the nanocellulose used is CNC or cellulose nanofiber.

2.1.4 Cetyltrimethylammonium Bromide Modified Cellulose Nanocrystals

Cellulose nanocrystals have also been alternatively reported to be modified with quaternary ammonium surfactant such as cetyltrimethylammonium bromide. Ranjbar et al. had developed cetyltrimethylammonium bromide modified CNC by adding varying amounts of cetyltrimethylammonium bromide [43]. The modified CNCs obtained were studied for the removal of Congo red. Among the various ratios of cetyltrimethylammonium bromide to CNC used, the sample possessing 0.25/1 w/w ratio showed the maximum adsorption capacity of 448 mg/g for Congo red. The adsorbed Congo red dye was afterwards desorbed with the help of ethanol where the adsorbent material was found to retain 85% of its actual adsorption capacity even after 5 cycles of regeneration.

2.1.5 Succinylated Cellulose Nanocrystals

Cellulose nanocrystals were mixed with different loadings of succinic anhydride in N, N-dimethylacetamide medium [9]. The resultant white precipitate of cellulose nanocrystal succinate obtained was neutralized with sodium bicarbonate and washed with water. The efficacy of the cellulose nanocrystal succinate in the removal of methylene blue was tested. Adsorption studies demonstrated a direct proportionality between the loading of succinic anhydride in the modified CNCs and the percentage of methylene blue removal from water. The adsorption capacity of methylene blue increased significantly with increased carboxylic acid content in CNC, which was in turn resulted in a better binding between carboxylic acid groups and sulphur of methylene blue. The material exhibited an adsorption capacity of 84.1 mg/g with 93.2% removal for methylene blue.

In another report, succinylated CNC was prepared from the acid hydrolysis of medical absorbent cotton followed by a reaction with succinic anhydride in pyridine medium. The sodic form of succinylated CNC was obtained by treating succinylated CNC with sodium bicarbonate. The maximum adsorption capacities of Pb^{2+} and Cd^{2+} ions using succinylated CNC were 367.6 mg/g and 259.7 mg/g, respectively, which was achieved by complexation process. The maximum adsorption capacities of Pb^{2+} and Cd^{2+} ions using the sodic form of succinylated CNC were calculated to be 465.1 mg/g and 344.8 mg/g, respectively, wherein the metal removal mechanism involved an ion exchange process.

2.2 Metal Oxide Modified Cellulose Nanocrystals

Apart from adopting functionalizing/modifying CNCs using organic moieties, inorganic compounds have also been used in the attempts executed to reach enhanced dye adsorption capacity.

For instance, nano zinc oxide can be incorporated into CNC to instigate better dye adsorption. CNCs were obtained by using bamboo powder as the cellulose source and the CNCs were mixed with zinc nitrate salt and sodium hydroxide [12]. After raising the solution pH to 8.5, the reaction mixture was kept under mechanical stirring for 30 min. The product obtained was named as ZnO/CNC8.5. In two other synthetic trials, cellulose nanocrystals were mixed with zinc chloride and sodium chloride. The pH of the mixture was adjusted to 10.5 and 11 using sodium hydroxide solution. The reaction contents were then heated at 80 °C for 24 h in a Teflon-lined stainless steel autoclave. The reaction products were tagged as ZnO/CNC10.5 and ZnO/CNC11. The dye removal ability of the nanohybrids developed was evaluated using two cationic dyes viz. methylene blue and malachite green. The dye removal percentage of ZnO/CNC10.5 and ZnO/CNC11 were 85.8% and 84.3%, respectively, both of which were lower in comparison to that of raw CNCs (91.08%). The nanohybrid ZnO/CNC8.5 showed the maximum dye removal of 93.55% among the synthesized nanohybrids due to the minimal quantity of zinc oxide present. It was deduced that

there was a lowering of dye adsorption with an increment in ZnO content. The observation also indicated the removal of cationic dyes was driven by the binding with surface carboxyl groups available in the CNCs.

Likewise, another work discussing the preparation of zinc oxide/CNC was reported by Oyewo et al. [31]. In this work, CNC was isolated from saw dust and zinc oxide/CNC nanocomposite was prepared by adding zinc oxide suspension to CNC and stirring for 24 h. The resulting air-dried nanocomposite was used for the removal of methylene blue. A comparative study carried out suggested an improved dye removal for the nanocomposite over raw CNC and native zinc oxide. 150 mg of the nanocomposite showed 97.5% removal for methylene blue. Desorption data received revealed ~60% of desorption on the usage of 2.5 M sodium chloride.

2.3 Cellulose Nanocrystals/Zeolitic Imidazolate Framework-8 Nanohybrids

Instead of functionalizing CNCs, in a recent work, hybrid hollow microspheres comprised of CNCs and zeolitic imidazolate framework-8 were reported for the adsorption of malachite green [25]. By virtue of the porous structures available in the nanohybrid, it was endowed with a very high surface area of 1240 m²/g. The adsorption capacity of the nanohybrid was also as high as 1060.2 mg/g. The very huge adsorption capacity of the nanohybrid is aided by its high surface area and the hydrophilicity offered by CNC shell layers. The sample after carbonization was shown to function as an efficient photocatalyst towards the degradation of methylene blue in the presence of solar light.

3 Textile Water Treatment by Photocatalysis

Photocatalysis is a very crucial water treatment process adopted globally, which involves degradation/conversion of harmful chemicals to safe chemicals in presence of a specific catalyst and light irradiation. Either UV light sourced from various lamps or visible light is normally utilized for the photocatalytic reaction to occur. A common light source used in many reports is the sun, which can help in the cost reduction of the process. Cellulose nanocrystals have been widely reported to be active photocatalysts in combination with well-known nano titania and nano zinc oxide. In this section, the applications of CNC-based materials towards the photocatalytic degradation of textile dyes.

3.1 *CNC/Titanium Dioxide Nanohybrids as Photocatalysts*

Nano titanium dioxide, undoubtedly is the most sought-after material by researchers working around the globe, when it comes to preparing photocatalysts. A variety of nanocomposite materials have been developed by combining titanium dioxide nanoparticles with CNCs to apply as photocatalysts in dye degradation. In an earlier research work, highly active titania nanocrystals were synthesized using CNC as morphology controlling agent [36]. CNCs were prepared by the acid hydrolysis of natural cotton fiber and mixed with titanium tetrachloride for different time intervals at various temperatures ranging from 40 to 80 °C. The TEM analysis clearly indicated that the crystalline phase of the materials was strongly influenced by temperature and experimental duration. Samples obtained were further applied in the photocatalytic degradation of methyl orange under high pressure mercury lamp irradiation. The authors concluded that the samples with cubic titania nanocrystals displayed relatively enhanced photocatalytic performance (degradation rate of 100%) than the samples with flower-like titania nanocrystals (degradation rate of 40%). This work was further extended by the same research group with the introduction of polyethylene terephthalate (PET) to CNC and titania [37]. At the initial step, CNCs prepared from cotton fibers were grafted on the PET fabric. In the following step, titania/PET nanohybrids were synthesizing by hydrolyzing titanium tetrachloride in presence of CNC-grafted PET fabric at 70 °C. The photocatalytic discoloration of methyl orange was tested even though there was no quantitative data provided on the percentage dye degradation. The experimental results showed that the methyl orange stain on the titania/PET vanished almost completely after exposing it to sunlight for 10 h, thus making it a good self-cleaning fabric.

N-doped mesoporous titania was synthesized by using urea of variable loading as N-source with and without employing CNC as template [3]. In the presence of visible light and solar light irradiation, titania prepared with N-doping and CNC template showed better photocatalytic activity in the degradation of methyl orange and other pollutants like phenol and nitrobenzene than the sample prepared without CNC template. Using CNC as template, hierarchically nanostructured titania was synthesized via hydrothermal synthetic strategy using various acids [4]. The prepared titania was calcined and then gold nanoparticles were loaded into the calcined titania. The photoactivity exhibited by titania, calcined titania and Au loaded calcined titania was examined for the degradation of methyl orange in presence of white light. The calcination process was expected to increase the photocatalytic activity of titania in degrading methyl orange and the addition of gold nanoparticles also helped in getting a better photocatalytic performance with an optimal Au loading.

3.2 CNC/Zinc Oxide Nanohybrids as Photocatalysts

CNC/ZnO nanohybrids were fabricated using a single-pot synthetic strategy using commercial microcrystalline cellulose and zinc nitrate as precursors [60]. It is claimed that the proposed method following Fischer esterification and precipitation is relatively simpler to other preparations reported earlier. Also, through the method followed, strong electronic interactions were expected between CNC and zinc oxide, which could be further exploited in photocatalysis. The nanohybrid prepared was tested for its photocatalytic activity using methylene blue as a model dye. Under UV irradiation, in a span of 10 min, 93% of the dye underwent decomposition proving the photocatalytic efficiency of the nanohybrid developed. A possible mechanism for the photocatalytic degradation of dye in presence of the developed nanohybrids and UV light irradiation is depicted in Fig. 4. Similar to this work, CNC/ZnO nanohybrids were prepared by adopting a single step hydrothermal methodology using microcrystalline cellulose and zinc chloride as precursors [1]. The nanohybrids with different zinc loading exhibited sheet-like morphologies and were employed as photocatalysts in the degradation of methylene blue. Under mercury-lamp irradiation rendering 500 W power, 95% degradation of methylene blue was shown by the sample denoted as CNC-ZnO_{5.0} (nanohybrid synthesized from 5 mmol of zinc chloride). By virtue of their structural stability, the nanohybrids displayed good recyclability where the turnover frequency values calculated were more or less the same for all the three cycles of dye degradation.

Nanohybrids composed of spherical cellulose nanocrystals and flower-like zinc oxide rod nanoclusters were developed and their antibacterial and photocatalytic

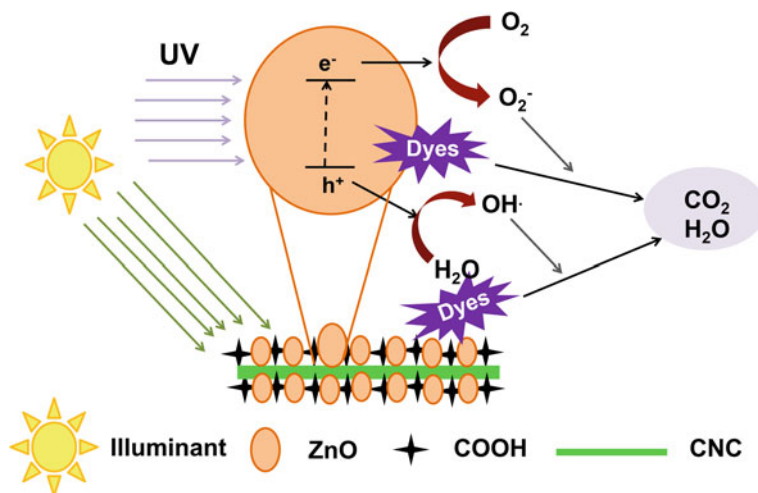


Fig. 4 Mechanism for the photocatalytic degradation of dyes using CNC/ZnO nanohybrids in presence of UV light (Redrawn from Yu et al. [60])

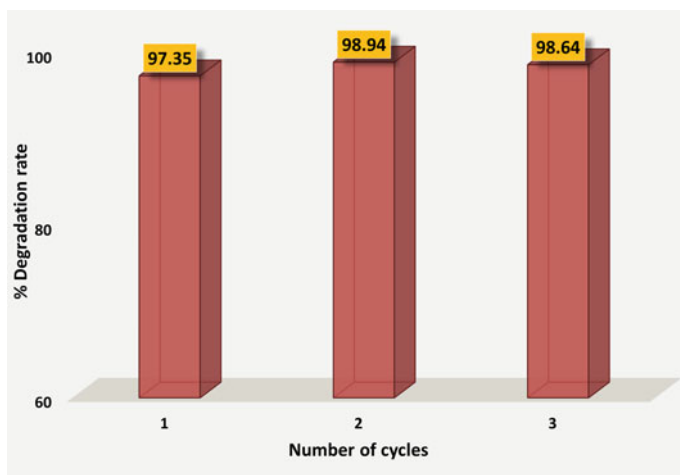


Fig. 5 Degradation ratio for cycled photocatalytic degradation (Redrawn from [59])

activity were explored [59]. Here, CNC was used as a substrate for the growth of zinc oxide nanorods. By altering reaction temperatures and pH, various nanohybrids were obtained. Among the prepared samples, the sample labelled as A-100/11 was found to exhibit a distinctive morphology possessing flower-like nanorod clusters, which also displayed stable photocatalytic activity. The ability to exhibit efficient adsorption (~97%) and subsequent decomposition of methylene blue was attributed to the high surface area achieved through the formation of flower-like morphology of A-100/11. From experiments, it was also revealed that the cycled degradation ratio did not vary significantly with the number of cycles (Fig. 5). The small variation in the degradation ratio was also surprisingly positive with the increase in number of cycles, which was justified as a result of the stable structure and the small size of the prepared nanohybrid.

A novel nanocomposite made up of zinc oxide and CNCs was proposed which had been prepared from garlic skin [27]. Initially, garlic skin extract was made use for the green synthesis of zinc oxide nanoparticles. In the next step, cellulose was isolated from the left-over garlic peel through step wise treatment processes. From the isolated cellulose, CNCs were prepared via acid hydrolysis. The nanocomposite prepared was shown to exhibit 88.62% degradation of methylene blue under sunlight as against 65.87% degradation obtained with bare zinc oxide nanoparticles, thus showing an improved photocatalytic performance by the incorporation of CNCs. The solution pH was observed to play a vital role in the photocatalysis and 9 was the solution pH at which the maximum dye degradation occurred. Very recently, Mg/CNC doped zinc oxide nanoparticles were synthesized in order to be utilized in photocatalytic applications [15]. Mg doping aids in widening the band gap of zinc oxide nanostructures, which is well-known in the literature. CNCs were prepared from the acid hydrolysis of microcrystalline cellulose and zinc oxide nanoparticles

were prepared by co-precipitation method. The nanomaterial developed was further used in the degradation of methylene blue under visible light. Based on the solution pH maintained, methylene blue underwent degradation to different extents. The dye degradation rates were 65%, 83% and 98% in neutral, acidic and basic medium, respectively.

Smart double stimuli responsive polypropylene non-woven fabric was prepared from CNC/ZnO nanohybrids and triblock copolymer brushes comprising of hydroxyethyl methacrylate, dimethylaminoethyl methacrylate and methacrylamide-azobenzene monomers [55]. The developed multifunctional fabric exhibited photocatalytic activity in degrading methylene blue under UV light irradiation. A reduction of 91.20% in the initial concentration of methylene blue was noticed after 3 h of irradiation. Using the developed fabric, removal of Cu^{2+} ion was also investigated, where the highest Cu^{2+} ion removal rate attained was 74.10% at a pH of 10.

In a latest work published, heterojunction-based photocatalytic system is reported using CNCs. Heterojunction is an interface created between two different semiconductor materials. Nanocomposites made up of CNC derived from saw dust, zinc oxide and titania were developed and used for the photocatalytic degradation of methyl blue [34]. A maximum degradation of methyl blue (98.52%) was recorded at a pH of 6 using the CNC-metal oxide nanocomposite.

Besides using titania and zinc oxide with CNC, iron oxide derived by employing CNC as a template also was used as a photocatalyst in dye degradation [22]. Mesoporous α -ferric oxide materials were prepared with CNC as a template and without CNC, via hydrothermal route. The materials thus synthesized were analyzed for their photoactivity in degrading methylene blue under visible light irradiation. From the degradation studies, the mesoporous α -ferric oxide prepared using CNC was observed to possess high photocatalytic activity as the dye degradation rate reached 58% in 180 min. On the other hand, the sample prepared without CNC showed a degradation rate of 23% under the same degradation conditions. The enhancement in the photoactivity of the former sample was due to the morphological properties introduced by using CNC as a template.

4 Textile Water Treatment by Membrane Filtration

Membrane filtration is one of the commercially adopted methods for the effective removal of pollutants from textile wastewater due to its ease of operability and efficiency. Membrane filtration assists in pressure-driven separation of undesirable contaminants from water, by employing a semi permeable thin layer of material known as a membrane. In the past few years, several research articles reporting the usage of filtration membranes constructed from CNCs have been published. Exhaustive reviews on the usance of nanocellulose-based membranes in water purification are available elsewhere [26, 46].

In 2020, Greshkewich et al. had reported the development of melamine formaldehyde functionalized CNCs incorporated hard wood pulp membranes with varied

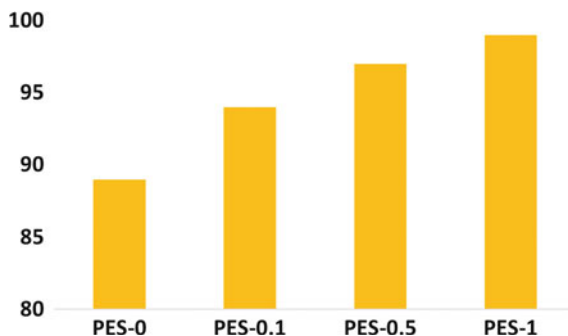
loading of CNCs [11]. The wet tensile index of the functionalized membranes raised up to the nanofiller loading of 14 wt%. Beyond this loading, the wet tensile index was found to drop. During the filtration experimentation, stacked modified membranes of 20 layers were used to get better removal efficiency. The MF functionalized CNC incorporated hard wood pulp membranes showed selectivity towards the removal of anionic dyes. From the filtration studies, it was found that modified hard wood pulp membrane with 14% nanofiller showed maximum removal of methyl orange (61% on using 20 membranes).

Biocomposite membranes comprised of CNCs and chitosan were developed through freeze drying and compacting process [20]. Their dye removal performance was tested with few cationic dyes in order to facilitate the electrostatic forces between negative charges of CNCs and positive charges of dyes. The ultrafiltration membranes exhibited removal efficiencies of 98%, 90% and 78% for the dyes Victoria blue, methyl violet and rhodamine 6G, respectively. The authors proposed that the dye adsorption mechanism was based upon electrostatic interactions and hydrogen bonding between the adsorbent and the adsorbate. It was also noted that the freeze-drying process rendered higher dye removal capacities, it had a negative impact on the mechanical strength of the membranes. From the same research group, multilayered membranes were synthesized by dip coating cellulose nanofibers with CNCs possessing sulphate or carboxylate groups to be utilized for metal ion removal [19]. Using the native cellulose nanofibers and sulphate and carboxyl functionalized CNC modified membranes, the removal efficiency of Ag^+ , Cu^{2+} and $\text{Fe}^{3+}/\text{Fe}^{2+}$ ions were experimentally determined by adopting both static flow and cross flow modes. In case of Ag^+ ion, the metal removal efficiency remained higher using static mode (100%) over cross flow mode (77–94%). For the other metal ions, the cross flow mode (Cu^{2+} —94–99%; $\text{Fe}^{3+}/\text{Fe}^{2+}$ —95–100%) favoured higher metal removal in comparison to the static mode of operation (Cu^{2+} —13–19%; $\text{Fe}^{3+}/\text{Fe}^{2+}$ —26–20%). Surface adsorption and the subsequent microprecipitation were suggested as the possible mechanism for ion removal.

Rafeian et al. prepared membranes consisting of polyethersulphone as matrix and amine functionalized CNCs as nanofillers at various loadings [41]. The separation efficiency of the developed membranes was verified by removing direct red-16 and Cu^{2+} ions from water. The removal efficiency of direct red 16 dye determined by the dead end filtration method was 89% using pristine polyethersulphone membrane, which was raised to 99% on using the CNC embedded membrane (1 wt% loading of modified CNC). There was a proportional rise in the dye removal efficacy corresponding to the loading of modified CNC, which has been graphically presented in Fig. 6. Metal removal studies done simultaneously using the membranes also demonstrated the same trend in increasing Cu^{2+} removal rates with increased CNC loading. The dispersal of nanocrystals at the surface of the polyethersulphone membrane and the presence of a large number of nitrogen-containing groups on the surface account for the improved efficiency of removal of copper ions and direct red-16 after modification.

CNC incorporated thin film nanofiltration membranes made up of polyethyleneimine and trimesoyl chloride were tested for the removal of Cu^{2+}

Fig. 6 Direct red 16 removal efficiency as a function of modified CNC loading



and Pb^{2+} ions from aqueous solutions [14]. The inclusion of CNCs as nanofillers was performed to enhance hydrophilicity and permeability of the pristine thin film membranes. The membranes showed a metal rejection efficiency of 98% from $CuSO_4$ solution, 96.5% from $CuCl_2$ solution and 90.8% for $PbCl_2$ solution.

4.1 Textile Water Treatment by Coagulation-Flocculation

Coagulation-flocculation is a popular water treatment process which implements the addition of special compounds to water in order to induce the clumping of small and fine particles to form filterable larger flocs (Fig. 7). Even though agglomeration is an issue observed while cellulose nanocrystals, reports are available on the exploitation of CNCs in the coagulation-flocculation process because they are biodegradable and will not cause pollution in the environment. In addition, it is inferred from previous reports that CNCs used after functionalization with improved surface polarity and hydrophobicity lead to better flocculation efficiency, when used as flocculants. It is well established that functionalizing these nanocrystals hikes their flocculation ability and in turn better pollutant removal efficiency [45].

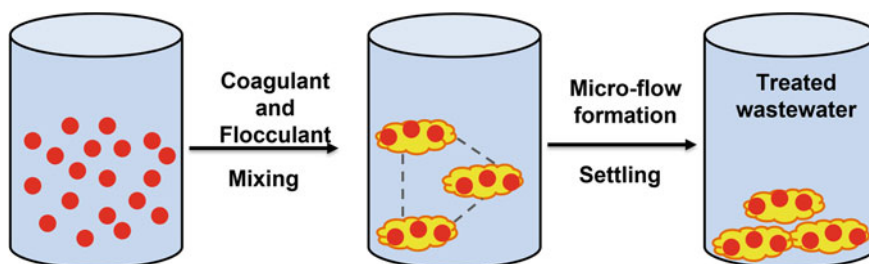


Fig. 7 Diagrammatic representation of coagulation-flocculation in water treatment (Redrawn from weponline.com) [57]

Carboxylated CNCs were prepared from microcrystalline cellulose via a single step citric acid/hydrochloric acid hydrolysis with varying extraction time [61]. Among the samples extracted, CNCs obtained at 4 h of hydrolysis time (CNCs-4H) had maximum carboxyl contents, higher crystallinity and increased suspension stability. As a result, CNCs-4H displayed superior coagulation-flocculation capability to kaolin suspension with a turbidity removal of 80.9%. CNCs-4H also functioned as an excellent adsorbent of methylene blue where the highest dye removal percentage attained was 92.8. The abundance of carboxyl groups in the modified CNCs accounted for the improved flocculation/adsorption behaviour manifested by the CNCs.

As in the previous case, carboxyl groups enriched cellulose nanocrystals modified by ascorbic acid and citric acid with dendritic morphology were synthesized via two-step grafting protocols [48]. The potential of the synthesized carboxyl enriched CNCs were further investigated as both adsorbent and coagulant-flocculant. From the experimental results, the CNCs with multibranched structure exhibited remarkable coagulation-flocculation capacity to kaolin suspension, where a turbidity reduction of 95.4% was attained. At the same time, the CNCs with multicarboxyl groups removed 87.8% of methylene blue efficiently through adsorption. The high removal efficiency achieved was attributed to the crystalline nature of the CNCs and the availability of plenty of anionic carboxyl groups in the surface.

Jiang et al. reported the use of poly(acryloyloxyethyltrimethyl ammonium chloride) grafted CNC as a flocculant for the removal of neutral reactive blue 19 [17]. The removal of dye was explained based on the charge neutralization mechanism. From the trials, it was deduced that the polymer grafted CNCs with higher cationicity required less amount for maximum colour removal. For a wide pH window, the color removal efficiency was above 80% with the highest value obtained at pH of 7. The crystallinity of the polymer grafted CNCs was found to accelerate the growth and precipitation of the flocs. With a settling period of 1 h, the colour removal efficiency achieved was 95% using the polymer grafted CNCs.

CNC isolated from sawdust was modified with sodium nitrite and sodium bicarbonate in two steps to introduce carboxylate anions in the surface of the modified CNCs [33]. The modified CNC was used in the removal of Ni^{2+} and Cd^{2+} ions by coagulation in the next step. The simple modification done on CNC was expected to lead to a reduction in the solubility of CNC in water and facilitate complexation with metal ions by dative bonds. As anticipated, the modification performed resulted in improved metal binding capacity, which was evident from the enormous removal capacities achieved for Ni^{2+} ions (956.6 mg/g) and Cd^{2+} ions (2207 mg/g). The zeta potential measurements proved a negative charge density on the coagulant which promoted the efficient removal of metal ions.

Hexadecyltrimethylammonium bromide functionalized sawdust-derived CNC was developed and used as a coagulant in water treatment [29]. The highly porous material displaying rod-like morphology was effective in reducing turbidity at lower initial turbidity levels and relatively lower pH. From the jar test results, it could be concluded that the turbidity reduction was directly proportional to reaction time and coagulant dose.

5 Conclusion

Treatment methodologies involving different mechanisms have been adopted so far to treat textile wastewater. The latest addition made to the list of materials employed in water purification is cellulose nanocrystals. Owing to their attractive characteristics and ease of functionalization, cellulose nanocrystals and their derivatives have been vastly utilized in removing various contaminants from textile wastewater obtained at the end of so many processing steps. The main focus of this book chapter was to compile the latest research inputs corresponding to the application of various cellulose nanocrystal-based materials in textile wastewater treatment. It is apparent that the renewable and biodegradable nature and ease of functionalization offered by cellulose nanocrystals are the major reasons for their predominant use in this field. However, in many instances, the biodegradability of the modified cellulose nanocrystals has not been clearly analyzed and disclosed. This approach therefore is in general questionable with respect to attaining biodegradability using cellulose nanocrystals.

References

1. Abdalkarim SYH, Yu HY, Wang C et al (2018) Green synthesis of sheet-like cellulose nanocrystal–zinc oxide nanohybrids with multifunctional performance through one-step hydrothermal method. *Cellulose* 25:6433–6446. <https://doi.org/10.1007/s10570-018-2011-0>
2. Bethke K, Palantöken S, Andrei V et al (2018) Functionalized cellulose for water purification, antimicrobial applications, and sensors. *Adv Funct Mater* 28:1800409. <https://doi.org/10.1002/adfm.201800409>
3. Chen X, Kuo DH, Lu D (2016) N-doped mesoporous TiO₂ nanoparticles synthesized by using biological renewable nanocrystalline cellulose as template for the degradation of pollutants under visible and sun light. *Chem Eng J* 295:192–200. <https://doi.org/10.1016/j.cej.2016.03.047>
4. Chen T, Wang Y, Wang Y, Xu Y (2015) Biotemplated synthesis of hierarchically nanostructured TiO₂ using cellulose and their applications in photocatalysis. *RSC Adv* 5:1673–1679. <https://doi.org/10.1039/C4RA13955K>
5. Cheng M, Qin Z, Chen Y et al (2017) Efficient extraction of cellulose nanocrystals through hydrochloric acid hydrolysis catalyzed by inorganic chlorides under hydrothermal conditions. *ACS Sustain Chem Eng* 5:4656–4664. <https://doi.org/10.1021/acssuschemeng.6b03194>
6. Choudhury RR, Sahoo SK, Gohil JM (2020) Potential of bioinspired cellulose nanomaterials and nanocomposite membranes thereof for water treatment and fuel cell applications. *Cellulose* 27:6719–6746. <https://doi.org/10.1007/s10570-020-03253-z>
7. Deng D, Lamssali M, Aryal N et al (2020) Textiles wastewater treatment technology: a review. *Water Environ Res* 92:1805–1810. <https://doi.org/10.1002/wer.1437>
8. Dong L, Deng R, Xiao H et al (2019) Hierarchical polydopamine coated cellulose nanocrystal microstructures as efficient nanoadsorbents for removal of Cr(VI) ions. *Cellulose* 26:6401–6414. <https://doi.org/10.1007/s10570-019-02529-3>
9. Emam HE, Shaheen TI (2019) Investigation into the role of surface modification of cellulose nanocrystals with succinic anhydride in dye removal. *J Polym Environ* 27:2419–2427. <https://doi.org/10.1007/s10924-019-01533-9>

10. Fan X-M, Yu H-Y, Wang D-C et al (2019) Facile and green synthesis of carboxylated cellulose nanocrystals as efficient adsorbents in wastewater treatments. *ACS Sustain Chem Eng* 7:18067–18075. <https://doi.org/10.1021/acssuschemeng.9b05081>
11. Grishkewich N, Mohammed N, Wei S et al (2020) Dye removal using sustainable membrane adsorbents produced from melamine formaldehyde-cellulose nanocrystals and hard wood pulp. *Ind Eng Chem Res* 59:20854–20865. <https://doi.org/10.1021/acs.iecr.0c04033>
12. Guan Y, Yu H-Y, Abdalkarim SYH et al (2019) Green one-step synthesis of ZnO/cellulose nanocrystal hybrids with modulated morphologies and superfast adsorption of cationic dyes. *Int J Biol Macromo* 132:51–62. <https://doi.org/10.1016/j.ijbiomac.2019.03.104>
13. He X, Male KB, Nesterenko PN et al (2013) Adsorption and desorption of methylene blue on porous carbon monoliths and nanocrystalline cellulose. *ACS Appl Mater Interfaces* 5:8796–8804. <https://doi.org/10.1021/am403222u>
14. Hoang MT, Pham TD, Verheyen D et al (2020) Fabrication of thin film nanocomposite nanofiltration membrane incorporated with cellulose nanocrystals for removal of Cu(II) and Pb(II). *Chem Eng J* 228:115998. <https://doi.org/10.1016/j.ces.2020.115998>
15. Ikram M, Mahmood A, Haider A et al (2021) Dye degradation, antibacterial and in-silico analysis of Mg/cellulose-doped ZnO nanoparticles. *Int J Biol Macromo* 185:153–164. <https://doi.org/10.1016/j.ijbiomac.2021.06.101>
16. Jain P, Varshney S, Srivastava S (2017) Site-specific functionalization for chemical speciation of Cr(III) and Cr(VI) using polyaniline impregnated nanocellulose composite: equilibrium, kinetic, and thermodynamic modeling. *Appl Water Sci* 7:1827–1839. <https://doi.org/10.1007/s13201-015-0356-1>
17. Jiang X, Lou C, Hua F et al (2020) Cellulose nanocrystals-based flocculants for high-speed and high-efficiency decolorization of colored effluents. *J Clean Prod* 251:119749. <https://doi.org/10.1016/j.jclepro.2019.119749>
18. Jin L, Li W, Xu Q, Sun Q (2015) Amino-functionalized nanocrystalline cellulose as an adsorbent for anionic dyes. *Cellulose* 22:2443–2456. <https://doi.org/10.1007/s10570-015-0649-4>
19. Karim Z, Claudpierre S, Grahn M et al (2016) Nanocellulose based functional membranes for water cleaning: tailoring of mechanical properties, porosity and metal ion capture. *J Membr Sci* 514:418–428. <https://doi.org/10.1016/j.memsci.2016.05.018>
20. Karim Z, Mathew AP, Grahn M et al (2014) Nanoporous membranes with cellulose nanocrystals as functional entity in chitosan: removal of dyes from water. *Carbohydr Polym* 112:668–676. <https://doi.org/10.1016/j.carbpol.2014.06.048>
21. Kusmono, Listyanda RF, Wildan MW, Ilman MN (2020) Preparation and characterization of cellulose nanocrystal extracted from ramie fibers by sulfuric acid hydrolysis. *Heliyon* 6:e05486. <https://doi.org/10.1016/j.heliyon.2020.e05486>
22. Liang H, Liu K, Ni Y (2016) Cellulose nanocrystals-assisted hydrothermal synthesis of mesoporous α -Fe₂O₃ for photocatalysis. *J Ceram Process Res* 17:990–993. <https://doi.org/10.36410/jcpr.2016.17.9.990>
23. Lin J, Lin F, Chen X et al (2019) Sustainable management of textile wastewater: a hybrid tight ultrafiltration/bipolar-membrane electro dialysis process for resource recovery and zero liquid discharge. *Ind Eng Chem Res* 58:11003–11012. <https://doi.org/10.1021/acs.iecr.9b01353>
24. Lombardo S, Thielemans W (2019) Thermodynamics of adsorption on nanocellulose surfaces. *Cellulose* 26:249–279. <https://doi.org/10.1007/s10570-018-02239-2>
25. Ma J, Hu J, Tang Y et al (2020) In-situ preparation of hollow cellulose nanocrystals/zeolitic imidazolate framework hybrid microspheres derived from Pickering emulsion. *J Colloid Interf Sci* 572:160–169. <https://doi.org/10.1016/j.jcis.2020.03.076>
26. Mautner A (2020) Nanocellulose water treatment membranes and filters: a review. *Polym Int* 69:741–751. <https://doi.org/10.1002/pi.5993>
27. Modi S, Fulekar MH (2020) Synthesis and characterization of zinc oxide nanoparticles and zinc oxide/cellulose nanocrystals nanocomposite for photocatalytic degradation of Methylene blue dye under solar light irradiation. *Nanotechnol Environ Eng* 5:1–12. <https://doi.org/10.1007/s41204-020-00080-2>

28. Mohammed N, Lian H, Islam MS et al (2021) Selective adsorption and separation of organic dyes using functionalized cellulose nanocrystals. *Chem Eng J* 417:129237. <https://doi.org/10.1016/j.cej.2021.129237>
29. Nkalane A, Oyewo OA, Leswifi T, Onyango MS (2019) Application of coagulant obtained through charge reversal of sawdust-derived cellulose nanocrystals in the enhancement of water turbidity removal. *Mater Res Express* 6:105060
30. Obele CM, Ejimofor MI, Atuanya CU, Ibenta ME (2021) Cassava stem cellulose (CSC) nanocrystal for optimal methylene blue bio sorption with response surface design. *Curr Opin Green Sustain Chem* 4:100067. <https://doi.org/10.1016/j.crgsc.2021.100067>
31. Oyewo OA, Adeniyi A, Sithole BB, Onyango MS (2020b) Sawdust-based cellulose nanocrystals incorporated with ZnO nanoparticles as efficient adsorption media in the removal of Methylene Blue dye. *ACS Omega* 5:18798–18807. <https://doi.org/10.1021/acsomega.0c01924>
32. Oyewo OA, Elemike EE, Onwudiwe DC, Onyango MS (2020a) Metal oxide-cellulose nanocomposites for the removal of toxic metals and dyes from wastewater. *Int J Biol Macromol* 164:2477–2496. <https://doi.org/10.1016/j.ijbiomac.2020.08.074>
33. Oyewo OA, Mutesse B, Leswifi TY, Onyango MS (2019) Highly efficient removal of nickel and cadmium from water using sawdust-derived cellulose nanocrystals. *J Environ Chem Eng* 7:103251. <https://doi.org/10.1016/j.jece.2019.103251>
34. Oyewo OA, Nevondo NG, Onwudiwe DC, Onyango MS (2021) Photocatalytic degradation of methyl blue in water using sawdust-derived cellulose nanocrystals-metal oxide nanocomposite. *Inorg Organomet Polym* 31:2542–2552. <https://doi.org/10.1007/s10904-020-01847-5>
35. Panchal P, Ogunsona E, Mekonnen T (2019) Trends in advanced functional material applications of nanocellulose. *Processes* 7:1–27. <https://doi.org/10.3390/pr7010010>
36. Peng XY, Ding EY (2012) Novel synthesis of TiO₂ nanocrystals induced by nanocrystal cellulose. *Appl Mech Mater* 117–119:944–948. <https://doi.org/10.4028/www.scientific.net/AMM.117-119.944>
37. Peng X, Ding E, Xue F (2012) In situ synthesis of TiO₂/polyethylene terephthalate hybrid nanocomposites at low temperature. *Appl Surf Sci* 258:6564–6570. <https://doi.org/10.1016/j.apsusc.2012.03.077>
38. Pinkert A, Marsh KN, Pang S, Staiger MP (2009) Ionic liquids and their interaction with cellulose. *Chem Rev* 109:6712–6728. <https://doi.org/10.1021/cr9001947>
39. Pinto AH, Taylor JK, Chandradat R et al (2020) Wood-based cellulose nanocrystals as adsorbent of cationic toxic dye, Auramine O, for water treatment. *J Environ Chem Eng* 8:104187. <https://doi.org/10.1016/j.jece.2020.104187>
40. Putro JN, Santoso SP, Soetaredjo FE et al (2019) Nanocrystalline cellulose from waste paper: adsorbent for azo dyes removal. *Environ Nanotechnol Monit Manag* 12:100260. <https://doi.org/10.1016/j.enmm.2019.100260>
41. Rafieian F, Jonoobi M, Yu Q (2019) A novel nanocomposite membrane containing modified cellulose nanocrystals for copper ion removal and dye adsorption from water. *Cellulose* 26:3359–3373. <https://doi.org/10.1007/s10570-019-02320-4>
42. Ranby BG (1951) Fibrous macromolecular systems. Cellulose and muscle. The colloidal properties of cellulose micelles. *Discuss Faraday Soc* 11:158–164. <https://doi.org/10.1039/DF9511100158>
43. Ranjbar D, Raeiszadeh M, Lewis L et al (2020) Adsorptive removal of Congo red by surfactant modified cellulose nanocrystals: a kinetic, equilibrium, and mechanistic investigation. *Cellulose* 27:3211–3232. <https://doi.org/10.1007/s10570-020-03021-z>
44. Sadeghifar H, Filpponen I, Clarke SP et al (2011) Production of cellulose nanocrystals using hydrobromic acid and click reactions on their surface. *J Mater Sci* 46:7344–7355. <https://doi.org/10.1007/s10853-011-5696-0>
45. Shak KPY, Pang YL, Mah SK (2018) Nanocellulose: recent advances and its prospects in environmental remediation. *Beilstein J Nanotechnol* 9:2479–2498. <https://doi.org/10.3762/bjnano.9.232>
46. Sharma PR, Sharma SK, Lindström T, Hsiao BS (2020) Nanocellulose-enabled membranes for water purification: perspectives. *Adv Sustain Syst* 4:1–28. <https://doi.org/10.1002/advs.201900114>

47. Shirvanimoghaddam K, Motamed B, Ramakrishna S, Naebe M (2020) Death by waste: fashion and textile circular economy case. *Sci Total Environ* 718:137317. <https://doi.org/10.1016/j.scitotenv.2020.137317>
48. Song ML, Yu HY, Chen LM et al (2019) Multibranch strategy to decorate carboxyl groups on cellulose nanocrystals to prepare adsorbent/flocculants and Pickering emulsions. *ACS Sustain Chem Eng* 7:6969–6980. <https://doi.org/10.1021/acssuschemeng.8b06671>
49. Suhas, Gupta VK, Carrott PJM et al (2016) Cellulose: a review as natural, modified and activated carbon adsorbent. *Bioresour Technol* 216:1066–1076. <https://doi.org/10.1016/j.biortech.2016.05.106>
50. Svagan AJ, Busko D, Avlasevich Y et al (2014) Photon energy upconverting nanopaper: a bioinspired oxygen protection strategy. *ACS Nano* 8:8198–8207. <https://doi.org/10.1021/nn502496a>
51. Tan KB, Reza AK, Abdullah AZ et al (2018) Development of self-assembled nanocrystalline cellulose as a promising practical adsorbent for methylene blue removal. *Carbohydr Polym* 199:92–101. <https://doi.org/10.1016/j.carbpol.2018.07.006>
52. Tran A, Boott CE, MacLachlan MJ (2020) Understanding the self-assembly of cellulose nanocrystals—toward chiral photonic materials. *Adv Mater* 32:1–15. <https://doi.org/10.1002/adma.201905876>
53. Vanderfleet OM, Osorio DA, Cranston ED (2017) Optimization of cellulose nanocrystal length and surface charge density through phosphoric acid hydrolysis. *Philos Trans A Math Phys Eng Sci* 376. <https://doi.org/10.1098/rsta.2017.0041>
54. Voisin H, Bergström L, Liu P, Mathew A (2017) Nanocellulose-based materials for water purification. *Nanomaterials* 7(3):57. <https://doi.org/10.3390/nano7030057>
55. Wang DC, Yang X, Yu HY et al (2020a) Smart nonwoven fabric with reversibly dual-stimuli responsive wettability for intelligent oil-water separation and pollutants removal. *J Hazard Mater* 383:121123. <https://doi.org/10.1016/j.jhazmat.2019.121123>
56. Wang G, Zhang J, Lin S et al (2020b) Environmentally friendly nanocomposites based on cellulose nanocrystals and polydopamine for rapid removal of organic dyes in aqueous solution. *Cellulose* 27:2085–2097. <https://doi.org/10.1007/s10570-019-02944-6>
57. Wilson LD (2014) An overview of coagulation-flocculation technology. *Water conditioning and purification international*. <https://wceponline.com/2014/04/17/overview-coagulation-flocculation-technology/>
58. Yang X, Liu H, Han F et al (2017) Fabrication of cellulose nanocrystal from *Carex meyeriana* Kunth and its application in the adsorption of methylene blue. *Carbohydr Polym* 175:464–472. <https://doi.org/10.1016/j.carbpol.2017.08.007>
59. Yang RT, Yu HY, Song ML et al (2016) Flower-like zinc oxide nanorod clusters grown on spherical cellulose nanocrystals via simple chemical precipitation method. *Cellulose* 23:1871–1884. <https://doi.org/10.1007/s10570-016-0907-0>
60. Yu HY, Chen GY, Wang YB, Yao JM (2014) A facile one-pot route for preparing cellulose nanocrystal/zinc oxide nanohybrids with high antibacterial and photocatalytic activity. *Cellulose* 22:261–273. <https://doi.org/10.1007/s10570-014-0491-0>
61. Yu HY, Zhang DZ, Lu FF, Yao J (2016) New approach for single-step extraction of carboxylated cellulose nanocrystals for their use as adsorbents and flocculants. *ACS Sustain Chem Eng* 4:2632–2643. <https://doi.org/10.1021/acssuschemeng.6b00126>

Carbon Materials for Dye Removal from Wastewater



Sarita Rai, Anindita De, Mridula Guin, and N. B. Singh

1 Introduction

Increasing population, urbanization, and industrial revolution are the main causes of pollution. The main sources of pollution include agricultural activities, municipal wastewater, wastewater discharge from industries, etc. [9, 111]. The main pollutants such as dyes, heavy metal ions, and different microorganisms in the water are very harmful for human health, environment, and all aquatic systems. This threatens global water security. Dyes are used in food, textile, paper, tanning, pharmaceutical, and many other industries to color their products. Nearly there are 10,000 dyes with an annual production of more than 7×10^5 t. These dyes are toxic and injurious to human health, soil, environment, etc. Therefore, decontamination of dyes from water is a must. Different techniques have been used for the remediation of pollutants from polluted water [16, 62]. Presently conventional methods are being used, which require large investments and produce huge amounts of sludge. Ion exchange, reverse osmosis, chemical precipitation, ultra-filtration, flocculation, photochemical, electrochemical, biological, advanced oxidation process, adsorption, and nanofiltration techniques are being used at the industrial scale, for the decontamination of dyes and heavy metal ions from wastewater [111, 132]. However, most of the techniques have limitations because of non-biodegradability and high energy requirements [19].

S. Rai

Department of Chemistry, Dr. Harisingh Gour University, Sagar, India

A. De (✉) · M. Guin · N. B. Singh (✉)

Department of Chemistry and Biochemistry, Sharda University, Greater Noida, India

e-mail: anindita.de@sharda.ac.in

N. B. Singh

e-mail: n.b.singh@sharda.ac.in

N. B. Singh

Research and Development Cell, Sharda University, Greater Noida, India

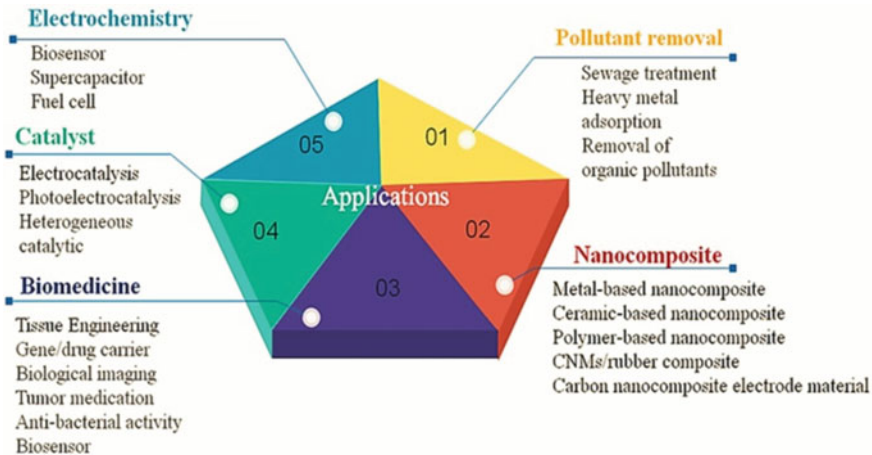


Fig. 1 Applications of carbon materials [87]

In some major techniques, there are low removal efficiency and high production of sewage sludge [68]. Therefore, low cost and efficient adsorbents are being searched. One of the most economical and convenient methods is adsorption. Different types of adsorbents such as agricultural waste, industrial waste, activated carbon, clay materials, zeolites, red mud, iron oxide, sugarcane bagasse, rice husk, fly ash, nano-materials (NMs), and nanocomposites (NCs) have been used for remediation of dyes from aqueous medium [37]. The traditional and most abundant adsorbent is carbon. The most common carbon materials generally used as adsorbents to remove dye are activated carbon (AC). The use of activated carbon as an adsorbent has a number of benefits such as high removal efficiency for organic and inorganic pollutants in higher concentrations [4]. Presently carbon in other forms such as carbon nanotubes, grapheme, carbon quantum dots, functionalized carbons nanotubes and graphene, nanocomposites of carbon, etc. [42] are used for different applications (Fig. 1) [87] including as adsorbents for dye removal. In this chapter, different types of carbon materials and their dye removal efficiencies have been discussed in detail.

2 Water Pollutants

Water pollutants are synthetic and natural compounds/ ions which enter into the ecosystem through different activities and are responsible for harmful effects. Pollutants can be broadly divided into: (1) inorganic and (2) organic pollutants. These pollutants are further divided into different types of pollutants (Fig. 2).

These pollutants, when entering water bodies, even in small quantities, deteriorate the quality of water and may have hazardous effects on animals, plants, human health, and aquatic organisms. Further dyes give color, mostly nondegradable, and more

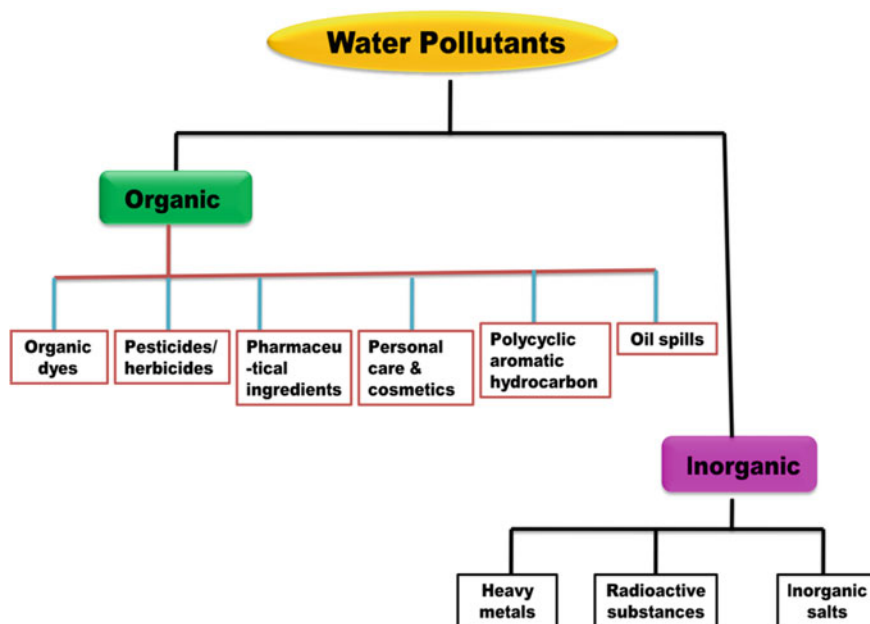


Fig. 2 Types of pollutants

hazardous. Thus, the removal of these dyes from wastewater/industrial effluent is important. First, a brief account of dyes and their toxic effects will be discussed.

3 Dyes and Their Harmful Effects

Dyes are colored substances that are used to give colors to different types of materials. Basically, there are two types of dyes—natural and synthetic. Natural dyes are obtained from plants, animals, and minerals. Aromatic compounds which attract electromagnetic energy in the wavelength range of 350–700 nm are colored. Colors are due to chromophores and auxochromes. Some representative chromophores are “quinoid rings and $-C=O$, $-NO_2$, $-C=N-$, $-C=C$, $-N=N-$, while auxochromes are $-COOH$, $-OH$, $-SO_3H$, and $-NH_3$ ” [58]. Dyes are classified by their chromophore color, structure, origin, and applications in the color index suggested by “The American Association of Textile Chemists and the Global Society of Colorists,” as shown in Fig. 3 [74].

Chemical structures of dyes are given in a number of research papers [15]. Chemical structures of some dyes are given in Figs. 4, 5 and 6.

Most of the dyes even in small amounts are toxic in nature [12] and the toxic effects are shown in Fig. 7 [134]. Dyes hinder sunlight penetration in water and destroy aesthetic quality. They are responsible for different types of diseases. Dyes in food

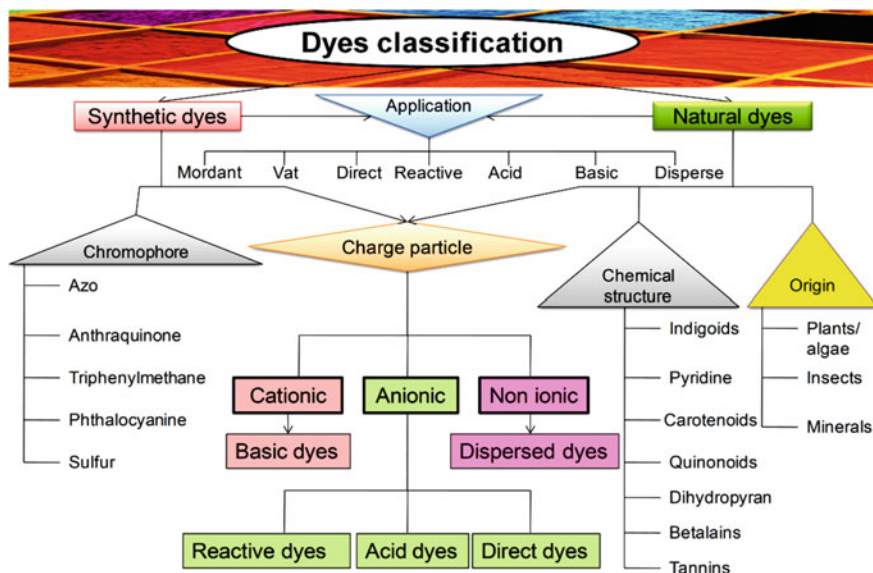


Fig. 3 Classification of dyes [74]

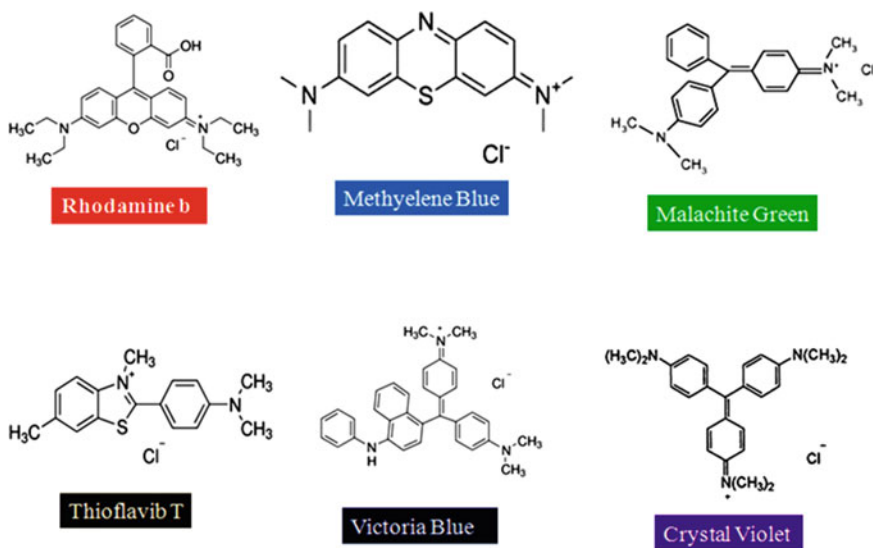


Fig. 4 Cationic dyes (chemical book, 18162-48-6, 872-50-4)

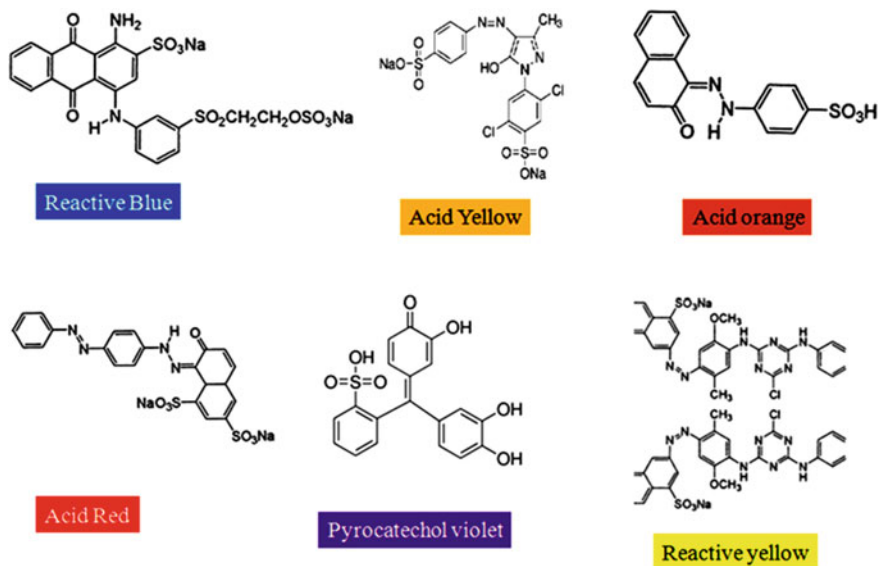


Fig. 5 Anionic dyes (chemical book, 18162-48-6, 872-50-4)

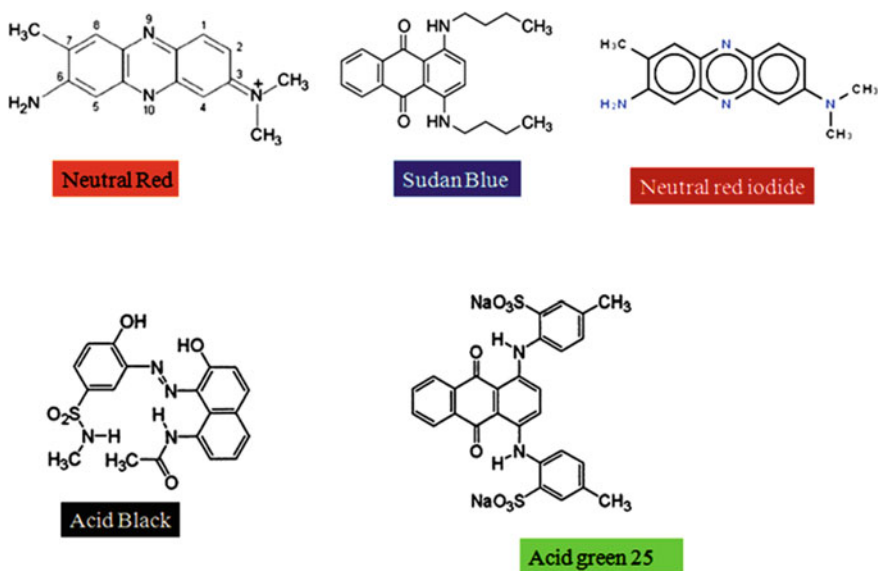


Fig. 6 Neutral dyes (chemical book, 18162-48-6, 872-50-4)

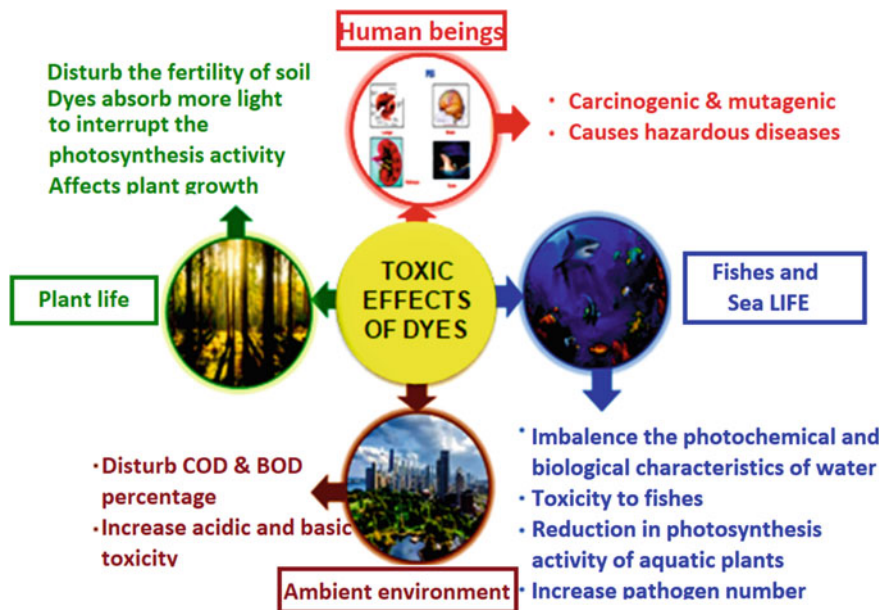


Fig. 7 Toxic effects of dyes [134]

affect the proper functioning of different organs of the human body. Many dyes are mutagenic and carcinogenic and damage different organs in human bodies. Therefore, dyes present in water is a serious threat, hence their removal from wastewater or domestic water is essential.

4 Methods of Removal of Dyes from Water

There are basically three techniques such as: (i) chemical, (ii) physical, and (iii) biological for the treatment of wastewater (Fig. 8) [134]. The advantages and disadvantages of each technique are also given in Fig. 8. Among different remediation methods, adsorption is easy to operate, cost-effective, efficient and eco-friendly and can remove different pollutants without producing toxic by-products [134].

5 Carbon Materials

Carbon is one of the most important elements on this planet and has a number of applications. Activated carbons and carbon-based nanomaterials have unique

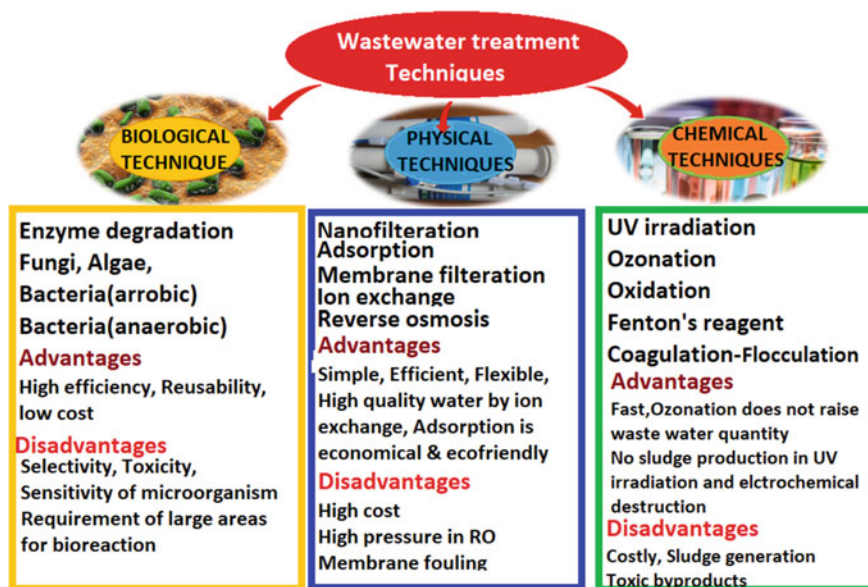


Fig. 8 Wastewater treatment methods—advantages and disadvantages [134]

properties, which make them important. In recent years, a number of carbon materials such as carbon nanotubes, functionalized carbon nanotubes, graphene, reduced graphene, carbon nanofibers, carbon nanohorns, graphene oxides, carbon nanoribbons, graphite-carbon nitride (g-C₃N₄), etc. have been synthesized. Figure 9 gives a

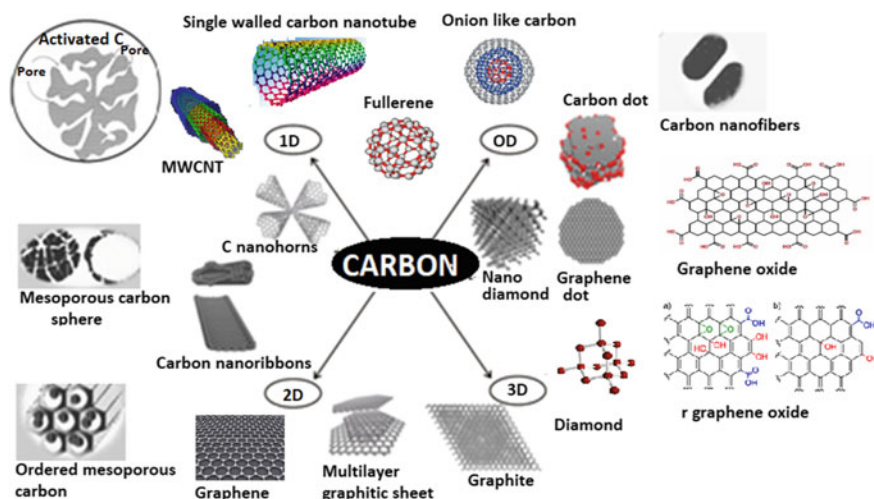


Fig. 9 Carbon materials



Fig. 10 Fabrication of carbon materials [44]

large family of carbon nanostructures [112]. Because of their high surface area and porous character, carbon materials are good adsorbents and that is why used in water remediation.

Since the 1900s, a number of methods have been developed (Fig. 10) [44, 112] for the synthesis of carbon materials particularly carbon nanomaterials but still methods are required to synthesize cost-effective carbon materials.

5.1 Toxicity of Carbon Materials

The toxic nature of nanomaterials depends on the chemical and physical features such as surface charge, structure, shape, particle size, solubility, catalytic activity, active functionalities on the surface, surface coatings, and surface area [114]. Due to their small size, nanomaterials can easily enter through cell membranes into living organisms resulting in cell damage/death. Nanomaterials, particularly carbon, have a large surface area, which allows the adherence on the surface, increasing toxicity and reactivity. Studies have shown that graphene oxide has the highest average toxicity

Table 1 Carbon nanomaterials and their toxic effects

Carbon materials	Results
C ₆₀	ROS produced attack organisms
	Electrons are exchanged with nucleotides
	Inflammation is produced in rat lung tissue
GRA	Cytotoxicity due to the oxidative stress reaction
	Fish cells metabolic activity is affected
	Cell wall of the algae cell is damaged
	Destroying physiological characteristics of the lungs,
	Neurotoxicity to zebrafish embryo
	Affect fetal growth and development
GO	Damage to cells
	Fecundity of <i>Spodoptera litura</i> is reduced
MWCNTs	DNA repair mechanism
	Cytotoxicity against HL-60 cells
	Bacterial and fungi growth is affected
	Inhibit microorganisms activity in the soil
SWCNTs	<i>Artemia salina</i> development in seawater is affected
CNT	Can enter the body causing granuloma and inflammation in the lungs

(52.24%) among carbon materials. However, surface functionalization decreases the toxic behavior. While using carbon materials, particularly carbon nanomaterials, in removing dyes from water, all precautions should be taken. The toxic effects of some carbon nanomaterials are given in Table 1 [87].

The mechanism of toxic effects of carbon on cells is mostly due to oxidative stress (Fig. 11) [87].

6 Removal of Dyes

6.1 Removal of Dyes by Activated Carbon (AC)

Dye is one of the major ingredients in various industries, which includes food, textile, leather, packaging, pharmaceutical, paper and pulp, etc. With the progress of industrialization, the production of dyes is happening at a fast rate. Most of the dyes are nonbiodegradable, extremely stable, and toxic in nature. It is reported that every year tons and tons of dyes are discharged in the aquatic environment. Thus, dye removal from wastewater is a matter of serious concern. Several methods are available for the treatment of dyes from water bodies. The use of conventional methods

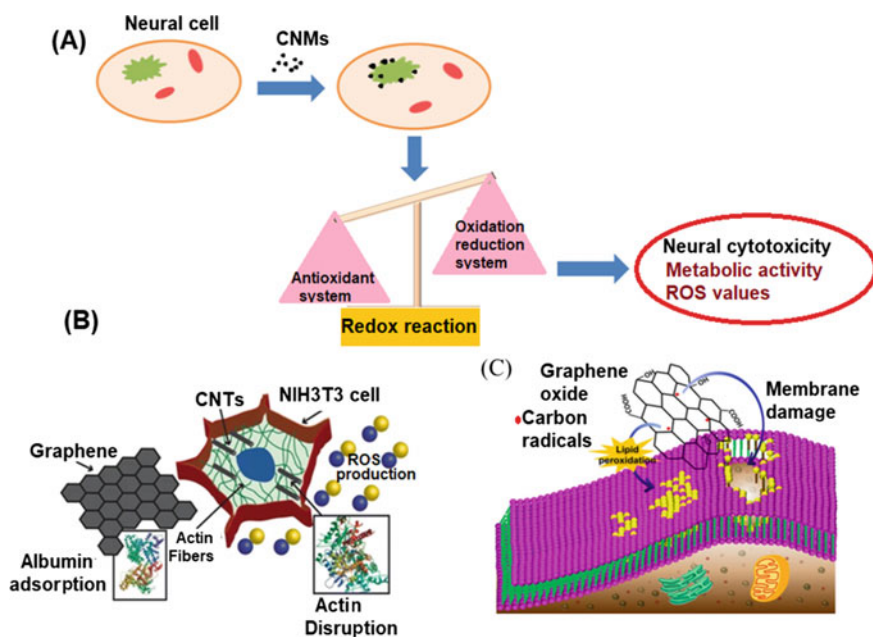


Fig. 11 Toxic effects of carbon on cells

is restricted because of the high demand for energy and associated high cost, generation of secondary pollution by hazardous spent catalysts, and membrane fouling. Although these methods have their own pros and cons, among them adsorption method is the most attractive method as it is economical, easy, simple to design, and reusability of reagents is possible. Activated carbon is being used as the most effective adsorbent for long. The comparison of the effectiveness of activated carbon as an adsorbent with other methods for dye removal is given in Table 2. Highly porous

Table 2 Performance comparison of activated carbon with other methods

Method	Removal of dye	Cost/energy requirement	Disinfection property	Generation of by-product
Activated carbon	High	Moderate	No	No
Zeolite	High/specific	Varied cost	No	No
Ozonation	High	Low to medium	Yes	Yes
Oxidation	Moderate	Low to medium	Yes	Yes
Nano filtration or RO filtration	High	High	No	No

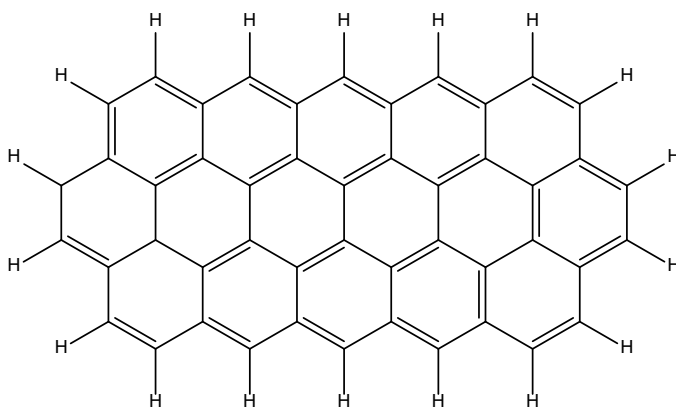
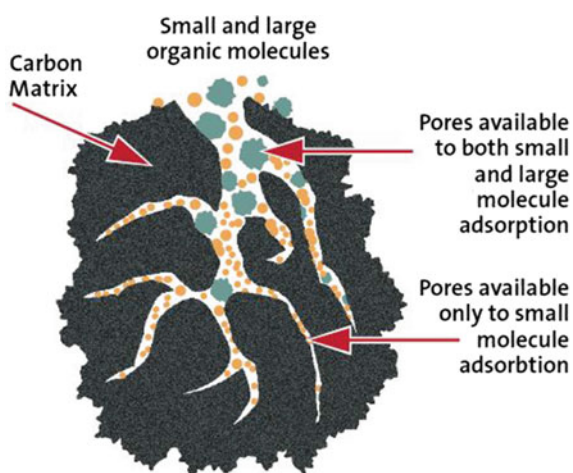


Fig. 12 Molecular structure of activated carbon

nature and large surface area are responsible for high adsorption by AC. The molecular structure of AC consists of highly disturbed graphite crystallite (Fig. 12). The presence of carbon atoms with varying degrees of saturation, oxidation state, and micropores with variable size play a key role in dye adsorption. AC with different pore sizes is shown in Fig. 13. In general, two types of ACs are present; one is granular activated carbon (GAC) and the other one is powdered activated carbon (PAC). The toxic dyes are more effectively removed by PAC than GAC. Conventionally activated carbon is prepared from high carbon content materials in different physical forms, for example, wood, coconut shell, coal, etc. [100, 106]. However, to make the process more cost-effective currently scientists are producing activated carbon using agricultural and industrial wastes. After synthesis, they are activated through various physical or chemical methods.

Fig. 13 Activated carbon with varying pores



6.1.1 Factors Affecting the Adsorption Capacity of ACs

ACs with good adsorbing capacity have high porous structure leading to a large specific surface area. The surface area and the concentration of pores can be modified using various activating agents. Larger pore size relates to larger pore volume, which is directly linked to higher adsorption capacity. The nature of the starting material and the nature of the produced activated carbon, nature of adsorbate, and adsorption reaction conditions play important role in removing the maximum amount of dye in a shorter time by the activated carbons.

The primary functional groups that are found to be present in the activated carbon include hydroxyl, carbonyl, carboxyl, phenol, lactone, and quinone. The functional-group-containing oxygen groups imparts acidic nature to the surface and improves adsorption capacity. The dye molecules adsorb over the surface of activated carbon through weak intermolecular interactions such as dispersion force or van der Waals force. The aromatic dyes bind via π - π stacking interactions whereas the ionic dyes via strong electrostatic interactions.

6.1.2 Precursor Material

A large number of carbonaceous materials with high carbon content are used for the manufacturing of activated carbons. The efficiency of the adsorption is dependent on several conditions, e.g., the nature of precursor material, the basic features of the adsorbents, identity of the adsorbate, chemistry of interaction between adsorbate and adsorbent. It is very difficult to assess the adsorption efficiency of the activated carbons prepared from different sources because of varied experimental environments. However in general it is observed that ACs produced from agricultural wastes and biomasses perform better for adsorption than the ACs generated from municipal and industrial sources [43].

6.1.3 Nature of AC

The adsorption efficiency of ACs is controlled by its porous structure involving pore size, pore volume, and surface area. The pores present in ACs can vary from less than a nanometer to a few thousand nanometers. Three different pores are available in activated carbon for performing different functions according to their sizes. The smallest pores are the micropores with a size less than 2 nm. They display the highest adsorption capacity due to their high surface area. Various solvents and volatile compounds are retained on microporous AC. Mesopores have size between 2 and 50 nm and are useful in retaining molecules, whose size falls between micropores and macropores. Macropores have a size of more than 50 nm which secures the quick adsorption of large size adsorbate and directs them further toward smaller pores of AC.

The BET surface area, ash content, distribution of pores, pore-volume, size of the particle whether granular or powdered, surface charge, presence of functional groups, and associated polarity are important criteria for determining the adsorption capacity of ACs. The high ash content of activated carbon is not beneficial for adsorption over AC.

6.1.4 Nature of Adsorbate

The molecular size of adsorbate is a deciding factor for adsorption. The larger the size of the dye molecules, the better the adsorption efficiency. The polarity of the functional groups present in the organic dye molecules also plays an important role. The lower the polarity or the hydrophilicity of the organic dyes higher is the adsorption on AC.

6.1.5 Adsorption Condition

Temperature, pH, ionic strength of the solution, contact time, initial dosage of adsorbate, concentration of adsorbent all have significant contribution toward the adsorption efficiency.

(a) Adsorbent dosage

When the dosage of AC is increased, the adsorption of dyes becomes more up to a certain limit and then decreases or remains almost constant at a higher dosage. Because the adsorption capacity is directly proportional to the number of adsorption sites. Increasing the concentration of AC leads to faster adsorption of dyes with lower energy requirements.

(b) Initial concentration of dye

The efficiency of adsorption process is dependent on the initial concentration of dyes. Several research works indicate that the adsorption efficiency diminishes by increasing the dye concentration. This is justified by the saturation of the accessible binding sites of AC. The driving force of mass transfer in adsorption is the unoccupied sites of the adsorbent, which is controlled by the dynamic equilibrium.

(c) Contact time

Optimizing the contact time in the adsorption process is important from a technical and economical point of view. At the initial stage, the rate of adsorption is high because of the dynamic nature of the adsorption process. The amount of the dyes adsorbed increases with an increase in contact time but remains unaltered or decreases after attaining equilibrium. The saturation of the active sites after the equilibrium results in the decrease of the rate of adsorption.

(d) pH

Table 3 Important physical and chemical properties of AC

BET surface area	500–3362 m ² /g
Specific mass	120–240 g/m ²
Density	0.5–2200
Pore volume	0.08–1.5 cm ³ /g
Average pore diameter	0.2–50 nm
Porosity	0.4–0.92
Adsorption capacity	5–5000 mg/g
Ash content	0.2–37%

Acidic and basic nature of the solution is a crucial factor in dye adsorption. Variation of pH of dye solution affects the efficiency of adsorption by modifying the surface properties of adsorbent (AC) by protonation. Further, the polarity of dye molecules can be altered by changing the pH of the dye solution. At acidic pH, the functional groups of ACs attain a positive charge resulting in strong adsorption of anionic dyes while weak adsorption of cationic dyes. The reverse phenomena are observed at basic pH conditions. The pH value at which surface charge is zero is defined as pH_{pzc} and is an important parameter in understanding adsorption capacity. It has been observed that the pH > pH_{pzc} will create a negative surface charge and be beneficial for cationic dye adsorption and pH < pH_{pzc} is ideal for anionic dye adsorption due to the positive charge on the surface.

(e) Temperature

Temperature is another critical factor in the adsorption process. It has been noticed that adsorption capacity improves with an increase in temperature. This may be due to the increased rate of diffusion of dyes towards the active sites of AC. With increasing temperature, more active sites are created over the adsorbent.

(f) Physical and chemical properties of AC

The adsorption efficiency of AC is associated with various physical and chemical properties. Extent of porosity, pore width, BET surface area, polarity, hydrophobicity, surface charge, acid/base nature, presence of functional groups, and hetero atoms are some of the important factors that control the extent of adsorption. Some selected physical and chemical parameters of AC are given in Table 3.

6.1.6 Modified AC for Dye Removal

The regeneration and reusability of AC is a serious issue for economic feasibility. The solution to the problem is given by the use of magnetic separation using magnetic nanoparticles blended AC. Numerous research has been performed on magnetic AC for effective removal of dyes [53, 54, 66, 76, 77, 102, 120, 124]. Integration of

magnetic nanoparticles with AC leads to better recovery and separation of the adsorbent. Various iron-oxide-based nanoparticles such as $\text{Fe}_3\text{O}_4/\text{CoFe}_2\text{O}_4$, $\alpha\text{-Fe}_2\text{O}_3$, NiFe_2O_3 , CeO_2 , $\text{Au}/\text{Fe}_3\text{O}_4$, etc. are reported in this field. A number of NMs such as ZnO , CuO , PbO , TiO_2 , SnO_2 , MgO , $\text{Zn}(\text{OH})_2$, Ce-TiO_2 , CuI-CuO , etc. loaded ACs have been investigated for their synergistic feature of adsorption process [21, 34–36, 78, 80, 84, 89, 90, 99, 107]. The physicochemical properties of AC get improved upon integration with nanometal oxides.

6.2 Agricultural Based ACs

As discussed in the previous sections, most of the commercially available ACs (CAC) are prepared from coal, petroleum, and lignocellulose-based materials. The major challenge faced by the CAC is the use of expensive precursor materials. Further, the coal- and petroleum-based starting materials are nonrenewable and create environmental issues. The huge demand for AC for environment and water remediation needs to increase the supply of AC. To bridge the demand and supply gap, new carbon materials with desired adsorption capabilities are explored. In this regard, the abundant availability of agricultural wastes gained popularity in producing highly porous AC. Agricultural wastes in general contribute significantly to environmental pollution. The benefit of biomass synthesized AC are: (1) They are economical as the precursors and are of low cost (2) The waste is getting revalorized (3) They are from renewable resources and (4) Environment friendly as the combustion of AC does not increase the CO_2 level.

The agricultural waste used for the synthesis of ACs can be classified into two categories: woody materials and nonwoody materials. Among nonwoody materials, various soft materials such as avocado peel, orange peel, waste tomato, waste, grape, waste pineapple, rice husk, corn cob, sugarcane bagasse, coir pith, rambutan, etc. are used for the synthesis of high absorbent ACs. On the other hand, in the woody material category, palm shell, coconut shell, walnut shell, fox nut shell, apricot stone, olive stone, cashew nut shell, etc. are investigated for producing ACs. Table 4 lists some ACs prepared from woody and nonwoody agricultural wastes. The specific surface area of the synthesized ACs is significantly dependent on the type of materials and nature of activating agents. The specific surface area is the determining factor of the activity, adsorption efficiency, and catalytic abilities of the ACs. Thus, it cannot be inferred which agricultural waste will be the most effective for producing AC as an adsorbent for dye removal from wastewater. Each of them has its own specific adsorbing characteristic. However, the ACs generated from agricultural wastes have tremendous potential for efficiently removing hazardous dyes from the water body.

Table 4 Nonwoody and woody agricultural waste materials of AC for dye removal

Precursor of AC	Activating agent	Name of dye	Specific surface area (m ² /g)	References
<i>Nonwoody waste materials</i>				
Avocado peel	H ₃ PO ₄	Naphthol blue black, reactive black 5, basic blue 41	87.52	[82]
Tomato waste	ZnCl ₂	Methylene blue, metanil yellow	1093	[105]
Grape waste	ZnCl ₂	Methylene blue, metanil yellow	1455	[104]
Pineapple waste	ZnCl ₂	Methylene blue	914.67	[70]
Orange peel	H ₃ PO ₄	Methylene blue and Rhodamine B	1090	[29]
Orange peel	H ₂ SO ₄ + NaHCO ₃	Methylene blue	–	[118]
Rice husk	H ₂ SO ₄	Crystal violet, direct orange, and magenta	98.27	[123]
Jerusalem artichoke stalk-based	ZnCl ₂	Methylene blue, methyl orange	1632	[136]
Corn cob	H ₃ PO ₄	Methylene blue	1809	[140]
Pomegranate peel	ZnCl ₂ , HNO ₃	Direct blue 106		[8]
Apple pulp and peel	H ₃ PO ₄	Methylene blue	1103 (pulp)/1552(peel)	[48]
Hazelnut bagasse	ZnCl ₂	Acid blue 350	1489	[20]
<i>Thevetia peruviana</i>	H ₃ PO ₄	Methylene blue, basic green 4, acid violet 49, reactive orange 4, direct blue 71	862.39	[13]
Cattail	H ₃ PO ₄	Neutral red, malachite green	1279	[109]
Rambutan	NaOH	Acid yellow 17	971.54	[81]
Flamboyant pods	NaOH	Acid yellow 6, acid yellow 23, acid red 18	2854	[122]
Pomelo Skin	NaOH	Methylene blue, acid blue 15	1335	[31]

(continued)

Table 4 (continued)

Precursor of AC	Activating agent	Name of dye	Specific surface area (m ² /g)	References
Date palm leaflets	KOH	Methylene blue	823	[26]
Sugarcane bagasse	ZnCl ₂	Basic dye	–	[27]
Sugarcane bagasse pith	ZnCl ₂ and H ₃ PO ₄	Reactive orange	–	[7]
Prickly pear peels, broccoli stems, white sapote seeds	H ₃ PO ₄	Acid blue 74, direct blue 80, basic blue 9, basic violet 3	1025 (prickly pear peels), 1177 (broccoli stems), 1043 (white sapote seeds)	[86]
Coir pith	ZnCl ₂	Acid brilliant blue, ACID violet, methylene blue, rhodamine B, direct red 12B, Congo red, Procion red, Procion orange	910	[79]
<i>Woody waste materials</i>				
Fox nutshell	ZnCl ₂	Methylene blue	2869	[60]
Palm shell waste	NaOH	Methylene blue	731.50	[129]
Macore fruit	NaOH	Methylene blue, Methyl orange	229.51	[2]
Spent coffee grounds	KOH	Methylene blue, acid orange 7	704.23	[56]
Holm oak acorn	H ₃ PO ₄	Orange 30	968	[121]
Coconut Shell	Red mud + lime + KOH + Al(NO ₃) ₃ + Na ₂ SO ₄	Reactive violet 5	–	[98]
Coconut shell	H ₃ PO ₄	Reactive blue 19	–	[1]
Cashew nut shell	KOH + TiO ₂	Brilliant green and Methylene blue	–	[94]
Apricot stones	H ₃ PO ₄ + HNO ₃	Methylene blue, methyl orange	359.40	[22]
Olive stone	–	Methylene blue	–	[45]
Walnut and poplar woods	H ₃ PO ₄	Acid red 18	–	[47]

(continued)

Table 4 (continued)

Precursor of AC	Activating agent	Name of dye	Specific surface area (m ² /g)	References
Peanut sticks wood	HCl and HNO ₃	Methylene blue	218.89	[34]
Peanut shell	Pyrolysis/MW + Pyrolysis	Direct black 38 and reactive red 141	371.10 (pyrolysis)/395.80 (MW + pyrolysis)	[33]
Quinoa husk	KOH	Malachite green, rhodamine B, methylene blue, methyl violet, methyl orange	1713	[110]
Walnut and almond shell	ZnCl ₂	Methylene blue	714 (almond)	[117]
Waste coffee grounds	FeCl ₃	Rhodamine B, methylene blue, methyl orange	1910	[128]

6.2.1 Synthesis of AC from Agricultural Wastes

The synthetic procedure of ACs from agricultural wastes involves an activation process by two different techniques: physical and chemical methods. In the physical method, carbonization of the precursor is performed at a high temperature and then CO₂ gas is passed to make it porous and increase its surface area. This method is also called as pyrolysis process due to the use of high temperature. Alternatively, chemical activation involves simultaneous activation and carbonization process. Here the activating agents are mixed with the precursor and heated at high temperature as required. Thus, the chemical activation process modifies both the physical and chemical properties of the precursor material to produce the AC. The chemical activation method produces a better porous structure due to the lower temperature requirement. Various reagents such as NaOH, KOH, HCl, H₂SO₄, H₃PO₄, ZnCl₂, K₂CO₃, etc. are used as activating agents. Figure 14 describes different steps, that are followed in the preparation of ACs from agricultural wastes.

6.3 Carbon Nanotubes (CNTs)

In addition to AC from various sources, CNTs (carbon nanotubes) are emerging as advanced adsorbents for dye removal [61]. Over the past few years, nanotechnology has revolutionized the removal of pollutants from water. CNTs have conducive physicochemical properties that help in water remediation processes. The structural diversity, selectivity, chemical stability, and large surface area of CNTs are the guiding factors that stand out in comparison with conventional adsorbents for dye

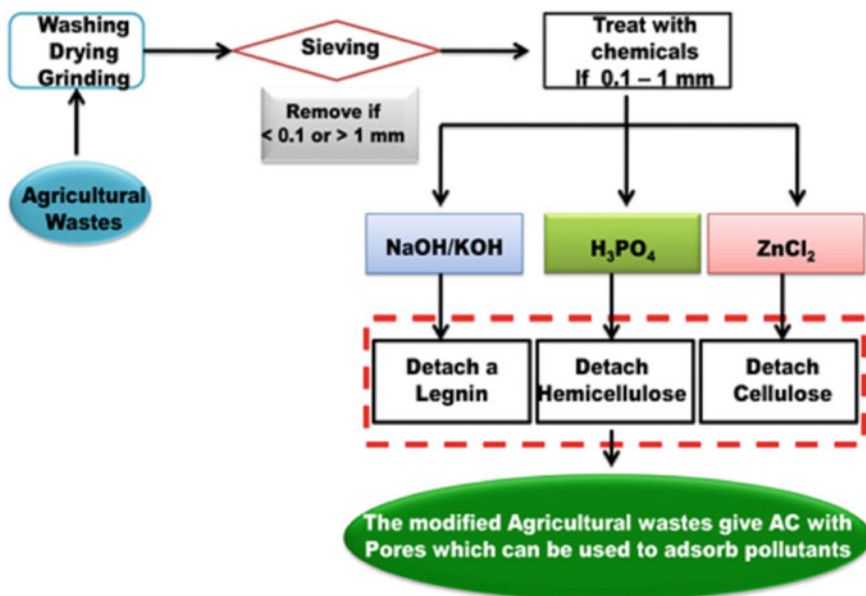


Fig. 14 Synthesis of AC from agricultural wastes

removal. In addition to that, the nanodimension of the CNTs provides large surface area, numerous sorption sites, adjustable pore size, faster intra-particle diffusion, and low-temperature requirement for further modifications. The strong affinity of CNTs toward organic dyes makes them far better adsorbents than other commonly available adsorbents. Both single-walled carbon nanotubes (SWCNTs) and multi-walled carbon nanotubes (MWCNTs) are investigated for dye removal applications. The surface area of SWCNTs is higher than MWCNTs and thus the efficiency of dye adsorption is higher in SWCNTs. However, MWCNTs are economically several times more affordable compared to SWCNTs. Consequently, scientists are directed towards making cost-effective adsorbents by surface functionalization of MWCNTs. Functionalization of MWCNTs or making composites with metal oxide nanoparticles improves adsorption capacity manifolds.

There are four different possible sites of adsorption in CNTs: (1) internal sites inside the hollow tube, (2) interstitial spaces between the walls, (3) the groove space between the peripheral bundles, and (4) external active surface area. The pollutants get trapped on the surface through various driving forces including electrostatic interaction, π - π stacking interaction, charge transfer interaction, and hydrophobic interaction.

Prola et al. [91] studied the adsorption of direct blue 53 dye on MWCNTs and powdered ACs (PAC). They have justified the higher adsorption capabilities of MWCNTs due to the textural similarities between the dye molecule and MWCNTs. The textural behavior of CNTs can be tailored according to the type of pollutants

by various methods. The morphology also plays a significant role in adsorption efficiency. For example, dyes belonging to the polynuclear aromatic category with planar geometry such as rhodamine B, alizarine red, acridine orange, and anthracene are strongly adsorbed over the CNT surface. Contrarily, the nonplanar category of aromatic dyes such as Orange G, xylenol orange, 1-(2-pyridylazo)-2-naphthol can bind weakly to the surface of CNTs. Further, non-conjugated, nonplanar dyes such as diiodofluorescein, bromothymol blue have the least affinity toward adsorption over CNT.

Thermodynamic aspects of four different azo dye adsorption over MWCNTs and AC are investigated by Ferreira et al. [30]. Their results indicate that the adsorption capacity of MWCNTs is 5.6 times higher than AC. A recent report by Abualnaja et al. has shown the promising features of MWCNTs for adsorbing Inmate violet 2R dye with a regeneration capacity of 91.71% after three cycles [3].

6.4 Modified/Functionalized CNTs

The surface of CNTs can be modified by introducing various functional groups according to the nature of the pollutants and intended application. Functionalized CNTs are more efficient in removing organic dyes. Various modification methods are available such as oxidation, alkali activation, incorporation of magnetic particles, blending with zero-valent iron, modification with nanometal oxide, modification with polymer, immobilization of CNT, chemical functionalization, composite with other carbon-based adsorbents, etc. Among them, oxidized MWCNTs are found to be very effective against dye removal from water [71, 137, 139].

To enhance the adsorption characteristics of CNTs, tremendous efforts have been made to minimize the hydrophobic features of CNTs by making composites with nanometal oxides, polymers, and other materials. The sorption capacities of these composites are several times higher than the pristine CNTs. A magnetic nanocomposite of MWCNTs using Fe_3O_4 particles is reported for adsorption of cationic dyes [25]. The composite MWCNT-COOH-cysteamine prepared by surface modification with cysteamine is proved to be an excellent adsorbent for amido 10B dye [101]. Functionalizations of MWCNTs can be of two types: covalent and noncovalent (Fig. 15) [55].

The functionalization can be tailored to add selectivity to the adsorption process. The noncovalent surface modification through π - π stacking interactions or van der Waals interaction is preferable as it preserves the structure of CNT. Novel interfacial properties are generated through functionalization, which were missing in the pristine form. A large variety of functional groups can be introduced over the surface of CNTs [115]

Numerous metal oxide doped CNTs are investigated for pollutant adsorption processes. Doping of alumina, titania, zinc oxide, iron oxide [11, 17, 24, 88], etc. has shown tremendous adsorption capacity compared to their non-doped counterparts. Duan et al. reported photocatalytic performance of titania-doped MWCNTs

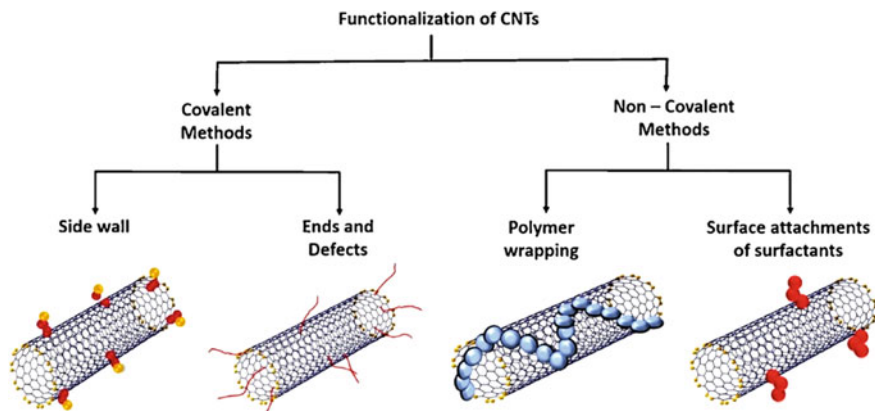


Fig. 15 Functionalization of CNT

for degradation of methyl orange dye. Their results indicated better performance of MWCNTs/TiO₂ composites over untreated MWCNTs due to the faster recombination timescale. Magnetite-loaded MWCNTs displayed electrostatic and π - π stacking interaction while adsorbing methylene blue dye (Fig. 16) [6]. Another independent work by Liu et al. used MWCNTs/TiO₂ composites synthesized through

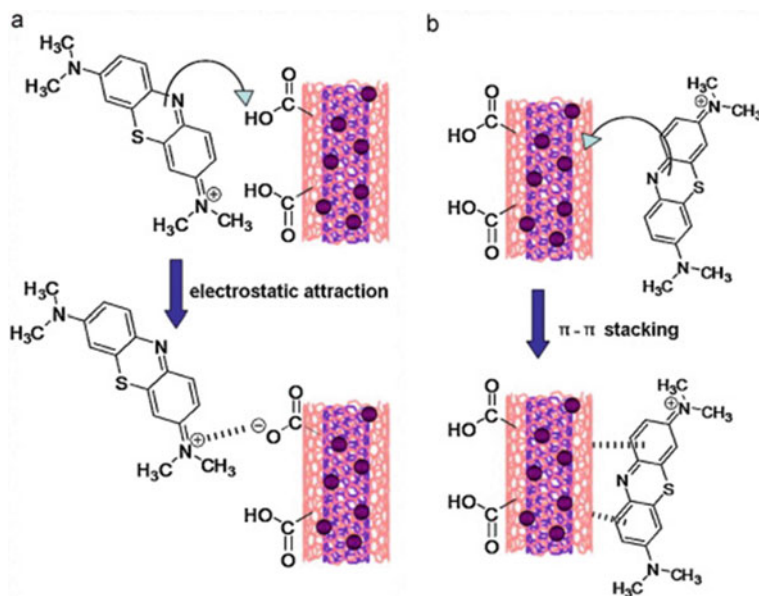


Fig. 16 Adsorption of dye over functionalized CNT [6]

the hydrothermal method for methylene blue dye removal [67]. Another interesting research on photodegradation of malachite green and methylene blue dye has been reported by Tarigh et al. [116]. Hu et al. have investigated a water-soluble hyperbranched polyamine functionalized MWCNTs for adsorption of three different organic dyes, e.g., methylene blue, methyl violet, and malachite green [49]. A number of CNT-based composites for dye removal have been reported [42]. Studies have indicated that composites of CNT-chitosan, CNT-ACF (AC fiber), CNT-Fe₃O₄, CNT-dolomite, CNT-cellulose, and CNT-graphene are excellent absorbents for various pollutants. A composite of polyaniline (PANI)-encapsulated MWCNTs is reported as an efficient adsorbent for alizarin yellow R dye [131]. Recently functionalized CNTs have been reported for water treatment processes [10, 50, 52, 95, 124]. Dye removal using various CNT-based adsorbents is given in Table 5 [103].

6.5 Magnetic Carbon Nanotubes

Carbon-based materials can be mixed with magnetic nanoparticles to get porous and stable materials having unique magnetic properties. These materials have various multidisciplinary applications. Various methods for the preparation of magnetic carbon nanotubes are summarized in Table 6.

MWCNTs are preferred over SWCNTs and magnetization is done using γ -Fe₂O₃ or Fe₂O₃. The synthesized magnetic nanotubes can be dispersed in water and can be separated with the help of a magnetic field. Multi-walled carbon nanotube (MWCNT) filled with γ -Fe₂O₃ have been used for the adsorptive removal of methylene blue and neutral red with a maximum adsorption capacity of 42.3 g/g and 77.5 mg/g, respectively. High-resolution transmission electron microscopic (HR-TEM) images showed that maghemite particles of size ~10 nm are inserted into the nanotubes. Whereas, the XRD spectrum indicated the presence of γ -Fe₂O₃. The material is attracted strongly toward an external magnet and can again be redispersed by the removal of the magnetic field thus making the separation step easy [93].

In a similar manner, MWCNTs modified by Fe₂O₃ or Fe₃O₄ nanoparticles were prepared by a wet chemical method. XRD pattern showed the presence of maghemite, hematite, and magnetite, and the diameter of the carbon nanotube was found to be 58 nm. This magnetic material was then used for adsorptive removal of thionine, crystal violet, and janus green B with about 98–99% efficiency [69]. Some other examples of these techniques are methylene blue removal [38] and methyl orange removal [14] by γ -Fe₂O₃ modified MWCNT.

6.6 Carbon-Nanotube-Based Buckypaper

Buckypapers are an entangled web of CNTs that is self-supported and have a flexible morphology apart from being chemically and physically stable. They also have

Table 5 Dye removal using various CNT-based adsorbents [103]

Types of CNT	Modification	Surface area (m ² /g)	Treated dye	Capacity (mg/g)
MWCNTs	Without modification	270	Acid red 18	167
MWCNTs	Without modification	217	Acid red 183 (AR183), reactive blue 4 (RB4)	AR183: 45 RB4: 59
MWCNTs	Without modification	–	Alizarin red S (ARS), Morin	ARS:161 Morin: 26
MWCNTs	Without modification	–	Maxilon blue	261
MWCNTs	Without modification	40	Congo red	352
MWCNTs	Without modification	181	Reactive red M-2BE	336
MWCNTs	Without modification	270	Malachite green	143
MWCNTs	Without modification	233	Acid blue 161	458
MWCNTs	Magnetic CNT-iron oxide composite	62	Methylene blue (MB), neutral red (NR), Brilliant Cresyl blue (BSB)	MB: 12 NR: 10 BSB: 6
MWCNTs	Oxidized	–	Methyl orange	306
MWCNTs	Composite with chitosan hydrogel beads	238	Congo red	450
MWCNTs	Magnetic nanocomposites of MWCNT and Fe ₃ C	39	Direct red 23	86
MWCNTs	Graphene coated MWCNT hybrid with graphene oxide	79	Methylene blue	88
MWCNTs	Composite with Fe ₂ O ₃ NPs	114	Methylene blue (MB), neutral red (NR)	MB: 42 NR: 78
MWCNTs	Starch coated magnetic iron oxide nanocomposites	133	Methyl orange (MO), methylene blue (MB)	MB: 94 MO: 136
MWCNTs	Modified with cysteamine (MWCNT-COOH-Cysteamine)	–	Amido black 10B	131
MWCNTs	Guar gum and iron oxide NP grafted MWCNTs	–	Methylene blue (MB), neutral red (NR)	MB: 62 NR: 90
SWCNTs	Without modification	700	Reactive blue 29	496
SWCNTs	Pristine and oxidized	400	Basic Red 46	38

(continued)

Table 5 (continued)

Types of CNT	Modification	Surface area (m ² /g)	Treated dye	Capacity (mg/g)
SWCNTs	Without modification	More than 700	Reactive Red 120	426

Table 6 Various methods for the preparation of magnetic carbon nanotubes and their potential application

Fabrication method	Properties	Applications
Hydrothermal	Optical and electrical properties	Pollutant adsorbent Magnetic storage medium
Sol-gel		
Self-assembly		
Pyrolysis	Field emission properties	Electrochemical sensor, gas sensor, supercapacitor
Electrospinning		
Template method		
Chemical vapor deposition	Chemical properties	Microwave adsorbent, magnetic hyperthermia
Arc discharge		
Capillary action		

interesting thermal, mechanical, and electrical properties, which make them useful in various fields such as sensors, actuators, radio-frequency filter, and environmental remediation. The buckypaper has a very disordered structure with CNTs which are held together by van der Waals and π - π interactions. The structure is highly porous and 60–70% of the total volume of the buckypaper is occupied by pores [96].

Buckypapers are typically produced by the dry method or wet method. In the dry method of preparation micro-sized hydrocarbons such as trichloro benzene are used as raw material and nickel and iron are used as catalysts under high-pressure environment. The membrane produced is comparatively large in size but has severe limitations in terms of the high amount of residual catalyst formation. The wet approach to fabrication is thought to be better than the dry approach due to better control over the composition. The wet method involves synthesis and filtration. In the first step, CNTs and surfactants are mixed thoroughly and homogenized using ultrasonication. Then the suspension is washed and filtered until a mat form is obtained and the material is free from mixed solvent. Commonly used surfactants are sodium dodecyl-sulfate and triton X-100. The quality of bucky paper depends on the suspension and the filter mat. Moreover, the buckypaper can further be functionalized to enhance its reactivity. The size of the bucky paper produced by this method is smaller although the method is not cost-effective.

Most of the research on CNT-based buckypaper is focused on the desalination of water and not too many reports on dye removal by buckypaper are known. In one of the works, Lau et al. fabricated a Jicama peroxidase stabilized buckypaper/polyvinyl alcohol membrane for removal of methyl blue [63]. The membrane can remove the

dye with more than 99% efficiency within 183 min with a flow rate of 2 mL/min and an H_2O_2 :dye ratio of 75:1.

6.7 Metal-Doped Porous Carbon Materials

Metal doping refers to the deposition of fine distribution of metal particles on the porous carbonaceous materials onto the pore channels. The overall integrity of the carbonaceous materials remains the same after the deposition; however, the surface properties are enhanced and as a consequence, the adsorption efficiency for dye also increases. Moreover, the selectivity of the materials is also increased due to the coordination of the doped metal with the carbon matrix. Metal doping can incorporate magnetic properties to the material and thus make the regeneration process easier. The doping could be by single as well as double metals and commonly used metals are iron, cobalt, nickel, aluminum, lanthanum, zinc, etc. As far as the mechanism is concerned, the metal ions coordinated with the acidic or basic functional groups present on the surface of the carbonaceous material, followed by in situ oxidation to form metal oxides (Fig. 17) [132].

6.7.1 Single-Metal-Doped Porous Carbon Materials

Among single-metal-doped porous carbon material, transition metals having magnetic properties such as iron, cobalt, and nickel are particularly favored because of the ease of separation of the adsorbent. Moreover, magnetic-metal-doped materials

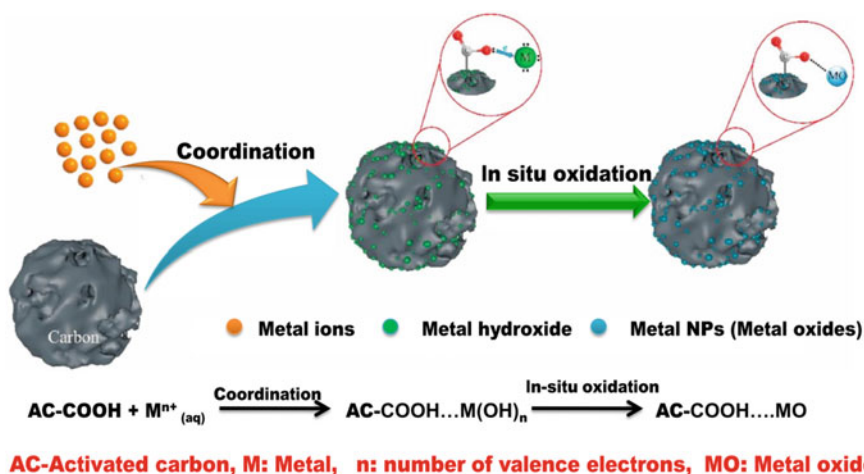


Fig. 17 Interaction between the carbonaceous material and metal on doping [132]

develop super paramagnetism. Almost all these materials show excellent adsorption behavior. Kim et al. have prepared granular AC modified with ferrous chloride to enhance the efficacy of methylene blue removal from wastewater. It was observed that adsorption capacity was increased from 175.4 to 238.1 mg/g on modification [59]. More examples of dye removal by magnetically enhanced porous carbon material are listed in Table 7. Many of these studies have also been focused on the regeneration of the adsorbent materials. For example, shell-based powdered AC modified with ferric nitrate was prepared and used for methyl orange removal with enhanced regeneration ability. It was reported that although the efficiency of the material for dye removal decreases from 384.62 to 303.03 mg/g, the modified material is easier to separate due to its magnetic property (Do et al. 2011). Table 7 contains the list of magnetic-metal-doped porous carbon materials for dye removal [132].

6.7.2 Nonmagnetic Metal-Doped Porous Carbon Materials

In addition to magnetic metal, porous carbon material can be doped with nonmagnetic metals also. Rare-earth elements such as lanthanides have a high affinity for organic compounds through the interaction of f orbitals. Goscianska et al. modified the ordered mesoporous carbon (OMC) with lanthanum chloride by template method and used it for the removal of methyl orange from wastewater. It was reported that adsorption capacity increases with an increase in lanthanum concentration although surface area and pore volumes decreased. This indicated that there is a strong interaction between lanthanum and the dye other than physisorption [39]. Similar observations are also obtained in the adsorptive removal of sunset yellow by cerium modified OMC [40]. Similarly, neodymium embedded OMC was used to enhance the efficiency (~40%) of adsorbent for removal of sunset yellow [5].

Doping with non-rare earth metals has also been studied. Palladium, silver, and zinc doped AC were used for the removal of bromophenol red dye and the adsorption efficiencies were found to be 143 mg/g, 240 mg/g, and 200 mg/g, respectively. This is due to differences in interactions of different metals with the dye. The same authors also reported the preparation of zinc doped AC by ultrasonic method for removal of sunset yellow with 588.8 mg/g efficiency in 20 min [34]. A comprehensive list of nonmagnetic-metal-doped porous; carbon material used for dye removal is given in Table 8.

The overall properties of the adsorbent materials, not only depend on the nature of the metal but also on the structure and properties of the porous carbon material used. The acid–base interaction between the dye molecule and the adsorbent is increased on metal doping and resulting in an increase in acidity. Moreover, the change in surface charge due to metal doping also influences electrostatic interaction between the dye molecule and the adsorbent. Both of these factors facilitate the adsorption process in addition to the π – π interaction between the aromatic moiety of the dye and the porous carbon material. Thus, both nonmagnetic and magnetic-metal-doped carbon materials are better compared to raw carbon material [132].

Table 7 List of magnetic-metal-doped porous carbon material for dye removal [132]

Adsorbing material	Doping method	Dyes	Magnetic behavior	Efficiency	Regeneration
Fe-AC	Ultrasound and microwave-assisted	MB	Superparamagnetic	259	Easily separated
Fe/fruit peels AC	Soak-calcination	MB Congo red Rhodamine B		183.05 ± 58.51 500.55 ± 174.96 270.71 ± 83.26	5 cycles (stay above 90%) 5 cycles (stay above 95%) 5 cycles (stay above 93%)
Fe ₃ O ₄ /AC	Solvothermal reduction	MO		324	Easily separated
C ₀ /C microrods	Direct carbonization	MB, acid fuchsin malachite green		13,960 11,610 4893	5 cycles (stay above 95%) 5 cycles (stay above 95%) 5 cycles (stay above 95%)
Fe-GAC	Impregnation	Methylene blue		238.1	–
10Fe ₃ O ₄ /PAC-HINO ₃	Impregnation	MO		303.03	5 cycles (stay above 65%)
Fe-AC	Wet oxidation	MB		30.61	–

Table 8 Adsorption capacity of various nonmagnetic-metal-doped porous carbon materials to dyes [132]

Adsorbent material	Doping method	Dye	Efficiency (mg/g)	Regeneration
ZnO-NRs-AC	Ultrasonic method	MB	588.8	–
Cu ₂ O-NP-AC	Hydrothermal	Sunset yellow	113	–
CuS-NP-AC	Heating	MB	208.3	–
Zn(OH) ₂ -NP-AC	Ultrasonic method	Sunset yellow	83.3–114.9	–
Al-CNTs-2.0	Hydrothermal	MO	69.7	–
Bi ₂ O ₃ @GO	Sonochemical method	Rhodamine B	320	8 cycles (stay above 78%)
Cu-AC	Ultrasound and microwave	MO	377.358	5 cycles (decreased gradually)
Zr/N-OMC	Direct carbonization	MB Erythrosine	492 286	–
MHPCM	Impregnation	MB Direct black 38	1585.7 438.6	–
Mg/NeC	Pyrolysis	MO	384.61	7 cycles (from 384.61 to 351.78 mg/g)

6.7.3 Bimetal-Doped Porous Carbon Material

Magnetic metals such as iron, nickel, etc. can magnetize the material thereby helping in regeneration; while metals such as copper, zinc, and cerium have a strong affinity toward N, O, S, etc. and can interact strongly with the dye molecule. Thus, doping with two metals instead of one can increase the efficiency and selectivity of the material further. Iron, cerium co-doped AC material was prepared by microwave heating and used for adsorptive removal of methylene blue dye from wastewater. It was reported that the surface area and pore volume are reduced significantly on codoping with two metals, however, the adsorption efficiency is enhanced by 27.31% compared to raw AC due to the synergistic action of both the metals. The regenerations also become easier [17]. NiO and ZnO codoped carbon fibers were used for adsorptive removal of Congo red dye from wastewater. The doped materials have an efficiency of 613 mg/g compared to 167 mg/g for untreated carbon fiber. The removal efficiency decreased by 1.4% even after 5 cycles [17]. Removal of malachite green by bimetallic Fe–Mg codoped AC was reported by Guo et al. The bimetallic carbon material has good adsorption efficiency and separability [41]. Similar studies have also been reported by other researchers [51, 72].

6.8 Graphene- and Graphene-Oxide-Based Adsorbent Material for Dye Removal

Graphene is an sp^2 hybridized, covalently bonded single sheet aromatic hydrocarbon in which hexagonal rings are arranged in a honeycomb crystal lattice structure (Fig. 18). Because of its remarkable properties such as high surface-to-volume ratio, excellent transparency, good conductivity and mechanical strength, graphene and its derivatives found applications in various fields of science and technology [119]. Conventional AC is a very good adsorbent material that has been used for the past many decades for the adsorptive removal of pollutants including organic dyes. However, they have severe limitations due to chemical rigidity and high cost for regeneration. Graphene and its derivatives, on the other hand, are a very good choice because of the large surface-to-volume ratio and the presence of strong π - π interaction and hydrophobic effect, which will reinforce the adsorption process. Reduction of graphene oxide does not produce graphene back, instead reduced graphene oxide is formed which has a carbon to oxygen ratio of 246:1 in comparison to 2:1 in graphene oxide (GO) [138].

Due to its hydrophobic nature, graphene is not dispersed in water. Hence, to increase its hydrophilicity, graphene is converted to composite or oxidized to form graphene oxide (GO). Oxidation of graphene renders it with functional groups such as hydroxyl, carboxyl, epoxy, carbonyl, etc. which creates a negative charge on the surface and thus makes it hydrophilic. Graphene and graphene oxide can further be functionalized with specific organic reagents.

Bismuth-oxide-embedded graphene oxide prepared by the sonochemical method has been used for the removal of rhodamine B with enhanced efficiency (320 mg/g) compared to unmodified graphene oxide. It is due to strong hydrogen bonding on the surface of graphene oxide on the incorporation of the metal oxide. The aggregation and oxidation of the surface can also be avoided in presence of bismuth oxide [85].

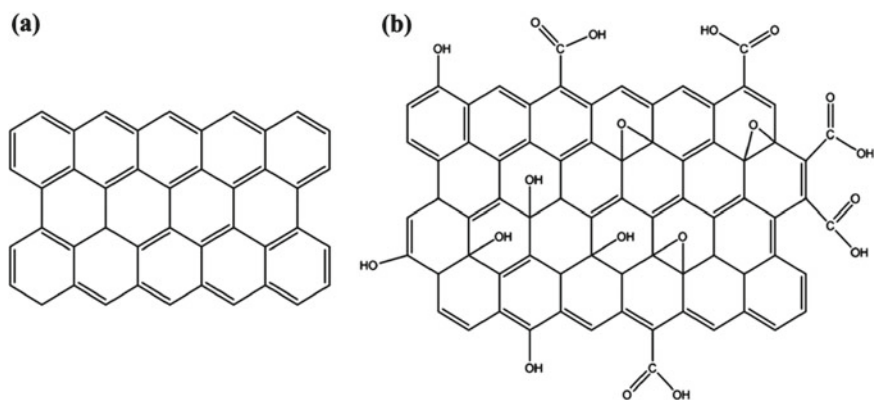


Fig. 18 Structure of **a** graphene and **b** graphene oxide

Chang et al. synthesized $\text{CoFe}_2\text{O}_4/\text{GO}$ composite, which showed selective adsorption behavior of cationic dye over anionic dyes. The composite material showed better efficiency for cationic dye adsorption than pure graphene but the efficiency of adsorption of anionic dye remained the same even after doping (Chang et al. 2020). Many natural polymers such as chitosan, xylan, insulin, and κ -carrageenan can form a stable composite with graphene or graphene oxide. For example, three biopolymer-GO nanocomposites have been prepared and used for the removal of methylene blue, rhodamine 6G, orange II, and acid fuchsin (Fig. 19). The material showed the highest efficiency for methylene blue (769 mg/g) and followed the Langmuir adsorption isotherm model. The adsorption process was found to be spontaneous, exothermic, and highly dependent on the pH and other conditions [92].

The GO-chitosan hydrogel composite is reported to remove methylene blue and eosin Y dyes from an aqueous solution. The capacity for methylene blue removal is 390 mg/g, for pure GO it is 387 mg/g, and for chitosan beads the capacity is 99 mg/g. The composite material was used as a column packing and the dyes could be removed by passing dye solution through it. The material was further improved by magnetization and the adsorption capacity became 95.16 mg/g. The process was exothermic and spontaneous and desorption was performed with 0.5 M NaOH and 90% dye could be recycled [18, 28]. Graphene-oxide-wrapped magnetite nanoclusters were used as a recyclable functional hybrid for fast and highly efficient removal of rhodamine B [32].

A comprehensive list of graphene- and graphene-oxide-based dye removal system are listed in Table 9.

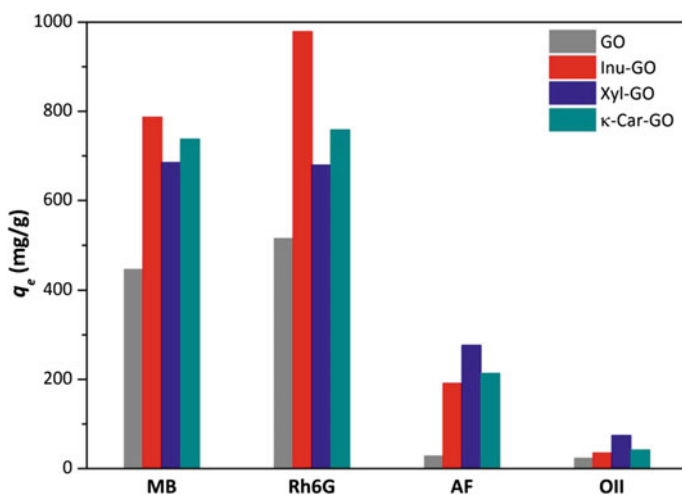


Fig. 19 Adsorption capacity GO and three GO-biopolymer composites for methylene blue (MB), rhodamine 6G(Rh6G), orange II(OII), and acid fuchsin (AF) [92]

Table 9 List of graphene- and graphene-oxide-based dye removal systems [119]

Composite	Dye	Adsorption capacity	Regeneration
GO	Methylene blue	1.939 mg mg ⁻¹	37% with acetic acid, 30% ammonia in ethanol
Chitosan-GO	Methylene blue, Methylene orange	1.60, 0.80 mmol g ⁻¹	>90% after 5 cycles, acidic/alkaline eluent
Graphene-Fe ₃ O ₄	Methylene blue	43.82	5 cycles (decreases with each cycle)
Amide-functionalized MOF/GO	Methylene blue	97% in 15 min	4 cycles
GO	Acridine orange	2158 mg g ⁻¹ , 95%	–
Layered GO	Methylene blue, Methylene green	350 and 248 mg g ⁻¹	–
rGO	Methylene green	77%	–
rGO-based hydrogels	Methylene blue, Rhodamine-B	~100%, ~97%	~ 100%, ~ 80%
rGO–TiO ₂ hybrids (sheets, nanotubes)	MB	83.26, 75.36 mg g ⁻¹ , 90%	–
Polystyrene/Fe ₃ O ₄ /GO	RhB	13.8 mg g ⁻¹	Magnetic separation
GO–Fe ₃ O ₄ hybrid	MB and neutral red (NR)	167.2 and 171.3 mg g ⁻¹	Magnetic separation
GO–chitosan hydrogels (GO–CS)(GO–CS10–10:1 w/w)	MB and eosin Y	387,326 mg g ⁻¹	Filtration
GO-sodium alginate	Methylene blue	833.33 mg/gm	–
PDA/GO	Methylene blue	2.18 g g ⁻¹	–
GO-magnetic cyclodextrin	Methylene blue	228.5 mg/g	Magnetic separation
rGO-supported ferrite	Methylene blue, rhodamine-B	35, 23 mg g ⁻¹ , ~100%, 92%	Magnetic separation

6.9 Multifunctional 3D Carbon Nanomaterials Superstructures

Carbon nanomaterials have extensively been used for environmental remediation but a direct release of carbon nanoparticles in the environment is not preferred due to environmental concerns [139]. In order to tackle these problems, carbon nanomaterials are combined with other materials to form a three-dimensional multifunctional superstructure. This amalgamation can ensure environmental safety and also generate new functionalities. The conversion of nanomaterials to three-dimensional structures is performed using a self-assembly method, template-assisted methods, and 3D

printing methods [135]. Different types of carbon-nanomaterial-based superstructures such as foams, sponges, aerogel, hydrogels have been successfully fabricated and utilized for adsorptive removal of oil spills, organic compounds, and dyes. The three-dimensional carbon nanomaterial-based porous sponges, foams, and aerogels are suitable for the removal of oil spills due to their superhydrophobic and superoleophobic surface and high amount of oil wettability [133]. On the other hand, hydrogels are more versatile and can be used against any type of pollutants.

Chen et al. fabricated 3D carbon aerogel materials by combining two-dimensional graphene oxide nanosheet and one oxidized carbon nanotubes via a self-assembly process. This material can adsorb several different types of pollutants including methylene blue dye (Fig. 20) [108].

The authors observed that there is a synergistic effect between graphene oxide and carbon nanomaterial in the ‘three-dimensional hydrogel producing a greater number of adsorption sites, large surface area, greater porosity, greater interspace, and as a consequence better adsorptive capacity. The adsorption efficiency for methylene blue is 685 mg/g and 94.47% of the dye could be recovered by desorption [108]. In another work, a graphene-based aerogel was constructed with gelatin by in situ reducing self-assembly method. The aerogel was then used for the removal of rhodamine B, methylene blue, crystal violet, and neutral red with an order of rhodamine B > methylene blue > crystal violet > neutral Red [65]. Chen et al. synthesized three-dimensional

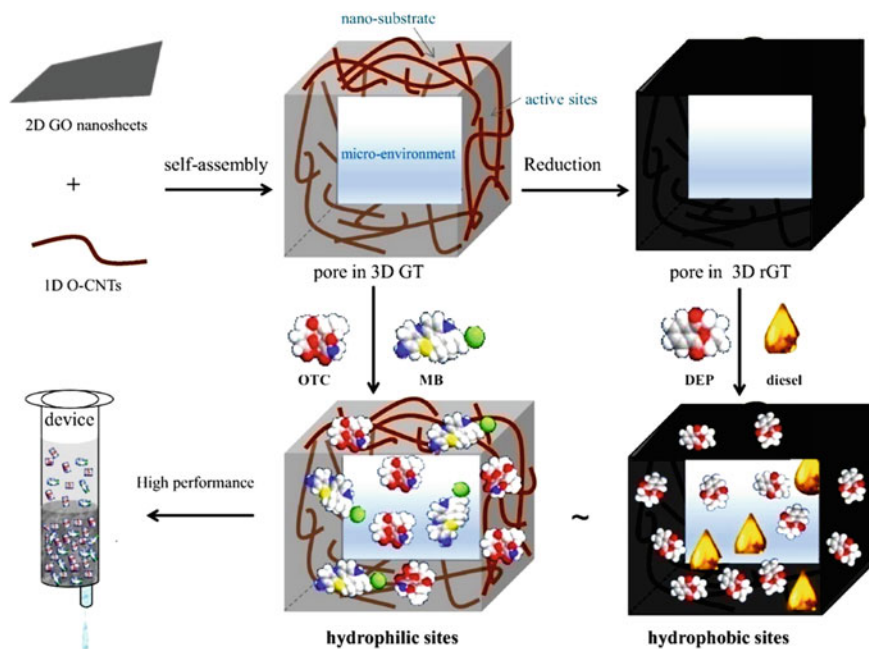


Fig. 20 The synergistic effect of GO and CNTs in 3D GTs' structure and adsorption performance [108]

graphene sheets with chitosan to generate both the positively charged and negatively charged surface for successful adsorption of methylene blue (cationic dye) and eosin Y (anionic dye) with more than 300 mg/g efficiency [18]. A cheese-like foam of three-dimensional carbon–boron–nitride was synthesized by Liu et al. following a simple heating method. The material has a very small pore size (2–100 nm) and hydrophobic and lipophilic character. Because of the presence of boron and nitrogen, a strong interaction is established between the active site on the three-dimensional material and organic dyes containing an aromatic ring. This adsorbent material can remove different types of pollutants including Congo red and methylene blue with 408 mg g⁻¹ and 307 mg g⁻¹ efficiency [64]. Thus, there are many such examples of carbon nanomaterials such as graphene, graphene oxide, carbon nanotubes, and nanofibers embedded into three-dimensional polymeric networks of hydrogels and their application in dye removal from wastewater [97].

6.10 Carbon-Based Nano/Micromotors for Adsorption of Dyes from Wastewater

An artificial nano/micromotor is a highly sophisticated device that can self-propagate in an aqueous medium by utilizing physical and biochemical energy into mechanical force. These devices can either be powered by fuel such as H₂O₂, water, acid, NaBH₄, etc., or energy sources such as light, sound, electric, or magnetic field [23, 113, 125]. Maria-Hormigos et al. fabricated carbon nanotube ferrite–manganese dioxide tubular micromotors for the removal of remazol brilliant blue R dye from industrial wastewater. The inside MnO₂ layer in the micromotor can decompose H₂O₂ catalytically to produce oxygen gas and hydroxyl radicals which degrades the dye into CO₂ and H₂O. The scaffold of the micromotor is produced by carbon and Fe₂O₃ which generates defects in it resulting in roughness of the outer surface and thus creating more radicals. The presence of Fe₂O₃ in the outer layer can also ensure better separability [73].

Another remarkable example of self-propel micromotor is hydrothermally produced carbon-MnO₂ micromotor used for catalytic degradation of methylene blue. Carbon-based micro/nanomotors have not been used so far for adsorptive removal of pollutants due to the high cost of production. However, due to their self-propagating properties, they are better than the static adsorbent [46].

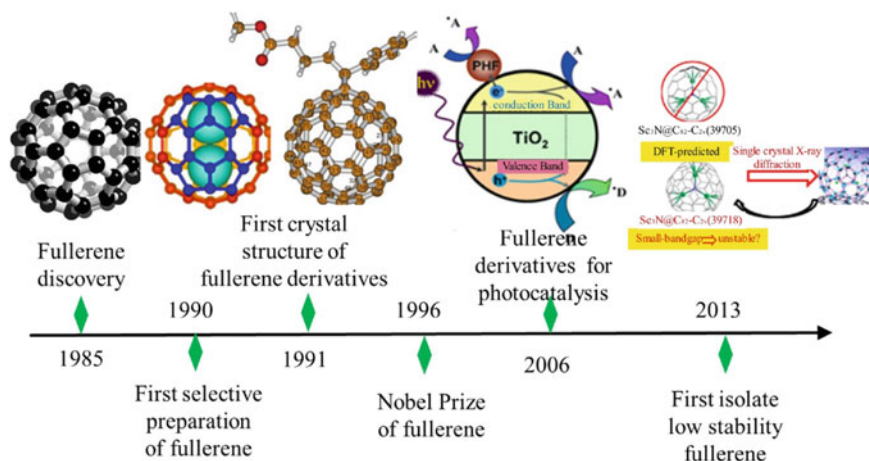


Fig. 21 Fullerene and its derivatives are used as an adsorbent as well as a photocatalyst for the removal of many dyes from solution [83]

6.11 Removal of Dyes by C₆₀ Fullerenes

Fullerene is a zero-dimensional structured carbon material and has a number of applications including dye adsorption [44]. The discovery of fullerenes and their derivatives are illustrated in Fig. 21 [83]. Depending on the functionalization, adsorption of dyes may occur via electrostatic interaction, π - π bonding, and hydrogen bonding.

6.12 Removal of Dyes by Nanodiamond

Nanodiamond (ND) is a form of carbon-based nanoparticles, offering diamond properties on a nanometer scale. It was discovered in the 1960s by the former Soviet scientists. ND is available with an average diameter of ~ 5 nm with narrow size distribution and relatively large surface area. It is used in a number of fields including water purification [57]. A number of dyes such as azo dye AO7 have been removed from ND by using the adsorption technique [127]. It is suggested that ND is a suitable adsorbent for textile dyes even at neutral pH. The unique surface chemistry of ND has made it a competitive candidate for carbon-based nanoparticles. Polymer/ND (PND) (nano-) composites are being used in a number of areas including dye removal and water purification in an effective manner. Synthesis, fabrication, and applications of PND are given in Fig. 22 [57]. However, it is a new field, so only limited work has been done.

Oxidized nanodiamond (OND) and unoxidized ND (UND) have been used for the removal of methyl orange (MO) and methylene blue (MB) dyes and results have shown that UND performs much better than OND (Fig. 23) [75].

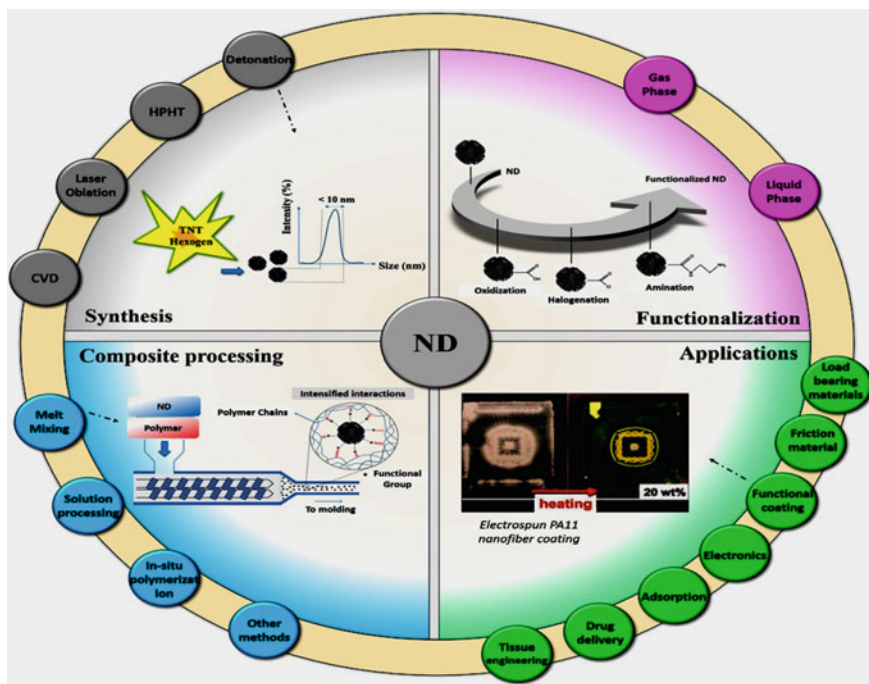


Fig. 22 Synthesis and applications of PND [57]

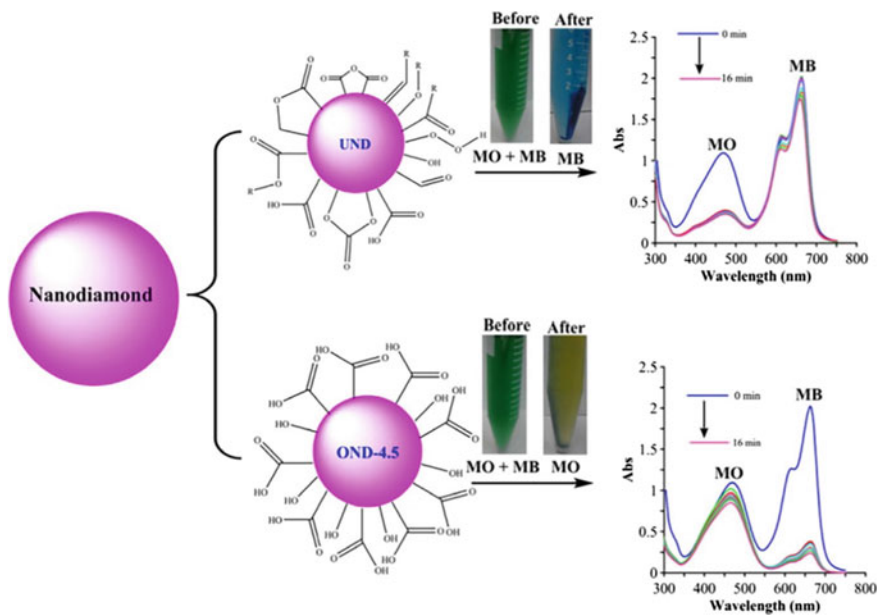


Fig. 23 Removal of MO and MB by ND [75]

7 Conclusions

Due to the industrial revolution and population growth, water has become highly polluted and harmful to living beings. One of the most toxic materials polluting water is dye. A number of methods have been used for the removal of dyes from water but the adsorbent technique is found to be the most efficient and economical. For this purpose, a suitable adsorbent with a high surface area is required. In recent years, different types of carbon materials have been used for dye removal. In this chapter, types of dyes and different carbon materials have been discussed. Effects of different parameters such as initial concentrations of dyes, solution pH, temperature, functionalization of carbon materials, doping in carbons, etc. have been discussed for the removal of dyes. Considering the type of dyes and carbon materials, it can be inferred that number of factors should be taken into account while the adsorption capacity of various carbon materials for dye removal is evaluated from an economic point of view.

References

1. Abdulraheem G, Bala S, Muhammad S, Abdullahi M (2015) Kinetics, equilibrium and thermodynamics studies of CI Reactive Blue 19 dye adsorption on coconut shell based AC. *Int Biodeterior Biodegradation* 102:265–273
2. Aboua KN, Yobouet YA, Yao KB, Gone DL, Trokourey A (2015) Investigation of dye adsorption onto AC from the shells of Macoré fruit. *J Environ Manag* 156:10–14
3. Abualnaja KM, Alprol AE, Ashour M, Mansour AT (2021) Influencing Multi-Walled Carbon nanotubes for the removal of Ismate violet 2R dye from wastewater: isotherm, kinetics, and thermodynamic studies. *Appl Sci* 11(11):4786–4812
4. Agbozu IE, Emoruwa FO (2014) Batch adsorption of heavy metals (Cu, Pb, Fe, Cr and Cd) from aqueous solutions using coconut husk. *Afr J Environ Sci Technol* 8(4):239–246
5. Ahmad ZU, Yao L, Wang J, Gang DD, Islam F, Lian Q, Zappi ME (2019) Neodymium embedded ordered mesoporous carbon (OMC) for enhanced adsorption of sunset yellow: characterizations, adsorption study and adsorption mechanism. *Chem Eng J* 359:814–826
6. Ai L, Zhang C, Liao F, Wang Y, Li M, Meng L, Jiang J (2011) Removal of methylene blue from aqueous solution with magnetite loaded multi-wall carbon nanotube: kinetic, isotherm and mechanism analysis. *J Hazard Mater* 198:282–290
7. Amin NK (2008) Removal of reactive dye from aqueous solutions by adsorption onto ACs prepared from sugarcane bagasse pith. *Desalination* 223(1–3):152–161
8. Amin NK (2009) Removal of direct blue-106 dye from aqueous solution using new ACs developed from pomegranate peel: adsorption equilibrium and kinetics. *J Hazard Mater* 165(1–3):52–62
9. Anastopoulos I, Karamesouti M, Mitropoulos AC, Kyzas GZ (2017) A review for coffee adsorbents. *J Mol Liq* 229:555–565
10. Aslam MMA, Kuo HW, Den W, Usman M, Sultan M, Ashraf H (2021) Functionalized carbon nanotubes (CNTs) for water and wastewater treatment: preparation to application. *Sustainability* 13(10):5717. <https://doi.org/10.3390/su13105717>
11. Asmaly HA, Saleh TA, Laoui T, Gupta VK, Atieh MA (2015) Enhanced adsorption of phenols from liquids by aluminum oxide/carbon nanotubes: comprehensive study from synthesis to surface properties. *J Mol Liq* 206:176–182. <https://doi.org/10.1016/j.molliq.2015.02.028>

12. Bagotia N, Sharma AK, Kumar S (2020) A review on modified sugarcane bagasse biosorbent for removal of dyes. *Chemosphere* 129309
13. Baseri JR, Palanisamy PN, Sivakumar P (2012) Preparation and characterization of AC from *Thevetia peruviana* for the removal of dyes from textile waste water. *Adv Appl Sci Res* 3(1):377–383
14. Bayazit ŞS (2014) Magnetic multi-wall carbon nanotubes for methyl orange removal from aqueous solutions: equilibrium, kinetic and thermodynamic studies. *Sep Sci Technol* 49(9):1389–1400
15. Benkhaya S, M'rabet S, El Harfi A (2020) A review on classifications, recent synthesis and applications of textile dyes. *Inorg Chem Commun* 115:107891
16. Bulgariu L, Escuder LB, Bello OS, Nisar MJ, Adegoke KA, Michael FA, Anastopoulos K (2019) The utilization of leaf-based adsorbents for dyes removal: A review. *J Mol Liq* 276:728–747
17. Chen S, Tang S, Sun Y, Wang G, Chen H, Yu X, Su Y, Chen G (2018) Preparation of a highly porous carbon material based on quinoa husk and its application for removal of dyes by adsorption. *Materials* 11(8):1407. <https://doi.org/10.3390/ma11081407>
18. Chen Y, Chen L, Bai H, Li L (2013) Graphene oxide–chitosan composite hydrogels as broad-spectrum adsorbents for water purification. *J Mater Chem A* 1(6):1992–2001
19. Chukwu UJ, John EP, Kalagbor AI (2017) Adsorption of Cu^{2+} and Fe^{2+} from single metal ion solution using unmodified and formaldehyde modified kola-nut (*Cola nitida*) testa. *OSR J Appl Chem (IOSR-JAC)* 10(12):12–18
20. Demiral H, Demiral I, Karabacakoglu B, Tümsük F (2008) Adsorption of textile dye onto AC prepared from industrial waste by ZnCl_2 activation. *J Int Environ Appl Sci* 3(5):381–389
21. Dil EA, Ghaedi M, Asfaram A, Mehrabi F, Bazrafshan AA, Tayebi L (2019) Synthesis and application of Ce-doped TiO_2 nanoparticles loaded on activated carbon for ultrasound-assisted adsorption of basic red 46 dye. *Ultrason Sonochem* 58:104702
22. Djlani C, Zaghdoudi R, Djazi F, Boucekima B, Lallam A, Modarressi A, Rogalski M (2015) Adsorption of dyes on activated carbon prepared from apricot stones and commercial activated carbon. *J Taiwan Inst Chem Eng* 53:112–121
23. Dong R, Zhang Q, Gao W, Pei A, Ren B (2016) Highly efficient light-driven TiO_2 –Au Janus micromotors. *ACS nano* 10(1):839–844
24. Duan Q, Lee J, Liu Y, Qi H (2016) Preparation and photocatalytic performance of MWCNTs/ TiO_2 nanocomposites for degradation of aqueous substrate. *J Chem* <https://doi.org/10.1155/2016/1262017>
25. Duman O, Tunç S, Polat TG, Bozoğlan BK (2016) Synthesis of magnetic oxidized multi-walled carbon nanotube- κ -carrageenan- Fe_3O_4 nanocomposite adsorbent and its application in cationic methylene blue dye adsorption. *Carbohydr Polym* 147:79–88
26. El-Shafey EI, Ali SNF, Al-Busafi S, Al-Lawati HAJ (2016) Preparation and characterization of surface functionalized activated carbons from date palm leaflets and application for methylene blue removal. *J Environ Chem Eng* 4:2713–2724
27. Fabon MB, Legaspi GJ, Leyesa K, Macawile MC (2013) Removal of basic dye in water matrix using AC from sugarcane bagasse. In: *International conference on innovations in engineering and technology*, pp 198–201
28. Fan L, Luo C, Li X, Lu F, Qiu H, Sun M (2012) Fabrication of novel magnetic chitosan grafted with graphene oxide to enhance adsorption properties for methyl blue. *J Hazard Mater* 215:272–279
29. Fernandez ME, Nunell GV, Bonelli PR, Cukierman AL (2014) Activated carbon developed from orange peels: batch and dynamic competitive adsorption of basic dyes. *Ind Crops Prod* 62:437–445
30. Ferreira GMD, Ferreira GMD, Hespanhol MC, de Paula Rezende J, dos Santos Pires AC, Gurgel LVA, da Silva LHM (2017) Adsorption of red azo dyes on multi-walled carbon nanotubes and AC: a thermodynamic study. *Colloids Surf A: Physicochem Eng Asp* 529:531–540

31. Foo KY, Hameed BH (2011) Microwave assisted preparation of AC from pomelo skin for the removal of anionic and cationic dyes. *Chem Eng J* 173(2):385–390
32. Ganesan V, Louis C, Damodaran SP (2018) Graphene oxide-wrapped magnetite nanoclusters: a recyclable functional hybrid for fast and highly efficient removal of organic dyes from wastewater. *J Environ Chem Eng* 6(2):2176–2190
33. Georjin J, Dotto GL, Mazutti MA, Foletto EL (2016) Preparation of AC from peanut shell by conventional pyrolysis and microwave irradiation-pyrolysis to remove organic dyes from aqueous solutions. *J Environ Chem Eng* 4(1):266–275
34. Ghaedi M, Ansari A, Habibi MH, Asghari AR (2014) Removal of malachite green from aqueous solution by zinc oxide nanoparticle loaded on activated carbon: kinetics and isotherm study. *J Ind Eng Chem* 20(1):17–28
35. Ghaedi M, Ghaedi AM, Mirtamizdoust B, Agarwal S, Gupta VK (2016) Simple and facile sonochemical synthesis of lead oxide nanoparticles loaded activated carbon and its application for methyl orange removal from aqueous phase. *J Mol Liq* 213:48–57
36. Ghaedi M, Nasab AG, Khodadoust S, Rajabi M, Azizian S (2014) Application of activated carbon as adsorbents for efficient removal of methylene blue: kinetics and equilibrium study. *J Ind Eng Chem* 20:2317–2324
37. Ghasemi E, Heydari A, Sillanp M (2019) Central composite design for optimization of removal of trace amounts of toxic heavy metal ions from aqueous solution using magnetic Fe₃O₄ functionalized by guanidine acetic acid as an efficient nano-adsorbent. *Micro Chem J* 147:133–141
38. Gong JL, Wang B, Zeng GM, Yang CP, Niu CG, Niu QY, Zhou WJ, Liang Y (2009) Removal of cationic dyes from aqueous solution using magnetic multi-wall carbon nanotube nanocomposite as adsorbent. *J Hazard Mater* 164(2–3):1517–1522
39. Goscianska J, Marciniak M, Pietrzak R (2014) Mesoporous carbons modified with lanthanum (III) chloride for methyl orange adsorption. *Chem Eng J* 247:258–264
40. Goscianska J, Marciniak M, Pietrzak R (2015) Ordered mesoporous carbons modified with cerium as effective adsorbents for azo dyes removal. *Sep Purif Technol* 154:236–245
41. Guo F, Jiang X, Li X, Jia X, Liang S, Qian L (2020) Synthesis of MgO/Fe₃O₄ nanoparticles embedded AC from biomass for high-efficient adsorption of malachite green. *Mater Chem Phys* 240:122240
42. Gupta VK, Kumar R, Nayak A, Saleh TA, Barakat MA (2013) Adsorptive removal of dyes from aqueous solution onto carbon nanotubes: a review. *Adv Coll Interface Sci* 193:24–34
43. Gupta VK, Nayak A, Bhushan B, Agarwal S (2015) A critical analysis on the efficiency of ACs from low-cost precursors for heavy metals remediation. *Crit Rev Environ Sci Technol* 45(6):613–668
44. Gusain R, Kumar N, Ray SS (2020) Recent advances in carbon nanomaterial-based adsorbents for water purification. *Coord Chem Rev* 405:213111
45. Hazzaa R, Hussein M (2015) Adsorption of cationic dye from aqueous solution onto AC prepared from olive stones. *Environ Technol Innov* 4:36–51
46. He X, Büchel R, Figi R, Zhang Y, Bahk Y, Ma J, Wang J (2019) High-performance carbon/MnO₂ micromotors and their applications for pollutant removal. *Chemosphere* 219:427–435. <https://doi.org/10.1016/j.colsurfa.2017.06.021>
47. Heibati B, Rodriguez-Couto S, Al-Ghouthi MA, Asif M, Tyagi I, Agarwal S, Gupta VK (2015) Kinetics and thermodynamics of enhanced adsorption of the dye AR 18 using ACs prepared from walnut and poplar woods. *J Mol Liq* 208:99–105
48. Hesas RH, Arami-Niya A, Daud WMAW, Sahu JN (2013) Preparation and characterization of AC from apple waste by microwave-assisted phosphoric acid activation: application in methylene blue adsorption. *BioResources* 8(2):2950–2966
49. Hu L, Yang Z, Wang Y, Li Y, Fan D, Wu D, Wei Q, Du B (2017) Facile preparation of water-soluble hyperbranched polyamine functionalized multiwalled carbon nanotubes for high-efficiency organic dye removal from aqueous solution. *Sci Rep* 7(1):1–13
50. Hu X, Zou C, Zou X (2019) The formation of supramolecular carbon nanofiber via amidation reaction on the surface of amino single walled carbon nanotubes for selective adsorption

- organic pollutants. *J Colloid Interface Sci* 542:112–122. <https://doi.org/10.1016/j.jcis.2019.01.130>
51. Hu H, Wageh S, Al-Ghamdi AA, Yang S, Tian Z, Cheng B, Ho W (2020) NiFe-LDH nanosheet/carbon fiber nanocomposite with enhanced anionic dye adsorption performance. *Appl Surf Sci* 511:145570
 52. Ibrahim RK, El-Shafie A, Hin LS, Mohd NSB, Aljumaily MM, Ibrahim S, AlSaadi MA (2019) A clean approach for functionalized carbon nanotubes by deep eutectic solvents and their performance in the adsorption of methyl orange from aqueous solution. *J Environ Manag* 235:521–534. <https://doi.org/10.1016/j.jenvman.2019.01.070>
 53. Jiang W, Zhang L, Guo X, Yang M, Lu Y, Wang Y, Zheng Y, Wei G (2021) Adsorption of cationic dye from water using an iron oxide/AC magnetic composites prepared from sugarcane bagasse by microwave method. *Environ Technol* 42(3):337–350
 54. Juang RS, Yei YC, Liao CS, Lin KS, Lu HC, Wang SF, Sun AC (2018) Synthesis of magnetic Fe₃O₄/AC nanocomposites with high surface area as recoverable adsorbents. *J Taiwan Inst Chem Eng* 90:51–60
 55. Jun LY, Mubarak NM, Yee MJ, Yon LS, Bing CH, Khalid M, Abdullah EC (2018) An overview of functionalised carbon nanomaterial for organic pollutant removal. *J Ind Eng Chem* 67:175–186. <https://doi.org/10.1016/j.jiec.2018.06.028>
 56. Jung KW, Choi BH, Hwang MJ, Jeong TU, Ahn KH (2016) Fabrication of granular ACs derived from spent coffee grounds by entrapment in calcium alginate beads for adsorption of acid orange 7 and methylene blue. *Biores Technol* 219:185–195
 57. Karami P, Khasraghi SS, Hashemi M, Rabiei S, Shojaei A (2019) Polymer/nanodiamond composites—a comprehensive review from synthesis and fabrication to properties and applications. *Adv Colloid Interface Sci* 269:122–151
 58. Khan FSA, Mubarak NM, Tan YH, Khalid M, Karri RR, Walvekar R, Abdullah EC, Nizamuddin S, Mazari SA (2021) A comprehensive review on magnetic carbon nanotubes and carbon nanotube-based buckypaper-heavy metal and dyes removal. *J Hazard Mater* 125375
 59. Kim JR, Santiano B, Kim H, Kan E (2013) Heterogeneous oxidation of methylene blue with surface-modified iron-amended AC
 60. Kumar A, Jena HM (2016) Removal of methylene blue and phenol onto prepared AC from Fox nutshell by chemical activation in batch and fixed-bed column. *J Clean Prod* 137:1246–1259
 61. Kumar GV, Rajeev K, Arunima N, Saleh TA, Barakat MA (2013) Adsorptive removal of dyes from aqueous solution onto carbon nanotubes: a review. *Adv Coll Interface Sci* 193–194:24–34
 62. Kumari P, Alam M, Siddiqi WA (2019) Usage of nanoparticles as adsorbents for waste water treatment an emerging trend. *Sustain Mater Technol* 22:00128
 63. Lau YJ, Karri RR, Mubarak NM, Lau SY, Chua HB, Khalid M, Jagadish P, Abdullah EC (2020) Removal of dye using peroxidase-immobilized Bucky paper/polyvinyl alcohol membrane in a multi-stage filtration column via RSM and ANFIS. *Environ Sci Pollut Res* 27(32):40121–40134
 64. Liu Z, Fang Y, Jia H, Wang C, Song Q, Li L, Lin J, Huang Y, Yu C, Tang C (2018) Novel multi-functional cheese-like 3D carbon-BN as a highly efficient adsorbent for water purification. *Sci Rep* 8(1):1–11
 65. Liu C, Liu H, Xu A, Tang K, Huang Y, Lu C (2017) In situ reduced and assembled three-dimensional graphene aerogel for efficient dye removal. *J Alloy Compd* 714:522–529
 66. Liu X, Tian J, Li Y, Sun N, Mi S, Xie Y, Chen Z (2019) Enhanced dyes adsorption from wastewater via Fe₃O₄ nanoparticles functionalized AC. *J Hazard Mater* 373:397–407
 67. Liu X, Wang X, Xing X, Li Q, Yang J (2015) Visible light photocatalytic activities of carbon nanotube/titanic acid nanotubes derived-TiO₂ composites for the degradation of methylene blue. *Adv Powder Technol* 26(1):8–13
 68. Luo Z, He Y, Zhi D, Luo L, Sun Y, Khan E, Wang L, Peng Y, Zhou Y, Tsang DCW (2019) Current progress in treatment techniques of triclosan from wastewater: a review. *Sci Total Environ* 696:13399
 69. Madrakian T, Afkhami A, Ahmadi M, Bagheri H (2011) Removal of some cationic dyes from aqueous solutions using magnetic-modified multi-walled carbon nanotubes. *J Hazard Mater* 196:109–114

70. Mahamad MN, Zaini MAA, Zakaria ZA (2015) Preparation and characterization of AC from pineapple waste biomass for dye removal. *Int Biodeterior Biodegradation* 102:274–280
71. Mahmoodian H, Moradi O, Shariatzadeha B, Salehf TA, Tyagi I, Maity A, Asif M, Gupta VK (2015) Enhanced removal of methyl orange from aqueous solutions by poly HEMA–chitosan-MWCNT nano-composite. *J Mol Liq* 202:189–198
72. Miandad R, Kumar R, Barakat MA, Basheer C, Aburiazaiza AS, Nizami AS, Rehan M (2018) Untapped conversion of plastic waste char into carbon-metal LDOs for the adsorption of Congo red. *J Colloid Interface Sci* 511:402–410
73. Miandad R, Kumar R, Barakat MA, Basheer C, Aburiazaiza AS, Nizami AS, Rehan M (2018) Untapped conversion of plastic waste char into carbon-metal LDOs for the adsorption of Congo red. *J Colloid Interface Sci* 511:402–410
74. Mishra S, Cheng L, Maiti A (2020) The utilization of agro-biomass/byproducts for effective bio-removal of dyes from dyeing wastewater: a comprehensive review. *J Environ Chem Eng* 104901
75. Molavi H, Shojaei A, Pourghaderi A (2018) Rapid and tunable selective adsorption of dyes using thermally oxidized nanodiamond. *J Colloid Interface Sci* 524:52–64
76. Moosavi S, Gan S, Zakaria S (2019) Functionalized cellulose beads with AC Fe₃O₄/CoFe₂O₄ for cationic dye removal. *Cellul Chem Technol* 53:815–825
77. Moosavi S, Lai CW, Gan S, Zamiri G, AkbarzadehPivehzhani O, Johan MR (2020) Application of efficient magnetic particles and AC for dye removal from wastewater. *ACS Omega* 5(33):20684–20697
78. Myneni VR, Kala NS, Kanidarapu NR, Vangalapati M (2019) Modelling and optimization of methylene blue adsorption onto magnesium oxide nanoparticles loaded onto AC (MgONP-AC): response surface methodology and artificial neural networks. *Mater Today: Proc* 18:4932–4941
79. Namasivayam C, Sangeetha D (2006) Recycling of agricultural solid waste, coir pith: removal of anions, heavy metals, organics and dyes from water by adsorption onto ZnCl₂ activated coir pith carbon. *J Hazard Mater B* 135:449–452
80. Nekouei F, Noorzadeh H, Nekouei S, Asif M, Tyagi I, Agarwal S (2016) Removal of malachite green from aqueous solutions by cuprous iodide–cupric oxide nano-composite loaded on AC as a new sorbent for solid phase extraction: isotherm, kinetics and thermodynamic studies. *J Mol Liq* 213:360–368
81. Njoku VO, Foo KY, Asif M, Hameed BH (2014) Preparation of ACs from rambutan (*Nephelium lappaceum*) peel by microwave-induced KOH activation for acid yellow 17 dye adsorption. *Chem Eng J* 250:198–204
82. Palma C, Lloret L, Puen A, Tobar M, Contreras E (2016) Production of carbonaceous material from avocado peel for its application as alternative adsorbent for dyes removal. *Chin J Chem Eng* 24(4):521–528
83. Pan Y, Liu X, Zhang W, Liu Z, Zeng G, Shao B, Liang Q, He Q, Yuan X, Huang D, Chen M (2020) Advances in photocatalysis based on fullerene C60 and its derivatives: properties, mechanism, synthesis, and applications. *Appl Catal B* 265:118579
84. Pargoletti E, Pifferi V, Falcioni L, Facchinetti G, Depaolini AR, Davoli E, Marelli M, Cappelletti G (2019) A detailed investigation of MnO₂ nanorods to be grown onto AC. High efficiency towards aqueous methyl orange adsorption/degradation. *Appl Surf Sci* 472:118–126
85. Patent Application Publication US 2013/0147788A1 (2013)
86. Peláez-Cid AA, Herrera-González AM, Salazar-Villanueva M, Bautista-Hernández A (2016) Elimination of textile dyes using ACs prepared from vegetable residues and their characterization. *J Environ Manag* 181:269–278
87. Peng Z, Liu X, Zhang W, Zeng Z, Liu Z, Zhang C, Liu Y, Shao B, Liang Q, Tang W, Yuan X (2020) Advances in the application, toxicity and degradation of carbon nanomaterials in environment: a review. *Environ Int* 134:105298
88. Potirak, Pecharapa W, Techittheera W (2014) Microwave-assisted synthesis of ZnO/MWCNT hybrid nanocomposites and their alcohol-sensing properties. *J Exp Nanosci* 9(1):96–105. <https://doi.org/10.1080/17458080.2013.820848>

89. Prajapati AK, Mondal MK (2020) Comprehensive kinetic and mass transfer modeling for methylene blue dye adsorption onto CuO nanoparticles loaded on nanoporous AC prepared from waste coconut shell. *J Mol Liq* 307:112949
90. Prajapati AK, Mondal MK (2020) Comprehensive kinetic and mass transfer modeling for methylene blue dye adsorption onto CuO nanoparticles loaded on nanoporous activated carbon prepared from waste coconut shell. *J Mol Liq* 307:112949
91. Prola LD, Machado FM, Bergmann CP, de Souza FE, Gally CR, Lima EC, Adebayo MA, Dias SL, Calvete T (2013) Adsorption of Direct Blue 53 dye from aqueous solutions by multi-walled carbon nanotubes and AC. *J Environ Manag* 130:166–175
92. Qi Y, Yang M, Xu W, He S, Men Y (2017) Natural polysaccharides-modified graphene oxide for adsorption of organic dyes from aqueous solutions. *J Colloid Interface Sci* 486:84–96
93. Qu S, Huang F, Yu S, Chen G, Kong J (2008) Magnetic removal of dyes from aqueous solution using multi-walled carbon nanotubes filled with Fe₂O₃ particles. *J Hazard Mater* 160(2–3):643–647
94. Ragupathy S, Raghu K, Prabu (2015) Synthesis and characterization of TiO₂ loaded cashew nut shell AC and photocatalytic activity on BG and MB dyes under sunlight radiation. *Spectrochim Acta Part A: Mol Biomol Spectrosc* 138:314–320
95. Rajabi M, Mahanpoor K, Moradi O (2017) Removal of dye molecules from aqueous solution by carbon nanotubes and carbon nanotube functional groups: critical review. *RSC Adv* 7(74):47083–47090
96. Rashid M, Ralph SF (2017) Carbon nanotube membranes: synthesis, properties, and future filtration applications. *Nanomaterials* 7(5):99
97. Ray SS, Gusain R, Kumar N (2020) Carbon nanomaterial-based adsorbents for water purification: fundamentals and applications. Elsevier
98. Ribas MC, Adebayo MA, Prola LD, Lima EC, Cataluña R, Feris LA, Puchana-Rosero MJ, Machado FM, Pavan FA, Calvete T (2014) Comparison of a homemade cocoa shell AC with commercial AC for the removal of reactive violet 5 dye from aqueous solutions. *Chem Eng J* 248:315–326
99. Roosta M, Ghaedi M, Sahraei R, Purkait MK (2015) Ultrasonic assisted removal of sunset yellow from aqueous solution by zinc hydroxide nanoparticle loaded AC: optimized experimental design. *Mater Sci Eng C* 52:82–89
100. Ruiz B, Ferrera-Lorenzo N, Fuente E (2017) Valorisation of lignocellulosic wastes from the candied chestnut industry. Sustainable ACs for environmental applications. *J Environ Chem Eng* 5(2):1504–1515
101. Sadegh H, Zare K, Maazinejad B, Shahryari-Ghoshekandi R, Tyagi I, Agarwal S, Gupta VK (2016) Synthesis of MWCNT-COOH-Cysteamine composite and its application for dye removal. *J Mol Liq* 215:221–228
102. Saleh TA, Al-Absi AA (2017) Kinetics, isotherms and thermodynamic evaluation of amine functionalized magnetic carbon for methyl red removal from aqueous solutions. *J Mol Liq* 248:577–585
103. Sarkar B, Mandal S, Tsang YF, Kumar, Kim KH, Ok YS (2018) Designer carbon nanotubes for contaminant removal in water and wastewater: a critical review. *Sci Total Environ* 612:561–581
104. Saygılı H, Güzel F, Önal Y (2015) Conversion of grape industrial processing waste to AC sorbent and its performance in cationic and anionic dyes adsorption. *J Clean Prod* 93:84–93
105. Saygılı H, Güzel F (2016) High surface area mesoporous AC from tomato processing solid waste by zinc chloride activation: process optimization, characterization and dyes adsorption. *J Clean Prod* 113:995–1004
106. Shahbazi D, Mousavi SA, Nayeri D (2020) Low-cost AC: characterization, decolorization, modeling, optimization and kinetics. *Int J Environ Sci Te* 17(1):3935–3946
107. Shamsizadeh A, Ghaedi M, Ansari A, Azizian S, Purkait MK (2014) Tin oxide nanoparticle loaded on AC as new adsorbent for efficient removal of malachite green-oxalate: non-linear kinetics and isotherm study. *J Mol Liq* 195:212–218

108. Shen Y, Zhu X, Zhu L, Chen B (2017) Synergistic effects of 2D graphene oxide nanosheets and 1D carbon nanotubes in the constructed 3D carbon aerogel for high performance pollutant removal. *Chem Eng J* 314:336–346
109. Shi Q, Zhang J, Zhang C, Li C, Zhang B, Hu W, Xu J, Zhao R (2010) Preparation of AC from cattail and its application for dyes removal. *J Environ Sci* 22(1):91–97
110. Siji C, Shanshan T, Yang S, Gang W, Huan C, Xiaoxiao Y, Yingjie S, Singh A, Sharma RK, Agrawal M, Marshall FM (2010) Health risk assessment of heavy metals via dietary intake of food stuffs from the wastewater irrigated site of a dry tropical area of India. *Food Chem Toxicol* 48:611–619
111. Singh NB, Garima N, Agrawal S, Rachna (2018) Water purification by adsorbents a: review. *Environ Technol Innov* 11:187–240
112. Sinha S, Gusain RR, Kumar N (2020) Carbon nanomaterials: synthesis, functionalization, and properties. Carbon nanomaterial-based adsorbents for water purification in fundamentals and applications. <https://doi.org/10.1016/B978-0-12-821959-1.00007-6>
113. Solovev AA, Sanchez S, Pumera M, Mei YF, Schmidt OG (2010) Magnetic control of tubular catalytic microbots for the transport, assembly, and delivery of micro-objects. *Adv Func Mater* 20(15):2430–2435
114. Sukhanova A, Bozrova S, Sokolov Berestovoy M, Karaulov A, Nabiev I (2018) Dependence of nanoparticle toxicity on their physical and chemical properties. *Nanoscale Res Lett* 13(1):1–21
115. Syrgiannis Z, Melchionna M, Prato M (2014) Covalent carbon nanotube functionalization. In: Kobayashi S, Mullen K (eds) *Encyclopedia of polymeric nanomaterials*. Springer, Berlin, pp 1–8. https://doi.org/10.1007/978-3-642-36199-9_363-1
116. Tarigh GD, Shemirani F, Maz'hari NS (2015) Fabrication of a reusable magnetic multi-walled carbon nanotube–TiO₂ nanocomposite by electrostatic adsorption: enhanced photodegradation of malachite green. *RSC Adv* 5:35070–35079. <https://doi.org/10.1039/c4ra1>
117. Teimouri Z, Salem A, Salem S (2019) Regeneration of wastewater contaminated by cationic dye by nanoporous AC produced from agriculture waste shells. *Environ Sci Pollut Res* 26(8):7718–7729
118. Teka T, Enyew S (2014) Study on effect of different parameters on adsorption efficiency of low cost activated orange peels for the removal of methylene blue dye. *Int J Innov Sci Res* 8:106–111. ISSN 2351-8014
119. Thakur K, Kandasubramanian B (2019) Graphene and graphene oxide-based composites for removal of organic pollutants: a review. *J Chem Eng Data* 64(3):833–867
120. Tuzen M, Sari A, Saleh TA (2018) Response surface optimization, kinetic and thermodynamic studies for effective removal of rhodamine B by magnetic AC/CeO₂ nanocomposite. *J Environ Manag* 206:170–177
121. Un UT, Ates F, Erginel N, Ozcan O, Oduncu E (2015) Adsorption of disperse orange 30 dye onto AC derived from holm oak (*Quercus Ilex*) acorns: a 3k factorial design and analysis. *J Environ Manag* 155:89–96
122. Vargas AM, Cazetta AL, Martins AC, Moraes JC, Garcia EE, Gauze GF, Costa WF, Almeida VC (2012) Kinetic and equilibrium studies: adsorption of food dyes Acid Yellow 6, Acid Yellow 23, and Acid Red 18 on AC from flamboyant pods. *Chem Eng J* 181:243–250
123. Verma VK, Mishra AK (2010) Kinetic and isotherm modeling of adsorption of dyes onto rice husk carbon. *Global NEST J* 12(2):190–196
124. Wang Y, Chen J, Tang W, Xia D, Liang Y, Li X (2019) Modeling adsorption of organic pollutants onto single-walled carbon nanotubes with theoretical molecular descriptors using MLR and SVM algorithms. *Chemosphere* 214:79–84. <https://doi.org/10.1016/j.chemosphere.2018.09.074>
125. Wang H, Pumera M (2015) Fabrication of micro/nanoscale motors. *Chem Rev* 115(16):8704–8735
126. Wang F, Zhang J, Jia DM (2019) Facile synthesis of shell-core structured Fe₃O₄@ACS as recyclable magnetic adsorbent for methylene blue removal. *J Dispersion Sci Technol* 40(12):1736–1743

127. Wang H-D, Yang Q, Niu CH, Badealldiko (2012) Adsorption of azo dye onto nanodiamond surface. *Diamond Relat Mater* 26:1–6
128. Wen X, Liu H, Zhang L, Zhang J, Fu C, Shi X, Chen X, Mijowska E, Chen MJ, Wang DY (2019) Large-scale converting waste coffee grounds into functional carbon materials as high-efficient adsorbent for organic dyes. *Biores Technol* 272:92–98. <https://doi.org/10.1016/j.biotech.2018.10.011>
129. Wong KT, Eu NC, Ibrahim S, Kim H, Yoon Y, Jang M (2016) Recyclable magnetite-loaded palm shell-waste based AC for the effective removal of methylene blue from aqueous solution. *J Clean Prod* 115:337–342
130. Wu HC, Chang X, Liu L, Zhao F, Zhao Y (2010) Chemistry of carbon nanotubes in biomedical applications. *J Mater Chem* 20(6):1036–1052. <https://doi.org/10.1039/b911099m>
131. Wu K, Yu J, Jiang X (2018) Multi-walled carbon nanotubes modified by polyaniline for the removal of alizarin yellow R from aqueous solutions. *Adsorpt Sci Technol* 36(1–2):198–214
132. Xiao W, Jiang X, Liu X, Zhou W, Garba ZN, Lawan I, Wang L, Yuan Z (2021) Adsorption of organic dyes from wastewater by metal-doped porous carbon materials. *J Clean Prod* 124773
133. Xu X, Mredha MTI, Cui J, Vlassak JJ, Jeon I (2018) Hydrogel bowls for cleaning oil spills on water. *Water Res* 145:640–649
134. Yadav S, Yadav A, Bagotia N, Sharma AK, Kumar S (2021) Adsorptive potential of modified plant-based adsorbents for sequestration of dyes and heavy metals from wastewater—a review. *J Water Process Eng* 42:102148
135. Yang K, Wang J, Chen X, Zhao Q, Ghaffar A, Chen B (2018) Application of graphene-based materials in water purification: from the nanoscale to specific devices. *Environ Sci Nano* 5(6):1264–1297
136. Yu L, Luo YM (2014) The adsorption mechanism of anionic and cationic dyes by Jerusalem artichoke stalk-based mesoporous AC. *J Environ Chem Eng* 2(1):220–229
137. Zare K, Gupta VK, Moradi O, Makhlof ASH, Sillanpää M, Nadagouda MN, Sadegh H, Shahryari-Ghoshekandi R, Pal A, Wang ZJ, Tyagi I (2015) A comparative study on the basis of adsorption capacity between CNTs and AC as adsorbents for removal of noxious synthetic dyes: a review. *J Nanostruct Chem* 5(2):227–236
138. Zare K, Sadegh H, Shahryari-ghoshekandi R, Maazinejad B, Ali V, Tyagi I, Agarwal Zhao J, Wang Z, White JC, Xing B (2014) Graphene in the aquatic environment: adsorption, dispersion, toxicity and transformation. *Environ Sci Technol* 48(17):9995–10009
139. Zare K, Sadegh H, Shahryari-ghoshekandi R, Maazinejad B, Ali V, Tyagi I, Agarwal S, Gupta VK (2015) Enhanced removal of toxic Congo red dye using multi walled carbon nanotubes: kinetic, equilibrium studies and its comparison with other adsorbents. *J Mol Liq* 212:266–271
140. Zhu GZ, Deng XL, Hou M, Sun K, Zhang YP, Li P, Liang FM (2016) Comparative study on characterization and adsorption properties of activated carbons by phosphoric acid activation from corncob and its acid and alkaline hydrolysis residues. *Fuel Process Technol* 144:255–261

Polysaccharide-Composites Materials as Adsorbents for Organic Dyes



Paulo V. O. Toledo  and Denise F. S. Petri 

1 Introduction

Colourants are natural or synthetic molecules used to change the colour of materials, products, or surfaces. They are applied in a plethora of situations, from bench experiments to large-scale industrial production of food, packaging, painting, and textiles [1–3]. Colourants are classified according to their solubility in water as dyes (soluble) and pigments (insoluble); each one of them demands different procedures of fixation and finishing. Dye molecules show intense colour because of electronic transitions promoted by conjugated π linkages in their structures. The presence of heteroatoms in the dye molecules not only induces excitation gaps compatible with the absorption of visible light but also allows charge stabilization, favouring the solubility in water [2, 4]. On the other hand, these structural features make dissolved dyes hard to be removed from aqueous media, enable their permeation into living tissues due to hydrophobic interactions with cell membranes, and affect cellular metabolism due to possible electrostatic interactions.

“Clean water and sanitation” is one of the 17 Sustainable Development Goals of the United Nations [5]. Due to the importance of clean water for life, the period 2018–2028 was set as the International Decade for Action “Water for Sustainable Development” [6]. These facts clearly show that world leaders are concerned with the issue of clean water on our planet. Due to human and industrial activities, large amounts of contaminants can be found in wastewater. Dyes belong to a class of

P. V. O. Toledo · D. F. S. Petri (✉)

Fundamental Chemistry Department, Institute of Chemistry, University of São Paulo, Av. Prof. Lineu Prestes 748, São Paulo 05508-000, Brazil
e-mail: dfsp@iq.usp.br

P. V. O. Toledo

e-mail: paulo.vinicius.toledo@usp.br

contaminants, which stem mainly from the textile industry [7]. Hence, feasible strategies are highly important to ensure the efficiency and safety of water purification. Adsorption is one of the simplest and most versatile methods to remove impurities from water [8]. Specificity, low cost, and the possibility of recycling adsorbents are important parameters to be considered.

Polysaccharides are potential candidates for the development of adsorbents because they are biodegradable, non-toxic, and abundant. Combining polysaccharides with reinforcing fillers results in composite materials with superior performance. This chapter compiles the literature research over the last 20 years on polysaccharides composites designed for the removal of dyes from wastewater. It allows identifying the most common dyes and the most frequent polysaccharide-base composites used for the removal of dyes. Furthermore, it is fundamental to prospect alternative natural dyes and novel polysaccharide-based composites. Biomass-based composites were not included in this review because biomass might contain not only polysaccharides (cellulose and hemicellulose), but also lignin and minerals.

1.1 State of the Art

Polysaccharides constitute a major family of biosynthetic polymer class present in the composition of wood (cellulose and hemicellulose), fruits and seed (starch, galactomannan, and pectin), arthropod exoskeleton (chitin), algae (alginates, carrageenan, and agars), and bacteria (cellulose, alginate, xanthan, gellan) [9]. According to IUPAC, a composite is a “multicomponent material comprising multiple, different (non-gaseous) phase domains in which at least one type of phase domain is a continuous” [10]. This review focuses on polysaccharide composites, in which polysaccharides are the continuous phase and the dispersed phase are particles with intrinsic properties that contribute to the adsorption process. Literature research was based on Web of Science® using the combination of “*sorption*” and “*composite*” and “*dye*” in *all fields*, for the period 2000–2021, refined by the type of particle (Fig. 1). The interest in this research field increased considerably in the last decade, probably motivated by the growing environmental concerns.

The most common composites for dye adsorption have magnetic particles, which include magnetite (Fe_3O_4), maghemite ($\gamma\text{-Fe}_2\text{O}_3$), and undefined ferrite (FeO_x) particles. The reason for this is, in contrast to diamagnetic materials, the magnetic materials can be easily recovered by approaching a magnet. The second most popular family of composites for dye sorption contains carbon-based materials, such as oxidized graphene (GO), graphite, carbon nanotubes (CN), and other activated carbon (AC), biochar, and fly ash. Clays are interesting fillers because of their native charges, which can interact with the polymer matrix improving the adsorption capacity of the adsorbent [11, 12], for instance, attapulgite (APT), bentonite (BNT), clinoptilolite (CNPT), kaolinite (KLT), laponite (LPT), montmorillonite (MMT), sepiolite (SPT), and vermiculite (VMT). TiO_2 nanoparticles are interesting fillers not only because they offer a large surface area, but also because under UV light they generate electrons

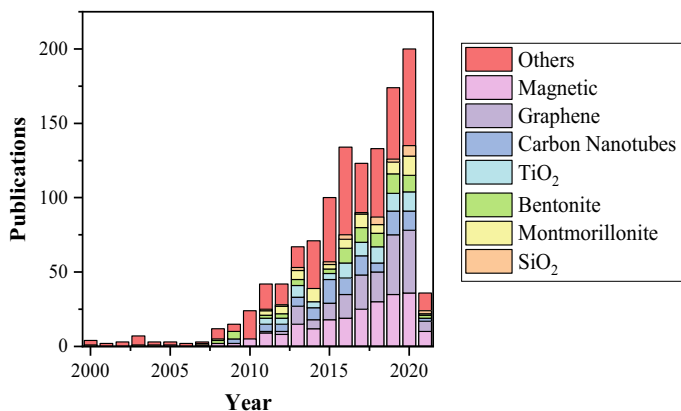


Fig. 1 Graphic of publications over time in years for “composite” and “sorption” and “dye” and “family of composite”: “magnetic” (pink), “graphene” (purple), “carbon nanotubes” (blue), “titanium dioxide” (cyan), “bentonite” (green), “montmorillonite” (yellow), “silicon dioxide” (orange) and others composites (red)

from the valence band, which react with O_2 to form superoxide radicals or hydroperoxide radicals [13]. Such radicals promote photobleaching of adsorbed dyes like methylene blue [14] or reactive red 141 [15].

Figure 2 shows the research refinement according to the “name of polysaccharide” used in the composites, one should notice that the term “polysaccharide” itself is a fraction of the total. Research studies involving chitosan (Chi), alginate (Alg),

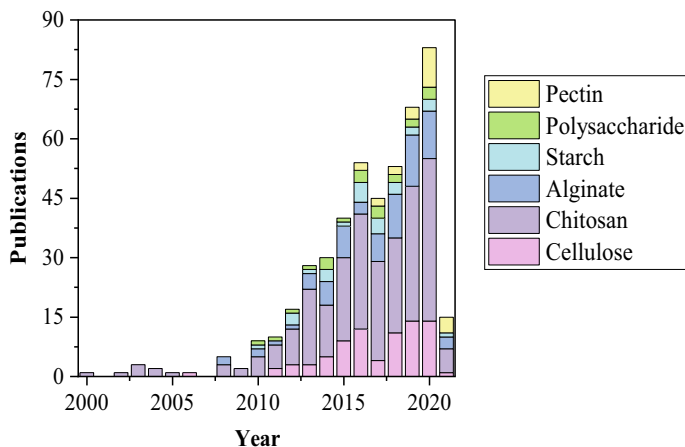


Fig. 2 Graphic of publications over time in years for “composite” and “sorption” and “dye” and “name of polysaccharide”: “cellulose” (pink), “chitosan” (purple), “alginate” (blue), “starch” (cyan), “polysaccharide” (green), and “pectin” (yellow)

and cellulose (Cel) together represented more than 80% of the total number of publications. This numeric asymmetry can be justified by their abundance and by the fact that they are not demanded by the food and beverage industry, as in the case of starch (Sta), pectin, xanthan, and gellan [9, 16]. In this context, the use of Chi in composites dominates because it stems from chitin, which is mainly extracted from bio-waste (crustaceans' shells). The use of biomass to gain materials dedicated to the environmental issue is one of the pillars of a sustainable economy.

Figure 3 shows the number of publications as a function of time for the research including the terms “composite” and “sorption” and “polysaccharides”, after refinement for the most frequent dyes. Remarkably most reports investigated the adsorption of methylene blue (MB), Congo red (CR), methyl orange (MO), rhodamine (Rh), malachite green (MG), and crystal violet (CV). These six dyes represent examples of the major families of organic dyes: MB is a thiazine compound; CR and MO are azo compounds; malachite green and CV are triphenyl compounds, and Rh are xanthene compounds. However, one should note that dyes are classified in eight families, based on the dyeing procedures, namely, acid (MO), basic (CV, MB+, Rh), direct (CR), disperse, reactive, solvent, sulphur, and vat [2, 17, 18]. The dye families disperse, solvent, and vat dyes are partially or insoluble in water and are used mainly for printing applications; if they are present in wastewater, they might be recovered by precipitation instead of by adsorption. On the other hand, reactive dyes have this name due to a fast and highly effective colouring, enabled by the presence of many functional groups in their molecules [2, 17]. The reading of the listed “polysaccharide composites for dye sorption” publications reported 102 distinct dyes, where malachite green was slightly less common than remazol black B (RBI). Most of the dyes are reported by their Colour Index names, a system defined as “family” + “colour” + “number”.

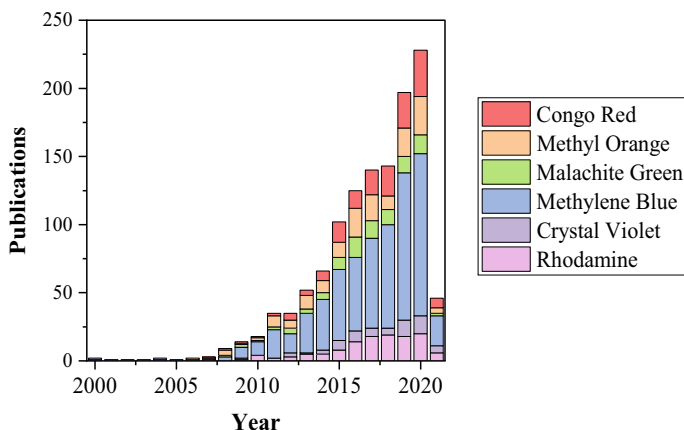


Fig. 3 The number of publications as a function of time (years) for the terms “composite” and “sorption” and “polysaccharides”, after refinement for the most common dyes: rhodamine, crystal violet, methylene blue, malachite green, methyl orange, and congo red

Amongst the most common dyes, methylene blue (MB) concentrates the most publications; it might be related to its particular photoactive properties. Under exposure to visible light (633 nm) methylene blue molecules achieve singlet and triplet excited states. The excited states can react with O_2 or undergo spontaneous decay [19], acting as a drug for photodynamic therapy. Both processes cause discolouration of methylene blue. For instance, the exposure of adsorbed MB molecules to a 3 mW laser beam for 15 min is enough to observe the bleaching [20]. This particular feature enables the recycling of adsorbents used for MB removal by the simple exposure to sunlight, although it may be a slower process than the traditional methods used for the recycling of adsorbents. MB molecules avoid adsorbing on hydrophobic substrates [21]. Water molecules in contact with hydrophilic substrates can assume three different states: (i) the tightly bound water molecules (non-freezing water), (ii) an intermediate state of water molecules that freeze below 0 °C, and (iii) free water [22]. The increase of intermediate water on cellulose-based hydrogels favoured the adsorption of MB and Rhodamine [23].

The adsorption of congo red (CR) on cellulose fibres has been used as an indirect method to estimate the surface area of the fibres [24]. The interactions between CR polar and charged groups and cellulose hydroxyl groups and hydrophobic interactions favour the adsorption process [25]. CR dye molecules also proved to mediate the adsorption of cholesterol oxidase [26] and lipase [27] on hydrophilic poly(ethylene glycol) modified surfaces.

1.2 Properties of Dyes

Table 1 comprises the physicochemical properties, toxicity, and applications of the most common dyes; the data were extracted from the PubChem database and USA Pharmacopoeia. The constant of dissociation (K_a) is important not only for the dyeing process but also for the adsorption process because it informs about the charge in the dye molecules as a function of pH [3, 28, 29]. The determination of K_a is dependent on the molecular symmetry and the technique utilized for its determination [30–32]. Hence, protocols for the estimation of K_a based on comparative molecular structure were developed. The most important contributions on simple molecules due to α and β positions concerning the polarization centre, while π conjugation could extend this contribution over large molecules [33]. Figure 4 represents the chemical structures of the most common dyes.

1.3 Adsorption

Adsorption is the increase in the concentration of dissolved molecules (adsorbate) at the interface of a condensed and/or a liquid phase due to intermolecular forces [10]. Physical adsorption is a reversible process, where the adsorbates are attached to the

Table 1 Physicochemical properties and final applications of the most common dyes: λ_{\max} UV–Vis, pK_a , and LD_{50} stand for maximal absorbance wavelength, $\log(K_a)$, and lethal dose to kill 50% of a group of test animals, respectively

	Congo red	Crystal violet	Methylene blue	Methyl orange	Remazol black B	Rhodamine B
CAS	573-58-0	548-62-9	61-73-4	547-58-0	17095-24-8	81-88-9
M_w (g/mol)	696.66	407.99	319.85	327.33	991.8	472.09
Solubility (g/L)	116 (25 °C)	50 (20 °C)	44 (20 °C)	50 (20 °C)	550 (20 °C)	15 (20 °C)
λ_{\max} (nm)	498	590	665	464 (pH 2) 507 (pH 5)	220	558
pK_a	4.1	3.29, 3.78, 4.26	2.6, 11.2	3.40, 3.76	6.9	3.7
Oral LD_{50} (mg/kg)	143 (human)	420 (rat)	3500 (mice)	60 (rat)	5000 (rat)	887 (mice)
Potential health effects	Carcinogenic teratogenic	Serious eye damage Carcinogenic mutagenic	Abdominal sore, vomit, and fever Reproductive disorders Mutagenic	Skin and respiratory irritation Chronic toxicity Mutagenic	Skin and respiratory irritation	Irritation of respiratory tract, skin, eyes Carcinogenic teratogenic
Application	Dyestuff Leather Textile	Dyestuff Leather Laundry activity Textiles	Dyestuff Food Laundry activity Leather Natural sources Plastic Textile	Food packages Laboratory Laundry activity Leather Paper Textiles	Leather Personal Care Printing Textiles	Dyestuff Food Laundry Leather Natural sources Plastic Textile

adsorbent by van der Waals forces, hydrophobic interactions, hydrogen bonds, or electrostatic interactions. Chemical adsorption is an irreversible process, where the adsorbates are covalently bound to the substrate. The adsorption processes can be studied in column or batch experiments. In fixed-bed column adsorption studies, the effluent (dye solution or wastewater) flows through the adsorbent (fixed-bed column) under constant flow. The concentration of effluent that comes out of the column as a function of time represents the breakthrough curve. The mass transport from the liquid phase to the adsorbent (column) depends mainly on the flow rate, column height, and adsorbate initial concentration. The breakthrough curves under different experimental conditions are important to optimize the operational conditions and to scale up to treat large amounts of wastewater [34]. However, the performance evaluation of polysaccharide composites as adsorbents for dyes often involves batch adsorption studies and small volumes of adsorbate (dye) solution. In batch adsorption studies the adsorbent and adsorbate solution are kept in contact (under shaking) until equilibrium conditions are achieved, at constant temperature (isotherm).

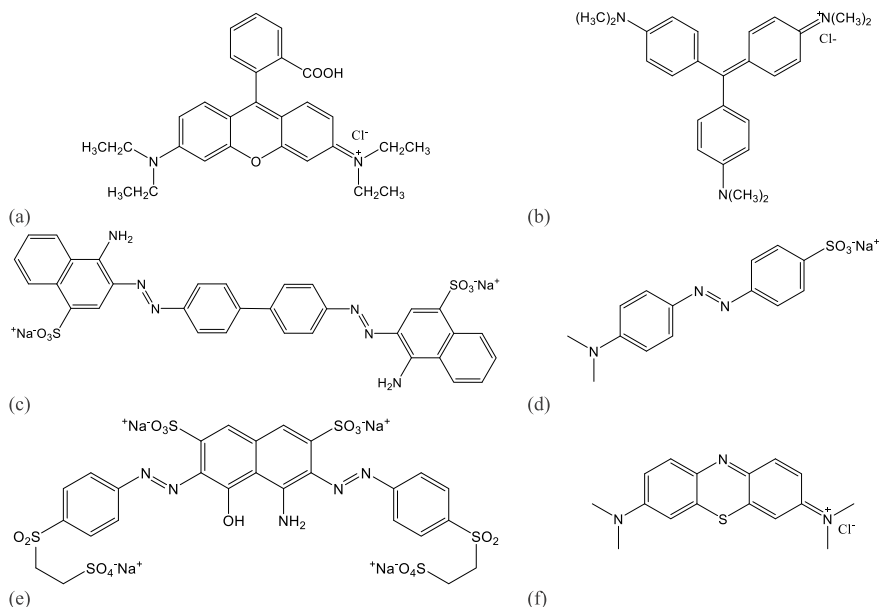


Fig. 4 The chemical structure of the most common dyes: **a** rhodamine B, **b** crystal violet, **c** congo red, **d** methyl orange, **e** remazol black, **f** methylene blue

The adsorption isotherm represents the variation of adsorbed amount as a function of adsorbate concentration at equilibrium conditions over a range of concentrations and a fixed amount of adsorbent. Parameters such as pH, ionic strength, temperature, concentration range, the dose of adsorbent can be varied to gain deeper comprehension about the interactions between adsorbate and adsorbent. For instance, if the adsorption is driven by electrostatic interaction, (i) the increase of ionic strength (by the addition of salt to the medium) brings about charges screening and consequent reduction of the adsorbed amount or (ii) in case the adsorbent (or adsorbate) molecules carry ionizable groups, depending on the pH, the groups are not ionized, reducing the adsorbed amount. If the adsorption process is endothermic, the adsorption will be favoured at a high temperature.

Different models can be applied to batch adsorption isotherms; fitting the experimental data to the models helps to understand the mechanism involved in the adsorption process. Comprehension of the adsorption mechanism is fundamental to achieve high adsorption efficiency. Many literature reports present the fittings of experimental batch adsorption isotherms with Langmuir, Freundlich, and Dubinin-Radushkevich model functions. In a recent review, the different models for batch adsorption experiments were presented and discussed [35]. Briefly, the Langmuir model considers the reversible formation of a monolayer (the adsorbate interacts only with the adsorbent) on a homogeneous surface (all binding sites have the same energy). The empirical Freundlich model is not restricted to monolayers (the adsorbate may interact with an adsorbent or with itself) and the adsorbent might carry adsorbing sites with

different energies. The semi-empirical Dubinin-Radushkevich model was developed for microporous adsorbents, like activated carbon, and considers the effect of the increasing concentration of adsorbate over the energy of interaction with adsorbent. The reduced chi-square statistics (variance of the fit divided by the average variance) is a criterion to choose the model that better fits the experimental adsorption isotherm [36].

Most systems (adsorbate/adsorbent) reported in this literature compilation fitted the experimental adsorption isotherms with the Langmuir model [35]:

$$Q_e = \frac{Q_{\max} K_L}{1 + K_L C_e} \quad (1)$$

where K_L is the Langmuir adsorption constant, Q_{\max} is the maximal adsorption capacity and Q_e is the adsorption capacity at equilibrium:

$$Q_e = \frac{C_0 - C_e}{m} \times v \quad (2)$$

where C_0 and C_e are the initial and equilibrium concentration, respectively, m is the mass of adsorbent and v is the volume of adsorbate solution.

Thus, to compare the different systems, in the forthcoming sections, the maximal adsorption capacity (Q_{\max}) will be presented along with the experimental parameters dye concentration range, contact time, medium (ionic strength, pH), amount, and surface area of the adsorbent, and temperature used for the batch adsorption studies [2, 17]. In most cases, the adsorption experiments were performed in the absence of buffer, the pH was simply adjusted with NaOH or HCl, as needed. Although the systematic batch adsorption studies are important to understand the interactions between composites and dyes, the real contaminated wastewater might present different adsorption behaviour in comparison to that of the synthetic dye solutions. Real wastewater samples might be a complex mixture composed of many inorganic ions (high ionic strength) and organic interferents (chelating agents) that screen the interaction between dye and composites.

2 Alginate-Based Composites

Alginic acid is an unbranched block copolymer of β -(1 \rightarrow 4) linked D-mannuronic acid (m) and α -(1 \rightarrow 4) linked L-guluronic acid (g) (Fig. 5a), extracted mainly from brown seaweeds [37]. Typically, the ratio D-mannuronic acid: L-guluronic acid (m:g) is 2.0:1.0; however, alginic acid from *Laminaria hyperborean* can reach m:g of 1.0:2.3. *Pseudomonas aeruginosa* and *Azotobacter vinelandii* can also produce alginic acid with m:g ratios ranging from 2.0:1.0 to 1.0:2.3 [9, 38]. Alginic acid can undergo the exchange of H^+ by Na^+ ions, resulting in the salt Na-alginate. In the presence of

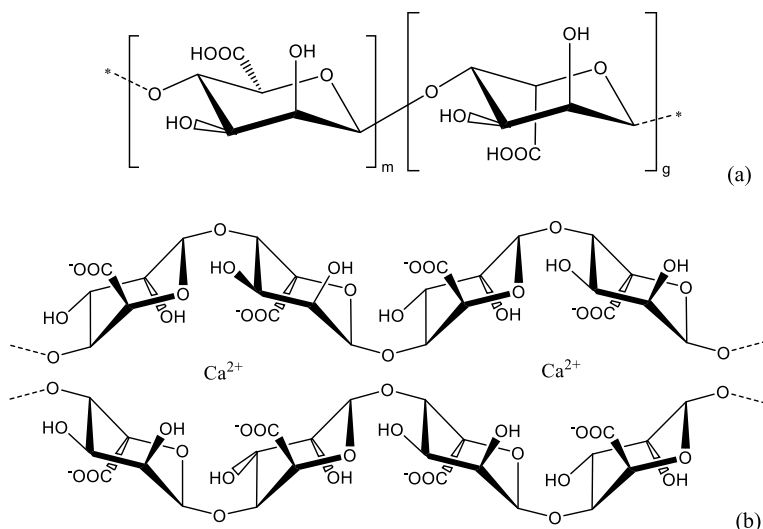


Fig. 5 Representation of **a** the chemical structure of the alginate as a copolymer of $\beta(1\text{--}4)$ D-mannuronic acid (m block) and $\alpha(1\text{--}4)$ L-guluronic acid (g block), **b** the “egg-box model” formed between guluronate blocks and Ca^{2+} ions

divalent (or multivalent) cations, such as Ca^{2+} , alginate chains form the “egg box junctions” (Fig. 5b) due to electrostatic interactions between Ca^{2+} ions and L-guluronate residues [39]. One simple strategy to prepare alginate-based composites is to disperse the fillers in the alginate solution and then drip the resulting dispersion into the CaCl_2 solution. Using this strategy, Sun and Fugetsu entrapped graphene oxide (GO) particles into the alginate beads for further removal of acridine orange; the presence of GO increased the Q_{\max} value by 50% [40]. Similarly, magnetic nanoparticles were dispersed in alginate solution and then precipitated into magnetic beads upon contact with CaCl_2 solution [41–44]. The chemical crosslinking of alginate is less common and related to films and multiform hydrogels, using alkylsilanes [45], acrylamides [46–48], and other grafting polymers [49].

Clays are hydrated aluminium silicates with multiple negatively charged sites for cation capture along with their structure, according to unitary cell, cells disposition in layers, and the number of layers [11]. Alginate and clays tend to repel each other due to their intrinsic negative charges [50]. One strategy to reduce the repulsion is to use a nonionic surfactant to screen the charges, allowing more homogeneous solutions [51, 52] or crosslinking via multivalent cation co-precipitation.

The adsorption of dyes on alginate-based composites is primarily driven by electrostatic interactions. Most of the articles presented in Table 2 reported an optimum pH solution higher than 5; at this condition, conjugated amine and azo groups of the dye molecules are protonated and can interact with the alginate carboxylate groups [45, 46, 52–60]. The addition of concentrated acid promotes the protonation of the

Table 2. Dyes, alginate-based composites, and the experimental conditions used for the adsorption experiments (filler content in the composite, temperature, pH, contact time, adsorbent dose, maximum concentration (C_{max}), maximum adsorption capacity (Q_{max}), adsorption/desorption cycles (reuse times) and desorption medium), along with the corresponding references

Dye	Composite	wt%	Temp (°C)	pH	Time (min)	Dose (g/L)	C_{max} (mg/L)	Q_{max} (mg/g)	Reuse	Desorption	References
Acid blue 25	Alg/MINPP-SiO ₂	50.0	22	4.0	150	2.0	300.0	5	–	–	Jabli and Hassine [45]
Acridine orange	CaAlg/GO	33.1	20	5.1	180	0.3	–	1234	–	–	Sun and Fugetsu [40]
Basic blue 41	CaAlg + PVA/ZnO	–	Room	Neutral	120	5.0	100	20.6	–	–	Elkady and Hassan [67]
Basic blue 41	CaAlg/NiZnFeO _x	–	25	8.0	180	0.2	–	25	–	–	Mahmoodi [43]
Basic red 18								56			
Basic violet 16	CaAlg/Zr[W(VO ₃)]	x	40	10.0	80	0.3	100	10.7	–	–	Elkady et al. [68]
Crystal violet	ZnAlg/AC	50.0	30	5.0	60	1.0	20	1.1603	–	–	Duraipandian et al. [69]
							40	1.5913			
							60	2.0015			
							80	0.3495			
							100	0.7279			
Crystal violet	CaAlg/BNT	28.6	30	8.0	360	1.0	300	263.14	–	–	Fabryanty et al. [55]
		37.5						308.83			

(continued)

Table 2 (continued)

Dye	Composite	wt%	Temp (°C)	pH	Time (min)	Dose (g/L)	C _{max} (mg/L)	Q _{max} (mg/g)	Reuse	Desorption	References
Crystal violet	CaAlg + RSP/BNT	44.4	30	4.0	480	1.0	800	462.61	–	–	Laysandra et al. [51]
Crystal violet	Alg/AM + MBA/GO	2.5	30	8.0	200	1.0	5000	100.3	10 x	HCl 1 M	Pashaei-Fakhri et al. [46]
Crystal violet	CaAlg/BNT + CNT	50 + 0	25	7.0	30	1.5	600	266.42	6 x	HCl 0.1 M	Patanjali et al. [60]
		40 + 10						398.14			
Methyl orange	CaAlg/Fe ₃ O ₄ + AC	69.7 + 2.75	Room	6.7	2880	35.3	1.637	432.1	–	–	Rocher et al. [44]
Methylene blue	Alg-g-PAA-co-AM/CNPT	–	–	–	1440	2.0	200	94.34	5 x	HCl 0.1 M	Rashidzadeh et al. [48]
Methylene blue	CaAlg + Husk/FeO _x	–	20	6.0	210	0.1	500	344	–	NaCl 1%	Alver et al. [41]
Methylene blue	CaAlg/BNT + AC	33.3 + 33.3	30	6.0	1800	0.8	500	756.97	6 x	H ₃ COH	Benhouria et al. [53]
Methylene blue	FeAlg/γ-Fe ₂ O ₃	–	25	4.0–10.0	2880	1.0	230	905.5	6 x	HNO ₃ 0.1 M	Boukhalifa et al. [54]

(continued)

Table 2 (continued)

Dye	Composite	wt%	Temp (°C)	pH	Time (min)	Dose (g/L)	C _{max} (mg/L)	Q _{max} (mg/g)	Reuse	Description	References
Methylene blue	CaAlg/NiFe ₂ O ₄	16.0	25	6.5	180	2.0	–	1243	–	–	Cojocar et al. [42]
Methylene blue	CaAlg/CNPT	71.4	25	–	1440	1.0	820	401.68	–	–	Dinu et al. [70]
		83.3						452.25			
Methylene blue	Alg/MNPP-SiO ₂	50.0	22	6.0	150	2.0	300.0	1.82	–	–	Jabli and Hassine [45]
Methylene blue	CaAlg/GO	5.0	25	7.0	5	0.5	80	181.81	–	–	Li et al. [71]
Methylene blue	CaAlg/NiZnFeO _x	–	25	8.0	180	0.2	–	106	–	–	Mahmoodi [43]
Methylene blue	CaAlg/CNT + MFA	10.0	25	10.0	2880	1.0	100	10.26	3 x	HCl 0.1 M	Mallakpour et al. [61]
Methylene blue	CaAlg/BNT + CNT	50 + 0	25	7.0	30	1.5	600	267.14	6 x	HCl 0.1 M	Patanjali et al. [60]
		40 + 10						400.55			
Methylene blue	CaAlg/BNT	10.0	25	7.0	2880	1.0	300	972.29	6 x	HCl 0.01 M	Oussalah and Boukerroui [62]
		20.0						805.55			
		30.0						670.54			

(continued)

Table 2 (continued)

Dye	Composite	wt%	Temp (°C)	pH	Time (min)	Dose (g/L)	C _{max} (mg/L)	Q _{max} (mg/g)	Reuse	Desorption	References
Methylene blue	CaAlg/Hectonite	80.0	25	12.0	900	2.0	800	785.45	6 x	H ₃ COH	Pawar et al. [72]
Methylene blue	Alg/Cel-KLT	–	25	7.0	2880	0.5	2000	512.8	5 x	HCl 0.3 M	Qian et al. [64]
Methylene blue	Alg/PAM/MMT	2.0	25	–	–	1.0	1000	2639	–	–	Qiu et al. [47]
Methylene blue	CaAlg/Fe ₃ O ₄ + AC	69.7 + 2.75	Room	6.7	2880	35.3	1.599	14,544	–	–	Rocher et al. [44]
Methylene blue	CaAlg/SiO ₂	75.0	20	5.0	300	4.0	700	228.07	5 x	HCl 0.1 M	Shi et al. [65]
Methylene blue	CuAlg/AC	50.0	30	10.0	970	0.2	250	446.43	–	–	Wang et al. [73]
Methylene blue	CaAlg/AC	25.0	25	5.0–11.0	1440	0.25	500	1210.7	–	–	Wang et al. [74]
Methylene blue	CaAlg + Chi/PVA/MMT	4.3	30	8.0	600	2.0	70	137.15	5 x	–	Wang et al. [66]
Methylene blue	Alg/Fe ₃ O ₄ -S-GO	6.3	21	5.4	360	1.0	500	789.7	–	–	Yap et al. [75]
Methylene green	Alg-g-PVFA-co-PAA/BNT	–	30	7.0	1440	–	300	2725	6 x	H ₃ CCOCH ₃	Subhan et al. [49]

(continued)

Table 2 (continued)

Dye	Composite	wt%	Temp (°C)	pH	Time (min)	Dose (g/L)	C _{max} (mg/L)	Q _{max} (mg/g)	Reuse	Description	References
Reactive black 5	Alg/PAM/GO	10.0	30	8.0	90	1.0	600	555.28	5 x	HCl 0.1 M	Shan et al. [76]
Rhodamine 6G	CaAlg/NiFe ₂ O ₄	16.0	25	6.5	180	2.0	–	845	–	–	Cojocarú et al. [42]
Rhodamine 6G	CaAlg/BNT	50.0	30	6.0	1440	1.0	800	429.5	5 x	H ₂ O	Gomri et al. [56]
Rhodamine B	CaAlg/HAPT	38.5	25	7.0	150	20	200	480	3 x	HCl 0.1 M	Oladipo and Gazi [59]
Rhodamine B	CaAlg/BNT + CNT	50 + 0	25	7.0	70	1.5	175	73.76	6 x	HCl 0.1 M	Patanjali et al. [60]
		40 + 10						111.56			
Rhodamine B	CaAlg + RSP/TiO ₂	–	30	2.0	480	2.5	300	100	3 x	NaOH 1 M	Singh [52]
Victoria blue	BaAlg/AC	–	30	4.0	50	0.4	20	1.9463	–	–	Kumar et al. [57]

The survey in the Web of Science combined the terms “alginate” + “composites” + “dye” + “sorption”

Legend AC Activated carbon; AM Acrylamide; BNT Bentonite; CNT Carbon nanotube; CNPT Clinoptilolite; GO Graphene oxide; HAPT Hydroxyapatite; KLT Kaolinite; MBA N-methylene bisacrylamide; MFA Magnesium fluorohydroxyapatite; MMT Montmorillonite; MNPP 4-methyl-2-naphthalen-2-yl-N-propylpentanamide; PAA Poly(acrylic acid); PVA Poly(vinyl alcohol); PVFA Poly(N-vinyl formamide-co-acrylic acid); RSP Rarasaponin

carboxylate groups of alginates and, consequently, reduces the electrostatic interactions with the dye molecules. Therefore, rinsing the dye saturated alginate-clay adsorbent with a strong acid favours the desorption of cationic dyes for the adsorbent recycling [46, 48, 52–54, 60–65]. On the other hand, the desorption of rhodamine (anionic leuco dye) can be favoured by rinsing with concentrate alkali [52]. Wang and co-workers investigated the adsorption of a cationic dye on alginate-PVA/MMT beads using various complementary techniques (EDS and XPS); they concluded that under mild conditions, the adsorption is equally driven by polar and electrostatic interactions [66].

Carbon-based materials such as graphene oxide (GO), carbon nanotubes (CNT), and activated carbon (AC) are less hydrophilic than the clays because they carry fewer charges than the clays. As a consequence, the pre-dispersion in water is more difficult, reducing the amounts of suspended GO [46, 71, 77], CNT [60, 61], and AC [44, 53, 57, 69, 73, 74, 78] that build the composites. The content of AC particles in alginate composites is generally smaller than that of clays (max of 10 wt% for carbon-based particles against min of 33 wt% of clays). Nevertheless, alginate-carbon materials composites seem to be more efficient adsorbent than the composites of alginate-charged fillers [42, 44, 75]. Durapandian and co-workers showed that Zn-alginate/CA composites were more efficient towards the removal of crystal violet from dilute solutions (20–60 mg/L) [69].

In some composites, the content of alginate in the composite was smaller than the filler content [44, 70, 72]. The dye desorption can be promoted by screening effects [41] or by the addition of other polar solvents [49, 53, 72]. In general, the reusability of the adsorbents was evaluated in batch studies with many adsorption/desorption cycles, where the final recycling removal efficiency varied from 85 to 50% of the original values. One important point seldom addressed in the literature regards the amount of eluent necessary to recover the adsorbents. If the amount of eluent necessary to recover the adsorbent is too large, maybe it is not an advantage because it will generate large amounts of the contaminated eluent. If the volume of eluent required to regenerate the adsorbent is small, then the resulting eluent is a concentrated dye solution that can be either returned to the textile industry or incinerated.

Mahmoodi investigated the adsorption of three different basic dyes separately and in binary mixtures on ferrite-alginate composites; the Q_{\max} values determined in the binary systems were up to fivefold smaller than the Q_{\max} values determined for isolated dye systems [43]. These findings show that the adsorption behaviour of more complex systems, as real industrial wastewater, might be different from that of simple systems prepared in the laboratory. The increase of temperature favoured some adsorption processes on alginate-based composites [51–53, 55, 65, 73]. However, the increase of temperature decreased the adsorbed amount of dyes on some alginate-based composites, turning the variation of the adsorption-free energy less negative [42, 45, 73]. Adsorption experiments using adsorbents based on pure polysaccharide (control) are important to show the contribution of the filler on the adsorption process. Nevertheless, only a few studies presented the adsorptive capacity of the control adsorbent [40, 46, 55, 57, 63, 74].

For the treatment of large volumes of contaminated wastewater, fixed bed column adsorption tends to be more efficient. The dynamic adsorption of rhodamine B on hydroxyapatite/alginate composites was more efficient at low flow rates [59]. Despite microbeads being widely used for chromatography and filtration purposes, materials in their size range, when packed in the column, leave free volume to the solution permeation without interaction with the composite. The continuous sorption experiments help to optimize the operational conditions for wastewater purification. However, the adsorption capacity of a given adsorbent packed in a column not necessarily is the same as that in batch experiments, because the contact time and the number of available binding sites on the adsorbent might be different; consequently, it is not trivial to correlate batch studies with column studies.

3 Chitosan-Based Composites

Chitin is composed of *N*-acetyl-D-glucosamine residues linked by β -(1 \rightarrow 4)-glycosidic linkages. It occurs in nature as the main structural element of arthropods exoskeleton and cell walls of fungi, so it is usually associated with proteins and cell pigments. Chitin is insoluble in water, but its deacetylation generates β -(1 \rightarrow 4)-D-glucosamine residues, which are soluble under acid conditions [79]. Chemical (acid or alkali) hydrolysis [80] or enzymatic hydrolysis [81] are common deacetylation processes. Depending on the source and reaction conditions, the degree of deacetylation might range from 60 to 99% with an average of 80% [82]. When the degree of deacetylation is 75% or more, the resulting copolymer of β -(1 \rightarrow 4)-*N*-acetyl-D-glucosamine and deacetylated β -(1 \rightarrow 4)-D-glucosamine, represented in Fig. 6, is named chitosan [83]. Chitosan properties depend on the polymerization degree and the degree of deacetylation because its solubility relies upon the swelling of the acetylated units (subject to crystallization) and solvation of the deacetylated units (subject to the protonation of primary amine groups and repulsion amongst blocks) [79].

The presence of primary amine groups makes chitosan a natural polycation in pH > 5 with the ability to form complexes with many transition metals [79, 84, 85], offering a route to physical crosslinking [45, 86]. Chitosan is a versatile platform for the synthesis of amphoteric compounds via grafting reactions with chloro-alkyl

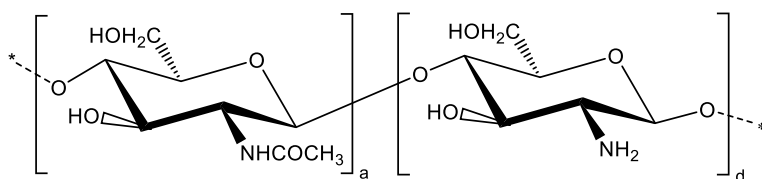


Fig. 6 Representation of the chemical structure of chitosan, a copolymer of β -(1 \rightarrow 4)-*N*-acetyl-D-glucosamine and β -(1 \rightarrow 4) D-glucosamine units

acids [87–89], sulphonation in the presence of sulphuric and sulphurous acids [90], crosslinking between the polymer and the hybrid material [91–95], and creation of an interconnected polymer network [89]. Table 3 comprises reports about chitosan-based composites for dye adsorption. The composites can be prepared using one of the strategies cited above or a combination of them, as recently reviewed by Pereira et al. [28].

As a polycation, chitosan chains repel cations and attract anions, promoting precipitation under adequate conditions due to competition for hydration or neutralization. Remarkably, clays as layered hydrated aluminium silicates show polyanion characteristics [11] and are modified to avoid precipitation in contact with chitosan [89, 90, 116, 137], unless flocculation is intended to physically crosslink the composite materials [98, 101, 102, 106, 118, 129, 144, 155]. The structure of the materials resulting from the mixture of polycation and polyanion is dependent on the mixing conditions. The homogeneous structure is favoured by low concentration, moderate ionic strength, and pH close to point of zero charges, whereas the heterogeneous structure is favoured by higher molecular weight, fast pouring of the solutions, and low molecular shear [156].

Chitosan-based composites are the most common for dye adsorption. The preference for chitosan can be explained by the electrostatic attraction to negatively charged fillers, which increases the stability of the composites; noteworthy, the reported point of zero charges for many reported composites range from 6.0 to 8.0 [58, 84, 87, 89–91, 94, 95, 100, 101, 103, 108, 109, 116, 118, 120, 135, 140, 142, 146, 150, 151, 154]. The chemical composition of chitosan allows producing composites as beads upon precipitation induced by alkali solution [95, 96, 123, 127], as powders, flakes, and other composites without defined form [87, 122, 126, 133, 148]. In many cases, chitosan-based composites have high (<50 wt%) filler contents [84, 98, 104, 107, 113, 136, 144, 152, 153, 155].

The mechanisms of adsorption might be complex and rely on different interactions between the composites and dyes. The attempt to unveil the adsorption mechanism makes use of the addition of competitor cations (Cd^{2+} , Pb^{2+} , Ni^{2+} , and Cu^{2+}) on the adsorption [116], multi-response optimization models [144], fittings to many adsorption models [113, 155], solid-state NMR analyses of dye loaded composites [100] and XPS analyses of the dye loaded composite in comparison to unloaded [58, 148]. In most cases, concentrated NaOH solution is used to recover the chitosan-based adsorbents. Under alkaline conditions, chitosan amine groups are deprotonated and hydroxyl groups might be deprotonated, and many dye molecules are negatively charged (Table 1). Thus, the desorption is efficient due to electrostatic repulsion between chitosan chains and negatively charged dye molecules. In cases where the adsorption is driven by polar and hydrophobic interactions, ethanol or EDTA proved to be efficient to recover the adsorbents [94, 104, 133].

The increase of temperature led to the increasing of the amount of adsorbed dye on some chitosan-based composites [103, 108, 120, 125, 127, 128, 131, 133, 136, 147, 148, 157]; on other composites, heating the systems brought about the decrease of adsorbed amount [84, 93, 96, 106, 113, 129, 138]. Noteworthy, adsorption processes driven by electrostatic interactions presented an increase [133] as well as a decrease

Table 3 Dyes, chitosan-based composites, and the experimental conditions used for the adsorption experiments (filler content in the composite, temperature, pH, contact time, adsorbent dose, maximum concentration (C_{max}), maximum adsorption capacity (Q_{max}), adsorption/desorption cycles (reuse times) and desorption medium), along with the corresponding references

Dye	Composite	wt%	Temp (°C)	pH	Time (min)	Dose (g/L)	C_{max} (mg/L)	Q_{max} (mg/g)	Reuse	Desorption	References
Acid blue 25	Chi-MNPP-SiO ₂	50.0	20	5.0	150	1.5	200	2.092	–	–	Jabli [96]
Acid blue 29	Chi/AC	–	30	3.0	300	1.0	350	345.1	5 x	pH 10.0	Auta and Hameed [97]
Acid fuchsin	Chi/MMT	80.0	40	5.0	90	5.0	–	15.28	–	–	Cao et al. [98]
Acid orange 7	Chi-La(III)/MMT	25.0	30	3.0	40	2.0	150	28.728	–	–	Sirajudheen and Meenakshi [99]
Acid orange 7	Chi/PMMA-SiO ₂	16.8	25	6.7	2880	0.5	631	87.58	–	–	Blachnio et al. [87]
Acid orange 8			25				656	72.87			
Acid orange 8	Chi/SiO ₂	90.0	25	5.5	2880	0.5	656	87.44	–	–	Budnyak et al. [100]
Acid red 1	Chi/Alunite	33.3	Room	3.0	40	0.2	100	646.96	20 x	NaOH 0.01 M	Akar et al. [101]
Acid red 1	Chi/PMMA-SiO ₂	16.8	25	8.5	2880	0.5	509	45.85	–	–	Blachnio et al. [87]
Acid red 1	Chi/Rectorite	14.3	Room	3.0	240	1.0	300	104.15	–	–	Feng and Xu [102]
Acid red 1	Chi/GO + HAPT	16.7 + 16.7	30	2.0	90	2.0	300	41.326	3 x	NaOH 0.1 M	Sirajudheen et al. [103]

(continued)

Table 3 (continued)

Dye	Composite	wt%	Temp (°C)	pH	Time (min)	Dose (g/L)	C _{max} (mg/L)	Q _{max} (mg/g)	Reuse	Desorption	References
Acid red 22	Chi/Fe ₃ O ₄ + GO	–	Room	3.0	150	0.8	50	24.87	4 x	CH ₃ CH ₂ OH	Sheshmani and Mashhadi [104]
Acid red 88	Chi/PMMA-SiO ₂	16.8	25	8.0	2880	0.5	721	192.18	–	–	Blachnio et al. [87]
Acid yellow 221	Chi/Fe ₃ O ₄ + GO	–	Room	6.0	45	2.5	500	303	–	–	Manatunga et al. [105]
Alizarine red	Chi-SO ₃ -BNT	50.0	30	8.0	40	–	500	131.58	–	–	Khapre and Jugade [90]
Amaranth red	Chi/BNT	16.7	25	2.0	360	0.2	500	362.1	3 x	NaOH 0.1 M	Dotto et al. [106]
Amaranth red	Chi/ZrO ₂ + Fe ₃ O ₄	33.3 + 33.3	25	2.0	1440	1.0	200	99.6	–	–	Jiang et al. [107]
Basic red 2	Chi/GO	50.0	25	4.0	60	0.5	600	279.6	–	–	Debnath et al. [108]
Brilliant green	Chi/HAPT	–	Room	7.0	60	0.9	80	49.1	–	–	Ragab et al. [109]
Congo red	Chi/FeO _x	–	25	7.0	120	0.3	3000	1724.1	–	NaOH 1.25 M	Hui et al. [86]
Congo red	Chi/FeO _x	–	25	7.5	1440	0.2	100	12.86	–	–	Kloster et al. [110]
Congo red	Chi/Manganite	–	30	4.5	360	0.5	100	200	–	–	Kochkina et al. [111]

(continued)

Table 3 (continued)

Dye	Composite	wt%	Temp (°C)	pH	Time (min)	Dose (g/L)	C_{\max} (mg/L)	Q_{\max} (mg/g)	Reuse	Description	References
Congo red	Chi/GO + HAPT	16.7 + 16.7	30	2.0	90	2.0	300	43.065	3 x	NaOH 0.1 M	Sirajudheen et al. [103]
Congo red	Chi/SiO ₂	20.0	25	-	3000	0.6	-	152.84	-	-	Wang et al. [112]
		50.0						150.22			
		80.0						155.37			
Congo red	Chi/Fe ₃ O ₄ + DMT	60.0	25	6.0	660	1.0	1400	1111	5 x	NaOH 0.5 M	Zheng et al. [113]
Crystal violet	Chi/TiO ₂ + KLT	45.0	45	x	150	2.0	60	111.11	-	-	Vardikar et al. [114]
Crystal violet	Chi/Fe ₃ O ₄ -SiO ₂	-	20	7.0	1440	1.0	1400	86.6	5 x	HCl 0.1 M	Yan et al. [115]
Direct green 6	Chi-Y(III)/fly ash	97.6	25	6.0	60	1.0	3800	627	3 x	NaOH 0.1 M	Li and Ren [84]
Direct rose FRN	Chi/clay	-	30	10.0	40	0.1	100	17.42	-	HCl 0.1 M	Kausar et al. [116]
Direct orange 2GL	Chi/Fe ₃ O ₄ + DMT	60.0	25	6.0	660	1.0	1400	1250	5 x	NaOH 0.5 M	Zheng et al. [113]
Direct red 23								1429			
Direct yellow R								909.1			

(continued)

Table 3 (continued)

Dye	Composite	wt%	Temp (°C)	pH	Time (min)	Dose (g/L)	C_{max} (mg/L)	Q_{max} (mg/g)	Reuse	Desorption	References
Eosin yellow	Chi/GO	90.0	25	7.2	2160	–	–	230	–	–	Chen et al. [117]
Indigo carmine	Chi/HAPT + MMT	10 + 10	25	6.24	90	1.0	200	243.18	3 x	NaOH 3.0 M	Joudi et al. [118]
Malachite green	Chi/ZnO	50.0	25	8.0	180	15.0	9.3	11	–	–	Muinde et al. [119]
Methyl blue	Chi/EDTA/Fe ₃ O ₄	10.0	30	2.0	240	3.3	300	459.9	8 x	NaOH 0.5 M	Chen et al. [91]
Methyl blue	Chi/HAPT + MMT	10 + 10	25	6.24	90	1.0	200	168.52	3 x	NaOH 3.0 M	Joudi et al. [118]
Methyl blue	Chi/ATT	–	25	10.0	720	0.5	200	161.29	5 x	HAc 1.0 M	Zhou et al. [120]
Methyl orange	Chi/AC	28.6	30	7.0	4320	0.4	28	21.96	3 x	NaOH 0.5 M	Chen and He [121]
Methyl orange	Chi/MgO	50.0	Room	8.0	5	0.5	300	175.4	5 x	–	Haldorai et al. [122]
Methyl orange	Chi/Fe ₃ O ₄	16.7	Room	8.0	5	0.5	300	90.3	5 x	–	Haldorai and Shim [123]
Methyl orange	Chi/HAPT + MMT	10 + 10	25	6.24	60	1.0	200	137.5	3 x	NaOH 3.0 M	Joudi et al. [118]
Methyl orange	Chi/Fe ₂ O ₃	20.0	37	2.9	540	1.0	60	28.94	–	–	Jiang et al. [124]

(continued)

Table 3 (continued)

Dye	Composite	wt%	Temp (°C)	pH	Time (min)	Dose (g/L)	C_{max} (mg/L)	Q_{max} (mg/g)	Reuse	Desorption	References
Methyl orange	Chi/mwCNT	80.0	35	7.0	300	0.7	55	400	–	–	Mahmoodian et al. [125]
Methyl orange	Chi/GTA/Fe ₃ O ₄	–	25	6.0	120	0.33	655	834.7	5 x	NaOH 0.1 M	Li et al. [93]
Methyl orange	Chi/Fe ₃ O ₄ + MOF	20 + 1	25	–	750	0.4	200	76.5	–	–	Liu et al. [126]
		20 + 2						82.8			
		20 + 3						100.1			
		20 + 4						108.7			
		20 + 5						117.6			
Methyl orange	Chi/GO	1.5	25	7.0	100	0.5	210	315.98			Ouyang et al. [127]
Methyl orange	Chi/ZnO	50.0	30	3.0	105	0.5	100	58.82	4 x	NaOH 0.1 M	Yuvaraja et al. [128]
Methyl orange	Chi/alumina	77.8	25	6.0	90	8.0	400	32.669	–	–	Zhang et al. [129]
Methyl orange	Chi/DMT	–	20	5.0	60	2.0	50	35.12	6 x	–	Zhao et al. [130]
Methyl orange	Chi/Fe ₃ O ₄ + DMT	60.0	25	6.0	660	1.0	1400	769.2	5 x	NaOH 0.5 M	Zheng et al. [113]

(continued)

Table 3 (continued)

Dye	Composite	wt%	Temp (°C)	pH	Time (min)	Dose (g/L)	C _{max} (mg/L)	Q _{max} (mg/g)	Reuse	Desorption	References
Methyl violet	Chi-g-PAA/GO	–	Room	5.0	1080	1.1	2000	303.0	–	–	Hongduo et al. [88]
Methylene blue	Chi/AC	–	30	7.0	300	1.0	350	197.3	5 x	pH 3.0	Auta and Hameed [97]
Methylene blue	Chi/Alg + AC	50.0	30	8.0	100	1.0	300	259.81	5 x	–	Auta and Hameed [131]
Methylene blue	Chi/GO	90.0	25	6.8	3480	–	–	350	–	–	Chen et al. [117]
Methylene blue	Chi/EDTA/Fe ₃ O ₄	10.0	30	2.0	240	3.3	300	404.4	8 x	NaOH 0.5 M	Chen et al. [91]
Methylene blue	Chi/BNT	16.7	25	10.0	360	0.2	500	496.5	2 x	HCl 0.1 M	Dotto et al. [106]
Methylene blue	Chi-Fe ₃ O ₄ /GO	12.5 + 37.5	30	10.0	–	2.0	–	180.83	–	–	Fan et al. [132]
Methylene blue	Chi/βCD/GO	–	25	11	80	0.4	–	84.32	5 x	CH ₃ CH ₂ OH	Fan et al. [133]
Methylene blue	Chi-SiO ₂ /ZnO	–	25	7.0	160	1.0	550	293.3	–	–	Hassan et al. [134]
Methylene blue	Chi + biomass/AC	33.3	30	8.0	120	1.0	100	302.02	–	–	Idohou et al. [135]
Methylene blue	Chi-MNPP-SiO ₂	50.0	20	5.0	150	1.5	200	0.725	–	–	Jabli [96]

(continued)

Table 3 (continued)

Dye	Composite	wt%	Temp (°C)	pH	Time (min)	Dose (g/L)	C_{\max} (mg/L)	Q_{\max} (mg/g)	Reuse	Desorption	References
Methylene blue	Chi/Fe ₃ O ₄ + AC	33.3 + 33.3	25	7.73	1440	1.0	500	200	–	–	Karaer and Kaya [136]
Methylene blue	sucChi-g-PAA/ATT	–	30	6.0	30	0.4	800	135.14	–	pH 2	Li et al. [137]
Methylene blue	Chi-g-PAA/VMT	10.0	30	7.0	240	0.25	1200	1682.18	–	–	Liu et al. [138]
Methylene blue	Chi/Manganite	–	30	6.5	360	0.5	100	40.01	–	–	Mokhtar et al. [139]
Methylene blue	Chi/GO	23.0	22	7.0	1440	0.4	320	402.6	–	–	Sabzevari et al. [140]
Methylene blue	Chi/AA-MBA/Fe ₃ O ₄	1.3	40	8.0	1440	1.0	30	20.25	–	–	Vieira et al. [141]
Methylene blue	Chi-g-PAA/ATT	–	30	5.0	60	0.1	–	1848	–	pH 2	Wang et al. [89]
Methylene blue	Chi/Fe ₃ O ₄ -SiO ₂	–	20	7.0	1440	1.0	1400	33.6	5 x	HCl 0.1 M	Yan et al. [115]
Methylene blue	Chi/Fe-biochar	–	Room	–	1440	2.0	20	6.8	–	–	Zhou et al. [142]
Orange G	Chi/SiO ₂	<16.8	25	5.9	2880	0.5	814.27	54.28	–	–	Blachnio et al. [87]
Orange II	Ce(III)Chi	–	20	2.0	2880	20.0	100	202.84	–	–	Zhu et al. [85]

(continued)

Table 3 (continued)

Dye	Composite	wt%	Temp (°C)	pH	Time (min)	Dose (g/L)	C_{max} (mg/L)	Q_{max} (mg/g)	Reuse	Desorption	References
Reactive black 5	Chi + Cel/TiO ₂	–	30	3.0	30	10.0	300	0.606	–	–	El-Zawahry et al. [143]
Reactive black 5	Chi/MMT	54.8	50	3.0	240	0.4	400	293.46	–	–	Li et al. [144, 145]
Reactive black 5	Chi/FeO _x	14.3	25	6.0	120	–	120	163.93	–	–	Parsaeian et al. [146]
Reactive black 5	Chi/GO	25	25	3.0	1440	1.0	50	205	–	pH 12	Travlou et al. [147]
Reactive black 5	Chi/FeO _x + GO	16.7 + 33.3	25	3.0	1440	1.0	50	368	–	pH 12	Travlou et al. [148]
Reactive black 5	Chi/Fe ₃ O ₄ + GO	–	Room	3.0	150	0.8	50	23.83	4 x	H ₃ CH ₂ OH	Sheshmani and Mashhadi [104]
Reactive blue 19	Chi/GMA/FeO _x	–	Room	3.0	180	2.5	626.5	107.1	3 x	NaOH 0.5 M	Elwakeel et al. [92]
Reactive blue 19	Chi/FeO _x	–	25	1.6	100	2.0	626.5	276.3	4 x	NaOH 0.5 M	Elwakeel et al. [149]
Reactive blue 19	Chi/GO	50.0	–	4.0	120	1.0	400	560.9	–	–	Jawad et al. [150]
Reactive blue 19	Chi/TPP/KLT	50.0	30	4.0	–	0.6	400	687.2	–	–	Jawad and Abdulhameed [151]

(continued)

Table 3 (continued)

Dye	Composite	wt%	Temp (°C)	pH	Time (min)	Dose (g/L)	C _{max} (mg/L)	Q _{max} (mg/g)	Reuse	Description	References
Reactive blue 19	Chi/Fe ₃ O ₄ + AC	33.3 + 33.3	25	6.64	1440	1.0	500	250	-	-	Karaer and Kaya [136]
Reactive blue 19	Chi/GO	66.7	30	4.0	60	1.0	60	40	-	-	Mohamadi et al. [152]
Reactive blue 19	Chi/TPP/MMT	1.0	25	3.0	600	2.5	1600	290.7	-	-	Pereira et al. [95]
		5.0	25	3.0	600	2.5	1600	334.8			
		15.0	25	3.0	600	2.5	1600	308.6			
		25.0	25	3.0	600	2.5	1600	308.6			
Reactive blue 222	Chi/MMT	54.8	50	3.0	240	0.4	400	325.94	-	-	Li et al. [144]
Reactive orange 16	Chi/Fe ₃ O ₄	60 + 20	30	4.0	660	0.08	150	66.9	-	-	Jawad et al. [153]
Reactive orange 16	Chi/EGDE/TiO ₂	50.0	40	4.0	300	0.02	250	1407.4	-	-	Abdulhameed et al. [154]
Reactive red 2	Chi/Fe ₃ O ₄ + AC	33.3	Room	3.0	10	0.4	30	378	20 x	NaOH 0.01 M	Akar et al. [101]
Reactive red 2	Chi/GO + HAPT	16.7 + 16.7	30	2.0	90	2.0	300	40.031	3 x	NaOH 0.1 M	Sirajudheen et al. [103]
Reactive red 2	Chi-La(III)/MMT	25.0	30	2.0	40	2.0	150	35.932	-	-	Sirajudheen and Meenakshi [99]

(continued)

Table 3 (continued)

Dye	Composite	wt%	Temp (°C)	pH	Time (min)	Dose (g/L)	C_{\max} (mg/L)	Q_{\max} (mg/g)	Reuse	Description	References
Reactive red 136	Chi/MMT	55.0	20	3.0	135	0.4	320	473.79	15 x	NaOH 0.05 M	Li et al. [155]
Reactive red 136	Chi/MMT	54.8	40	3.0	240	0.4	400	473.92	–	–	Li et al. [144]
Reactive yellow 145	Chi/MMT	54.8	50	3.0	240	0.4	400	363.33	–	–	Sheshmani and Mashhadi [104]
Rhodamine 6G	Chi-g-PAA/GO	–	Room	5.0	1080	1.1	2000	476.19	–	–	Hongduo et al. [88]
Rhodamine B	Chi/EDTA/FeO _x -GO	–	33	7.5	5	0.2	250	1085.3	7 x	EDTA 0.1 M	Marnani and Shahbazi [94]
Rhodamine B	Chi/Ag-HAPT	30.0	Room	7.0	120	0.5	20	40.11	3 x	H ₂ SO ₄ 0.1 M	Li et al. [145]
Tartrazine yellow	Chi/ZrO ₂ + Fe ₃ O ₄	33.3 + 33.3	25	2.0	1440	1.0	200	47.3	–	–	Jiang et al. [107]
Yellow 7GL	Chi/Fe ₃ O ₄ + SiO ₂	–	20	7.0	1440	1.0	1400	26.3	5 x	HCl 0.1 M	Yan et al. [115]

The survey in the Web of Science combined the terms “chitosan” + “composites” + “dye” + “sorption”

Legend: AC Activated carbon; AM Acrylamide; ATT Attapulgit; β CD β -cyclodextrine; BNT Bentonite; CNT Carbon nanotube; DMT Diatomite; EDTA Ethylenediamine tetraacetic acid; EGDE Ethyleneglycol diglycidyl ether; GMA Glycidyl methacrylate; GO Graphene oxide; GTA Glutaraldehyde; HAPT Hydroxyapatite; KLT Kaolinite; MBA *N*-methylene bisacrylamide; MFA Magnesium fluorohydroxyapatite; MMT Montmorillonite; MNPP 4-methyl-2-naphthalen-2-yl-*N*-propylpentanamide; MOF Metal-organic framework; PAA Poly(acrylic acid); PMMA Poly(methyl methacrylate); PVA Poly(vinyl alcohol); PVFA Poly(*N*-vinyl formamide-co-acrylic acid); RSP Rarasaponin; TPP Tripolyphosphate; VMT vermiculite

[84, 138] of the adsorbed amount upon temperature increase. The increase of the ionic strength weakened the adsorption of dyes on chitosan-based composites [120, 131, 138, 157], which involved electrostatic interactions. However, the increase of ionic strength favoured the H bonding-driven adsorption of dyes on chitosan composites [147, 148]. A few reports compared the adsorption of the dye on pure chitosan or pure filler with that of the chitosan composite [90, 95, 96, 110–112, 127, 141].

Table 3 shows that in general, the presence of graphene oxide (GO) nanoplatelets increased the adsorption capacity of chitosan-based composites, as in the case of alginate-based composites. Most magnetic chitosan-based composites presented high efficiency to adsorb different dyes. Chitosan forms composites with a variety of clays; the adsorption capacity of the resulting composite is dependent on the surface area of clay particles. Table 3 shows composites of rectorite [102] or alunite [101] and chitosan for the adsorption of acid red 1 (AR1). Composites of chitosan and diatomite, porous siliceous mineral particles, presented high Q_{\max} values towards different dyes [113, 130].

4 Cellulose-Based Composites

Cellulose is a linear polysaccharide of β -(1 \rightarrow 4)-linked D-glucopyranosyl repeating units, a non-reducing end, and a reducing end, as depicted in Fig. 7 [158]. Cellulose is a very important polymer because its annual biosynthesis amounts to 1.3 billion metric tons [159] mainly from plants. The crystallinity and degree of polymerization of cellulose depend on its source and the process of purification. Cotton and bacterial cellulose are the natural sources with the highest contents of cellulose (higher than 90%), whereas the cellulose content in natural fibres might range from 45 to 55%.

Cellulose is insoluble in water. Not only the intra- and intermolecular H bonds, but also the hydrophobic interactions hinder the solubility of cellulose in water [160]. Cellulose can be modified by chemical reactions to enhance its solubility in water. Cellulose ethers are nontoxic water-soluble cellulose derivatives with applications as rheology controllers, thickeners, emulsifiers in food, drug, and paint formulations [161]. The chemical nature of the substituent, the degree of the substitution (DS, up to three by glucopyranose unit), and the degree of polymerization will define

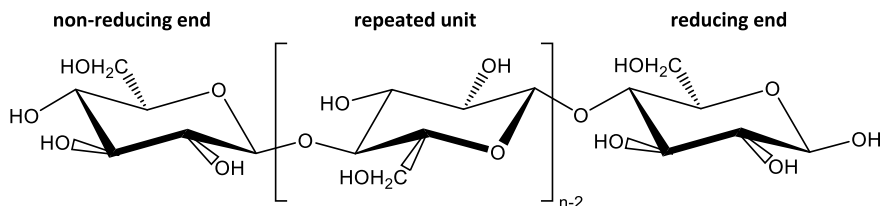


Fig. 7 Representation of the structure of cellulose, a linear polysaccharide of β -(1 \rightarrow 4)-D-glucose repeating units, a non-reducing end, and a reducing end [158]

the properties of cellulose ethers, like solubility in water and affinity for dissolved molecules [162].

Amongst the cellulose ethers, carboxymethyl cellulose (CMC) is one of the most used for the preparation of composites. The reaction of alkali-activated cellulose with chloroacetic acid results in a derivative that behaves as a polyanion at pH higher than 4. The degree of carboxymethylation should be larger than 0.7 to achieve complete solubility in water. For a cationic dye like methylene blue, CMC is supposed to present a more pronounced uptake [163–166] in comparison to cellulose-based composites [167–172]. However, the interactions between CMC and fillers or other polymers might involve electrostatic interactions or ion–dipole interactions, reducing the number of CMC carboxylate groups available for the cationic dye adsorption [173]. Table 4 shows examples of CMC-composites with adsorption capacity smaller or similar [174–177] to that of cellulose-based composites [177–180]. One should notice that very high concentrations of dye [163, 165, 177, 178, 181] and small dosage of adsorbents [91, 165, 178, 179] might induce to multilayer adsorption of dye molecules by π - π stacking and high Q_{\max} values.

Effects due to net charges are also related to the loading/entrapment of clay [64, 168, 179, 186, 190, 193], to the binding with other polymers [177, 195, 200] and/or other particles [181, 182, 187, 191, 192, 201]. The influence of charges is remarkable when comparing the adsorption efficiency of some cellulose/carbon composites [170, 176, 182, 185, 197, 198], the phenomenon also seen in some chitosan-based [103, 104, 121, 142, 152], and alginate-based composites [57, 69]. The adsorption of dyes on cellulose acetate-based composites [184, 197] containing nanocellulose particles (CNC and CNF, hydrophilic) [199, 203, 208] is driven by polar interactions, yielding Q_{\max} approximately 100 mg_{dye}/g_{sorbent}. CNC produced by the hydrolysis of cellulose with sulphuric acid carries sulphate groups, which favour the adsorption of positively charged dyes, as methylene blue [210].

Cellulose composites are strongly related to the valorization of biomass wastes by mixing them directly with a second polymer [41, 64, 135, 167, 190] or by the valorization of their sub-products [185, 198].

5 Starch and Other Polysaccharide-Based Composites

Starch is composed of amylose, a polysaccharide with α -(1→4)-linked D-glucopyranosyl repeating units, and amylopectin, a highly branched macromolecule with α -(1→4)-linked D-glucose backbone and about 5% of α -(1→6) branch linkages [211]. Starch is produced by green plants for energy storage and is the main source of carbohydrates for humankind. Despite nutritional relevance, some research groups developed starch-based composites for dye adsorption. Table 5 shows starch-based composites and the corresponding Q_{\max} values. The combination of starch and nanosheets of graphene oxide (GO) seems to yield composites with the highest Q_{\max} values, indicating that the large surface area of nanofillers plays an important role in dye removal efficiency. Crosslinked potato starch combined with graphene

Table 4 Dyes, cellulose-based composites, and the experimental conditions used for the adsorption experiments (filler content in the composite, temperature, pH, contact time, adsorbent dose, maximum concentration (C_{\max}), maximum adsorption capacity (Q_{\max}), adsorption/desorption cycles (reuse times) and desorption medium), along with the corresponding references

Dye	Polysaccharide composite	wt%	Temp (°C)	pH	Time (min)	Dose (g/L)	C_{\max} (mg/L)	Q_{\max} (mg/g)	Reuse	Desorption	References
Acid red 1	CMC/Fe ₃ O ₄ + GO	–	30	7.0	40	2.0	300	46,234	5 x	NaOH 0.1 M	Sirajudheen et al. [182]
Acidol red 2BE	CMC/BNT	50.0	23	5.0	180	1.0	200	71.42	–	–	Leshaf et al. [183]
Acid scarlet	CA/MMT	60.0	20	1.0	720	0.5	125	85.7	–	–	Zhou et al. [184]
Acid yellow 220	CMC/HAPT	–	Room	6.0	90	2.5	500	200	–	–	Manatunga et al. [105]
Bromocresol green	SiO ₂ /Chi-CMC-Chi	–	Room	12.0	120	25.0	–	12.02	–	–	Ghiorghita et al. [173]
Basic red 46	Cel-GO/Fe ₃ O ₄	0 + 5.0	Room	11	60	3	60	15.22	–	H ₂ O	Rahimi et al. [185]
		1.0 + 5.0						19.8			
Congo red	CNC-Chi/Fe ₃ O ₄ -ATT	–	25	5.5	240	0.2	500	230	5 x	NaOH 0.1 M	Chen et al. [186]
Congo red	SiO ₂ /Chi-CMC-Chi	–	–	12.0	120	25.0	–	9.49	–	–	Ghiorghita et al. [173]
Congo red	CNF/Fe@FeS	–	25	5.0	240	0.5	400	111.1	5 x	NaOH 0.5 M	Sankaramakrishnan et al. [187]
Congo red	Cel/BNT	10.0	30	7.0	90	1.0	50	24.2	–	–	Santoso et al. [188]
		20.0						34.03			

(continued)

Table 4 (continued)

Dye	Polysaccharide composite	wt%	Temp (°C)	pH	Time (min)	Dose (g/L)	C_{max} (mg/L)	Q_{max} (mg/g)	Reuse	Description	References
		30.0						45.77			
Congo red	CMC/Fe ₃ O ₄ + GO	–	30	7.0	40	2.0	300	45,098	5 x	NaOH 0.1 M	Sirajudheen et al. [182]
Congo red	CMC/PAn/TiO ₂	10.0	25	2.6	24	2.8	100	94.3	5 x	NaOH 1.0 M	Tanzifi et al. [189]
Congo red	LignoCel/MMT	–	30	10.0	360	0.4	800	102.32	–	NaOH 0.1 M	Wang et al. [190]
Congo red	CA + Chi/Fe ₃ O ₄ + TiO ₂	15.0	Room	3.0	120	0.5	100	74.2			ZabihSahebi et al. [191]
Congo red	Cel/Fe ₃ O ₄ + AC	30.8 + 7.7	25	4.0	900	1.0	–	66.09	5 x	NaOH 0.1 M	Zhu et al. [192]
Crystal violet	Cel/GO	–	25	9.0	–	0.8	40	19.23	5 x	HCl 4 vol%	Nayl et al. [170]
Drimarine yellow HF	Cel/Clay	98.4	30	2.0	120	2.0	100	48.97	3 x	HAc 1 wt%	Kausar et al. [193]
Eosin yellow	CMC/GO	8.0	20	2.0	120	1.2	100	65.7	5 x	–	Liu et al. [176]
Malachite green	Cel-g-PAM/MMT	10.0	30	7.0	240	1.0	10	172.4	–	–	Peighambardoust et al. [194]
Malachite green	CMC-PVA-NaAlg/zeolite	5.0	25	10.0	220	50.0	10	29.58	5 x	HCl 0.1 M	Radoor et al. [195]
Methylene blue	Cel/SiO ₂	–	25	8.0	1440	2.0	100	78.75	–	–	Ali [196]

(continued)

Table 4 (continued)

Dye	Polysaccharide composite	wt%	Temp (°C)	pH	Time (min)	Dose (g/L)	C _{max} (mg/L)	Q _{max} (mg/g)	Reuse	Description	References
Methylene blue	CA/AC	33.3	25	7.0	3000	0.4	200	158	8 x	pH 2	Bai et al. [197]
Methylene blue	Bagasse/CaAlg/biochar	–	30	7.4	180	1.0	50	68.39	–	–	Biswas et al. [167]
Methylene blue	Cel/GO	10.0	25	6.0	3000	0.4	220	452.49	3 x	HCl 0.2 M	Chen et al. [178]
Methylene blue	Cel/CaAlg-ATT	–	25	8.0	2160	1.25	15	11.23	3 x	H ₂ SO ₄ 0.1 M	Chen et al. [168]
Methylene blue	CMC/PVA/BNT	12.5	40	8.00	180	1.0	250	163.93	4 x	HCl 0.1 M	Dai et al. [174]
Methylene blue	CMC/GO	25.0	25	10.0	300	1.0	250	183.23	9 x	H ₃ CH ₂ COH	Eltaweil et al. [175]
Methylene blue	Cel/MMT	–	30	8.0	240	0.5	170	338.8	4 x	H ₃ CH ₂ COH	Hu et al. [179]
Methylene blue	CMC/GO/Chi	50.0	25	6.0	4320	0.4	600	3190.1	5 x	HCl 0.1 M	Huang et al. [163]
Methylene blue	Cel/Fe ₃ O ₄	20.0	25	9.0	120	1.0	1000	1105.7	–	HCl 0.1 M	Li et al. [181]
Methylene blue	CMC-g-PAA/APT	5.0	30	7.0	30	0.5	1200	2094.8	–	–	Liu et al. [164]
		20.0						1979.48			(continued)

Table 4 (continued)

Dye	Polysaccharide composite	wt%	Temp (°C)	pH	Time (min)	Dose (g/L)	C_{max} (mg/L)	Q_{max} (mg/g)	Reuse	Desorption	References
Methylene blue	CMC/GO	8.0	20	6.0	120	1.2	100	58.24	-	-	Liu et al. [176]
Methylene blue	Cel/GO	1.0	-	-	1440	2.0	100	12.13	-	-	Liu et al. [198]
		10.0						46.35			
Methylene blue	CNF/PVA/MMT	30.0	50	10.0	360	1.2	250	67.2	-	-	Luo et al. [199]
Methylene blue	CMC/AA + MBA/Fe ₃ O ₄	20.0	25	7.0	90	0.33	350	1081.6	-	-	Malatji et al. [165]
Methylene blue	Cel/GO	-	25	7.0	-	0.8	40	35.71	5 x	HCl 4 vol%	Nayl et al. [170]
Methylene blue	CMC-EPTAC-Clay	10.0	30	7.0	60	62.5	200	909	-	-	Peng et al. [166]
Methylene blue	Cel-PDMA-Chi/Fe ₃ O ₄	-	Room	6.0	150	-	200	828.3	-	HCl 1 M	Peng et al. [177]
Methylene blue	Cel/KLT	-	25	7.0	2880	0.5	2000	93.7	5 x	HCl 0.3 M	Qian et al. [64]
Methylene blue	Cel(III)/GO	0.5	Room	6.0	90	1.2	20	78.493	-	-	Ren et al. [171]
Methylene blue	CNC/PAA/Fe ₃ O ₄	-	25	7.2	180	4.0	20	332	5 x	NaOH 0.1 M	Samadder et al. [200]

(continued)

Table 4 (continued)

Dye	Polysaccharide composite	wt%	Temp (°C)	pH	Time (min)	Dose (g/L)	C_{max} (mg/L)	Q_{max} (mg/g)	Reuse	Description	References
Methylene blue	CNF/Fe@FeS	–	25	7.0	240	0.5	160	200	5 x	NaOH 0.5 M	Sankaramakrishnan et al. [187]
Methylene blue	Cel/AC	1.0	35	7.0	1440	–	100	71.41	–	–	Somsesta et al. [172]
		2.0						74.1			
		3.0						110.35			
Methylene blue	Cel-Fe ₃ O ₄ /GO	30.4 + 3.6	25	5.0	840	1.0	100	70.03	5 x	NaOH 0.1 M	Shi et al. [201]
Methylene blue	Cel/GO	4.5	25	7.0	70	1.0	160	245.1	7 x	H ₂ O	Wang et al. [202]
Methylene blue	Cel-S-GO	1.8	25	7.0	70	1.0	160	273.97	7 x	H ₂ O	Wang et al. [202]
		2.8						349.65			
		3.6						361.01			
		4.5						421.94			
Methylene blue	CNF/GO	25.0	–	–	360	–	220	112.2	–	–	Wang et al. [203]
Methylene blue	CA + Chi/Fe ₃ O ₄ + TiO ₂	15.0	Room	3.0	120	0.5	100	97.6	–	–	ZabihSahebi et al. [191]

(continued)

Table 4 (continued)

Dye	Polysaccharide composite	wt%	Temp (°C)	pH	Time (min)	Dose (g/L)	C_{max} (mg/L)	Q_{max} (mg/g)	Reuse	Desorption	References
Methyl orange	Cel/GMA/Fe ₃ O ₄ + AC	–	25	3.0	180	0.4	50	98.33	5 x	HCl 0.1 M	Huang et al. [204]
Methyl orange	CMC-g-PDMAEMA/BNT	80.0	Room	6.9	60	2.0	300	155.76	5 x	pH 9	Li et al. [205]
Methyl violet	CMC/AM-TEMED/zeolite	–	25	7.0	90	0.4	–	44.51	3 x	HCl 0.01 M	Karadağ et al. [206]
Rhodamine B	CA/AC	33.3	25	7.0	3000	0.4	200	33.4	–	pH 8	Bai et al. [197]
Rhodamine B	Cel/Clay I	14.3	25	2.0	120	2.0	100	47.112	–	–	Kausar et al. [207]
Rhodamine B	Cel/Clay II	14.3	25	2.0	120	2.0	100	50.138	–	–	–
Rhodamine B	Cel/Fe ₃ O ₄	20.0	25	7.0	120	1.0	1000	127.1	5 x	HCl 0.1 M	Li et al. [181]
Rhodamine B	CNC/GO	11.0	30	–	–	–	30	86.4	42 x	CH ₃ CH ₂ COH	Tian et al. [208]
Rhodamine B	CMC/GO	–	Room	–	1440	2.0	300	161.29	–	–	Xiang et al. [209]
Reactive red 2	CaCMC/Fe ₃ O ₄ + GO	–	30	7.0	40	2.0	300	47.327	5 x	NaOH 0.1 M	Sirajudheen et al. [182]

The survey in the Web of Science combined the terms “cellulose” + “composites” + “dye” + “sorption”

Legend AA Acrylic acid; AC Activated carbon; AM Acrylamide; ATT Attapulgit; BNT Bentonite; CA Cellulose acetate; CMC Carboxymethyl cellulose; CNC Cellulose nanocrystals; CNF Cellulose nanofibres; CNT Clonopitilolite; DMAEM Diatomite; EPTAC Ethylenediamine tetraacetic acid; GMA Glycidyl methacrylate; GO Graphene oxide; GTA Glutaraldehyde; HAPT Hydroxyapatite; KLT Kaolinite; MBA N-methylene bisacrylamide; MMT Montmorillonite; MOF Metal-organic framework; PAA Poly(acrylic acid); PAn Poly(aniline); PDMA Pyromellitic dianhydride; PDMAEMA Poly(2-(dimethylamino)ethyl methacrylate); PMMA Poly(methyl methacrylate); PVA Poly(vinyl alcohol); TEMED Tetramethylethylenediamine

Table 5 Dyes, composites containing starch or other less frequent polysaccharides, and the experimental conditions used for the adsorption experiments (filler content in the composite, temperature, pH, contact time, adsorbent dose, maximum concentration (C_{max}), maximum adsorption capacity (Q_{max}), adsorption/desorption cycles (reuse times) and desorption medium), along with the corresponding references

Dye	Polysaccharide composite	wt%	Temp (°C)	pH	Time (min)	Dose (g/L)	C_{max} (mg/L)	Q_{max} (mg/g)	Reuse	Desorption	References
Methylene blue	Gum ghatti/TiO ₂	3.0	25	7.0	60	0.2	800	1305.38	3 x	CH ₃ CH ₂ OH	Mittal and Ray [215]
Basic red 2	iCar/AM + MBA/MMT	10.0	25	–	5760	–	17.5	4.56			Karadağ et al. [216]
Crystal violet	kCar/LPT	1 x	24	5.5	1440	1.0	200	108.1	5 x	KCl 0.5 M	Mahdavia et al. [217]
		2 x						160.0			
		4 x						172.3			
Methylene blue	kCar + CMC/MMT	16.7	30	6	180	1	500	10.75	5 x	Ethanol 98 vol % HCl 0.01 M	Liu et al. [169]
Methylene blue	kCar-g-P(AM-co-MAA)/zeolite	4.0	25	7	1440	0.4	500	661.91	6 x	H ₃ CCOCH ₃	Mittal et al. [218]
Methylene blue	kCar/AM + MBA/BNT	–	25	11.0	60	0.4	20	156.25	5 x	H ₃ CCOCH ₃	Pourjavadi et al. [219]
Rhodamine B	Locust gum/GO	20	Room	3	1440	0.25	100	514.5	10 x	NaOH 0.1 M	Li et al. [220]
Basic yellow 28	Pectin/MMT	10.0	20	2.0	120	0.3	80	131.5	–	HOCH	Nesic et al. [221]
Crystal violet	Pullulan/PDA/MMT	11.3	37	x	300	1.0	300	103.78	6 x	HCl 0.1 M	Qi et al. [222]
		22.7						112.45			

(continued)

Table 5 (continued)

Dye	Polysaccharide composite	wt%	Temp (°C)	pH	Time (min)	Dose (g/L)	C _{max} (mg/L)	Q _{max} (mg/g)	Reuse	Desorption	References
		34.0						97.46			
		45.3						89.37			
Acid scarlet	Starch/MMT	5.0	25	7.4	15	0.01	100	43.7	–	–	Kochkina et al. [111]
Congo red	Starch + PAA/Fe ₃ O ₄	33.3	25	5.0	300	–	200	31.847	7 x	NaOH 0.1 M	Saberi et al. [223]
Brilliant blue X	Starch/clay	10.0	20	–	40	50.0	–	112.4	–	–	Xing et al. [224]
		20.0						122.0			
		30.0						89.3			
Basic blue 17	Starch/AA + MBA/KLT	0.5	25	–	5760	60.0	18.35	7.462	–	–	Karadağ et al. [225]
		1.0						10.137			
		1.5						7.709			
		2.0						6.884			
Crystal violet	Starch-g-MA/CaCO ₃	2 x	25	5.5	120	5.0	10	0.536	–	–	Bakshi and Darvishi [214]
Crystal violet	Starch-g-MA/Egg CaCO ₃	1 x	25	5.5	120	5.0	10	0.988	–	–	Bakshi and Darvishi [214]
		2 x						0.932			
		3 x						1.33			

(continued)

Table 5 (continued)

Dye	Polysaccharide composite	wt%	Temp (°C)	pH	Time (min)	Dose (g/L)	C _{max} (mg/L)	Q _{max} (mg/g)	Reuse	Description	References
Methylene blue	Starch-GTA-GO	5.0	45	9.0	210	0.35	–	500	3 x	pH 4.0	Bhattacharyya et al. [212]
Methylene blue	Starch-g-MA/CaCO ₃	2 x	25	5.5	120	5.0	10	1.53	–	–	Bakshi and Darvishi [214]
Methylene blue	Starch-g-MA/Egg CaCO ₃	1 x	25	5.5	120	5.0	10	1.66	–	–	Bakshi and Darvishi [214]
		2 x	25	5.5	120	5.0	10	1.71			
		3 x	25	5.5	120	5.0	10	1.38			
Methyl violet	Starch/Fe ₃ O ₄ + clay	14.3 + 57.1	25	9.0	150	1.5	100	29.67	–	–	Ansari Mojarad et al. [226]
Methyl violet	Starch + PAA/Fe ₃ O ₄	33.3	25	7.4	300	–	200	23.584	7 x	CH ₃ CH ₂ OH	Saberi et al. [223]
Malachite green	Starch-g-PAM/GO + HAPT	1.0	25	10.0	240	1.0	200	287	5 x	HNO ₃ 0.5 M	Hosseinzadeh and Ramin [213]
		3.0						261			
		5.0						297			
Methyl violet	Starch/Fe ₃ O ₄ + clay	14.3 + 57.1	25	9.0	150	1.5	100	29.67	–	–	Ansari Mojarad et al. [226]

(continued)

Table 5 (continued)

Dye	Polysaccharide composite	wt%	Temp (°C)	pH	Time (min)	Dose (g/L)	C _{max} (mg/L)	Q _{max} (mg/g)	Reuse	Desorption	References
Methyl violet	Starch + PAA/Fe ₃ O ₄	33.3	25	7.4	300	–	200	23.584	7 x	CH ₃ CH ₂ OH	Saberi et al. [223]
Janus green B	Xanthan/AM + MBA/SPT	25.0	25	–	5760	–	1022	1425	–	–	Karadağ et al. [227]
		16.8						2442			
		12.5						3143			
		10.0						3169			
Methylene blue	Xanthan-co-PAA/GO	–	25	5	120	0.5	200	793.65	–	–	Makhado et al. [228]
Methyl violet								1052.63			
Methylene blue	Xanthan/SiO ₂	30	25	8.0	–	0.8	100	432.9	3 x	H ₂ SO ₄	Thakur et al. [229]

The survey in the Web of Science combined the terms “polysaccharide” or “starch” + “composites” + “dye” + “sorption”

Legend AC Activated carbon; AM Acrylamide; ATT Attapulgitic; BNT Bentonite; CA Cellulose acetate; Car Carrageenan; CMC Carboxymethyl cellulose; GO Graphene oxide; GTA Glutaraldehyde; HAPT Hydroxyapatite; KLT Kaolinite; LPT Lepidolite; MBA N-methylene bisacrylamide; MMT Montmorillonite; MOF Metal-organic framework; PAA Poly(acrylic acid); PDA Polydopamine; SPT Sepiolite

oxide (GO) resulted in composites with Q_{\max} of 500 mg/g towards methylene blue (MB) [212]. Cassava starch crosslinked with polyacrylamide (PAM) in the presence of GO nanosheets and hydroxyapatite (HAPT) showed Q_{\max} of 297 mg/g of malachite green [213]. Wheat starch, poly(sodium methacrylate), P(NaMA), and eggshell particles or CaCO_3 formed composites for the adsorption of MB and crystal violet (CV); in comparison to composites prepared with CaCO_3 , those prepared with eggshell particles provided larger adsorption capacity due to the intrinsic porosity of eggshells [214]. Composites of starch and other polysaccharides (κ -carrageenan, pectin, pullulan, xanthan) and clays presented high affinity for less common (BY28, JGB) and common (CV) dyes, as shown in Table 5.

6 Future Trends

The results presented in this book chapter demonstrated that the interest in developing polysaccharide-based composites for dye removal from wastewater increased considerably during the last decade. This tendency should remain for the next decade since clean water has become increasingly scarce on our planet. The topic “Polysaccharides-based composites for dye removal” offers opportunities to improve the composites, making them more functional, and creating less hazardous dyes. Figure 8 depicts some strategies regarding new processes and products based on biological or natural sources.

The increase of composite functionality might be achieved by the combination of polysaccharides with sunlight-photoactive fillers. For instance, the incorporation of active nanofillers as TiO_2 , which not only improves the mechanical properties of the composites but also promotes the photobleaching of the dyes under UV light, is surely a path to follow. Another promising strategy is the incorporation of microorganisms able to discolour textile effluents [230] into the composites. Bacteria, fungi, algae, and yeast can biodegrade a plethora of organic dyes [231]. The attachment of active microorganisms to the composites would provide an in situ degradation of the adsorbed dye. In both cases, is fundamental to study the toxicity evaluation of the products resulting from the dye degradation.

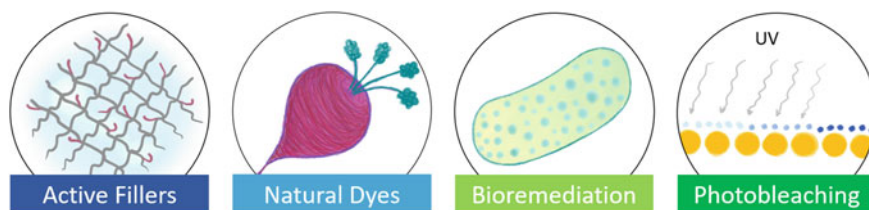


Fig. 8 Some possible strategies to mitigate problems related to effluents contaminated by organic dyes: preparation of composites with active fillers, which can be photocatalysts for the degradation of adsorbed dyes or microorganisms that biodegrade dyes, and the development of new natural dyes

Since the beginning, humankind has used natural dyes [232]. The accidental discovery of the first synthetic dye in 1856 by William Henry Perkin started a new era of mass production of synthetic dyes [1]. Since then the use of natural dyes decreased due to the cost and the amount necessary to supply the demand. Now the concerns about environmental impact and the importance of clean water bring us back to the natural dyes. The development of new natural dyes is an increasing trend for the new decade due to their biodegradability and low toxicity, reducing the environmental impact caused by synthetic dyes. For instance, recently a new chemical route transformed beetroot pigment (betalains) from red to orange or magenta to blue [233]. This new dye, named BeetBlue, dissolves in water and other solvents and is nontoxic. All over the world, companies combine technologies and innovations to achieve sustainable production of natural dyes for the textile industry. *EarthColors*[®] is a trademark for dyes produced from non-edible agricultural or herbal waste. In India, a country with traditional textile industry, companies like *Ama Herbals* and *Bio Dye Goa* offer a plethora of natural dyes. These trends point at a promising next decade with novel dyestuff based on old nature.

References

1. Bechtold T, Mussak R (2009) Handbook of natural colorants. Wiley, Chichester. <https://doi.org/10.1002/9780470744970>
2. Hunger K (ed) (2002) Industrial dyes, 1st edn. Wiley, Frankfurt. <http://doi.org/10.1002/3527602011>
3. Sabnis RW (2010) Handbook of biological dyes and stains. Wiley. <http://doi.org/10.1002/9780470586242>
4. Nassau K (1998) The fifteen causes of color. In: AZimuth. Elsevier Masson SAS, pp 123–168. [http://doi.org/10.1016/S1387-6783\(98\)80007-X](http://doi.org/10.1016/S1387-6783(98)80007-X)
5. Spencer J (2021) The sustainable development goals. Des Glob Challenges Goals 12–25. <https://doi.org/10.4324/9781003099680-3>
6. United Nations Secretary (2017) Water action decade 2018–2028, New York. Available at <http://digitallibrary.un.org/record/859143>
7. Berradi M, Hsissou R, Khudhair M et al (2019) Textile finishing dyes and their impact on aquatic environs. Heliyon 5. <https://doi.org/10.1016/j.heliyon.2019.e02711>
8. Crini G, Lichtfouse E (2019) Advantages and disadvantages of techniques used for wastewater treatment. Environ Chem Lett 17:145–155. <https://doi.org/10.1007/s10311-018-0785-9>
9. Voragen ACJ, Rolin C, Marr BU et al (2003) Polysaccharides. In: Ullmann's encyclopedia of industrial chemistry. Wiley-VCH Verlag GmbH & Co. KGaA, Weinheim, Germany
10. McNaught AD, Wilkinson A (eds) (2019) The IUPAC compendium of chemical terminology, 2nd edn. International Union of Pure and Applied Chemistry (IUPAC), Oxford, UK. <https://doi.org/10.1351/goldbook>
11. Theng BKG (2012c) The clay minerals. In: Developments in clay science, 2nd edn. Elsevier B.V., pp 3–45. <http://doi.org/10.1016/B978-0-444-53354-8.00001-3>
12. Theng BKG (2012d) Polysaccharides. In: Developments in clay science, pp 351–390. <http://doi.org/10.1016/B978-0-444-53354-8.00011-6>
13. Banerjee S, Pillai SC, Falaras P et al (2014) New insights into the mechanism of visible light photocatalysis. J Phys Chem Lett 5:2543–2554. <https://doi.org/10.1021/jz501030x>
14. Toledo PVO, Marques LR, Petri DFS (2019) Recyclable Xanthan/TiO₂ composite cryogels towards the photodegradation of Cr(VI) ions and methylene blue dye. Int J Polym Sci. <https://doi.org/10.1155/2019/8179842>

15. Frizzo MS, Betega K, Poffo CM et al (2021) Highly enhanced adsorption and photocatalytic performance of TiO₂ quantum dots synthesized by microwaves for degradation of reactive red azo dye. *J Nanoparticle Res* 23:113. <https://doi.org/10.1007/s11051-021-05237-x>
16. Nguyen TTH, Qureshi D, Lim S et al (2021) Introduction to polysaccharides. In: Food, medical, and environmental applications of polysaccharides. Elsevier, pp 3–46. <https://doi.org/10.1016/B978-0-12-819239-9>
17. Burkinshaw SM (2016) Physico-chemical aspects of textile coloration. Wiley, Chichester. <https://doi.org/10.1002/9781118725658>
18. Sabnis RW (2015) Handbook of fluorescent dyes and probes, 1st edn. Wiley. <http://doi.org/10.1002/9781119007104>
19. Tardivo JP, Del Giglio A, De Oliveira CS et al (2005) Methylene blue in photodynamic therapy: from basic mechanisms to clinical applications. *Photodiagn Photodyn Ther* 2:175–191. [https://doi.org/10.1016/S1572-1000\(05\)00097-9](https://doi.org/10.1016/S1572-1000(05)00097-9)
20. Martins BF, de Toledo PVO, Petri DFS (2017) Hydroxypropyl methylcellulose based aerogels: synthesis, characterization and application as adsorbents for wastewater pollutants. *Carbohydr Polym* 155:173–181. <https://doi.org/10.1016/j.carbpol.2016.08.082>
21. Toledo PVO, Petri DFS (2019) Hydrophilic, hydrophobic, Janus and multilayer xanthan based cryogels. *Int J Biol Macromol* 123:1180–1188. <https://doi.org/10.1016/j.ijbiomac.2018.11.193>
22. Hatakeyama T, Hatakeyama H (2017) Heat capacity and nuclear magnetic relaxation times of non-freezing water restrained by polysaccharides, revisited. *J Biomat Sci* 28:1215–1230. <http://doi.org/10.1080/09205063.2017.1291551>
23. Toledo PVO, Bernardinelli OD, Sabadini E, Petri DFS (2020) The states of water in tryptophan grafted hydroxypropyl methylcellulose hydrogels and their effect on the adsorption of methylene blue and rhodamine B. *Carbohydr Polym* 248:116765. <https://doi.org/10.1016/j.carbpol.2020.116765>
24. Ougiya H, Hioki N, Watanabe K, Morinaga Y, Yoshinaga F, Samejima M (1998) Relationship between the physical properties and surface area of cellulose derived from adsorbates of various molecular sizes. *Biosci Biochemol Biochem* 62:1880–1884. <https://doi.org/10.1271/bbb.62.1880>
25. Mazeau K, Wyszomirski M (2012) Modelling of Congo red adsorption on the hydrophobic surface of cellulose using molecular dynamics. *Cellulose* 19:1495–1506. <https://doi.org/10.1007/s10570-012-9757-6>
26. Silva RA, Carmona-Ribeiro AM, Petri DFS (2013) Enzymatic activity of cholesterol oxidase immobilized onto polymernanoparticles mediated by Congo red. *Colloids Surf B* 110:347–355. <http://doi.org/10.1016/j.colsurfb.2013.03.024>
27. Silva RA, Carmona-Ribeiro AM, Petri DFS (2014) Catalytic behavior of lipase immobilized onto Congo red and PEG-decorated particles. *Molecules* 19:8610–8628. <https://doi.org/10.3390/molecules19068610>
28. Pereira AGB, Rodrigues FHA, Paulino AT et al (2021) Recent advances on composite hydrogels designed for the remediation of dye-contaminated water and wastewater: a review. *J Clean Prod* 284. <https://doi.org/10.1016/j.jclepro.2020.124703>
29. Sabnis RW (2007) Handbook of acid-base indicators. CRC Press, San Francisco. <https://doi.org/10.1201/9780849382192>
30. De Araujo RE, Gomes ASL, De Araújo CB (2000) Measurements of pK_a of organic molecules using third-order nonlinear optics. *Chem Phys Lett* 330:347–353. [https://doi.org/10.1016/S0009-2614\(00\)01108-8](https://doi.org/10.1016/S0009-2614(00)01108-8)
31. Impert O, Katafias A, Kita P et al (2003) Kinetics and mechanism of a fast leuco-methylene blue oxidation by copper(ii)-halide species in acidic aqueous media. *J Chem Soc Dalton Trans* 3:348–353. <https://doi.org/10.1039/b205786g>
32. Stratton SG, Taumoeofolau GH, Purnell GE et al (2017) Tuning the pK_a of fluorescent rhodamine pH probes through substituent effects. *Chem A Eur J* 23:14064–14072. <https://doi.org/10.1002/chem.201703176>

33. Perrin DD, Dempsey B, Serjeant EP (1981) pK a prediction for organic acids and bases. Springer, Netherlands. <https://doi.org/10.1007/978-94-009-5883-8>
34. Patel H (2019) Fixed-bed column adsorption study: a comprehensive review. *Appl Water Sci* 9:45–62. <https://doi.org/10.1007/s13201-019-0927-7>
35. Al-Ghouti MA, Da'ana DA (2020) Guidelines for the use and interpretation of adsorption isotherm models: a review. *J Hazard Mater* 393:122383. <https://doi.org/10.1016/j.jhazmat.2020.122383>
36. Tran HN, You SJ, Hosseini-Bandegharaei A, Chao HP (2017) Mistakes and inconsistencies regarding adsorption of contaminants from aqueous solutions: a critical review. *Water Res* 120:88–116. <https://doi.org/10.1016/j.watres.2017.04.014>
37. Sabra W, Deckwer WD (2004) Alginate—a polysaccharide of industrial interest and diverse biological functions. In: Dumitriu S (ed) *Polysaccharides. Structural diversity and functional versatility*, 2nd edn. CRC Press, Boca Raton/USA, pp 515–533. <https://doi.org/10.1201/9781420030822-25>
38. Izydorczyk M, Cui S, Wang Q (2005) Polysaccharide gums. In: *Food carbohydrates*. CRC Press. <http://doi.org/10.1201/9780203485286.ch6>
39. Morris ER, Rees DA, Thom D (1980) Characterisation of alginate composition and block-structure by circular dichroism. *Carbohydr Res* 81:305–314. [https://doi.org/10.1016/S0008-6215\(00\)85661-X](https://doi.org/10.1016/S0008-6215(00)85661-X)
40. Sun L, Fugetsu B (2014) Graphene oxide captured for green use: influence on the structures of calcium alginate and macroporous alginic beads and their application to aqueous removal of acridine orange. *Chem Eng J* 240:565–573. <https://doi.org/10.1016/j.cej.2013.10.083>
41. Alver E, Metin AÜ, Brouers F (2020) Methylene blue adsorption on magnetic alginate/rice husk bio-composite. *Int J Biol Macromol* 154:104–113. <https://doi.org/10.1016/j.ijbiomac.2020.02.330>
42. Cojocaru C, Humelnicu AC, Samoila P et al (2018) Optimized formulation of NiFe₂O₄@Ca-alginate composite as a selective and magnetic adsorbent for cationic dyes: experimental and modeling study. *React Funct Polym* 125:57–69. <https://doi.org/10.1016/j.reactfunctpolym.2018.02.008>
43. Mahmoodi NM (2013) Magnetic ferrite nanoparticle-alginate composite: synthesis, characterization and binary system dye removal. *J Taiwan Inst Chem Eng* 44:322–330. <https://doi.org/10.1016/j.jtice.2012.11.014>
44. Rocher V, Siaugue JM, Cabuil V, Bee A (2008) Removal of organic dyes by magnetic alginate beads. *Water Res* 42:1290–1298. <https://doi.org/10.1016/j.watres.2007.09.024>
45. Jabli M, Hassine BB (2018) Improved removal of dyes by [sodium alginate/4-methyl-2-(naphthalen-2-yl)-*N*-propylpentanamide-functionalized ethoxy-silica] composite gel beads. *Int J Biol Macromol* 117:247–255. <https://doi.org/10.1016/j.ijbiomac.2018.04.194>
46. Pashaei-Fakhri S, Peighambaroust SJ, Foroutan R et al (2021) Crystal violet dye sorption over acrylamide/graphene oxide bonded sodium alginate nanocomposite hydrogel. *Chemosphere* 270:129419. <https://doi.org/10.1016/j.chemosphere.2020.129419>
47. Qiu H, Qiu Z, Wang J et al (2014) Enhanced swelling and methylene blue adsorption of polyacrylamide-based superabsorbents using alginate modified montmorillonite. *J Appl Polym Sci* 131:1–9. <https://doi.org/10.1002/app.40013>
48. Rashidzadeh A, Olad A, Salari D (2015) The effective removal of methylene blue dye from aqueous solutions by NaAlg-g-poly(acrylic acid-co-acryl amide)/clinoptilolite hydrogel nanocomposite. *Fibers Polym* 16:354–362. <https://doi.org/10.1007/s12221-015-0354-9>
49. Subhan H, Alam S, Shah LA et al (2021) Sodium alginate grafted poly(*N*-vinyl formamide-co-acrylic acid)-bentonite clay hybrid hydrogel for sorptive removal of methylene green from wastewater. *Colloids Surf A Physicochem Eng Asp* 611:125853. <https://doi.org/10.1016/j.col surfa.2020.125853>
50. Theng BKG (2012) Negatively charged polymers (Polyanions). *Dev Clay Sci* 4:111–127. <https://doi.org/10.1016/B978-0-444-53354-8.00004-9>
51. Laysandra L, Fabryanty R, Ju YH et al (2019) Renewable rarasaponin-bentonite-alginate composite with sponge-like structure and its application for crystal violet removal from aqueous solution. *Desalin Water Treat* 160:354–365. <https://doi.org/10.5004/dwt.2019.24196>

52. Singh V (2015) Mesoporous titania spheres derived from sodium alginate-gum acacia composite beads: efficient adsorbent for “Reactive blue H5G” dye. *J Environ Chem Eng* 3:2727–2737. <https://doi.org/10.1016/j.jece.2015.09.021>
53. Benhouria A, Islam MA, Zaghoulane-Boudiaf H et al (2015) Calcium alginate-bentonite-activated carbon composite beads as highly effective adsorbent for methylene blue. *Chem Eng J* 270:621–630. <https://doi.org/10.1016/j.cej.2015.02.030>
54. Boukhalfa N, Boutahala M, Djebri N, Idris A (2019) Kinetics, thermodynamics, equilibrium isotherms, and reusability studies of cationic dye adsorption by magnetic alginate/oxidized multiwalled carbon nanotubes composites. *Int J Biol Macromol* 123:539–548. <https://doi.org/10.1016/j.ijbiomac.2018.11.102>
55. Fabryanty R, Valencia C, Soetaredjo FE et al (2017) Removal of crystal violet dye by adsorption using bentonite–alginate composite. *J Environ Chem Eng* 5:5677–5687. <https://doi.org/10.1016/j.jece.2017.10.057>
56. Gomri F, Finqueneisel G, Zimny T et al (2018) Adsorption of Rhodamine 6G and humic acids on composite bentonite–alginate in single and binary systems. *Appl Water Sci* 8:1–10. <https://doi.org/10.1007/s13201-018-0823-6>
57. Kumar M, Tamilarasan R, Sivakumar V (2013) Adsorption of Victoria Blue by carbon/Ba/alginate beads: kinetics, thermodynamics and isotherm studies. *Carbohydr Polym* 98:505–513. <https://doi.org/10.1016/j.carbpol.2013.05.078>
58. Lai KC, Lee LY, Hiew BYZ et al (2020) Utilisation of eco-friendly and low cost 3D graphene-based composite for treatment of aqueous Reactive Black 5 dye: characterisation, adsorption mechanism and recyclability studies. *J Taiwan Inst Chem Eng* 114:57–66. <https://doi.org/10.1016/j.jtice.2020.09.024>
59. Oladipo AA, Gazi M (2016) Uptake of Ni²⁺ and rhodamine B by nano-hydroxyapatite/alginate composite beads: batch and continuous-flow systems. *Toxicol Environ Chem* 98:189–203. <https://doi.org/10.1080/02772248.2015.1115506>
60. Patanjali P, Mandal A, Chopra I, Singh R (2020) Adsorption of cationic dyes onto biopolymer-bentonite composites: kinetics and isotherm studies. *Int J Environ Anal Chem* 1–23. <https://doi.org/10.1080/03067319.2020.1849660>
61. Mallakpour S, Behranvand V, Mallakpour F (2021) Adsorptive performance of alginate/carbon nanotube-carbon dot-magnesium fluorohydroxyapatite hydrogel for methylene blue-contaminated water. *J Environ Chem Eng* 9:105170. <https://doi.org/10.1016/j.jece.2021.105170>
62. Oussalah A, Boukerroui A (2020) Removal of cationic dye using alginate–organobentonite composite beads. *Euro-Mediterranean J Environ Integr* 5:1–10. <https://doi.org/10.1007/s41207-020-00199-3>
63. Pei Y, Guo D, An Q et al (2018) Hydrogels with diffusion-facilitated porous network for improved adsorption performance. *Korean J Chem Eng* 35:2384–2393. <https://doi.org/10.1007/s11814-018-0181-y>
64. Qian LW, Yang MX, Zhang SF et al (2018) Preparation of a sustainable bioadsorbent by modifying filter paper with sodium alginate, with enhanced mechanical properties and good adsorption of methylene blue from wastewaters. *Cellulose* 25:2021–2036. <https://doi.org/10.1007/s10570-018-1674-x>
65. Shi J, Zhang H, Yu Y et al (2020) Adsorption properties of calcium alginate-silica dioxide hybrid adsorbent to methylene blue. *J Inorg Organomet Polym Mater* 30:2114–2125. <https://doi.org/10.1007/s10904-019-01357-z>
66. Wang W, Zhao Y, Bai H et al (2018) Methylene blue removal from water using the hydrogel beads of poly(vinyl alcohol)-sodium alginate-chitosan-montmorillonite. *Carbohydr Polym* 198:518–528. <https://doi.org/10.1016/j.carbpol.2018.06.124>
67. Elkady M, Hassan H (2015) Equilibrium and dynamic profiles of azo dye sorption onto innovative nano-zinc oxide biocomposite. *Curr Nanosci* 11:805–814. <https://doi.org/10.2174/1573413711666150415003115>
68. Elkady MF, Shokry Hassan H, El-Sayed EM (2015) Basic violet decolorization using alginate immobilized nanozirconium tungstovanadate matrix as cation exchanger. *J Chem.* <https://doi.org/10.1155/2015/385741>

69. Duraipandian J, Rengasamy T, Vadivelu S (2017) Experimental and modeling studies for the removal of crystal violet dye from aqueous solutions using eco-friendly *Gracilaria corticata* seaweed activated carbon/Zn/alginate polymeric composite beads. *J Polym Environ* 25:1062–1071. <https://doi.org/10.1007/s10924-016-0879-z>
70. Dinu MV, Lazar MM, Dragan ES (2017) Dual ionic cross-linked alginate/clinoptilolite composite microbeads with improved stability and enhanced sorption properties for methylene blue. *React Funct Polym* 116:31–40. <https://doi.org/10.1016/j.reactfunctpolym.2017.05.001>
71. Li Y, Du Q, Liu T et al (2013) Methylene blue adsorption on graphene oxide/calcium alginate composites. *Carbohydr Polym* 95:501–507. <https://doi.org/10.1016/j.carbpol.2013.01.094>
72. Pawar RR, Lalmunsiam GP et al (2018) Porous synthetic hectorite clay-alginate composite beads for effective adsorption of methylene blue dye from aqueous solution. *Int J Biol Macromol* 114:1315–1324. <https://doi.org/10.1016/j.ijbiomac.2018.04.008>
73. Wang Y, Li Y, Zhang X, Zheng H (2020) Removal of methylene blue from water by copper alginate/activated carbon aerogel: equilibrium, kinetic, and thermodynamic studies. *J Polym Environ* 28:200–210. <https://doi.org/10.1007/s10924-019-01577-x>
74. Wang B, Gao B, Wan Y (2019) Comparative study of calcium alginate, ball-milled biochar, and their composites on aqueous methylene blue adsorption. *Environ Sci Pollut Res* 26:11535–11541. <https://doi.org/10.1007/s11356-018-1497-1>
75. Yap PL, Hassan K, Auyoong YL et al (2020) All-in-one bioinspired multifunctional graphene biopolymer foam for simultaneous removal of multiple water pollutants. *Adv Mater Interfaces* 7:1–14. <https://doi.org/10.1002/admi.202000664>
76. Shan C, Wang L, Li Z et al (2019) Graphene oxide enhanced polyacrylamide-alginate aerogels catalysts. *Carbohydr Polym* 203:19–25. <https://doi.org/10.1016/j.carbpol.2018.09.024>
77. Sun Q, Fu CW, Aguila B et al (2018) Pore environment control and enhanced performance of enzymes infiltrated in covalent organic frameworks. *J Am Chem Soc* 140:984–992. <https://doi.org/10.1021/jacs.7b10642>
78. Yang M, Wang L, Cheng Y et al (2019) Light- and pH-responsive self-healing hydrogel. *J Mater Sci* 9983–9994. <https://doi.org/10.1007/s10853-019-03547-z>
79. Rinaudo M (2006) Chitin and chitosan: properties and applications. *Prog Polym Sci* 31:603–632. <https://doi.org/10.1016/j.progpolymsci.2006.06.001>
80. Roberts GAF (1992) Preparation of chitin and chitosan. *Chitin Chem* 54–84. https://doi.org/10.1007/978-1-349-11545-7_2
81. Kaczmarek MB, Struszczyk-Swita K, Li X et al (2019) Enzymatic modifications of chitin, chitosan, and chitooligosaccharides. *Front Bioeng Biotechnol* 7. <https://doi.org/10.3389/fbioe.2019.00243>
82. No HK, Meyers SP (1995) Preparation and characterization of chitin and chitosan—a review. *J Aquat Food Prod Technol* 4:27–52. https://doi.org/10.1300/J030v04n02_03
83. Yeul VS, Rayalu SS (2013) Unprecedented chitin and chitosan: a chemical overview. *J Polym Environ* 21:606–614. <https://doi.org/10.1007/s10924-012-0458-x>
84. Li B, Ren Z (2020) Superior adsorption of direct dye from aqueous solution by Y(III)-chitosan-doped fly ash composite as low-cost adsorbent. *J Polym Environ* 28:1811–1821. <https://doi.org/10.1007/s10924-020-01728-5>
85. Zhu T, Huang W, Zhang L et al (2017) Adsorption of Cr(VI) on cerium immobilized cross-linked chitosan composite in single system and coexisted with Orange II in binary system. *Int J Biol Macromol* 103:605–612. <https://doi.org/10.1016/j.ijbiomac.2017.05.051>
86. Hui M, Shengyan P, Yaqi H et al (2018) A highly efficient magnetic chitosan “fluid” adsorbent with a high capacity and fast adsorption kinetics for dyeing wastewater purification. *Chem Eng J* 345:556–565. <https://doi.org/10.1016/j.cej.2018.03.115>
87. Blachnio M, Budnyak TM, Derylo-Marczewska A et al (2018) Chitosan-silica hybrid composites for removal of sulfonated azo dyes from aqueous solutions. *Langmuir* 34:2258–2273. <https://doi.org/10.1021/acs.langmuir.7b04076>
88. Hongduo T, Liu Y, Li B et al (2020) Preparation of chitosan graft polyacrylic acid/graphite oxide composite and the study of its adsorption properties of cationic dyes. *Polym Sci Ser A* 62:272–283. <https://doi.org/10.1134/S0965545X20030141>

89. Wang L, Zhang J, Wang A (2011) Fast removal of methylene blue from aqueous solution by adsorption onto chitosan-g-poly (acrylic acid)/attapulgite composite. *Desalination* 266:33–39. <https://doi.org/10.1016/j.desal.2010.07.065>
90. Khapre MA, Jugade RM (2020) Hierarchical approach towards adsorptive removal of Alizarin Red S dye using native chitosan and its successively modified versions. *Water Sci Technol* 82:715–731. <https://doi.org/10.2166/wst.2020.376>
91. Chen B, Zhao H, Chen S et al (2019) A magnetically recyclable chitosan composite adsorbent functionalized with EDTA for simultaneous capture of anionic dye and heavy metals in complex wastewater. *Chem Eng J* 356:69–80. <https://doi.org/10.1016/j.cej.2018.08.222>
92. Elwakeel KZ, El-Bindary AA, Ismail A, Morshidy AM (2016) Sorptive removal of Remazol Brilliant Blue R from aqueous solution by diethylenetriamine functionalized magnetic macroreticular hybrid material. *RSC Adv* 6:22395–22410. <https://doi.org/10.1039/c5ra26508h>
93. Li K, Li P, Cai J et al (2016) Efficient adsorption of both methyl orange and chromium from their aqueous mixtures using a quaternary ammonium salt modified chitosan magnetic composite adsorbent. *Chemosphere* 154:310–318. <https://doi.org/10.1016/j.chemosphere.2016.03.100>
94. Marnani NN, Shahbazi A (2019) A novel environmental-friendly nanobiocomposite synthesis by EDTA and chitosan functionalized magnetic graphene oxide for high removal of Rhodamine B: adsorption mechanism and separation property. *Chemosphere* 218:715–725. <https://doi.org/10.1016/j.chemosphere.2018.11.109>
95. Pereira FAR, Sousa KS, Cavalcanti GRS et al (2017) Green biosorbents based on chitosan-montmorillonite beads for anionic dye removal. *J Environ Chem Eng* 5:3309–3318. <https://doi.org/10.1016/j.jece.2017.06.032>
96. Jabli M (2020) Synthesis, characterization, and assessment of cationic and anionic dye adsorption performance of functionalized silica immobilized chitosan bio-polymer. *Int J Biol Macromol* 153:305–316. <https://doi.org/10.1016/j.ijbiomac.2020.02.323>
97. Auta M, Hameed BH (2013) Coalesced chitosan activated carbon composite for batch and fixed-bed adsorption of cationic and anionic dyes. *Colloids Surf B Biointerfaces* 105:199–206. <https://doi.org/10.1016/j.colsurfb.2012.12.021>
98. Cao CY, Zhang T, Cong Q (2017) Adsorption of acid fuchsin onto the chitosan–montmorillonite composite. *Mar Georesources Geotechnol* 35:799–805. <https://doi.org/10.1080/1064119X.2016.1240277>
99. Sirajudheen P, Meenakshi S (2020) Lanthanum (III) incorporated chitosan-montmorillonite composite as flexible material for adsorptive removal of azo dyes from water. *Mater Today Proc* 27:318–326. <https://doi.org/10.1016/j.matpr.2019.11.040>
100. Budnyak TM, Błachnio M, Slabon A et al (2020) Chitosan deposited onto fumed silica surface as sustainable hybrid biosorbent for acid orange 8 dye capture: effect of temperature in adsorption equilibrium and kinetics. *J Phys Chem C* 124:15312–15323. <https://doi.org/10.1021/acs.jpcc.0c04205>
101. Akar ST, San E, Akar T (2016) Chitosan-alunite composite: an effective dye remover with high sorption, regeneration and application potential. *Carbohydr Polym* 143:318–326. <https://doi.org/10.1016/j.carbpol.2016.01.066>
102. Feng T, Xu L (2013) Adsorption of acid red onto chitosan/rectorite composites from aqueous solution. *RSC Adv* 3:21685–21690. <https://doi.org/10.1039/c3ra43384f>
103. Sirajudheen P, Karthikeyan P, Ramkumar K, Meenakshi S (2020) Effective removal of organic pollutants by adsorption onto chitosan supported graphene oxide-hydroxyapatite composite: a novel reusable adsorbent. *J Mol Liq* 318:114200. <https://doi.org/10.1016/j.molliq.2020.114200>
104. Sheshmani S, Mashhadi S (2018) Potential of magnetite reduced graphene oxide/chitosan nanocomposite as biosorbent for the removal of dyes from aqueous solutions. *Polym Compos* 39:E457–E462. <https://doi.org/10.1002/pc.24608>
105. Manatunga DC, De Silva RM, De Silva KMN, Ratnaweera R (2016) Natural polysaccharides leading to super adsorbent hydroxyapatite nanoparticles for the removal of heavy metals and dyes from aqueous solutions. *RSC Adv* 6:105618–105630. <https://doi.org/10.1039/c6ra22662k>

106. Dotto GL, Rodrigues FK, Tanabe EH et al (2016) Development of chitosan/bentonite hybrid composite to remove hazardous anionic and cationic dyes from colored effluents. *J Environ Chem Eng* 4:3230–3239. <https://doi.org/10.1016/j.jece.2016.07.004>
107. Jiang H, Chen P, Luo S et al (2013) Synthesis of novel biocompatible composite $\text{Fe}_3\text{O}_4/\text{ZrO}_2$ /chitosan and its application for dye removal. *J Inorg Organomet Polym Mater* 23:393–400. <https://doi.org/10.1007/s10904-012-9792-7>
108. Debnath S, Parashar K, Pillay K (2017) Ultrasound assisted adsorptive removal of hazardous dye Safranin O from aqueous solution using crosslinked graphene oxide-chitosan (GO-CH) composite and optimization by response surface methodology (RSM) approach. *Carbohydr Polym* 175:509–517. <https://doi.org/10.1016/j.carbpol.2017.07.088>
109. Ragab A, Ahmed I, Bader D (2019) The removal of Brilliant Green dye from aqueous solution using nano hydroxyapatite/chitosan composite as a sorbent. *Molecules* 24. <https://doi.org/10.3390/molecules24050847>
110. Kloster GA, Mosiewicki MA, Marcovich NE (2019) Chitosan/iron oxide nanocomposite films: effect of the composition and preparation methods on the adsorption of congo red. *Carbohydr Polym* 221:186–194. <https://doi.org/10.1016/j.carbpol.2019.05.089>
111. Kochkina NE, Skobeleva OA, Khokhlova YV (2017) Investigation of cationic starch/Na-montmorillonite bionanocomposite adsorbent prepared by vibration milling for acid dye removal. *Part Sci Technol* 35:259–264. <https://doi.org/10.1080/02726351.2016.1153546>
112. Wang J, Zhou Q, Song D et al (2015) Chitosan-silica composite aerogels: preparation, characterization and Congo red adsorption. *J Sol-Gel Sci Technol* 76:501–509. <https://doi.org/10.1007/s10971-015-3800-7>
113. Zheng L, Wang C, Shu Y et al (2015) Utilization of diatomite/chitosan-Fe (III) composite for the removal of anionic azo dyes from wastewater: equilibrium, kinetics and thermodynamics. *Colloids Surf A Physicochem Eng Asp* 468:129–139. <https://doi.org/10.1016/j.colsurfa.2014.12.015>
114. Vardikar HS, Bhanvase BA, Rathod AP, Sonawane SH (2018) Sonochemical synthesis, characterization and sorption study of Kaolin-Chitosan-TiO₂ ternary nanocomposite: advantage over conventional method. *Mater Chem Phys* 217:457–467. <https://doi.org/10.1016/j.matchem.2018.07.014>
115. Yan H, Li H, Yang H et al (2013) Removal of various cationic dyes from aqueous solutions using a kind of fully biodegradable magnetic composite microsphere. *Chem Eng J* 223:402–411. <https://doi.org/10.1016/j.cej.2013.02.113>
116. Kausar A, Naeem K, Tariq M et al (2019) Preparation and characterization of chitosan/clay composite for direct Rose FRN dye removal from aqueous media: comparison of linear and non-linear regression methods. *J Mater Res Technol* 8:1161–1174. <https://doi.org/10.1016/j.jmrt.2018.07.020>
117. Chen Y, Chen L, Bai H, Li L (2013) Graphene oxide-chitosan composite hydrogels as broad-spectrum adsorbents for water purification. *J Mater Chem A* 1:1992–2001. <https://doi.org/10.1039/c2ta00406b>
118. Joudi M, Nasserlah H, Hafdi H et al (2020) Synthesis of an efficient hydroxyapatite-chitosan-montmorillonite thin film for the adsorption of anionic and cationic dyes: adsorption isotherm, kinetic and thermodynamic study. *SN Appl Sci* 2:1–13. <https://doi.org/10.1007/s42452-020-2848-3>
119. Muinde VM, Onyari JM, Wamalwa B, Wabomba JN (2020) Adsorption of malachite green dye from aqueous solutions using mesoporous chitosan-zinc oxide composite material. *Environ Chem Ecotoxicol* 2:115–125. <https://doi.org/10.1016/j.enceco.2020.07.005>
120. Zhou Q, Gao Q, Luo W et al (2015) One-step synthesis of amino-functionalized attapulgite clay nanoparticles adsorbent by hydrothermal carbonization of chitosan for removal of methylene blue from wastewater. *Colloids Surf A Physicochem Eng Asp* 470:248–257. <https://doi.org/10.1016/j.colsurfa.2015.01.092>
121. Chen X, He L (2017) Microwave irradiation assisted preparation of chitosan composite microsphere for dye adsorption. *Int J Polym Sci*. <https://doi.org/10.1155/2017/2672597>

122. Haldorai Y, Kharismadewi D, Tuma D, Shim JJ (2015) Properties of chitosan/magnetite nanoparticles composites for efficient dye adsorption and antibacterial agent. *Korean J Chem Eng* 32:1688–1693. <https://doi.org/10.1007/s11814-014-0368-9>
123. Haldorai Y, Shim JJ (2014) An efficient removal of methyl orange dye from aqueous solution by adsorption onto chitosan/MgO composite: a novel reusable adsorbent. *Appl Surf Sci* 292:447–453. <https://doi.org/10.1016/j.apsusc.2013.11.158>
124. Jiang R, Fu Y-Q, Zhu H-Y et al (2012) Removal of methyl orange from aqueous solutions by magnetic maghemite/chitosan nanocomposite films: adsorption kinetics and equilibrium. *J Appl Polym Sci* 125:E540–E549. <https://doi.org/10.1002/app.37003>
125. Mahmoodian H, Moradi O, Shariatzadeha B et al (2015) Enhanced removal of methyl orange from aqueous solutions by poly HEMA-chitosan-MWCNT nano-composite. *J Mol Liq* 202:189–198. <https://doi.org/10.1016/j.molliq.2014.10.040>
126. Liu L, Ge J, Yang LT et al (2016) Facile preparation of chitosan enwrapping Fe₃O₄ nanoparticles and MIL-101(Cr) magnetic composites for enhanced methyl orange adsorption. *J Porous Mater* 23:1363–1372. <https://doi.org/10.1007/s10934-016-0195-y>
127. Ouyang A, Wang C, Wu S et al (2015) Highly porous core-shell structured graphene-chitosan beads. *ACS Appl Mater Interfaces* 7:14439–14445. <https://doi.org/10.1021/acsami.5b03369>
128. Yuvaraja G, Chen DY, Pathak JL et al (2020) Preparation of novel aminated chitosan Schiff's base derivative for the removal of methyl orange dye from aqueous environment and its biological applications. *Int J Biol Macromol* 146:1100–1110. <https://doi.org/10.1016/j.ijbiomac.2019.09.236>
129. Zhang J, Zhou Q, Ou L (2012) Kinetic, isotherm, and thermodynamic studies of the adsorption of methyl orange from aqueous solution by chitosan/alumina composite. *J Chem Eng Data* 57:412–419. <https://doi.org/10.1021/je2009945>
130. Zhao P, Zhang R, Wang J (2017) Adsorption of methyl orange from aqueous solution using chitosan/diatomite composite. *Water Sci Technol* 75:1633–1642. <https://doi.org/10.2166/wst.2017.034>
131. Auta M, Hameed BH (2014) Chitosan-clay composite as highly effective and low-cost adsorbent for batch and fixed-bed adsorption of methylene blue. *Chem Eng J* 237:352–361. <https://doi.org/10.1016/j.cej.2013.09.066>
132. Fan L, Luo C, Sun M et al (2012) Preparation of novel magnetic chitosan/graphene oxide composite as effective adsorbents toward methylene blue. *Bioresour Technol* 114:703–706. <https://doi.org/10.1016/j.biortech.2012.02.067>
133. Fan L, Luo C, Sun M et al (2013) Synthesis of magnetic β -cyclodextrin-chitosan/graphene oxide as nanoadsorbent and its application in dye adsorption and removal. *Colloids Surf B Biointerfaces* 103:601–607. <https://doi.org/10.1016/j.colsurfb.2012.11.023>
134. Hassan H, Salama A, El-ziaty AK, El-Sakhawy M (2019) New chitosan/silica/zinc oxide nanocomposite as adsorbent for dye removal. *Int J Biol Macromol* 131:520–526. <https://doi.org/10.1016/j.ijbiomac.2019.03.087>
135. Idohou EA, Fatombi JK, Osseni SA et al (2020) Preparation of activated carbon/chitosan/Carica papaya seeds composite for efficient adsorption of cationic dye from aqueous solution. *Surf Interfaces* 21:100741. <https://doi.org/10.1016/j.surfin.2020.100741>
136. Karaer H, Kaya I (2016) Synthesis, characterization of magnetic chitosan/active charcoal composite and using at the adsorption of methylene blue and reactive blue4. *Microporous Mesoporous Mater* 232:26–38. <https://doi.org/10.1016/j.micromeso.2016.06.006>
137. Li Q, Zhao Y, Wang L, Ai Qin W (2011) Adsorption characteristics of methylene blue onto the *N*-succinyl-chitosan-g-polyacrylamide/attapulgit composite. *Korean J Chem Eng* 28:1658–1664. <https://doi.org/10.1007/s11814-011-0037-1>
138. Liu Y, Zheng Y, Wang A (2010) Enhanced adsorption of Methylene Blue from aqueous solution by chitosan-g-poly (acrylic acid)/vermiculite hydrogel composites. *J Environ Sci* 22:486–493. [https://doi.org/10.1016/S1001-0742\(09\)60134-0](https://doi.org/10.1016/S1001-0742(09)60134-0)
139. Mokhtar A, Abdelkrim S, Djelad A et al (2020) Adsorption behavior of cationic and anionic dyes on magadiite-chitosan composite beads. *Carbohydr Polym* 229:115399. <https://doi.org/10.1016/j.carbpol.2019.115399>

140. Sabzevari M, Cree DE, Wilson LD (2018) Graphene oxide-chitosan composite material for treatment of a model dye effluent. *ACS Omega* 3:13045–13054. <https://doi.org/10.1021/acs.omega.8b01871>
141. Vieira T, Artifon SES, Cesco CT et al (2021) Chitosan-based hydrogels for the sorption of metals and dyes in water: isothermal, kinetic, and thermodynamic evaluations. *Colloid Polym Sci* 299:649–662. <https://doi.org/10.1007/s00396-020-04786-2>
142. Zhou Y, Gao B, Zimmerman AR et al (2014) Biochar-supported zerovalent iron for removal of various contaminants from aqueous solutions. *Bioresour Technol* 152:538–542. <https://doi.org/10.1016/j.biortech.2013.11.021>
143. El-Zawahry MM, Abdelghaffar F, Abdelghaffar RA, Hassabo AG (2016) Equilibrium and kinetic models on the adsorption of Reactive Black 5 from aqueous solution using Eichhornia crassipes/chitosan composite. *Carbohydr Polym* 136:507–515. <https://doi.org/10.1016/j.carbpol.2015.09.071>
144. Li J, Cai J, Zhong L et al (2018) Adsorption of reactive dyes onto chitosan/montmorillonite intercalated composite: multi-response optimization, kinetic, isotherm and thermodynamic study. *Water Sci Technol* 77:2598–2612. <https://doi.org/10.2166/wst.2018.221>
145. Li L, Iqbal J, Zhu Y et al (2018) Chitosan/Ag-hydroxyapatite nanocomposite beads as a potential adsorbent for the efficient removal of toxic aquatic pollutants. *Int J Biol Macromol* 120:1752–1759. <https://doi.org/10.1016/j.ijbiomac.2018.09.190>
146. Parsaeian MR, Dadfarnia S, Haji Shabani AM, Hafezi Moghaddam R (2020) Green synthesis of a high capacity magnetic polymer nanocomposite sorbent based on the natural products for removal of Reactive Black 5. *Int J Environ Anal Chem* 1–15. <https://doi.org/10.1080/03067319.2020.1748612>
147. Travlou NA, Kyzas GZ, Lazaridis NK, Deliyanni EA (2013) Graphite oxide/chitosan composite for reactive dye removal. *Chem Eng J* 217:256–265. <https://doi.org/10.1016/j.cej.2012.12.008>
148. Travlou NA, Kyzas GZ, Lazaridis NK, Deliyanni EA (2013) Functionalization of graphite oxide with magnetic chitosan for the preparation of a nanocomposite dye adsorbent. *Langmuir* 29:1657–1668. <https://doi.org/10.1021/la304696y>
149. Elwakeel KZ, El-Bindary AA, Ismail A, Morshidy AM (2017) Magnetic chitosan grafted with polymerized thiourea for remazol brilliant blue R recovery: effects of uptake conditions. *J Dispers Sci Technol* 38:943–952. <https://doi.org/10.1080/01932691.2016.1216436>
150. Jawad AH, Abdulhameed AS, Malek NNA, ALOthman ZA (2020) Statistical optimization and modeling for color removal and COD reduction of reactive blue 19 dye by mesoporous chitosan-epichlorohydrin/kaolin clay composite. *Int J Biol Macromol* 164:4218–4230. <https://doi.org/10.1016/j.ijbiomac.2020.08.201>
151. Jawad AH, Abdulhameed AS (2020) Facile synthesis of crosslinked chitosan-tripolyphosphate/kaolin clay composite for decolorization and COD reduction of remazol brilliant blue R dye: optimization by using response surface methodology. *Colloids Surf A Physicochem Eng Asp* 605:125329. <https://doi.org/10.1016/j.colsurfa.2020.125329>
152. Mohamadi MB, Ejazi H, Azadbakht F (2019) Using composite chitosan-graphene oxide to eliminate reactive blue 19 from water solutions: the study of adsorption kinetics and reaction thermodynamics. *Desalin Water Treat* 155:341–349. <https://doi.org/10.5004/dwt.2019.23816>
153. Jawad AH, Malek NNA, Abdulhameed AS, Razuan R (2020) Synthesis of magnetic chitosan-fly ash/Fe₃O₄ composite for adsorption of reactive orange 16 dye: optimization by Box-Behnken design. *J Polym Environ* 28:1068–1082. <https://doi.org/10.1007/s10924-020-01669-z>
154. Abdulhameed AS, Jawad AH, Mohammad AKT (2019) Synthesis of chitosan-ethylene glycol diglycidyl ether/TiO₂ nanoparticles for adsorption of reactive orange 16 dye using a response surface methodology approach. *Bioresour Technol* 293:122071. <https://doi.org/10.1016/j.biortech.2019.122071>
155. Li J, Cai J, Zhong L et al (2019) Adsorption of reactive red 136 onto chitosan/montmorillonite intercalated composite from aqueous solution. *Appl Clay Sci* 167:9–22. <https://doi.org/10.1016/j.clay.2018.10.003>

156. Theng BKG (2012) Positively charged polymers (Polycations). *Dev Clay Sci* 4:129–151. <https://doi.org/10.1016/B978-0-444-53354-8.00005-0>
157. Rathinam K, Singh SP, Arnusch CJ, Kasher R (2018) An environmentally-friendly chitosan-lysozyme biocomposite for the effective removal of dyes and heavy metals from aqueous solutions. *Carbohydr Polym* 199:506–515. <https://doi.org/10.1016/j.carbpol.2018.07.055>
158. French AD (2017) Glucose, not cellobiose, is the repeating unit of cellulose and why that is important. *Cellulose* 24:4605–4609. <https://doi.org/10.1007/s10570-017-1450-3>
159. Krässig H, Schurz J, Steadman RG et al (2004) Cellulose. In: Ullmann's encyclopedia of industrial chemistry. Wiley. http://doi.org/10.1002/14356007.a05_375.pub2
160. Medronho B, Romano A, Miguel MG et al (2012) Rationalizing cellulose (in)solubility: reviewing basic physicochemical aspects and role of hydrophobic interactions. *Cellulose* 19:581–587. <https://doi.org/10.1007/s10570-011-9644-6>
161. Thielking H, Schmidt M (2006) Cellulose ethers. Ullmann's encyclopedia of industrial chemistry. Wiley-VCH Verlag GmbH & Co. KGaA, Weinheim, Germany, pp 1–2
162. Tundisi LL, Mostaço GB, Carricondo PC, Petri DFS (2021) Hydroxypropyl methylcellulose: physicochemical properties and ocular drug delivery formulations. *Eur J Pharm Sci* 159:105736. <https://doi.org/10.1016/j.ejps.2021.105736>
163. Huang T, Shao YW, Zhang Q et al (2019) Chitosan-cross-linked graphene oxide/carboxymethyl cellulose aerogel globules with high structure stability in liquid and extremely high adsorption ability. *ACS Sustain Chem Eng* 7:8775–8788. <https://doi.org/10.1021/acssuschemeng.9b00691>
164. Liu Y, Wang W, Jin Y, Wang A (2011) Adsorption behavior of methylene blue from aqueous solution by the hydrogel composites based on attapulgite. *Sep Sci Technol* 46:858–868. <https://doi.org/10.1080/01496395.2010.528502>
165. Malatji N, Makhado E, Ramohlola KE et al (2020) Synthesis and characterization of magnetic clay-based carboxymethyl cellulose-acrylic acid hydrogel nanocomposite for methylene blue dye removal from aqueous solution. *Environ Sci Pollut Res* 27:44089–44105. <https://doi.org/10.1007/s11356-020-10166-8>
166. Peng N, Hu D, Zeng J et al (2016) Superabsorbent cellulose-clay nanocomposite hydrogels for highly efficient removal of dye in water. *ACS Sustain Chem Eng* 4:7217–7224. <https://doi.org/10.1021/acssuschemeng.6b02178>
167. Biswas S, Mohapatra SS, Kumar U et al (2020) Batch and continuous closed circuit semi-fluidized bed operation: removal of MB dye using sugarcane bagasse biochar and alginate composite adsorbents. *J Environ Chem Eng* 8:103637. <https://doi.org/10.1016/j.jece.2019.103637>
168. Chen X, Song X, Sun Y (2016) Attapulgite nanofiber-cellulose nanocomposite with core-shell structure for dye adsorption. *Int J Polym Sci* 2016:1–9. <https://doi.org/10.1155/2016/2081734>
169. Liu C, Omer AM, Ouyang XK (2018) Adsorptive removal of cationic methylene blue dye using carboxymethyl cellulose/k-carrageenan/activated montmorillonite composite beads: isotherm and kinetic studies. *Int J Biol Macromol* 106:823–833. <https://doi.org/10.1016/j.ijbiomac.2017.08.084>
170. Nayl AA, Abd-Elhamid AI, Abu-Saied MA et al (2020) A novel method for highly effective removal and determination of binary cationic dyes in aqueous media using a cotton-graphene oxide composite. *RSC Adv* 10:7791–7802. <https://doi.org/10.1039/c9ra09872k>
171. Ren F, Li Z, Tan WZ et al (2018) Facile preparation of 3D regenerated cellulose/graphene oxide composite aerogel with high-efficiency adsorption towards methylene blue. *J Colloid Interface Sci* 532:58–67. <https://doi.org/10.1016/j.jcis.2018.07.101>
172. Somsesta N, Sricharoenchaikul V, Aht-Ong D (2020) Adsorption removal of methylene blue onto activated carbon/cellulose biocomposite films: equilibrium and kinetic studies. *Mater Chem Phys* 240:122221. <https://doi.org/10.1016/j.matchemphys.2019.122221>
173. Ghiorghita C-A, Bucatariu F, Dragan ES (2018) Novel silica/polyelectrolyte multilayer core-shell composite microparticles with. *Cellul Chem Technol* 52:663–672. Available at [https://www.cellulosechemtechnol.ro/pdf/CCT7-8\(2018\)p.663-672.pdf](https://www.cellulosechemtechnol.ro/pdf/CCT7-8(2018)p.663-672.pdf)

174. Dai H, Huang Y, Huang H (2018) Eco-friendly polyvinyl alcohol/carboxymethyl cellulose hydrogels reinforced with graphene oxide and bentonite for enhanced adsorption of methylene blue. *Carbohydr Polym* 185:1–11. <https://doi.org/10.1016/j.carbpol.2017.12.073>
175. Eltaweil AS, Elgarhy GS, El-Subruiti GM, Omer AM (2020) Carboxymethyl cellulose/carboxylated graphene oxide composite microbeads for efficient adsorption of cationic methylene blue dye. *Int J Biol Macromol* 154:307–318. <https://doi.org/10.1016/j.ijbiomac.2020.03.122>
176. Liu J, Chu H, Wei H et al (2016) Facile fabrication of carboxymethyl cellulose sodium/graphene oxide hydrogel microparticles for water purification. *RSC Adv* 6:50061–50069. <https://doi.org/10.1039/c6ra06438h>
177. Peng S, Liu Y, Xue Z et al (2017) Modified nanoporous magnetic cellulose–chitosan microspheres for efficient removal of Pb(II) and methylene blue from aqueous solution. *Cellulose* 24:4793–4806. <https://doi.org/10.1007/s10570-017-1463-y>
178. Chen L, Li Y, Hu S et al (2016) Removal of methylene blue from water by cellulose/graphene oxide fibres. *J Exp Nanosci* 11:1156–1170. <https://doi.org/10.1080/17458080.2016.1198499>
179. Hu Y, Chen C, Yang L et al (2019) Handy purifier based on bacterial cellulose and Camontmorillonite composites for efficient removal of dyes and antibiotics. *Carbohydr Polym* 222:115017. <https://doi.org/10.1016/j.carbpol.2019.115017>
180. Wang S, Ma X, Zheng P (2019c) Sulfo-functional 3D porous cellulose/graphene oxide composites for highly efficient removal of methylene blue and tetracycline from water. *Int J Biol Macromol* 140:119–128. <https://doi.org/10.1016/j.ijbiomac.2019.08.111>
181. Li B, Zhang Q, Pan Y et al (2020) Functionalized porous magnetic cellulose/Fe₃O₄ beads prepared from ionic liquid for removal of dyes from aqueous solution. *Int J Biol Macromol* 163:309–316. <https://doi.org/10.1016/j.ijbiomac.2020.06.280>
182. Sirajudheen P, Nikitha MR, Karthikeyan P, Meenakshi S (2020) Perceptive removal of toxic azo dyes from water using magnetic Fe₃O₄ reinforced graphene oxide–carboxymethyl cellulose recyclable composite: adsorption investigation of parametric studies and their mechanisms. *Surf Interfaces* 21:100648. <https://doi.org/10.1016/j.surfin.2020.100648>
183. Leshaf A, Ziani Cherif H, Benmansour K (2019) Adsorption of acidol red 2BE-NW dye from aqueous solutions on carboxymethyl cellulose/organo-bentonite composite: characterization, kinetic and thermodynamic studies. *J Polym Environ* 27:1054–1064. <https://doi.org/10.1007/s10924-019-01395-1>
184. Zhou C-H, Zhang D, Tong D-S et al (2012) Paper-like composites of cellulose acetate–organo-montmorillonite for removal of hazardous anionic dye in water. *Chem Eng J* 209:223–234. <https://doi.org/10.1016/j.cej.2012.07.107>
185. Rahimi K, Mirzaei R, Akbari A, Mirghaffari N (2018) Preparation of nanoparticle-modified polymeric adsorbent using wastage fuzzes of mechanized carpet and its application in dye removal from aqueous solution. *J Clean Prod* 178:373–383. <https://doi.org/10.1016/j.jclepro.2017.12.213>
186. Chen X, Cui J, Xu X et al (2020) Bacterial cellulose/attapulgitic magnetic composites as an efficient adsorbent for heavy metal ions and dye treatment. *Carbohydr Polym* 229:115512. <https://doi.org/10.1016/j.carbpol.2019.115512>
187. Sankaramakrishnan N, Singh N, Srivastava I (2020) Hierarchical nano Fe(0)@FeS doped cellulose nanofibres derived from agrowaste—potential bionanocomposite for treatment of organic dyes. *Int J Biol Macromol* 151:713–722. <https://doi.org/10.1016/j.ijbiomac.2020.02.155>
188. Santoso SP, Kurniawan A, Soetaredjo FE et al (2019) Eco-friendly cellulose–bentonite porous composite hydrogels for adsorptive removal of azo dye and soilless culture. *Cellulose* 26:3339–3358. <https://doi.org/10.1007/s10570-019-02314-2>
189. Tanzifi M, Tavakkoli Yarak M, Karami M et al (2018) Modelling of dye adsorption from aqueous solution on polyaniline/carboxymethyl cellulose/TiO₂ nanocomposites. *J Colloid Interface Sci* 519:154–173. <https://doi.org/10.1016/j.jcis.2018.02.059>
190. Wang M, Wang L, Wang A (2013) Characterization and Congo Red uptake capacity of a new lignocellulose/organic montmorillonite composite. *Desalin Water Treat* 51:7120–7129. <https://doi.org/10.1080/19443994.2013.791782>

191. ZabihSahebi A, Koushkbaghi S, Pishnamazi M et al (2019) Synthesis of cellulose acetate/chitosan/SWCNT/Fe₃O₄/TiO₂ composite nanofibers for the removal of Cr(VI), As(V), methylene blue and Congo red from aqueous solutions. *Int J Biol Macromol* 140:1296–1304. <https://doi.org/10.1016/j.ijbiomac.2019.08.214>
192. Zhu HY, Fu YQ, Jiang R et al (2011) Adsorption removal of congo red onto magnetic cellulose/Fe₃O₄/activated carbon composite: equilibrium, kinetic and thermodynamic studies. *Chem Eng J* 173:494–502. <https://doi.org/10.1016/j.cej.2011.08.020>
193. Kausar A, Shahzad R, Iqbal J et al (2020) Development of new organic-inorganic, hybrid bionanocomposite from cellulose and clay for enhanced removal of Dimarine Yellow HF-3GL dye. *Int J Biol Macromol* 149:1059–1071. <https://doi.org/10.1016/j.ijbiomac.2020.02.012>
194. Peighambardoust SJ, Aghamohammadi-Bavil O, Foroutan R, Arsalani N (2020) Removal of malachite green using carboxymethyl cellulose-g-polyacrylamide/montmorillonite nanocomposite hydrogel. *Int J Biol Macromol* 159:1122–1131. <https://doi.org/10.1016/j.ijbiomac.2020.05.093>
195. Radoor S, Karayil J, Jayakumar A et al (2021) An efficient removal of malachite green dye from aqueous environment using ZSM-5 zeolite/polyvinyl alcohol/carboxymethyl cellulose/sodium alginate bio composite. *J Polym Environ*. <https://doi.org/10.1007/s10924-020-02024-y>
196. Ali SM (2018) Fabrication of a nanocomposite from an agricultural waste and its application as a biosorbent for organic pollutants. *Int J Environ Sci Technol* 15:1169–1178. <https://doi.org/10.1007/s13762-017-1477-x>
197. Bai Q, Xiong Q, Li C et al (2017) Hierarchical porous cellulose/activated carbon composite monolith for efficient adsorption of dyes. *Cellulose* 24:4275–4289. <https://doi.org/10.1007/s10570-017-1410-y>
198. Liu Z, Li D, Dai H, Huang H (2017) Enhanced properties of tea residue cellulose hydrogels by addition of graphene oxide. *J Mol Liq* 244:110–116. <https://doi.org/10.1016/j.molliq.2017.08.106>
199. Luo J, Ma X, Zhou X, Xu Y (2021) Construction of physically crosslinked cellulose nanofibrils/alkali lignin/montmorillonite/polyvinyl alcohol network hydrogel and its application in methylene blue removal. *Cellulose* 1. <https://doi.org/10.1007/s10570-021-03847-1>
200. Samadder R, Akter N, Roy AC et al (2020) Magnetic nanocomposite based on polyacrylic acid and carboxylated cellulose nanocrystal for the removal of cationic dye. *RSC Adv* 10:11945–11956. <https://doi.org/10.1039/d0ra00604a>
201. Shi H, Li W, Zhong L, Xu C (2014) Methylene blue adsorption from aqueous solution by magnetic cellulose/graphene oxide composite: equilibrium, kinetics, and thermodynamics. *Ind Eng Chem Res* 53:1108–1118. <https://doi.org/10.1021/ie4027154>
202. Wang S, Ma X, Zheng P (2019) Sulfo-functional 3D porous cellulose/graphene oxide composites for highly efficient removal of methylene blue and tetracycline from water. *Int J Biol Macromol* 140:119–128. <https://doi.org/10.1016/j.ijbiomac.2019.08.111>
203. Wang Z, Song L, Wang Y et al (2021) Construction of a hybrid graphene oxide/nanofibrillated cellulose aerogel used for the efficient removal of methylene blue and tetracycline. *J Phys Chem Solids* 150:109839. <https://doi.org/10.1016/j.jpcs.2020.109839>
204. Huang X, Zhan X, Wen C et al (2018) Amino-functionalized magnetic bacterial cellulose/activated carbon composite for Pb²⁺ and methyl orange sorption from aqueous solution. *J Mater Sci Technol* 34:855–863. <https://doi.org/10.1016/j.jmst.2017.03.013>
205. Li W, Zuo P, Xu D et al (2017) Tunable adsorption properties of bentonite/carboxymethyl cellulose-g-poly(2-(dimethylamino) ethyl methacrylate) composites toward anionic dyes. *Chem Eng Res Des* 124:260–270. <https://doi.org/10.1016/j.cherd.2017.06.034>
206. Karadağ E, Yel B, Kundakçı S, Üzümlü ÖB (2017) Synthesis and application of acrylamide/sodium vinylsulfonate/carboxymethyl cellulose/zeolite hybrid hydrogels as highly swollen effective adsorbents for model cationic dye removal. *Desalin Water Treat* 74:402–414. <https://doi.org/10.5004/dwt.2017.20613>

207. Kausar A, Shahzad R, Asim S et al (2021) Experimental and theoretical studies of Rhodamine B direct dye sorption onto clay-cellulose composite. *J Mol Liq* 328:115165. <https://doi.org/10.1016/j.molliq.2020.115165>
208. Tian S-Y, Guo J-H, Zhao C et al (2018) Preparation of cellulose/graphene oxide composite membranes and their application in removing organic contaminants in wastewater. *J Nanosci Nanotechnol* 19:2147–2153. <https://doi.org/10.1166/jnn.2019.15808>
209. Xiang C, Wang C, Guo R et al (2019) Synthesis of carboxymethyl cellulose-reduced graphene oxide aerogel for efficient removal of organic liquids and dyes. *J Mater Sci* 54:1872–1883. <https://doi.org/10.1007/s10853-018-2900-5>
210. Toledo PVO, Martins BF, Pirich CL, Sierakowski MR, Teixeira Neto E, Petri DFS (2019) Cellulose based cryogels as adsorbents for organic pollutants. *Macromol Symp* 383:1800013. <https://doi.org/10.1002/masy.201800013>
211. Pérez S, Bertoft E (2010) The molecular structures of starch components and their contribution to the architecture of starch granules: a comprehensive review. *Starch Stärke* 62:389–420. <https://doi.org/10.1002/star.201000013>
212. Bhattacharyya A, Banerjee B, Ghorai S et al (2018) Development of an auto-phase separable and reusable graphene oxide-potato starch based cross-linked bio-composite adsorbent for removal of methylene blue dye. *Int J Biol Macromol* 116:1037–1048. <https://doi.org/10.1016/j.ijbiomac.2018.05.069>
213. Hosseinzadeh H, Ramin S (2018) Fabrication of starch-graft-poly(acrylamide)/graphene oxide/hydroxyapatite nanocomposite hydrogel adsorbent for removal of malachite green dye from aqueous solution. *Int J Biol Macromol* 106:101–115. <https://doi.org/10.1016/j.ijbiomac.2017.07.182>
214. Bakhshi H, Darvishi A (2016) Preparation and evaluation of hydrogel composites based on starch-g-PNaMA/eggshell particles as dye biosorbent. *Desalin Water Treat* 57:18144–18156. <https://doi.org/10.1080/19443994.2015.1087344>
215. Mittal H, Ray SS (2016) A study on the adsorption of methylene blue onto gum ghatti/TiO₂ nanoparticles-based hydrogel nanocomposite. *Int J Biol Macromol* 88:66–80. <https://doi.org/10.1016/j.ijbiomac.2016.03.032>
216. Karadağ E, Hasgül B, Kundakci S, Üzüüm ÖB (2014) A study of polymer/clay hybrid composite sorbent-based AAm/SMA hydrogels and semi-IPNs composed of κ -carrageenan and montmorillonite for water and dye sorption. *Adv Polym Technol* 33. <http://doi.org/10.1002/adv.21432>
217. Mahdavinia GR, Rahmani Z, Mosallanezhad A et al (2016) Effect of magnetic laponite RD on swelling and dye adsorption behaviors of κ -carrageenan-based nanocomposite hydrogels. *Desalin Water Treat* 57:20582–20596. <https://doi.org/10.1080/19443994.2015.1111808>
218. Mittal H, Al Alili A, Alhassan SM (2020) High efficiency removal of methylene blue dye using κ -carrageenan-poly(acrylamide-co-methacrylic acid)/AQSOA-Z05 zeolite hydrogel composites. *Cellulose* 27:8269–8285. <https://doi.org/10.1007/s10570-020-03365-6>
219. Pourjavadi A, Bassampour Z, Ghasemzadeh H et al (2016) Porous Carrageenan-g-polyacrylamide/bentonite superabsorbent composites: swelling and dye adsorption behavior. *J Polym Res* 23:1–10. <https://doi.org/10.1007/s10965-016-0955-z>
220. Li K, Lei Y, Liao J, Zhang Y (2021) A facile synthesis of graphene oxide/locust bean gum hybrid aerogel for water purification. *Carbohydr Polym* 254:117318. <https://doi.org/10.1016/j.carbpol.2020.117318>
221. Nestic AR, Velickovic SJ, Antonovic DG (2014) Novel composite films based on amidated pectin for cationic dye adsorption. *Colloids Surf B Biointerfaces* 116:620–626. <https://doi.org/10.1016/j.colsurfb.2013.10.031>
222. Qi X, Zeng Q, Tong X et al (2021) Polydopamine/montmorillonite-embedded pullulan hydrogels as efficient adsorbents for removing crystal violet. *J Hazard Mater* 402:123359. <https://doi.org/10.1016/j.jhazmat.2020.123359>
223. Saberi A, Alipour E, Sadeghi M (2019) Superabsorbent magnetic Fe₃O₄-based starch-poly(acrylic acid) nanocomposite hydrogel for efficient removal of dyes and heavy metal ions from water. *J Polym Res* 26. <https://doi.org/10.1007/s10965-019-1917-z>

224. Xing G, Liu S, Xu Q, Liu Q (2012) Preparation and adsorption behavior for brilliant blue X-BR of the cost-effective cationic starch intercalated clay composite matrix. *Carbohydr Polym* 87:1447–1452. <https://doi.org/10.1016/j.carbpol.2011.09.038>
225. Karadağ E, Hasgül B, Kundakci S, Üzüüm ÖB (2014) Novel composite sorbent AAm/MA hydrogels containing starch and kaolin for water sorption and dye uptake. *Bull Mater Sci* 37:1637–1646. <https://doi.org/10.1007/s12034-014-0723-9>
226. Ansari Mojarad A, Tamjidi S, Esmaili H (2020) Clay/starch/Fe₃O₄ nanocomposite as an efficient adsorbent for the removal of methyl violet dye from aqueous media. *Int J Environ Anal Chem* 1–22. <https://doi.org/10.1080/03067319.2020.1845665>
227. Karadağ E, Ödemiş H, Kundakçi S, Üzüüm ÖB (2016) Swelling characterization of acrylamide/zinc acrylate/xanthan gum/sepiolite hybrid hydrogels and its application in sorption of Janus Green B from aqueous solutions. *Adv Polym Technol* 35:248–259. <https://doi.org/10.1002/adv.21547>
228. Makhado E, Pandey S, Ramontja J (2018) Microwave assisted synthesis of xanthan gum-cl-poly (acrylic acid) based-reduced graphene oxide hydrogel composite for adsorption of methylene blue and methyl violet from aqueous solution. *Int J Biol Macromol* 119:255–269. <https://doi.org/10.1016/j.ijbiomac.2018.07.104>
229. Thakur S, Pandey S, Arotiba OA (2017) Sol-gel derived xanthan gum/silica nanocomposite—a highly efficient cationic dyes adsorbent in aqueous system. *Int J Biol Macromol* 103:596–604. <https://doi.org/10.1016/j.ijbiomac.2017.05.087>
230. Jamee R, Siddique R (2019) Biodegradation of synthetic dyes of textile effluent by microorganisms: an environmentally and economically sustainable approach. *Eur J Microbiol Immunol* 9:114–118. <https://doi.org/10.1556/1886.2019.00018>
231. Jadhav I, Vasniwal R, Shrivastava D, Jadhav K (2016) Microorganism-based treatment of azo dyes. *J Environ Sci Technol* 9:188–197. <https://doi.org/10.3923/jest.2016.188.197>
232. Yusuf M, Shabbir M, Mohammad F (2017) Natural colorants: historical, processing and sustainable prospects. *Nat Products Bioprospect* 7:123–145. <https://doi.org/10.1007/s13659-017-0119-9>
233. Freitas-Dörr BC, Machado CO, Pinheiro AC et al (2020) A metal-free blue chromophore derived from plant pigments. *Sci Adv* 6:eaz0421. <http://doi.org/10.1126/sciadv.aaz0421>

Application of Agricultural Wastes for Cationic Dyes Removal from Wastewater



Abdullahi Haruna Birniwa, Abdulsalam Salisu Abubakar, Habibun Nabi Muhammad Ekramul Mahmud, Shamsul Rahman Mohamed Kutty, Ahmad Hussaini Jagaba, Shehu Sa'ad Abdullahi, and Zakariyya Uba Zango

1 Introduction

As the population grew, so did the demand for textiles, resulting in an increase in textile waste, textiles are the materials used for human being, and its the second most essential requirement for life and protection from the elements. However, as the world's population grows, so does the demand for textiles, resulting in a rise in textile waste. The planet now faces a major problem of sustainable textile waste management due to the linear way that textile systems operate. Pre-consumer and

A. H. Birniwa (✉)

Department of Chemistry, Sule Lamido University Kafin Hausa, Kafin-Hausa, Jigawa State, Nigeria

e-mail: birniwa01@gmail.com

H. N. M. E. Mahmud

Department of Chemistry, University Malaya, Kuala Lumpur, Malaysia

e-mail: ekramul@um.edu.my

A. S. Abubakar

Department of Pure and Industrial Chemistry, Bayero University Kano, Kano, Nigeria

S. R. M. Kutty · A. H. Jagaba

Department of Civil and Environmental Engineering, Universiti Teknologi PETRONAS, Bandar Seri Iskandar, Perak Darul Ridzuan, Malaysia

A. H. Jagaba

Department of Civil Engineering, Abubakar Tafawa Balewa University, Bauchi, Nigeria

S. S. Abdullahi

Department of Polymer Technology, Hussaini Adamu Federal Polytechnic Kazaure, Kazaure, Jigawa State, Nigeria

School of Chemical Sciences, Universiti Sains Malaysia, USM Pulau Pinang, Gelugor, Malaysia

Z. U. Zango

Department of Chemistry, Al-Qalam University Katsina, Katsina, Katsina State, Nigeria

© The Author(s), under exclusive license to Springer Nature Singapore Pte Ltd. 2022

239

S. S. Muthu and A. Khadir (eds.), *Textile Wastewater Treatment*, Sustainable Textiles:

Production, Processing, Manufacturing & Chemistry,

https://doi.org/10.1007/978-981-19-2832-1_9

post-consumer clothing wastes are divided into two categories, Pre-consumer wastes are those produced during textile processing, while post-consumer wastes are those that have outlived their usefulness [1, 2]. Colored compounds that are chemically bound to a substrate are known as dyes, As a result, the desired color is transferred to the substance, and the chemical bond strength is increased (fastness). Dyes are non-biodegradable and resistance to certain chemical reagents, oxidizing agents, and heat due to their chemical composition [3]. Decolorizing effluents after they have been introduced into the marine system is a major undertaking. The use of a mordant can improve the dye's consistency with the substrate, pigments can also be used as dyeing agents, pigments, on the other hand, bind to each other by physical adsorption, mechanical retention, or the forming of covalent bonds [1, 2]. Organic dye molecules are made up of extraordinary delocalized electronic structures of conjugate double bonds chemistry. Toxic dyes, such as acidic and basic dyes, can be present in industrial wastewater [3], radioactive dyes released into the atmosphere by the clothing, dyestuffs, leather, paper, foodstuffs, cosmetics, rubber, plastics, and paint industries pose a health risk to humans [4, 5]. Textiles require a significant amount of water and are polluted by dangerous poisonous substances such as inorganic compounds, synthetic fibers are used in phases, colourings of fabric dyeing are referred to as dyestuffs, salt is a suitable standard of salt that improves the affinity of dye molecules. In today's dyeing methods, gross dyestuff remains unfixed at a rate of 280 kilotons per year, 90% of fabric dyeing colorants have an LD50 value. (lethal dosage, 50%) of less than 2000 mg/kg according to a survey conducted by "Ecological and Toxicological Association of the Dyestuffs Manufacturing Industry" [6–9]. Because of the constant use of water by clothing, paint, rubber, chemical, medicinal, and urban wastewater companies, environmental scientists have encountered problems on a global scale, organic dye contamination of water supply poses a serious danger to the environment [10–13]. Industrial wastes that are often associated with wastewater treatment schemes are liquid wastes, value-added components such as ingredients feedstock, cleaning and washing agents, by-products, plasticizers, and solvents, may also be used in dissolved or dispersed forms in industrial effluents, velocity and flow volume, environmental conditions, toxic and chemical elements, and microbiological material are all characteristics of effluents [14–17]. The dye molecules in the water pose a serious threat to the atmosphere, including carcinogenic potential, mutagenicity, and kidney, liver, brain, and human reproductive system malfunction, about 10,000 various varieties of marketable coloring agent, with an average output of thousands of tones (700,000), are released into the river and sea sources lacking being properly handled, it also has a significant impact on photosynthetic behavior in marine plants by reducing sunlight delivery through water and disrupting the metabolic process of living things [13, 14, 18–23].

Dye molecules are transported from the wastewater to a solid region during the adsorption process, and can then be regenerated for further use. Synthetic sorbents for dye removal are more expensive, and they necessitate a separate procedure for waste treatment and disposal. Agro-wastes (that includes plant, microbes and animal biomass), on the other hand, are a viable choice of converting waste to wealth for the adsorption of dyestuff in wastewater [13].

Dye-contaminated wastewater is treated using a variety of approaches (biological, chemical, and physical) [13, 14, 24–27], ion exchange, adsorption, membrane phase (ultrafiltration, microfiltration, nano-filtration, and reverse osmosis), precipitation and flocculation-coagulation are all part of the physical system (electrocoagulation) chemical coagulation, fenton oxidation, ozonation, membrane processes, and adsorption are the most popular approaches for removing dyes from wastewater [4, 5, 28]. Irradiation and the oxidative mechanism are two biological processes (oxidative process with sodium hypochlorite, hydrogen peroxide, photo, ozonation electrochemical and oxidation process process). Fungal decolorization, microbe depletion, algae decolorization, Biological treatment includes adsorption by live or dead microbial biomass, or industrial biomass, as well as enzyme-mediated dye reduction. Agricultural/ biowaste is inexpensive, plentiful (every inhabited place on the planet generates biowaste), and can be used to make adsorbents, nanomaterials is made from agricultural waste such as peels, leaves, and seeds using thermal treatment [24].

There are other agricultural waste that are used in so many application like in making composite [29–31]. Adsorption has rapidly gained interest in the treatment of wastewater due to its low cost, ease of operation, high-quality filtered effluents, and easy to handle [4, 32–37]. Adsorption, has a number of benefits, including ease of use, high performance, and the absence of hazardous by-products [24], where the benefits and drawbacks of each method are weighed, adsorption seems to be the better option; as a result, several study groups have focused on it. Adsorbents are the most important component of adsorption, and a variety of materials have been used for this purpose, because of their abundance and low cost, traditional adsorbents such as bentonite, clay, montmorillonite, and zeolite, have received a lot of attention. Seeking substitute methods and raw materials to make good adsorbent were critical at this stage [38–41].

There's not been a detailed analysis of the role of agro-waste materials in biosorption dye extraction from textile wastewater, in this chapter, we present a selection of studies on the removal of the most widely identified cationic dyes from agricultural waste, primarily leaves, stems, roots, and flower/fruit, to have a better understanding of the most common patterns and causes associated with this type of substance, the sorption capacity, isotherm, influencing factors, efficiency, and so on were documented. This chapter presents a current overview of using agricultural waste as adsorbents to dissolve dyes, with a broad variety of adsorption methods using environmentally friendly Agro-Waste material for dyeing wastewater treatment.

2 Classification of Dyes

A dye is a colored organic compound that may permanently bind to the fiber through chemical or physical bonding between the dye's groups and the fiber's groups, the dye must be resistant to glare, scratching, and water in order to be commercially viable, dyestuff is not necessarily a colored compound. The wavelength of light striking the retina of the eye causes a physiological phenomenon known as color, as light

with a wavelength in the visible region of the electromagnetic spectrum strikes the retina of the eye, the illusion of color is produced” [42]. The chromophores, which provide color, and the auxochromes, which not only complement the chromophore but also make the molecule soluble in water and have improved affinity (to attach) to the fibers, are the two main components of dye molecules. The color of the dye is determined by the chromophores, while the strength of the color is determined by the auxochromes. “The chromophore group is a basic configuration consisting of conjugated double bonds containing delocalized electrons. The chromogen, which has an aromatic structure normally contains benzene, naphthalene, or anthracene rings, is a part of the chromogen–chromophore structure along with auxochromes. The presence of ionizing groups known as auxochromes results in a much stronger alternation of the maximum absorption of the compound and provides a bonding affinity”. Some common auxochrome groups include $-\text{COOH}$, $-\text{HSO}_3$, $-\text{NH}_3$, and $-\text{OH}$ [43].

Dyes can be classified in many ways, the main classification is based on Natural sources of dyes (this further subdivided into origin source as plant/algae, insects or minerals sources), synthetic sources of dyes (this subdivided based on the possession of chromophore such as anthraquinone, azo, phthlocyanine, triphylmethene or sulfur) and classification based on application (this includes acid, basic direct, disperse mordant reactive or vat), this classification further sub divided into based on chemical structure (betalains, carotenoids, dihydropyran, indigoids, pyridine quinonoids, and tannins), based on the charge they possessed (anionic cationic non-ionic), organic chemists categorize them based on their shared parent structure (chemical classification). The dyer, who is only interested in securing the dye to the fabric, divides them into categories based on how they are applied. Figure 1 summarizes the various dye classifications. Lee et al. [44] divides textile dyes into three categories: anionic (direct, acid, and reactive dyes), cationic (all basic dyes), and nonionic (all nonionic dyes) (dispersed dyes). For this chapter we are going to give more emphasis to the cationic dyes in particular. For more details about dye and pigment classification you can read on *Removal of dyes and pigments from industrial effluents* [14].

3 Cationic Dyes

Cationic dyes breakdown in aqueous solution producing positively charged ions which are water soluble, and attach to salt groups of the fiber molecules which then strongly bond to them and stain them. Malachite green (MG), BR₂, simple blue 41, crystal violet, and MB, rhodamine B, methylene green, and MB are examples of cationic dyes, MB is a cationic dye that is causing the most concern among researchers. Cationic dyes are substrate to treated nylon, polyester, inks paper and polyacrylonitrile, chemical type related to this class of dye are (h) acridine, anthraquinone, azine, azo, cyanine, diazahemicyanine, diphenylmethane, hemicyanin, oxazine, triarylmethane, xanthenes, etc. Garlic root can be used as a low-cost adsorbent, but it will not strip dyes from agricultural wastewater, according to Tran

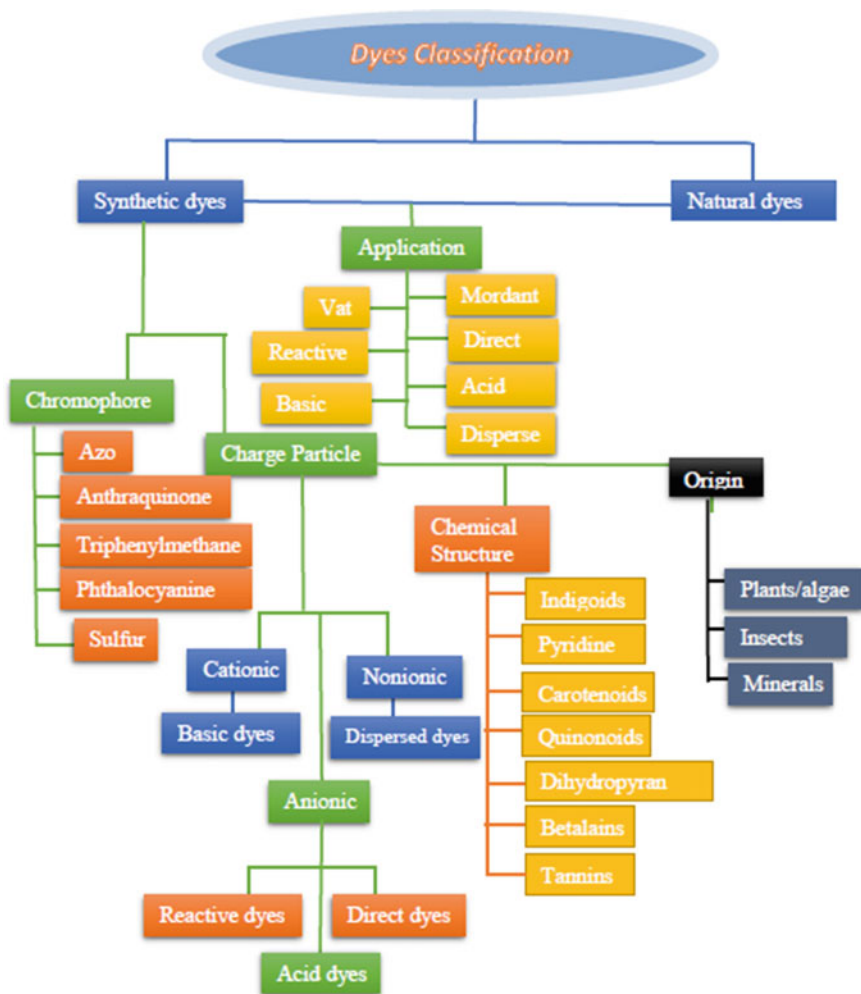


Fig. 1 Schematic representation of dye classification

and his co-authors, reducing environmental emissions is critical in an era where the dye is commonly used. They come to the conclusion that there is no need to abandon researching and developing farm waste as dye adsorbents, the following some important cationic dyes are discussed.

3.1 *Methylene Blue (MB)*

MB is a cationic dye with the molecular formula ($C_{16}H_{18}ClN_3S \cdot 3H_2O$) and a molecular mass of $319.85 \text{ g mol}^{-1}$ as shown in Table 1 and a maximum absorption wavelength of 663 nm. Methyl thioninium chloride is both a drug and a pigment. It is the most dispersible coloring and noxious colorant, burning sensation, causing methemoglobinemia, disorderly breath, mental confusion, necrosis of the tissue, nausea, quadriplegia, and jaundice in humans and animals [13, 45–47]. With an LD50 (mg/kg) of 1180, it was treated with low-cost raw or modified farming waste products before being released into the atmosphere.

3.2 *Malachite Green (MG)*

$C_{23}H_{25}N_2$ and $364.911 \text{ g mol}^{-1}$ (max = 617 nm) are the molecular formula and molecular mass of MG, a cationic dye, it is poisonous to a variety of marine and terrestrial species, as well as humans, and presents significant health risks. Mutagenesis, carcinogenesis, respiratory syndromes, and damaging effects on the eyes, kidney, liver, and skin are just a few of the serious health effects, anemia, blood coagulation, dyscrasia, and leukocytosis are among the post-exposure symptoms identified by MG [48, 49].

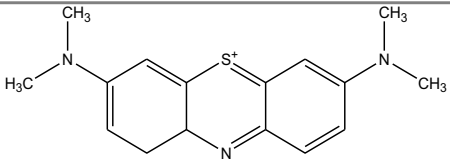
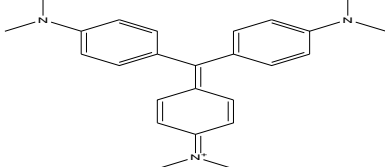
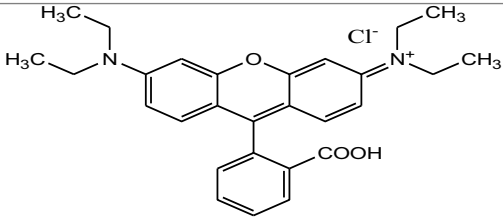
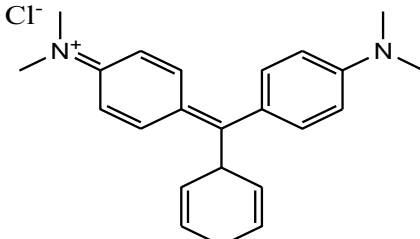
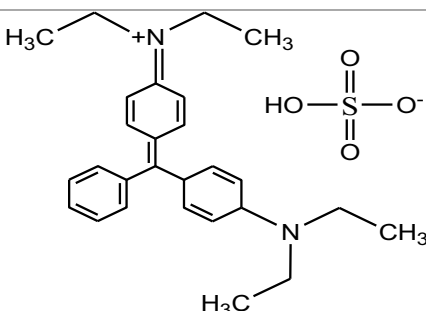
3.3 *Crystal Violet (CV)*

CV is a dye that is cationic ($C_{25}N_3H_{30}Cl$) with a molecular mass of $407.978 \text{ g mol}^{-1}$ and a maximum absorption wavelength of 590 nm, in vitro clastogenic influence, mitotic toxicity, hepatocarcinoma. This powerful carcinogen causes, reticular cell sarcoma, fish tumors, and other cancers [50]. Furthermore, it harms the respiratory and gastrointestinal processes of humans [51].

3.4 *Brilliant Green (BG)*

The BG dye is another type of cationic dye with the molecular mass of 475.6 g mol^{-1} and the molecular formula ($C_{27}H_{34}N_2O_4S$) and have a maximum absorption wavelength of 625 nm. It's widely used in simple clothing dye, and it poses a number of environmental health hazards, including nausea, diarrhea, vomiting, dermatitis, and respiratory tract inflammation [52].

Table 1 Chemical structure and molecular weight of several cationic dyes

S. No.	Name of dye	Chemical structure	Molar mass (g/mol)
1	Methylene Blue		319.85
2	Crystal violet		407.978
3	Rhodamine -B (RhB)		479.02
4	Malachite Green (MG)		364.911
5	Brilliant green (BG)		475.6

3.5 Rhodamine-B (RhB)

RhB is a cationic dye with a molecular mass of $479.02 \text{ g mol}^{-1}$ and a maximum wavelength of 544 nm ($\text{C}_{28}\text{H}_{31}\text{ClN}_2\text{O}_3$), it's a carcinogenic xanthine dye that pollutes the environment as humans and animals eat it, health threats include reproductive and developmental toxicity, neurotoxicity, chronic toxicity, scalp, visual impairment, and respiratory tract inflammation. As a result, major steps to treat dye-contaminated effluents have been taken, with the aim of ensuring environmental protection for future generations [53, 54].

4 Agricultural Waste Used in Adsorption of Cationic Dyes Removal

The environment is seriously harmed by the improper disposal of waste provided by agricultural sectors, as such, proper waste management is a current need, in recent years, scientists have tried to solve the issue by using these wastes as a dye adsorbent material, which has shown to be successful, agricultural waste is cost-effective, environmentally sound, and plentiful, and it has the ability to supplement other commercial activated carbon (AC), furthermore, it needs less packaging, is nonhazardous, and has a low manufacturing cost, furthermore, it needs less packaging, is nonhazardous, and has a low manufacturing cost. Materials that can economically expel toxins from dirty water are seeing a lot of attention these days, as a result, academics and environmental scientists are focusing their efforts on the use of low-cost industrial waste products in dye removal treatments, adsorption is a surface phenomenon in which the intensity of a certain ingredient rises at the interface between two phases, causing mixtures to separate [55], adsorption methods have become one of the most commonly used physicochemical procedures for successful removal of dyes from polluted wastewater due to their low cost, abundant raw material availability, and high quality, since toxic pollutants inhibit cell activity and cause cell formation to stop, contaminant removal by dead biomass has an advantage over live organisms [56]. Commercially available AC is expensive for many small-scale businesses, and its use necessitates regeneration and reactivation procedures, to address these issues, researchers are concentrating their efforts on generating AC from crop residues, which is seen as a promising material for eliminating contaminants.

Agricultural materials such as seeds, fruit peel, flowers, leaves, stem bark, algal biomass, fish scales, fungi, and bacteria biomass are used as the majority of adsorbents for dye adsorption, but in this chapter, we will concentrate on plant sources only. Agronomic yields extracted from floras are lignocellulosic (contains lignin, hemicelluloses and cellulose) and contain a variety of functional groups such as hydroxyl, carboxyl, and others that serve as active sorption sites. The dye sorption potential of sorbents with high cellulose and lignin content is particularly high [57]. Selecting an appropriate adsorbent after evaluating the surface characteristics is

needed for a successful sorption operation. Enabled adsorbents (derived from agricultural production) use the van-der-Waals force or the London dispersion force during surface contact with sorbate. The efficacy of cationic dye removal from aqueous media using adsorbents derived from plant leaves, stems, seeds, fruit peel, vine, base, algal residue, waste of animals, and bacteria/fungi biomass has been discussed sequentially in this chapter.

5 Leaves

The plant leaves are made up of biomolecules including cellulose, hemicellulose, pectin, which lignin, and are the primary photosynthetic tissue. Various functional groups in these biomolecules, such as amino, carboxyl, carbonyl, hydroxyl, and nitro, act as receptors and help in the interactive biosorption of dye molecules from an aqueous medium, leaf-based bio-materials should be used as effective biosorbents for the removal of various dyestuffs (ionic or non-ionic) from contaminated water because the binding affinity of such functional groups with dye molecules is inevitably dependent on the laboratory conditions, which can be dissociated or non-dissociated [58]. To clear dust and other impurities, the raw leaves are first washed with tap, distilled, or deionized water, the washed and dried leaves are ground into a powder and sieved to isolate the desired particle size for biosorption, Several studies on the decolorization of different dyes using leaf-based adsorbents have recently been performed with very reliable results published in the literature Das et al. [59] used *Butea monosperma* leaf powder as a biosorbent to remove methylene blue dye from an aqueous solution, within 120 min, the authors recorded a maximal dye removal efficiency of 98.7% with an adsorbent dosage of 0.5 g/L against an initial dye concentration of 100 mg/L at pH 8. Surprisingly, the biosorbent had an 80% desorption potential in the first loop and could be reused twice for dye removal. Furthermore, leaf-based biosorbents can be changed into activated carbon or bio composite materials via physical or chemical methods to boost dye-binding affinity or biosorption capability. Akar et al. [60] conducted a research using spent tea leaves as a waste material to generate activated carbon (STAC), malachite green (MG) was removed from aqueous solutions using STAC as a low-cost adsorbent, at 45°C, the STAC had the highest adsorption potential (256.4 mg g⁻¹). STAC successfully separated 94% of malachite green from aqueous solution, and adsorption is beneficial under the operating conditions investigated. Up to pH 4, the amount of adsorbed malachite green increased, but remained constant above that point. The Langmuir isotherm suited the experimental results the most, the MG adsorption on STAC was governed by pseudo-second-order kinetics. The removal of MB dye with *Apium graveolens* residue modified with H₂SO₄ was successful. The Freundlich adsorption isotherm, which adopted the PSO model of kinetics, was considered to be the best match for the experimental results. 476.19 mg g⁻¹ was discovered to be the maximum adsorption capacity (MAC). The mechanism seems to be exothermic and random, according to the thermodynamic analysis [61]. Pirbazari et al. [62] studied the adsorption of

methylene blue (MB) from aqueous solution by alkali treated Foumanat tea waste (ATFTW) from agriculture biomass. Complexation and ion exchange tend to be the primary mechanisms for MB adsorption, according to FTIR data. The Langmuir, Sips, Redlich-Peterson, and Freundlich equations were used to suit the adsorption isotherm results, and the Langmuir adsorption power, Q_{max} , was determined to be 461 mg g^{-1} . The adsorption of MB increases as the temperature rises from 303 to 323 K, indicating that the mechanism is endothermic. ATFTW used pseudo-second order reaction kinetics based on Lagergren equations to remove MB, the adsorption of MB on the ATFTW was primarily governed by external mass transport, with particle diffusion serving as the rate-limiting step, according to mechanism studies.

The pericarp of *Sapindus mukorossi* (reetha) was used by Samal et al. [63] as a biosorbent modified chemically and physically for the removal of methyl violet (MV) dye. It was characterized by using advanced analytical methods such as BET, FE-SEM, FTIR, and EDX analysis. The CCD model was used to refine the different parameters (sorbent dosage, pH, and dye concentration). The biosorbent that has been thermally treated had maximum dye removal ability (95%) at pH 4 with an adsorbent dosage of 0.1 g L^{-1} and an MV concentration of 28 mg L^{-1} in 150 min. Bello et al. [64] investigated the use of chemically modified activated carbon obtained from gmelina aborea leaves (GALAC) as an adsorbent for the elimination of Rhodamine B (Rh-B) dye from aqueous solutions. The Langmuir isotherm model best defined RhB dye adsorption on GALAC, with a maximum monolayer coverage of 1000 mg g^{-1} and an R^2 value of 0.9999. GALAC had a carbon content of 82.81% by weight and 91.2% by atom, which is needed for high adsorption capability, according to the EDX report. The PSO kinetic model was best suited by adsorption kinetic results, thermodynamic parameters for GALAC showed that the RhB dye removal from aqueous solutions was random and endothermic.

Astuti et al. [65] used thermal conversion of pineapple crown leaf waste to make the enabled carbon that has been magnetized adsorbent and tested its effectiveness for removing methyl violet dye from aqueous solution. The authors found that a $0.3 \text{ g}/50 \text{ mL}$ dosage of micro and mesoporous adsorbent could extract 100% of the original 50 mg/L dye concentration from the solution at pH 5 after 180 min of contact time. The dye sorption absorption was found to be lower in the strong acid medium (pH 1) due to adsorbent surface protonation, and higher in the pH 5–11 range due to the development of soluble hydroxy complexes between the dye and the adsorbent. Also under the magnetic effect, enabled carbon that has been magnetized has a benefit in terms of pollutant isolation. Zaidi et al. [66] looked at the dye adsorption potential of cellulose isolated from *Artocarpus odoratissimus* leaves to clear MV and CV from an aqueous solution. They discovered that at atmospheric pH 4.78 and 6.08, the adsorbent had a gross adsorption capacity of 239 and 187 mg/g for CV and MV, respectively, and that it could regenerate best in an alkaline medium for five rounds. Zaidi et al. in another research [67] studied the adsorption of malachite green dye onto *Artocarpus odoratissimus* (Tarap) leaves, the leaves' surfaces were modified with a strong base, sodium hydroxide (NaOH). The Redlich–Peterson model was the perfect choice for the isotherm. The value of Tarap leaves increased from 254.9 to 422.0 mg/g after adjustment based on monolayer adsorption using the Langmuir model, and

increased by threefold while using the Sips model. Contact time, ionic strength, pH, temperature, and initial dye concentrations were all investigated as affecting parameters on adsorption. Thionine adsorption on tea waste and rice husk has been used for dye therapy [68, 69]. Oil palm fronds, tendu leaves (*Diospyros melanoxylon*), tea leaves, and pistachio shells were used to clear the cationic dye Janus green [70, 71]. Ruby S2G and brilliant 2BE and were stripped using coconut epicarp and sugar cane bagasse [72, 73]. These cationic dyes involve hydrogen bonding interactions and intra-particle diffusion, which are affected by the pH and ionic strength of the medium. The prevalent negative charge on the adsorbent surface forms electrostatic attraction with the cationic dyes in mildly acidic medium ($\text{pH} > 4.5$), maximizing dye adsorption. Natural or chemically modified leaf-derived adsorbents have a high potential for extracting dye from aqueous media under different ionic pressures, as well as good desorption and reusability, according to the literature.

6 Stem Biomass

The stem is the most valuable part of a plant, and it's used in a variety of industries including wood carving, pulp, and paper. During industrial processing (selection, sorting, and other processes), some waste is produced that goes un-used and needs additional cost and effort to dispose of herbaceous plant stems are left in fields untouched to decompose. The easily available lignocellulosic stem biomass may be used as an adsorbent in effluent dye removal. In order to investigate the stain-elimination potential of adsorbents isolated from raw or activated/modified carbon obtained from stem biomass, a number of studies have been carried out, the biosorption capacity plant stem of *Ananas comosus* for the abstraction of cationic Basic Blue-3 from aqueous solution was investigated by Chan et al. [74]. After two consecutive cycles of sorption-desorption, the biosorbent's total sorption capacities for basic blue-3 dyes were found to be 58.983 mg/g at pH 10 after 120 min, which was found to be reduced by 20%. This thermodynamic experiments suggest that an exothermic adsorption process might be affected by a higher temperature.

Using an aqueous solution and *Artocarpus odoratissimus*'s axis stem, Kooh et al. [75] studied the adsorption of the methyl violet-2B dye was investigated, at pH 4.2 and 65 °C, the investigators discovered that a 0.04 g adsorbent dose extracts 87.2% of the original dye concentration of 50 mg/L in 120 min, with a median absorption of 263.7 mg/g. Increases in temperature from 25 to 65 degrees Celsius increased dye biosorption, while raising the medium's ionic concentration from 0 to 0.8 mol/L had the opposite effect. Sugarcane bagasse modified with magnetic pyromellitic dianhydride (PMDA) and immature sugarcane activated with H_2SO_4 , MB [76] and its corresponding adsorption capacity of 304.90 mg/g were removed. Oloo et al. [77] investigated the function of *Rhizophora mucronata* stem-barks in the biosorption of crystal violet dye from aqueous solution, they achieved a maximum dye biosorptive efficacy of 99.8% after 60 min of interaction, adsorbent biosorption efficacy rises with adsorbent dosage, initial dye concentration, and contact time, then falls

with particle size and biosorbent ionic pressure. The adsorptive potential of activated carbon isolated from *Cornulaca monacantha* stem for the removal of malachite green dye from aqueous solution was investigated by Sharma et al. [78]. According to the scientists, the adsorbent's total dye removal efficiency was 97.07% against a starting dye dose of 100 mg/L, with an overall uptake capacity of 133.33 mg/g in an alkaline (pH 12) medium. Machrouhi et al. [79] studied the adsorption ability of activated carbons from *Thapsia transtagana* stems for the elimination of MB and MV dyes from wastewater. After 145 min at 500 °C, they discovered that the maximal adsorption capacities for respective dyes with an impregnation ratio of 2 g/g were 219.70 and 1137.80 mg/g. They discovered that the impregnation ratio and activation temperature were the two most significant parameters that positively affected the activation mechanism. To adsorb safranin O and safranin (SBP), the biosorbent *Salvadora persica* (Miswak) powder (SP) and dried sugar beet pulp were used. With an adsorption potential of 17.3 mg g⁻¹ 603 for SP and 147 mg g⁻¹ for SBP, both sorbents were considered a suitable alternative to the industrial activated carbon. In SP, Langmuir and Freundlich were used to analyze the investigational results, with SBP and the PSO being the best fit for both [79, 80].

Bello et al. [81] used free radical graft co-polymerization of sodium acrylate and acrylamide to create banana pseudo-stem cellulose-based super-adsorbent hydrogels, they studied the ability of super-adsorbent hydrogels to remove methylene blue dyes and found that the Overall uptake was 124 mg/g, with maximal desorption for both dyes of >96%, resulting in improved hydrogel usage. Other agricultural wastes, such as walnut shells [82], sawdust biomasses [83], tarap leaves [67], spent tea leaves [60], cattail biomass [84], coffee beans [85], luffa aegyptica peel [86], maize cob [86], coconut coir [87], and rice husk [87], were also used to remove cationic Malachite Green from aqueous solutions.

6.1 Flower, Fruit Peel, and Seed Biomass

Researchers have spent years attempting to reclaim and eliminate these agricultural wastes, which may be by removing the necessary bio-components or repurposing the leftover for other manufacturing purposes. Preparation of biosorbents and derived adsorbents for wastewater treatment, as well as the processing of feed or fertilizer.

Reproductive organs of Plants develop into flowers, fruit peels, and seeds. Flowers make up the majority of the waste produced by ornamental and spiritual establishments. Fruit peels and seeds are sorted as waste in the majority of food treating sectors and in the majority of kitchen garbage bins, the active biomolecules in these pollution by-products are beneficial to people's health [50, 73].

Numerous researchers have studied the adsorbents extracted from these agro-products for the successful elimination of cationic dyes from aqueous media, as shown in Table 2.

Saeed et al. [88] investigated the biosorptive potential of grapefruit peel for the elimination of CV cationic dye from wastewater. The biosorbent made from peels

Table 2 Decolorization of different dyes by different types of biomass

Dyes	Plant	Optimum Exper. Con.: CT, Dose, pH, Temp., rpm	Adsorption cap./ % Removal	Desorption	Isotherm	Kinetics	References
<i>Leaves</i>							
Methylene blue	Bamboo	20 min, 10 mg/L, 6,	88.00%		Freundlich	PSO	[93]
Methylene blue	Butea monosperma	120 min, 100 mg/L, 8, 25 °C, 150 rpm	99.00%	After at 2nd cycle 80%	Freundlich		[59]
Methylene blue	Banana leaves		48.00%				[94]
Methylene blue	Banana leaves	250 mg/L, 4, 30 °C	110 mg/g				[95]
Methylene blue	Ficus palmata	80 min, 15 mg/L, 7, 313 k,	98%/6.89 mg/g	54%	Freundlich	PSO	[96]
Methyl violet	Eucalyptus	10 min, 10 mg/L, 7, 40 °C, 200 rpm	98%		Freundlich	PSO	[97]
Methyl violet	Pineapple	180 min, 20 mg/L, 5, 25 °C, 120 rpm	31.24 mg/g		Redlich-Peterson		[65]
Safarin	Phlomis cancellata Bunge	39.96 min, 100 mg/L, 9, 25 °C, 331 rpm	99.6		Lamgmuir	PFO	[98]
<i>STEM</i>							
Crystal violet	Rhizophora mucronata	60 min, 100 mg/L, 7, 25 °C	99.80%		Freundlich	PSO	[77]
Malachite green	Cornulaca monacantha	120 min, 100 mg/L, 6, 30 °C, 140 rpm	97%, 45 mg/g	After 6th cycle 54%	Lamgmuir	PSO	[78]
Malachite green	Sugercane baggase Biochar	52 min, 0.5 g, 7.5,	3000 mg/L				[99]

(continued)

Table 2 (continued)

Dyes	Plant	Optimum Exper. Con.: CT, Dose, pH, Temp., rpm	Adsorption cap./ % Removal	Desorption	Isotherm	Kinetics	References
Malachite green	Sugercane baggase (SB)		157.2 mg g ⁻¹		Langmuir		[67]
Malachite green	Banana pith carbon	24 h, 4,	48.20%				[23]
Malachite green	Banana stalk AC	120 min, 8, 303 k,	142 mg/g				[100]
Methylene blue	Banana Pseudo stem	450 min, 100 mg/L, 7, 25 °C, 120 rpm	333.3 mg/g	After 1st cycle 98%	Freundlich	PSO	[81]
Methylene blue	Banana pith	120 min, 25 mg/L,	89%		Langmuir	PSO	[101]
Methylene blue	Banana pith carbon	24 h, 4,	93.3%				[23]
Methylene blue	Banana stalk waste	7, 30 °C	243.90 mg/g		Langmuir	PSO	[102]
Methylene blue	Agava sisalana	20 min, 300 mg/L, 8, 328 k, 200 rpm	553 mg/g		Freundlich		[103]
Methylene blue	Bagasse	60 min, 0.5 g/50 mL, 700 °C	132 g/mg				[104]
Methyl violet	Thapsia transtagana	145 min, 500 mg/L, 6, 25 °C	141 mg/g		Langmuir		[79]
Methyl violet	Banana pith carbon	24 h, 4,	37%				[23]
Methyl violet- 2B	Artocarpus odoratissimus	120 min, 500 mg/L, 2, 65 °C, 250 rpm	87%/264 mg/g	After 5th cycle 45 mg/g			[75]
Rhodamine-B	Banana pith carbon	24 h, 3.2,	83%				[23]
Rhodamine-B	Banana pith	4	87%				[105]
Rhodamine-B	Sugercane baggase	1 g/L	65.5 mg/g				[106]

(continued)

Table 2 (continued)

Dyes	Plant	Optimum Exper. Con.: CT, Dose, pH, Temp., rpm	Adsorption cap./ % Removal	Desorption	Isotherm	Kinetics	References
Safarin	Pseudo stem Banana	90 min, 40 mg/L, 7.5, 20 °C,	21.7 mg/g				[107]
<i>Flower, fruit peel, & seed</i>							
Crystal violet	grape fruit peel	60 min, 100 mg/L, 6, 30 °C, 100 rpm	266 mg/g	After 1st cycle 98%	Langmuir	PSO	[88]
Crystal violet	cotton linter (sponges)	2 h, 298 k, 7,	76.63 mg/g,	After 12th 70.94% cycle	Langmuir	PSO	[108]
Malachite green	Borassus aethiopicum flower	4 h, 100 mg/L, 6.8, 300 k	48.5 mg/g				[89]
Methylene blue	Nerium oleander, Pergularia tomentosa and Populus tremula seeds	90 min, 60 mg/L, 6, 22 °C, 100 rpm	280, 145, 168 mg/g		Freundlich	PSO	[57]
Methylene blue	Banana peel	3 h, 100 mg/L, 4-8, 20 °C	18.7 mg/g				[109]
Methylene blue	Banana peel	25 oC	225 mg/g				[110]
Methylene blue	Banana peel Activated	3 h, 100 mg/L, 4-8, 20 °C	19.7 mg/g				[109]
Methylene blue	Banana peel Activated	120 min, 4,	94%				[111]
Methylene blue	Banana peel AC	24 h, 1000 mg/L, 9, 25 °C,	620 mg/g				[112]

(continued)

Table 2 (continued)

Dyes	Plant	Optimum Exper. Con.: CT, Dose, pH, Temp., rpm	Adsorption cap./ % Removal	Desorption	Isotherm	Kinetics	References
Methylene blue	Banana peel AC	150 min, 25 °C	225 mg/g				[113]
Methylene blue	Banana peel AC	25 °C	1263 mg/g				[110]
Methylene blue	Banana peel AC	6, 22 °C	455 mg/g				[114]
Methylene blue	Banana fruit bunch AC-H ₃ PO ₄		76 mg/g				[115]
Methylene blue	Banana fruit bunch AC-KOH		71 mg/g				[115]
Methylene blue	Banana fruit bunch AC-Untreated		70 mg/g				[115]
Methylene blue	cotton linter (sponges)	2 h, 298 k, 11,	123.46 mg/g,	After 12th cycles 77.04%	Langmuir	PSO	[108]
Methylene blue	Sugercane Bagasse (SB)		90.11 mg/g				[116]
	SB modified		571.4 mg/g				[116]
<i>Root</i>							
Auramine O	Ipomoea aquatica	120 min, 1000 mg/L, 6, 25 °C, 250 rpm	456 mg/g	After 5th cycle 75%	Sips model	PSO	[117]
Gentian violet/Crystal violet	Banyan aerial root	9 h, 500 mg/L, 6, 318 k, 180 rpm	457 mg/g		Langmuir	PSO	[118]
Malachite green	Allium Sativa L	2 h, 50 g/L, 25 °C, 200 rpm	233 mg/g		Langmuir	PSO	[119]

(continued)

Table 2 (continued)

Dyes	Plant	Optimum Exper. Con.: CT, Dose, pH, Temp., rpm	Adsorption cap./ % Removal	Desorption	Isotherm	Kinetics	References
Malachite green	Cassava	120 min, 0.05 g/L, 4, 25 oC, 300 rpm	933 mg/g				[120]

was found to be successful, removing 96% of the dye in 60 min. The equilibrium mechanism adopted the Langmuir isotherm, and the data from kinetics studies was found to be best suited for a pseudo-second-order model. The peel-sorbent was also reusable and could be regenerated using a 1 M NaOH solution with a dye recovery rate of 98.25%.

The sorption of this dye malachite green using activated carbon obtained from *Borassus aethiopicum* flower biomass was investigated by Nethaji et al. [89], the authors demonstrated that the adsorbent could remove 99 of the sample in a slightly alkaline pH medium, 95%, and 78 of dye molecules for initial 100 m, 600 m, and 1000 m dye concentrations respectively, involving both intra-particle and boundary layer diffusion of dye molecules.

Shakoor et al. [90] used the peel of *Citrus limetta* to remove the Methylene Blue stain, with a maximum sorption capacity of 227.3 mg g⁻¹, the experimental findings were ideally suited to the pseudo-second-order (PSO) kinetics and Langmuir isotherm model. With time and equilibrium dye concentration, the adsorption capacity increases, the removal efficiency of the adsorbent improves from 94.61 to 97.1 in the concentration range (0.4–2.0 g L⁻¹) of the adsorbent, this may be due to an increase in surface area and the number of adsorption binding sites. The Gibbs energy was negative, indicating an exothermic and random adsorption operation, using biochar corn straw-derived backed zero-valent iron NPs (nZVI) composite, the MG dye was successfully removed from the aqueous solution [91]. The charge has a big impact on the adsorption performance on the adsorbent surface, the composite has a very good dye removal performance after just 20 min (99.9%), adsorption is a spontaneous and endothermic operation, the MAC was discovered to be 515.77 mg g⁻¹.

To extract RhB and MO dyes, Xiaoyan and collaborators used corncob as a raw material and mixed furfural agricultural manufacturing waste, since there are functional groups bearing oxygen on the surface of the mesoporous system, the furfural residue (FR) has a high removal ability, with 37.93 mg g⁻¹ as its maximum adsorption capacity, the adsorption data adopted the Freundlich isotherm. The PSO kinetic model accurately represented the adsorption mechanism, and thermodynamic tests confirmed that the process was spontaneous and exothermic. The reusability of the raw material is critical from an industrial standpoint, by the fifth step, the RhB dye removal efficiency had decreased, indicating that the adsorbent had a strong recycling capacity [92].

White rice husk ash (WRHA) [121] was used to successfully clear the BG dye from the aqueous solution, the MAC was estimated to be 85.56 mg g⁻¹ at 320 K. The most reliable model was discovered to be the PSO model, showing that the adsorption is completely chemical. In the range of concentrations of 3–100 mg L⁻¹, more than 96.92% of the dye was eliminated at a fixed adsorbent dosage of 5 g L⁻¹. The activation energy of the chemisorption process was estimated at 50 kJ mol⁻¹, meaning that it is the rate-controlling stage of the adsorption process. The adsorption mechanism was exothermic, and no significant improvements in the adsorbent's internal structure were found during the process, as shown by ΔH° and ΔS° .

Acetic acid is used as an activator in the production of AC by *Pinus roxburghii* (PRCAC), the initial dye concentration (60 ppm), temperature (25 °C), pH (6), are the best adsorption parameters for MG. The MAC of the adsorbent was calculated by the Langmuir model to be 250 mg g⁻¹. The adsorbed potential of PRCAC decreased from 93 to 83% subsequently just 5 rounds, according to desorption studies [122].

The MG was adsorption removed by the coffee husk dependent biosorbent (ACH), an important improvement in dye removal efficiency (96%) was found when the adsorbent dose was increased to 0.5 g L⁻¹. Murthi et al. calculated the adsorbent's MAC to be 263 mg g⁻¹, and found that the PSO kinetic model and sips isotherm model matched the experimental results better, with $R^2 > 0.98$ [123]. The Adsorption mechanism was also discovered to be endothermic, practicable, and random. At pH 6.8 and a q_e value of 185 mg g⁻¹, the MAC of MG on ACH (74%) was observed, the removal efficiency decreased after pH (7) when it comes to dye adsorption, pH is extremely important [123].

Terminalia arjuna with an adsorption potential of 45.99 mg g⁻¹, sawdust (TASD) was discovered to be an excellent adsorbent. The adsorption potential improved as the dye concentration was increased, and equilibrium was reached in 120 min, for successful adsorption of the pH of the medium should be greater than 5 when using crystal violet dye as an adsorbent. The kinetics experimental data preceded the PFO with a k_1 value of 0.013 min⁻¹, according to the findings. The adsorption was accompanied by the Freundlich isotherm model, suggesting multilayer cooperative adsorption, the reaction was endothermic and spontaneous [124].

At 80° C, the orange peel (OP) was treated with FeCl₃ and FeCl₂, and precipitated with 10% ammonia. The OP's adsorption properties were improved by the magnetization process, at higher temperatures and pH, the adsorbent had better adsorbed properties. The Langmuir isotherm, which has monolayer uptake capacity (MOP) of 555.6 mg g⁻¹ for and 138.9 mg g⁻¹ for OP, is supplemented by the PSO model, which has monolayer sorption capacity of 555.6 mg g⁻¹ for MOP and 138.9 mg g⁻¹ for OP, suits the equilibrium data well, MOP demonstrated outstanding renewability by up to 5 cycles as compared to OP. MOP had a higher equilibrium adsorption potential than OP, with a value of 46.94 mg g⁻¹. The adsorption of the crystal violet onto the orange peel is endothermic in nature and it is followed by an increase in power [125].

To further clear MB stain from textile effluents, cashew nut shells were used as a low-cost adsorbent, at pH 10, with an adsorbent dosage of 2.1486 gL⁻¹ and an initial dye concentration of 50 mg L⁻¹, and an equilibrium period of 63 min, the appropriate optimum parameters were determined using reaction surface methodology (RSM) [126].

The activated carbon extracted from sour cherry stones (*Prunus cerasus* L.) with SBET was found to extract yellow 18 (Y₁₈), a cationic dye with V_{total} of 1704 m²g⁻¹ and 0.984 cm³ g⁻¹, respectively. The adsorption potential was 75.76 mg g⁻¹ at 318 K, with the pH and temperature of the solution playing a role [68, 69].

For the adsorption of the BG dye, Aichour and Zaghouane [127] used lemon peel waste (LP), Algerian montmorillonite (Mt), and industrial AC, while AC has a higher adsorption capability, its high cost has restricted its use. The Langmuir and PSO

models suit the adsorption isotherm and kinetic well, with MACs of 229,150, and 826 mg g⁻¹ for MT, LP, and AC, respectively. According to thermodynamic experiments, the values of ΔH° and ΔG° were negative, suggesting that the adsorption mechanism was spontaneous and exothermic reaction. The high degree of spontaneously during dye adsorption onto the bio adsorbent is due to the positive value of ΔS° .

Chen et al. [128] used sludge-rice husk biochar to study the adsorption of the dye methylene blue. The dye sorption mechanism was discovered to include surface involvement, $-\pi-\pi$ interactions, electrostatic interactions, and hydrogen bonds, with a sorption capability of 22.59 mg/g as determined by the Langmuir isotherm.

For the MB dye sorption capacity, Asma et al. [129] used the Mangosteen peel as a source of AC and ZnCl₂ as an activating agent, temperature, impregnation time, calcination time, and ratio both had an effect on the surface properties. Mesoporous AC has the largest surface size, pore depth, and pore diameter (1622m²g⁻¹; 1.805 cm₃ g⁻¹; and 4.4 nm), making it a strong contender for a variety of environmental applications, the MB adsorption on AC was represented using the Lagergren pseudo-first-order and PSO models. The Langmuir isotherm was followed in this situation, and the MAC was found to be 1192 mg g⁻¹, revealing the endothermic and random presence of MB on the AC.

Cucurbita pepo seed husks' biosorptive properties for removing cationic dyes (basic violet-10 and basic red-46) from aqueous medium were investigated by Kowalkowska and Jozwiak [130], they found that the seed husk absorbed 96.01 and 163.39 mg/g of basic violet-10 and basic red-46 dyes, respectively. The sorption capacity differed because cationic dyes have the capacity to form additional hydrogen bonds with the polysaccharides in seed husk. According to published findings, the reproductive parts of plants as agro-waste may be used to treat dyeing wastewater, reducing energy loss and providing a profitable income for food industries.

6.2 Root Biomass

Plant roots are in charge of extracting water and minerals from the soil or water, all of which are needed for plant growth, the roots of aquatic plants, in particular, are designed to live in water and can therefore be used to extract dissolved nutrients from an aqueous medium. Just a few roots (carrots, sweet potatoes, and others) are edible, so the non-edible roots are left to decompose. To minimize dye loss, the adsorbent obtained from the roots of a few aquatic plants was investigated for the removal of dyes from aqueous media, as shown in Table 2.

Kallel et al. [131] designed predicted values were very similar to the real values, they used an adsorbent with garlic straw, which removed the dye with a proficiency of 85% in just 200 min at pH 7. With an adsorbent dose of 0.04 g/10 mL and an IDC of 100 mg mL⁻¹, the MAC was found to be 256.41 mg g⁻¹. The sorption equilibrium was evaluated using Langmuir's, Freundlich's, and Temkin isotherm models, and the essence of adsorption was discovered to be exothermic.

Fan et al. [118] investigated the sorbent behavior of modified banyan aerial roots for the elimination of gentian violet dye from aqueous solutions, with a bio sorbent dosage of 0.02 g/L, they achieved a maximal sorption potential of 456.64 mg/g in 540 min and adsorptive equilibrium results that followed the Langmuir isotherm in endothermic adsorption studies with electrostatic interaction. Aerial root grinding resulted in significant structural non-uniformity at the bio sorbent surface as well as a lower crystallinity of 21.79, indicating the biosorbents exceptionally high reactivity. Lu et al. [117] studied the sorption of auramine-O dye using root powder from *Ipomoea aquatica* as a adsorbent. The root powder had a dye sorption potential of 455.74 mg/g, with successful dye removal of 75% after the fifth sorption–desorption stage, and the kinetic results adopted a PSO model with a rate constant of 1.92 g mmol/min, according to the authors. Furthermore, the batch process was used to remove dye from polluted water using *Musa acuminata* (MA) peels and *Solanum tuberosum* (ST), when compared to MA peels, the ash content of ST peels is lower, and the water content is higher, SEM analysis revealed the porous nature of the adsorbents. Which was shown to be beneficial in the handling of water containing dye molecules. Adsorption tests showed that rising the adsorbent dose increases percent sorption in both cases. In an acidic medium, both adsorbents demonstrated stronger adsorption. It was also discovered that the sorption of MA rises over time, although there was no discernible difference in the peels of ST. At 30 °C and 10 °C, the maximal adsorption of ST and MA was observed. The Langmuir isotherm was found to be more applicable in the isothermal experiments, with R^2 values of 0.854 for ST and 0.7508 for MA. In both cases, the PSO is used, with MACs of 83.31 mg g⁻¹ for ST and 87.24 mg g⁻¹ for MA [132].

The hydrothermal treatment system was used to remove RhB dye from water using agricultural waste such as bamboo shoot shell (BSS) and cassava slag (HCS), with a MAC of 105.3 mg g⁻¹ and excellent regeneration efficiency, HCS will extract 96% of the dye. At 25 °C adsorption equilibrium period of around 20 min, the MAC of BSS was found to be 85.8 mg g⁻¹, In both cases, the adsorption mechanism may be well described by PSO kinetics. Enthalpy, entropy, and Gibbs free energy were determined using the Van der Hoff equation, with the temperature, the endothermic nature of the process was mirrored in the increased adsorption of dye onto HCS [133, 134]. Similarly, using various farm wastes as an adsorbent, several research articles confirmed the elimination of MB dye. Carrot leaves and stems (CLP&CSP) [135], potato stems and leaves [136], foumanat tea waste [62], luffa actangula carbon [137], coconut shell [137], corn stalks [138], hawthorn kernels [139], raw peach shell [140], carica papaya [140], palm trees and date stones [141], tea waste [69], rejected tea [142], wheat straw [143]. It has been discovered that there are very few findings in the literature on the use of root biomass as a biosorbent for dye removal. The root biomass contains enough cellulose, suberin, starch sheath, and other active functional groups such as amino, carboxyl, carbonyl, and nitro, making it a strong biosorbent for dye removal from aqueous media.

7 Factors affecting dye sorption

The final dye sorption capacity of AC is determined by the conditions under which dye adsorption takes place. Dye sorption is influenced by a number of factors, including dye initial concentration, temperature, pH, in the effluent, and chemical structure of the dye.

7.1 Adsorbent Dosage

The adsorbent dosage capacity is determined by the quantity of adsorbent dose used for the removal of dyes under specified optimal conditions. Dye adsorption usually improves when the adsorbent dosage increased due to the presence of more adsorbent active sites. Adsorption dosage can be affected by the adsorbent-adsorbate solution with various adsorbent quantities added to the set starting dye concentration and mixed together for a balance time [58]. Generally, with increasing adsorbent dose, the percentage of dye removal rises. At first, the rate of increase in the percentage of dye removal was shown to be quick and decreased as the dosage rose. The reason for this occurrence is the fact that adsorbate (dye) is more easily accessible in the less adsorbent dosage and thus the extraction of adsorbent per unit weight is larger. With the increase of adsorbent dosage, adsorption is less proportional due to the lack of saturation at many sites during adsorption [144]. However, the improvement in removal efficiency following a particular dosage is negligible in relation to the dose increase. This is due to a very rapid superficial adsorption of the adsorbent surface is produced in the solution at a greater adsorbent concentration than at a lower dosage of the adsorbent. Thus, the quantity of dye adsorbed per unit mass of adsorbent is decreased with increasing adsorbent dosage, producing q_e decreases [145–149].

7.2 Effect of pH on Dye Sorption Capacity

It's crucial to figure out what pH a certain carbonaceous adsorbent works best for adsorption capacity. The pH of the dye solution has a major effect for dye uptake in the case of dye binding by electrostatic reaction, with the largest dye uptake happening at the pH where the adsorbent and molecules of dye have good sensitivity. The maximal affinity can be determined using the adsorbent's zeta potential. To absorb cationic dyes, the carbonaceous material must be negatively charged, while to bind anionic dyes, the adsorbent must be positively charged. The pH of the effluent has no effect on dye binding through Van der Waal strength, hydrogen bonding, or hydrophobic-hydrophobic interaction, and adsorption takes place over a wider pH spectrum. The best pH for adsorbent dye binding is determined by the activation processes and carbon feed stocks used.

7.3 Contact Time

This ensures the maximum adsorption of an adsorbent at suitable operating conditions. In that time, the amount of adsorbed materials onto the adsorbents makes a state of dynamic equilibrium with the number of desorbed materials. Adsorbent–adsorbate solution with a set adsorbent condition and initial concentration of dye may be applied to the impact of contact time on dye adsorption and shaken to balance over a different time interval. The rate of color removal often rises to some degree with an increase in contact time. Further increase in contact time does not improve absorption since dyes are deposited in adsorbent material at the accessible adsorption site (Ansari and Mosayebzadeh 2010). The dye value that is desorbed by the adsorbent is now in a condition of dynamic balance with the dye quantity adsorbed to the adsorbent. The time needed to achieve this balance is called the equilibrium time and the dye adsorption at the equilibrium time represents the adsorbent's maximal adsorption capacity under those operating conditions [148–151].

7.4 Effect of Temperature and Pressure

According to Le Chatelier's principles, the increase of temperature and decrease of pressure enhanced the rate of adsorption, heat is consumed in the process at this time, which favors adsorption. Temperature is another important element in adsorption research, as it reveals much about the system involved in the sorption process. In general, temperature has two major effects on the adsorption process, since the viscosity of the solution decreases as the temperature rises, the diffusion rate of adsorbed molecules increases through the external boundary layer and in the internal pore of the adsorbent particle. Similarly, changes in the adsorption system's temperature cause changes in the adsorbent's equilibrium potential for a given adsorbent [152, 153]. The temperature at which dye adsorption occurs is also important in the dye adsorption capacities of carbonaceous materials. It's possible to have endothermic or exothermic interactions with dye molecules and adsorbent. Dye molecules diffuse and bind to the adsorbent due to the constant thermal motion of atoms and molecules, which is dependent on the energy available. The increase in temperature provides thermal energy, which increases dye molecule molecular motion and drives diffusion through the adsorbent.

7.5 Effect of Dye Concentration

The data of initial and final ions concentrations are used to calculate the adsorption capacity of an adsorbent [151, 154]. However, if the initial ion concentration increases for a specified amount of adsorbent dosage, then the removal efficiency

will be decreasing due to the presence of a higher number of dye per unit mass of adsorbents. The adsorption potential would be determined by the dye concentration in the wastewater. Because of the low concentration of the dye, it is possible the dye adsorption won't reach saturation, and the adsorbent may be underutilized. The dye adsorption potential rises as the dye content in the effluent rises until the adsorbent's dye-binding sites are saturated, at which stage there is no increase in dye-binding concentration since the dye-binding sites are completely packed with dye molecules. Furthermore, as the concentration of those cationic dye in the wastewater increases, the dye adsorption efficiency decreases due to adsorption site saturation on the adsorbent's surface.

7.6 Effect of Pore Volume and Particle Size of Adsorbent

The pore volume of an adsorbent is essential in dye adsorption because it enables the most dye molecules to bind to it. The surface area of adsorbed materials is also affected by particle size, which has a significant impact on the adsorption process. Since ions will enter the pore structure of the adsorbent when the external surface area is high, the adsorption process is accelerated [155]. As the pore size of a porous material is greater than 1.7 times the size of the adsorbate molecule, repulsion between the adsorbate molecules increases dramatically, necessitating higher adsorption energies [156]. The most powerful pores are 1.7^{e6} times the size of the adsorbate molecule [157]. As a result, the dye sorption is governed by the pore capacity of the adsorbents rather than their surface area [158].

8 Dye Adsorption Isotherm and Kinetic Modeling

8.1 Dye Adsorption Isotherm Models

The Langmuir, Freundlich, and Temkin, models are the most popular isotherm models used to explain the adsorption of cationic dyes by adsorbent. They're useful for determining how dye molecules are dispersed at equilibrium on the solid adsorbent and in the liquid phases. Adsorption isotherms are used to describe the association of the dye molecule with the carbonaceous adsorbent, as well as adsorption equilibrium and the dye attaching active sites on the adsorbent [159]. The adsorption isotherm explains the volume of adsorbate on the carbonaceous adsorbent surface as a result of its amount at a constant temperature.

The best match for dye adsorption by adsorbents is determined by comparing the R^2 values obtained from the adsorption models. The affinity between the adsorbate and the adsorbent surface determines how well the adsorbate interacts with the adsorbent substance. The adsorption process starts until the adsorbate and adsorbent

come into contact, and continues until the adsorbate on the adsorbent surface and the adsorbate left in the aqueous solution enter equilibrium. The amount of adsorbate leaving the adsorbent surface at this point would be equal to the amount adsorbed to the adsorbent surface. The term “adsorption isotherm” refers to the phenomena that defines the adsorption processes between the adsorbate on the adsorbent surface (that is, adsorption number, Q_e) and the adsorbate in the aqueous phase (equilibrium concentration, C_e). By varying the quantity of adsorbent, the initial concentration of solute, and the volume of liquid, the number of adsorbate ions per unit mass of the adsorbent (Q_e) and the equilibrium concentration of the adsorbate remaining in the aqueous phase (C_e) can be obtained over a wide range. Equation: To determine the equilibrium metal uptake Q_e , use the following formula:

$$Q_e = \frac{(C_i - C_e)V}{m} \quad (1)$$

where V is the volume of the solution, C_i and C_e are initial and equilibrium concentrations, and m is the dry mass of adsorbent [160–162].

Isotherm models are used to fit the adsorption equilibrium data by plotting Q_e against C_e . Once the models fit the isotherm data, the adsorption properties such as maximum adsorption amount, affinity constant, thermodynamic parameters, and the mechanism of the adsorption can be obtained for the adsorption process. Such information allows the evaluation or prediction of the performance of the adsorption process and is useful to optimize the use of the adsorbent in its intended applications. The two widely used models for describing the experimental isotherm data were developed by renowned scientists namely Langmuir and Freundlich model [162, 163].

The Langmuir isotherm model

For monolayer adsorption onto a surface with a finite number of equivalent sorption sites, the Langmuir isotherm model is accurate. It is based on the premise that any adsorption site is equal, regardless of whether neighboring sites are occupied or not. The Langmuir model is based on four assumptions: all adsorption sites are equal and can only accommodate one molecule, the surface is energetically homogeneous and adsorbed molecules do not interact, there are no phase transitions, and at maximum adsorption, only a monolayer appears [160]. According to the Langmuir model, adsorption energy is constant and unchanged by surface coverage. When a monolayer of dye molecules covers the adsorption surface, maximum adsorption occurs. In the other hand, certain adsorbates adsorb on certain parts of the surface. The equation that represents the model is as follows:

$$\frac{C_e}{Q_e} = \frac{C_e}{Q_{\max}} + \frac{1}{Q_{\max}k_L} \quad (2)$$

k_L (L/g) is a constant related to adsorption power and energy of adsorption, and Q_{\max} (mg/g) is the maximal adsorption capacity equivalent to total monolayer coverage. The parameters representing the Langmuir model can be determined from the slope and intercept by plotting Ce/Q_e versus C_e .

The dimensionless separation factor, R_L , can be used to express the favorability of an adsorption mechanism as follows:

$$R_L = \frac{1}{1 + k_L C_o} \quad (3)$$

This shows that for favorable adsorption, $0 < R_L < 1$, while $R_L > 1$ represents unfavorable adsorption, $R_L = 1$ represents linear adsorption and $R_L = 0$ means the adsorption is irreversible.

The Freundlich isotherm model

The experimental Freundlich model also takes into account the adsorbent's monomolecular layer coverage of the solute. However, it is assumed that the adsorbent has a heterogeneous surface, with different binding sites.

The Freundlich Equation, which is strictly analytical and dependent on sorption on a heterogeneous surface, is:

$$Q_e = k_F (C_e)^{1/n} \quad (4)$$

The Freundlich Equation can be linearized in logarithmic form as expressed below:

$$\ln Q_e = \ln k_F + \frac{1}{n} \ln C_e \quad (5)$$

The Freundlich constants k_F (L/g) and n , which represent the adsorption potential and strength, respectively, are used. The Freundlich constants are calculated using experimental data and the intercept and slope of the linear plot of $\ln Q_e$ versus $\ln C_e$.

8.2 Adsorption Kinetic Models

Adsorption kinetics defines the solute uptake rate, which controls the residence time of adsorbate uptake at the liquid–solid interface, including the diffusion mechanism [148, 164]. The pseudo-first-order and pseudo-second-order models are commonly used kinetic models of adsorption [165].

Pseudo-first-order kinetic model

Lagergren [166] proposed a pseudo-first-order Equation based on significant potential for the sorption of a liquid/solid structure. It is assumed that the difference in

the saturation concentration and the volume of solid absorption with time is directly proportional to the rate of change of sorbate uptake with time. In liquid phase sorption, the Lagergren Equation is the most commonly used rate equation. The following is the pseudo-first-order rate model:

$$\log(Q_e - Q_t) = \log Q_e - \frac{k_1}{2.303}t \quad (6)$$

The Lagergren rate constant of adsorption is k_1 (min^{-1}), the maximum adsorption power is Q_e (mg/g), and the volume of adsorption at time t is Q_t (mg/g) (min). The intercepts and slope of the plot of $\log(Q_e - Q_t)$ versus t are used to evaluate the values of k_1 and Q_e [167].

Pseudo-second-order kinetic model

The pseudo-second-order kinetics is based on the premise that the rate-limiting step could be chemical sorption or chemisorption involving valance force by sharing or swapping electrons between the adsorbate and the adsorbent [167].

The sorption data were also studied by pseudo-second-order kinetic, which is expressed as follows:

$$\frac{t}{Q_t} = \frac{1}{k_2 Q_e^2} + \frac{t}{Q_e} \quad (7)$$

k_2 is the pseudo-second-order adsorption rate constant (g/mg min), and k_2 and Q_e were estimated from the intercepts and slope of the t/Q_t versus t plot.

9 Conclusion

The current study covers a wide range of adsorbents, including agricultural by-products, activated carbon derived from biomass, and biosorbents, all of which can be used directly, modified, processed, and extracted for the removal of cationic dyes from contaminated wastewater using adsorption technology. The number of studies in this field is on a daily basis, showing that this industry has a bright future. Because of its abundant availability, low cost, eco-friendly, and biodegradable material, agro-waste has drawn researchers for the development of environmental treatment systems. However, no comprehensive study of the efficacy of biosorbents and co-substrates, as well as related technical shortcomings such as additional carbon and color loading in bio-treated water, viability, and expense, has been undertaken to date. Agro-waste biomass (whether untreated or modified) has a high potential for extracting various dyes from an aqueous solution, according to a dye biosorption study. The biosorptive ability of porous biosorbents with cellulosic content and active surface functional

groups (such as hydroxyl, carbonyl, carboxyl, amino) for dyes has been demonstrated. Langmuir and pseudo-second-order models were used as dominant isotherm and kinetic models, respectively, to analyze the fundamental mechanism operative between the adsorbent and the adsorbate of the system. The majority of biosorption kinetic processes used a pseudo-second-order kinetic model, with adsorption equilibrium results that equally correlated monolayer or multilayer adsorption isotherms. Agricultural waste material performed much higher as an adsorbent as compared to other forms of adsorbents. When comparing sorbent materials, price is an important consideration. The cost of AC made from farm wastes is said to be poor as compared to other adsorbents. Furthermore, industrial wastes as a potential adsorbent have a greater adsorption ability than other adsorbents. This chapter shows that agricultural by-products can be used as powerful and affordable adsorbents in the near future for a wide variety of applications.

References

1. Amaike M, Yamamoto H (2006) Preparation of polypyrrole by emulsion polymerization using hydroxypropyl cellulose. *Pol J* 38:703–709
2. Roy M, Saha, R (2021) Dyes and their removal technologies from wastewater: a critical review. *Intell Environ Data Monit Pollut Manage* 127–160 (Elsevier). <https://doi.org/10.1016/b978-0-12-819671-7.00006-3>
3. Amer WA, Omran MM, Rehab AF, Ayad MM (2018) Acid green crystal-based in situ synthesis of polyaniline hollow nanotubes for the adsorption of anionic and cationic dyes †. <https://doi.org/10.1039/c8ra02236d>
4. Vijayakumar G, Tamilarasan R, Dharmendirakumar M (2011) Adsorption, Kinetic, Equilibrium and Thermodynamic studies on the removal of basic dye Rhodamine-B from aqueous solution by the use of natural adsorbent perlite. *J Mater Environ Sci* 3:157–170
5. Sharma V, Rekha P, Mohanty P (2016) Nanoporous hypercrosslinked polyaniline: an efficient adsorbent for the adsorptive removal of cationic and anionic dyes. *J Mol Liq* 222:1091–1100
6. Mishra S, Cheng L, Chemical AM-J (2020) The utilization of agro-biomass/byproducts for effective bio-removal of dyes from dyeing wastewater: a comprehensive review. (*Elsevier*)
7. Vikrant K et al (2018) Recent advancements in bioremediation of dye: current status and challenges. *Biores Technol* 253:355–367
8. Huang G, Wang W, Liu G (2015) Simultaneous chromate reduction and azo dye decolourization by *Lactobacillus paracase* CL1107 isolated from deep sea sediment. *J Environ Manage* 157:297–302
9. Mishra S, Maiti A (2020) Biological methodologies for treatment of textile wastewater. 77–107. https://doi.org/10.1007/978-3-030-38152-3_6
10. Gupta VK, Ali I, Saini VK (2007) Defluoridation of wastewaters using waste carbon slurry. *Water Res* 41:3307–3316
11. Gupta VK, Jain R, Varshney S, Saini VK (2007) Removal of Reactofix Navy Blue 2 GFN from aqueous solutions using adsorption techniques. *J Colloid Interface Sci* 307:326–332
12. Gupta VK, Mohan D, Suhas, Singh KP (2006) Removal of 2-aminophenol using novel adsorbents. *Ind Eng Chem Res* 45:1113–1122
13. Bushra R, Mohamad S, Alias Y, Jin Y, Ahmad M (2021) Current approaches and methodologies to explore the perceptive adsorption mechanism of dyes on low-cost agricultural waste: a review. *Microporous Mesoporous Mater* 319:111040
14. Gürses A, Güneş K, Şahin E (2021) Removal of dyes and pigments from industrial effluents. *Green Chem Water Rem Res Appl*. <https://doi.org/10.1016/b978-0-12-817742-6.00005-0>

15. Jagaba AH et al (2021) Sequencing batch reactor technology for landfill leachate treatment: a state-of-the-art review. *J Environ Manage* 282:111946
16. Jagaba AH et al (2021) A systematic literature review of biocarriers: Central elements for biofilm formation, organic and nutrients removal in sequencing batch biofilm reactor. *J Water Process Eng* 42:102178
17. Mustafa HM, Hayder G, Jagaba AH, Jagaba AH (2021) Microalgae: a renewable source for wastewater treatment and feedstock supply for biofuel generation. 11:7431–7444 ([researchgate.net](https://www.researchgate.net))
18. Lee J-W, Choi S-P, Thiruvenkatachari R, Shim W-G, Moon H (2005) Evaluation of the performance of adsorption and coagulation processes for the maximum removal of reactive dyes. (*Elsevier*). <https://doi.org/10.1016/j.dyepig.2005.03.008>
19. Vinu R, Madras G (2009) Kinetics of sonophotocatalytic degradation of anionic dyes with Nano-TiO₂. *Environ Sci Technol* 43:473–479
20. Ferreira AM, Coutinho JAP, Fernandes AM, Freire MG (2014) Complete removal of textile dyes from aqueous media using ionic-liquid-based aqueous two-phase systems. (*Elsevier*) <https://doi.org/10.1016/j.seppur.2014.02.036>
21. Güneş E, Dinçer AR, Gü Nes ḂY, Karakaya N, Gü Nes E (2006) Comparison of activated carbon and bottom ash for removal of reactive dye from aqueous solution Comparison of activated carbon and bottom ash for removal of reactive dye from aqueous solution. (*Elsevier*). <https://doi.org/10.1016/j.biortech.2006.03.009>
22. Tian X, Wu B, Li J (2008) The exploration of making acidproof fracturing proppants using red mud. *J Hazard Mater* 160:589–593
23. Kadirvelu K et al (2003) Utilization of various agricultural wastes for activated carbon preparation and application for the removal of dyes and metal ions from aqueous solutions. *Bioresour Technol* 87:129–132
24. Kadhom M, Albayati N, Alalwan H, Al-Furaiji M (2020) Removal of dyes by agricultural waste. *Sustain Chem Pharm* 16:100259
25. Robinson T, McMullan G, Marchant R, Nigam P, Remediation of dyes in textile e, uent: a critical review on current treatment technologies with a proposed alternative. (*Elsevier*). <https://www.sciencedirect.com/science/article/pii/S0960852400000808>
26. Ahmad A et al (2015) Recent advances in new generation dye removal technologies: novel search for approaches to reprocess wastewater. *RSC Adv* 5:30801–30818
27. Mishra S, Cheng L, Maiti A (2021) The utilization of agro-biomass/byproducts for effective bio-removal of dyes from dyeing wastewater: a comprehensive review. *J Environ Chem Eng* 9:104901
28. Patra BN, Majhi D (2015) Removal of anionic dyes from water by potash alum doped polyaniline: investigation of kinetics and thermodynamic parameters of adsorption. *J Phys Chem B* 119:8154–8164
29. Birniwa AH, Mahmud HNME (2019) Study on physico-mechanical behaviour of acacia nilotica (gum tree) and glass fiber blend reinforced epoxy resin composite. 10:46–53
30. Abdullahi SS, Birniwa AH, Chadi AS, Mohammad REA, Mamman S (2020) Effect of fiber surface modification on the mechanical properties of rice husk/glass fiber reinforcement epoxy resin hybrid composite. *Niger Res J Chem Sci* 8:147–162. <http://www.unn.edu.ng/nigerian-research-journal-of-chemical-sciences/>
31. Birniwa AH, Sa'ad Abdullahi S, Zango ZU, Ahmad F, Abdullahi MA (2021) Studies on physico-mechanical behaviour of sawdust/glass fiber reinforced epoxy hybrid composites. 2 (slujst.com.ng). <https://slujst.com.ng/index.php/jst/article/view/136>
32. Attallah O, Al-Ghobashy M, Nobsen, M., Salem MY (2016) Removal of cationic and anionic dyes from aqueous solution with magnetite/pectin and magnetite/silica/pectin hybrid nanocomposites: kinetic, isotherm and. (pubs.rsc.org)
33. Nasir Labaran A, Uba Zango Z, Armaya U, Garba ZN (2019) Rice husk as biosorbent for the adsorption of methylene blue. *Sci World J* 14
34. Funmilayo Babamale H, Uba Zango Z, Shehu Imam S, Ibrahim Muhammad A (2021) Environmental remediation view project removal of orange G dye from aqueous solution by adsorption: a short review. *J Environ Treat Tech* 9:318–327

35. Jagaba AH et al (2022) Kinetics of pulp and paper wastewater treatment by high sludge retention time activated sludge process 49(2)
36. Abdullahi SSA, Musa H, Habibu S, Birniwa AH, Mohammad REA (2022) Facile synthesis and dyeing performance of some disperse monomeric and polymeric dyes on nylon and polyester fabrics, *J Bull Chem Soc Ethiop.* 35:3:485–497
37. Jagaba AH, Kutty SRM, Noor A, Isah AS, Lawal IM, Birniwa AH, Usman AK, Kilaco AU, Abubakar S (2022) Kinetics of pulp and paper wastewater treatment by high sludge retention time activated sludge process. *J Hunan Univ Nat Sci* 49:2
38. Crini G, Ndongo Peindy H (2006) Adsorption of C.I. basic blue 9 on cyclodextrin-based material containing carboxylic groups. *Dye Pigment* 70:204–211
39. Mu B, Wang A (2016) Adsorption of dyes onto palygorskite and its composites: a review. *J Environ Chem Eng* 4:1274–1294
40. Karadag D et al (2007) Basic and reactive dye removal using natural and modified zeolites basic and reactive dye removal using natural and modified zeolites basic and reactive dye removal using natural and modified zeolites. *Artic J Chem Eng Data* 52:2436–2441
41. Abbas MN, Alalwan HA (2019) Catalytic oxidative and adsorptive desulfurization of heavy naphtha fraction. *Korean Chem Eng Res* 57:283–288
42. Iranifam M, Zarei M (2011) Decolorization of CI Basic Yellow 28 solution using supported ZnO nanoparticles coupled with photoelectro-Fenton process. (*Elsevier*)
43. Nidheesh PV, Gandhimathi R, Ramesh ST (2013) Degradation of dyes from aqueous solution by Fenton processes: a review. *Environ Sci Pollut Res* 20:2099–2132
44. Kaur H (2011) A review on applicability of naturally available adsorbents for the removal of hazardous dyes from aqueous waste. 183:151–195 (Springer)
45. Mohammed N, Grishkewich N, Berry RM, Tam KC (2015) Cellulose nanocrystal–alginate hydrogel beads as novel adsorbents for organic dyes in aqueous solutions. *Cellulose* 22:3725–3738
46. Kang S et al (2018) Removal of methylene blue from water with montmorillonite nanosheets/chitosan hydrogels as adsorbent. *Appl Surf Sci* 448:203–211
47. Asfaram A, Ghaedi M, Hajati S, Goudarzi A, Bazrafshan AA (2015) Simultaneous ultrasound-assisted ternary adsorption of dyes onto copper-doped zinc sulfide nanoparticles loaded on activated carbon: optimization by response surface methodology. *Spectrochim Acta Part A Mol Biomol Spectrosc* 145:203–212
48. Sartape A, Mandhare A, Jadhav V (2017) Removal of malachite green dye from aqueous solution with adsorption technique using *Limonia acidissima* (wood apple) shell as low cost adsorbent. (*Elsevier*)
49. Yonar ME, Yonar SM (2010) Changes in selected immunological parameters and antioxidant status of rainbow trout exposed to malachite green (*Oncorhynchus mykiss*, Walbaum, 1792). *Pestic Biochem Physiol* 97:19–23
50. Lellis B, Fávoro-Polonio CZ, Pamphile JA, Polonio JC (2019) Effects of textile dyes on health and the environment and bioremediation potential of living organisms. *Biotechnol. Res. Innov.* 3:275–290
51. Mani S, Bharagava RN (2016) Exposure to crystal violet, its toxic, genotoxic and carcinogenic effects on environment and its degradation and detoxification for environmental safety. *Rev Environ Contam Toxicol* 237:71–104
52. Ragab A, Ahmed I, Bader D (2019) The removal of brilliant green dye from aqueous solution using nano hydroxyapatite/chitosan composite as a sorbent. *Molecules* 24:847 (*mdpi.com*)
53. Li Q et al (2015) Removal of Rhodamine B from wastewater by modified *Volvariella volvacea*: batch and column study. *RSC Adv* 5:25337–25347
54. Jedynak K, Wideł D (2019) Removal of rhodamine b (a basic dye) and acid yellow 17 (an acidic dye) from aqueous solutions by ordered mesoporous carbon and commercial activated carbon. (*mdpi.com*)
55. Pradhananga RR et al (2017) Wool carpet dye adsorption on Nanoporous carbon materials derived from agro-product. 3:12. (*mdpi.com*)

56. Kodal SP, Aksu Z (2017) Cationic surfactant-modified biosorption of anionic dyes by dried *Rhizopus arrhizus*. *Environ Technol (United Kingdom)* 38:2551–2561
57. Sebeia N, Jabli M, Ghith A (2019) *Populus tremula*, *Nerium oleander* and *Pergularia tomentosa* seed fibers as sources of cellulose and lignin for the bio-sorption of methylene blue. (*Elsevier*)
58. Salleh MAM, Mahmoud DK, Karim WAWA, Idris A (2011) Cationic and anionic dye adsorption by agricultural solid wastes: a comprehensive review. *Desalination* 280:1–13
59. Das M, Samal AK, Mehar N (2020) *Butea monosperma* leaf as an adsorbent of methylene blue: recovery of the dye and reuse of the adsorbent. *Int J Environ Sci Technol* 17:2105–2112
60. Akar E, Altinişik A, Seki Y (2013) Using of activated carbon produced from spent tea leaves for the removal of malachite green from aqueous solution. *Ecol Eng* 52:19–27
61. Pradhan P (2020) Preparation and characterization of films from Chicken feathers for dye adsorption. (*Elsevier*)
62. Ebrahimiyan Pirbazari A, Saberikhah E, Badrouh M, Emami MS (2014) Alkali treated Foumanat tea waste as an efficient adsorbent for methylene blue adsorption from aqueous solution. *Water Resour Ind* 6:64–80
63. Samal K, Raj N, Mohanty K (2019) Saponin extracted waste biomass of *Sapindus mukorossi* for adsorption of methyl violet dye in aqueous system. *Surf Interfaces* 14:166–174
64. Bello OS et al (2020) Rhodamine B dye sequestration using *Gmelina aborea* leaf powder. *Heliyon* 6:e02872
65. Astuti W et al (2019) Thermal conversion of pineapple crown leaf waste to magnetized activated carbon for dye removal adsorption of [AuCl₄]-on ultrasonically and mechanical-stirring assisted Mg/Al-NO₃ hydrotalcite-magnetite. (*Elsevier*). <https://doi.org/10.1016/j.biotech.2019.121426>
66. Zaidi NAHM, Lim LBL, Usman A (2018) *Artocarpus odoratissimus* leaf-based cellulose as adsorbent for removal of methyl violet and crystal violet dyes from aqueous solution. *Cellulose* 25:3037–3049
67. Zaidi NAHM, Lim LBL, Usman A (2019) Enhancing adsorption of malachite green dye using base-modified *Artocarpus odoratissimus* leaves as adsorbents. 13:211–223
68. Dezhampannah H, Mohammad-Khah A, Aghajani, N (2013) Equilibrium and thermodynamic studies of thionine adsorption from aqueous solution onto rice husk. *Chem Bull* <https://citeseerx.ist.psu.edu/viewdoc/download?doi=10.1.1.832.4965&rep=rep1&type=pdf>
69. Madrakian T, Afkhami A, Ahmadi M (2012) Adsorption and kinetic studies of seven different organic dyes onto magnetite nanoparticles loaded tea waste and removal of them from wastewater samples. *Spectrochim Acta Part A Mol Biomol Spectrosc* 99:102–109
70. Leng Chew T, Husni H (2019) Oil palm frond for the adsorption of Janus Green dye. *Mater Today Proc* 16:1766–1771
71. Nagda GK, Ghole VS (2011) Removal of Janus Green dye from aqueous solution by phosphoric acid carbonized agro-industrial waste. 37:38 (*thaiscience.info*)
72. Da Silva LG et al (2011) Adsorption of Brilliant Red 2BE dye from water solutions by a chemically modified sugarcane bagasse lignin. *Chem Eng J* 168:620–628
73. Vieira AP et al (2011) Removal of textile dyes from aqueous solution by babassu coconut epicarp (*Orbignya speciosa*). *Chem Eng J* 173:334–340
74. Chan S-L, Tan YP, Abdullah AH, Ong S-T (2016) Equilibrium, kinetic and thermodynamic studies of a new potential biosorbent for the removal of basic blue 3 and Congo red dyes: Pineapple (*Ananas comosus*) plant stem. *J Taiwan Inst Chem Eng* 61:306–315
75. Kooh MRR, Dahri MK, Lim LBL (2017) Removal of the methyl violet 2B dye from aqueous solution using sustainable adsorbent *Artocarpus odoratissimus* stem axis. *Appl Water Sci* 7:3573–3581
76. Yu JX et al (2012) A situ co-precipitation method to prepare magnetic PMDA modified sugarcane bagasse and its application for competitive adsorption of methylene blue and basic magenta. *Bioresour Technol* 110:160–166
77. Oloo CM, Onyari JM, Wanyonyi WC, Wabomba JN, Muinde VM (2020) Adsorptive removal of hazardous crystal violet dye from aqueous solution using *Rhizophora mucronata* stem-barks: equilibrium and kinetics studies. *Environ Chem Ecotoxicol* 2:64–72

78. Sharma A, Sharma G, Kuma A, Siddiqi ZM, Pathania D (2016) Exclusion of organic dye using neoteric activated carbon prepared from *Cornulaca monacantha* stem: equilibrium and thermodynamics studies. *Mater Sci Forum* 875:1–15
79. Machrouhi A et al (2019) Statistical optimization of activated carbon from *Thapsia transtagana* stems and dyes removal efficiency using central composite design. *J Sci Adv Mater Devices* 4:544–553
80. Malekbala MR, Hosseini S, Kazemi Yazdi S, Masoudi Soltani S, Malekbala MR (2012) The study of the potential capability of sugar beet pulp on the removal efficiency of two cationic dyes. *Chem Eng Res Des* 90:704–712
81. Bello K, Sarojini K, Narayana B, Rao A, Byrappa K (2017) A study on adsorption behavior of newly synthesized banana pseudo-stem derived superabsorbent hydrogels for cationic and anionic dye removal from effluents. *Carbohydr Polym* 181:605–615
82. Hajjaligol S, Masoum S (2019) Optimization of biosorption potential of nano biomass derived from walnut shell for the removal of Malachite Green from liquids solution: experimental design approaches. *J Mol Liq* 286:110904
83. Deniz F, Kepekci RA (2017) Bioremoval of Malachite green from water sample by forestry waste mixture as potential biosorbent. 32:172–178 (*Elsevier*)
84. Yu M, Han Y, Li J, Wang L (2017) CO₂-activated porous carbon derived from cattail biomass for removal of malachite green dye and application as supercapacitors. *Chem Eng J* 317:493–502
85. Baek M-H, Olakitan Ijagbemi C, Kim D-S (2010) Removal of malachite green from aqueous solution using degreased coffee bean. *J Hazard Mater* 176:820–828
86. Mashkoo F, Nasar A (2019) Preparation, characterization and adsorption studies of the chemically modified *Luffa aegyptica* peel as a potential adsorbent for the removal of malachite green from aqueous solution. *J Mol Liq* 274:315–327
87. Uma, Banerjee S, Sharma YC (2013) Equilibrium and kinetic studies for removal of malachite green from aqueous solution by a low cost activated carbon. *J Ind Eng Chem* 19:1099–1105
88. Saeed A, Sharif M, Iqbal M (2010) Application potential of grapefruit peel as dye sorbent: Kinetics, equilibrium and mechanism of crystal violet adsorption. *J Hazard Mater* 179:564–572
89. Nethaji S, Sivasamy A, Thennarasu G, Saravanan S (2010) Adsorption of Malachite Green dye onto activated carbon derived from *Borassus aethiopicum* flower biomass. *J Hazard Mater* 181:271–280
90. Shakoor S, Nasar A (2016) Removal of methylene blue dye from artificially contaminated water using citrus limetta peel waste as a very low cost adsorbent. *J Taiwan Inst Chem Eng* 66:154–163
91. Eltaweil AS, Ali Mohamed H, Abd El-Monaem EM, El-Subruiti GM (2020) Mesoporous magnetic biochar composite for enhanced adsorption of malachite green dye: Characterization, adsorption kinetics, thermodynamics and isotherms. *Adv Powder Technol* 31:1253–1263
92. Chen S et al (2019) Study on the adsorption of dyestuffs with different properties by sludge-rice husk biochar: adsorption capacity, isotherm, kinetic, thermodynamics and mechanism. *J Mol Liq* 285:62–74
93. Kuntari K (2018) Utilization of bamboo leaves wastes for methylene blue dye adsorption. 2026:020062 (*aip.scitation.org*)
94. Susial P, Perez Peña P (2013) Preparation of activated carbons from banana leaves by chemical activation with phosphoric acid. adsorption of methylene blue. (*Redalyc*) <http://www.redalyc.org/articulo.oa?id=62029966021>
95. Krishni RR, Foo KY, Hameed BH (2014) Adsorptive removal of methylene blue using the natural adsorbent-banana leaves. *Desalin Water Treat* 52:6104–6112
96. Fiaz R, Hafeez M, Mahmood R (2019) *Ficus palmata* leaves as a low-cost biosorbent for methylene blue: thermodynamic and kinetic studies. *Water Environ Res* 91:689–699
97. Nooraee Nia N, Rahmani M, Kaykhaii M, Sasani M (2017) Evaluation of eucalyptus leaves as an adsorbent for decolorization of Methyl Violet (2B) dye in contaminated waters: thermodynamic and Kinetics model. *Model Earth Syst Environ* 3:825–829

98. Heydari S, Zaryabi MH, Ghiassi H (2019) Statistical optimization of removal of safranin dye from aqueous system using biosorbent obtained from leaves of *phlomis cancellata bunge* by response surface methodology. *Iranian Chem Soc Anal Bioanal Chem* 6. <https://iranjournals.nlai.ir/handle/123456789/99409>
99. Vyavahare GD et al (2018) Response surface methodology optimization for sorption of malachite green dye on sugarcane bagasse biochar and evaluating the residual dye for phyto and cytogenotoxicity. *Chemosphere* 194:306–315
100. Bello O, Agarry SE, Bello OS, Ahmad MA, Ahmad N (2012) Adsorptive features of banana (*Musa paradisiaca*) stalk-based activated carbon for malachite green dye removal Related papers Ackee apple (*Blighia sapida*) seeds: a novel adsorbent for the removal of Congo Red dye. *Chem Ecol* 28:153–167
101. El-Maghraby A, Taha NA (2014) Equilibrium and kinetic studies for the removal of cationic dye using banana pith. *Adv Environ Res* 3:217–230
102. Hameed BH, Mahmoud DK, Ahmad AL (2008) Sorption equilibrium and kinetics of basic dye from aqueous solution using banana stalk waste. *J Hazard Mater* 158:499–506
103. Vargas, V. H., Paveglio, R. R., Pauletto, P. de S., Salau, N. P. G. & Dotto, L. G. Sisal fiber as an alternative and cost-effective adsorbent for the removal of methylene blue and reactive black 5 dyes from aqueous solutions. *Chem. Eng. Commun.* **207**, 523–536 (2020).
104. Thi N, Hanh H (2020) Sorption of methylene blue in aqueous solutions by adsorption material from bagasse. *7:11572–11578*
105. Namasivayam C, Kanchana N, Yamuna RT (1993) Waste banana pith as adsorbent for the removal of rhodamine-B from aqueous solutions. *Waste Manag* 13:89–95
106. Zhang Z, O'Hara IM, Kent GA, Doherty WOS (2013) Comparative study on adsorption of two cationic dyes by milled sugarcane bagasse. *Ind Crops Prod* 42:41–49
107. de Sousa AÉA et al (2014) Adsorption of safranin on pseudostem banana fibers. *Sep Sci Technol* 49:2681–2688
108. Ma M et al (2020) Effective removal of cation dyes from aqueous solution using robust cellulose sponge. *J Saudi Chem Soc* 24:915–924
109. Amel K, Hassen MA, Kerroum D (2012) Isotherm and kinetics study of biosorption of cationic dye onto banana peel. *Energy Procedia* 19:286–295
110. Ma J (2015) Adsorption of methylene blue and Orange II pollutants on activated carbon prepared from banana peel. *J Porous Mater* 22:301–311
111. Gautam, S. & Khan, S. H. removal of methylene blue from waste water using banana peel as adsorbent. (*ijset.net*) www.ijset.net.
112. Hashem FS, Amin MS, Hashem F, Amin M (2016) Adsorption of methylene blue by activated carbon derived from various fruit peels removal of some heavy metals and organic dyes pollutants using activated carbon derivatives from fruits husks. *Des WatTreat.* 57:22573–22584
113. Kong W, Highly adsorptive mesoporous carbon from biomass using molten-salt route. (*Springer*)
114. Nowicki P, Kazmierczak-Razna J, Pietrzak R (2016) Physicochemical and adsorption properties of carbonaceous sorbents prepared by activation of tropical fruit skins with potassium carbonate. *Mater Des* 90:579–585
115. Seshadri S, Sugumaran P, Priya Susan V, Ravichandran P, Seshadri S (2012) Production and characterization of activated carbon from banana empty fruit bunch and *Delonix regia* Fruit Pod. *J Sustain Energy Environ* 3. <https://www.researchgate.net/publication/236694681>
116. Aruna, Bagotia N, Sharma AK, Kumar S (2021) A review on modified sugarcane bagasse biosorbent for removal of dyes. *Chemosphere* 268
117. Lu YC, Priyantha N, Lim LBL (2020) *Ipomoea aquatica* roots as environmentally friendly and green adsorbent for efficient removal of Auramine O dye. *Surf Interfaces* 20:100543
118. Fan H, Ma Y, Wan J, Pollution YW-ES (2020) Removal of gentian violet and rhodamine B using banyan aerial roots after modification and mechanism studies of differential adsorption behaviors

119. Ren H, Zhang R, Wang Q, Pan H, Wang Y (2016) Garlic root biomass as novel biosorbents for malachite green removal: Parameter optimization, process kinetics and toxicity test. *Chem Res Chinese Univ* 32:647–654
120. Beakou BH, El Hassani K, Houssaini MA, Belbahloul M, Oukani E, Anouar A (2017) A novel biochar from Manihot esculenta Crantz waste: application for the removal of Malachite Green from wastewater and optimization of the adsorption process. (*iwaponline.com*) <https://doi.org/10.2166/wst.2017.332>
121. Tavlieva MP, Genieva SD, Georgieva VG, Vlaev LT (2013) Kinetic study of brilliant green adsorption from aqueous solution onto white rice husk ash. *J Colloid Interface Sci* 409:112–122
122. Sharma G et al (2019) Honeycomb structured activated carbon synthesized from Pinus roxburghii cone as effective bioadsorbent for toxic malachite green dye. *J Water Process Eng* 32:100931
123. Murthy T, Gowrishankar B (2019) Studies on batch adsorptive removal of malachite green from synthetic wastewater using acid treated coffee husk: equilibrium, kinetics and thermodynamic studies. (*Elsevier*)
124. Shakoor S, Nasar A (2018) Adsorptive decontamination of synthetic wastewater containing crystal violet dye by employing Terminalia arjuna sawdust waste. *Groundw Sustain Dev* 7:30–38
125. Ahmed M, Mashkoor F, Nasar A (2020) Development, characterization, and utilization of magnetized orange peel waste as a novel adsorbent for the confiscation of crystal violet dye from aqueous solution. *Groundw Sustain Dev* 10:100322
126. Subramanian R, Kumar Ponnusamy S (2015) Novel adsorbent from agricultural waste (cashew NUT shell) for methylene blue dye removal: optimization by response surface methodology. *Water Resour Ind* 11:64–70
127. Aichour A, Zaghouane-Boudiaf H (2019) Highly brilliant green removal from wastewater by mesoporous adsorbents: Kinetics, thermodynamics and equilibrium isotherm studies. *Microchem J* 146:1255–1262
128. Chen X et al (2019) Effective removal of methyl orange and rhodamine B from aqueous solution using furfural industrial processing waste: Furfural residue as an eco-friendly biosorbent. *Colloids Surfaces Physicochem Eng Asp* 583:123976
129. Nasrullah A et al (2019) Mangosteen peel waste as a sustainable precursor for high surface area mesoporous activated carbon: Characterization and application for methylene blue removal. *J Clean Prod* 211:1190–1200
130. Kowalkowska A, Józwiak T (2019) Utilization of pumpkin (Cucurbita pepo) seed husks as a low-cost sorbent for removing anionic and cationic dyes from aqueous solutions. (*deswater.com*) <https://doi.org/10.5004/dwt.2019.24761>
131. Kallel F et al (2016) Sorption and desorption characteristics for the removal of a toxic dye, methylene blue from aqueous solution by a low cost agricultural by-product. *J Mol Liq* 219:279–288
132. de Hoyos-Martinez P, Merle J, Labidi J, Charrier-El Bouhtoury F (2019) Tannins extraction: a key point for their valorization and cleaner production tannins ex-traction: a key point for their valorization and cleaner production. *J Clean Prod* 206
133. Hou Y et al (2019) Hydrothermal conversion of bamboo shoot shell to biochar: Preliminary studies of adsorption equilibrium and kinetics for rhodamine B removal. *J Anal Appl Pyrolysis* 143:104694
134. Wu J, Yang J, Huang G, Xu C, Lin B (2020) Hydrothermal carbonization synthesis of cassava slag biochar with excellent adsorption performance for Rhodamine B. *J Clean Prod* 251:119717
135. Kushwaha AK, Gupta N, Chattopadhyaya MC (2014) Removal of cationic methylene blue and malachite green dyes from aqueous solution by waste materials of Daucus carota. *J Saudi Chem Soc* 18:200–207
136. Gupta N, Kushwaha AK, Chattopadhyaya MC (2016) Application of potato (Solanum tuberosum) plant wastes for the removal of methylene blue and malachite green dye from aqueous solution. *Arab J Chem* 9:S707–S716

137. Siddiqui SH (2018) The removal of Cu^{2+} , Ni^{2+} and Methylene Blue (MB) from aqueous solution using Luffa Actangula Carbon: Kinetics, thermodynamic and isotherm and response methodology. *Groundw Sustain Dev* 6:141–149
138. Tang Y et al (2019) Adsorption performance and mechanism of methylene blue by H_3PO_4 -modified corn stalks. *J Environ Chem Eng* 7:103398
139. Akköz Y, Coşkun R, Delibaş A (2019) Preparation and characterization of sulphonated bio-adsorbent from waste hawthorn kernel for dye (MB) removal. *J Mol Liq* 287:110988
140. Markovi S et al (2015) Application of raw peach shell particles for removal of methylene blue. 3:16–724 (*Elsevier*)
141. Belala Z, Jeguirim M, Belhachemi M, Addoun F, Trouvé G (2011) Biosorption of basic dye from aqueous solutions by date stones and palm-trees waste: Kinetic, equilibrium and thermodynamic studies. (*Elsevier*). <https://doi.org/10.1016/j.desal.2010.12.009>
142. Hameed BH, Nasuha N, Hameed BH (2011) Adsorption of methylene blue from aqueous solution onto NaOH-modified rejected tea. Want more papers like this? Adsorption of methylene blue from aqueous solution onto NaOH-modified rejected tea. *Acad Chem Eng J* 166:783–786
143. Han R et al (2010) Characterization of modified wheat straw, kinetic and equilibrium study about copper ion and methylene blue adsorption in batch mode. *Carbohydr Polym* 79:1140–1149
144. Bhatnagar A, Jain A, Gupta (2003) VA comparative assessment of adsorbents prepared from industrial wastes for the removal of cationic dye. (*diva-portal.org*)
145. Han R et al (2007) Biosorption of methylene blue from aqueous solution by fallen phoenix tree's leaves. *J Hazard Mater* 141:156–162
146. Saifuddin MN, Kumaran P (2005) Removal of heavy metal from industrial wastewater using chitosan coated oil palm shell charcoal. (*scielo.conicyt.cl*)
147. El-Said AG, Badawy NA, Garamon SE (2012) Adsorption of cadmium (II) and mercury (II) onto natural adsorbent rice husk ash (RHA) from aqueous solutions: study in single and binary system. *Int J Chem*
148. Azouaou N, Sadaoui Z, Djaafri A, Mokaddem H (2010) Adsorption of cadmium from aqueous solution onto untreated coffee grounds: equilibrium, kinetics and thermodynamics. *J Hazard Mater* 184:126–134
149. Birniwa AH, Abubakar AS, Huq AKO, Mahmud HNME (2021) Polypyrrole-polyethyleneimine (PPy-PEI) nanocomposite: an effective adsorbent for nickel ion adsorption from aqueous solution. *J Macromol Sci Part A Pure Appl Chem* 58:206–217
150. Martínez M et al (2006) Removal of lead(II) and cadmium(II) from aqueous solutions using grape stalk waste. *J Hazard Mater* 133:203–211
151. Montazer-Rahmati MM, Rabbani P, Abdolali A, Keshkar AR (2011) Kinetics and equilibrium studies on biosorption of cadmium, lead, and nickel ions from aqueous solutions by intact and chemically modified brown algae. *J Hazard Mater* 185:401–407
152. Wang S, Boyjoo Y, Choueib A, Zhu ZH (2005) Removal of dyes from aqueous solution using fly ash and red mud. *Water Res* 39:129–138
153. Olatunji MA, Khandaker MU, Mahmud HNME, Amin YM (2015) Influence of adsorption parameters on cesium uptake from aqueous solutions- a brief review. *RSC Adv* 5:71658–71683
154. Mukhopadhyay M, Noronha SB, Suraishkumar GK (2007) Kinetic modeling for the biosorption of copper by pretreated *Aspergillus niger* biomass. *Bioresour Technol* 98:1781–1787
155. Stejskal J, Trchová M (2018) Conducting polypyrrole nanotubes: a review. *Chem Pap* 72:1563–1595
156. Ekramul HNM, Obidul Huq AK, Rosiyah Y (2016) The removal of heavy metal ions from wastewater/aqueous solution using polypyrrole-based adsorbents: a review. *RSC Adv* 6:14778–14791
157. Branton P, Bradley RH, Bradley RH (2011) Effects of active carbon pore size distributions on adsorption of toxic organic compounds. *Adsorption* 17:293–301
158. Hassan MM, Carr CM (2021) Biomass-derived porous carbonaceous materials and their composites as adsorbents for cationic and anionic dyes: a review. *Chemosphere* 265:129087

159. Cao C et al, In situ preparation of magnetic Fe₃O₄/chitosan nanoparticles via a novel reduction–precipitation method and their application in adsorption of reactive azo dye ()
160. Langmuir I (1918) The adsorption of gases on plane surfaces of glass, mica and platinum. *J Am Chem Soc* 40:1361–1403
161. Shen W et al (2009) Adsorption of Cu(II) and Pb(II) onto diethylenetriamine-bacterial cellulose. *Carbohydr Polym* 75:110–114
162. Foo KY, Hameed BH (2010) Insights into the modeling of adsorption isotherm systems. *Chem Eng J* 156:2–10
163. Juang RS, Tseng RL, Wu FC, Lin SJ (1996) Use of chitin and chitosan in lobster shell wastes for color removal from aqueous solutions. *J Environ Sci Heal—Part A Toxic/Hazardous Subst Environ Eng* 31:325–338
164. Olatunji MA, Khandaker MU, Mahmud HNME (2018) Adsorption kinetics, equilibrium and radiation effect studies of radioactive cesium by polymer-based adsorbent. *J Vinyl Addit Technol* 24:347–357
165. Tseng RL, Wu FC, Juang RS (2010) Characteristics and applications of the Lagergren's first-order equation for adsorption kinetics. *J Taiwan Inst Chem Eng* 41:661–669
166. Lagergren S (1898) Zur theorie der sogenannten adsorption gelöster stoffe
167. Ho YS, McKay G (1999) Comparative sorption kinetic studies of dye and aromatic compounds onto fly ash. *J Environ Sci Heals Part A Toxic/Hazardous Subst Environ Eng* 34:1179–1204 (1999)
168. Jagaba AH, Kutty SRM, Hayder G, Baloo L, Noor A, Yaro NSA, Saeed AAH, Lawal IM, Birniwa AH, Usman AK (2021) A systematic literature review on waste-to-resource potential of palm oil clinker for sustainable engineering and environmental applications. *Mater* 14(16):4456
169. Jagaba AH, Kutty SRM, Salih GH, Noor A, Md Hafiz MFUB, Yaro NSA, Saeed AAH, Lawal IM, Birniwa AH, Kilaco AU (2021) Palm oil clinker as a waste by-product: utilization and circular economy potential. <https://doi.org/10.5772/intechopen.97312>
170. Birniwa AH, Abdullahi SSA, Yakasai MY, Ismaila A (2021). Studies on physico-mechanical behaviour of kenaf/glass fiber reinforced epoxy hybrid composites. *Bull Chem Soc Ethiop* 35(1):171–184

Application of Aromatic-Based Synthetic Macromolecules in Textile Wastewater



Jumina, Yehezkiel Steven Kurniawan, and Anggit Fitria

1 Introduction

Dyes and pigments are indispensable day-to-day essentials in human activity since dyes and pigments play pivotal roles especially for textile industries, cosmetic formulations, leather processing, paper and paint manufacturing, and plastic production [96, 110]. In 2015, the annual world production of dyes and pigments reached 700,000 tonnes. However, the estimated amount of leaked dyes and pigments during the industrial processes yielding up to 15% of dyes and pigments in the textile wastewater, amounting to 105,000 tonnes/year, which represent a significant potential bio-hazard [4]. The textile industry, for example, produces a large amount of liquid waste that contains synthetic dyes which are inevitable because not all colors remain attached to the textiles. The resulting textile wastewater is not readily biodegradable, thus, textile wastewater becomes a serious health threat to the environment and human life [30, 40].

Synthetic dyes are categorized as toxic and create potentially carcinogenic waste [67]. In the long-term exposure, there will be a definite possibility for human contamination, which can cause respiratory and skin problems. Other symptoms that can be experienced include itching, watery eyes, sneezing, asthma symptoms, skin irritation, and nasal congestion [40]. Additionally, synthetic dyes significantly damage the aesthetic quality of water bodies, as well as increase biochemical and chemical

Jumina (✉) · Y. S. Kurniawan · A. Fitria
Department of Chemistry, Faculty of Mathematics and Natural Sciences, Universitas Gadjah
Mada, Sekip Utara Bulaksumur, Yogyakarta 55281, Indonesia
e-mail: jumina@ugm.ac.id

Y. S. Kurniawan
e-mail: yehezkiel.steven.k@mail.ugm.ac.id

A. Fitria
e-mail: anggit.fitria@mail.ugm.ac.id

oxygen requirements. Furthermore, synthetic dyes inhibit plant growth, damage the food chain, and cause bioaccumulation of toxins, which will increase toxicity, mutagenicity and carcinogenicity in living organisms. Therefore, serious attention should be given to textile wastewater treatment [2].

2 Synthetic Dyes

Several synthetic dyes have been widely applied in textile industries. Synthetic dyes are mainly produced from aromatic hydrocarbons derived from coals and crude oils through a petrochemical process [41]. Several functional groups such as nitro, nitroso, cyano, azo, anthraquinone, and phthalocyanine are introduced as a chromophore to give strong absorption signals at visible light region (400–800 nm). Therefore, synthetic dyes gave a stronger color intensity and higher chemical stability than natural dyes [67].

In general, synthetic dyes can be categorized into two major classes, i.e. cationic and anionic dyes according to their charges. On the other hand, synthetic dyes can be categorized also according to the generated color in the solution such as red, yellow, orange, black, brown, violet, blue, and green. The commonly used red synthetic dyes are acid scarlet 3R, alizarin red S, basic fuchsin, butyl rhodamine B, congo red, eosin-y, methyl red, neutral red, rhodamine 6G, rhodamine B, rose bengal, and safranin T. The chemical structures of red synthetic dyes are shown in Fig. 1. The commonly used yellow and orange synthetic dyes are acid orange 5, acridine orange, auramine O, metanil yellow, methyl orange, Orange I, Orange II, reactive yellow 42, and titan yellow [36]. The chemical structures of yellow and orange synthetic dyes are shown in Fig. 2.

The commonly used black, brown, and violet synthetic dyes are Bismarck brown Y, crystal violet, direct black 38, direct violet 51, methyl violet, reactive black 5, and reactive black 45. The chemical structures of black, brown, and violet synthetic dyes are shown in Fig. 3. The commonly used blue and green synthetic dyes are brilliant green, bromophenol blue, Chicago sky blue 6B, direct blue 15, direct blue 71, Evans blue, malachite green, methyl green, methylene blue, reactive blue 19, toluidine blue, and Victoria blue B [36]. The chemical structures of blue and green synthetic dyes are shown in Fig. 4. Meanwhile, the molecular formulas and molecular weights of synthetic dyes are listed in Table 1.

The existence of synthetic dyes can be easily detected according to the generated colors since the synthetic dyes are highly stable and give a strong colored solution even at a concentration below 1 mg L^{-1} [41]. The potential for water pollution becomes worse because almost all synthetic dyes are rapidly soluble at high concentrations in the water [110]. Consequently, water pollution has become a global problem and textile wastewater treatment must be carefully considered for a sustainable future [8, 66]. The easiest way to prevent water pollution is an efficient textile wastewater treatment, thus, the discharge of synthetic textiles to the main streams can be suppressed [116].

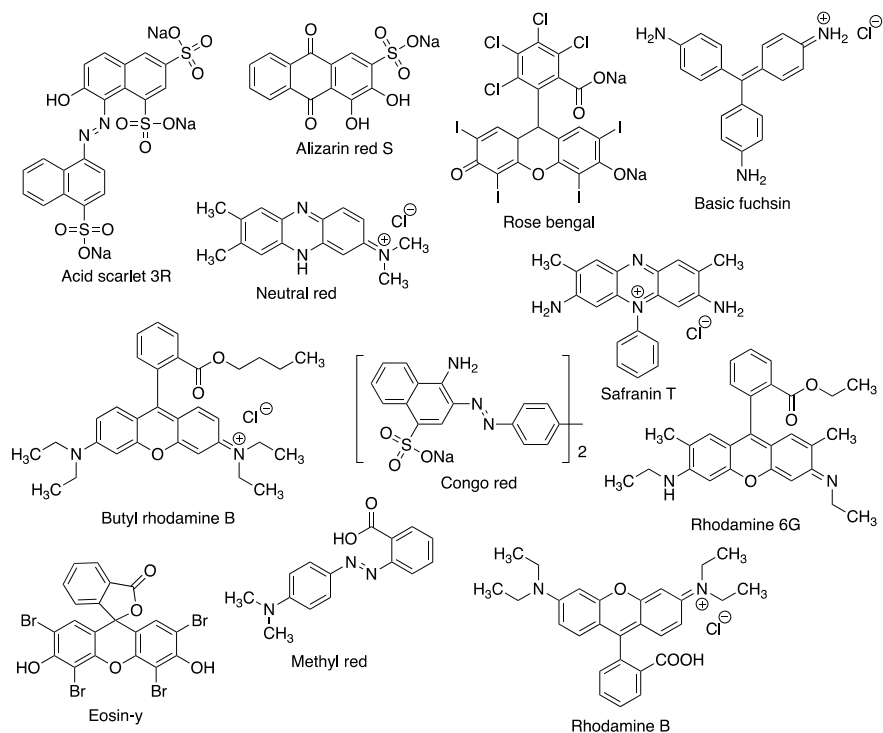


Fig. 1 The chemical structures of red synthetic dyes, i.e. acid scarlet 3R, alizarin red S, basic fuchsin, butyl rhodamine B, congo red, eosin-y, methyl red, neutral red, rhodamine 6G, rhodamine B, rose bengal, and safranin T

A number of textile wastewater treatment technologies have been introduced and developed such as adsorption, coagulation, precipitation, membrane filtration, photocatalysis, and bioremediation [2, 5, 7, 13, 31, 48, 64, 97, 102]. Among these technologies, adsorption is the simplest, cheapest, and most convenient technique for a large-scale process [2]. The adsorption process is a mass transfer phenomenon in which the adsorbate (in this case, synthetic dyes) accumulates on the surface of the adsorbent materials [21, 114]. Ideal adsorbent materials should have a high maximum adsorption capacity (q_{\max}), a high selectivity, and an easy regeneration process [22]. Among the hundreds of adsorbent materials, aromatic-based synthetic macromolecules such as calixarenes and carbon nanotubes nearly fulfil all of the mentioned requirements; thus, an ideal adsorption process can be established for a real textile wastewater treatment [99, 129, 131].

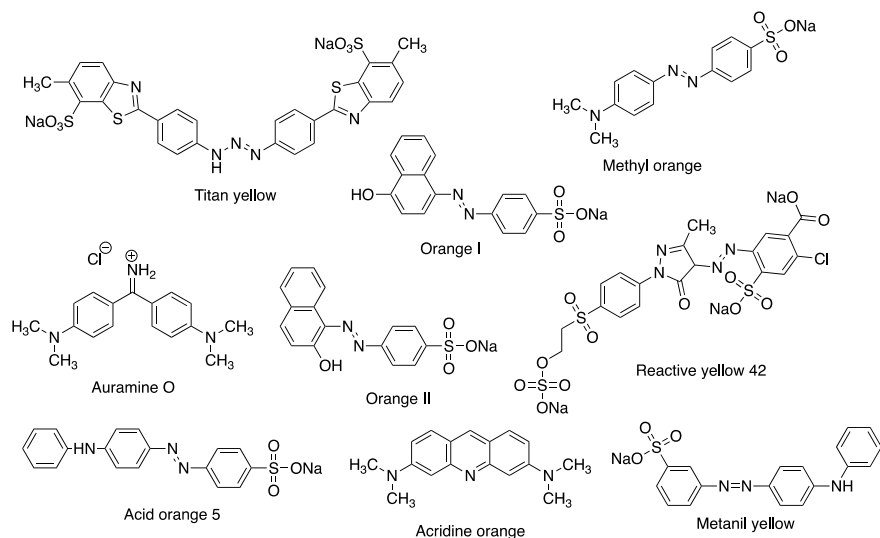


Fig. 2 Chemical structures of yellow and orange synthetic dyes, i.e. acid orange 5, acridine orange, auramine O, metanil yellow, methyl orange, Orange I, Orange II, reactive yellow 42, and titan yellow

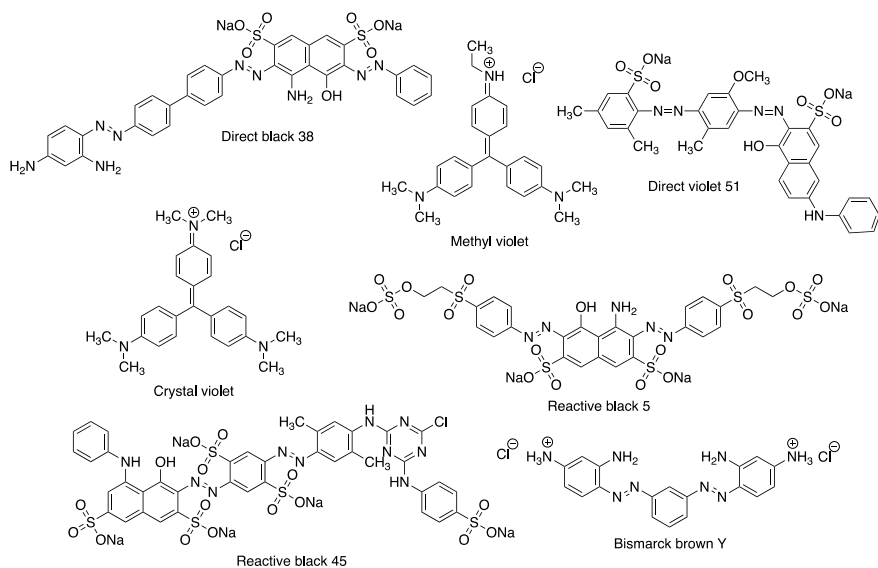


Fig. 3 Chemical structures of black, brown, and violet synthetic dyes, i.e. Bismarck brown Y, crystal violet, direct black 38, direct violet 51, methyl violet, reactive black 5, and reactive black 45

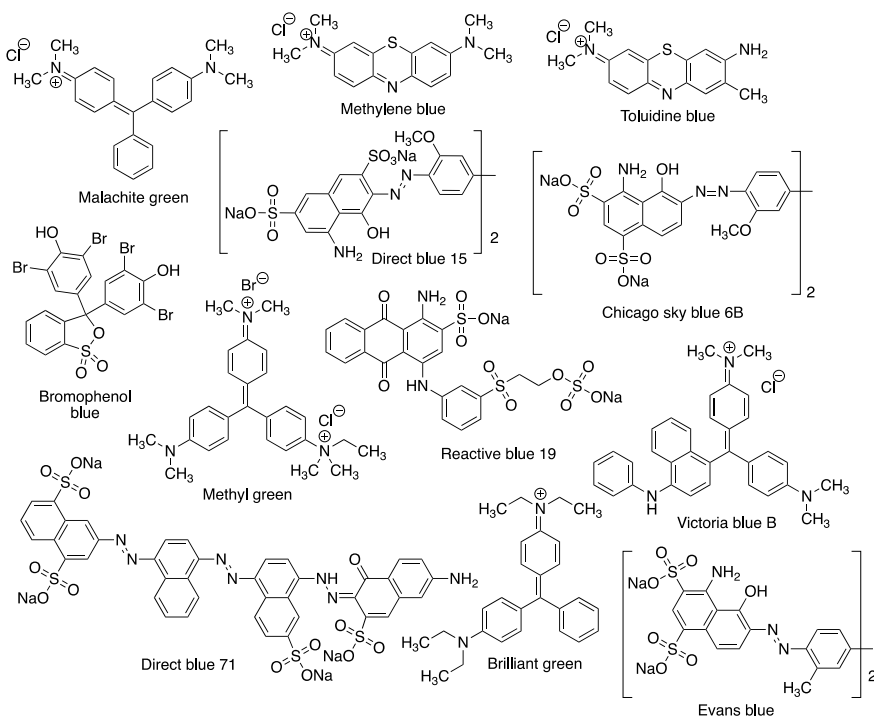


Fig. 4 Chemical structures of blue and green synthetic dyes, i.e. brilliant green, bromophenol blue, Chicago sky blue 6B, direct blue 15, direct blue 71, Evans blue, malachite green, methyl green, methylene blue, reactive blue 19, toluidine blue, and Victoria blue B

3 Aromatic-Based Synthetic Macromolecules

3.1 Calixarenes

Calixarenes are macrocyclic host compounds exhibiting unique and selective molecular discrimination abilities [88]. Calixarenes belong to the third generation of supramolecules after crown ether and cyclodextrin [25]. The general structure of calixarene is shown in Fig. 5. Extensive attention is focused on the research of calixarenes because of their gram-scale synthesis process, easy chemical modification, excellent selectivity, rigid chemical scaffold, and high stability [44]. Furthermore, calixarenes are able to interact with the guest compounds through electrostatic, hydrogen bonding, and π - π stacking interactions [60].

The first synthesis of calixarene was reported by A. von Bayer in 1872 and then about a century later, C.D. Gutsche coined the term of calixarene in 1970 [106]. From that year, the calixarene era was started and calixarenes have been widely applied in separation science, catalytic reaction, chemosensors, drug delivery agent, electronic material, and membrane polymers [61, 62, 65, 105, 113, 128]. These

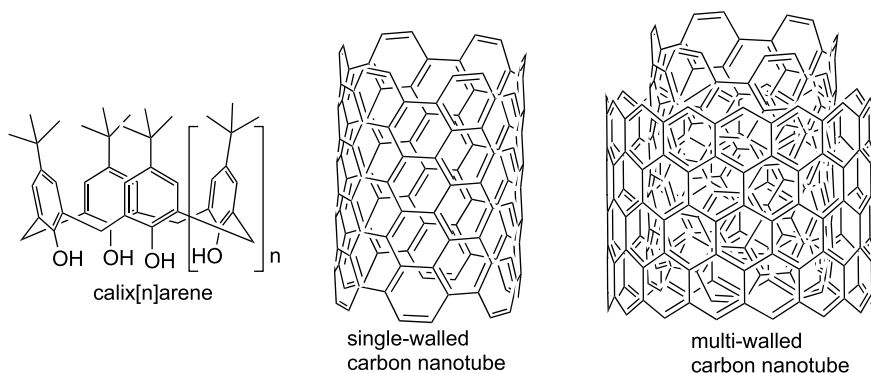
Table 1 Commonly used synthetic dyes over the past several years

No.	Name	Molecular formula	Molecular weight (g mol ⁻¹)
1	Acid orange 5	C ₁₈ H ₁₄ N ₃ NaO ₃ S	375.38
2	Acid scarlet 3R	C ₂₀ H ₁₁ N ₂ Na ₃ O ₁₀ S ₃	604.47
3	Acridine orange	C ₁₇ H ₁₉ N ₃	265.35
4	Alizarin red S	C ₁₄ H ₇ NaO ₇ S	342.26
5	Auramine O	C ₁₇ H ₂₂ ClN ₃	303.83
6	Basic fuchsin	C ₁₉ H ₁₈ ClN ₃	323.82
7	Bismarck brown Y	C ₁₈ H ₂₀ ClN ₈	419.31
8	Brilliant green	C ₂₇ H ₃₄ N ₂ O ₄ S	482.63
9	Bromophenol blue	C ₁₉ H ₁₀ Br ₄ O ₅ S	669.96
10	Butyl rhodamine B	C ₃₂ H ₃₉ ClN ₂ O ₃	535.12
11	Chicago sky blue 6B	C ₃₄ H ₂₄ N ₆ Na ₄ O ₁₆ S ₄	992.80
12	Congo red	C ₃₂ H ₂₂ N ₆ Na ₂ O ₆ S ₂	696.66
13	Crystal violet	C ₂₅ H ₃₀ ClN ₃	407.98
14	Direct black 38	C ₃₄ H ₂₅ N ₉ Na ₂ O ₇ S ₂	781.70
15	Direct blue 15	C ₃₄ H ₂₄ N ₆ Na ₄ O ₁₆ S ₄	992.80
16	Direct blue 71	C ₄₀ H ₂₃ N ₇ Na ₄ O ₁₃ S ₄	1029.9
17	Direct violet 51	C ₃₂ H ₂₇ N ₅ Na ₂ O ₈ S ₂	719.70
18	Eosin-y	C ₂₀ H ₆ Br ₄ Na ₂ O ₅	691.86
19	Evans blue	C ₃₄ H ₂₄ N ₆ Na ₄ O ₁₄ S ₄	960.81
20	Malachite green	C ₂₃ H ₂₅ ClN ₂	364.91
21	Metanil yellow	C ₁₈ H ₁₄ N ₃ NaO ₃ S	375.38
22	Methyl green	C ₂₇ H ₃₅ BrClN ₃	458.47
23	Methyl orange	C ₁₄ H ₁₄ N ₃ NaO ₃ S	327.33
24	Methyl red	C ₁₅ H ₁₅ N ₃ O ₂	269.30
25	Methyl violet	C ₂₄ H ₂₈ ClN ₃	407.99
26	Methylene blue	C ₁₆ H ₁₈ ClN ₃ S	319.85
27	Neutral red	C ₁₅ H ₁₇ ClN ₄	288.78
28	Orange I	C ₁₆ H ₁₁ N ₂ NaO ₄ S	350.30
29	Orange II	C ₁₆ H ₁₁ N ₂ NaO ₄ S	350.32
30	Reactive black 5	C ₂₆ H ₂₁ N ₅ Na ₄ O ₁₉ S ₆	991.80
31	Reactive black 45	C ₃₉ H ₂₆ ClN ₁₀ Na ₅ O ₁₆ S ₅	1201.4
32	Reactive blue 19	C ₂₂ H ₁₆ N ₂ Na ₂ O ₁₁ S ₃	626.50
33	Reactive yellow 42	C ₁₉ H ₁₄ ClN ₄ Na ₃ O ₁₂ S ₃	690.94
34	Rhodamin 6G	C ₂₈ H ₃₁ N ₂ O ₃ Cl	479.01
35	Rhodamine B	C ₂₈ H ₃₁ ClN ₂ O ₃	479.02
36	Rose bengal	C ₂₀ H ₂ Cl ₄ I ₄ Na ₂ O ₅	1017.6

(continued)

Table 1 (continued)

No.	Name	Molecular formula	Molecular weight (g mol^{-1})
37	Safranin T	$\text{C}_{20}\text{H}_{19}\text{ClN}_4$	350.84
38	Titan yellow	$\text{C}_{28}\text{H}_{19}\text{N}_5\text{Na}_2\text{O}_6\text{S}_4$	695.72
39	Toluidine blue	$\text{C}_{15}\text{H}_{16}\text{ClN}_3\text{S}$	270.37
40	Victoria blue B	$\text{C}_{33}\text{H}_{32}\text{ClN}_3$	506.08

**Fig. 5** General structures of calixarenes and carbon nanotubes

remarkable applications are due to host–guest interactions between the calixarene derivatives and targeted compounds [72]. Because of that, hundreds of calixarenes have been designed, synthesized, evaluated, and developed over the past several years [49, 50, 63, 95, 125].

Calixarenes have been successfully applied for the removal of dyes from textile wastewater. Since the dye compounds are mainly constructed by aromatic and ionizable functional groups, the derivatives of calixarenes can be utilized as the adsorbent material. The aromatic moieties of dyes interact with the aromatic rings of calixarene through π - π stacking, while the ionizable functional groups of dyes interact with phenolic and/or other polar groups of calixarenes through either hydrogen bonding or electrostatic interaction [3]. Moreover, calixarenes are recognized for their size-exclusion selectivity allowing only a specific dye to be adsorbed during the separation process [90]. Therefore, the calixarenes have been reported for their outstanding adsorption capability and selectivity for the removal of dyes from textile wastewater.

3.2 Carbon Nanotubes

Another aromatic-based synthetic macromolecule with an outstanding adsorption capability for dyes removal is the carbon nanotube. Similar to calixarenes, carbon

nanotube material is composed of polycyclic aromatic frameworks with an organized π conjugation system [24]. Carbon nanotubes are defined as a nanomaterial with a polycyclic aromatic framework of graphene and/or graphite in a cylinder form with a hemisphere end structure. Carbon nanotubes were discovered by Iijima and Ichihashi in 1991 [45]. In general, carbon nanotubes are classified into two major classes: single- and multi-walled carbon nanotubes [46]. The general structures of carbon nanotubes are shown in Fig. 5. Carbon nanotubes are generally prepared through arc evaporation, electrolysis, chemical vapor deposition, flame synthesis, and laser ablation methods. Among the preparation methods, arc evaporation and laser ablation methods are able to produce a near-perfect structure of carbon nanotubes [77].

Carbon nanotubes are widely useful advanced materials in various aspects such as electronic, catalyst, and advanced materials [108]. Carbon nanotubes consist of graphene or graphitic sheets that have π conjugations resulting in a high hydrophobic surface. The existence of the hydrophobic active sites causes the surface of carbon nanotubes to play an important role in the adsorption process. Adsorption of dye on carbon nanotubes occurred through mainly hydrophobic, and π - π stacking interactions. The adsorption sites may locate in the external grooves, interstitial channels, internal sites, and outer surface sites of carbon nanotubes. The chemical interactions might have a role simultaneously or individually in the adsorption process of synthetic dyes from the textile wastewater [99].

4 Removal of the Synthetic Dyes from Aquatic Environmental Samples Using Aromatic-Based Synthetic Macromolecules

4.1 Removal of the Synthetic Dyes from Aquatic Environmental Samples Using Calixarenes

Functionalized calixarenes and the corresponding composite materials have been designed and evaluated for the adsorption of synthetic dyes. The chemical structures of functionalized calixarenes are shown in Fig. 6. At first, the applications of calixarenes for a single synthetic dye molecule are reviewed and then followed by a description of simultaneous adsorption of several synthetic dyes. At the end of the section, the summarized data on the adsorbent material, adsorbed synthetic dyes, pH and q_{max} values are listed in Table 2.

A composite material of calix[n]arene **1** on starch support through an epichlorohydrin linker has been evaluated for butyl rhodamine B adsorption. The composite material exhibited the q_{max} value of $2.43 \times 10^{-2} \text{ mol g}^{-1}$ which is much higher than the starch support ($1.08 \times 10^{-3} \text{ mol g}^{-1}$) at pH 9.0. The regeneration of adsorbent material was easily performed by an eluting ethanol and water mixture at 4:1 volume ratio. Furthermore, the composite material did not lose the adsorption capability after the ten-cycle adsorption process, which was remarkable [17].

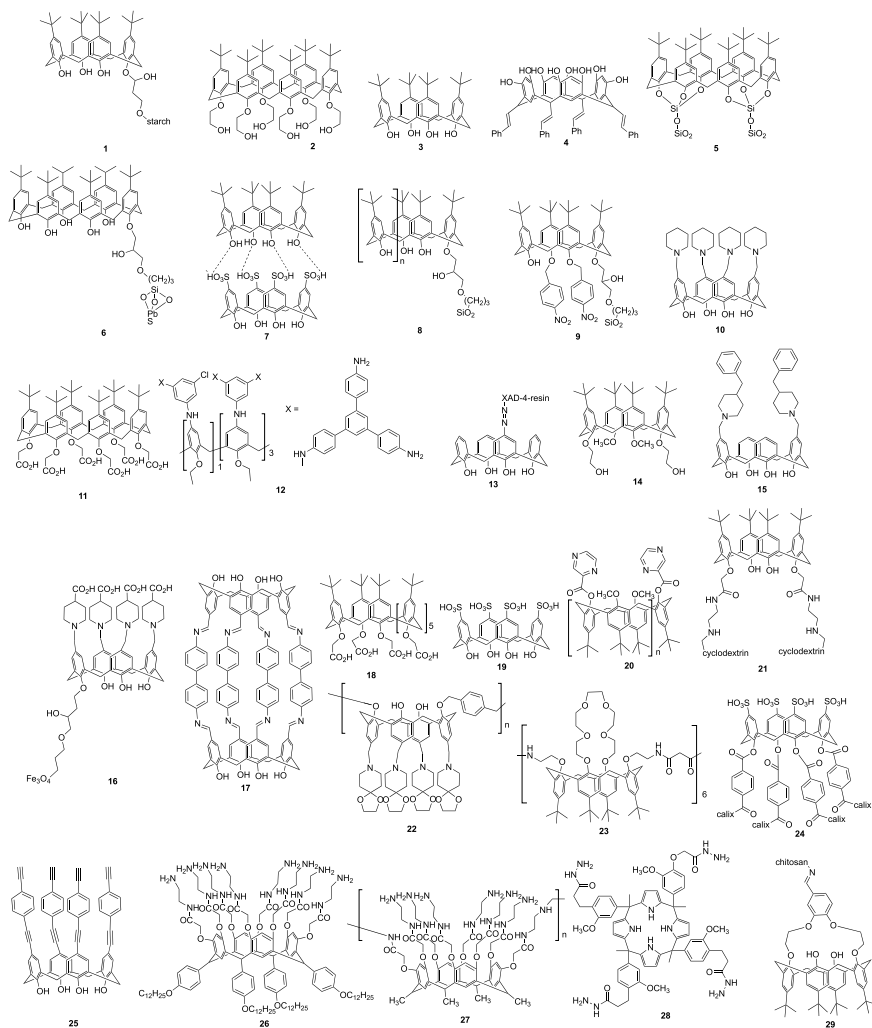


Fig. 6 Chemical structures of functionalized calixarenes

Another calix[6]arene derivative **2** with ether and alcohol functional groups was employed for methyl red removal from the aqueous media [78]. The methyl red was selectively extracted (99%) while the other dyes (methylene blue, methyl green, and methyl violet) were extracted in less percentages (28–45%). The removal percentage of methyl red using calix[6]arene (99%) was higher than D2EHPA (65%), Cyanex301 (85%), and tetrabutylammonium bromide (95%) as the commercial extraction agents [57, 74, 84]. The preconcentration process of methyl red can be achieved by transporting methyl red from the donor solution at pH 5.5 to the acceptor solution at

Table 2 Summary of adsorption conditions and maximum adsorption capacity value of synthetic dyes using calixarenes

No.	Material	Analyte	pH	q_{\max} (mol g ⁻¹)	References
1	Starch-calix[8]arene (200 mg)	Butyl rhodamine B (50 mL, 0.04 mM)	9.0	2.43×10^{-2}	[17]
2	Calix[6]arene (15 mg)	Methyl red (10 mL, 0.03 mM)	5.5	1.65×10^{-5}	[78]
3	Chitosan-calix[4]arene (20 mg)	Reactive yellow 42 (25 mL, 0.15 mM)	4.0	2.80×10^{-4}	[39]
4	C-cinnamal calix[4]resorcinarene (100 mg)	metanil yellow (10 mL, 0.03 mM)	3.0	5.67×10^{-5}	[26]
5	Silica-calix[6]arene (75 mg)	Direct black 38 (10 mL, 0.02 mM)	9.0	2.43×10^{-6}	[53]
6	PbS-calix[6]arene (44 mg)	Methylene blue (10 mL, 0.06 mM)	6.0	1.72×10^{-5}	[101]
7	Alginate-graphene oxide-calix[4]arene (10 mg)	Methylene blue (10 mL, 0.30 mM)	4.0	5.32×10^{-4}	[81]
8	Silica gel-calix[8]arene (200 mg)	Methylene blue (200 mL, 0.06 mM)	8.0	6.53×10^{-4}	[16]
9	Silica-calix[4]arene (20 mg)	Methylene blue (20 mL, 0.06 mM)	12	6.65×10^{-4}	[117]
10	Silica-calix[4]arene (75 mg)	Reactive blue 19 (10 mL, 0.02 mM)	4.0	8.62×10^{-3}	[51]
11	Calix[6]arene (25 mg)	Chicago sky blue 6B, Evans blue, and direct blue 15 (10 mL, 0.02 mM)	5.0	Chicago sky blue 6B: 7.12×10^{-6} Evans blue: 6.00×10^{-6} Direct blue 15: 3.60×10^{-6}	[91]

(continued)

Table 2 (continued)

No.	Material	Analyte	pH	q_{\max} (mol g ⁻¹)	References
12	Calix[4]arene polymer (5 mg)	Methylene blue and toluidine blue (50 mL, 0.10 mM)	7.0	Methylene blue: 5.65×10^{-3} Toluidine blue: 8.01×10^{-3}	[68]
13	Amberlite XAD-4-calix[4]arene (100 mg)	Congo red, reactive black-5, and reactive black-45 (10 mL, 0.02 mM)	Congo red: 6.0 Reactive black-5: 11 Reactive black-45: 3.0	Congo red: 1.58×10^{-5} Reactive black-5: 1.61×10^{-5} Reactive black-45: 1.17×10^{-5}	[52]
14	Amberlite XAD-4-calix[4]arene (5 mg)	Methylene blue, methyl green, and methyl violet (25 mL, 0.03 mM)	6.0	Methylene blue: 2.78×10^{-6} Methyl green: 2.27×10^{-6} Methyl violet: 3.63×10^{-6}	[79]
15	Calix[4]arene (10 mg)	Chicago sky blue 6B and orange II (10 mL, 0.02 mM)	3.0–9.0	Chicago sky blue 6B: 1.94×10^{-5} Orange II: 1.98×10^{-5}	[4]
16	Fe ₃ O ₄ -calix[4]arene (5 mg)	Evans blue and Chicago sky blue 6B (5 mL, 0.01 mM)	2.5	Evans blue: 1.39×10^{-2} Chicago sky blue 6B: 1.75×10^{-2}	[11]
17	Two-dimensional covalent organic framework (7.5 mg)	Methylene blue and rhodamine B (15 mL, 0.01 mM)	7.0	Methylene blue: 1.16×10^{-4} Rhodamine B: 8.35×10^{-5}	[29]
18	Calix[8]arene (10 mg)	Direct violet 51, methyl orange, orange II, and reactive black 5 (10 mL, 0.02 mM)	11	Direct violet 51: 1.54×10^{-5} Methyl orange: 8.00×10^{-6} Orange II: 1.60×10^{-5} Reactive black 5: 9.40×10^{-6}	[34]

(continued)

Table 2 (continued)

No.	Material	Analyte	pH	q_{\max} (mol g ⁻¹)	References
19	Hydrogel calix[4]arene (3 mg)	Neutral red, methylene blue, and eosin-y (20 mL, 500 ppm)	7.0	Neutral red: 1.82×10^{-3} Methylene blue: 7.19×10^{-4} Eosin-y: 6.16×10^{-4}	[86]
20	Calix[8]arene (25 mg)	Evans blue, orange II, reactive black 5, methyl orange, and Chicago sky blue 6B (10 mL, 0.02 mM)	3.0	Evans blue: 7.84×10^{-6} Orange II: 7.04×10^{-6} Reactive black 5: 7.68×10^{-6} Methyl orange: 6.88×10^{-6} Chicago sky blue 6B: 7.84×10^{-6}	[35]
21	β -cyclodextrin-calix[4]arene (100 mg)	Methylene blue and basic fuchsin (25 mL, 140 ppm)	9.0	Methylene blue: 5.94×10^{-5} Basic fuchsin: 9.47×10^{-5}	[127]
22	Calix[4]arene (25 mg)	Chicago sky blue 6B, Evans blue, and direct blue 15 (10 mL, 0.02 mM)	8.0	Chicago sky blue 6B: 7.84×10^{-6} Evans blue: 7.68×10^{-6} Direct blue 15: 7.84×10^{-6}	[3]
23	β -cyclodextrin-calix[4]arene (25 mg)	Methyl orange, direct blue 71, titan yellow, and Orange II (10 mL, 0.03 mM)	11.0	Methyl orange: 8.28×10^{-6} Direct blue 71: 8.40×10^{-6} Titan yellow: 8.52×10^{-6} Orange II: 8.28×10^{-6}	[122]
24	Mesoporous calix[4]arene (15 mg)	Methylene blue, crystal violet, brilliant green, and rhodamine B (15 mL, 0.01 mM)	7.0	$\sim 9.5 \times 10^{-6}$	[129]

(continued)

Table 2 (continued)

No.	Material	Analyte	pH	q_{\max} (mol g ⁻¹)	References
25	Porous calix[4]arene (5 mg)	Methylene blue, congo red, and rhodamine B (10 mL, 0.50 mM)	7.0	Methylene blue: 1.95×10^{-3} Congo red: 9.66×10^{-4} Rhodamine B: 1.01×10^{-3}	[112]
26	Calix[4]resorcinarene (10 mg)	Congo red, acid orange 5, and methyl orange (4 mL, 0.02 mM)	7.0	Congo red: 2.91×10^{-5} Acid orange 5: 3.48×10^{-4} Methyl orange: 2.90×10^{-5}	[56]
27	Calix[4]resorcinarene (1 mg)	Congo red, methyl orange, and acid orange 5 (4 mL, 0.002 mM)	7.0	Congo red: 8.97×10^{-4} Methyl orange: 1.14×10^{-3} Acid orange 5: 1.32×10^{-3}	[109]
28	Calix[4]pyrrole (5 mg)	Methylene blue and methyl orange (2 mL, 0.10 mM)	7.0	Turnover number for methylene blue degradation: 3.79×10^{-4} Turnover number for methyl orange degradation: 3.85×10^{-4}	[58]
29	Chitosan-crown-calix[4]arene (10 mg)	Brilliant green, victoria blue B, neutral red, and Orange I (10 mL, 1.00 mM)	Brilliant green, victoria blue, neutral red: 9.0 Orange I: 5.0	Brilliant green: 1.64×10^{-3} Victoria blue B: 1.86×10^{-3} Neutral red: 1.95×10^{-3} Orange I: 1.78×10^{-3}	[120]

pH 12. By employing this process, methyl red can be selectively removed from the industrial wastewater samples with 99.5–99.9% purity, which was remarkable [78].

Copolymer material of chitosan and *p*-tert-butylcalix[4]arene **3** was utilized for reactive yellow 42 dye adsorption from the aqueous solution. The copolymer material adsorbed reactive yellow 42 according to a pseudo-second-order kinetic model at pH 4.0 within 135 min. The pH 4.0 was suitable to protonate amine functional groups of chitosan; thus, the reactive yellow 42 dye was adsorbed through electrostatic

interactions. Since the copolymer material has a random and heterogenous structure, the adsorption process is time-consuming (135 min). However, the reaction rate constant of copolymer material ($3.63 \times 10^{-4} \text{ g mg}^{-1} \text{ min}^{-1}$) was still 1.50 times faster than the unmodified chitosan material ($2.42 \times 10^{-4} \text{ g mg}^{-1} \text{ min}^{-1}$). The copolymer material yielded the q_{\max} value of $2.80 \times 10^{-4} \text{ mol g}^{-1}$ which was higher than activated hyacinth ($6.62 \times 10^{-6} \text{ mol g}^{-1}$), activated reeds ($1.17 \times 10^{-5} \text{ mol g}^{-1}$), and copolymer of eugenol ($1.83 \times 10^{-5} \text{ mol g}^{-1}$) [39].

Utilization of *C*-cinnamal calix[4]resorcinarene **4** was reported for metanil yellow adsorption. The *C*-cinnamal calix[4]resorcinarene was prepared from a cyclocondensation reaction between cinnamaldehyde and resorcinol. The metanil yellow adsorption reached optimum condition at pH 3.0. At pH lower than 3.0, the metanil yellow was protonated and the ion exchange interaction was suppressed. On the other hand, at pH higher than 3.0, the hydroxyl groups of *C*-cinnamal calix[4]resorcinarene was deprotonated and the electrostatic repulsion hindered the metanil yellow adsorption process. From the isotherm adsorption experiment, the q_{\max} value of metanil yellow was $5.67 \times 10^{-5} \text{ mol g}^{-1}$ [26].

Immobilized calix[6]arene **5** on the silica resin material was effective for the removal of direct black 38 dye. The immobilization reaction was conducted in toluene using triethylamine as the base catalyst. The best pH for direct black 38 removal percentage (91%) was achieved at pH 9.0. The adsorption mechanism happened with the aid of sodium cations. The sodium ion was chelated by the lower rim of calix[6]arene and then the sulfonate group of direct black 38 was locked by the electrostatic interaction with a sodium ion, as well as π - π stacking interactions with aromatic rings of calix[6]arene. The resin material exhibited 70% removal of direct black 38 from the real textile wastewater samples. Furthermore, the resin material can be regenerated by removing the adsorbed dyes by using an acidic solution [53].

The composite material of lead(II) sulfide and calix[6]arene **6** was reported for methylene blue adsorption. The composite material was prepared by connecting lead(II) sulfide with calix[6]arene **6** with 3-glycidopropyltrimethoxysilane as the linker agent. The average size of the composite material was less than 30 nm with a point of zero charge at pH 7.28. At pH lower than 7.28, the composite material has positive zeta potential charges on the surface of adsorbent material. On the other hand, at a pH higher than 7.28, the composite material has negative zeta potential charges on the surface of adsorbent material [101].

The experimental condition was optimized by a response surface methodology and the optimum adsorption condition was achieved by using 44 mg composite material at pH 6.0 at 304 K. The optimum pH value (6.0) was achieved below the point of zero charge of the composite material demonstrating that the adsorption process mainly happened through π - π stacking and hydrogen bonds rather than electrostatic interaction. The methylene blue adsorption followed the Langmuir model with the q_{\max} value of $1.72 \times 10^{-5} \text{ mol g}^{-1}$. The q_{\max} value ($1.72 \times 10^{-5} \text{ mol g}^{-1}$) was higher than natural zeolite ($1.61 \times 10^{-5} \text{ mol g}^{-1}$), wood material ($1.48 \times 10^{-5} \text{ mol g}^{-1}$), carbon material ($1.28 \times 10^{-5} \text{ mol g}^{-1}$), and activated carbon ($8.03 \times 10^{-6} \text{ mol g}^{-1}$), which was remarkable [9, 32, 33, 38]. The regeneration of the composite material was

done by eluting 0.75 M HNO₃. The composite material did not lose the adsorption capability after the four-cycle adsorption process, which was remarkable [101].

The nanocomposite material between alginate, graphene oxide, and calix[4]arenes **7** has been reported for methylene blue removal from the aqueous solution. The nanocomposite material was prepared through a cross-link reaction and followed by an agitation process. The nanocomposite material was stable up to 490 K from the TGA analysis. The optimum adsorption condition for methylene blue was achieved using 10 mg adsorbent material at pH 4.0 within 1 h adsorption process. The adsorption kinetics followed the pseudo-second-order model with a rate constant of 46 mg mg⁻¹ min⁻¹. Meanwhile, the methylene blue adsorption followed the Langmuir model yielding the q_{\max} value of 5.32×10^{-4} mol g⁻¹ [81].

Additionally, composite material between calix[n]arene **8** and silica gel with 3-glycidoxypropyltrimethoxysilane as the linker agent was effective for methylene blue removal from the aqueous media. The composite material was prepared through a reflux method for 6 h under alkaline condition using NaH as the base. Through the reflux method, as much as 0.4 mmol g⁻¹ calix[n]arene was successfully impregnated on the silica gel as the support. The calix[4]arene composite material gave slower (160 min) and lower q_{\max} value (9.38×10^{-5} mol g⁻¹) than the calix[6]arene- (80 min, 5.03×10^{-4} mol g⁻¹) and calix[8]arene-composite (2 min, 6.53×10^{-4} mol g⁻¹) materials. A wider calix[n]arene was able to accommodate more methylene blue compounds on the calix[n]arene cavity during the adsorption process. The q_{\max} value of methylene blue adsorption using calix[4]arene-, calix[6]arene-, and calix[8]arene-composite materials was in good order with the size of the calixarene cavity [16].

The q_{\max} value of calix[8]arene-composite (6.53×10^{-4} mol g⁻¹) was higher than sawdust (1.53×10^{-5} mol g⁻¹), marine seaweed (1.63×10^{-5} mol g⁻¹), orange peel (1.83×10^{-5} mol g⁻¹), rice husk (3.09×10^{-5} mol g⁻¹), silica (3.50×10^{-5} mol g⁻¹), and date pits (5.41×10^{-5} mol g⁻¹) [6, 20, 47, 54, 85, 89, 119]. Furthermore, the q_{\max} value (6.53×10^{-4} mol g⁻¹) was also higher than the dead biomass (5.79×10^{-5} mol g⁻¹), lemon peel (9.06×10^{-5} mol g⁻¹), hazelnut shell (1.29×10^{-4} mol g⁻¹), yellow passion fruit (1.40×10^{-4} mol g⁻¹), fly ash (2.36×10^{-4} mol g⁻¹), sewage sludge (3.59×10^{-4} mol g⁻¹), and coir pith (3.76×10^{-4} mol g⁻¹) adsorbent materials, which was remarkable [14, 28, 55, 59, 92, 93, 111].

The composite material of silica-calix[4]arene **9** was investigated for methylene blue removal. The preparation of composite material was done by using 3-glycidoxypropyltrimethoxysilane under alkaline condition. The amount of calix[4]arene derivative in 1 g of composite material was up to 0.34 mmol. The composite material was stable up to 470 K. The composite material adsorbed 93% of methylene blue through electrostatic interaction between nitro functional group and the positive charge of methylene blue at pH 12 [117].

The bare silica material and calix[4]arene derivative itself only adsorbed 61 and 41% of methylene blue using the same adsorbent mass and experimental condition. A higher adsorption percentage of the composite material (93%) demonstrated a synergistic effect between silica and calix[4]arene derivative, which was remarkable. The adsorption kinetics followed the second-order kinetic model with a rate

constant of $32 \text{ mg mg}^{-1} \text{ min}^{-1}$. Meanwhile, the isotherm adsorption followed the Langmuir model with a q_{max} value of $6.65 \times 10^{-4} \text{ mol g}^{-1}$. The composite material has been applied for the simulated textile wastewater samples. The composite material adsorbed 40–75% of methylene blue from the simulated textile wastewater samples, which was remarkable [117].

The composite material of silica-piperidine-calix[4]arene **10** has been investigated for reactive blue 19 dye adsorption in the fixed-bed experiment. The composite material with 0.4 mmol g^{-1} calix[4]arene was prepared through the reflux method under alkaline condition using trimethylamine as the homogeneous catalyst. The adsorption process was favorable at a pH region of 2.0–4.0 giving the q_{max} value of $8.62 \times 10^{-3} \text{ mol g}^{-1}$ according to the Langmuir model. The composite material exhibited 69–98% removal percentages of reactive blue 19 dye removal from three independent wastewater samples, which was remarkable [51].

Utilization of carboxylic acid type of calix[6]arene **11** for adsorption of Chicago sky blue 6B, Evans blue, and direct blue 15 dyes has been reported. The *p*-tert-butylcalix[6]arene was reacted with methyl bromoacetate in acetone and then hydrolyzed with potassium hydroxide in ethanol. The adsorption percentage for Chicago sky blue 6B, Evans blue, and direct blue 15 dyes at pH 5.0 was 89, 75, and 45%, respectively. The adsorption percentages were not significantly changed at a pH range of 3.5–8.5. The synthetic dyes were adsorbed through hydrogen bonds between carboxylic acid groups of calix[6]arene and sulfonate groups of dyes at acidic condition. On the other hand, the adsorption of dyes was facilitated by sodium cations in an alkaline condition; thus, the adsorption percentages were maintained [91].

Calix[4]arene **12** polymers exhibit high adsorption capability for methylene blue and toluidine blue removal. The polymer material was prepared through a coupling reaction between chloro-substituted calix[4]arene and amino-substituted calix[4]arene under an alkaline condition in 45% yield. The polymer material has a surface area and a pore volume of $122 \text{ m}^2 \text{ g}^{-1}$ and 0.1 mL g^{-1} , respectively. The polymer material rapidly adsorbed methylene blue and toluidine blue dyes with adsorption percentage of 99.4–99.6% within 5 min [68].

The q_{max} values were 5.65×10^{-3} and $8.01 \times 10^{-3} \text{ mol g}^{-1}$ for methylene blue and toluidine blue dyes, respectively. Selective adsorption was achieved only for methylene blue and toluidine blue, while the other dyes, i.e. rhodamine B, crystal violet, and fluorescein were hardly adsorbed. The favorable dyes adsorption mainly happened through electrostatic, hydrogen bonds, and π - π stacking interactions. The regeneration of the composite material was easily carried out by washing the polymer material with methanol. The composite material did not lose the adsorption capability after the four-cycle adsorption process, which was remarkable [68].

The composite material of calix[4]arene **13** on the Amberlite XAD-4 support was evaluated for the adsorption process of congo red, reactive black 5, and reactive black 45 dyes. The composite material was prepared through a consecutive chemical reaction, i.e. nitration, reduction, diazotization, and coupling reaction through -N=N-linkage. As much as 72% of congo red, 82% of reactive black 5, and 60% of reactive

black 45 were adsorbed at pH 6, 11, and 3, respectively, using the composite material [52].

Immobilization of calix[4]arene **14** on Amberlite XAD-4 support has been also applied for the adsorption of methylene blue, methyl orange, methyl green, methyl violet, and eosin dyes. The adsorbent material contained 0.05 mmol g⁻¹ of calix[4]arene **14**. The adsorbent material (5 mg) adsorbed 90% of each methylene blue, methyl green, and methyl violet dyes, however, other dyes were hardly adsorbed demonstrating high selectivity of calix[4]arene **14** at pH 6.0. The adsorption process fits well with the Freundlich model yielding 0.89, 1.04, and 1.25 mol g⁻¹ as the q_{\max} values of methylene blue, methyl green, and methyl violet, respectively [79].

The q_{\max} value for methylene blue adsorption (0.89 mol g⁻¹) was much higher than the unmodified Amberlite XAD-4 resin adsorbent (6.0×10^{-6} mol g⁻¹) and activated carbon (3.7×10^{-6} mol g⁻¹) materials [103, 126]. Meanwhile, the q_{\max} value for methyl green adsorption (1.04 mol g⁻¹) was much better than NiFe₂O₄-carbon nanotubes (2.4×10^{-6} mol g⁻¹) and activated carbon (1.0×10^{-5} mol g⁻¹) materials [10, 37]. On the other hand, the q_{\max} value for methyl violet adsorption (1.25 mol g⁻¹) was higher than wood sawdust (1.2×10^{-5} mol g⁻¹), carbon nanotubes (1.1×10^{-4} mol g⁻¹), and activated carbon (3.7×10^{-6} mol g⁻¹) materials [83, 87]. Furthermore, the adsorbent material adsorbed 99% of each methylene blue, methyl green, and methyl violet dyes from the real textile wastewater samples, which was remarkable. The regeneration of adsorbent material was easily performed by eluting 0.6 M HCl solution. The adsorbent material still exhibited 90% adsorption percentage of synthetic dyes after the five-cycle process [79].

Calix[4]arene **15** owing to benzylpiperidine functional group has been evaluated for the removal of Chicago sky blue 6B and orange II dyes. The calix[4]arene exhibit 97–99% of both dyes removal in each individual system within 15 min process at pH 3.0–9.0. The inclusion of both Chicago sky blue 6B and orange II dyes was facilitated by π - π stacking and electrostatic interactions between the negative charge of sulfonate groups with the positive charge of piperidine groups. The combination of both interactions was absent in the monomer structure; thus, the removal percentage (97–99%) was eight times higher than the monomer structure (12%) due to the chelating ability of calix[4]arene **15**, which was remarkable [4].

Composite adsorbent material of calix[4]arene with magnetite (Fe₃O₄) **16** was investigated for the removal of Evans blue and Chicago sky blue 6B dyes. The adsorbent material was prepared by mixing Fe₃O₄ and calix[4]arene with the presence of [3-(2,3-epoxypropoxy)-propyl]-trimethoxysilane as the linker agent in acetonitrile as the reaction media. From the spectroscopic calculation, the composite material was composed of 34% calix[4]arene and 66% Fe₃O₄ materials. The adsorbent material (5 mg) exhibited a rapid and efficient adsorption process of Evans blue and Chicago sky blue 6B dyes at 95% adsorption percentage within 15 min at pH 2.5. At pH 2.5, the piperidine heterocyclic ring was protonated, making the nitrogen atoms possible to interact with the negatively charge-sulfonate functional groups of either Evans blue or Chicago sky blue 6B dye [11].

The adsorption of Evans blue and Chicago sky blue 6B dyes using the composite adsorbent material **16** followed the Langmuir model with a q_{\max} value of 1.39×10^{-2}

and $1.75 \times 10^{-2} \text{ mol g}^{-1}$, respectively. The obtained q_{max} value using the composite adsorbent material **16** was higher than the β -cyclodextrin polymers with 9.58×10^{-3} and $1.06 \times 10^{-2} \text{ mol g}^{-1}$ for Evans blue and Chicago sky blue 6B, respectively [123]. The regeneration of the composite material was conducted by eluting 0.1 M NaOH. The composite material did not lose the adsorption capability after the ten-cycle adsorption process, which was remarkable [11].

A two-dimensional covalent organic framework serves as an ideal platform for dyes adsorption due to their tunable pore functionality, high stability, and well-organized structure. Two-dimensional covalent organic framework **17** was obtained from the reaction between *p*-carbaldehyde-calix[4]arene and benzidine compounds in chloroform as the reaction media. By using two different experimental conditions, the covalent organic framework was generated in fiber-like and sphere-like structure in 25% yield. Both materials were stable up to 650 K. Surfaces of fiber-like and sphere-like adsorbent materials were composed of negative charges of -45 and -41 mV, respectively [29].

When utilizing the two-dimensional covalent organic framework as the adsorbent material was taken into account, the adsorbent material (7.5 mg) strongly adsorbed the cationic dyes such as methylene blue and rhodamine B. The adsorption of methylene blue and rhodamine B dyes rapidly and selectively occurred by using fiber-like adsorbent material within 1 min. In contrast, the sphere-like adsorbent material required 180 min to reach the same adsorption percentage (95%) due to its narrower surface area leading to a slower kinetic process. The experimental results agreed with the computational study that revealed the association of methylene blue and rhodamine B dyes in the fiber-like adsorbent material happened within 200 ns. The favorable adsorption yielded the q_{max} value of 1.16×10^{-4} and $8.35 \times 10^{-5} \text{ mol g}^{-1}$ for methylene blue and rhodamine B, respectively [29].

Evaluation of nitro and carboxylic acid derivatives of calix[n]arene for removal of direct violet 51, methyl orange, orange II, and reactive black 5 has been reported. The calix[8]arene derivatives **18** gave higher removal percentages (up to 80%) than calix[4]arene derivatives (up to 28%) due to larger cavity size. Furthermore, the carboxylic acid calix[4]arene derivative (40–80%) exhibited higher removal percentages than nitro derivatives (4–12%) due to the ion-exchange mechanism. The optimum condition for dyes removal was 1 h contact time at pH 11. Calix[8]arene **18** gave removal percentage of direct violet 51, methyl orange, orange II, and reactive black 5 at 77, 40, 80, and 47%, respectively. The simultaneous removal of the synthetic dyes occurred due to suitable ion-exchange interaction as well as π - π stacking and hydrogen bonds [34].

Hydrogel composite material of graphene oxide and calix[4]arene sulfonic acid **19** demonstrated a high adsorption capability for synthetic dyes removal. The hydrogel material was prepared from a mixture of graphene oxide, calix[4]arene sulfonic acid **19**, and L-cysteine under alkaline condition for 3 h at 360 K. The hydrogel material was composed mostly of water (90% weight); thus, the hydrogel material can be considered as an environmentally friendly material. When the hydrogel material was employed for the removal of synthetic dyes, the positively charged dyes (methylene blue and crystal violet) were adsorbed faster than the neutral dye (neutral red) and

much faster than negatively charged dyes (methyl orange and eosin-y). The reason was due to the presence of negatively charge sulfonic acid which could suitably interact with the positively charged dyes [86].

The q_{\max} values of neutral red, methylene blue, and eosin-y were 1.82×10^{-3} , 7.19×10^{-4} , and 6.16×10^{-4} mol g⁻¹, respectively. The q_{\max} value of methylene blue from an adsorption process using the hydrogel material (7.19×10^{-4} mol g⁻¹) was higher than reduced graphene oxide hydrogel (2.45×10^{-5} mol g⁻¹), graphene-Ag₃PO₄ (2.63×10^{-4} mol g⁻¹), reduced graphene oxide-ascorbic acid (5.31×10^{-4} mol g⁻¹), and graphene oxide itself (5.88×10^{-4} mol g⁻¹) [19, 70, 71, 118]. Meanwhile, the q_{\max} value of eosin-y using the hydrogel material (6.16×10^{-4} mol g⁻¹) was higher than graphene oxide-chitosan hydrogel (4.71×10^{-4} mol g⁻¹) due to the presence of calix[4]arene sulfonic acid [18].

The hydrogel material was simply regenerated by dipping the dyes-laden hydrogel material with copper(II) sulfate and hydrazine in water media to degrade the synthetic dyes. The hydrogel material did not lose the adsorption capability after the five-cycle adsorption process. Furthermore, an in situ degradation of a mixture of methylene blue, crystal violet, methyl orange, eosin-y, neutral red, congo red, bromophenol blue, rose bengal, rhodamine 6G, acridine orange, and bismarck brown Y dyes (at 500 ppm concentration each) was established at 360 K to obtain a colorless filtrate, which was remarkable [86].

Fast adsorption of Evans blue, orange II, reactive black 5, methyl orange, and Chicago sky blue 6B dyes was achieved within 10 min by using calix[n]arene owing to pyrazine-2-carboxylic acid moieties. The adsorption was favorable at pH 3.0 yielding 86–98% adsorption percentages by using calix[8]arene derivative **20**. In contrast, the calix[4]arene derivatives gave lower adsorption percentages (59–73%) due to limited space on its surface cavity. The aqueous solution with a pH value of 3.0 was suitable for protonation of pyrazine functional groups; thus, the adsorption of dyes occurred through the electrostatic interactions. The regeneration of the adsorbent material was done by eluting with a brine solution. The composite material did not lose the adsorption capability after the five-cycle adsorption process, which was remarkable [35].

The composite material of β -cyclodextrin and calix[4]arene **21** was employed as the adsorbent material for methylene blue and basic fuchsin dyes adsorption. The calix[4]arene was connected to β -cyclodextrin biomaterial through amide bonds in 70% yield. The adsorption process of methylene blue and basic fuchsin dyes was optimum at pH 9.0 yielding the q_{\max} value of 5.94×10^{-5} and 9.47×10^{-5} mol g⁻¹ for methylene blue and basic fuchsin dyes, respectively [127].

The calix[4]arene polymer material **22** was reported as an efficient adsorbent material for Chicago sky blue 6B, Evans blue, and direct blue 15 dyes. The adsorbent material was prepared by the polymerization process of calix[4]arene through the reaction between phenolic groups of calix[4]arene with *p*-dibromoxylene under alkaline condition. The yield of polymerization reaction was 70% and the polymer material was stable up to 450 K. The polymer material was employed as the adsorbent material yielding high removal percentages (96–98%) at pH 8.0. The Chicago sky

blue 6B, Evans blue, and direct blue 15 dyes were adsorbed through electrostatic, hydrogen bonds, and π - π stacking interactions [3].

The combination of β -cyclodextrin and calix[4]arene **23** as the adsorbent material was evaluated for the removal of methyl orange, direct blue 71, titan yellow, and Orange II dyes. The oligomer material was obtained in 65% yield with a molecular weight of 2150 g mol^{-1} and thermal stability up to 570 K. The adsorption percentage of methyl orange, direct blue 71, titan yellow, and Orange II was in a range of 69–71%. The q_{max} values of methyl orange, direct blue 71, titan yellow, and Orange II were obtained from the Langmuir isotherm model giving the value of 8.28×10^{-6} , 8.40×10^{-6} , 8.52×10^{-6} , and $8.28 \times 10^{-6} \text{ mol g}^{-1}$, respectively. The mechanism of dyes adsorption was driven by hydrogen bond, chelation, electrostatic, and hydrophobic interactions [122].

Application of mesoporous calix[4]arene **24** was used for the preconcentration process of synthetic dyes. The phenolic groups of *p*-sulfonic acid calix[4]arene was esterified with terephthaloyl chloride under the alkaline condition to form the calix[4]arene polymer material **24**. The surface area of the polymer material was $123 \text{ m}^2 \text{ g}^{-1}$ with around 3 nm pore size. Several synthetic dyes such as methylene blue, crystal violet, brilliant green, and rhodamine B were effectively preconcentrated by using the polymer membrane material. The removal percentages of the synthetic dyes were around 95%. The regeneration of the polymer membrane material was done by washing with ethanol. The polymer membrane material did not lose the adsorption capability after the five-cycle adsorption process, which was remarkable [129].

The porous material of calix[4]arene **25** was prepared through a Sonogoshira-Hagihara coupling reaction between *p*-bromo-calix[4]arene and 1,4-diethynylbenzene by using a palladium-based catalyst. The porous material has a very large surface area ($\sim 600 \text{ m}^2 \text{ g}^{-1}$); thus, this material rapidly and effectively adsorbed methylene blue, congo red, and rhodamine B dyes from the aqueous solution. As much as 95, 80, and 50% removal percentages were achieved within 5 min for methylene blue, congo red, and rhodamine B dyes, respectively [112].

After 15 min adsorption process, a quantitative ($\sim 100\%$) removal percentage was achieved for each dye in the individual experiment. The q_{max} value was 1.95×10^{-3} , 9.66×10^{-4} , and $1.01 \times 10^{-3} \text{ mol g}^{-1}$ for methylene blue, congo red, and rhodamine B dyes, respectively. The favorable dyes adsorption was mainly driven by a combination of hydrophobic, electrostatic, hydrogen bonds, and π - π stacking interactions with the amorphous surface of the porous material. The regeneration of the composite material was done by washing the porous material with 0.10 M HNO_3 . The composite material did not lose the adsorption capability after several adsorption cycles, which was remarkable [112].

Another group of metacyclophanes, i.e. calix[4]resorcinarenes, calix[4]pyrrole, and crown-calix[4]arene have also been studied for the dyes adsorption process. Functionalized calix[4]resorcinarene **26** with dodecyloxybenzyl substituent was reported for congo red, acid orange 5, and methyl orange dyes. The methyl orange was 98% adsorbed while the quantitative adsorption percentage (99–100%) for congo red and acid orange 5 was achieved using calix[4]resorcinarene **26**, which was remarkable. The dyes were adsorbed through both electrostatic interaction and hydrogen

bonds. The q_{\max} values for congo red, acid orange 5, and methyl orange dyes were 2.91×10^{-5} , 3.48×10^{-4} , and 2.90×10^{-5} mol g⁻¹, respectively [56].

The nitrogenated calix[4]resorcinarene **27** polymer material has been applied for the adsorption process of congo red, methyl orange, and acid orange 5 dyes. The polymer material was obtained in 65% yield from calix[4]resorcinarene derivative with diethylenetriamine in a solvent mixture of methanol and toluene. The polymer material was stable up to 490 K. The q_{\max} values of congo red, methyl orange, and acid orange 5 dyes were 8.97×10^{-4} , 1.14×10^{-3} , and 1.32×10^{-3} mol g⁻¹, respectively. The synthetic dyes were adsorbed mainly through hydrogen bonds and electrostatic interactions [109].

A composite material consisting of calix[4]pyrrole **28** and palladium nanoparticles has been applied for methylene blue and methyl orange degradation process. The zeta potential charge of the composite material was -26.2 mV; thus, this composite material was appropriate for the removal of methylene blue and methyl orange which are categorized as cationic dyes. Within 12 min, as much as 90% and 95% of methylene blue and methyl orange dyes were degraded to yield a colorless filtrate. The degradation mechanism occurred through an electron transfer process from sodium borohydride to the composite material; thus, the reduction of azo functional groups happened [58].

From the mass spectra analysis, the methylene blue was degraded to form phenol and amine compound, while methyl orange was degraded to form aniline and benzenesulfonic acid. The turnover number for the dyes removal process using the composite material was 3.79×10^{-4} and 3.85×10^{-4} for methylene blue and methyl orange, respectively. The regeneration of the composite material was done by washing the composite material with a mixture of water and acetone. The composite material did not lose the adsorption capability after the six-cycle adsorption process, which was remarkable [58].

A composite material between chitosan and crown-calix[4]arene **29** has been evaluated for the adsorption of brilliant green, Victoria blue B, neutral red, and Orange I dyes. The composite material was prepared through an imine connection between carbaldehyde-crown-calix[4]arene and amino groups of chitosan. Around 22% of crown-calix[4]arene was successfully impregnated on the chitosan material. The optimum pH value was achieved at pH 9.0 for brilliant green, Victoria blue B, and neutral red dyes, while the optimum pH value for orange I was found at pH 5.0 [120].

The composite material exhibited higher adsorption percentages (75–90%) than the bare chitosan (45–60%). The q_{\max} values for brilliant green, Victoria blue B, neutral red, and Orange I were 1.64×10^{-3} , 1.86×10^{-3} , 1.95×10^{-3} , and 1.78×10^{-3} mol g⁻¹, respectively. The regeneration of the composite material was done by washing the composite material with HCl and followed by NaOH solution. The composite material did not lose the adsorption capability after the five-cycle adsorption process, which was remarkable [120].

4.2 Removal of the Synthetic Dyes from Aquatic Environmental Samples Using Carbon Nanotubes

Functionalized carbon nanotube materials have been prepared and investigated for the adsorption of synthetic dyes. At first, the application of carbon nanotubes for a single synthetic dye molecule was reviewed and then followed by a description of the simultaneous adsorption of several synthetic dyes. At the end of the section, the summarized data on the adsorbent material, adsorbed synthetic dyes, pH and q_{max} values are listed in Table 3.

Nanoadsorbent materials consisting of single- and multi-walled carbon nanotubes were investigated against adsorption of Alizarin red S. The q_{max} values produced by single- and multi-walled carbon nanotubes were 9.1×10^{-4} and 3.9×10^{-4} mol g⁻¹, respectively. The equilibrium time required for single-walled carbon nanotubes (65 min) was faster than the multi-walled carbon nanotubes (100 min). The adsorption process was carried out at a temperature of 318 K with an optimal pH of 2.0 which causes the carbon nanotubes to be positively charged so that the electrostatic interactions can occur with negatively charged Alizarin red S [73].

Single-walled carbon nanotubes consist of an independent cylinder form thus having a larger and more open surface structure compared to the multi-walled carbon nanotubes. Because of that, single-walled carbon nanotubes exhibit a higher adsorption capability than multi-walled carbon nanotubes indeed. However, from the economic point of view, the preparation of single-walled carbon nanotubes is a costly process. In contrast, bulk synthesis of multi-walled carbon nanotubes is available at a cheaper production price and multi-walled carbon nanotubes are less toxic for aquatic organisms [104]. Therefore, researchers give more attention to the design and application of multi-walled carbon nanotube materials for a real application for wastewater treatment [77].

Multi-walled carbon nanotubes were also employed to adsorb acid scarlet 3R, auramine O, and crystal violet synthetic dyes. The q_{max} values for acid scarlet 3R, auramine O, and crystal violet were 4.1×10^{-2} , 8.0×10^{-2} , and 6.0×10^{-2} mol g⁻¹, respectively. The optimum adsorption condition was found at pH 7.0 with an equilibrium time of 60 min. The adsorbent material can be reused after the adsorbent regeneration process [107]. Furthermore, in other reports, multi-walled carbon nanotubes were also able to adsorb methyl orange, eosin-y, crystal violet, acridine orange, congo red and reactive black 5 at pH 6.0 yielding a q_{max} value of 1.2×10^{-4} , 2.3×10^{-4} , 4.0×10^{-4} , 1.5×10^{-3} , 3.7×10^{-4} , and 5.5×10^{-5} mol g⁻¹, respectively [27, 69, 75, 121, 124].

Multi-walled carbon nanotubes in a hydrogel form were recently investigated for the adsorption of safranin T, crystal violet, malachite green, and methylene blue dyes. The adsorption was carried out at an optimum condition of pH 7.0 with an equilibrium time of 90 min which fit well with the pseudo-second-order adsorption kinetics model. The q_{max} values for safranin T, crystal violet, malachite green, and methylene blue were 2.6×10^{-3} , 2.4×10^{-3} , 2.3×10^{-3} , and 1.6×10^{-3} mol g⁻¹, respectively, in the range of 293–313 K. The hydrogel material can be used for three

Table 3 Summary of adsorption condition and maximum adsorption capacity value of synthetic dyes using carbon nanotubes

Material	Analyte	pH	q_{\max} (mol g ⁻¹)	References
Single- and multi-walled carbon nanotubes (30 mg)	Alizarin red S (20 mL, 2.92 mM)	2.0	Single-walled: 9.1×10^{-4} Multi-walled: 3.9×10^{-4}	[73]
Multi-walled carbon nanotubes (40 mg)	Acid scarlet 3 R, auramine O, and crystal violet (100 mL, 10 ppm)	7.0	Acid scarlet 3R: 4.1×10^{-2} Auramine O: 8.0×10^{-2} Crystal violet: 6.0×10^{-2}	[107]
Multi-walled carbon nanotubes (15 mg)	Methyl orange (50 mL, 0.06 mM)	2.3	1.2×10^{-4}	[121]
Multi-walled carbon nanotubes (100 mg)	Eosin-y and acridine orange (50 mL)	7.0	Eosin-y: 2.3×10^{-4} Acridine orange: 1.5×10^{-3}	[124]
Multi-walled carbon nanotubes (15 mg)	Crystal violet (20 mL, 0.05 mM)	7.0	4.0×10^{-4}	[75]
Multi-walled carbon nanotubes (10 mg)	Congo red (10 mL, 0.29 mM)	6.0	3.7×10^{-4}	[27]
Multi-walled carbon nanotubes (2500 mg)	Reactive black 5 (100 mL, 0.04 mM)	7.0	5.5×10^{-5}	[69]
Multi-walled carbon nanotube hydrogel (50 mg)	Safranin T, crystal violet, malachite green, and methylene blue (50 mL, 1000 ppm)	7.0	Safranin T: 2.6×10^{-3} Crystal violet: 2.4×10^{-3} Malachite green: 2.3×10^{-3} Methylene blue: 1.6×10^{-3}	[80]
Multi-walled carbon functionalized thiol (20 mg)	Methylene blue (20 mL, 0.13 mM)	6.0	3.1×10^{-4}	[100]

(continued)

Table 3 (continued)

Material	Analyte	pH	q_{\max} (mol g ⁻¹)	References
Oxidized multi-walled carbon nanotubes (10 mg)	Malachite green (25 mL, 0.08 mM)	5.0	Oxidized multi-walled carbon nanotube: 5.4×10^{-5} Multi-walled carbon nanotube: 1.3×10^{-5}	[23]
Magnetite-multi-walled carbon nanotubes (50 mg)	Crystal violet and methylene blue (50 mL, 20 ppm)	6.0	Crystal violet: 5.6×10^{-4} Methylene blue: 1.5×10^{-4}	[98]
Magnetite-chitosan-multi-walled carbon nanotubes (30 mg)	Methyl orange (50 mL, 0.12 mM)	4.3	2.6×10^{-4}	[130]
Starch-multi-walled carbon nanotubes (50 mg)	Methyl orange and methylene blue (100 mL, 1.0 mM)	7.0	Methyl orange: 4.2×10^{-4} Methylene blue: 2.9×10^{-4}	[15]
Chitosan-poly-2-hydroxyethyl methacrylate-multi-walled carbon nanotubes (10 mg)	Methyl orange (15 mL, 0.11 mM)	4.0	1.9×10^{-3}	[76]
Magnetite-chitosan-silica-multi-walled carbon nanotubes (50 mg)	Reactive blue 19 and direct blue 71 (50 mL, 50 ppm)	Reactive blue 19: 2.0 Direct blue 19: 6.8	Reactive blue 19: 1.7×10^{-3} Direct blue 19: 6.8×10^{-4}	[1]
Water-soluble hyperbranched polyamine functionalized multiwalled carbon nanotubes nanocomposite (5 mg)	Methylene blue, malachite green, and methyl violet (10 mL, 0.12 mM)	6.0	Methylene blue: 2.5×10^{-3} Malachite green: 2.3×10^{-3} Methyl violet: 2.4×10^{-3}	[43]

(continued)

Table 3 (continued)

Material	Analyte	pH	q_{\max} (mol g ⁻¹)	References
Polyethersulfone-multi-walled carbon nanotubes (100 mg)	Rhodamine B and crystal violet (100 mL, 100 ppm)	6.0	Rhodamine B: 2.0×10^{-3} Crystal violet: 2.1×10^{-3}	[94]
β -cyclodextrin-multi-walled carbon nanotubes (10 mg)	Methylene blue and methyl orange (20 ppm)	8.0	Methylene blue: 2.8×10^{-4} Methyl orange: 3.0×10^{-4}	[82]
Copolymer acrylic acid- <i>N</i> -isopropyl acrylamide-multi-walled carbon nanotubes (50 mg)	Rhodamine B, crystal violet, and methylene blue (50 mL, 50 ppm)	8.0	Rhodamine B: 4.8×10^{-4} Crystal violet: 7.0×10^{-4} Methylene blue: 9.4×10^{-4}	[42]
Magnetite-alginate-oxidized multi-walled carbon nanotubes (700 mg)	Methylene blue (100 mL, 0.72 mM)	5.0	2.8×10^{-3}	[12]

times after being regenerated without losing the adsorption capability, which was remarkable [80].

Multi-walled carbon nanotubes functionalized with thiol functional groups were tested for methylene blue dye removal. The adsorption was done at optimum conditions at pH 6.0 and 298 K with 60 min contact time. The adsorbent material followed the Langmuir isotherm model. The q_{\max} value for methylene blue adsorption by using multi-walled carbon nanotubes functionalized with thiol functional groups (3.1×10^{-4} mol g⁻¹) was much higher than the unmodified one (7.4×10^{-6} mol g⁻¹) [100].

Effort on the further modification of multi-walled carbon nanotubes has been given to improve the adsorption capability for synthetic dyes adsorption. Oxidation of multi-walled carbon nanotubes by using oxidation agents such as HNO₃ and NaOCl generates hydroxyl and/or carboxylic acid functional groups on the surface of multi-walled carbon nanotubes thus increasing the surface area of carbon nanotubes from 115 to 158 m² g⁻¹ [115]. The increment of the surface area gave a positive effect on the adsorption capability of multi-walled carbon nanotubes. The q_{\max} value of unmodified carbon nanotubes for malachite green adsorption was 1.3×10^{-5} mol g⁻¹ while oxidized carbon nanotubes exhibited a four-time higher q_{\max} value (5.4×10^{-5} mol g⁻¹), which was remarkable [23].

Another modification is the preparation of a composite material between multi-walled carbon nanotubes and other organic/inorganic materials. The combination of

magnetite and multi-walled carbon nanotubes increased the surface area of multi-walled carbon nanotubes to $145 \text{ m}^2 \text{ g}^{-1}$. The improvement of the surface area enhanced the adsorption capability of crystal violet and methylene blue dyes. The q_{max} value for crystal violet adsorption was slightly improved from 4.0×10^{-4} to $5.6 \times 10^{-4} \text{ mol g}^{-1}$ while the q_{max} value for methylene blue adsorption was significantly improved from 7.4×10^{-6} to $1.5 \times 10^{-4} \text{ mol g}^{-1}$ [98].

A different structure of synthetic dye gives different adsorption preference for modified multi-walled carbon nanotubes. The chemical structure of crystal violet is larger than methylene blue, thus adsorption of crystal violet is sterically hindered by multi-walled carbon nanotubes thus the adsorption mechanism mainly happened through hydrophobic interactions. In contrast, methylene blue with a smaller chemical structure was able to infiltrate the structure of the adsorbent material and then trapped with strong interactions with magnetite structure [98].

A composite material consisting of magnetite, chitosan, and multi-walled carbon nanotubes showed a higher adsorption capacity for the adsorption of methyl orange in the distilled water media. The adsorption isotherm of methyl orange followed the Langmuir model while the adsorption kinetics fitted well with the pseudo-second-order kinetic model. The q_{max} value for methyl orange adsorption was slightly improved from 1.2×10^{-4} to $2.6 \times 10^{-4} \text{ mol g}^{-1}$ compared to the unmodified carbon nanotubes material. The adsorbent material can be easily separated through filtration with the aid of a magnet thus the adsorbent material can be reused for a further adsorption process [130].

The combination of starch and multi-walled carbon nanotubes increased the biocompatibility and hydrophilicity properties, as well as surface area enhancement (from 115 to $133 \text{ m}^2 \text{ g}^{-1}$). The composite material gave higher adsorption capability towards methyl orange and methylene blue dyes in the aqueous solution. The q_{max} value for methyl orange adsorption was increased from 1.2×10^{-4} to $4.2 \times 10^{-4} \text{ mol g}^{-1}$ compared to the unmodified carbon nanotubes material. On the other hand, the q_{max} value for methylene blue adsorption was improved from 7.4×10^{-6} to $2.9 \times 10^{-4} \text{ mol g}^{-1}$ compared to the unmodified carbon nanotubes material. The enhancement of the adsorption capacity of synthetic dyes mainly occurred due to the better dispersion ability of multi-walled carbon nanotubes due to higher hydrophilicity and surface area [15].

A composite material consisting of chitosan, poly-2-hydroxyethyl methacrylate and multi-walled carbon nanotubes were employed as the adsorbent material for the removal of methyl orange. The q_{max} value for methyl orange adsorption using the composite material was improved 15 times fold from 1.2×10^{-4} to $1.9 \times 10^{-3} \text{ mol g}^{-1}$. Furthermore, the composite material can be regenerated by the desorption process of methyl orange at pH 13. The adsorption mechanism was reported to be happened through hydrogen bonds and electrostatic interactions between methyl orange with chitosan and poly-2-hydroxyethyl methacrylate, together with π - π stacking interactions between methyl orange and multi-walled carbon nanotubes [76].

A combination of magnetite, chitosan, silica, and multi-walled carbon nanotubes in a composite material has been prepared for the adsorption of reactive blue 19 and

direct blue 71. The composite material was prepared through a gelation technique employing glutaraldehyde as the linker agent. The optimum pH for reactive blue 19 dye adsorption was found at pH 2 while the optimum pH for direct blue 71 dye adsorption was found at pH 6.8. The adsorption isotherm of both reactive blue 19 and direct blue 71 dyes followed the Langmuir model yielding the q_{\max} value of 1.7×10^{-3} and 6.8×10^{-4} mol g⁻¹, respectively. The adsorption mechanism of reactive blue 19 and direct blue 71 dyes adsorption happened mainly through electrostatic, hydrogen bonds, and π - π stacking interactions [1].

A nanocomposite of water-soluble hyperbranched polyamine functionalized multi-walled carbon nanotubes has been used for the adsorption of organic dyes, i.e. methylene blue, malachite green, and methyl violet. Each adsorbent had an efficient removal value of more than 90% for each dye with an optimum pH of 6.0. The contact time of the nanocomposite material for methylene blue adsorption was 10 min, while the adsorption of malachite green and methyl violet required 120 min. The q_{\max} values for methylene blue, malachite green, and methyl violet were 2.5×10^{-3} , 2.3×10^{-3} , and 2.4×10^{-3} mol g⁻¹, respectively. Adsorption kinetics followed a pseudo-second-order model, while the adsorption isotherm followed the Langmuir model. The adsorbent regeneration was conducted by using a mixture of ethanol and water. Furthermore, the nanocomposite adsorbent material did not lose the adsorption capability after the five-cycle adsorption process [43].

Composite material from polyethersulfone and multi-walled carbon nanotubes has been evaluated for the adsorption of rhodamine B and crystal violet. The composite material was prepared using triethylenediamine as the linker agent through an impregnation method. The composite material gave high adsorption capacity for rhodamine B and crystal violet adsorption. The q_{\max} value for rhodamine B and crystal violet adsorption was 2.0×10^{-3} and 2.1×10^{-3} mol g⁻¹, respectively. Compared to the unmodified multi-walled carbon nanotubes, the composite material has a higher thermal and chemical stability, as well as a larger surface area and stronger antifouling properties [94].

On the other hand, composite material between β -cyclodextrin and multi-walled carbon nanotubes has been used for the adsorption of methylene blue and methyl orange. The composite material was produced through an impregnation reaction by using glycine as the linker agent. The q_{\max} value for methylene blue adsorption was improved from 7.4×10^{-6} to 2.8×10^{-4} mol g⁻¹ compared to the unmodified carbon nanotubes material. On the other hand, the q_{\max} value for methyl orange adsorption was slightly improved from 1.2×10^{-4} to 3.0×10^{-4} mol g⁻¹ compared to the unmodified carbon nanotubes material. The adsorption mechanism was reported to be happened through hydrogen bondings between synthetic dyes with β -cyclodextrin, together with π - π stacking interactions between synthetic dyes and multi-walled carbon nanotubes [82].

Copolymerization of acrylic acid and *N*-isopropyl acrylamide together with multi-walled carbon nanotubes and magnetite have been prepared through a chain transfer copolymerization reaction. The composite material was evaluated for rhodamine B, crystal violet, and methylene blue dyes adsorption. The q_{\max} value for rhodamine B, crystal violet, and methylene blue adsorption was found to be 4.8×10^{-4} , $7.0 \times$

10^{-4} , and $9.4 \times 10^{-4} \text{ mol g}^{-1}$, respectively. The adsorption mechanism occurred via hydrogen bonds and electrostatic interactions. The composite material was easily regenerated by washing with HNO_3 . Furthermore, the composite material can be reused for up to five-cycle process [42].

Recently, composite material from magnetite, alginate, and oxidized multi-walled carbon nanotubes was prepared and applied for methylene blue adsorption. The composite material gave 380 times higher q_{max} value ($2.8 \times 10^{-3} \text{ mol g}^{-1}$) than the unmodified multi-walled carbon nanotubes ($7.4 \times 10^{-6} \text{ mol g}^{-1}$), which was remarkable. The methylene blue adsorption was found to be a spontaneous and endothermic reaction from the thermodynamic data. The regeneration of the composite material was done by washing the porous material with 0.10 M HNO_3 . The composite material did not lose the adsorption capability after the six-cycle process, which was remarkable [12].

5 Conclusions

Aromatic-based synthetic macromolecules, i.e. calixarenes and carbon nanotubes are found to be suitable adsorbent materials for dyes adsorption and removal from the textile wastewater. Adsorption of synthetic dyes using aromatic-based synthetic macromolecules offers an easy and simple operation process as well as high adsorption capability and selectivity. The calixarenes possess a strong binding affinity with synthetic dyes mainly through hydrogen bonds and electrostatic interactions. On the other hand, the carbon nanotube materials serve as an adsorbent material for synthetic dyes mainly through π - π stacking and hydrophobic interactions. Furthermore, the aromatic-based synthetic macromolecules are easily regenerated by either adjustment of the pH value or solvent washing; thus, a consecutive adsorption process for dyes removal from textile wastewater is possible for a real-life application.

Acknowledgements Financial support from the Directorate of Research, Technology and Community Services, KEMDIKBUDRISTEK, The Republic of Indonesia, through the PTUPT Scheme for the budget year 2020–2022 is greatly acknowledged.

References

1. Abbasi M (2017) Synthesis and characterization of magnetic nanocomposite of chitosan/SiO₂/carbon nanotubes and its application for dyes removal. *J Clean Prod* 145:105–113. <https://doi.org/10.1016/j.clepro.2017.01.046>
2. Afroze S, Sen TK (2018) A review on heavy metal ions and dye adsorption from water by agricultural solid waste adsorbents. *Water Air Soil Pollut* 229:225. <https://doi.org/10.1007/s11270-018-3869-z>

- Akceylan E, Bahadir M, Yilmaz M (2009) Removal efficiency of a calix[4]arene-based polymer for water-soluble carcinogenic direct azo dyes and aromatic amines. *J Hazard Mater* 162:960–966. <https://doi.org/10.1016/j.jhazmat.2008.05.127>
- Akceylan E, Erdemir S (2015) Carcinogenic direct azo dye removal from aqueous solution by amino-functionalized calix[4]arenes. *J Incl Phenom Macrocycl Chem* 82:471–478. <https://doi.org/10.1007/s10847-015-0518-7>
- Alotaibi NF, Nassar AM, Alrwailli GM, Elnasr TAS, Zeid EFA (2019) Selective, efficient and complete precipitation of anionic dyes in aqueous solutions using Ag@PbCO₃ nanocomposite. *Inorg Nano-metal Chem* 49:395–400. <https://doi.org/10.1080/24701556.2019.1661463>
- Annadurai G, Juang RS, Lee DJ (2002) Use of cellulose-based wastes for adsorption of dyes from aqueous solutions. *J Hazard Mater* 92:263–274. [https://doi.org/10.1016/S0304-3894\(02\)00017-1](https://doi.org/10.1016/S0304-3894(02)00017-1)
- Ariyanti D, Iswanti D, Sugita P, Nurhidayat N, Effendi H, Ghazali AA, Kurniawan YS (2020) Highly selective phenol biosensor utilizing selected *Bacillus* biofilm through an electrochemical method. *Makara J Sci* 24:24–30. <https://doi.org/10.7454/mss.v24i1.11726>
- Aryal N, Wood J, Rijal I, Deng D, Jha MK, Boadu AO (2020) Fate of environmental pollutants: a review. *Water Environ Res* 92:1587–1594. <https://doi.org/10.1002/wer.1404>
- Aygun A, Yenisoay-Karakas S, Duman I (2003) Production of granular activated carbon from fruit stones and nutshells and evaluation of their physical, chemical and adsorption properties. *Microporous Mesoporous Mater* 66:189–195. <https://doi.org/10.1016/j.micromeso.2003.08.028>
- Bahgat M, Farghali AA, Rouby WE, Khedr M, Ahmed MYM (2013) Adsorption of methyl green dye onto multi-walled carbon nanotubes decorated with Ni nanoferrite. *Appl Nanosci* 3:251–261. <https://doi.org/10.1007/s13204-012-0127-3>
- Bhatti AA, Oguz M, Yilmaz M (2017) Magnetizing calixarene: azo dye removal from aqueous media by Fe₃O₄ nanoparticles fabricated with carboxylic-substituted calix[4]arene. *J Chem Eng Data* 62:2819–2825. <https://doi.org/10.1021/acs.jced.7b00128>
- Boukhalfa N, Bouthala M, Djebri N, Idris A (2019) Kinetics, thermodynamics, equilibrium isotherms, and reusability studies of cationic dye adsorption by magnetic alginate/oxidized multiwalled carbon nanotubes composites. *Int J Bio Macromol* 123:539–548. <https://doi.org/10.1016/j.ijbiomac.2018.11.102>
- Butler EB, Hung YT, Mulamba O (2017) The effects of chemical coagulants on the decolorization of dyes by electrocoagulation using response surface methodology (RSM). *Appl Water Sci* 7:2357–2371. <https://doi.org/10.1007/s13201-016-0410-7>
- Cengiz S, Cavas L (2008) Removal of methylene blue by invasive marine seaweed: *Caulerpa racemosa* var. *cylindracea*. *Bioresour Technol* 99:2357–2363. <https://doi.org/10.1016/j.biortech.2007.05.011>
- Chang PR, Zheng P, Liu B, Anderson DP, Yu J, Ma X (2011) Characterization of magnetic soluble starch-functionalized carbon nanotubes and its application for the adsorption of the dyes. *J Hazard Mater* 186:2144–2150. <https://doi.org/10.1016/j.jhazmat.2010.12.119>
- Chen M, Chen Y, Diao G (2010) Adsorption kinetics and thermodynamics of methylene blue onto p-tert-butyl-calix[4,6,8]arene-bonded silica gel. *J Chem Eng Data* 55:5109–5116. <https://doi.org/10.1021/je1006696>
- Chen M, Shang T, Fang W, Diao G (2011) Study on adsorption and desorption properties of the starch grafted p-tert-butyl-calix[n]arene for butyl rhodamine B solution. *J Hazard Mater* 185:914–921. <https://doi.org/10.1016/j.jhazmat.2010.09.107>
- Chen Y, Chen L, Bai H, Li L (2013) Graphene oxide-chitosan composite hydrogels as broad-spectrum adsorbents for water purification. *J Mater Chem A* 1:1992–2001. <https://doi.org/10.1039/C2TA00406B>
- Cheng Z, Liao J, He B, Zhang F, Zhang F, Huang X, Zhou L (2015) One-step fabrication of graphene oxide enhanced magnetic composite gel for highly efficient dye adsorption and catalysis. *ACS Sustain Chem Eng* 3:1677–1685. <https://doi.org/10.1021/acssuschemeng.5b00383>

20. Choy KKH, McKay G, Porter JF (1999) Sorption of acid dyes from effluents using activated carbon. *Resour Conser Recycl* 27:57–71. [https://doi.org/10.1016/S0921-3449\(98\)00085-8](https://doi.org/10.1016/S0921-3449(98)00085-8)
21. Crini G, Lichtfouse E (2019) Advantages and disadvantages of techniques used for wastewater treatment. *Environ Chem Lett* 17:145–155. <https://doi.org/10.1007/s10311-018-0785-9>
22. Crini G, Lichtfouse E, Wilson LD, Morin-Crini N (2019) Conventional and non-conventional adsorbents for wastewater treatment. *Environ Chem Lett* 17:195–213. <https://doi.org/10.1007/s10311-018-0786-8>
23. Derakhshan MS, Moradi O (2014) The study of thermodynamics and kinetics methyl orange and malachite green by SWCNTs, SWCNT-COOH and SWCNT-NH₂ as adsorbents from aqueous solution. *J Ind Eng Chem* 20:3186–3194. <https://doi.org/10.1016/j.jiec.2013.11.064>
24. Dutta DP, Venugopalan R, Chopade S (2017) Manipulating carbon nanotubes for efficient removal of both cationic and anionic dyes from wastewater. *ChemistrySelect* 2:3878–3888. <https://doi.org/10.1002/slct.201700135>
25. Espanol ES, Villamil MM (2019) Calixarenes: generalities and their role in improving the solubility, biocompatibility, stability, bioavailability, detection, and transport of biomolecules. *Biomolecules* 9:90. <https://doi.org/10.3390/biom9030090>
26. Etika SB, Nasra E (2021) Utilization of C-cinnamal calix[4]resorcinarene as adsorbent for methanil yellow. *J Phys Conf Ser* 1788:012012. <https://doi.org/10.1088/1742-6596/1788/1/012012>
27. Ferreira GMD, Ferreira GMD, Hespanhol MC, Rezende JP, Pires ACS, Gurgel LVA, Silva LHM (2017) Adsorption of red azo dyes on multi-walled carbon nanotubes and activated carbon: a thermodynamic study. *Colloids Surf A* 529:531–540. <https://doi.org/10.1016/j.colsurfa.2017.06.021>
28. Ferrero F (2007) Dye removal by low cost adsorbents: hazelnut shells in comparison with wood sawdust. *J Hazard Mater* 142:144–152. <https://doi.org/10.1016/j.jhazmat.2006.07.072>
29. Garai B, Shetty D, Skorjanc T, Gandara F, Naleem N, Varghese S, Sharma SK, Baias M, Jagannathan R, Olson MA, Kirmizialtin S, Trabolsi A (2021) Taming the topology of calix[4]arene-based 2D-covalent organic frameworks: interpenetrated vs noninterpenetrated frameworks and their selective removal of cationic dyes. *J Am Chem Soc* 143:3407–3415. <https://doi.org/10.1021/jacs.0c12125>
30. Garg T, Hamilton SE, Hochard JP, Kresch EP, Talbot J (2018) (Not so) gently down the stream: river pollution and health in Indonesia. *J Environ Econ Manage* 92:35–53. <https://doi.org/10.1016/j.jeem.2018.08.011>
31. Ghadhbani MY, Majidi HS, Rashid KT, Alsahy QF, Lakshmi DS, Salih IK, Figoli A (2020) Removal of dye from a leather tanning factory by flat-sheet ultrafiltration (UF) membrane. *Membranes* 10:47. <https://doi.org/10.3390/membranes10030047>
32. Ghaedi M, Nasab AG, Khodadoust S, Rajabi M, Azizian S (2014) Application of activated carbon as adsorbents for efficient removal of methylene blue: kinetics and equilibrium study. *J Ind Eng Chem* 20:2317–2324. <https://doi.org/10.1016/j.jiec.2013.10.007>
33. Ghaedi M, Kokhdan SN (2015) Removal of methylene blue from aqueous solution by wood millet carbon optimization using response surface methodology. *Spectrochim Acta A Mol Biomol Spectrosc* 136:141–148. <https://doi.org/10.1016/j.saa.2014.07.048>
34. Gungor O, Yilmaz A, Memon S, Yilmaz M (2008) Evaluation of the performance of calix[8]arene derivatives as liquid phase extraction material for the removal of azo dyes. *J Hazard Mater* 158:202–207. <https://doi.org/10.1016/j.jhazmat.2008.01.060>
35. Gungor O (2019) Efficient removal of carcinogenic azo dyes by novel pyrazine-2-carboxylate substituted calix[4,8]arene derivatives. *Supramol Chem* 31:776–783. <https://doi.org/10.1080/10610278.2020.1711908>
36. Gupta VK, Khamparia S, Tyagi I, Jaspal D, Malviya A (2015) Decolorization of mixture of dyes: a critical review. *Glob J Environ Sci Manage* 1:71–94. <https://doi.org/10.7508/GJESM.2015.01.007>
37. Gustavo L, Reis TD, Robaina NF, Pacheco WF, Cassella RJ (2011) Separation of malachite green and methyl green cationic dyes from aqueous medium by adsorption on amberlite XAD-2 and XAD-4 resins using sodium dodecylsulfate as carrier. *Chem Eng J* 171:532–540. <https://doi.org/10.1016/j.cej.2011.04.024>

38. Han R, Zhang J, Han P, Wang Y, Zhao Z, Tang M (2009) Study of equilibrium, kinetic and thermodynamic parameters about methylene blue adsorption onto natural zeolite. *Chem Eng J* 145:496–504. <https://doi.org/10.1016/j.cej.2008.05.003>
39. Handayani DS, Purnawan C, Pranoto HS, Hilmiyana D (2016) Adsorption of Remazol yellow FG from aqueous solution on chitosan-linked P-T-butylcalix[4]arene. *IOP Conf Ser Mater Sci Eng* 107:012011. <https://doi.org/10.1088/1757-899X/107/1/012011>
40. Hassaan MA, Nemr A (2017) Health and environmental impacts of dyes: mini review. *Am J Environ Sci* 1:64–67. <https://doi.org/10.11648/j.ajese.20170103.11>
41. Holkar CR, Jadhav AJ, Pinjari DV, Mahamuni NM, Pandit AB (2016) A critical review on textile wastewater treatments: possible approaches. *J Environ Manage* 182:351–366. <https://doi.org/10.1016/j.jenvman.2016.07.090>
42. Hosseinzadeh S, Hosseinzadeh H, Pashaei S, Khodaparast Z (2018) Synthesis of magnetic functionalized MWCNT nanocomposite through surface RAFT co-polymerization of acrylic acid and *N*-isopropyl acrylamide for removal of cationic dyes from aqueous solutions. *Ecotoxicol Environ Saf* 161:34–44. <https://doi.org/10.1016/j.ecoenv.2018.05.063>
43. Hu L, Yang Z, Wang Y, Li Y, Fan D, Wu D, Wei Q, Du B (2017) Facile preparation of water-soluble hyperbranched polyamine functionalized multiwalled carbon nanotubes for high-efficiency organic dye removal from aqueous solution. *Sci Rep* 7:3611. <https://doi.org/10.1038/s41598-017-03490-6>
44. Huang F, Anslyn EV (2015) Introduction: supramolecular chemistry. *Chem Rev* 115:6999–7000. <https://doi.org/10.1021/acs.chemrev.5b00352>
45. Iijima S, Ichihashi T (1993) Single-shell carbon nanotubes of 1-nm diameter. *Nature* 363:603–605. <https://doi.org/10.1038/363603a0>
46. Iijima S (2002) Carbon nanotubes: past, present, and future. *PhyB* 323:1–5. [https://doi.org/10.1016/S0921-4526\(02\)00869-4](https://doi.org/10.1016/S0921-4526(02)00869-4)
47. Janos P, Buchtova H, Ryznarova M (2003) Sorption of dyes from aqueous solutions onto fly ash. *Water Res* 37:4938–4944. <https://doi.org/10.1016/j.watres.2003.08.011>
48. John J, Dineshran R, Hemalatha KR, Dhassiah MP, Gopal D, Kumar A (2020) Biodecolorization of synthetic dyes by a halophilic bacterium *Salinivibrio* sp. *Front Microbiol* 11:594011. <https://doi.org/10.3389/fmicb.2020.594011>
49. Jumina J, Priastomo Y, Setiawan HR, Mutmainah M, Kurniawan YS, Ohto K (2020) Simultaneous removal of lead(II), chromium(III) and copper(II) heavy metal ions through an adsorption process using C-phenylcalix[4]pyrogallolarene material. *J Environ Chem Eng* 8:103971. <https://doi.org/10.1016/j.jece.2020.103971>
50. Jumina J, Setiawan HR, Triono S, Kurniawan YS, Siswanta D, Zulkarnain AK, Kumar N (2020) The C-arylcalix[4]pyrogallolarene sulfonic acid: a novel and efficient organocatalyst material for biodiesel production. *Bull Chem Soc Jpn* 93:252–259. <https://doi.org/10.1246/bcsj.20190275>
51. Junejo R, Memon S, Memon FN, Memon AA, Durmaz F, Bhatti AA, Bhatti AA (2019) Thermodynamic and kinetic studies for adsorption of reactive blue (RB-19) dye using calix[4]arene-based adsorbent. *J Chem Eng Data* 64:3407–3415. <https://doi.org/10.1021/acs.jced.9b00223>
52. Kamboh MA, Solangi IB, Sherazi STH, Memon S (2009) Synthesis and application of calix[4]arene based resin for the removal of azo dyes. *J Hazard Mater* 172:234–239. <https://doi.org/10.1016/j.jhazmat.2009.06.165>
53. Kamboh MA, Bhatti AA, Solangi IB, Sherazi STH, Memon S (2014) Adsorption of direct black-38 azo dye on p-tert-butylcalix[6]arene immobilized material. *Arab J Chem* 7:125–131. <https://doi.org/10.1016/j.arabjc.2013.06.033>
54. Kannan N, Sundaram MM (2001) Kinetics and mechanism of removal of methylene blue by adsorption on various carbons: a comparative study. *Dyes Pigm* 51:25–40. [https://doi.org/10.1016/S0143-7208\(01\)00056-0](https://doi.org/10.1016/S0143-7208(01)00056-0)
55. Kavitha D, Namasivayam C (2007) Experimental and kinetic studies on methylene blue adsorption by coir pith carbon. *Bioresour Technol* 98:14–21. <https://doi.org/10.1016/j.biotech.2005.12.008>

56. Kazakova EK, Morozova JE, Mironova DA, Kononov AI (2012) Sorption of azo dyes from aqueous solutions by tetradodecyloxybenzylcalix[4]resorcinarene derivatives. *J Incl Phenom Macro Chem* 74:467–472. <https://doi.org/10.1007/s10847-011-0075-7>
57. Kazemi P, Peydayesh M, Bandegi A, Mohammadi T, Bakhtiari O (2013) Pertraction of methylene blue using a mixture of D2EHPA/M2EHPA and sesame oil as a liquid membrane. *Chem Papers* 67:722–729. <https://doi.org/10.2478/s11696-013-0374-0>
58. Kongor A, Panchal M, Athar M, Vora M, Makwana B, Jha PC, Jain V (2020) Calix[4]pyrrole stabilized PdNPs as an efficient heterogeneous catalyst for enhanced degradation of water-soluble carcinogenic azo dyes. *Catal Lett* 151:548–558. <https://doi.org/10.1007/s1056-020-03304-x>
59. Kumar KV, Porkodi K (2006) Relation between some two- and three-parameter isotherm models for the sorption of methylene blue onto lemon peel. *J Hazard Mater* 138:633–635. <https://doi.org/10.1016/j.jhazmat.2006.06.078>
60. Kumar R, Sharma A, Singh H, Suating P, Kim HS, Sunwoo K, Shim I, Gibb BC, Kim JS (2019) Revisiting fluorescent calixarenes: from molecular sensors to smart materials. *Chem Rev* 119:9657–9721. <https://doi.org/10.1021/acs.chemrev.8b00605>
61. Kurniawan YS, Sathuluri RR, Iwasaki W, Morisada S, Kawakita H, Ohto K, Miyazaki M, Jumina J (2018) Microfluidic reactor for Pb(II) ion extraction and removal with amide derivative of calix[4]arene supported by spectroscopic studies. *Microchem J* 142:377–384. <https://doi.org/10.1016/j.microc.2018.07.001>
62. Kurniawan YS, Sathuluri RR, Ohto K, Iwasaki W, Kawakita H, Morisada S, Miyazaki M, Jumina J (2019) A rapid and efficient lithium-ion recovery from seawater with tripropylmonoacetic acid calix[4]arene derivative employing droplet-based microfluidic reactor system. *Sep Purif Technol* 211:925–934. <https://doi.org/10.1016/j.seppur.2018.10.049>
63. Kurniawan YS, Ryu M, Sathuluri RR, Iwasaki W, Morisada S, Kawakita H, Ohto K, Maeki M, Miyazaki M, Jumina J (2019) Separation of Pb(II) ion with tetraacetic acid derivative of calix[4]arene by using droplet-based microreactor system. *Indones J Chem* 19:368–375. <https://doi.org/10.22146/ijc.34387>
64. Kurniawan YS, Anggraeni K, Indrawati R, Yuliati L (2020) Functionalization of titanium dioxide through dye sensitizing method utilizing red amaranth extract for phenol photodegradation. *IOP Conf Ser Mater Sci Eng* 902:012029. <https://doi.org/10.1088/1757-899X/902/1/012029>
65. Kurniawan YS, Sathuluri RR, Ohto K (2020b) Droplet microfluidic device for rapid and efficient metal separation using host-guest chemistry. In: Ren Y (ed) *Advances in microfluidic technologies for energy and environmental applications*. IntechOpen, London, pp 1–19. <https://doi.org/10.5772/intechopen.89846>
66. Kurniawan YS, Priyanga KTA, Krisbiantoro PA, Imawan AC (2021) Green chemistry influences in organic synthesis: a review. *J Mult App Nat Sci* 1:1–12. <https://doi.org/10.47352/jmans.v1i1.2>
67. Lellis B, Polonio CZF, Pamphile JA, Polonio JC (2019) Effects of textile dyes on health and the environment and bioremediation potential of living organisms. *Biotechnol Res Innov* 3:275–290. <https://doi.org/10.1016/j.biori.2019.09.001>
68. Li H, Huang H, Yan X, Liu C, Li L (2021) A calix[4]arene-crosslinked polymer for rapid adsorption of cationic dyes in water. *Mater Chem Phys* 263:124295. <https://doi.org/10.1016/j.matchemphys.2021.124295>
69. Luca PD, Chiodo A, Macario A, Siciliano C, Nagy JB (2021) Semi-continuous adsorption processes with multi-walled carbon nanotubes for the treatment of water contaminated by an organic textile dye. *Appl Sci* 11:1687. <https://doi.org/10.3390/app11041687>
70. Ma J, Chen C, Yu F (2016) Self-regenerative and self-enhanced smart graphene/Ag₃PO₄ hydrogel adsorbent under visible light. *New J Chem* 40:3208–3215. <https://doi.org/10.1039/C5NJ03404C>
71. Ma J, Sun Y, Zhang M, Yang M, Gong X, Yu F, Zheng J (2017) Comparative study of graphene hydrogels and aerogels reveals the important role of buried water in pollutant adsorption. *Environ Sci Technol* 51:12283–12292. <https://doi.org/10.1021/acs.est.7b02227>

72. Ma J, Zhang Y, Zhao B, Jia Q (2020) Supramolecular adsorbents in extraction and separation techniques: a review. *Anal Chim Acta* 1122:97–113. <https://doi.org/10.1016/j.aca.2020.04.054>
73. Machado FM, Carmalin SA, Lima EC, Dias SLP, Prola LDT, Saucier C, Jauris IM, Zanella I, Fagan SB (2016) Adsorption of alizarin red s dye by carbon nanotubes: an experimental and theoretical investigation. *J Phys Chem C* 120:18296–18306. <https://doi.org/10.1021/acs.jpcc.6b03884>
74. Madaeni SS, Jamali Z, Islami N (2011) Highly efficient and selective transport of methylene blue through a bulk liquid membrane containing Cyanex 301 as carrier. *Sep Purif Technol* 81:116–123. <https://doi.org/10.1016/j.seppur.2011.07.004>
75. Madrakian T, Afkhami A, Ahmadi M, Bagheri H (2011) Removal of some cationic dyes from aqueous solutions using magnetic-modified multi-walled carbon nanotubes. *J Hazard Mater* 196:109–114. <https://doi.org/10.1016/j.jhazmat.2011.08.078>
76. Mahmoodian H, Moradi O, Shariatzadeha B, Salehf TA, Tyagi I, Maity A, Asif M, Gupta VK (2015) Enhanced removal of methyl orange from aqueous solutions by polyHEMA-chitosan-MWCNT nano-composite. *J Mol Liq* 202:189–198. <https://doi.org/10.1016/h.molliq.2014.10.040>
77. Mashkoo F, Nasar A, Inamuddin (2020) Carbon nanotube-based adsorbents for the removal of dyes from waters: a review. *Environ Chem Lett* 18:605–629. <https://doi.org/10.1007/s10311-020-00970-6>
78. Memon FN, Memon S, Minhas FT (2014) Rapid transfer of methyl red using calix[6]arene as a carrier in a bulk liquid membrane. *C R Chim* 17:577–585. <https://doi.org/10.1016/j.crci.2013/09.015>
79. Memon FN, Memon S (2015) Sorption and desorption of basic dyes from industrial wastewater using calix[4]arene based impregnated material. *Sep Sci Technol* 50:1135–1146. <https://doi.org/10.1080/01496395.2014.965831>
80. Meng Y, Miao L (2019) Adsorption of dyes using multi-walled carbon nanotube hydrogel. *Chem Res Chin Univ* 35:311–318. <https://doi.org/10.1007/s40242-019-8228-0>
81. Mohammadi A, Doctorsafaei AH, Zia KM (2018) Alginate/calix[4]arenes modified graphene oxide nanocomposite beads: preparation, characterization, and dye adsorption studies. *Int J Biol Macromol* 120:1353–1361. <https://doi.org/10.1016/j.ijbiomac.2018.09.136>
82. Mohammadi A, Veisi P (2018) High adsorption performance of β -cyclodextrin-functionalized multi-walled carbon nanotubes for the removal of organic dyes from water and industrial wastewater. *J Environ Chem Eng* 6:4634–4643. <https://doi.org/10.1016/j.jece.2018.07.002>
83. Mohddin AT, Hameed BH (2010) Adsorption of methyl violet dye on acid modified activated carbon: isotherms and thermodynamics. *J Appl Sci Environ Sani* 5:151–160
84. Muthuraman G, Ibrahim M (2013) Use of bulk liquid membrane for the removal of Cibacron red FN-R from aqueous solution using TBAB as a carrier. *J Ind Eng Chem* 19:444–449. <https://doi.org/10.1016/j.jiec.2012.08.025>
85. Namasivayam C, Radhika R, Suba S (2001) Uptake of dyes by a promising locally available agricultural solid waste: coir pith. *Waste Manage* 21:381–387. [https://doi.org/10.1016/S0956-053X\(00\)00081-7](https://doi.org/10.1016/S0956-053X(00)00081-7)
86. Narula A, Rao CP (2019) Hydrogel of the supramolecular complex of graphene oxide and sulfonatocalix[4]arene as reusable material for the degradation by spectroscopy and microscopy. *ACS Omega* 4:5731–5740. <https://doi.org/10.1021/acsomega.9b00545>
87. Ofomaja AE, Ho YS (2008) Effect of temperatures and pH on methyl violet biosorption by *Mansonia* wood sawdust. *Biores Tech* 99:5411–5417. <https://doi.org/10.1016/j.biortech.2007.11.018>
88. Ohto K (2010) Review of the extraction behavior of metal cations with calixarene derivatives. *Solvent Extr Res Des, Jpn* 17:1–18
89. Otero M, Rozada F, Calvo LF, Garcia AI, Moran A (2003) Kinetic and equilibrium modeling of the methylene blue removal from solution by adsorbent materials produced from sewage sludges. *Biochem Eng* 15:59–68. [https://doi.org/10.1016/S1369-703X\(02\)00177-8](https://doi.org/10.1016/S1369-703X(02)00177-8)

90. Ovsyannikov A, Solovieva S, Antipin I, Ferlay S (2017) Coordination polymers based on calixarene derivatives: structures and properties. *Coord Chem Rev* 352:151–186. <https://doi.org/10.1016/j.ccr.2017.09.004>
91. Ozmen EY, Erdemir S, Yilmaz M, Bahadir M (2007) Removal of carcinogenic direct azo dyes from aqueous solutions using calix[n]arene derivatives. *Clean* 35:612–616. <https://doi.org/10.1002/clean.200700033>
92. Pavan FA, Lima EC, Dias SLP, Mazzocato AC (2008) Methylene blue biosorption from aqueous solutions by yellow passion fruit waste. *J Hazard Mater* 150:703–712. <https://doi.org/10.1016/j.jhazmat.2007.05.023>
93. Pekkuz H, Uzun I, Guzel F (2008) Kinetics and thermodynamics of the adsorption of some dyestuffs from aqueous solution by poplar sawdust. *Bioresour Technol* 99:2009–2017. <https://doi.org/10.1016/j.biortech.2007.03.014>
94. Peydayesh M, Mohammadi T, Bakhtiari O (2018) Effective treatment of dye wastewater via positively charged TETA-MWCNT/PES hybrid nanofiltration membranes. *Sep Purif Technol* 194:488–502. <https://doi.org/10.1016/j.seppur.2017.11.070>
95. Priyanga KTA, Kurniawan YS, Yuliati L (2020) Synthesis and characterizations of C-3-nitrophenylcalix[4]resorcinarene as a potential chemosensor for La(III) ions. *IOP Conf Ser Mater Sci Eng* 959:012014. <https://doi.org/10.1088/1757-899X/959/1/012014>
96. Priyanga KTA, Kurniawan YS, Yuliati L, Purwono B, Wahyuningih TD, Lintang HO (2021) Novel Schiff base azo-imine for ultra-sensitive and highly selective fluorescent chemosensor of Fe³⁺ ions. *Luminescence*. <https://doi.org/10.1002/bio.4049>
97. Priyanga KTA, Kurniawan YS, Yuliati L (2021) Effect of calcination temperature on the photocatalytic activity of Zn₂Ti₃O₈ materials for phenol photodegradation. *Bull Chem React Eng Catal* 16:196–204. <https://doi.org/10.9767/bcrec.16.1.10322.196-204>
98. Qu S, Huang F, Yu S, Chen G, Kong J (2008) Magnetic removal of dyes from aqueous solution using multi-walled carbon nanotubes filled with Fe₂O₃ particles. *J Hazard Mater* 160:643–647. <https://doi.org/10.1016/j.jhazmat.2008.03.037>
99. Rajabi M, Mahanpoor K, Moradi O (2017) Removal of dye molecules from aqueous solution by carbon nanotubes and carbon nanotube functional groups: critical review. *RSC Adv* 7:47083–47090. <https://doi.org/10.1039/c7ra09377b>
100. Robati D, Mirza B, Ghazisaeidi R, Rajabi M, Moradi O, Tyagi I, Agarwal S, Gupta VK (2016) Adsorption behavior of methylene blue dye on nanocomposite multi-walled carbon nanotube functionalized thiol (MWCNT-SH) as new adsorbent. *J Mol Liq* 216:830–835. <https://doi.org/10.1016/j.molliq.2016.02.004>
101. Rosly NZ, Abdullah AH, Kamarudin MA, Ashari SE, Ahmad SAA (2021) *Int J Environ Res Public Health* 18:397. <https://doi.org/10.3390/ijerph18020397>
102. Sagita CP, Nulandaya L, Kurniawan YS (2021) Efficient and low-cost removal of methylene blue using activated natural kaolinite material. *J Mult Appl Nat Sci* 1:69–77. <https://doi.org/10.47352/jmans.v1i2.80>
103. Santhi T, Manonmani S, Smitha T (2010) Kinetics and isotherm studies on cationic dyes adsorption onto annona squamosa seed activated carbon. *Int J Eng Sci Tech* 2:287–295
104. Sarkar B, Mandal B, Tsang YF, Kumar P, Kim KH, Ok YS (2018) Designer carbon nanotubes for contaminant removal in water and wastewater: a critical review. *Sci Total Environ* 612:561–581. <https://doi.org/10.1016/j.scitotenv.2017.08.132>
105. Sathuluri RR, Kurniawan YS, Kim JY, Maeki M, Iwasaki W, Morisada S, Kawakita H, Miyazaki M, Ohto K (2018) Droplet-based microreactor system for stepwise recovery of precious metal ions from real metal waste with calix[4]arene derivatives. *Sep Sci Technol* 53:1261–1272. <https://doi.org/10.1080/01496395.2017.1366518>
106. Savyasachi AJ, Kotova O, Shanmugaraju S, Bradberry SJ, OMaille GM, Gunnlaugsson T (2017) Supramolecular chemistry: a toolkit for soft functional materials and organic particles. *Chem* 3:764–811. <https://doi.org/10.1016/j.chempr.2017.10.006>
107. Shabaan OA, Jahin HS, Mohamed GG (2020) Removal of anionic and cationic dyes from wastewater by adsorption using multiwall carbon nanotubes. *Arab J Chem* 13:4797–4810. <https://doi.org/10.1016/j.arabjc.2020.01.010>

108. Shahidi S, Moazzenchi B (2018) Carbon nanotube and its applications in textile industry—a review. *J Text Inst* 109:1653–1666. <https://doi.org/10.1080/00405000.2018.1437114>
109. Shalaeva YV, Morozova JE, Mironova DA, Kazakova EK, Kadirov MT, Nizameev IR, Konovalov AL (2015) Amidoamine calix[4]resorcinarenes-based oligomers and polymers as efficient sorbents of azo dyes from water. *Supramol Chem* 27:595–605. <https://doi.org/10.1080/10610278.2015.1046455>
110. Sharma K, Dalai AK, Vyas RK (2018) Removal of synthetic dyes from multicomponent industrial wastewaters. *Rev Chem Eng* 34:107–134. <https://doi.org/10.1515/revce-2016-0042>
111. Sharma YC, Uma (2010) Optimization of parameters for adsorption of methylene blue on a low-cost activated carbon. *J Chem Eng Data* 55:435–439. <https://doi.org/10.1021/je900408s>
112. Shetty D, Jahovic I, Raya J, Ravaux F, Jouiad M, Olsen JC, Trabolsi A (2017) An ultra-adsorbent alkyne-rich porous covalent polycalix[4]arene for water purification. *J Mater Chem A* 5:62–66. <https://doi.org/10.1039/C6TA08388A>
113. Shumatbaeva AM, Morozova JE, Syakaev VV, Shalaeva YV, Sapunova AS, Voloshina AD, Gubaidullin AT, Bazanova OB, Babaev VM, Nizameev IR, Kadirov MK, Antipin IS (2020) The pH-responsive calix[4]resorcinarene-mPEG conjugates bearing acylhydrazone bonds: synthesis and study of the potential as supramolecular drug delivery systems. *Colloids Surf A* 589:124453. <https://doi.org/10.1016/j.colsurfa.2020.124453>
114. Sikosana ML, Sikhwivhilu K, Moutloali R, Madyira DM (2019) Municipal wastewater treatment technologies: a review. *Procedia Manuf* 35:1018–1024. <https://doi.org/10.1016/j.promfg.2019.06.051>
115. Sobhanardakani S, Zandipak R, Sahraei R (2013) Removal of Janus Green dye from aqueous solutions using oxidized multi-walled carbon nanotubes. *Toxicol Environ Chem* 95:909–918. <https://doi.org/10.1080/02772248.2013.840379>
116. Sousa JCG, Riberio AR, Barbosa MO, Pereira FR, Silva AMT (2018) A review on environmental monitoring of water organic pollutants identified by EU guidelines. *J Hazard Mater* 344:146–162. <https://doi.org/10.1016/j.jhazmat.2017.09.058>
117. Temel F, Turkyilmaz M, Kucukcongar S (2020) Removal of methylene blue from aqueous solutions by silica gel supported calix[4]arene cage: investigation of adsorption properties. *Eur Polym J* 125:109540. <https://doi.org/10.1016/j.eurpolymj.2020.109540>
118. Tiwari JN, Mahesh K, Le NH, Kemp KC, Timilsina R, Tiwari RN, Kim KS (2013) Reduced graphene oxide-based hydrogels for the efficient capture of dye pollutants from aqueous solutions. *Carbon* 56:173–182. <https://doi.org/10.1016/j.carbon.2013.01.001>
119. Tsai WT, Hsien KJ, Yang JM (2004) Silica adsorbent prepared from spent diatomaceous earth and its application to removal of dye from aqueous solution. *J Colloid Interface Sci* 275:428–433. <https://doi.org/10.1016/j.jcis.2004.02.093>
120. Xiaoting F, Hongyu G, Fafu Y, Xiaoyan B (2015) Synthesis and dyes adsorption properties of calix[4]grown-grafted chitosan chelating polymer. *Chem Res Chin Univ* 31:1051–1055. <https://doi.org/10.1007/s40242-015-5242-8>
121. Yao Y, Bing H, Feifei X, Xiaofeng C (2011) Equilibrium and kinetic studies of methyl orange adsorption on multiwalled carbon nanotubes. *Chem Eng J* 170:82–89. <https://doi.org/10.1016/j.cej.2011.03.031>
122. Yilmaz A, Yilmaz E, Yilmaz M, Bartsch RA (2007) Removal of azo dyes from aqueous solutions using calix[4]arene and β -cyclodextrin. *Dyes Pigm* 74:54–59. <https://doi.org/10.1016/j.dyepig.2006.01.011>
123. Yilmaz E, Memon S, Yilmaz M (2010) Removal of direct azo dyes and aromatic amines from aqueous solutions using two β -cyclodextrin-based polymers. *J Hazard Mater* 174:592–597. <https://doi.org/10.1016/j.jhazmat.2009.09.093>
124. Yu H, Fugetsu B (2010) A novel adsorbent obtained by inserting carbon nanotubes into cavities of diatomite and applications for organic dye elimination from contaminated water. *J Hazard Mater* 177:138–145. <https://doi.org/10.1016/j.jhazmat.2009.12.007>
125. Zadmand R, Hokmabadi F, Jalali MR, Akbarzadeh A (2020) Recent progress to construct calixarene-based polymers using covalent bonds: synthesis and applications. *RSC Adv* 10:32690. <https://doi.org/10.1039/d0ra05707j>

126. Zhang X, Li A, Jiang Z, Zhang Q (2006) Adsorption of dyes and phenol from water on resin adsorbents: effect of adsorbate size and pore size distribution. *J Hazard Mater* 137:1115–1122. <https://doi.org/10.1016/j.jhazmat.2006.03.061>
127. Zhang X, Shi L, Xu G, Chen C (2013) Synthesis of β -cyclodextrin-calix[4]arene coupling product and its adsorption of basic fuchsin and methylene blue from water. *J Incl Phenom Macrocycl Chem* 75:147–153. <https://doi.org/10.1007/s10847-012-0155-3>
128. Zhang Y, Su K, Hong Z, Han Z, Yuan D (2019) Robust cationic calix[4]arene polymer as an efficient catalyst for cycloaddition of epoxides with CO₂. *Ind Eng Chem Res* 59:7247–7254. <https://doi.org/10.1021/acs.iecr.9b05312>
129. Zhao Q, Liu Y (2018) Macrocycl crosslinked mesoporous polymers for ultrafast separation of organic dyes. *Chem Commun* 54:7362–7365. <https://doi.org/10.1039/C8CC04080J>
130. Zhu HY, Jiang R, Xiao L, Zeng GM (2010) Preparation, characterization, adsorption kinetics and thermodynamics of novel magnetic chitosan enwrapping nanosized γ -Fe₂O₃ and multi-walled carbon nanotubes with enhanced adsorption properties for methyl orange. *Bioresour Technol* 101:5063–5069. <https://doi.org/10.1016/j.biortech.2010.01.107>
131. Zhu Z, Liu D, Ren Q, Tan Y, Chen Y, Zhang Y (2019) Microcapsule dispersion of poly(calix[4]arene-piperazine) for hazardous metal cations removal from wastewater. *Iran Polym J* 28:697–706. <https://doi.org/10.1007/s13726-019-00739>

Synthesis of Hydroxyapatite Nanoparticle from Papermill Sludge



A. Geethakarathi

1 Introduction

1.1 General

The exponential growth and proliferation in industrial and urban sector have led to great demand for utilization of resources, thereby causing increased waste production. Critical issues are faced by the society in managing and disposing these wastes in an economic and sustainable manner. Stringent legislation and regulations have banned most of the conventional disposal method [3]. To attain these sustainable strategies, development of innovative techniques to recover and reuse the industrial wastes and byproducts have become significant. Among many industries, this chapter focuses on the recovery and utilization of pulp and paper industry sludge to attain circular economy and industrial symbiosis. Paper industry is one of the diversified industries next to textile, tanning and automobile sector, consuming high natural resources (wood pulp), chemicals, water and energy. Consequently, higher level of greenhouse gases such as CO₂, sludge, lime mud and furnace ash is released.

The paper industry is expanding particularly in Asia and South America with the high usage of paper and is quadrupled over the past 50 years. The worldwide paper production has reached 400 MT by 2014 and is expected to reach up to 550 MT by the next 30 years [14]. The paper consumption is at unsustainable levels with negative impacts on forest, surface and sub-surface water quality, air quality and other climatic changes. Besides, high volume of greenhouse gas emission with high energy utilization, paper mills generate large amount of sludge from various treatment process of paper manufacturing units.

A. Geethakarathi (✉)

Department of Civil Engineering, Kumaraguru College of Technology, Coimbatore, Tamilnadu, India

e-mail: geethakarathi.a.ce@kct.ac.in

1.2 Papermill Manufacturing Process

The paper mill sludge constitutes of organic components (wood, cellulose and organic binders) and inorganic components such as calcium carbonate, paper additives and other heavy metal impurities [26]. India contributes to about 3.18% of global paper production (408 million tons per annum) as per Indian Paper Industry, 2016. 13 million tons of paper, paper board and newsprint are manufactured per year in India. Conversion of raw fibrous wood into pulp followed by pulp into paper are the basic steps involved in paper production. The paper manufacturing industry involves a series of stages including raw material processing and handling, bleaching and chemical recovery and the schematic representation is shown in Fig. 1.

1.3 Waste Generation and Characterization of Paper Mill Industry

Every tone of paper produces about 40–50 kg of dry sludge on an average from a paper industry. The sludge being the end derivative from pulp and paper industry is released from various operational stages such as paper processing and screening, deinking, pulping and bleaching process (Fig. 1). The characterization of sludge generated from various manufacturing units of a paper mill sludge is given in Table 1. The present disposal management practices of these sludge are landfilling, land application and other reclamation purposes [16, 29]. Mechanical dewatering is the commonly adopted method to improve and reduce the volume of solid content in the sludge (Table 2). Composting is one of the well-recognized disposal method of paper sludge to obtain effective end derivative used for soil stabilization.

This chapter highlights on sludge conversion into an effective and efficient material hydroxyapatite (HAp). The converted HAp has a wide range of application that would be used in water treatment technology to pave the way towards sustainable and circular economy. In specific, the paper sludge ash from the deinking process contains about 71% of calcium carbonate. From these CaCO_3 wastes, the calcium source required for the synthesis of hydroxyapatite can be prepared.

1.4 Extraction and Conversion of Calcium Carbonate from Sludge Ash to Calcium Hydroxide

The paper sludge ash (PSA) from deinking plant contains about 54% of calcium carbonate.

Decomposition of this calcium carbonate does not occur even at 800 °C incinerating temperature and remains as ash. The extraction of the calcium carbonate from the paper sludge ash is through the acid solvent followed by wet precipitation process

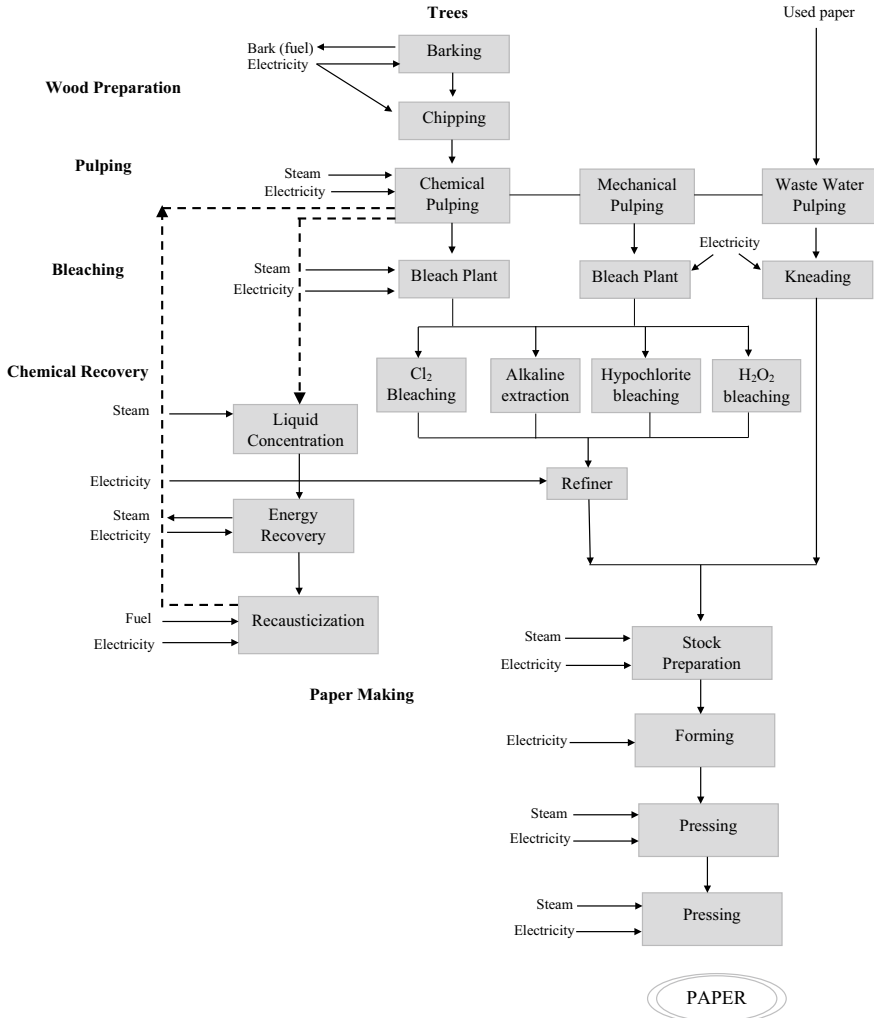


Fig. 1 Schematic layout of wastewater generation from various stages of pulp and paper manufacturing industry

[8, 25]. The precipitated and extracted calcium from PSA was about 71% of the sludge ash. In this process, solvents like acetic acid, hydrochloric acid, ammonium chloride, ammonium acetate, sodium citrate and ultra-pure water are used [25]. Out of all the solvents, acid behaves as the best solvent in calcium extraction. From the previous experimental works [2, 18, 37, 42, 46] carried out by many researchers, calcium hydroxide was found to be a very good calcium source in obtaining hydroxyapatite nanoparticle. Synthesis of calcium carbonate into HAp is not possible directly, hence it is necessary to convert CaCO_3 to $\text{Ca}(\text{OH})_2$ to use it as a calcium source

Table 1 General characteristics of primary and deinking paper sludge [19]

Parameters	Paper sludge	Deinking sludge
Moisture content (%)	8.18	2.91
Ash content of oven-dried sample (%)	19.50	53.62
Klason lignin content of oven-dried sample (%)	27.84	25.69
Halocellulose content of oven-dried sample (%)	62.73	42.88
pH	5.65	7.01
Acid buffering capacity, mmol NaOH/100 g	2.71	0.17
Base buffering capacity, mmol H ₂ SO ₄ /100 g	5.18	5.11

Table 2 Characterization of paper mill sludge considered under the study

Parameters	Values
Moisture content (%)	62.5 ± 0.01
pH	8.285 ± 0.5
Electrical conductivity (mS/cm)	1.73 ± 0.2
Loss of ignition (%)	24.96 ± 0.01
Ash content (%)	12.54 ± 0.03
Sodium (mg/L)	5.583 ± 0.02
Potassium (mg/L)	0.01

for further conversion into a nanostructured particle. The hydroxyapatite can be synthesized by various methods [28]. The most commonly followed methods in the synthesis of nano-crystalline HAp include precipitation, hydrothermal, hydrolysis, mechano-chemical and sol-gel.

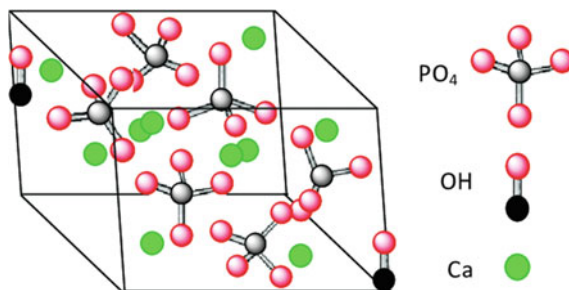
2 Hydroxyapatite Nanoparticle

2.1 Source and Application

Hydroxyapatite (HAp), is a naturally occurring mineral form of calcium apatite with the chemical formula $\text{Ca}_{10}(\text{PO}_4)_6(\text{OH})_2$ as represented in Fig. 2. HAp can be derived from natural or synthetic calcium resource possessing high pore, biocompatibility and are osteoconductive [5, 30]. Some of the natural calcium source used for HAp synthesis are coral, eggshell, limestone and seashell [6, 9]. Hydroxyapatite is the hydroxyl ion of the apatite group that can be replaced by fluoride, chloride or carbonate, producing fluorapatite or chlorapatite [12] has a hexagonal crystal system.

Pure hydroxyapatite powder is white, whereas the naturally occurring apatites have brown, yellow or green in colour. The Ca-HA, $\text{Ca}_{10}(\text{PO}_4)_6(\text{OH})_2$, is an insoluble calcium phosphate mineral, which is a major constituent of bones, teeth and are

Fig. 2 Structure of hydroxyapatite crystals [34]



found within pineal glands. The human body constitutes up to 70% by weight of bone as hydroxyapatite and are usually referred as 'bone mineral'. Dental enamel is composed of carbonated hydroxyapatite as the main mineral.

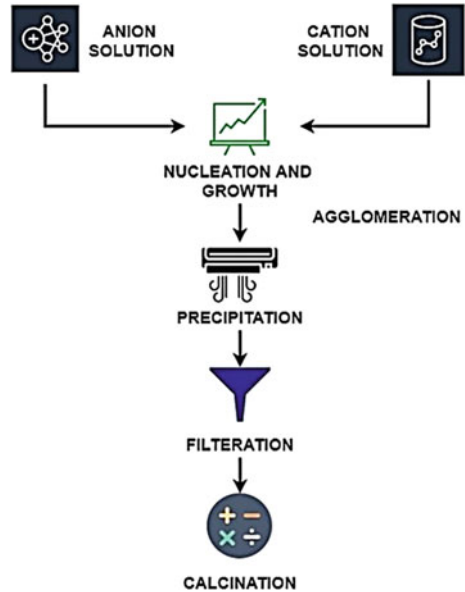
Calcium hydroxyapatite (HAp), has proved to be an efficient adsorbent in the removal of metal ions. The use of HAp has found to be significant in both environmental and industrial aspects in long-term containment of contaminants because of its high sorption capacity and high stability under reducing and oxidizing conditions [17]. The mechanism involved in sorption of HAp may be through ionic exchange reaction, surface complexion with phosphate, calcium and hydroxyl groups and co-precipitation of new partially soluble phases.

2.2 *Synthesis Methods*

Synthesis of HAp using different methods had been experienced and reported [2, 28, 37]. Common methods used to produce synthetic nano-crystalline HAp include precipitation [35], hydrothermal [49], hydrolysis, mechano-chemical and sol-gel [24] and are discussed below.

- i. Wet (chemical method)
 - Precipitation method
 - Hydrothermal techniques
 - Hydrolyses
- ii. Dry method (solid-state reaction)
- iii. Mechano-chemical method
- iv. Other methods like sol-gel, spray pyrolysis and electrochemical deposition.

Fig. 3 Schematic diagram of wet-chemical precipitation of HAp



2.2.1 Wet Chemical Method

Precipitation Method

Precipitation also known as wet precipitation is the most widely researched technique for HAp synthesis [18, 35]. This technique is chosen widely to synthesize HAp in contrast to other techniques due to its high amount of synthesis and cost effectiveness. In this method, calcium and phosphorus ions undergo a chemical reaction at controlled pH and temperature in an aqueous medium as illustrated in Fig. 3. The precipitated powder is calcined at high temperature to obtain a stoichiometric apatitic structure (Ca/P ratio as 1.67). Constant and slow titration are to be maintained to improve the homogeneity and stoichiometry of the mixture [38]. A decrease in solution pH below 9.0 would lead to the formation of Ca-deficient apatite structure.

Hydrothermal Techniques

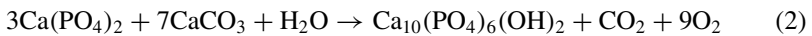
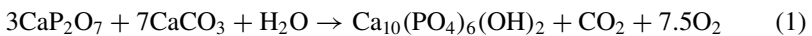
The hydrothermal technique [27, 49] was identified as an important method for the synthesis of ceramic and nanomaterials including HAp. Hydrothermal synthesis is a process that utilizes single or heterogeneous phase reactions in aqueous conditions at temperature and pressure greater than 25 °C and 100 kPa, respectively.

The application of high temperature and pressure results in the formation of a homogenous and crystallized powder with improved Ca/P ratio [49]. HAp prepared

from this method, has high purity with different shapes like spherical, rod, needle, hexagonal and spine like [21].

2.2.2 Dry Method

Solid-state synthesis or dry method is a relatively simple and low-cost procedure and does not require any solvent. The stability of the phases during the processing of ceramic materials are maintained in solid-state synthesis at high temperatures [22]. These methods are widely used for huge production of ceramics at lower precision control [23]. The heterogenous end product with lower diffusion coefficient is the main drawback of this method, especially in biomedical field. To overcome and homogenize the phase, longer calcination period is required. The two main reactions involved in the solid-state synthesis of HAp are as follows:



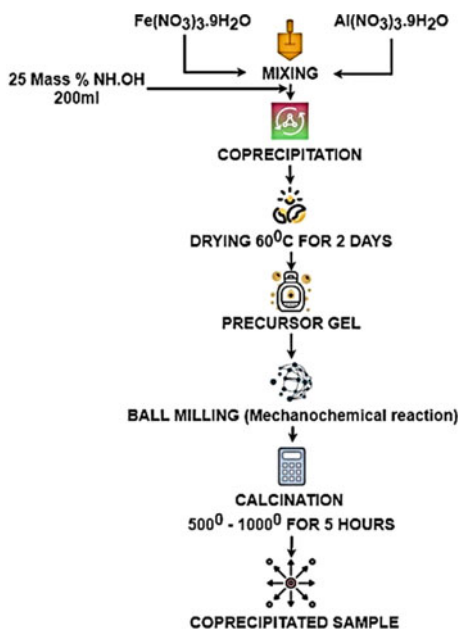
2.2.3 Mechano-chemical Method

The mechano-chemical process is also known as mechanical alloying. It is used for fabrication of Nano crystalline alloys and ceramics. In this method, the mechanical energy accelerates the structural and chemical changes of the precursor ions, thereby improving the kinetic performance [11]. Mechano-chemical method is simple to process and produce well defined structural advanced materials like HAp. The schematic representation of a mechano-chemical method is shown in Fig. 4. The stoichiometric ratio of the Ca and P, pH and the milling time are the main operational parameters to be considered in this process. The decrease in milling time leads to decrease in crystalline size.

2.2.4 Other Methods

The sol-gel [24] approach is an effective method for the synthesis of nano-structural HAp. The HAp synthesized by this method improves the contact and stability at the artificial bone interfaces with high purity and crystallinity. Though only limited attempts have been reported on the sol-gel processing, recent attention is seen towards the synthesis of HAp and other ceramic, fibre and coating materials [4]. The main disadvantages of this method are the yield of low homogeneous final product and the high cost of the raw materials. Recently, sol-gel method has been extensively used in development of biocompatible nanomaterials [44].

Fig. 4 Schematic representation of Mechano-chemical method



The monocrystal HAp prepared by molten salt growth method are grown from the molten phase (with a given composition) at high temperatures but are severely deformed due to high temperature gradients that occur during growth. This gel growth occurs in an aqueous phase containing Ca^{2+} and PO_4^{3-} ions under neutral condition at temperature around 37 °C [32, 33]. High porous calcium phosphate is used in the field of tissue engineering and drug delivery system. Electrospinning is one such method used in the production of ceramic fibres and calcium phosphate based scaffolds. A number of researchers have reported, synthesis of micro-porous ceramic structures with submicron fiber range using electrospinning.

3 Application of HAp in Environmental Remediation

HAp has been used in variety of fields such as biomedical, bone transplantation, protein synthesis, drug delivery system and other pharmaceutical industries due to their excellent biocompatible and osteoconductive nature [41, 48]. Moreover, HAp is substantially used in column separation technique, environmental management including air, water and soil. The shift towards circular and sustainable treatment technologies, had diverted research field into development of new and innovative materials to eliminate the contaminant in all three phases [36].

The unique properties of HAp like molecular arrangement, stoichiometric ratio, thermal stability, adsorption capacities, coagulation and ion exchange, had made

the application of HAp in the field of environmental management [20]. HAp has proven to be an excellent sorption material, especially in human body. It is also a cost-effective natural material with low water solubility, surface area and oxidizing condition. The diversified application of hydroxyapatite is due to its high degree of crystallinity and its correlation with its ion adsorption behaviour was reported in a study conducted by Stotzel et al. [39]. Usage of crystallized HAp in the nutrient recovery and removal in the advanced wastewater treatment process was found to be an alternative removal process of phosphorus and uranium removal in comparison with the granulated activated carbon, thereby confirming it to be a potential adsorbent [10]. In spite of its use in the surface water and wastewater treatment technologies, HAp has paved its way in the remediation of groundwater treatment too and is recognized as a potential reactive barrier to mitigate leaching.

In a work carried out by Sharanabasava et al. [37], nano-sized HAp nanoparticle was synthesized via wet chemical precipitation. $\text{Ca}(\text{OH})_2$ and ortho phosphoric acid (H_3PO_4) were used for extraction and synthesis process. Experiments were conducted under controlled environment parameters such as required pH, concentration of solutions and temperature as well. The variation in any of these parameters resulted change in the synthesized HAp obtained. The pore size of HAp was around 35–90 nm and was optimized subjecting it to different temperature conditions [2]. These optimized HAp nano-powders were subjected for further characterization and surface area analysis.

4 Development of Hydroxyapatite from Paper Mill Sludge

4.1 Processing of Raw Sludge

This chapter discusses on feasibility of deinking sludge produced as a by-product from the deinking plant. Wood, cellulose fibres and lignin are the major organic components present in the paper mill sludge [40]. The inorganic components of the paper mill sludge are kaolinite (clay) and calcium carbonate, which are used as paper additives. Inorganic components are usually predominant in sludge from printing paper and board production, whereas in the packaging paper industry sludge of a more organic character is typical. Paper Sludge Ash (PSA) is ash generated during the paper manufacturing process and is of alkaline nature. PSA obtained as a by-product has high volume of calcium-containing reagents, including calcium carbonate, which can be used as fillers or coating pigments to improve the paper quality.

4.2 Conversion of Sludge to Ash and Its Characterization

The dried paper sludge is converted to ash by incinerating at $800\text{ }^{\circ}\text{C} \pm 3\text{ }^{\circ}\text{C}$ (Fig. 5). At this temperature it is found that the organic matter present in sludge gets decomposed and the calcium carbonate exist in the ash after incineration.

The final loss of weight analysed by the TG-DTA curves for the converted ash from the paper sludge was found at $799.45\text{ }^{\circ}\text{C}$ and maintained a constant weight loss till $1200\text{ }^{\circ}\text{C}$ and is shown in Figs. 6 and 7. But the raw sludge was able to withstand a temperature of around $374.40\text{ }^{\circ}\text{C}$ due to the dominance of organic matter in the sludge composition [45].

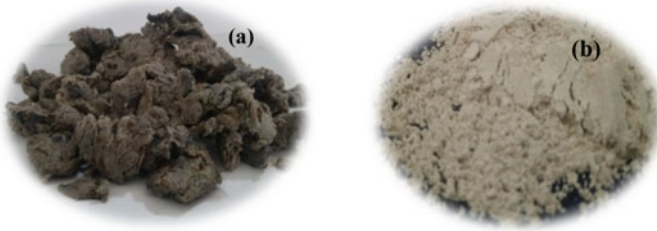


Fig. 5 Paper sludge (a) and paper sludge ash (b)

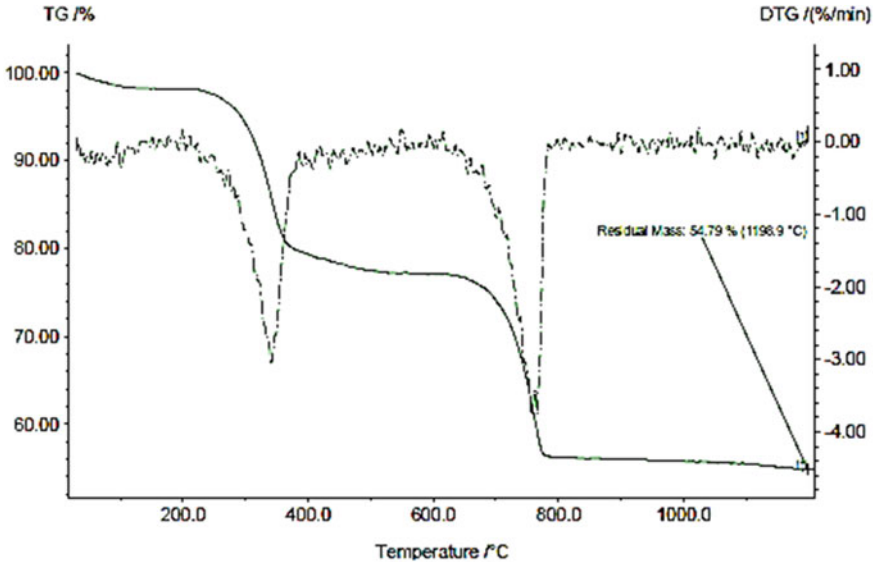


Fig. 6 TG-DTA profile curves of paper sludge

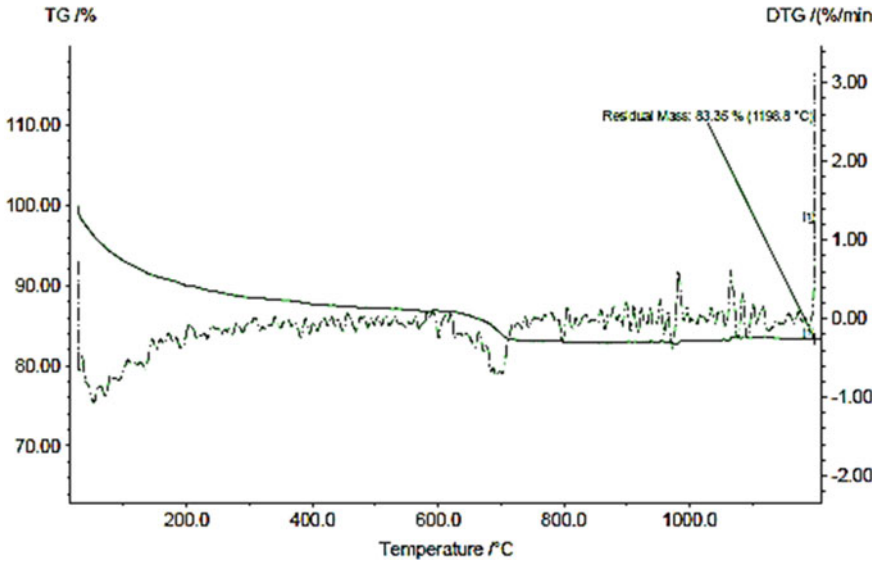


Fig. 7 TG–DTA profile curves of paper sludge ash

4.3 Synthesis and Characterization of Hydroxyapatite

4.3.1 Synthesis of Calcium Hydroxide

The paper sludge ash was made up to 1 M HCl in the ratio of 1:10—sludge to HCl to dissolve Ca, Si, Al and Mg compounds with pH maintained at 1. Non-soluble silicate components were filtered from the suspension to provide a clear liquid phase silicates precipitate at bottom. The extracted calcium carbonate is synthesized into calcium hydroxide by wet chemical precipitation method. By using calcium hydroxide as calcium source, hydroxyapatite is synthesized.

4.3.2 Synthesis of Hydroxyapatite

The hydroxyapatite was synthesized by wet chemical precipitation using calcium source as calcium hydroxide obtained from paper sludge ash and orthophosphoric acid as a phosphate source. Figure 8 shows the experimental setup for hydroxyapatite synthesis. The pH of the medium was maintained at 8.5 ± 0.25 °C by the addition of ammonium hydroxide. The entire experiment was conducted at a temperature between 40 and 45 °C. A continuous and homogenous stirring given to the aqueous medium turned the solution into milky white, which were kept for different aging time for 24 h and 48 h, respectively for precipitate formation.

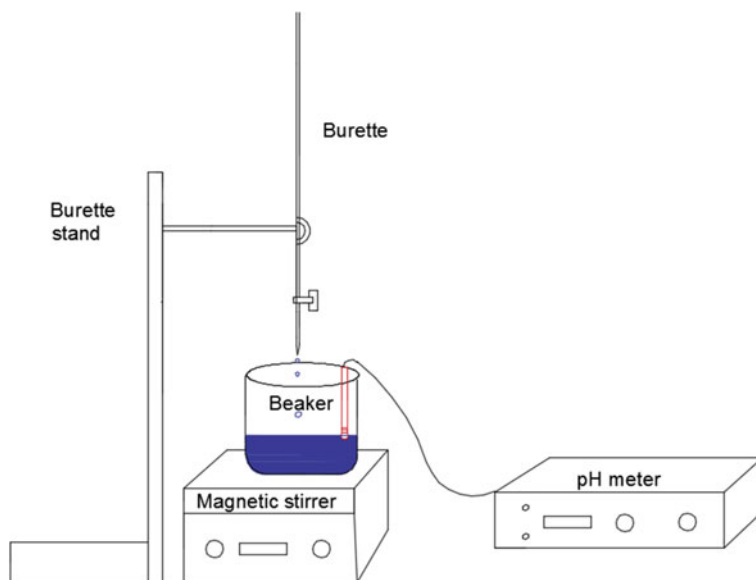


Fig. 8 Experimental setup for nano-hydroxyapatite synthesis

4.3.3 Characterization of Hydroxyapatite

Fourier Transform-Infrared Spectral Studies (FT-IR)

The purity and formation of the hydroxyapatite differs with the precipitate formed during different aging period.

The FT-IR spectra of the HAp for the aging period at 24 and 48 h are shown in Fig. 9. The peaks seen in the figure showed the formation of the apatite lattice and was confirmed by the stretching and flexural peaks at 3410.15 cm^{-1} . The calcium and phosphate group absorption bands were identified at 1014.5 and 550.50 cm^{-1} . The quantification of the calcium and phosphate for the different aging period also depends on the stoichiometric ratio of the two ions [23].

Thermal Analysis

The thermal gravimetric analysis (TGA) showed a weight loss in the temperature region up to $450\text{ }^{\circ}\text{C}$. The differential thermal analysis (DTA) showed exothermic peaks in the temperature region of $250\text{--}350\text{ }^{\circ}\text{C}$. The HAp under thermal decomposition for the different aging period resulted in residual masses of 85% and 76.35% , respectively and is interpreted from Figs.10 and 11. This proves the thermal stability of the synthesized hydroxyapatite.

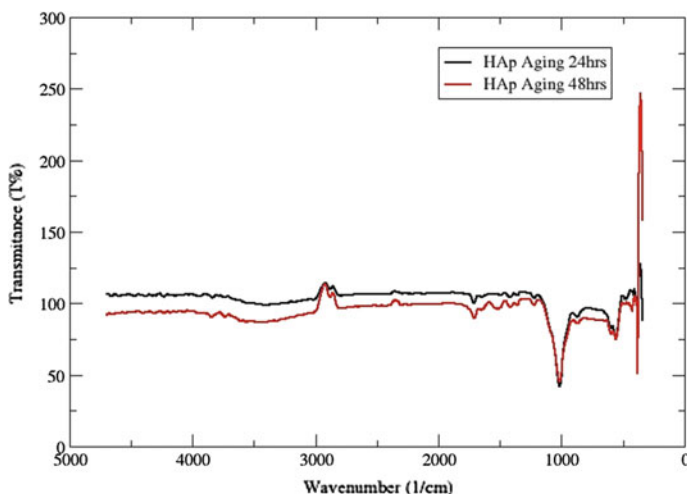


Fig. 9 FT-IR spectral analysis of synthesized hydroxyapatite during aging period of 24 h and 48 h

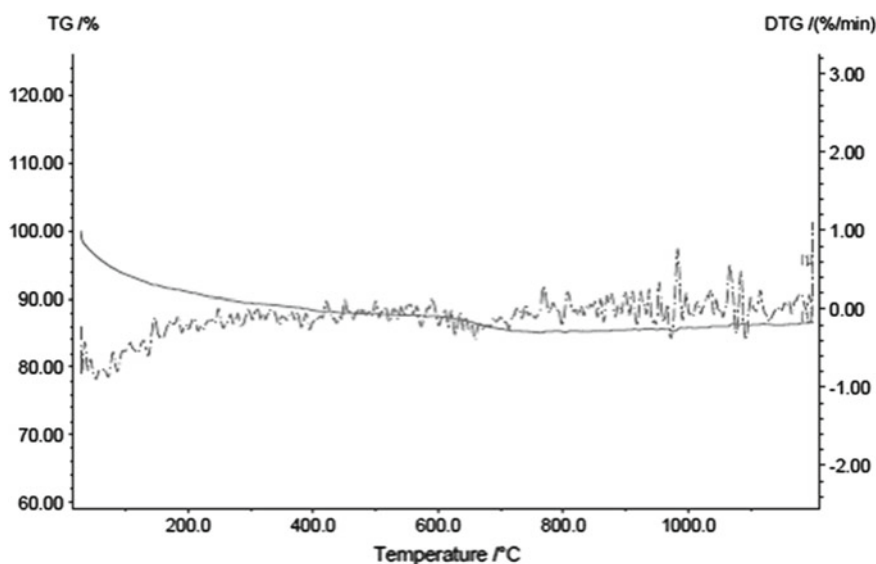


Fig. 10 TG-DTA profile curves of synthesized hydroxyapatite during aging period of 24 h

Brunauer–Emmett–Teller (BET) Isotherm

Brunauer–Emmett–Teller (BET) isothermal plot clearly depicts the molecular behaviour and kinetics due to adsorption of the gas molecule adhering to the HAp surface. The occupancy of the gas molecules determines the specific surface area

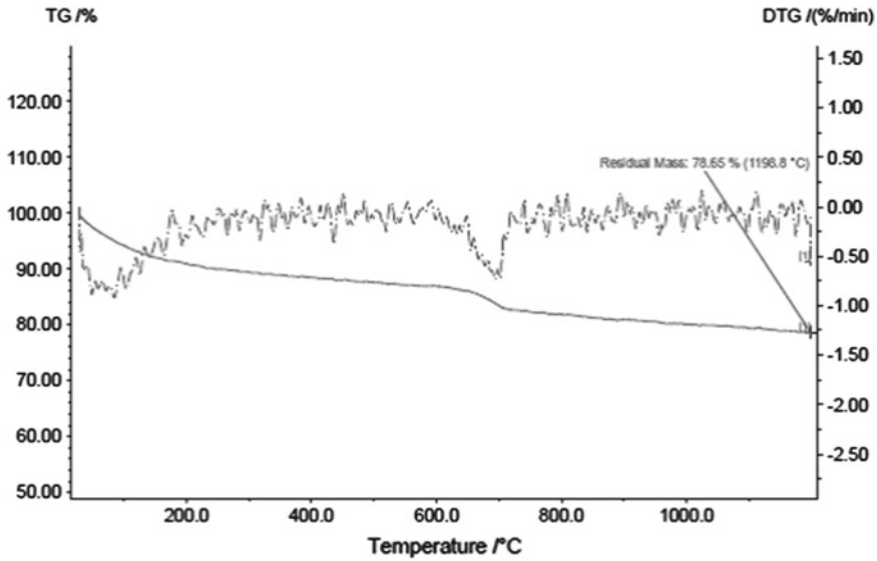
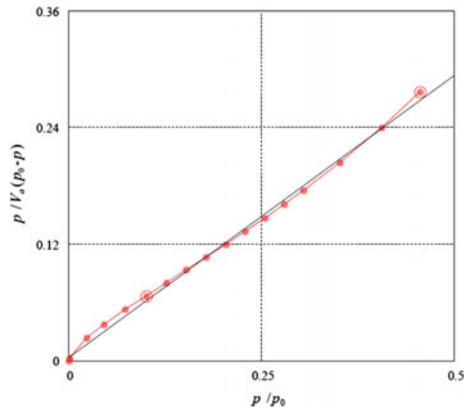


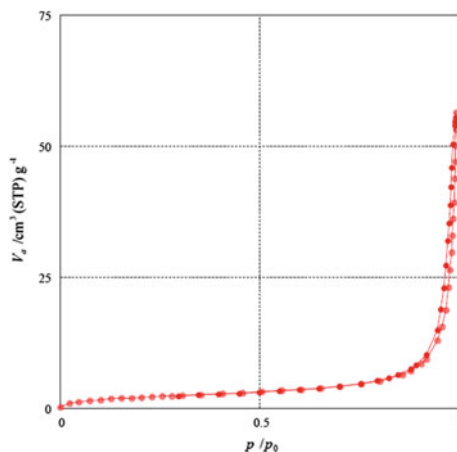
Fig. 11 TG–DTA profile curves of synthesized hydroxyapatite during aging period of 48 h

Fig. 12 BET isothermal plot of 24 h aged HAP



and the pore volume of the synthesized HAP. Based on the precipitation formed with respect to the aging period, 24 h aging yielded high purity HAP at an adsorption temperature of 77 K and saturated vapour pressure of 97.605 kPa in the presence of an inert N₂ atmosphere. The specific surface area, pore volume and pore diameter for 24 h aging period analyzed from the adsorption–desorption isothermal plot in Figs. 12 and 13 were 7.4425 m²/g, 0.00843 cm³/g and 45.422 nm, respectively.

Fig. 13
Adsorption/desorption
isothermal curves of 24 h
aged HAP



5 Conclusion

The usage of paper is very predominant among the Asian and South American countries. India being one among them accounting to about 2% of the paper and newsprint production. The disposal of the sludge generated by the pulp and paper mill is one of the challenges faced by the paper industry. This chapter has effectively discussed on the effective utilization of paper sludge, produced as the end product from paper mill effluent. The sludge ash constituting of high calcium source was extracted and synthesized to hydroxyapatite by wet chemical precipitation. The synthesized hydroxyapatite possessed an excellent adsorbent property such as porous nature, thermal stability and highly specific area. It specifically had very high capacity in removal of divalent heavy metal ion due to the presence of calcium and phosphate ions. The pore size of 45.422 nm confirmed the formation of nanoparticle sized Hydroxyapatite.

References

1. Abdullah R, Ishak CF (2015) Characterization and feasibility assessment of recycled paper mill sludge for land application in relation to the environment. *Int J Environ Res Public Health* 12:9314–9329. <https://doi.org/10.3390/ijerph120809314>
2. Abidi SSA, Murtaza Q (2013) Synthesis and characterization of nano-hydroxyapatite powder using wet chemical precipitation reaction. *J Mater Sci Technol* 30:307–310. <https://doi.org/10.1016/j.jmst.2013.10.011>
3. Agbeboh NI, Oladele IO, Daramola OO, Adediran AA, Olasukanmi OO, Tanimola MO (2020) Environmentally sustainable processes for the synthesis of hydroxyapatite. <https://doi.org/10.1016/j.heliyon.2020.e03765>
4. Agrawal K, Singh G, Puri D, Prakash S (2011) Synthesis and characterization of hydroxyapatite powder by sol-gel method for biomedical application. *J Miner Mater Charact Eng* 10(8):727–734. <https://doi.org/10.4236/jmmce.2011.108057>

5. Akram M, Ahmed R, Shakir I (2014) Extracting hydroxyapatite and its precursors from natural resources. *J Mater Sci* 49(4):1461–1475
6. Anee TK, Ashok M, Palanichamy M, Kalkura SN (2003) A novel technique to synthesize hydroxyapatite at low temperature. *Mater Chem Phys* 80:725–730
7. Apriant T (2018) Heavy metal ions adsorption from pulp and paper industry wastewater using zeolite/activated carbon-ceramic composite. In: International conference on science and applied science (ICSAS)
8. Blomquist M, Tomtegata (2001) Method of recovering Calcium from waste material or contaminated natural calcic material. Wipo IP Portal, WO/1998/013298
9. Cahyaningrum SE, Herdyastuty N, Devina B, Supangat D (2017) Synthesis and characterization of hydroxyapatite powder by wet precipitation method. In: International conference on chemistry and material science (IC2MS). <https://doi.org/10.1088/1757-899X/299/1/012039>
10. Chang H, Park N, Jang Y, Lim H, Kim W (2020) Application of the hydroxyapatite crystallization-filtration process to recover phosphorus from wastewater effluents. *Water Sci Technol* 81(11):2300–2310
11. Chatterjee T, Das AK, Lala S, Pradhan SK, Meikap MK (2019) Structural and electrical characterizations of hydrothermally grown hydroxyapatite polycrystals: a morphological hierarchy. *J Appl Phys* 125:225107 <https://doi.org/10.1063/1.5096452>
12. Cheng K, Weng W, Han G, Du P, Shen G, Yang J, Ferreira JMF (2003) The effect of triethanolamine on the formation of sol–gel derived fluoroapatite/hydroxyapatite solid solution. *J Mater Chem Phys* 78:767–771
13. Engin A, Girgin İ (2008) Synthesis of hydroxyapatite by using calcium carbonate and phosphoric acid in various water–ethanol solvent systems. *Cent Eur J Chem* 7:745–751
14. FAOSTAT (Food and Agriculture Organization of the United Nations—Statistics division) (2015) Domain forestry. <http://faostat3.fao.org/download/F/FO/E>
15. Fan X, Parker DJ (2003) Adsorption kinetics of fluoride on low-cost materials. *Water Res* 37:4929–4937. <https://doi.org/10.1016/j.watres.2003.08.014>
16. Faubert P, Barnabé S, Bouchard S, Côté R, Villeneuve C (2016) Pulp and paper mill sludge management practices: what are the challenges to assess the impacts on greenhouse gas emissions? *Resour Conserv Recycl* 108:107–133
17. Ferraz MP, Monteiro FJ, Manuel M (2004) Hydroxyapatite nanoparticles: a review of preparation methodologies. *J Appl Biomater Biomech* JABB 2(2):74–80
18. Ganachari SV, Bevinakatti AA, Yaradoddi JS (2016) Rapid synthesis, characterization, and studies of hydroxyapatite nanoparticles. *Adv Mater Sci Res* 1(1):9–13
19. Geng X, Zhang SY, Deng J (2007) Characteristics of paper mill sludge and its utilization for the manufacture of medium density fiberboard. *Wood Fiber Sci* 39(2):345–351
20. Ibrahim M, Labaki M, Giraudon J-M, Lamonier J-F (2020) Hydroxyapatite, a multifunctional material for air, water and soil pollution control: a review. *J Hazard Mater* 383:121139
21. Ines S, Neira Yury V, Kolen K (2009) An effective morphology control of hydroxyapatite crystals via hydrothermal synthesis. *Cryst Growth Des* 9(9):466–474
22. Jamil M, Elouatli B, Khallok H, Elouahli A, Gourri E, Ezzahmouly M, Abida F, Hatim Z (2018) Silicon substituted hydroxyapatite: preparation with solid-state reaction, characterization and dissolution properties. *J Mater Environ Sci* 9(8):2322–2327
23. Ji HL, Meisha LS (2013) Copolymer-mediated synthesis of hydroxyapatite nanoparticles in an organic solvent. *Am Chem Soc Langmuir* 29:10940–10944
24. Kim I-S, Kumata PN (2004) Sol–gel synthesis and characterization of nanostructured hydroxyapatite powder. *Mater Sci Eng B* 111:232–236. <https://doi.org/10.1016/j.mseb.2004.04.011>
25. Kim D, Kim M-J (2018) Calcium extraction from paper sludge ash using various solvents to store carbon dioxide. *KSCE J Civ Eng* 22:4799–480
26. Kuokkanen T, Nurmesniemi H, Poykio R, Kujala K, Kaakinen J, Kuokkanen M (2008) Chemical and leaching properties of paper mill sludge. *Chem Speciat Bioavailab* 20(2). <https://doi.org/10.3184/095422908X324480>

27. Liu F, Wang FP, Shimizu T, Igarashi K, Zhao L (2016) Hydroxyapatite formation on oxide films containing Ca and P by hydrothermal treatment. *Ceram Int* 32:527–531
28. Nayak AK (2010) Hydroxyapatite synthesis methodologies: an overview. *Int J Chemtech Res* 2(2):903–907
29. Pervaiz M, Sain M (2015) Recycling of paper mill biosolids: a review on current practices and emerging biorefinery initiatives. *CLEAN–Soil Air Water* 43(6):919–926. <https://doi.org/10.1002/clen.201400590>
30. Rahmayeni S, Zulhadjri Z, Jamarun N, Emriadi E, Arief S (2016) Synthesis of ZnO-NiFe₂O₄ magnetic nanocomposites by simple solvothermal method for photocatalytic dye degradation under solar light. *Oriental J Chem* 32(3):1411–1419. <https://doi.org/10.13005/ojc/320315>
31. Ravaglioli A, Krajewski A (1992) *Bioceramics: materials properties and applications*. Chapman & Hall, London
32. Rivera-Munoz E, Díaz JR, Rodríguez R, Brostow W, Castano VM (2001) Hydroxyapatite spheres with controlled porosity for eye ball prosthesis: processing and characterization. *J Mater Sci: Mater Med* 12:305–311
33. Rivera-Munoz EM, Huirache-Acuna R, Velázquez R, Alonso-Núñez G, EguíaEguía S (2011) Growth of hydroxyapatite nanoparticles on silica gels. *J Nanosci Nanotechnol* 11(6):5592–5598
34. Rujitanapanich S, Kumpapan P, Wanjanoi P (2014) Synthesis of hydroxyapatite from oyster shell via precipitation. *Energy Procedia* 56:112–117. <https://doi.org/10.1016/j.heliyon.2020.e03765>
35. Saeri MR, Afshar A, Ghorbani M, Ehsani N, Sorrell CC (2003) The wet precipitation process of hydroxyapatite. *Mater Lett* 57:4064–4069. [https://doi.org/10.1016/S0167-577X\(03\)00266-0](https://doi.org/10.1016/S0167-577X(03)00266-0)
36. Shaaban M, Van Zwieten L, Bashir S, Younas A, Nunez-Delgado A, Chhajro M, Kubar KA, Ali U, Rana MS, Mehmood MA (2018) A concise review of biochar application to agricultural soils to improve soil conditions and fight pollution. *J Environ Manag* 228:429–440
37. Sharanabasava V, Ganachari, Anjali A, Bevinakatti (2016) Rapid synthesis, characterization and studies of hydroxyapatite nanoparticles. *Adv Mater Sci Res* 1(1)
38. da Silva NMP, Espitalier F, Nzihou A (2005) Precipitation process of calcium phosphate from calcium carbonate suspension. *KONA Powder Part J*. <https://doi.org/10.14356/kona.2016002>
39. Stotzel C, Muller FA, Reinert F, Niederdraenk F, Barralet JE, Gbureck U (2009) Ion adsorption behaviour of hydroxyapatite with different crystallinities. *Colloids Surf B Biointerfaces* 74:91–95
40. Suriyanarayanan S, Mailappa AS, Jayakumar D, Nanthakumar K, Karthikeyan K, Balasubramanian S (2010) Studies on the characterization and possibilities of reutilization of solid wastes from a waste paper based paper industry. *Glob J Environ Res* 4:18–22
41. Surmeneva MA, Ivanova AA, Tian Q, Pittman R, Jiang W, Lin J, Liu HH, Surmenev RA (2019) Bone marrow derived mesenchymal stem cell response to the RF magnetron sputter deposited hydroxyapatite coating on AZ91 magnesium alloy. *Mater Chem Phys* 221:89–98
42. Ungureanu DN, Angelescu N (2011) Synthesis and characterization of hydroxyapatite nano powders by chemical precipitation. *AIP Conf Proc* 1961:030037 <https://doi.org/10.1063/1.5035239>
43. Ungureanu DN, Angelescu N (2011) Thermal stability of chemically precipitated hydroxyapatite nano powders. *Int J Biol Biomed Eng* 5(2)
44. Varma HK, Suresh BS (2005) Synthesis of calcium phosphate bio ceramics by citrate gel pyrolysis method. *Ceram Int* 31:109–114
45. Vasile E, Popescu LM, Piticescu RM, Burlacu A, Buruiana T (2021) Physico-chemical and biocompatible properties of hydroxyapatite based composites prepared by an innovative synthesis route. *Mater Lett* 79:85–88
46. Verwilghen C, Rio S, Nzihou A, Gauthier D, Flamant G, Sharrock PJ (2007) Preparation of high specific surface area hydroxyapatite for environmental applications. *J Mater Sci* 42(15):6062–6066
47. Wardhani S, Azkiya NI (2018) Synthesis of hydroxyapatite using precipitated calcium carbonate (PCC) from limestones. *Mater Sci Eng* 299

48. Weera suriya DRK, Wijesinghe W, Rajapakse RMG (2017) Encapsulation of anticancer drug copper bis (8-hydroxyquinoline) in hydroxyapatite for pH-sensitive targeted delivery and slow release. *Mater Sci Eng C* 71:206–213
49. Yoshimura M, Suda H (1994) Hydrothermal processing of hydroxyapatite: past, present, and future. *Hydroxyapatite Relat Mater* 45–72

Adsorptive Removal of Reactive Blue Dye by Cucumber Peel Adsorbent: Isotherm, Kinetics and Mass Transfer Studies



Gajendiran Vasu and Selvaraju Sivamani

1 Introduction

Dyes are substances added to fabric material which are making chemical bonds to impart colour to the cloth [18]. In ancient days, natural dyes, biodegradable in nature, are used and the use of natural dyes is not polluting the environment like synthetic dyes [24]. Synthetic dyes are chemical compounds, aromatic in nature and non-biodegradable because of their high thermal stability and photostability [14]. Due to the increase in demand, the production of textile products also increasing proportionally, and the use of synthetic dyes has together contributed to dye wastewater becoming one of the important sources of severe pollution problems in current times [3]. By considering the volume of effluent generated and its composition, the wastewater from textile industries is the most polluting one among all the industry sectors.

The disposal of wastewater produced from dyeing industries affects the soil, water bodies and aquatic life [6]. Dyes have the nature of absorbing and reflecting the sunlight in water, which affect the photosynthetic activity of algae present in the water bodies which are seriously affecting the food chain. Since the dyes are synthetic in nature, their breakdown products are carcinogenic, mutagenic, and toxic to life [13]. A report revealed that the dyeing industrial workers are affected with skin cancer, kidney cancer, urinary bladder cancer, and liver cancer. Dyes can cause skin allergy, skin irritation, eye allergy, and irritation in the mucus membrane and upper respiratory tract [7].

Treatment of wastewater from dyeing industries before disposing it is an essential and highly challenging one [15]. Though various physical and chemical treatment methods such as ozonation, electrochemical destruction, photochemical, membrane

G. Vasu (✉) · S. Sivamani
Engineering Department, University of Technology and Applied Sciences, Salalah, Oman
e-mail: vasu.g@sct.edu.com; gvasuchem@gmail.com

filtration, ion exchange, irradiation, and electrocoagulation methods are available, still there is demand for an economical method for removing the dyes from wastewater. Adsorption creates interest among the researchers because of its efficiency, simplicity in operation, and can remove the contaminant even at low concentrations. Adsorption is a separation operation which utilizes the attractive force that naturally exists between adsorbent and adsorbate molecules for separation [8]. Adsorbent is a solid on which adsorbate molecules are deposited. Adsorbate is solute from the solution which is being got adsorbed by the adsorbent used.

The choice of adsorbent is an important factor to make the adsorption the cheapest method. Recent studies reveal that the use of agricultural wastes as a source of adsorbent is the cheapest one for treating the dye containing wastewater [9]. Since agriculture is a main occupation in the developing countries, the production of agricultural waste is abundant, and its disposal has become a challenging task for farmers as it requires huge manpower. The place for disposing these agricultural wastes pose threat to the environment.

As cucumber contains antioxidants, vitamins, and minerals that help in weight loss and are suitable for reducing blood sugar, cucumber has become unavoidable in people dining throughout the world [11]. As the need for cucumber increases daily, the production of cucumber is increasing proportionally. Among the farmers, the cultivation of cucumber become popular, and they are producing several thousand tons of cucumber throughout the year. This generates a huge amount of cucumber waste [10].

In this study, cucumber peel is used as an adsorbent for the removal of copper from its aqueous solution. Batch studies were conducted by changing the parameters like pH, contact time, agitation speed, initial adsorbate concentration, and adsorbent dosage along with isotherm, kinetics, and mass transfer studies.

2 Literature Review

Basu et al. [4] studied the adsorption removal of lead from solution using cucumber peel adsorbent. Batch adsorption studies were performed by varying pH, temperature, time, initial adsorbate concentration, and co-ion effect on adsorption capacity. A maximum adsorption capacity of 133.6 mg/g was achieved at pH 5.0, 30 °C, and 60 min. Pseudo-second order kinetics and Langmuir isotherm fitted with the data. Co-ion effect was negligible. The adsorbent was characterized using Thermo Gravimetric Analysis (TGA), Scanning Electron Microscopy (SEM), Energy Dispersive X-ray Analysis (EDAX), X-ray Diffraction (XRD), Fourier Transform Infrared Analysis (FTIR), and zeta potential. Desorption studies were also executed using hydrochloric acid.

Basu et al. [5] studied the adsorption removal of cadmium from wastewater in a packed bed reactor using cucumber peel adsorbent. Continuous adsorption studies, by varying flow rates, bed height, and influent concentration were conducted at pH 5.0. The maximum percentage removal of 78.03% was achieved with an adsorption

capacity of 107.76 mg/g at 50 mg/L influent concentration, 20 mL/min flow rate, and 8.0 cm bed height. Adsorption pattern in continuous mode was studied, and Thomas model and Yoon–Nelson model fitted with the data. Desorption studies were executed successfully with 0.1 M HCl.

Stavrinou et al. [23] studied the percentage removal of cationic methylene blue (MB) and anionic Orange G (OG) dye from wastewater with cucumber peel adsorbent. Batch adsorption studies, by varying pH, adsorbent dosage, contact time, and dye concentration were conducted. A maximum adsorption capacity of 179.9 mg/g for MB at pH 6.0 and 40.5 mg/g for OG at pH 2.0 were achieved. Freundlich isotherm fitted with data for low MB concentration and Langmuir isotherm fitted with data for a high concentration of MB. For OG, Langmuir isotherm well fitted with the data. The adsorbent was characterized using Attenuated Total Reflectant Fourier Transform Infrared analysis (ATR-FTIR), N₂ sorption, SEM, and XRD. Adsorption kinetic models are studied and found chemisorption was the dominant mechanism.

Pandey et al. [16] investigated the percentage removal of divalent lead ions from an aqueous solution by using a cucumber peel. Batch adsorption studies, by varying conditions like pH, adsorbent dosage, and contact time on adsorption capacity were conducted. A maximum adsorption capacity of 28.25 mg/g was achieved at pH 5.0 for initial concentration of 25 mg/L at 25 °C was obtained. Pseudo-second order kinetics and Langmuir isotherm fitted with the data. Desorption studies with 1 M HNO₃ were also executed.

Mahmoodi et al. [12] investigated the adsorption removal of low-cost mesoporous activated carbon prepared from cucumber peel for removing single dye (MB), binary dyes ((MB + Malachite Green, MG) and (MB + Rhodamine B, RhB)), and ternary dye (MB + MG + RhB) from wastewater. Batch adsorption studies, by varying conditions like MB concentration, Activated carbon (AC) dosage, process time, temperature, and solution pH were conducted on adsorption capacity. Pseudo-second order kinetics and Langmuir isotherm fitted with the data. Thermodynamic data like Gibbs free energy (−15.14 kJ/mol), enthalpy (25.84 kJ/mol), and entropy (0.1327 J/mol) revealed that MB adsorption by the prepared AC was spontaneous endothermic and physical sorption respectively. The prepared AC was characterized by XRD, Field Emission Scanning Electron Microscopes (FESEM)/EDAX, TGA/Differential Thermal Analysis (DTA), FTIR, Brunauer-Emmet-Teller surface area analysis (BET)-Barret-Joyner-Halenda (BJH) pore size and volume analysis, X-ray Photoelectron Spectroscopy (XPS), particle size, and zeta potential analyses. The Artificial Neural Network (ANN) model was studied extensively and overlaps the experimental data due to the low divergence between actual and estimated data. Also, the prepared AC has the ability for removing dyes from binary (MB + MG and MB + RhB) and ternary (MB + MG + RhB) systems.

Saygılı and Güzel [19] studied the adsorption capacity of chemically modified cucumber peel adsorbents for removal of reactive black 5 and direct blue 7 dye from wastewater. Batch adsorption studies were conducted and the maximum adsorption capacity of 95.24 mg/g for reactive black 5 and 129.87 mg/g for direct blue 7 was achieved. Pseudo-second order kinetics and Langmuir isotherm fitted with the data. Thermodynamic studies revealed that the adsorption was spontaneous and

endothermic in nature. The adsorbent was characterized by FTIR, SEM, TGA, XRD, proximate and ultimate analyses, and pH_{zpc} measurements. Desorption studies were conducted using NH_3 and NaOH solutions.

Shakoor and Nasar [20] investigated the applicability of cucumber peel waste as low-cost adsorbent for the removal of methylene blue dye from wastewater. Batch adsorption studies on adsorbate removal varying parameters like adsorbent dose, contact time, initial dye concentration, particle size, pH, and temperature were conducted. Freundlich adsorption isotherm fitted with data shows that the adsorbent surface was heterogeneous in nature. The deviation from normal or ideal Langmuir adsorption has been explained considering non-idealized cooperative adsorption. Adsorption kinetics was found to obey pseudo-second order kinetics. Thermodynamic data was obtained indicating that the adsorption process is spontaneous and exothermic in nature. The values of ΔH° and ΔS° have been found to be negative which indicate that the feasibility of the process decreases with increasing temperature. The adsorbent was analysed by SEM and FTIR spectroscopy, Desorption studies were examined using HCl .

Akkaya and Güzel [1], conducted a batch study and investigated the adsorption removal of divalent copper and lead from their aqueous solution by using cucumber peel adsorbent. Batch adsorption studies by changing the variables like pH, biosorbent dosage, contact time, and initial adsorbate concentration were conducted. A maximum adsorption capacity of 88.50 and 147.06 mg/g for copper(II) and lead(II) ions, respectively, was achieved at pH 5.0, biosorbent dose of 0.1 g, contact time of 60 and 85 min, and initial concentration of 100 and 150 mg/L. Pseudo-second order kinetics and Langmuir isotherm fitted with the data. Thermodynamic parameters were examined and shows that the adsorption process was spontaneous and endothermic. Desorption studies were carried out with HCl .

Smitha et al. [21] examined the adsorption removal of acid black7 (acid dye) from wastewater by using low-cost adsorbent produced from cucumber peel. Batch adsorption studies by changing the parameters such as pH, contact time, adsorbent dosage, and initial adsorbate concentration were executed. A maximum percentage removal of 85% was achieved at pH 3.0, contact time of 55 min. and 1.0 mg/g of adsorbent dosage at an initial adsorbate concentration of 100 mg/L. Pseudo-second-order kinetics and Langmuir isotherm fitted with the data. FTIR, XRD, SEM, EDAX, and zeta potential measurements were characterized for the adsorbent.

Akkaya and Güzel [2] examined the removal of methylene blue (MB) from an aqueous solution by using low-cost adsorbent prepared from cucumber peel. Batch adsorption studies on varying parameters like pH, initial dye concentration, temperature, dye concentration, ionic strength, and adsorbent dosage were conducted. A maximum adsorption capacity of 111.11 mg g^{-1} at pH 6.42 was achieved. Pseudo-first-order kinetics fitted with data, thermodynamic studies were conducted and concluded that the biosorption was spontaneous and feasible. Desorption studies were also conducted with HCl and H_3PO_4 .

Rodríguez et al. [17] investigated the Chromium (VI) removal capacity of cucumber shell biomass. Batch studies by changing the variables like pH, contact time, temperature, and initial concentration of metal, biomass, and contaminated

niches were conducted. A complete Chromium (VI) removal was achieved at pH 1.0, 28 °C, 100 rpm by using 1.0 g of biomass for the initial metal concentration of 100 mg/L.

3 Materials and Methods

3.1 Preparation of Cucumber Peel (Adsorbent)

Fresh cucumber was purchased from the local market and peeled; the peel was washed with tap water for three times followed by distilled water three times. The washed cucumber peel was kept in a hot air oven at 70 °C for drying, periodically the weight of the peel was measured. Drying was continued until the constant weight of the peel reached. The dry cucumber peel was pulverized using mortar and pestle and stored in an airtight bottle for experimental uses.

3.2 Preparation of 1000 ppm Reactive Blue Dye Solution (Stock Solution)

One gram of reactive blue dye was taken and dissolved with 200 ml of distilled water. Then the solution was transferred to 1 l standard flask and distilled water was added up to the mark. Now the 1000 ppm reactive blue dye solution is ready to use.

3.3 Effect of pH

Five conical flasks were taken and labelled with pH 3, pH 5, pH 7, pH 9, and pH 11. 100 mL of 500 ppm reactive blue dye solution was taken in the first conical flask and the pH was measured and adjusted to 3 by adding 0.1 N Sulphuric acid with the help of a pH meter. 100 mL of 500 ppm of reactive blue dye solution was taken in the second conical flask and the pH was adjusted to 5 by adding 0.1 N Sulphuric acid with the help of a pH meter. Similarly, other conical flasks were taken with 100 mL of 500 ppm of reactive blue dye solution each and the pH was adjusted to 7, 9, and 11 by adding 0.1 N Sulphuric acid/ Sodium hydroxide. Weigh 0.5 g of cucumber peel adsorbent and add to each conical flask. Put the flasks in a water bath shaker and set the time for 30 min at 100 rpm (revolution per minute). After 30 min of shaking, the sample from each conical flask was filtered. The absorbance value for each sample after adsorption was measured by adsorption using Atomic Absorption Spectrophotometer (AAS).

3.4 Effect of Time

100 mL of 500 ppm adsorbate (Reactive blue dye solution) was taken in an Erlenmeyer's flask and the pH was adjusted to 7 by adding 0.1 N NaOH solution drop by drop manner. Then 0.5 g of adsorbent (cucumber peel powder) was added to the flask. The flask was kept in a water bath shaker for mixing at 100 rpm and at room temperature. After every 5 min, 10 mL of the sample from the flask was taken and filtered. The absorbance of the filtered sample was measured by using Atomic Absorption Spectrophotometer (AAS).

3.5 Effect of Initial Concentration

Five Erlenmeyer flasks were taken and numbered 1, 2, 3, 4 and 5. Each flask was taken with 100 mL of reactive blue dye solution with different concentrations as 100 ppm, 200 ppm, 300 ppm, 400 ppm, and 500 ppm, respectively. 0.5 g of Cucumber peel powder was added to each flask. The mixture is put in a water bath shaker and mix it for 25 min at 100 rpm and at room temperature. After 25 min of mixing the content from each flask was filtered and their absorbance was measured by using Atomic Absorption Spectrophotometer (AAS).

3.6 Effect of Adsorbent Dosage

Five Erlenmeyer flasks were taken and numbered as 1, 2, 3, and 4. 100 mL of 500 ppm reactive blue dye solution was taken in each flask and its pH was adjusted to 7 by using 0.1 N Sodium hydroxide. Cucumber peel adsorbents were added to the flasks in the order of 0.5 g, 1.0 g, 1.5 g, and 2.0 g. All the flasks were put in the water bath shaker and mix it for 25 min at 100 rpm and at room temperature. After 25 min, the sample from each flask was filtered and their absorbance was measured by using Atomic Absorption Spectrophotometer (AAS).

3.7 Effect of Agitation Speed

Four Erlenmeyer flasks were taken and numbered 1, 2, 3, and 4. All the flasks are filled with 100 mL of 500 ppm reactive blue dye solution and the pH of the sample in each flask was adjusted to 7 by adding 0.1 N Sodium hydroxide drop by drop. 0.5 g of Cucumber peel powder was added to each flask. The flask which numbered 1 was kept in a water bath shaker and mix it for 25 min at 50 rpm. Similarly, other flasks are kept in the water bath shaker and mix it for 25 min in the order of 100, 150, and

200 rpm. After mixing, the sample from each flask was filtered and the absorbance of each sample was measured by using Atomic Absorption Spectrophotometer (AAS).

3.8 Adsorption Calculations

The percentage of copper removal and adsorption capacity is used to evaluate the effectiveness of adsorption. They are given in Eqs. (1) and (2) as follows

$$\text{Percentage copper removal} = \frac{C_i - C_f}{C_i} \times 100\% \quad (1)$$

$$\text{Adsorption capacity } q = \frac{(C_i - C_f)V}{m} \frac{\text{mg adsorbate removed}}{\text{g adsorbent added}} \quad (2)$$

where C_i and C_f are initial and final concentrations of adsorbate, respectively, V is the volume of solution taken and m is the mass of adsorbent added. Equilibrium adsorption capacity is calculated as given in Eq. (2) at equilibrium time.

3.9 Adsorption Isotherms

Adsorption isotherm relates equilibrium adsorption capacity and concentration of adsorbate at a constant temperature. The maximum adsorption capacity can be calculated from the models developed for adsorption isotherms. The widely used isotherm models are developed by Langmuir and Freundlich. Langmuir adsorption isotherm is represented in Eq. (3) as follows:

$$\frac{1}{q_e} = \frac{K_L}{q_m C_e} + \frac{1}{q_m} \quad (3)$$

where q_e and C_e are equilibrium adsorption capacity and concentration, respectively, K_L is Langmuir constant and q_m is maximum equilibrium capacity.

Freundlich adsorption isotherm is represented in Eq. (4) as follows:

$$\ln q_e = \ln K_F + n \ln C_e \quad (4)$$

where K_F is Freundlich constant and n is adsorption intensity.

3.10 Adsorption Kinetics

Adsorption kinetics reveal the rate of adsorption of adsorbate on the adsorbent. It is also used to find the rate constant and order of adsorption. In general, adsorption follows pseudo kinetics, either first or second order. Pseudo-first order kinetics, proposed by Lagergren, is given in Eq. (5) is as follows:

$$\ln(q_e - q_t) = \ln q_e - k_1 t \quad (5)$$

where q_t is adsorption capacity at any time t , and k_1 is pseudo-first order constant.

Pseudo-second order kinetics, proposed by Blanchard, is given in Eq. (6) is as follows:

$$\frac{t}{q_t} = \frac{1}{k_2 q_e^2} + \frac{t}{q_e} \quad (6)$$

where k_2 is pseudo-second order constant.

3.11 Diffusion in Adsorption

The diffusional steps involved in adsorption are as follows: (i) Transfer from the interior of the adsorbate to the adsorbate-solvent interface; (ii) Movement across the adsorbate-solvent interface; (iii) Diffusion through the relatively stagnant liquid film surrounding the adsorbate; (iv) Transport through the bulk solvent; (v) Diffusion through the relatively stagnant liquid film surrounding the adsorbent; (vi) Movement across the adsorbate-adsorbent interface; (vii) Diffusion through the pores of adsorbent; and (viii) Transport through the surface of adsorbent to occupy the active site. Diffusion is due to two mechanisms: Intraparticle and liquid film diffusion.

Weber and Morris developed a model for the intraparticle diffusion mechanism in adsorption, as given in Eq. (7).

$$q_t = k' t^{0.5} + C \quad (7)$$

where k' is intraparticle diffusion constant and C is integral constant.

Elovich developed a model for liquid film diffusion mechanism in adsorption, as given in Eq. (8).

$$\ln(1 - F) = -k'' t \quad (8)$$

where k'' is liquid film diffusion constant and $F = q_t/q_e$.

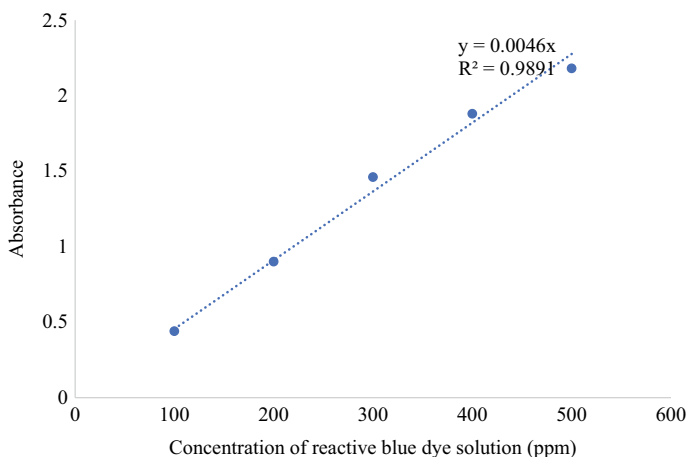


Fig. 1 Calibration graph for standard reactive blue dye solution

4 Results and Discussion

4.1 Calibration Curve

Figure 1 shows the calibration graph of standard reactive blue dye solution. A stock solution was prepared with a concentration of 1000 ppm. According to Lambert–Beer’s law, absorbance is directly proportional to the concentration of a standard solution with a proportionality constant of mass absorptivity. When the concentration of standard solution increased from 100 to 500 ppm, absorbance increases linearly with mass absorptivity of 0.0046 L/(mg cm). The value of R^2 of 0.9981 affirms that the prepared reactive blue dye solution follows Lambert–Beer’s law with a minimum deviation of 0.19%. Mass absorptivity is used in further experimental studies to calculate the concentration of a solution from absorbance.

4.2 Effect of pH

Figure 2 shows the effect of pH on the percentage removal of reactive blue dye from an aqueous solution by cucumber peel adsorbent. The percentage removal of reactive blue dye was studied with different pHs maintained at 3, 5, 7, 9 and 11. When pH increased from 3 to 5, percentage removal decreases from 92.6 to 92.3%. The percentage removal increases to 94.8% on a further increase of pH to 7. Again, a decline in percentage removal to 94.3% is observed when pH is increased to 9. Upon further elevation of pH to 11, the percentage removal dipped to 92.5%. From the

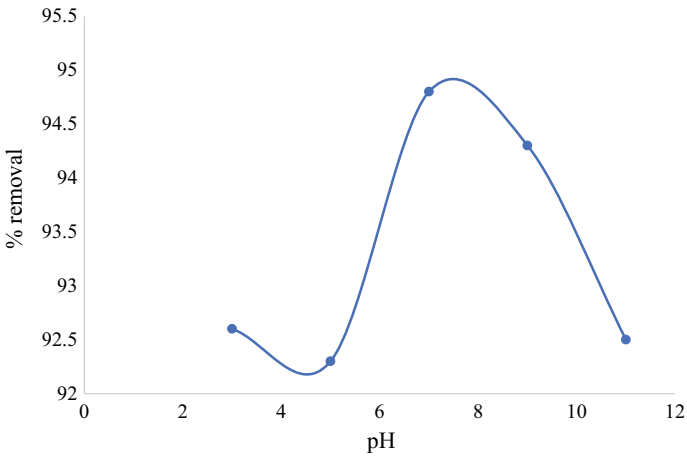


Fig. 2 Effect of pH on reactive blue dye removal using cucumber peel adsorbent

results, it was observed that a pH of 7 is an optimum value to achieve the maximum percentage of reactive blue dye removal of 94.8% using cucumber peel adsorbent.

4.3 Effect of Time

Figure 3 shows the effect of time on the percentage removal of reactive blue dye from an aqueous solution by cucumber peel adsorbent. The percentage removal of reactive

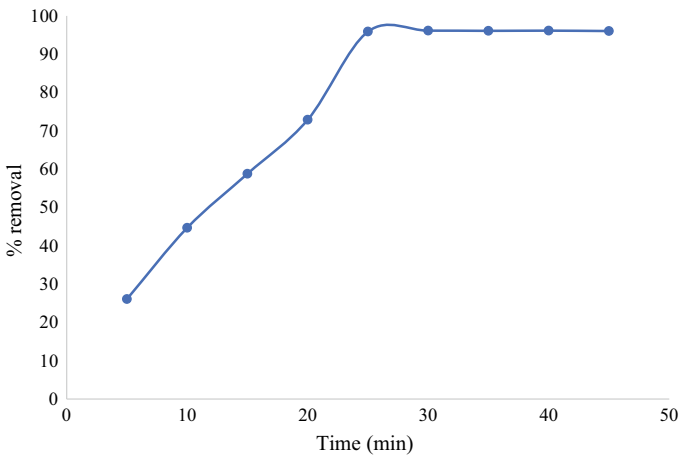


Fig. 3 Effect of time on reactive blue dye removal using cucumber peel adsorbent

blue dye was studied with various time intervals to achieve equilibrium. When time increased from zero to 5th minute, percentage removal increased from zero to 26.1%. The percentage removal further increases to 44.7, 58.8, 72.9, and 95.9% on a further increase of time to 10, 15, 20, and 25 min. After a further increase of time beyond 25 min, percentage removal becomes almost constant at around 96%, which means that equilibrium time is reached at 25 min. Equilibrium time is an important factor to study adsorption isotherm and kinetics. Also, it is an important criterion for the design of continuous and industrial adsorbers.

4.4 Effect of Initial Reactive Blue Dye Concentration

Figure 4 shows the effect of initial reactive blue dye concentration on the percentage removal of reactive blue dye from an aqueous solution by cucumber peel adsorbent. The percentage removal of reactive blue dye was studied with different initial reactive blue dye concentrations ranging from 100 to 500 ppm. Percentage reactive blue dye removal decreases with an increase in initial metal concentration because of loading adsorbate on the adsorbent. When initial reactive blue dye concentration increased from 100 to 200 ppm, percentage removal decreases from 79.69 to 58.84%. The percentage removal further decreases to 33.31% on a further increase of initial reactive blue dye concentration to 300 ppm. Again, a decline in percentage removal to 13.79% is observed when the initial reactive blue dye concentration is increased to 400 ppm. Upon further elevation of the initial reactive blue dye concentration to 500 ppm, the percentage removal dipped to 3.12%. Adsorption isotherm is studied from the effect of initial reactive blue dye concentration on percentage metal removal.

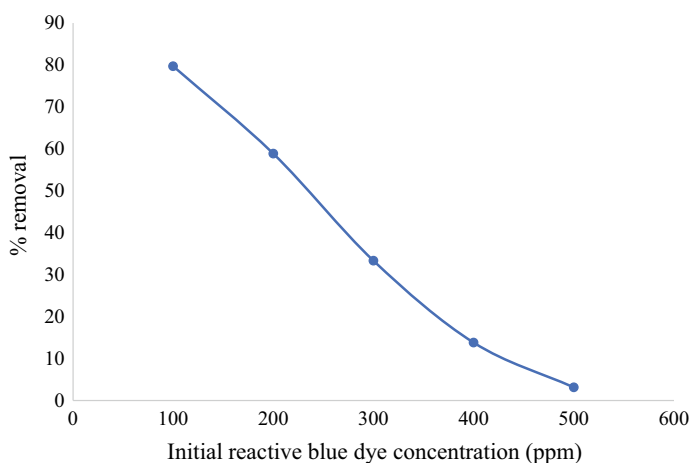


Fig. 4 Effect of initial reactive blue dye concentration on metal removal using cucumber peel adsorbent

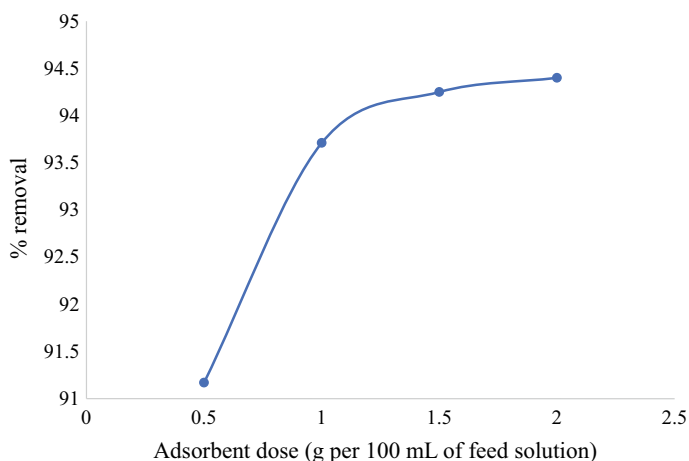


Fig. 5 Effect of adsorbent dosage on reactive blue dye removal using cucumber peel adsorbent

4.5 Effect of Adsorbent Dose

Figure 5 shows the effect of adsorbent dosage on the percentage removal of reactive blue dye from an aqueous solution by cucumber peel adsorbent. The percentage removal of reactive blue dye were studied with different adsorbent dosage maintained at 0.5, 1, 1.5, and 2 g per 100 mL of feed solution. When adsorbent dosage increased from zero to 0.5 g per 100 mL of the feed solution, percentage removal observed a steep increase from zero to 91.17%. The percentage removal increases to 93.71% on a further increase of initial reactive blue dye concentration to 1 g per 100 mL of feed solution. Again, a plateau is observed in percentage removal at 94.25% when the adsorbent dosage is increased to 1.5 g per 100 mL of feed solution. Upon further elevation of adsorbent dosage to 2 g per 100 mL of the feed solution, the percentage removal saturated at 94.4%. From the results, it was observed that an adsorbent dosage of 1.5 g per 100 mL of the feed solution is an optimum value to achieve a maximum percentage of reactive blue dye removal of 94.25% using cucumber peel adsorbent.

4.6 Effect of Agitation Speed

Figure 6 shows the effect of agitation speed on the percentage removal of reactive blue dye from an aqueous solution by cucumber peel adsorbent. The percentage removal of reactive blue dye was studied with different agitation speeds ranging from 50 to 200 rpm. When agitation speed increased from 50 to 100 rpm, percentage removal increases from 94.4 to 94.6%. The percentage removal increases to 94.7% on a further increase of agitation speed to 150 rpm. Again, an increase in percentage

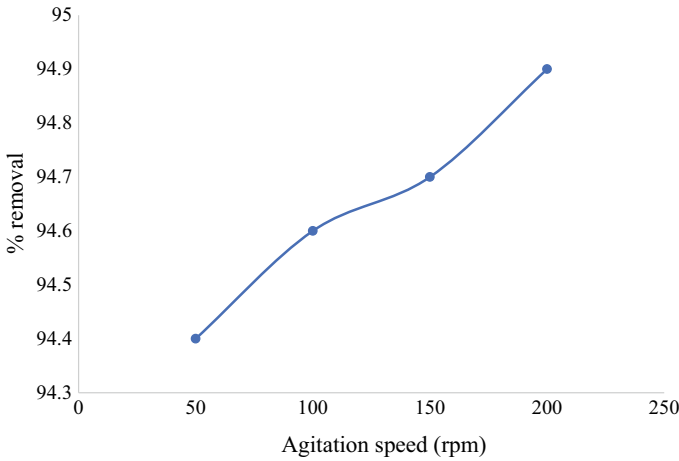


Fig. 6 Effect of agitation speed on reactive blue dye removal using cucumber peel adsorbent

removal to 94.9% is observed when agitation speed is increased to 200 rpm. From the results, it was observed that an agitation speed of 100 rpm is an optimum value to achieve maximum percentage reactive blue dye removal of 94.6% using cucumber peel adsorbent as the plateau is observed between 100 and 150 rpm.

4.7 Adsorption Isotherms

4.7.1 Langmuir Isotherm

Figure 7 shows Langmuir isotherm for reactive blue dye removal using cucumber peel adsorbent. A non-linear form of Langmuir isotherm is given in Eq. (9) as follows:

$$q_e = \frac{q_m C_e}{K_L + C_e} \quad (9)$$

From Fig. 7, the maximum adsorption capacity and Langmuir constant were calculated to be 59.17 mg/g and 26.87 L/mg, respectively. The value of R^2 of 0.9891 affirms that the experimental data fitted well with the Langmuir isotherm with a minimum deviation of 1.09%.

4.7.2 Freundlich Isotherm

Figure 8 shows Freundlich isotherm for reactive blue dye removal using cucumber peel adsorbent. A non-linear form of Freundlich isotherm is given in Eq. (10) as

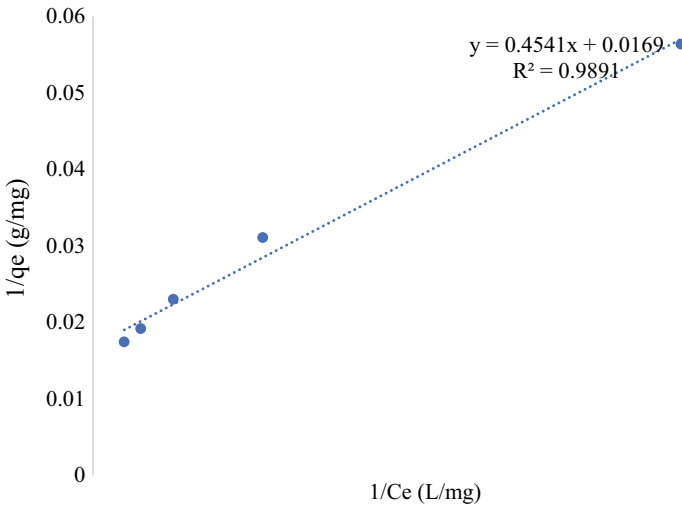


Fig. 7 Langmuir isotherm for reactive blue dye removal using cucumber peel adsorbent

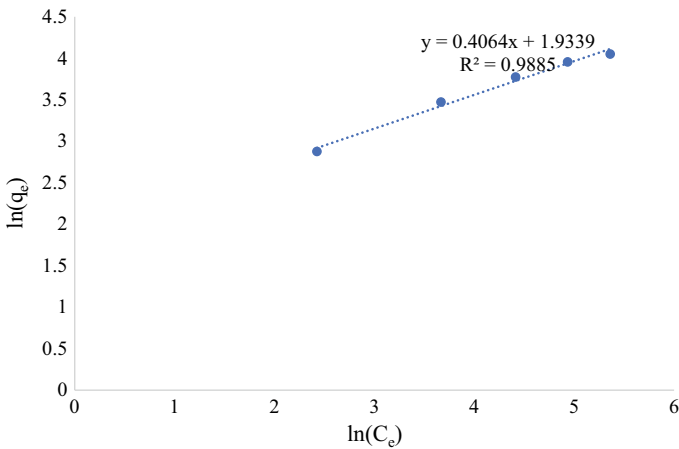


Fig. 8 Freundlich isotherm for reactive blue dye removal using cucumber peel adsorbent

follows:

$$q_e = K_F C_e^n \tag{10}$$

From Fig. 8, the Freundlich constant and adsorption intensity was calculated to be 6.916 and 0.4064, respectively. The value of adsorption intensity of 0.4064 reveals that the adsorption layer between adsorbate and adsorbent is not homogeneous, i.e., the interaction between adsorbate and adsorbent is not formed through a single layer

but multiple layers. Two layers of adsorbate are formed over the active sites of the adsorbent. The value of R^2 of 0.9885 affirms that the experimental data fitted well with the Freundlich isotherm with minimum deviation of 1.15%.

4.8 Adsorption Kinetics

4.8.1 Pseudo-first Order Kinetics

Figure 9 shows pseudo-first order kinetics for reactive blue dye removal using cucumber peel adsorbent. A non-linear form of pseudo-first order kinetics is given in Eq. (11) as follows:

$$\frac{q_e}{q_e - q_t} = e^{k_1 t} \tag{11}$$

From Fig. 9, rate constant and equilibrium adsorption intensity were calculated to be 0.0694 min^{-1} and 133.23 mg/g , respectively. The value of the rate constant of 0.0694 min^{-1} reveals that the adsorption rate is better when compared to 0.058 min^{-1} for crystal violet and 0.065 min^{-1} for rhodamine B using raw cucumber peel adsorbent [22]. The value of R^2 of 0.9915 affirms that the experimental data fitted well with pseudo-first order kinetics with a minimum deviation of 0.85%.

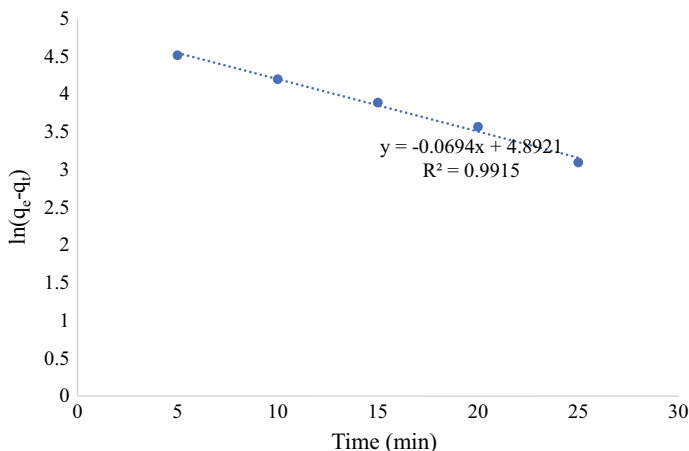


Fig. 9 Pseudo-first order kinetics for reactive blue dye removal using cucumber peel adsorbent

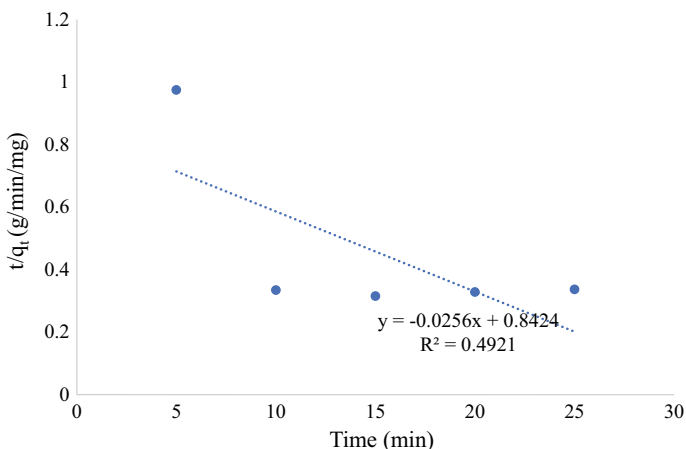


Fig. 10 Pseudo-second order kinetics for reactive blue dye removal using cucumber peel adsorbent

4.8.2 Pseudo-second Order Kinetics

Figure 10 shows pseudo-second order kinetics for reactive blue dye removal using cucumber peel adsorbent. A non-linear form of pseudo-second order kinetics is given in Eq. (12) as follows:

$$\frac{t}{q_t} = \frac{(1 + tk_2q_e)}{k_2q_e^2} \quad (12)$$

From Fig. 10, the value of R^2 of 0.4921 affirms that the experimental data does not fit well with pseudo-second order kinetics with a significant deviation of 50.79%. Hence, it is concluded that the adsorption kinetics follows the pseudo-first order model.

4.9 Diffusion in Adsorption

4.9.1 Intraparticle Diffusion

Figure 11 shows the intraparticle diffusion mechanism for reactive blue dye removal using cucumber peel adsorbent. From Fig. 11, the intraparticle diffusion constant was calculated to be $0.2 \text{ min}^{-0.5}$. The integral constant was calculated to be 100 mg/g . The value of the intraparticle diffusion constant of $0.2 \text{ min}^{-0.5}$ reveals that the adsorption mechanism is due to the interaction between adsorbate and adsorbent at the interface. Adsorption is better when compared to $0.193 \text{ min}^{-0.5}$ for crystal violet and 0.196 min^{-1} for rhodamine B using raw cucumber peel adsorbent. The value of

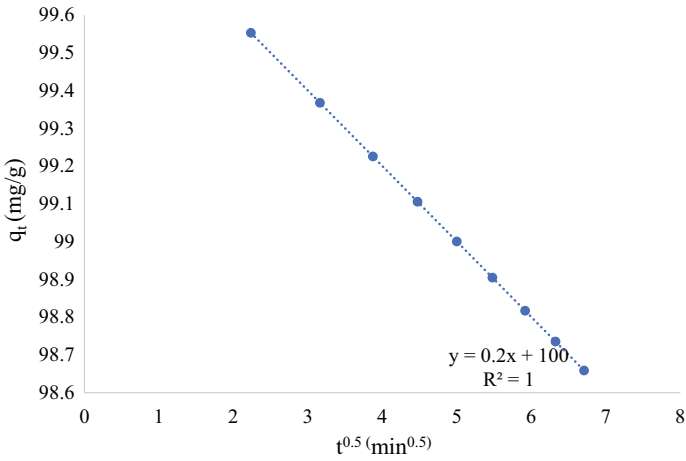


Fig. 11 Intraparticle diffusion mechanism for reactive blue dye removal using cucumber peel adsorbent

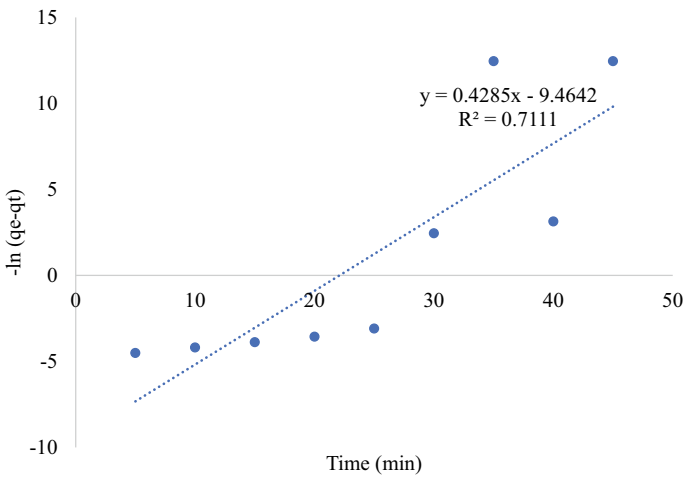


Fig. 12 Liquid film diffusion mechanism for reactive blue dye removal using cucumber peel adsorbent

R^2 of 1 affirms that the experimental data fitted well with the intraparticle diffusion mechanism with insignificant deviation.

4.9.2 Liquid Film Diffusion

Figure 12 shows the liquid film diffusion mechanism for reactive blue dye removal using cucumber peel adsorbent. From Fig. 12, the value of R^2 of 0.7111 affirms that the experimental data does not fit well with the liquid film diffusion mechanism with a significant deviation of 28.89%. Hence, it is concluded that the adsorption kinetics follow the intraparticle diffusion mechanism.

5 Conclusion

The present work aimed to study the applicability of raw cucumber peel adsorbent to remove reactive blue dye (cupric chloride) from its aqueous solution. The optimal values of pH 7, 25, min equilibrium time, 400 ppm initial reactive blue dye concentration, 1.5 g per 100 mL of the feed solution, and 100 rpm of agitation speed showed the maximum percentage reactive blue dye removal of around 95%. Adsorption isotherm follows Langmuir and Freundlich models. Adsorption kinetics reveals the fitting of experimental data to pseudo-first order model. Mass transfer or diffusion studies explore the intraparticle diffusional mechanism for the adsorption of reactive blue dye on cucumber peel adsorbent. Thus, cucumber peel could be utilized as a cost-effective adsorbent for the removal of reactive blue dye from its aqueous solution.

References

1. Akkaya G, Güzel F (2013) Optimization of copper and lead removal by a novel biosorbent: cucumber (*Cucumis sativus*) peels—kinetic, equilibrium, and desorption studies. *J Dispers Sci Technol* 34(10):1295–1307
2. Akkaya G, Güzel F (2014) Application of some domestic wastes as new low-cost biosorbents for removal of methylene blue: kinetic and equilibrium studies. *Chem Eng Commun* 201(4):557–578
3. AlProl AE (2019) Study of environmental concerns of dyes and recent textile effluents treatment technology: a review. *Asian J Fish Aquat Res* 1–18
4. Basu M, Guha AK, Ray L (2017) Adsorption of lead on cucumber peel. *J Clean Prod* 151:603–615
5. Basu M, Guha AK, Ray L (2019) Adsorption of cadmium ions by cucumber peel in continuous mode. *Int J Environ Sci Technol* 16(1):237–248
6. Chung KT (2016) Azo dyes and human health: a review. *J Environ Sci Health C* 34(4):233–261
7. Gita S, Hussan A, Choudhury TG (2017) Impact of textile dyes waste on aquatic environments and its treatment. *Environ Ecol* 35(3C):2349–2353
8. Jain S, Jain PK (2020) Classification, chemistry, and applications of chemical substances that are harmful to the environment: classification of dyes. In: *Impact of textile dyes on public health and the environment*. IGI Global, pp 20–49
9. Katheresan V, Kansedo J, Lau SY (2018) Efficiency of various recent wastewater dye removal methods: a review. *J Environ Chem Eng* 6(4):4676–4697

10. Khanna S, Rattan VK (2017) Removal of acid red 1 from aqueous waste streams using peel of *Cucumis sativus* fruit. Equilibrium studies. *J Chem Technol Metall* 52(5)
11. Kumar PS, Saravanan A (2017) Sustainable wastewater treatments in textile sector. In: Sustainable fibres and textiles. Woodhead Publishing, pp 323–346
12. Mahmoodi NM, Taghizadeh M, Taghizadeh A (2018) Mesoporous activated carbons of low-cost agricultural bio-wastes with high adsorption capacity: preparation and artificial neural network modeling of dye removal from single and multicomponent (binary and ternary) systems. *J Mol Liq* 269:217–228
13. Mani S, Chowdhary P, Bharagava RN (2019) Textile wastewater dyes: toxicity profile and treatment approaches. In: Emerging and eco-friendly approaches for waste management. Springer, Singapore, pp 219–244
14. Manzoor J, Sharma M (2020) Impact of textile dyes on human health and environment. In: Impact of textile dyes on public health and the environment. IGI Global, pp 162–169
15. Navya A, Nandhini S, Sivamani S, Vasu G, Sivarajasekar N, Hosseini-Bandegharai A (2020) Preparation and characterization of cassava stem biochar for mixed reactive dyes removal from simulated effluent. *Desalin Water Treat* 189:440–451
16. Pandey R, Ansari NG, Prasad RL, Murthy RC (2014) Pb (II) removal from aqueous solution by *Cucumis sativus* (Cucumber) peel: kinetic, equilibrium & thermodynamic study. *Am J Environ Prot* 2(3):51–58
17. Rodríguez IA, Zamarripa DMA, Pérez DJS, González JFC, Pérez ASR, Juárez VMM, Oviedo JT, Domínguez EE. The use of *Cucumis sativus* shell biomass in the removal of chromium (VI) in aqueous solution
18. Saravanakumar K, Senthilkumar R, Prasad DMR, Prasad BSN, Manickam S, Gajendiran V (2020) Batch and column arsenate sorption using *Turbinaria ornata* seaweed derived biochar: experimental studies and mathematical modeling. *Chem Select* 5(12):3661–3668
19. Saygılı GA, Güzel F (2017) Chemical modification of a cellulose-based material to improve its adsorption capacity for anionic dyes. *J Dispers Sci Technol* 38(3):381–392
20. Shakoor S, Nasar A (2017) Adsorptive treatment of hazardous methylene blue dye from artificially contaminated water using *Cucumis sativus* peel waste as a low-cost adsorbent. *Groundw Sustain Dev* 5:152–159
21. Smitha T, Santhi T, Makeswari M (2015) Adsorption of acid black-7 from synthetic aqueous solution onto *Cucumis sativus* peel. *J Chem Pharm Res* 7(4):1617–1625
22. Smitha T, Santhi T, Prasad AL, Manonmani S (2017) *Cucumis sativus* used as adsorbent for the removal of dyes from aqueous solution. *Arab J Chem* 10:S244–S251
23. Stavrinou A, Aggelopoulos CA, Tsakiroglou CD (2018) Exploring the adsorption mechanisms of cationic and anionic dyes onto agricultural waste peels of banana, cucumber and potato: adsorption kinetics and equilibrium isotherms as a tool. *J Environ Chem Eng* 6(6):6958–6970
24. Zaman A, Das P, Banerjee P (2016) Biosorption of dye molecules. In: Toxicity and waste management using bioremediation. IGI Global, pp 51–74

Application of Dried Fungus in Textile Wastewater



Ariani Dwi Astuti and Yonik Meilawati Yustiani

1 Introduction

Currently, industrial growth is growing rapidly, as evident from the number of growing small and large industries. As such, the people's standard of living can improve. However, industries may increase the level of air and water pollution. One industry that pollutes the environment is textiles, which generates wastewater with a high concentration of dyes and organic substances [72]. In 2012, global textile production was 140.84 million tons with a growth rate of 6.5%/year [33]. A report shows that the total consumption of textile goods can increase to 49 billion kg/year [49]. About 15–20% of the dyes used in textile manufacturing go unused and are dumped into bodies of water without being treated [38].

Dyes used in textile production are generally synthetic materials, which have molecules in the form of bonds from unsaturated organic compounds. When the dye used is not fully absorbed by the fiber, the fibers will become colored waste. The absorption of the dye by the fiber is affected by the dye's absorption rate. The absorption rate of the fiber to the dye varies according to the dye used. One of them is a reactive dye with an absorption rate of 50–90%. The loss of reactive dyes in the production process can reach up to 50%, which will become colored waste [55].

Several treatment methods are often used in dealing with textile waste, i.e., chemical, physical and biological processing. Coagulation-flocculation, adsorption and aerobic processes with the activated sludge method are examples of those processing

A. D. Astuti (✉)

Department of Environmental Engineering, Faculty of Landscape Architecture and Environmental Technology, Universitas Trisakti, Jakarta, Indonesia

e-mail: ariani_da@trisakti.ac.id

Y. M. Yustiani

Department of Environmental Engineering, Faculty of Engineering, Universitas Pasundan, Bandung, Indonesia

e-mail: yonik@unpas.ac.id

methods, respectively. However, color removal through the coagulation process has a disadvantage, i.e., excess production of chemical sludge. Thus, further processing of the sludge is required. The current sludge processing includes drying the sludge in a drying bed and then putting it in a sack. Therefore, it is necessary to find other alternatives to handle the textile industry's wastewater production.

The adsorption method is recorded as the better process for color removal. It's relatively simple in reactor design, inexpensive and effective in removing high dye concentrations. Adsorption is a mechanism of attaching a substance (adsorbate) to the surface of another substance (adsorbent) of the solid adsorbent. This adsorption process occurs due to the attractive force of molecules on the surface of the media. A widely used adsorption method in textile wastewater treatment is activated carbon [51], which has been used to remove dyes in liquid waste as it is proven to be very useful in treating color waste. However, the high price of activated carbon becomes an obstacle in its use. Another pollutant sorption method is processing through a biosorption process that utilizes both dead and live fungi [36]. Biosorption is the removal/recovery of pollutants using microorganisms, in the process of which absorption (sorption) is carried out by microorganisms [24]. Biosorption can take place in living or dead microorganisms. Dead biomass provides a better sorption result compared to live biomass [12]. Compared to the living ones, the dead fungus has several advantages, including a high level of resistance to the environment, a greater level of toxicity tolerance, and relatively fast regeneration for reuse [35]. A particular culture media is not needed to maintain its active conditions. The use of dried fungi is expected to be an alternative in removing dyestuff waste.

Fungi are usually widely used in food, beverage, and drug productions. Waste generated from these industries will contain a lot of molds. The fungus in this waste can be taken and used for processing industrial textile waste. These fungi can be either alive or dead. The *Rhizopus* sp, for example, is easily obtained from the Indonesian special cuisine *tempe*, a soybean fermentation cake. This fungus is expected to be an option to activated carbon in adsorbing dyes. Furthermore, the usage of fungi in the biosorption of textile wastes can also remove other pollutants such as salts and surfactants [67].

2 Dye Removal Using Fungus

2.1 Dye in Textile Wastewater

Azo dyes produce bright, vivid colors, and are primarily used in the production of colored cotton, leather, cosmetics, and food. Compared to organic dyes, azo dyes comprise the majority (over 3000 different varieties) of all textile dye substances manufactured owing to their easy and cost-efficient synthesis, stability, and the wide range of colors available [18]. They are utilized in various industries, including textiles, paper, food, leather, cosmetics, and medicines [66].

Adsorption approaches have gotten significant attention because they have a more excellent performance of decolorization for wastewater consisting of several dyes, including azo. When evaluating an adsorbent for dye removal, high affinity, component capacity, and regeneration ability are the main influential factors. Activated carbon is an attractive material for a wide type of dyes. Its high cost and difficulty in regeneration, however, limit its use in decolorization. Some scientists have utilized low-cost adsorbents such as peat, bentonite clay, fly ash, and polymeric resins to make the sorption process cost-effective. For the decolorization of textile wastewater, some scientists have used natural resources such as treated ginger water, groundnut shell-charcoal, date-stones, and potato-plant waste. However, several issues with these adsorbents have limited their use, including adsorbent recovery and/or disposal, slurry production, and the high price. As a result, adsorbents should be used in processes with low pollutant concentrations or when the adsorbent is inexpensive or easily regenerated [32].

2.2 Dried Fungus

Gymnomycota, Mastigomycota, and Amastigomycota are the three categories of fungi. Zygomycetes, Basidiomycetes, Ascomycetes, and Deuteromycetes are the four classes of Amastigomycota. Fungi are chemoheterotrophic microbes that can be parasitic or saprophytic. Some are single-celled, while others have cell walls and are filamentous. Fungi are vital for health and a sustainable ecosystem. Molds, mushrooms, and yeasts are the three types of fungi. The former two are filamentous in nature, whereas the latter are unicellular. These organisms are crucial in terms of biotechnology.

White rot fungus, brown rot fungi, and soft rot fungi are three forms of wood-rot fungi that exhibit a variety of enzymes and can breakdown a variety of wood types, depending on the type of decay. Pleurotus, Trametes, Phanerochaete, Lentinus, Ganoderma, and other genera of white rot fungi are among the most important. These can cause the lignin component of woody plants to breakdown, resulting in wood bleaching. They produce enzymes such as laccase, lignin peroxidase, and manganese peroxidase, which are all necessary for the breakdown of wood and other refractory and xenobiotic compounds such as dyes [73].

The fungal body structure, in general, its parts and functions are listed below:

- (a) Thallus is the overall form of the fungus because the fungus does not yet have true roots, stems, and leaves.
- (b) Fungal cell walls are composed of chitin and beta-glucan substances. Chitin is a carbohydrate polymer containing nitrogen and has an essential role in the color adsorption process by dried fungi.
- (c) Septa (singular: septum) is a dividing wall between one or more nuclei with other nuclei.

- (d) Hyphae (micrometers to meters) are rows of cells that form threads in multicellular fungi. It is known that there are aseptate hyphae, uninuclear septate hyphae, and multinucleated septate hyphae, based on the presence or absence of a septum or septa.
- (e) Pores are holes in the septa that allow the cytoplasm to move from cell to cell to distribute nutrients.
- (f) Haustoria is a modified form of hyphae possessed by fungi whose life is parasitic.
- (g) Mycelium is made up of hyphae that branch out, where spores are formed, and it is a means of reproduction and food.
- (h) The sporophore (fruiting body) is a clump of hyphae that emerges from the soil or weathered wood. Fruiting bodies can be found in a variety of fungi. Yeast cells range in size, widths of 1–5 μm , and lengths of 5–30 μm or more. Other types of mushrooms with fruiting bodies that measure 20–25 cm in diameter and 25–30 cm in length.
- (i) Fungi reproduce primarily through spores.
- (j) Extracellular hydrolytic enzymes break down food substances that are still complex compounds before being absorbed by fungi (Figs. 1 and 2).

Fungi are used to remove the color from textile waste in the biosorption process, both living and dead cells. Dried fungi are viable for treating textile wastewater because they reduce operational costs [68]. Biosorption has several advantages, including high efficiency, low-cost, good removal results, low recovery costs, and equipment availability.

Decolorization in living cells is more complicated than in dead cells, involving intracellular, extracellular oxidase, and biosorption. Operating conditions such as nutrient requirements, effect concentrations, and toxicity are closely related to living cells' processes. However, decolorization by dried fungi speeds up the process; dead cells have a high sorption capacity under most circumstances and the potential to be effective biosorbents. This chapter goes into detail about the ability of dead fungi to remove the color from textile wastewater.

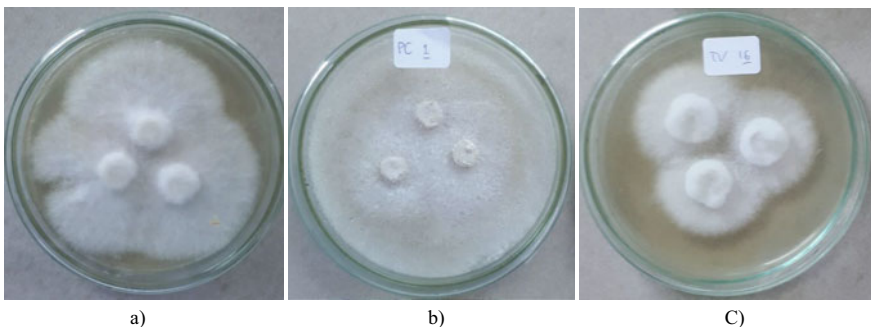


Fig. 1 Culture of white rot fungi **a** *Bjerkanthera adusta*, **b** *Phanerochaete chrysosporium*, **c** *Trametes versicolor*



Fig. 2 a *Bjerkandera adusta*, b *Trametes versicolor* (<https://commons.wikimedia.org/wiki/File:2011-09> and <https://commons.wikimedia.org/w/index.php?curid=25175312>)

2.3 Dried Fungus Preparation

The fungus must first be treated before being used in the adsorption process. Several dried-fungus pretreatment methods can improve biomass adsorption capacity. Physical and chemical pretreatment methods or a combination of both are used: physically through drying only; heat-drying or autoclaving-drying and chemically, through contact with organic or inorganic compounds such as formaldehyde or NaOH, H₂SO₄, HCl, NaHCO₃, and CaCl₂.

Twenty fungal endophytes were dried and tested for the capacity in breaking down azo dyes. Furthermore, those dyes decolorized at a rate of 97%, 56%, 48%, and 33%, for Remazol Brilliant Blue R., methyl red, congo red, and orange G, respectively, by this isolate's strain [48]. Another researcher employed dried fungi to remove methylene blue (MB) dye using Artist's Bracket (AB) mushrooms. They washed the fungi particles with deionized water and dried them at 105 °C for 24 h [47]. Asma et al. [9] discovered that the dried white rot fungus *Phanerochaete chrysosporium* ME446 performed better at removing colors than *Funalia trogii* ATCC 200800. The drying procedure for fungi is carried out at a temperature of 30 °C for 24 h. After 5 min, the adsorption effectiveness of dried algae was more significant than the adsorption efficiency of living algae [19].

The fungus' structure may be ruptured during autoclaving, exposing potential dye-binding sites. The porosity and surface area of *R. oryzae* biomass was measured by Gallagher et al. [29], who discovered that the autoclave process could disrupt particle structure [29]. The destruction may enhance the particles' surface area and monolayer quantity, as well as the porosity, exposing latent sites and thus increasing dye adsorption. Astuti and Muda [11] conducted a color removal study using artificial textile wastewater and *Bjerkandera adusta* with pretreatment autoclaving-drying; they obtained a color removal result of 53.55% [11].

Other pretreatments to obtain biosorbents can also be carried out by combining autoclaving and immersion such as 0.1 M NaOH, 0.1 M HCl, 0.1 M H₂SO₄, etc.

[28]. Basic Blue 9's biosorption capacity grew from 1.17 to 18.54 mg/g after autoclaving, while Acid Blue 29's sorption potency increased from 6.63 to 13.83 mg/g after 0.1 M H₂SO₄ pretreatment [28]. It shows approximately 100% biosorption potency enhancement. Another improvement was also performed in acid pretreatment of Acid Blue 29 as an anionic dye. The addition of a negative charge of fungus surface as media could change into positive in this treatment [64]. The combination of autoclaving with chemical pretreatment using HCl acid was also carried out by Astuti and Muda [10], which could increase the percentage of color removal from artificial textile wastewater from 53.55 to 81.3% using *Bjerkandera adusta* [10].

Zhou and Banks [71] increased the biosorption capacity by soaking *R. arrhizus* biomass with 2 M NaOH for 1 h. The relatively long the treatment, the more significant the increase in biosorption capacity. They argued that eliminating proteins and glucans from the cell wall would result in a higher amount of chitin/chitosan throughout the cell fraction. A mount of chitin can be converted to chitosan over time using a concentrated alkaline solution. *R. oryzae* was pretreated by heating using autoclave, calcium saturation, NaOH, and chitin/chitosan enhancement by Gallagher et al. [29], and all these processes improved the sorption capacity from 7 to 15%. Calcium was an excellent activating counter ion because due to its ease of substitution with dyes that formed more stable complexes, an increase in adsorption capacity by Ca²⁺ saturation suggested that *R. oryzae* had a poor affinity for Ca²⁺ ions; calcium was an excellent activating counter ion because it was easily replaced by dyes that formed more stable complexes. Pretreated with NaOH could result in anionic sites and expose the cell's chitin/chitosan complex by dissolving some biopolymers from the biomass particle surface, as chitin/chitosan was identified as the primary biosorbent of the colorant. Pretreated can be done by dissolving it in an acid-alkali solution to maximize chitin/chitosan in biomass.

The capacities and mechanisms of native and treated white rot fungus *Lentinus sajurcaju* for removing textile dye (i.e., Reactive Red-120) from an aqueous solution were evaluated by Yakup and Bayramoğlu [46]. The most excellent dye uptake was seen at pH 3.0 for all tested fungal biomass preparations. The dye uptake capabilities of the biosorbents were 117.8, 182.9, 138.6, and 57.2 mg/g for native and heat-treated (100 °C in 10 min), acid-treated (H₂SO₄), and base-treated (NaOH) dry fungal preparations, respectively [46]. Further research by Bayramoğlu and Yakup [14] resulted that the biosorption capabilities of native and heat-treated *Trametes Versicolor* were 101.1 and 152.3 mg/g for Direct Blue-1, and 189.7 and 225.4 mg/g for Direct Red-128, respectively.

3 Factors Affecting Dye Removal Using Dried Fungus

Adsorption is the separation of a compound from the solution attached to the media surface, in the contact area between the media and the solution. Desorption is the opposite of adsorption, which releases a compound from a solid where the compound is deposited or attached to it in the solution [53]. The adsorption and desorption

processes occur simultaneously. If the rate of adsorption is the same as that of desorption, then the condition is considered a state of achieving equilibrium.

Several factors influence the adsorption process [34, 37]:

- The physical condition of the adsorbent and adsorbate: surface area, pore dimension, molecular size, etc.
- Chemical characteristics of adsorbent and adsorbate: chemical composition, structure, polarity, etc.
- Solubility of substances and their concentration in solution
- The state of the liquid, such as temperature and pH
- The retention time of wastewater in the system.

Wastewater, in general, can be absorbed (adsorption power) by dissolved compounds, which are very varied and complex. The molecular structure of solubility affects the adsorption power. This effect can be seen as follows [25].

- Increasing the solubility of a material in a liquid will decrease its adsorption power
- Branched chains are easier to adsorb than long chains
- Groups that affect the adsorption power, including, i.e., hydroxyl groups, usually decrease the adsorption power depending on the molecular structure, amino groups usually decrease adsorption power, but with a greater effect, sulfonic groups usually reduce adsorption power, and nitro groups can increase the adsorption power
- Generally, robust ion solutions are more difficult to adsorb than weak ion solutions
- The amount of hydrolytic adsorption depends on the hydrolysis ability to form adsorbable acids or bases
- Large molecules are more easily adsorbed than small molecules with the same chemical properties
- Molecules with low polarity are easier to adsorb than high polarity.

Several factors that affect the biosorption process in removing color from textile wastewater are as follows.

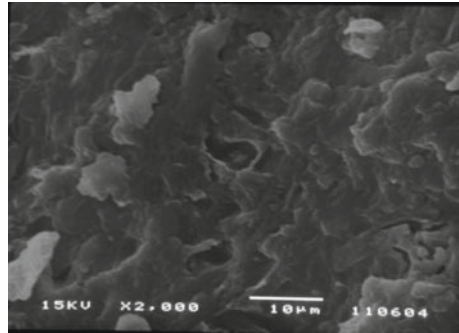
1. pH: the main parameter that can affect the biosorption capacity. Wastewater color and solubility of several types of dye can also be affected by pH. Thus, pH may influence the biosorption process that depends on the dye type. For anionic dyes, the biosorption process will increase with the decreasing pH [62]. In cationic dyes like Orllamar, the biosorption process increases with the increasing pH [15, 39]. In a study of dyes and metal adsorption from textile wastewater, it was found that the maximum process occurs at a pH of 5.5 for Methyl Orange, pH of 6 for Cr, and pH of 7 for Pb, an increase in pH can decrease the biosorption of the dyes [65].
2. Temperature: textile dyestuff wastewater generally has a high temperature of up to 60 °C. Thus, temperature becomes an essential factor that can affect the sorption process. The biosorption process will decrease with increasing temperature in anionic dyes (Remazol Black B reactive) [3]. The biosorption process will decrease with increasing temperature in cationic dyes of Violet 3

and Basic Yellow 23 [20, 21]. This is caused by a decrease in cell surface activity [3].

3. Initial concentration: a higher dye concentration may lead to higher biosorption capacity. The initial condition plays an essential role as a driving force to deal with resistance in mass, a transferring process of the dye between phases [2].
4. Salt: the dyeing process requires a lot of salt. The salt concentration in the textile industry wastewater is an essential factor affecting the biosorption process. High ionic strength resulting in strong sorption of humic acids by fungi is similar to the effect of strong ions of colloids [71]. At high ionic strength, the two layers between fungi biomass and humic acid will be pressed thinly, thereby increasing van der Waals bonds and causing increased biosorption.
5. Heavy metals: metal ions such as Cd^{2+} , Cu^{2+} , and Al^{3+} are often found in the wastewater of textile industries due to the usage of metal-containing dyes. These affect the humic acid adsorption by fungi, which can perform higher sorption in higher concentrations; the metal ions may link *Rhizopus arrizus* and humic acids, both negatively charged [71]. Therefore, the existence of metal ions can make a neutral condition of the surface charge and lower the repulsion strength among fungi and humic acids so that the bond increases.
6. Mixing speed: the absorption capacity of the biomass increases with the increasing speed of stirring. A study on the effect of the stirring rate of dye biosorption in activated sludge was conducted with a particle size of 300–600 μm [20, 21]. The biomass absorption capacity increased from 18 to 53 mg/g with an increase in stirring speed from 40 to 160 rpm. It was also found that the layer around the biomass particles lowering the sorption capacity and increasing speed can overcome this problem.
7. Contact Time: the biosorption rate is rapid at the beginning of contact between the dyes and adsorbent [12]. In general, the longer the contact duration, the more the adsorbed material. However, in a certain period, the adsorbent is saturated so that it does not adsorb effectively, and then desorption can occur.
8. Amount of adsorbent: the amount of adsorbent media is essential in the sorption process because it will determine the amount of dye to be removed. The more media used, the more dye will be absorbed. This occurs due to the increasing number of media surfaces available for the dye to stick. The amount of adsorbent that can remove a certain amount of dye will give the value of adsorption capacity. Media is said to be good if it can absorb a lot of dye in small quantities, which gives economic benefits [60].
9. Particle size: the biosorption kinetics are strongly related to the adsorbent surface area. The sorption capacity of the fungi may improve in a smaller particle grain size because the total surface area will be larger with smaller particle grains for the same amount of biomass. A wide surface area can also be formed as numerous pores can give more opportunity to the dye substances to attach to the media. Figure 3 shows the SEM of dried *Rhizopus* sp.

The use of live microorganisms for biosorption has several weaknesses is as follows [2]:

Fig. 3 Scanning electron microscopes (SEM) analysis of dried *Rhizopus* sp pores 2000× magnification [57]



- The difficulty in maintaining the biomass alive during the biosorption process because it will continue to require a nutritional intake
- It can affect the life of microorganisms if pollutants are toxic.

Several benefits of the use of dried microorganisms as an absorbent for wastewater treatment are as follows [2]:

- Dried organisms do not affect toxic waste
- Dried organisms do not need nutritional intake because they are dead
- It can be regenerated and reused.

The conditions that must be met by a biosorbent to adsorb pollutants are as follows [52, 54]:

- It has a very large ratio of surface area to weight
- It has a high affinity and selectivity to certain ions
- Available in large quantities and relatively inexpensive.

4 Mechanism of Dye Adsorption on Dried Fungus

The dye adsorption mechanism for dead cells is biosorption, characterized by physicochemical contact such as adsorption, deposition, and ion-exchange. The most crucial active ingredient is chitin/ chitosan. It was performed in the study of humic acid adsorption by *R. arrhizus* [71]. Another study showed that various physical mechanisms might occur during the biosorption process. The usage of *R. oryzae* in adsorbing Reactive Brilliant Red discovered that both the Freundlich and Langmuir isotherm models are suitable for biosorption, implying physical sorption through various mechanisms on a heterogeneous surface [29].

The Scanning Electron Microscopes (SEM) analysis was used to describe the morphological properties of the used adsorbent sample, including surface features. The surface porosity and structure/texture of the treated adsorbent were also projected. The adsorption capacity is determined by pore size distribution, particle size, and surface area [43].

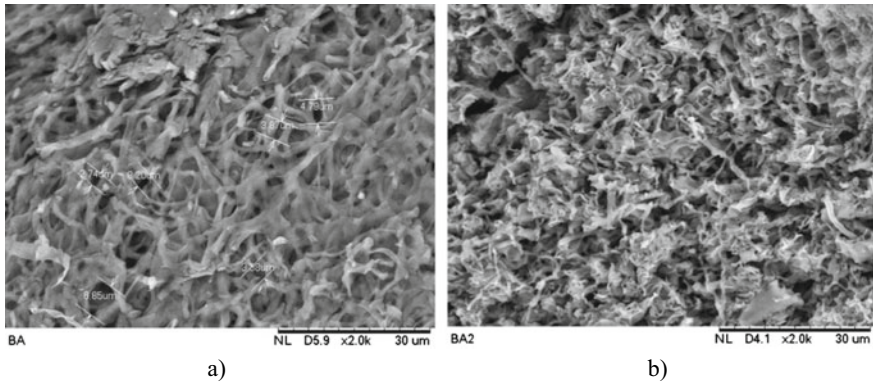


Fig. 4 Scanning electron microscopes (SEM) analysis *Bjerkandera adusta* using an autoclave **a** before and **b** after adsorption processes at 2000 \times magnification [11]

The SEM analysis of biosorbent *B. adusta* was performed at 2000 \times magnification before and after the artificial textile wastewater adsorption process [11]. The changes in the biosorbent after being added to the contaminant dye were observed (Fig. 3). Figure 4a and b depicts the morphology of the biosorbent *B. adusta*, highlighting the pores. The *B. adusta* cell wall appears shrunken and has more holes (Fig. 4b) than before contact (Fig. 4a), which tends to be more moisturized and supple. Biosorbent *B. adusta* had pores ranging in size from 2.74 to 8.30 μm , but after biosorption, they shrank to 1.31–2.14 μm . The dye that accumulates between *B. adusta* biosorbent is clearly visible in a crystalline form [11]. The findings of this study agree with those of Ririhena et al. [56], who used *S. cerevisiae* to study Cu^{2+} ion absorption [56].

Regeneration potency is one of the most valuable properties of sorbent media. Several solutions may perform as a regeneration solvent. Ethanol, methanol, and surfactants such as nonionic Tween and NaOH solvent can elute and regenerate fungal biomass [28].

To adsorb humic acid from *R. arrhizus* biosorbent, Zhou and Banks [71] utilized 0.1 M NaOH. The average efficiency of desorption was greater than 90%. According to the findings, *R. arrhizus* biomass can be used for various sorption–desorption processes with comparable results [71].

5 Kinetics of Dye Adsorption on Dried Fungus

Adsorption kinetics describes the rate of material adsorbed at constant environmental conditions, especially temperature. There are two kinetic models that often describe the biosorption process of this dye. The first model is Lagergren pseudo first-order, suitable for the initial biosorption process. The second model is the Ho and McKay pseudo second-order, which can describe biosorption process in a long range until

equilibrium occurs. The equilibrium is stated in the duration of 18 or 24 h in certain temperatures [50]. The adsorption isotherm is a description of a relationship between the solute adsorbed per unit mass and the equilibrium concentration. In the acid dye biosorption study using lyophilized *Cunninghamella elegans*, it was found that the appropriate kinetics were both models of pseudo first-order and second-order [58].

In addition, the adsorption isotherm also reveals the number of pores filled by the adsorbate. The adsorption isotherm was carried out to acquire data on the adsorption capacity of an adsorbent against solutes or adsorbates. Calculation using isotherm equations is conducted to determine this capacity. The Freundlich sorption isotherm and Langmuir sorption isotherms are often used for this purpose.

5.1 Types of Sorption Isotherms

The popular sorption isotherm types are Freundlich's and Langmuir's. Freundlich's sorption isotherm is developed on the assumption in which adsorption happens in a bilayer and affects a heterogeneous adsorbent surface, commonly used to describe dyes sorption [59]. This surface condition presumes that the adsorption rate differs according to the energy or strength of a specific location. Some locations or surfaces attract adsorbate strongly while some other sites do so weakly. Adsorption or desorption rates differ according to the energy/strength of the surface [40].

Freundlich sorption isotherm can be seen in the following equation [45]:

$$\frac{X}{M} = K_f \times C_{eq}^{1/n} \quad (1)$$

where K_f is Freundlich constant (mg/g), $1/n$ is constant, X/M is the weight of substance adsorbed on the adsorbate (mg/g), C_{eq} is a solution concentration at equilibrium (mg/L). K_f indicates the adsorption capacity while $1/n$ indicates adsorption intensity.

The sorption isotherm proposed by Langmuir has the assumption that adsorption occurs in one layer and is used on a homogeneous adsorbent surface. The homogeneous surface of the adsorbent states that the adsorption energy (the adsorption force between the surface and the adsorbed molecule) is the same for all locations [22].

Langmuir sorption isotherm can be seen in the following equation [69, 70]:

$$\frac{X}{M} = \frac{b \times q_m \times C_{eq}}{1 + b \times C_{eq}} \quad (2)$$

where b is Langmuir equilibrium value, X/M depicts the amount of substance adsorbed on the adsorbate (mg/g), C_{eq} is a concentration of solution at equilibrium (mg/L), q_m is a constant indicating the maximum weight of adsorbate per adsorbent. It gives an adsorption capacity in mg/g.

The condition of this isotherm type can be expressed in the adsorbent suitability constant (R_L), using this equation [31]:

$$R_L = \frac{1}{1 + (b \times C_0)} \quad (3)$$

where R_L is the adsorbent suitability value in the Langmuir isotherm equation, b is the Langmuir equilibrium constant. R_L is also expressed as a separation factor.

In describing the effect of the porous configuration of a sorption media, an isotherm model was developed for the monolayer condition [16]. This model is more general and not assuming homogeneity of media or constant sorption potential like other models.

$$q = q_{\max} \exp(-\beta \varepsilon^2) \quad (4)$$

where q_{\max} describes the capacity in a saturated state (mol/g), β is specific number (mol^2/kJ^2) associated with sorption energy. The Polanyi potential (ε) is calculated by Eq. 5.

$$\varepsilon = RT \ln \left(1 + \frac{1}{C_f} \right) \quad (5)$$

where R is gas constant (8.314 J/mol/K), and T is the absolute temperature (K).

In general, the Dubinin Radushkevich isotherm equation is frequently applied to determine the mean biosorption energy, which provides significant information about the chemical or physical character of the biosorption process [42]. Biosorption energy (E) is analyzed using Eq. 6.

$$E = \frac{1}{\sqrt{2B}} \quad (6)$$

Biosorption process follows the chemical ion-exchange when energy (E) shows between 8 and 16 kJ/mol. If E is more than 8 kJ/mol, it suggests the occurrence of physical activity of sorption.

5.2 Isotherm of Dye Biosorption on Dried Fungus

A study of isotherm equations determination on Remazol Golden Yellow 6 Color Removal by dried fungi of *Rhizopus* sp shows that the kinetics follow both the Freundlich and Langmuir isotherm mechanisms [57]. Furthermore, the constant of determination of Langmuir is more suitable rather than Freundlich. Aksu and Tezer

[3] conducted a study on the sorption of Remazol Black B dye using dried fungus *Rhizopus arrhizus*. The result suggests that the Freundlich isotherm pattern is more suitable for dye biosorption with varying concentrations and temperatures than the Langmuir pattern. However, the Langmuir pattern is also thought to be suitable for dye studies, given that the linear regression coefficient obtained is more than 0.95. Another study shows that the Freundlich model was found suitable for the sorption process of Everzol Black using *Rhizopus arrhizus* [30].

Calculation of biosorption energy in D-R isotherm of zinc ions results in a range of 9.81–11.16 kJ/mol using *C. utilis* and 10.15–12.33 kJ mol⁻¹ using *C. tropicalis*. It indicates that an ion-exchanging occurred chemically before the biosorption process [1].

6 Application of Dried Fungus in Textile Wastewater

The white rot fungi have a high potential for biosorption of contaminants like metals and dyes from wastewater and solutions. The only microorganisms capable of degrading wood components such as cellulose, lignin, and hemicellulose are white rot fungi.

Many studies (Table 1) have been carried out to see how ligninolytic fungi like *Phanerochaete chrysosporium* decolorize and degrade synthetic dyes [13], *Trametes versicolor* [4, 5], *Trametes trogii* [41], *Applatanum*, artist's bracket [47] and *Bjerkandera adusta* [10, 11]. In addition, fungi such as *Rhizopus* sp, *Rhizopus arrhizus* are also widely used for dye removal [5, 6, 8, 44, 57], *Saccharomyces cerevisiae* [7, 26], and *Aspergillus niger* [5]. Das et al. [23] reported removing the carcinogenic dye rhodamine B from wastewater using biomass from several fungi and yeasts. The biomass of *Rhizopus oryzae* MTCC 262 is the most effective of all the fungal species investigated [23].

Endophytic fungi can also remove the color of anthraquinone dyes. The high removal efficiency was shown more than 90% for Remazol Brilliant Blue R (RBBR) [48]. This proves that in addition to white rot fungi, endophytic fungi can also decolorize synthetic dyes and are potentially attractive for the removal of dye waste.

It was discovered that the flow rate and the concentration of dye in the inlet affect the sorption of each dye in the continuous application. The breakthrough curve rises as the flow rate rises, as did the breakpoint time and quantity of adsorbed dye, most likely due to insufficient dye liquid contact time in the column [6].

Initial concentration, pH, contact time, and biosorbent dosage are the most frequently modified parameters in the adsorption process. In general, the lower the pH, the better the color removal efficiency. However, Naghipour et al. [47] found that using artist's bracket fungi, they were able to remove 90% of methylene blue with a pH of 9 in the adsorption process. The increased absorption at lower pH values could be explained by the electrostatic interaction between negatively-charged dye anions and positively-charged cell surfaces.

Table 1 Studies on dyes removal using dried fungi

Kind of fungi	Kind of color	System	Color removal	Parameter of processes	References
<i>Applatanum</i> , Artist's bracket	Methylene blue	Batch	54.7–98.7% and 98.5–99.9%	pH 9, biosorbent dosage 2 g, temperature	[47]
<i>Bjerkandera adusta</i>	Artificial textile wastewater	Batch	53.55%	pH 4, size biosorbent 0.4 mm, biosorbent dosage 3 g, contact time 90 min	[11]
<i>Bjerkandera adusta</i>	Artificial textile wastewater	Batch	81.3%	pH 4, size biosorbent 0.4 mm, biosorbent dosage 3 gr, contact time 90 min	[10]
<i>Rhizopus sp</i>	Remazol Golden Yellow 6 Zat	Batch	70,922 mg/g biomass, 156,25 mg/g biomass and 243,902 mg/g biomass	pH 1.75, concentration 100 mg/L, biosorbent dosage 0.5 g	[57]
<i>Phanerocheate chrysosporium</i>	Reactive Blue 4 dye	Batch, continuous	211.6 mg/g and at a flow rate of 20 mL/h	pH 3, capacity of biosorbent 156.9–81.1 mg/g, biomass 211.6 mg, temperature 4, 25, 37 °C, initial concentration of 600 mg/L	[13]
<i>Candida sp.</i> , <i>C. tropicalis</i> , <i>C. lipolytica</i>	Remazol Blue	Batch		pH 2, initial concentration of 400 mg/L	[7]
<i>C. utilis</i> , <i>C. quilliermendii</i>	Remazol Blue	Batch		pH 2, initial concentration of 300 mg/L	[7]
<i>Saccharomyces cerevisiae</i> , <i>Schizosaccharomyces pombe</i> , <i>Kluyveromyces marxianus</i> , and <i>C. membranefaciens</i>	Remazol Blue	Batch		pH 2, initial concentration of 200 mg/L	[7]

(continued)

Table 1 (continued)

Kind of fungi	Kind of color	System	Color removal	Parameter of processes	References
<i>Alternaria alternata</i> CMERI F6	Congo Red Dye (600 mg/L)	Batch	99.99%	pH, temperature, contact time	[17]
<i>Saccharomyces cerevisiae</i>	Astrazone Blue	Batch	70 mg/g dried fungi,	pH	[26]
<i>Penicillium restrictum</i>	Reactive Black 5 (RB)	Batch	142 mg/g biomass	pH 1, contact time 75 min, biosorbent dosage 20 mg and dye concentrations 200 mg/L and T 35 °C	[27]
<i>Trametes trogl</i>	Methyl orange (980 mg/L) and Xylidine (480 mg/L)	Batch, fluid	75 and 96%	Contact time 24 h	[41]
<i>Fomes fomentarius</i> and <i>Phellinus igniarius</i>	Methylene blue (MB) and rhodamine B (RB)	Batch, fluid		204.38–232.73 mg/g and 25.12–36.82 mg/g for MB and RB	[63]
<i>Penicillium oxalicum</i> SAR-3	Azo dyes Acid Red 183, Direct Blue 15, and Direct Red 75	Batch, fluid	95–100%	Contact time 120 h, at pH 7.0	[61]
<i>Rhizopus arrhizus</i>	Methylene Blue (MB) and sodium dodecylsulfate (SDS)	Batch	370.3 mg/g dye	pH 10	[8]
<i>Trametes versicolor</i>	Acid Blue	Batch	471.6 mg/g dye	pH 3, initial dye concentration 500 mg/L	[4]
<i>Rhizopus arrhizus</i> , <i>Trametes versicolor</i> , <i>Aspergillus niger</i>	Gryfalan Black RL metal-complex dye	Batch	666.7 mg/g dye	pH 1–2	[5]
<i>Rhizopus arrhizus</i>	Gemacion (Procion) Red H-E7B (GR), Gemazol Turquoise Blue-G (GTB), Gemactive (Reactive) Black HFGR (GB)	Continuous	1007.8 mg/g for GR dye, 823.8 mg/g for GTB dye and 635.7 mg/g for GB dye	pH, temperature	[6]

(continued)

Table 1 (continued)

Kind of fungi	Kind of color	System	Color removal	Parameter of processes	References
<i>Rhizopus arrhizus</i>	Reactive orange 16 dye	Batch	200 mg/g		[44]

7 Conclusion

It was discovered among microorganisms, that fungi can play an effective role in decolorizing the wastewater of the textile industries and can be used for a variety of reasons, including cost-effectiveness, ease of access, environmental compatibility, and a shorter duration than other methods. In the application of dried fungi, the adsorption process to decolorize dye is divided into biosorbent preparation (physical and chemical) and the adsorption process itself. The most significant factors influencing color removal are pH, initial concentration, contact time, and biosorbent dosage. The types of fungi that can be used for dye removal are not limited to white rot fungi but also other types, such as single-celled and endophytic, which also have great potential for dye removal.

The right biosorbent selection affects not only adsorption capacity but also regeneration, waste management, and overall maintenance costs. In some special waste situations, cheap biosorbents with adequate adsorption capacity, such as dried fungus, may prove to be more appropriate than other, more expensive sorbents, such as activated carbon.

References

1. Ahmad MF, Haydar S, Quraishi TA (2013) Enhancement of biosorption of zinc ions from aqueous solution by immobilized *Candida utilis* and *Candida tropicalis* cells. *Int Biodeterior Biodegradation* 83:119–128. <https://doi.org/10.1016/j.ibiod.2013.04.016>
2. Aksu Z (2005) Application of biosorption for the removal of organic pollutants: a review. *Process Biochem* 40:997–1026. <https://doi.org/10.1016/j.procbio.2004.04.008>
3. Aksu Z, Tezer S (2000) Equilibrium and kinetic modelling of biosorption of removal Black B by *Rhizopus arrhizus* in a batch system: effect of temperature. *Process Biochem* 36(5):431–439. [https://doi.org/10.1016/S0032-9592\(00\)00233-8](https://doi.org/10.1016/S0032-9592(00)00233-8)
4. Aksu Z, Tatlı I, Tunc O (2008) A comparative adsorption/biosorption study of Acid Blue 161: effect of temperature on equilibrium and kinetic parameters. *Chem Eng J* 142:23–39. <https://doi.org/10.1016/j.cej.2007.11.005>
5. Aksu Z, Karabayır G (2008) Comparison of biosorption properties of different kinds of fungi for the removal of Gryfalan Black RL metal-complex dye. *Biosource Technol* 99:7730–7741. <https://doi.org/10.1016/j.biortech.2008.01.056>
6. Aksu Z, Çağatay ŞŞ, Gönen F (2007) Continuous fixed bed biosorption of reactive dyes by dried *Rhizopus arrhizus*: determination of column capacity. *J Hazard Mater* 143(1–2):362–371. <https://doi.org/10.1016/j.jhazmat.2006.09.039>
7. Aksu Z, Donmez G (2003) A comparative study on the biosorption characteristics of some yeasts for Remazol Blue reactive dye. *Chemosphere* 50:1075–1083. [https://doi.org/10.1016/S0045-6535\(02\)00623-9](https://doi.org/10.1016/S0045-6535(02)00623-9)
8. Aksu Z, Ertuğrul S, Dönmez G (2010) Methylene Blue biosorption by *Rhizopus arrhizus*: effect of SDS (sodium dodecylsulfate) surfactant on biosorption properties. *Chem Eng J* 158(3):474–481. <https://doi.org/10.1016/j.cej.2010.01.029>
9. Asma D, Kahraman S, Cing S, Yesilada O (2006) Adsorptive removal of textile dyes from aqueous solutions by dead fungal biomass. *J Basic Microbiol* 46(1):3–9. <https://doi.org/10.1002/jobm.200510602>
10. Astuti AD, Muda K (2020) Effect of pretreatment of biosorbent in biosorption: a comparative study. *J Environ Treat Tech* 8(3):894–899

11. Astuti AD, Muda K (2018) Biosorption process of synthetic textile waste-water using *Bjerkandera agusta* via response surface methodology (RSM). E3S Web Conf 68. <https://doi.org/10.1051/e3sconf/20186804020>
12. Ayele A, Haile S, Alemu D, Kamaraj M (2021) Comparative utilization of dead and live fungal biomass for the removal of heavy metal: a concise review. Hindawi Sci World J Article ID 5588111:10 p. <https://doi.org/10.1155/2021/5588111>
13. Bayramoğlu G, Çelik G, Arica MY (2006) Biosorption of Reactive Blue 4 dye by native and treated fungus *Phanerocheate chrysosporium*: batch and continuous flow system studies. J Hazard Mater 137:1689–1697. <https://doi.org/10.1016/j.jhazmat.2006.05.005>
14. Bayramoğlu G, Arica MY (2007) Biosorption of benzidine based textile dyes “Direct Blue 1 and Direct Red 128” using native and heat-treated biomass of *Trametes versicolor*. J Hazard Mater 143:135–143. <https://doi.org/10.1016/j.jhazmat.2006.09.002>
15. Boudechiche N, Mokaddem H, Sadaoui Z, Trari M (2016) Biosorption of cationic dye from aqueous solutions onto lignocellulosic biomass (*Luffa cylindrica*): characterization, equilibrium, kinetic and thermodynamic studies. Int J Ind Chem 7:167–180. <https://doi.org/10.1007/s40090-015-0066-4>
16. Brouers F, Al-Musawi TJ (2015) On the optimal use of isotherm models for the characterization of biosorption of lead onto algae. J Mol Liq 212:46–51. <https://doi.org/10.1016/j.molliq.2015.08.054>
17. Chakraborty S, Basak B, Dutta S, Bhunia B, Dey A (2013) Decolorization and biodegradation of congo red dye by a novel white rot fungus *Alternaria alternata* CMERI F6. Biores Technol 147:662–666. <https://doi.org/10.1016/j.biortech.2013.08.117>
18. Chang JS, Kuo TS, Chao YP, Ho JY, Lin PJ (2000) Azo dye decolorization with a mutant *Escherichia coli* strain. Biotechnol Lett 22(9):807–812. <https://doi.org/10.1023/A:1005624707777>
19. Cheng J, Yin W, Chang Z, Lundholm N, Jiang Z (2017) Biosorption capacity and kinetics of cadmium(II) on live and dead *Chlorella vulgaris*. J Appl Phycol 29(1):211–221. <https://doi.org/10.1007/s10811-016-0916-2>
20. Chu HC, Chen KM (2002) Reuse of activated sludge biomass: I. Removal of basic dyes from wastewater by biomass. Process Biochem 37(6):595–600. [https://doi.org/10.1016/S0032-9592\(01\)00234-5](https://doi.org/10.1016/S0032-9592(01)00234-5)
21. Chu HC, Chen KM (2002) Reuse of activated sludge biomass: II. The rate processes for the adsorption of basic dyes on biomass. Process Biochem 37(10):1129–1134. [https://doi.org/10.1016/S0032-9592\(01\)00326-0](https://doi.org/10.1016/S0032-9592(01)00326-0)
22. Cooney DO (1999) Adsorption design for wastewater treatment. Lewis Publisher, Boca Raton
23. Das SK, Bowal J, Das AR, Guha AK (2006) Adsorption behavior of Rhodamine B on *Rhizopus oryzae* biomass. Langmuir 22(1):7265–7272. <https://doi.org/10.1016/j.jhazmat.2009.06.156>
24. Dewi NK, Mubarak I, Yuniastuti A (2019) Biosorption of heavy metal pollution by *Enterobacter agglomerans*. Biosaintifika J Biol Biol Educ 11(2):289–295. <https://doi.org/10.15294/biosaintifika.v11i2.20471>
25. Eckenfelder WW (2000) Industrial water pollution control. McGraw-Hill series in pollution, vol 138, pp 358–367
26. Farah JY, El-gendy NS, Farahat LA (2007) Biosorption of Astrazone Blue basic dye from an aqueous solution using dried biomass of Baker’s yeast. J Hazard Mater 148:402–408. <https://doi.org/10.1016/j.jhazmat.2007.02.053>
27. Filik C, Kiran I, Ilhan S (2007) Biosorption of Reactive Black 5 dye by *Penicillium restrictum*: the kinetic study. J Hazard Mater 143:335–340. <https://doi.org/10.1016/j.jhazmat.2006.09.028>
28. Fu Y, Viraraghavan T (2001) Fungal decolorization of dye wastewaters: a review. Biores Technol 79:251–262. [https://doi.org/10.1016/S0960-8524\(01\)00028-1](https://doi.org/10.1016/S0960-8524(01)00028-1)
29. Gallagher KA, Healy MG, Allen SJ (1997) Biosorption of synthetic dye and metal ions from aqueous effluents using fungal biomass. Stud Environ Sci 66(C):27–50. [https://doi.org/10.1016/S0166-1116\(97\)80033-7](https://doi.org/10.1016/S0166-1116(97)80033-7)
30. Gül ÜD, Silah H (2014) Comparison of color removal from reactive dye contaminated water by systems containing fungal biosorbent, active carbon and their mixture. Water Sci Technol 70(7):1168–1175. <https://doi.org/10.2166/wst.2014.339>

31. Hall KR, Eagleton LC, Acrivos A, Vermuelen T (1966) Pore and solid-diffusion kinetics in fixed-bed adsorption under constant-pattern conditions. I & EC Fundam 5(2):212–233. <https://doi.org/10.1021/i160018a011>
32. Holkar CR, Jadhav AJ, Pinjari DV, Mahamuni NM, Pandit AB (2016) A critical review on textile wastewater treatments: possible approaches. J Environ Manag 182:351–366. <https://doi.org/10.1016/j.jenvman.2016.07.090>
33. Huang B, Zhao J, Geng Y, Tian Y, Jiang P (2017) Energy-related GHG emissions of the textile industry in China. Resour Conserv Recycl 119:69–77. <https://doi.org/10.1016/j.resconrec.2016.06.013>
34. Iftekhhar S, Ramasamy DL, Srivastava V, Asif MB, Sillanpää M (2021) Understanding the factors affecting the adsorption of Lanthanum using different adsorbents: a critical review. Chemosphere 204:413–430. <https://doi.org/10.1016/j.chemosphere.2018.04.053>
35. Javanbakht V, Alavi SA, Zilouei H (2014) Mechanisms of heavy metal removal using microorganisms as biosorbent. Water Sci Technol 69(9):1775–1787. <https://doi.org/10.2166/wst.2013.718>
36. Kabbout R, Taha S (2014) Biodecolorization of textile dye effluent by biosorption on fungal biomass materials. Phys Procedia 55:437–444. <https://doi.org/10.1016/j.phpro.2014.07.063>
37. Karimi S, Yaraki MT, Karri RR (2019) A comprehensive review of the adsorption mechanisms and factors influencing the adsorption process from the perspective of bioethanol dehydration. Renew Sustain Energy Rev 107:535–553. <https://doi.org/10.1016/j.rser.2019.03.025>
38. Kiran S, Huma T, Jalal F, Farooq T, Hameed A, Gulzar T, Bashir A, Rahmat M, Rahmat R, Rafique MA (2019) Lignin degrading system of *Phanerochaete chrysosporium* and its exploitation for degradation of synthetic dyes wastewater. Pol J Environ Stud 28(3):1749–1757. <https://doi.org/10.15244/pjoes/89575>
39. Kocaman S (2020) Synthesis and cationic dye biosorption properties of a novel low-cost adsorbent: coconut waste modified with acrylic and polyacrylic acids. Int J Phytorem 22(5):551–566. <https://doi.org/10.1080/15226514.2020.1741509>
40. Kumar KV, Gadipelli S, Wood B, Ramisetty KA, Stewart AA, Howard CA, Brett DJL, Rodriguez-Reinoso F (2019) Characterization of the adsorption site energies and heterogeneous surfaces of porous materials. J Mater Chem A 17:10104–10137. <https://doi.org/10.1039/C9TA00287A>
41. Levin L, Grassi E, Carballo R (2012) Efficient azoic dye degradation by *Trametes trogii* and a novel strategy to evaluate products released. Int Biodeterior Biodegradation 75:214–222. <https://doi.org/10.1016/j.ibiod.2012.10.005>
42. Liu Y, Liu YJ (2008) Biosorption isotherm, kinetics and thermodynamics. Sep Purif Technol 61(3):229–242. <https://doi.org/10.1016/j.seppur.2007.10.002>
43. Mahmoud MS (2016) Decolorization of certain reactive dye from aqueous solution using Baker's yeast (*Saccharomyces cerevisiae*) strain. Hous Build Natl Res Center J 12(1):88–98. <https://doi.org/10.1016/j.hbrcj.2014.07.005>
44. Mahony TO, Guibal E, Tobin JM (2002) Reactive dye biosorption by *Rhizopus arrhizus* biomass. Enzyme Microb Technol 31:456–463. [https://doi.org/10.1016/S0141-0229\(02\)00110-2](https://doi.org/10.1016/S0141-0229(02)00110-2)
45. Metcalf, Eddy (2004) Wastewater engineering treatment disposal, reuse, 3rd edn. McGraw-Hill Inc, Singapore
47. Naghipour D, Taghavi K, Moslemzadeh M (2016) Removal of methylene blue from aqueous solution by Artist's Bracket fungi: kinetic and equilibrium studies. Water Sci Technol 73(11):2832–2840. <https://doi.org/10.2166/wst.2016.147>
48. Ngieng NS, Zulkharnain A, Roslan HA, Husaini A (2013) Decolourisation of synthetic dyes by endophytic fungal flora isolated from senduduk plant (*Melastoma malabathricum*). ISRN Biotechnol 2013:1–7. <https://doi.org/10.5402/2013/260730>
49. Nimkar U (2018) A solution to the textile industry in a developing world. Green Sustain Chem 9:13–17. <https://doi.org/10.1016/j.cogsc.2017.11.002>
50. Notodarmojo S (2005) Pencemaran Tanah dan Air Tanah. Institute of Technology Bandung, Bandung

51. Patel H (2018) Charcoal as an adsorbent for textile wastewater treatment. *Sep Sci Technol* 53(17):2797–2812. <https://doi.org/10.1080/01496395.2018.1473880>
52. Pratiwi RR, Elystia S, Muria SR (2017) Biosorpsi Kromium (Cr) pada Limbah Cair Industri Elektroplating menggunakan Biomassa Ragi Roti (*Saccharomyces cerevisiae*). *Jom FTEKNIK* 4(1):1–7
53. Purwiantono F, Lestari P, Widodo W, Marlina M, Aprilia N (2017) Adsorption isotherm studies of Rhodamine B on citrus sinesis peel. *ICJR Indones J Chem Res* 2(1–2):47–53. <https://doi.org/10.20885/ijcr.vol2.iss1.art6>
54. Ratnawati E, Ermawati R, Naimah S (2010) Teknologi Biosorpsi oleh Mikroorganisme, Solusi Alternatif untuk Mengurangi Pencemaran Logam Berat. *Jurnal Kimia dan Kemasan* 32(1):34–40. <https://doi.org/10.24817/jkk.v32i1.2739>
55. Rehman K, Shahzad T, Sahar A, Hussain S, Mahmood F, Siddique MH, Siddique MA, Rashid MI (2018) Effect of Reactive Black 5 azo dye on soil processes related to C and N cycling. *PeerJ* 6:e4802. <https://doi.org/10.7717/peerj.4802>
56. Ririheha SAJ, Astuti AD, Fachrul MF, Silalahi MDS, Hadisoebroto R, Rinanti A (2018) Biosorption of heavy metal copper (Cu²⁺) by *Saccharomyces cerevisiae*. *IOP Conf Ser: Earth Environ Sci* 106(1). <https://doi.org/10.1088/1755-1315/106/1/012090>
57. Rusmaya D, Nugroho FD, Purwanti TA (2012) Penentuan Tipe Isoterm Sorpsi Zat Warna Remazol Golden Yellow 6 Menggunakan Jamur Mati *Rhizopus Sp* Hasil Isolasi Dari Tempe. *Infomatek* 14(1):39–50. <https://doi.org/10.23969/infomatek.v14i1.3950>
58. Russo ME, Di Natale F, Prigione V, Tigrini V, Marzocchella A, Varese GC (2010) Adsorption of acid dyes on fungal biomass: equilibrium and kinetics characterization. *Chem Eng J* 162:537–545. <https://doi.org/10.1016/j.cej.2010.05.058>
59. Ryczyńska-Tkaczyk K, Kornilowicz-Kowalska T (2016) Biosorption optimization and equilibrium isotherm of industrial dye compounds in novel strains of microscopic fungi. *Int J Environ Sci Technol* 13:2837–2846. <https://doi.org/10.1007/s13762-016-1111-3>
60. Salleh MAM, Mahmoud DK, Karim WAWA, Idris A (2011) Cationic and anionic dye adsorption by agricultural solid wastes: a comprehensive review. *Desalination* 280(1–3):1–13. <https://doi.org/10.1016/j.desal.2011.07.019>
61. Saroj S, Kumar K, Pareek N, Prasad R, Singh RP (2014) Biodegradation of azo dyes Acid Red 183, Direct Blue 15 and Direct Red 75 by the isolate *Penicillium oxalicum* SAR-3. *Chemosphere* 107:240–248. <https://doi.org/10.1016/j.chemosphere.2013.12.049>
62. Silva CEDF, Gonçalves AHdS, Abud AKdS (2016) Treatment of textile industry effluents using orange waste: a proposal to reduce color and chemical oxygen demand. *Water Sci Technol* 74(4):994–1004. <https://doi.org/10.2166/wst.2016.298>
63. Singh N, Mittal AK, Cornel P, Rother E (2006) Biosorption of dyes using dead macro fungi: effect of dye structure, ionic strength and pH. *Bioresource Technol* 97:512–521. <https://doi.org/10.1016/j.biortech.2005.02.045>
64. Srinivasan A, Viraraghavan T (2010) Decolorization of dye wastewaters by biosorbents: a review. *J Environ Manag* 91(10):1915–1929. <https://doi.org/10.1016/j.jenvman.2010.05.003>
65. Takeji M, Shaikh T, Mane N, Majumder DR (2014) Bioremediation of xenobiotics: use of dead fungal biomass as adsorbent. *IJRET: Int J Res Eng Technol* 3(1):565–570
66. Telke A, Kalyani D, Jadhav J, Govindwar S (2008) Kinetics and mechanism of Reactive Red 141 degradation by a bacterial isolate *Rhizobium radiobacter* MTCC 8161. *Acta Chim Slov* 55(2):320–329
67. Tigrini V, Prigione V, Giansanti P, Mangiavillano A, Pannocchia A, Varese GC (2010) Fungal biosorption, an innovative treatment for the decolourisation and detoxification of textile effluents. *Water* 2:550–565. <https://doi.org/10.3390/w2030550>
68. Tochwang L, Mishra VK, Passari AK, Singh BP (2019) Endophytic fungi: role in dye decolorization, pp 1–15. https://doi.org/10.1007/978-3-030-03589-1_1
69. Weber WJ, Digiano FA (1995) *Process dynamics in environmental system*. Wiley, New York
70. Weber TW, Chackravorti RK (1974) Pore and solid diffusion models for fixed bed adsorbents. *Amer Inst Chem Eng J* 20(2):228–238. <https://doi.org/10.1002/aic.690200204>

46. Yakup M, Bayramoğlu G (2007) Biosorption of Reactive Red-120 dye from aqueous solution by native and modified fungus biomass preparations of *Lentinus sajorçaju*. J Hazard Mater 149(2):499–507. <https://doi.org/10.1016/j.jhazmat.2007.04.021>
72. Yaseen DA, Scholz M (2019) Textile dye wastewater characteristics and constituents of synthetic effluents: a critical review. Int J Environ Sci Technol 16:1193–1226. <https://doi.org/10.1007/s13762-018-2130-z>
73. Yesilada O, Birhanli E, Geckil H (2018) Bioremediation and decolorization of textile dyes by white rot fungi and laccase enzymes. https://doi.org/10.1007/978-3-319-77386-5_5
71. Zhou JL, Banks CJ (1993) Mechanism of humic acid color removal from natural waters by fungal biomass biosorption. Chemosphere 27:607–620. [https://doi.org/10.1016/0045-6535\(93\)90096-N](https://doi.org/10.1016/0045-6535(93)90096-N)

Application of Waste Utilization in Textile Dye Removal



Arti Malviya and Dipika Jaspal

1 Introduction

Industrial sectors like textile, plastics, printing, tanning, rubber etc. widely use dyes to fabricate colored materials. The wastewater produced from these industrial units is continuously discharged into water bodies thereby deteriorating the quality of the water streams. The polluted natural water source becomes inefficient to facilitate aquatic life, wherein acts as light absorbers and interferes with the photosynthetic activity of the aquatic plants. The persistent nature of the dyes poses the danger of allergic impact, skin diseases, mutation and even cancer depending upon the exposure to the dye containing wastewater [3]. Color removal thus becomes a matter of acute concern environmentally, aesthetically and from the health perspective. The scientific community has always shouldered the responsibility to contribute to the wastewater treatment methods. In this regard, efforts are constantly being made to develop eco-friendly green methods for eradicating the dyes from wastewaters.

Among the treatment technologies, methods like Fenton process, photo-catalytic and electrochemical combined treatments, photo-catalytic degradation using UV/TiO₂, biodegradation, electrochemical degradation, chemical coagulation, ozonation, oxidation, chemical precipitation, ion-exchange, reverse osmosis and ultra-filtration have been explored. But adsorption technique is prominently employed due to its low cost, regeneration possibility, simple equipment and sludge

A. Malviya

Department of Engineering Chemistry, Lakshmi Narain College of Technology, Bhopal, Madhya Pradesh 462021, India

D. Jaspal (✉)

Department of Applied Science, Symbiosis Institute of Technology (SIT), Symbiosis International (Deemed University) (SIU), Lavale, Pune, Maharashtra 412115, India

e-mail: dipikaj@sitpune.edu.in

free operation [9]. In order to make adsorption technique more suitable and efficient, researchers have focused their hunt on agricultural waste materials and their potentiality.

A number of agricultural waste materials have been considered for the exclusion of different types of dyes (direct, reactive dyes, basic dyes, dispersive dyes) from aqueous solutions at different operating conditions till date. The chapter focuses on different types of agricultural wastes, their utilization routes and dye sequestration ability. Further in the chapter, the challenges in the utilization of agro-waste have been unfolded with an attainable solution.

2 Types of Agricultural Waste

Agricultural waste refers to the residue obtained from agricultural products either in raw condition or after their processing. This includes fruits, vegetable plants, meat, poultry, livestock, aquaculture, dairy products, agro-industrial products etc. (Fig. 1). The nature of the agricultural product, activity or processing decides whether the waste obtained will be of solid, liquid or semisolid nature. Cultivation activities are

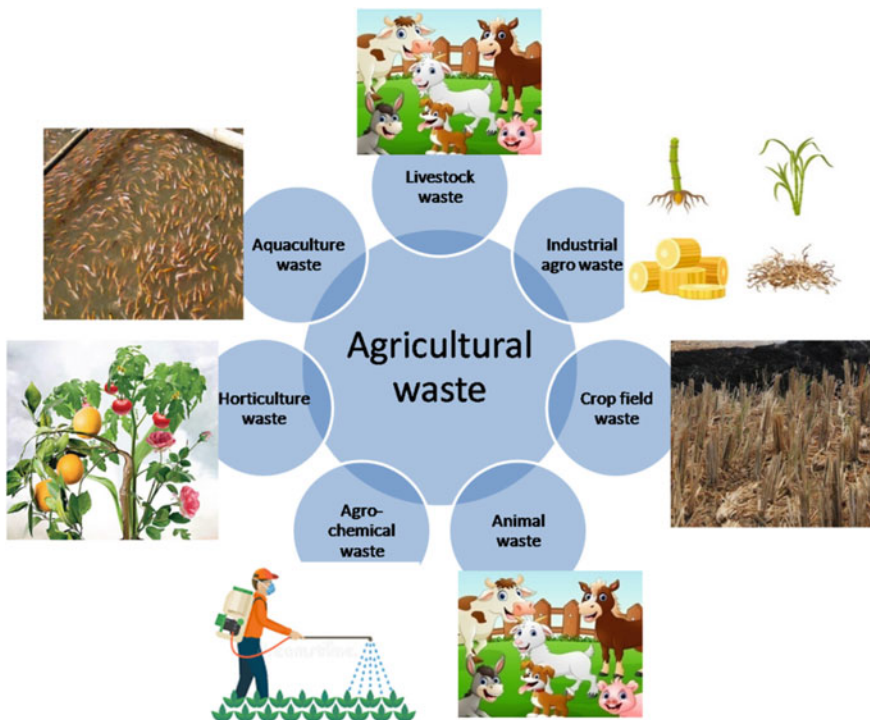


Fig. 1 Sources of agricultural waste

one of the major contributors to agricultural waste. According to Plant Protection Department, approximately 2% of the chemicals used for increasing fertility or as pesticides in the field remain in their packaging after their use. The packaging, containers or bottles add to the waste generated from the crop fields [62].

Waste from livestock includes manure, animal carcasses, organic materials and wastewater (75–79%). The peels of fruits/vegetables, hoofs and bones generated from the processing of the agricultural products/livestock adds to the waste production. Several wastes are generated from the crop fields like husks, crop residues, saw dust, weeds and pruning, stocks, hull, kernels, grass/plant cuttings etc. Agricultural fields contribute majorly to the waste generation due to different kinds of activities performed from land clearing till harvest. In the case of aquaculture, the type and amount of feed given decides the waste output. Furthermore, agro-based industrial residue significantly contributes to the agricultural load [12]. The solid waste generated is dumped indiscriminately or burnt resulting in contamination of soil and air pollution. The improper handling alters the climatic patterns as well which indirectly affects the food production. The untreated waste can generate greenhouse gases and have a negative impact on the fertility of the soil. These if discarded to the environment contribute only in increasing the organic load for the natural decomposers [45].

Research is being carried out to explore the potential of these waste substances and their utilization for several purposes for the benefit of mankind as well as for the sustainable environment.

3 Waste Utilization

Wastes of agricultural origin can be processed in a variety of ways in order to diminish their negative impact on the environment and human health (Fig. 2). They can either be rendered ineffective or stored inert or disposed off in an efficient manner. Waste utilization techniques result in the reduction of greenhouse gas emission, create jobs in the relevant field and help the production of non-conventional fuels. Some of the waste utilization technologies explored are as follows:

3.1 Combustion

This is one of the oldest methods of reducing biomass. On-site burning of residues decreases the soil carbon content and dries the soil [48]. Agricultural waste is usually burnt for heating, cooking, secondary fuel production, steam generation and for thermal applications. The greater the proper designing of the method utilized, the greater is the energy output obtained by the process. Improperly managed combustion process adds to greenhouse gases and increases air pollution [55].

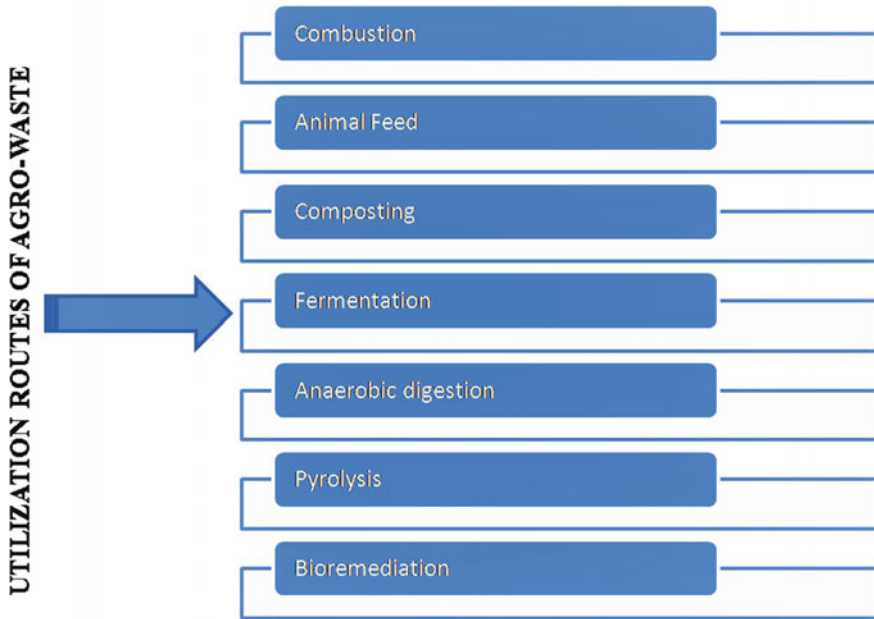


Fig. 2 Utilization of agricultural waste

3.2 *Animal Feed*

Fibrous crop waste including straw and stover is usually used as feed for the domestic animals. The residues of maize, sugar cane, sorghum, soyabean, wheat and vegetables are usually involved in animal feeding. This adds to the traditional way of increasing the livestock production and is a key livelihood resource for farmers.

3.3 *Composting*

One of the very efficient and eco-friendly waste utilization routes is the conversion of organic agricultural waste into manure. The formed manure greatly amends the soil characteristics, increases soil fertility, ion exchange capacity, water absorbing capacity and microbial population. But, the method is associated with large energy and cost input, transportation load, storage issues and odor related problems encountered during the conversion process.

3.4 Pyrolysis

It is a technique of anaerobic thermal decomposition of agricultural waste at elevated temperatures and in inert conditions. This technique generates bio-oil, char, fuel alcohol, and energy rich gaseous fuel. But the technique demands high energy and cost input and has the possible drawback of generating toxic air [36].

3.5 Bio-remediation

The newer approach for utilization of agricultural waste is by employing them for the removal of heavy metals [21, 51], pesticides [20], organics [11, 47] and colorants [68] and microbes [8]. Waste utilization for bioremediation offers the advantage of being cost effective and easy availability. The contaminants can be removed based on ion exchange, complexation process, adsorption or absorption or by precipitation.

4 Agricultural Waste for Dye Removal

4.1 Dyes and Their Toxicity

A dye is a coloring substance employed for imparting color or altering the color of different substances. Dyes are characterized by the presence of chromophores and auxochromes.

Indiscriminate and unplanned discharge of the effluent produced from the textile industries containing dyes alters the color, smell and taste, encourages chemisorptions and impairs biological and chemical characteristics of water bodies. The azo group containing dyes are difficult to get rid of due to strong bonding between nitrogen atoms. These dyes are found to drastically affect the soil profile and water quality and are mutagenic [27, 41], as observed by Khamparia et al. [32]. Nylon clothing initiates allergic reactions due to the dye, employed during its manufacture [35]. Various anionic dyes used in textiles pollute the water bodies and are substantially responsible for causing mutations in living systems. They alter the ecological balance and disturb the self-purification capacity of the water bodies [31, 13, 57]. Reactive dyes are found to be responsible agents in causing dermatitis and skin disorders [22]. Disperse dyes initiate sensitization of the skin and can cause allergic contact dermatitis [38], and tend to bio-accumulate in alga and higher plants [28]. Table 1 represents the different categories of dyes along with their toxicity.

Treatment of textile effluent thus becomes crucial and agricultural wastes act as promising substances for addressing the problem.

Table 1 Characterization of Dyes

Types of dyes	Category	Textile Substrate	Properties	Toxicity	Example	References
Basic dye	Cationic	Polyesters, jute, acrylics, linen, hemp	Water soluble, salts of organic bases, Soluble in alcohol, average to good fastness	Carcinogenic, eye damage/eye irritation, toxic to aquatic life with long lasting effects	Basic yellow 37	[35]
Acid dye	Anionic	Nylons, wool, silk	Water soluble, carboxylic or sulphuric acid salts, poor wash fastness	Carcinogenic, health hazards and ecological disorders	Acid blue 45, acid yellow 127	[31, 57]
Direct dye	Anionic	Cotton, protein fiber and cellulosic fabric	Water soluble, cheap, poor wet fastness	Carcinogenic	Direct red 216, direct blue 18	[46]
Reactive dye	Anionic	Cotton	Water soluble, halogen containing reactive group, powder as well as liquid	Dermatitis, asthma, eye damage/irritation	Reactive Red 195	[22]
Vat dye	Non ionic	Cellulosic fabric	Water insoluble, presence of keto group, attaches in leuco form, excellent fastness, costly	Mutagenic	Quinonic dye	[1, 60]
Disperse dye	Non ionic	Polyesters	Water insoluble, substituted azo, anthraquinone, or diphenylamine compound, low molecular weight, physically trapped in fibers	Allergenic, skin irritant carcinogenic	Disperse Red 60	[28, 38]

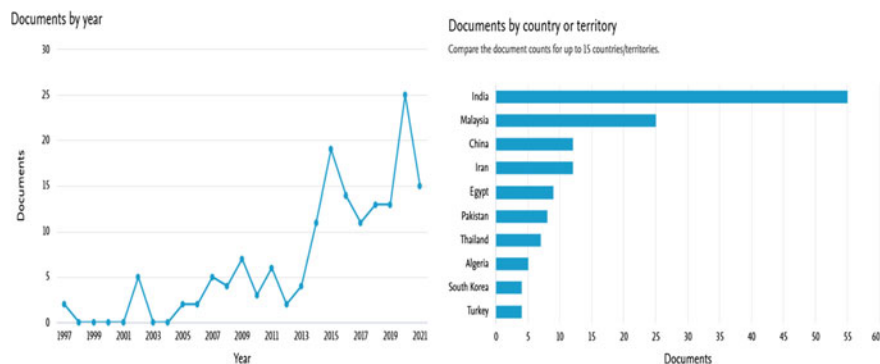


Fig. 3 Reported analytics on agro-waste as adsorbent for dye removal till date

4.2 Agricultural Waste for Textile Dye Removal

4.2.1 Dye Sequestration Using Different Adsorbents

The abundance, cost effectiveness and renewability of agro-waste have enabled them to behave as excellent materials for confiscation of the dyes from aqueous media [58].

Substantial research based on the harnessing of the potential of agro-waste for dye elimination has been carried out worldwide. Figure 3 depicts the number of investigations reported year wise, as well as country wise. It undoubtedly suggests a massive perspective provided by the biomass material for efficient environmental remediation which has been investigated by researchers worldwide.

Agricultural byproducts usually have no economic value unless they are valorized. The process of carbonization and physical or chemical activation is executed to develop activated carbon from agricultural waste. The conversion process proves to be economical, reduces the cost of waste disposal and shows superiority over conventional activated adsorbents. During the physical carbonization process, a non-porous material called char is obtained at a temperature of 1000 °C.

Further activation of char in presence of oxidizing gases occurs at about 900 °C which generates a highly porous structure having excellent efficiency to remove dyes. On the other hand chemical activation involves infusion with chemicals like zinc chloride, potash, caustic soda and phosphoric acid followed by heating. Chemical activation is much more favorable for developing the adsorbent as it is a low temperature single step process and the end product is greatly porous for efficient removal of dye from waste water [23].

Better adsorption capacities were achieved by modifying the agricultural waste as the process enhanced the active adsorption sites and also the porosity. The increase in the surface area along with the generation of new functional groups also contributes to the elimination enhancement. The investigations include the effect of operational parameters like contact time, pH and temperature to understand the operative mechanism in dye sequestration by agricultural biomass.

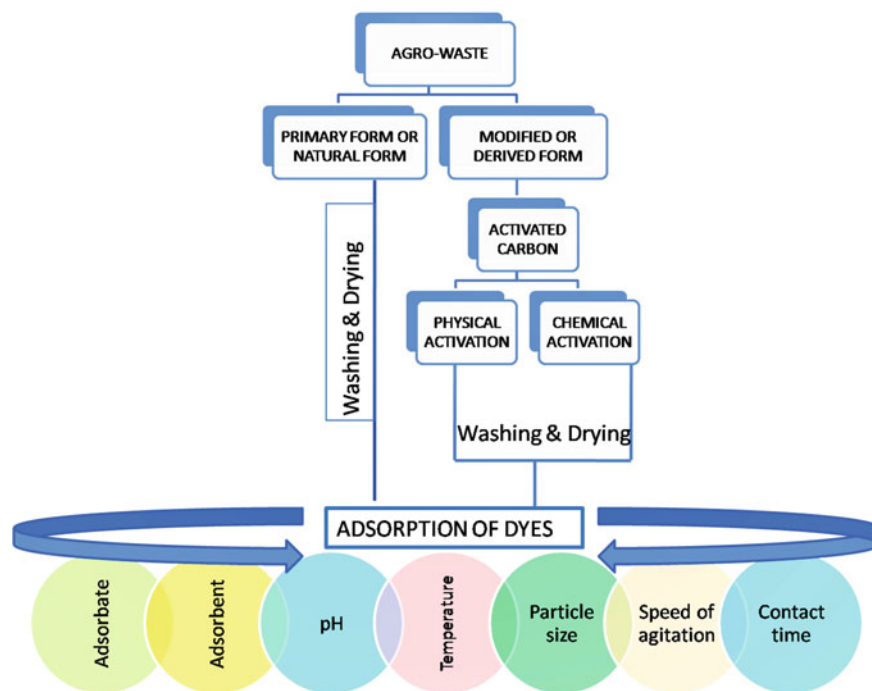


Fig. 4 Procedure of eradicating dye using agro-waste

The following figure illustrates the complete procedure involved in the study (Fig. 4).

Although a number of agricultural wastes are available as adsorbents, the selection of a suitable material is governed by its availability, cost and chemical composition (Table 2).

Lignin

The agro-industrial waste comprising of lignin has been employed by a number of researchers for the removal of textile dye either in its raw or modified form. Lignin is polymeric aromatic with alkyl phenols and three dimensional structures. Lignin is the chief structural component of the plant. The elimination and resurgence of cationic dyes like cationic red GTL, turquoise GB and cationic yellow X-5GL has been carried out by Liu and Hang [37] wherein endothermic adsorption has been reported. Synthetic dye, congo red elimination (71.8%) was achieved using waste wood biomass of Euroamerican poplar, and biosorption capacity was obtained as 3.3 mg g^{-1} . The Langmuir model fitted well with the biosorption data, and kinetics data confirmed pseudo second-order kinetics [63].

Table 2 Agricultural wastes for textile dye removal

Type of waste	Type of dye eliminated	References
Garlic peel, jack fruit peel, oil plant fiber and pineapple stem	Basic dyes	[23, 24]
Groundnut shell	Basic dyes	[39]
Cauliflower leaf powder	Basic dyes	[4]
Banana empty fruit bunch, Delonixregia fruit pod	Basic dyes	[64]
Rice hull	Azo dye	[18]
Sugarcane bagasse, rice straw, cotton stalk, and corn stalk	Reactive Dye	[17]
Coir pith	Reactive dye	[54, 56]
Rice husks	Basic dyes, synthetic dyes	[25, 50]
Tea waste	Basic dyes	[19]
Neem saw dust	Triarylmethane dye	[33]
Guava leaf waste	Thiazine dye	[49]
Jute waste	Basic dyes	[6],
Wheat straw	Anionic dye	[69]
Barley husk	Azo dye	[26]
Citrus waste	Reactive azo dye	[5, 53]
De-oiled soya	Azo dye, triarylmethane dyes	[41]
Saw dust	Basic dyes	[13]
Papaya seed	Cationic dye	[30]
Cotton hull, Sesame hull	Anionic dye	[66]

Sugarcane Bagasse

Pressed stalks from sugarcane are known as Bagasse. About 43% of the global production of waste sugar cane bagasse has been reported in Brazil. Most of the bagasse is used as fuel, as raw material for paper and fiberboard. The excess of bagasse, stored in the open air on incineration gives off soot and pollutes the air. Thus it is thoughtful to utilize it for environmental remediation. It is enriched with various elements like nitrogen, sodium, aluminum, calcium and magnesium which act as activators during the activation process of the adsorbent. Researchers have harnessed sugar cane agro-waste for sequestration of reactive dyes remazol black, blue and brilliant red [9].

Rice Husk

Rice husk is an agro industrial waste, and about 96% of it is produced in developing nations. It is the outer hard shielding jacket (20–25% of its weight) surrounding the

paddy grain and is obtained from the paddy during rice milling. This material has proved to be alternative and cheaper material in water management than commercially available activated carbon. Silica (15–20%) and carbon (30–50%) present in the rice husk imparts it the characteristic to adsorb dyes [25]. The operating variables investigated were contact time, pH, temperature, initial dye concentration etc. The monolayer adsorption capacity was obtained to be 40.5 mg/g at 25 °C. The adsorption process was established to be controlled by external mass transfer and intraparticle diffusion [50]. The authors suggested that the spent adsorbent can be disposed of by dewatering and drying and flaming with simultaneous recovery of the heat liberated. Dyes like acid violet 54, acid violet 17, acid blue, acid violet and acid red etc. were efficiently eradicated using rice husk as adsorbent.

Similarly, a Rice hull based adsorbent was investigated for the adsorptive removal of EBT (Eriochrome Black T) from an aqueous solution. The optimum conditions were obtained as 95 mg/L dye concentration, 2 g adsorbent dose and pH as 2, using Box–Behnken design. Pore diffusion was the limiting step in the adsorption process [18].

Groundnut Shell

Groundnut shell was employed by the researcher for its adsorptive characteristics of malachite green dye. Groundnut shell is carbonaceous and fibrous material having fuel value. But its disposal is of concern to the environmentalists. Thus, it is employed as an adsorbent in its modified form using zinc chloride by the researchers. Fibrous solid waste of groundnut shell was investigated for malachite green elimination and about 95% removal efficiency was observed. The simulation studies about the effect of temperature, pH, and contact time were carried out. Investigators reported 94.5% percent removal of dye in 30 min equilibrium time at an adsorbent dose of 0.5 g/L. BET equation was used to determine maximum adsorptive ability [39].

Saw Dust

Among the various agro-based adsorbents, saw dust is the most appealing material for decontamination. It has lignocellulose and hemicellulose for binding with colorants. Usually, the process of adsorption involves ion exchange, complex formation and hydrogen bonding. Various variables like temperature, concentration, pH and contact time were studied by the investigators to understand the adsorption profile of the textile dyes. The obtained data were analyzed using Langmuir and Freundlich isotherms and the best fit was observed with the Langmuir isotherm [13].

Banana Peel

Another investigation reported the elimination of methylene blue dye using banana empty fruit bunch and *Delonix regia* fruit pod carbonized at 450 °C and 400 °C respectively. The presence of phosphoric acid enhanced the reduction of the color [64]. The stalks of the banana consisted of cellulosic and lignin which have strong chemical adsorption capacity for cationic species like metal ions or organic bases.

Other Agro Wastes

Basic dyes like malachite green and methylene blue have been eradicated from the textile wastewaters by a number of researchers. Hameed et al. in their research revealed that Garlic peel, jack fruit peel, oil plant fiber and pineapple stem showed large adsorption potential for removing the colorant [24].

The porous structure of the leaf biomass was explored by a number of researchers [39]. Leaf biomass with characteristic functional groups attracted the dye molecules thereby effectively eliminating it [29]. The cauliflower leaf powder was investigated for the removal of methylene blue with an adsorption capacity of 149.22 mg/g at room temperature [4].

Wong et al. proved the potential of coffee waste for eradicating the reactive black 5 and congo red dyes from textile wastewater. The adsorption was monolayer with chemisorption as the rate-controlling step [68]. Barley husk was employed by researchers to eradicate the azo dyes and proved to be efficient to remove color as well as chemical oxygen demand from textile wastewater [26].

Sesame and cotton seed hulls were used for adsorption of acid red 114 from wastewater. The optimum conditions obtained for the process were pH 3, adsorbent dose of 3 g/L and equilibrium time of 4 h. They reported a greater adsorption capacity of sesame seed hull than cotton seed hull [66].

One of the cationic dyes (methylene blue) was removed using papaya seeds where intraparticle diffusion was operative. The interaction between the dye and adsorbent obeyed pseudo second-order kinetics and monolayer adsorption capacity was found to be 555 mg/g [30].

A number of investigators have studied the utilization of coir pith, an agricultural solid state waste for the elimination of textile dyes like rhodamine B, acid violet and procion orange [54, 56]. Researchers are constantly working to develop inexpensive and effortlessly available agro-based adsorbents according to their physical and chemical characteristics.

The sorption characteristics of different adsorbents vary according to the conditions of temperature, pH, agitation speed, other operative factors and experimental conditions. The comparison of adsorption capacities of the materials is thus difficult to interpret. However, studies reveal that nonconventional agro-based adsorbents are readily available, have a high capacity and good kinetics and thus act as efficient sequestering agents (Table 3).

Table 3 Reported absorption capacities and thermodynamic parameters

Agricultural waste	Maximum adsorption capacity (mg/g)	ΔH° (kJ mol ⁻¹)	ΔS° (JK ⁻¹ mol ⁻¹)	ΔG° (kJ mol ⁻¹)	References
Almond shells	58.13	64.059	253.740	-12.824	[40]
Almond leaves	22.96	-16.106	67.667	-4601.12	[44]
	7.77	-10.481	37.340	-788.312	
Gipto seed peel	36.14	-4.697	-11.083	-1.339	[2]
Wild gourd	166.66	-72.876	294.51	-7.283	[7]
Kutaj seed	144.92	-67.362	276.073	-6.472	
Sugarcane baggase	190	19.36	-31.57	-9.79	[43]
Corn cob	25.5	-14.324	28.853	-22.578	[65]
Cotton stick biomass	-	-12.66	-0.145	-2.1	[10]
Breadfruit seed	16	-23.30	-49.99	-1940.08	[14]
Mango bark	0.53	20.21	0.18	-20.40	[61]
Neem bark	0.36	25.25	0.13	-21.45	

4.3 Dye Desorption

The utilization of agricultural waste also offers the advantage of being recycled. The desorption characteristics of the adsorbent have been studied for their reusability. Desorption agents can either be acidic, basic or neutral. In one of the studies on the desorption of textile dyes from pinecone as adsorbent, the maximum desorption percentage for acid black 26 and acid blue 7 was obtained as 93 and 98%, respectively [9]. The desorption pattern was also influenced by pH [67]. Basic and neutral solutions had no significant effect on the desorption characteristics of crystal violet, while acetic acid showed about 50% desorption [34].

4.4 Mechanism of Elimination

The adsorption behavior is governed by various factors like the structure and size of the adsorbate, the surface characteristics of the adsorbent, steric influences along with interactive forces like van der Waals interaction and hydrogen bonding. The complexation between the dye and the adsorbent can be through strong bonding, ionic interaction or weak van der Waals forces. External transport is the rate limiting step in systems with improper mixing, small particle size and low concentrations

whereas intraparticle transfer governs the system with proper mixing, large particle diameter and high concentration. It is well reported that the mechanism of adsorptive exchange helps to distinguish between the particle and film diffusion. There are three steps involved in the process. Firstly, transport of the adsorbate ions from bulk to the external surface of the adsorbent (film diffusion). Secondly, transport of the adsorbate particles within the pores of the adsorbent (particle diffusion) and adsorption of the adsorbate ions on the interior surface and capillary spaces [41]. It was observed that the intraparticle diffusion process was predominant in the case of high adsorption rates, concentrations, and high adsorbent particle sizes [42]. The quantitative treatment of the sorption dynamics was in agreement with the annotations of Reichenberg [52].

5 Advantages and Disadvantages of Agro-Waste

The noticeable advantage of using agro-waste is its cost effectiveness with a high potential of removing contaminants including recalcitrant dyes when compared to other types of adsorbents and methods. The process is applicable to a large variety of target substrates. The efficiency of the process further improves when coupled with other advanced methods like nano-filtration and advanced oxidation [59]. The utilization of leftover residue from farms, poultry, aquaculture and industries based on agricultural processing diminishes the total organic load on the environment. This reduces the likelihood of destructive bio-amplification and air quality degradation.

The agro-waste definitely proves to be an efficient alternative over conventional methods but their selective nature towards contaminants limits their application. The cost input involved in the regeneration is also an important constraint. Large-scale utilization of agro-based adsorbents for textile effluent treatment is yet to be achieved as most of the studies carried out are lab based. The real situation implication is still being explored for a better understanding of the applicability of the agro-waste in combating the mentioned problem [15, 16].

6 Conclusion

The scientific community, industrialists, stakeholders, researchers as well as policy makers are working towards the preservation of the environment. The demand of the environmentalists for pollution free water bodies has compelled textile based industries to prioritize the decontamination process. Thus, exploration of agro-waste as a potential sequesting agent would benefit the environment as well as human life. Consistent efforts of the industrialist and researchers can facilitate utilization of agro-waste for strengthening socio economic conditions of the farmers and protection of the environment. The existing methods of textile wastewater treatment need to be supplemented with novel and robust techniques, cost effective equipments, and

regeneration methodology, aiming at the best utilization of agricultural based waste for textile water remediation.

References

1. Abioye HG, Aransiola A (2015) Bio-removal of vat dye from textile effluent by candida tropicalis and Candida apis isolated from soil. *Expert Opin Environ Biol* 4:3. <https://doi.org/10.4172/2325-9655.1000121>
2. Alene AN, Abate GY, Habte AT, Getahun DM (2021) Utilization of a novel low cost gibto (*lipinus albus*) seed peel waste for the removal of malachite green dye: equilibrium. Kinetic and thermodynamic studies. *J Chem* 1–16. <https://doi.org/10.1155/2021/6618510>
3. Amirza M, Mohd R, Rafidah H (2017) Application of agricultural wastes activated carbon for dye removal—an overview. *MATEC Web Conf* 103:06013. <https://doi.org/10.1051/mateconf/201710306013>
4. Ansari SA, Khan F, Ahmad A (2016) Cauliflower leave, an agricultural waste biomass adsorbent and its application for the removal of MB dye from aqueous solution: equilibrium, kinetics, and thermodynamic studies. *Int J Anal Chem* 10. <https://doi.org/10.1155/2016/8252354>
5. Asgher M, Bhatti HN (2010) Mechanistic and kinetic evaluation of biosorption of reactive azo dyes by free, immobilized and chemically treated *Citrus sinensis* waste. *Ecol Eng* 36:1660–1665. <https://doi.org/10.1016/j.ecoleng.2010.07.003>
6. Banerjee S, Dastidar MG (2005) Use of jute processing wastes for treatment of wastewater contaminated with dye and other organics. *Bioresour Technol* 96:1919–1928. <https://doi.org/10.1016/j.biortech.2005.01.039>
7. Basharat S, rehman R, Mahmud T, Basharat S, Mitu L (2020) Tartaric acid modified holarrhena antidysentrica and citrullus colocynthis biowaste for efficient eradication of crystal violet dye from water. *J Chem* 1–18. <https://doi.org/10.1155/2020/8862167>
8. Bhainsa KC, D'Souza SF (2008) Removal of copper ions by the filamentous fungus, *Rhizopusoryzae* from aqueous solution. *Bioresour Technol* 99:3829–3835. <https://doi.org/10.1016/j.biortech.2007.07.032>
9. Bharathi KS, Ramesh ST (2013) Removal of dyes using agricultural waste as low-cost adsorbents: a review. *Appl Water Sci* 3:773–790. <https://doi.org/10.1007/s13201-013-0117-y>
10. Bhatti HN, Sadaf S, Aleem A (2015) Treatment of textile effluents by low cost agricultural wastes: batch biosorption study. *J Anim and Plant Sci*. 25:284–289
11. Blachnio M, Derylo-Marczewska A, Charmas B, Zienkiewicz-Strzalka M, Bogatyrov V, Galaburda M (2020) Activated carbon from agricultural wastes for adsorption of organic pollutants. *Molecules* 25(21):5105. <https://doi.org/10.3390/molecules25215105>
12. Bracco S, Calicioglu O, Juan MGS, Flammini A (2018) Assessing the contribution of bioeconomy to the total economy: a review of national frameworks. *Sustainability* 10:1698. <https://doi.org/10.3390/su10061698>
13. Chikri R, Elhadiri N, Benchanaa M, Barek, EI Maguana Y (2020) Efficiency of sawdust as low-cost adsorbent for dyes removal. *J Chem* 2020:1–17. <https://doi.org/10.1155/2020/8813420>
14. Conrad EK, Nnaemeka OJ, Uchechi EE, Basil A, Veronica OO, Cynthia OE, Emeka OE (2016) Adsorption of congo red dye from aqueous solution using agricultural waste. *J Appl Chem* 9:39–51. <https://doi.org/10.9790/5736-0909013951>
15. Crini G, Eric L (2019) Advantages and disadvantages of techniques used for wastewater treatment. *Environ Chem Lett* 17:145–155. <https://doi.org/10.1007/s10311-018-0785-9>
16. Crini G, Lichtfouse E (2018) Wastewater treatment: an overview, chapter 1. In: Crini G, Lichtfouse E (eds) *Green adsorbents for pollutant removal—fundamentals and design, environmental*

- chemistry for a sustainable world, vol 1. Springer, Berlin, pp 1–21. https://doi.org/10.1007/978-3-319-92111-2_1
17. Darwesh O, Aya E, Mohamed A, Mohamed K (2021) Enhancing the efficiency of some agricultural wastes as low-cost adsorbents to remove textile dyes from their contaminated solutions. *Biomass Conver Biorefin* 1-10. <https://doi.org/10.1007/s13399-020-01142-w>
 18. de Luna MDG, Flores ED, Genuino DAD, Futralan CM, Meng-Wei W (2013) Adsorption of Eriochrome Black T (EBT) dye using activated carbon prepared from waste rice hulls—optimization, isotherm and kinetic studies. *J Taiwan Inst Chem Eng* 44:646–653
 19. Fan S, Tang J, Wang Y, Li H, Zhang H, Tang J, Wang Z, Li X (2016) Biochar prepared from co-pyrolysis of municipal sewage sludge and tea waste for the adsorption of methylene blue from aqueous solutions: Kinetics, isotherm, thermodynamic and mechanism. *J Mol Liq* 220:432–441. <https://doi.org/10.1016/j.molliq.2016.04.107>
 20. Gadd GM (1992) Metals and microorganisms: a problem of definition. *FEMS Microbiol Lett* 100:197–203
 21. Gaur N, Flora G, Yadav M, Tiwari A (2014) A review with recent advancements bioremediation-based abolition of heavy metals. *Environ Sci Processes Impacts* 162:180–193. <https://doi.org/10.1039/c3em00491k>
 22. Gelebo GG, Ahmed FE (2019) Removal of direct and reactive dyes from textile wastewater using *Moringa stenopetala* seed extract. *J Textile Eng Fashion Technol* 5(4):184–191. <https://doi.org/10.15406/jteft.2019.05.00200>
 23. Hameed BH, Ahmad AA (2009) Batch adsorption of methylene blue from aqueous solution by garlic peel, an agricultural waste biomass. *J Hazard Mater* 164:870–875. <https://doi.org/10.1016/j.jhazmat.2008.08.084>
 24. Hameed BH, El-Khaiary MI (2008) Removal of basic dye from aqueous medium using a novel agricultural waste material: pumpkin seed hull. *J Hazard Mater* 155:601–609. <https://doi.org/10.1016/j.jhazmat.2007.11.102>
 25. Han R, Ding D, Xu Y, Zou W, Wang Y, Li Y, Zou L (2008) Use of rice husk for the adsorption of Congo red from aqueous solution in column mode. *Bioresour Technol* 99(8):2938–2946. <https://doi.org/10.1016/j.biortech.2007.06.027>
 26. Haq I, Bhatti HN, Asgher MM (2011) Removal of solar red ba textile dye from aqueous solution by low cost barley husk: equilibrium, kinetic and thermodynamic study. *Can J Chem Eng* 89:593–600. <https://doi.org/10.1002/cjce.20436>
 27. Hassaan M, El Nemr A (2017) Health and environmental impacts of dyes: mini review. *Am J of Environ Sci Eng* 1:64–67. <https://doi.org/10.11648/j.ajese.20170103.11>
 28. Hausen BM (1993) Contact allergy to disperse blue 106 and blue 124 in black “velvet” clothes. *Contact Dermatitis* 28:169–173. <https://doi.org/10.1111/j.1600-0536.1993.tb03381.x>
 29. Immich APS, Ulson de Souza AA (2009) Removal of Remazol Blue dye from aqueous solutions with Neem leaves and evaluation of their toxicity with *Daphnia magna*. *J Hazard Mater* 164:1580–1585. <https://doi.org/10.1016/j.jhazmat.2008.09.019>
 30. Jong TS, Yoo CY, Kiew PL (2020) Feasibility study of methylene blue adsorption using magnetized papaya seeds. *Prog Energy Environ* 14(1):1–12
 31. Kabir FSM, RafaelC BS, Romeo LD, Kuttruff JT, Marx BD, Negulescu II (2019) Removal of acid dyes from textile wastewaters using fish scales by absorption process. *Clean Technol* 1:311–325. <https://doi.org/10.3390/cleantechnol1010021>
 32. Khamparia S, Jaspal D, Malviya A (2015) Optimization of adsorption process for removal of sulphonated di azo textile dye. *Green Chem Technol Lett* 1(01):61–66. <https://doi.org/10.18510/gctl.2015.119>
 33. Khattri SD, Singh MK (2009) Removal of malachite green from dye wastewater using neem sawdust by adsorption. *J Hazard Mater* 167:1089–1094. <https://doi.org/10.1016/j.jhazmat.2009.01.101>
 34. Kumar R, Ahmad R (2011) Biosorption of hazardous crystal violet dye from aqueous solution onto treated ginger waste TGW. *Desal* 265:112–118. <https://doi.org/10.1016/j.desal.2010.07.040>

35. Kyzas GZ, Christodoulou E, Bikiaris DN (2018) Basic dye removal with sorption onto low-cost natural textile fibers. *Processes* 6:166. <https://doi.org/10.3390/pr6090166>
36. Lee J, Yang X, Cho S-H, Kim J-K, Lee SS, Tsang D, Ok YS (2017) Pyrolysis process of agricultural waste using CO₂ for waste management, energy recovery, and biochar fabrication. *Appl Energy* 185:214–222. <https://doi.org/10.1016/j.apenergy.2016.10.092>
37. Liu MH, Hong SN, Huang JH, Zhan HY (2005) Adsorption/desorption behavior between a novel amphoteric granular lignin adsorbent and reactive red K-3B in aqueous solutions. *J Environ Sci China* 17:212–214
38. Mahmoudabadi TZ, Talebi P, Jalili M (2019) Removing Disperse red 60 and Reactive blue 19 dyes removal by using Alcearosea root mucilage as a natural coagulant. *AMB Expr* 9:113. <https://doi.org/10.1186/s13568-019-0839-9>
39. Malik R, Ramteke DS, Wate SR (2007) Adsorption of Malachite green on groundnut shell waste based powdered activated carbon. *Waste Manag* 27:1129–1138. <https://doi.org/10.1016/j.wasman.2006.06.009>
40. Melhaoui R, Miyah Y, Kodad S, Houmy N, Addi M, Abid M, Mihaoui A, Serghini-caid H, Lairini S, Tijani N, Elamrani A (2021) On the suitability of almond shells for the manufacture of a natural low cost bioadsorbent to remove brilliant green: kinetics and equilibrium isotherms study. *Sci World J* 2021:13. <https://doi.org/10.1155/2021/6659902>
41. Mittal A, Mittal J, Malviya A, Gupta VK (2010) Removal and recovery of chrysoidine Y from aqueous solutions by waste materials. *J Coll and Interf Sci* 344(2):497–507. <https://doi.org/10.1016/j.jcis.2010.01.007>
42. Neto VOS, Melo DQ, de Oliveira TC et al (2014) Evaluation of new chemically modified coconut shell adsorbents with tannic acid for Cu(II) removal from wastewater. *J Appl Polym Sci* 131(18):40744–40755. <https://doi.org/10.1002/app.40744>
43. Nilay Sharma N, Bk BKN (2013) Utilization of Sugarcane baggase, an agricultural waste to remove malachite green dye from aqueous solutions. *J Mater Environ Sci* 4(6):1052–1065
44. Nnaemeka OJ, Josphine OJ, Charles O (2016) Adsorption of basic and acidic dyes onto agricultural wastes. *Int Lett Chem* 70:12–26. <https://doi.org/10.18052/www.scipress.com/ILCPA.70.12>
45. Obi FO, Ugwuishiwu BO, Nwakaire JN (2016) Agricultural waste concept, generation utilization and management. *Niger J Technol* 35(4):957–964
46. Ouslimani N, Boureghda MZM (2018) Removal of direct dyes from wastewater by cotton fiber waste. *Int J Waste Resour* 8:330
47. Patricia O-O, Peter DA, Okechukwu O (2018) A review of the application of agricultural wastes as precursor materials for the adsorption of per- and polyfluoroalkyl substances: a focus on current approaches and methodologies. *Environ Technol Innov* 9:100–114. <https://doi.org/10.1016/j.eti.2017.11.005>
48. Perea-Moreno MA, Samerón-Manzano E, Perea-Moreno AJ (2019) Biomass as renewable energy: worldwide research trends. *Sustainability* 11(3):863. <https://doi.org/10.3390/su11030863>
49. Ponnusami V, Vikram S, Srivastava SN (2008) Guava (*Psidium guajava*) leaf powder: novel adsorbent for removal of methylene blue from aqueous solutions. *J Hazard Mater* 152:276–286. <https://doi.org/10.1016/j.jhazmat.2007.06.107>
50. Rahman IA, Saad B, Shaidan S, Rizal ESS (2005) Adsorption characteristics of malachite green on activated carbon derived from rice husks produced by chemical–thermal process. *J Bioresour Technol* 96:1578–1583. <https://doi.org/10.1016/j.biortech.2004.12.015>
51. Reddy DHK, Ramana DKV, Seshiah K, Reddy AR (2011) Biosorption of Ni(II) from aqueous phase by *Moringaoleifera* bark, a low cost biosorbent. *Desalination* 268:150–157. <https://doi.org/10.1016/j.desal.2010.10.011>
52. Reichenberg D (1953) Properties of ion-exchange resin in relation to their structure. III. Kinetics of exchange. *J Am Chem Soc* 75:589
53. Sadia S, Abu N (2016) Removal of methylene blue dye from artificially contaminated water using citrus limetta peel waste as a very low cost adsorbent. *J Taiwan Inst Chem Eng* 66:154–163. <https://doi.org/10.1016/j.jtice.2016.06.009>

54. Santhy K, Selvapathy P (2006) Removal of reactive dyes from wastewater by adsorption on coirpith activated carbon. *J Bioresour Technol* 97:1329–1336. <https://doi.org/10.1016/j.biortech.2005.05.016>
55. Shah MA, Khan MNS, Kumar V (2018) Biomass residue characterization for their potential application as biofuels. *J Therm Anal Calorim* 134:2137–2145. <https://doi.org/10.1007/s10973-018-7560-9>
56. Shankar D, Sivakumar D, Thiruvengadam M, Manojkumar M (2014) Colour removal in a textile industry wastewater using coconut coir pith. *Pollution Res* 33:499–503
57. Shoomaila L, Rabia R, Muhammad I, Shahis I, Ayesha Kanwal, Iliu M (2019) Removal of acidic dye from aqueous media using *Citrullus lanatus* peels: an agro waste-based adsorbent for environmental safety. *J Chem* 9. <https://doi.org/10.1155/2019/6704953>
58. Singh K, Kumar P, Srivastava R (2017) An overview of textile dyes and their removal techniques: Indian perspective. *Poll Res* 36:790–797
59. Sivakumar P, Palanisamy N (2010) Mechanistic study of dye adsorption on to a novel non-conventional low-cost adsorbent. *Adv Appl Sci Res* 1(1):58–65
60. Smelcerovic M, Dordevic D, Novakovic M, Mizdrakovic M (2010) Decolorization of a textile vat dye by adsorption on waste ash. *J Serb Chem Soc* 75(6):855–872. <https://doi.org/10.2298/JSC090717051K>
61. Srivastava R, Rupainwar DC (2011) A comparative evaluation for adsorption of dye on neem bark and mango bark powder. *Indian J Chem Technol* 1(8):67–75
62. Stephanie C, Bruce J, Peter J (2019) Pesticide removal from drinking water sources by adsorption: a review. *Environ Technol Rev* 8(1):1–24. <https://doi.org/10.1080/21622515.2019.1593514>
63. Stjepanovic M, Velic N, Galic A, Kosovic I, Jakovljevic T, Habuda-Stanic M (2021) From waste to biosorbent: removal of congo red from water by waste wood biomass. *Water* 13:279. <https://doi.org/10.3390/w13030279>
64. Sugumaran P, Susan VP, Ravichandran P, Seshadri S (2012) Production and characterization of activated carbon from banana empty fruit bunch and *Delonix regia* fruit pod. *J Sustain Ener Environ* 3:125–132
65. Suteu D, Malutan T, Bilba D (2011) Agricultural waste corn cob as a sorbent for removing reactive dye orange 16: equilibrium and kinetic study. *Cellulose Chem Technol* 45(5–6):413–420
66. Thinakaran N, Panneerselvam P, Baskaralingam P, Pulikesi M, Sivanesan S (2008) Removal of acid violet 17 from aqueous solutions by adsorption onto activated carbon prepared from sunflower seed hull. *J Hazard Mater* 154:204–212. <https://doi.org/10.1016/j.jhazmat.2007.05.076>
67. Vishal C, Singh VK (2016) Adsorption of safranin dye from aqueous solutions using a low-cost agro-waste material soybean hull. *Desalin Water Treat* 57(9):4122–4134. <https://doi.org/10.1080/19443994.2014.991758>
68. Wong S, Ghafar NA, Ngadi N, Fatina R, Ibrahim MI, Ramli M, Nor ASA (2020) Effective removal of anionic textile dyes using adsorbent synthesized from coffee waste. *Sci Rep* 10:2928. <https://doi.org/10.1038/s41598-020-60021-6>
69. Zhang W, Li H, Kan X, Dong L, Yan H, Jiang Z, Yang H, Li A, Cheng R (2012) Adsorption of anionic dyes from aqueous solutions using chemically modified straw. *Bioresour Technol* 117:40–47. <https://doi.org/10.1016/j.biortech.2012.04>

Correction to: Chitosan-Based Composite Beads for Removal of Anionic Dyes



Joydeep Dutta

Correction to:
Chapter “Chitosan-Based Composite Beads for Removal of Anionic Dyes” in: S. S. Muthu and A. Khadir (eds.), *Textile Wastewater Treatment, Sustainable Textiles: Production, Processing, Manufacturing & Chemistry*, https://doi.org/10.1007/978-981-19-2832-1_3

The original version of the book was published without figures and tables in the chapter “Chitosan-Based Composite Beads for Removal of Anionic Dyes”, which has now been provided figures and tables with captions are inserted in this chapter as in below:

The updated original version of this chapter can be found at https://doi.org/10.1007/978-981-19-2832-1_3

© The Author(s), under exclusive license to Springer Nature Singapore Pte Ltd. 2022
S. S. Muthu and A. Khadir (eds.), *Textile Wastewater Treatment, Sustainable Textiles: Production, Processing, Manufacturing & Chemistry*,
https://doi.org/10.1007/978-981-19-2832-1_15

C1

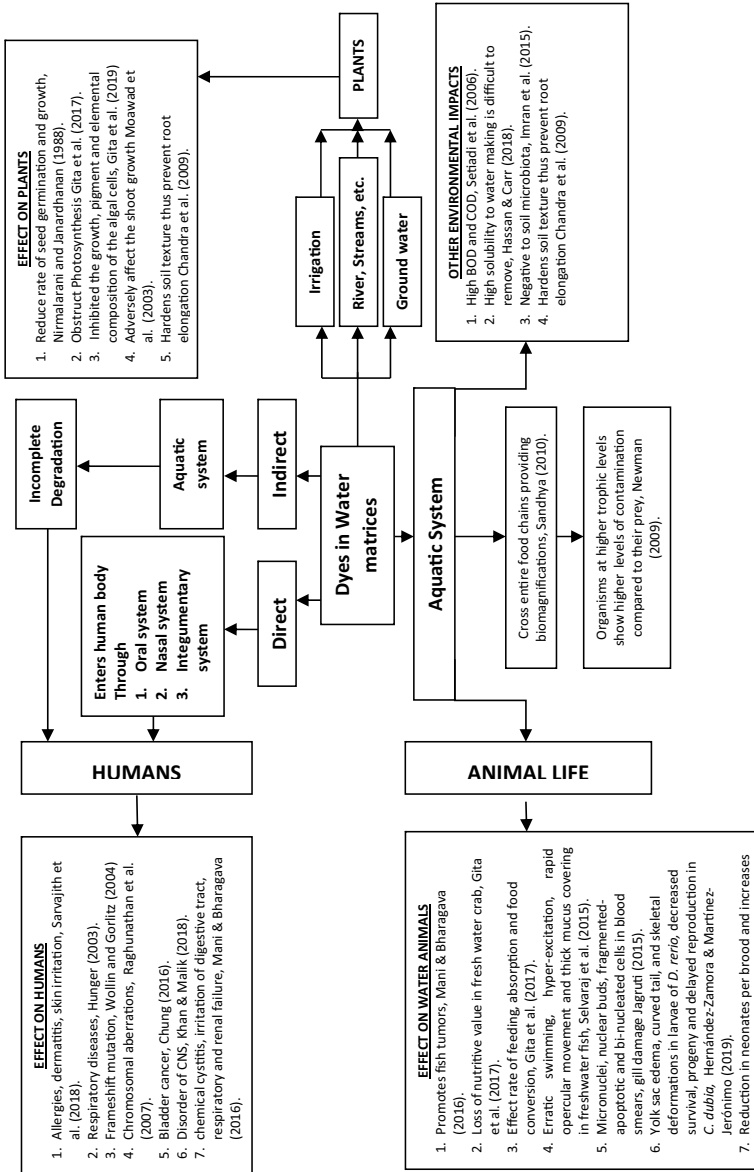


Fig. 1 Complex follow through of dyes in water matrices and their effect on the biological organisms

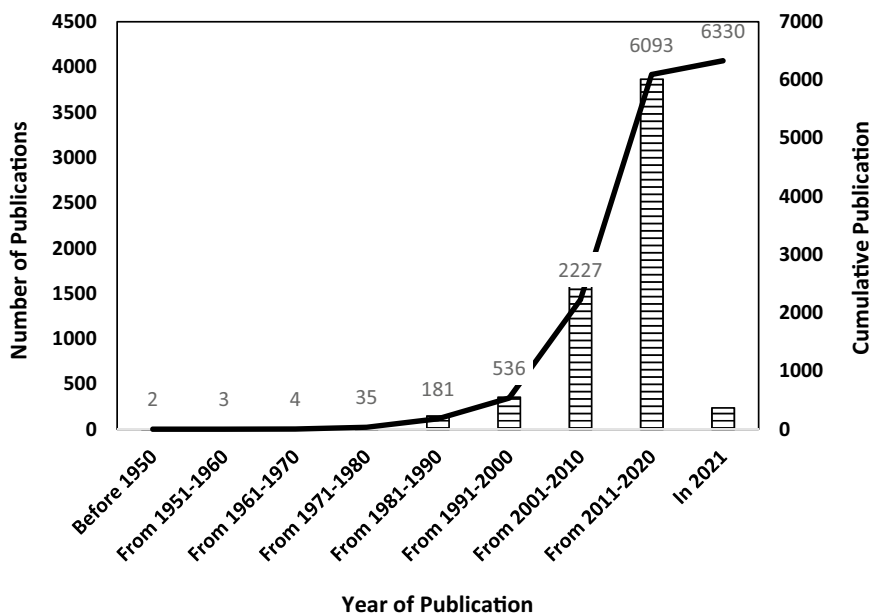


Fig. 2 Data from Pubmed (From Year 1928–2021), the number and cumulative publications related to Removal of textile Dyes from water matrices

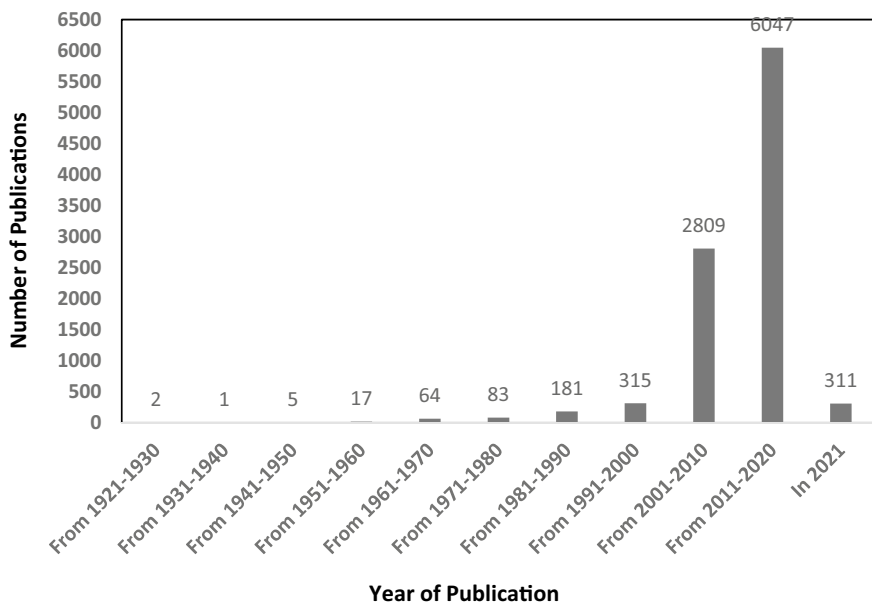


Fig. 3 Pubmed data shows work on adsorption of dyes from wastewater from 1923 to 2021

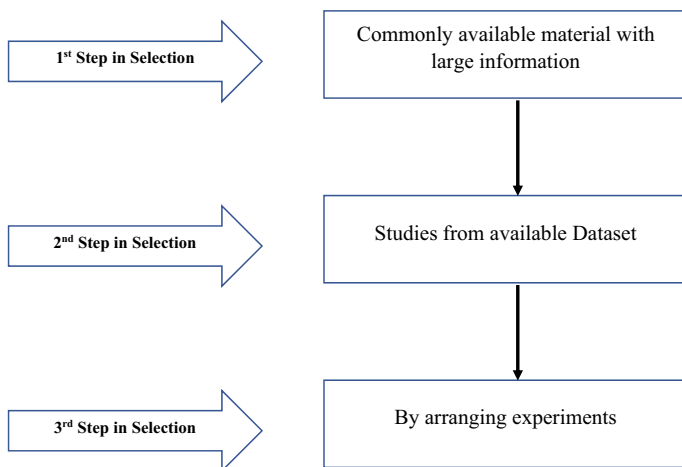


Fig. 4 Selection process of good adsorbent

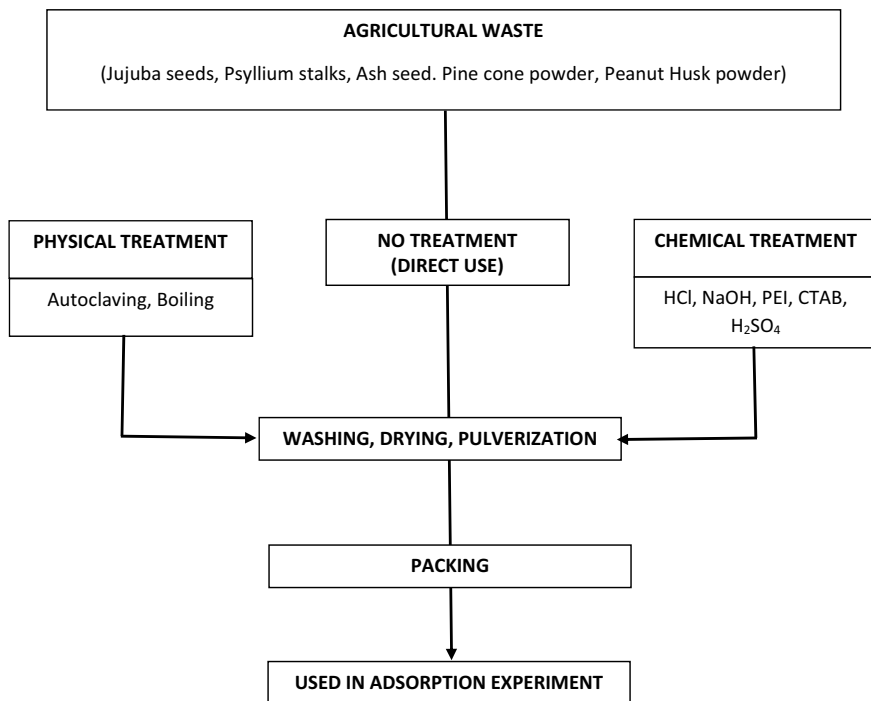


Fig. 5 Processing of agricultural waste before use for adsorption

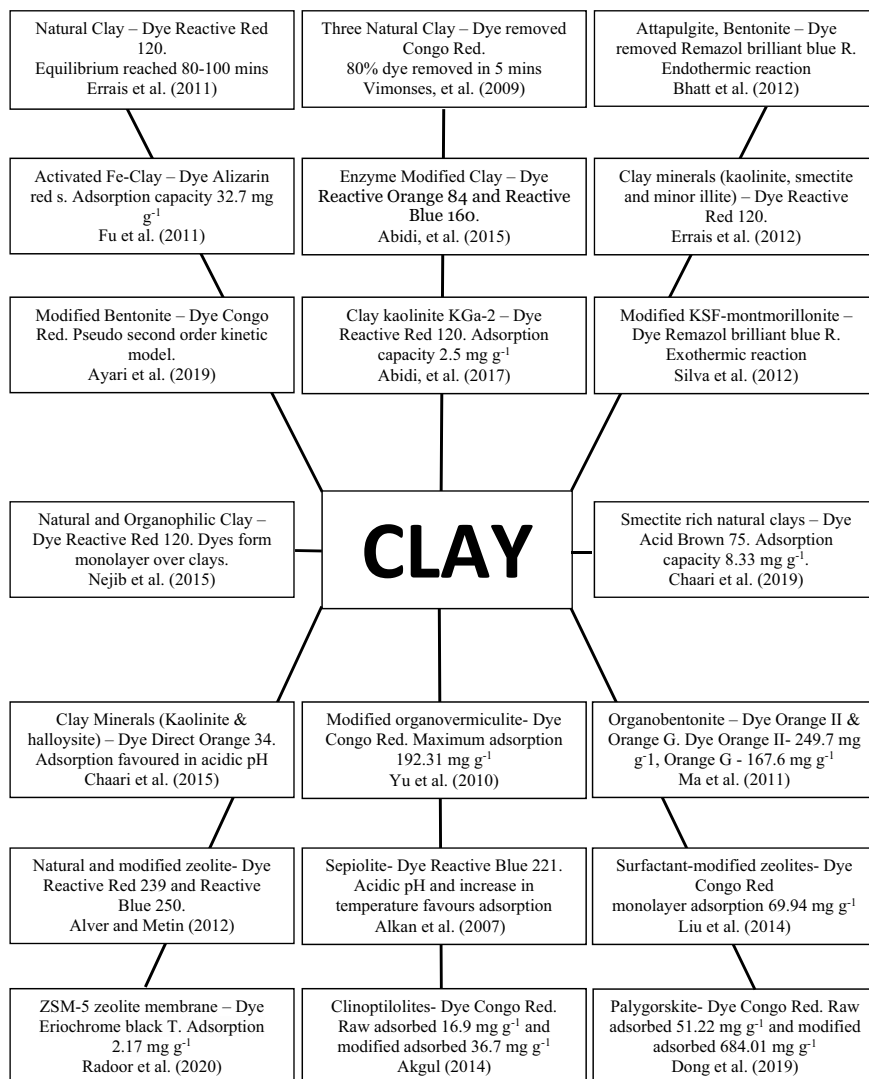


Fig. 6 Glimpse of modified and un-modified clays for adsorption of dyes

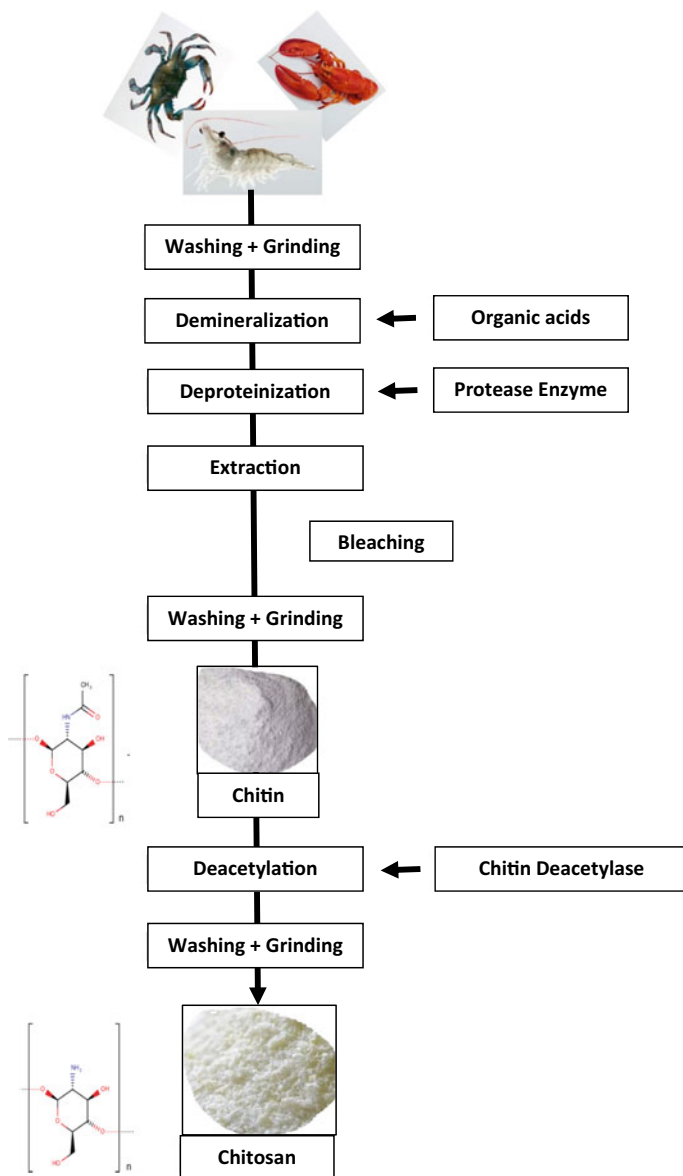


Fig. 7 Production process of chitin and chitosan from animal sources

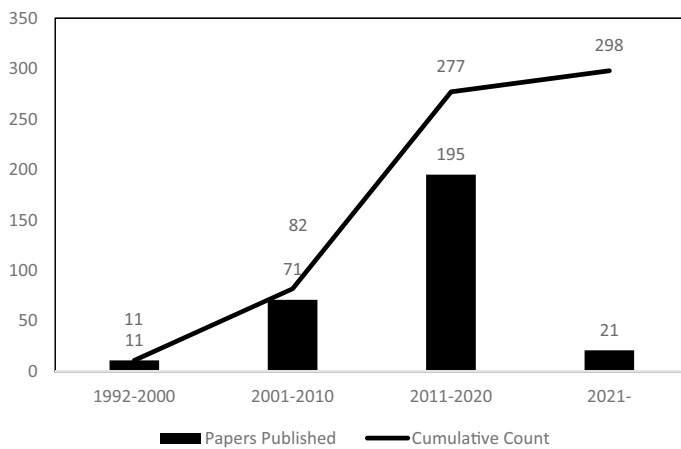


Fig. 8 Cumulative work with chitosan beads as adsorbent from 1992 to date as per Pubmed database

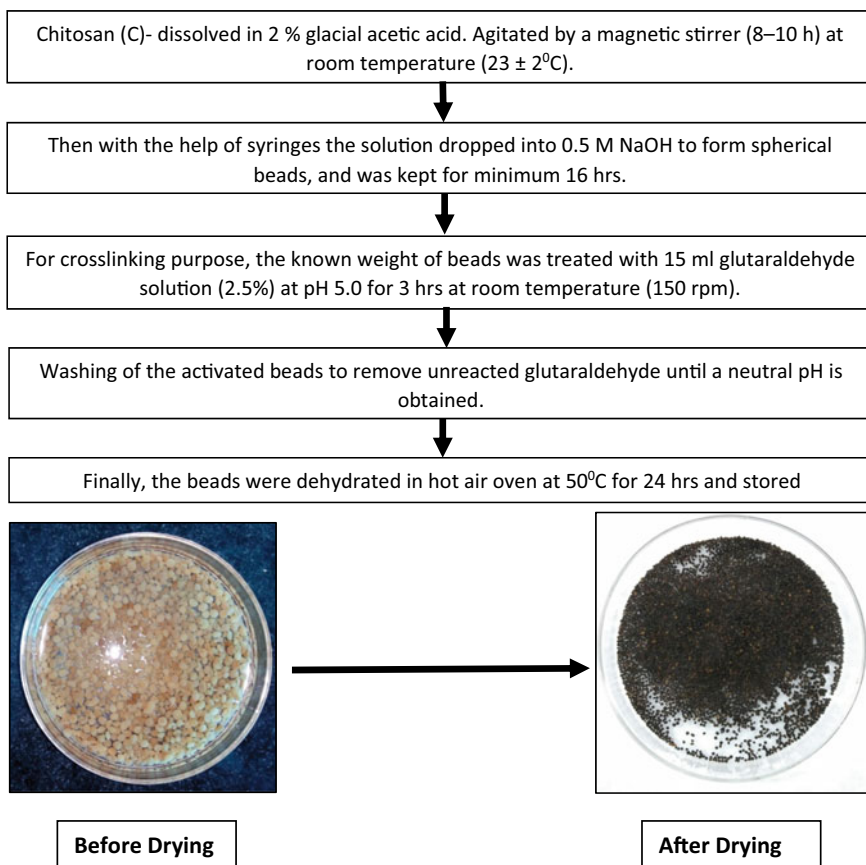


Fig. 9 Development of chitosan beads

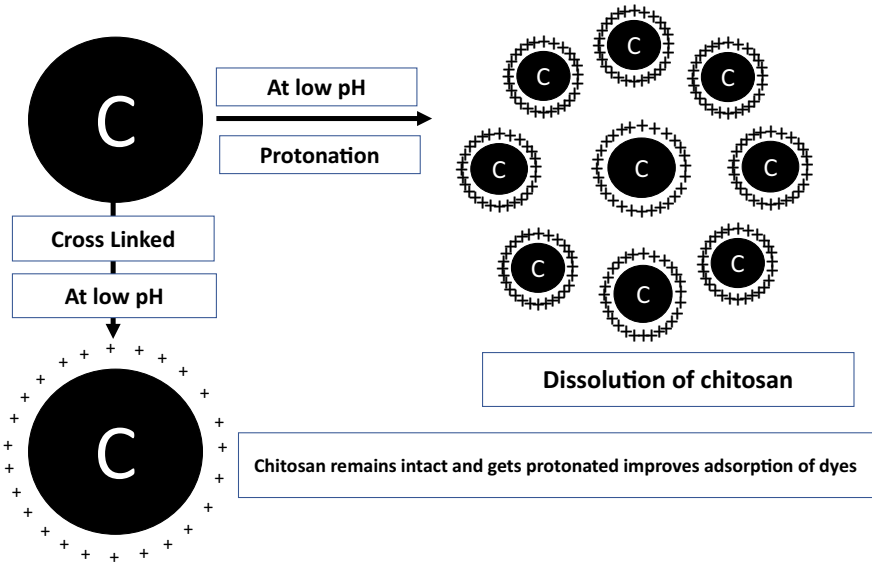


Fig. 10 Reaction of chitosan at low pH

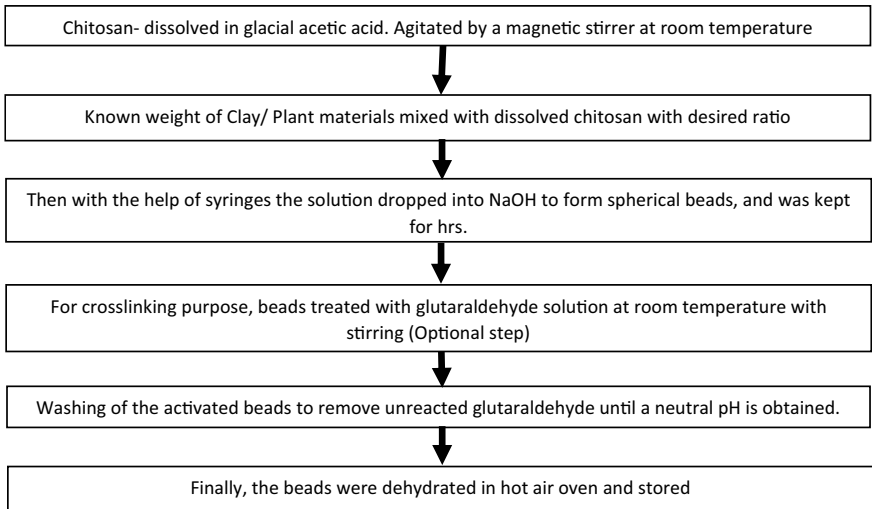


Fig. 11 Development of chitosan composite beads

Table 1 Advantages and disadvantages of adsorption

S. No.	Advantages	Disadvantages
1	Easy operation	Non selective method
2	Adaptable and can be shaped in different formats	Performance depends on the type of materials
3	Technologically simple	Several types of adsorbents required
4	Can be operated at different scenarios	Chemical modifications required of adsorbents for better results
5	Low energy requirements	Different operating conditions
6	Low economy involved (when raw materials used)	Elimination of the adsorbent after adsorption i.e. disposal
7	Used for wide range of contaminants and excellent ability	Costly when pyrolysis or other methods involved

Table 2 Adsorption capacities of dyes by some of the agricultural wastes

Agri waste	Dye	Adsorption capacity	References
Wood sawdust	Acid blue 25	5.92 mg g ⁻¹	Ho and McKay (1998a)
Coir pith	Congo red	2.6 mg g ⁻¹	Namasivayam and Kavitha (2002)
Peanut hull	Amaranth	14.9 mg g ⁻¹	Gong et al. (2005)
Peanut hull	Sunset yellow	13.99 mg g ⁻¹	Gong et al. (2005)
Peanut hull	Fast green	15.60 mg g ⁻¹	Gong et al. (2005)
Hazelnut shell	Acid blue 25	60.2 mg g ⁻¹	Ferro (2007)
Saw dust—cherry	Acid blue 25	31.98 mg g ⁻¹	Ferro (2007)
Saw dust—oak	Acid blue 25	27.85 mg g ⁻¹	Ferro (2007)
Saw dust—walnut	Acid blue 25	36.98 mg g ⁻¹	Ferro (2007)
Palm kernel fibre	BDH	38.6 mg g ⁻¹	Ofomaja and Ho (2007)
Almond shell	Direct red 80	90.09 mg g ⁻¹	Ardejani et al. (2008)
Sugar cane bagasse	Orange 16	34.48 mg g ⁻¹	Wong et al. (2009)
Sugar cane bagasse	Basic blue 3	37.59 mg g ⁻¹	Wong et al. (2009)
Neem bark	Malchite green	0.36 mg g ⁻¹	Srivastava and Rupainwar (2011)
Mango bark	Malchite green	0.53 mg g ⁻¹	Srivastava and Rupainwar (2011)
Jujuba seeds	Congo red	55.56 mg g ⁻¹	Reddy et al. (2012)
Walnut shell	Reactive brilliant red K-2BP	568.18 mg g ⁻¹	Cao et al. (2014)
Pristine sawdust	Reactive red 196	13.39	Doltabadi et al. (2016)
Wheat straw	Orange II	506 mg g ⁻¹	Lin et al. (2017)
Banana pseudo-stem	Methyl orange	124 mg g ⁻¹	Bello et al. (2018)
Banana peel	Orange G	20.9 mg g ⁻¹	Stavrinou et al. (2018)
Potato peel	Orange G	23.6 mg g ⁻¹	Stavrinou et al. (2018)
Cucumber peel	Orange G	40.5 mg g ⁻¹	Stavrinou et al. (2018)
Psyllium stalks	Coomassie brilliant blue	237.2 mg g ⁻¹	Periyaraman et al. (2019)
Tea waste	Acid blue 25	127.14 mg g ⁻¹	Jain et al. (2020)
Coffee	Reactive black 5	77.52 mg g ⁻¹	Wong et al. (2020)
Coffee	Congo red	34.36 mg g ⁻¹	Wong et al. (2020)

(continued)

Table 2 (continued)

Agri waste	Dye	Adsorption capacity	References
Eucalyptus bark	Remazol BB	34.10 mg g ⁻¹	Morais et al. (1999)
Mango seed kernel	Methylene blue	142.90 mg g ⁻¹	Kumar and Kumrana (2005)
Guava leaf powder	Methylene blue	95.10 mg g ⁻¹	Ponnusami et al. (2008)
Orange peel	Direct red 23	10.72 mg g ⁻¹	Arami et al. (2005)
Orange peel	Direct red 80	21.05 mg g ⁻¹	Arami et al. (2005)
Sugarcane bagasse	Methylene blue	34.20 mg g ⁻¹	Filho et al. (2007)
Sugarcane bagasse	Methylene blue	99.60 mg g ⁻¹	Raghuvanshi et al. (2004)

Table 3 Microorganisms as adsorbent

Organisms	Dye	Adsorbed mg g ⁻¹ /removal %	References
<i>Pichia carsonii</i>	Reactive black 5	25 mg g ⁻¹	Polman and Breckenridge (1996)
<i>B. subtilis</i>	Reactive yellow 2	2–97 mg g ⁻¹	
<i>E. coli</i>	Reactive blue 5	9–31 mg g ⁻¹	
<i>Aeromonas</i> sp.	Reactive red 22	114–146 mg g ⁻¹	
<i>P. luteola</i> ,	Reactive violet 2	80–113 mg g ⁻¹	
<i>S. aureus</i>		1–3 mg g ⁻¹	Hu (1996)
<i>Aspergillus niger</i>	Congo red	98.8%	Hamad and Saied (2021)
<i>Fomes fomentarius</i>	Methylene blue	204.38–232.73 mg g ⁻¹	Maurya et al. (2006)
<i>Phellinus igniarius</i>	Rhodamine B	25.12–36.82 mg g ⁻¹	Maurya et al. (2006)
<i>Trametes versicolor</i>	Acid violet 7	104.2 mg g ⁻¹	Wang and Yu (1998)
	Indigo carmine	51.0 mg g ⁻¹	
	Acid green 27	53.5 mg g ⁻¹	
<i>A. niger</i> (Autoclaved)	Basic blue 9	18.54 mg g ⁻¹	Fu and Viraraghavan (2000)
<i>A. niger</i> (Living)	Basic blue 9	1.17 mg g ⁻¹	
<i>Cunninghamella elegans</i>	Acid blue 62	300–600 mg g ⁻¹	Russo et al. (2010)
	Acid red 266		
	Acid yellow 49		
<i>Lentinus concinnus</i>	Reactive yellow 86	190.2 mg g ⁻¹	Bayramoglu and Yilmaz (2018)
<i>Rhizopus stolonifera</i>	Bromophenol blue	1111 mg g ⁻¹	Zeroual et al. (2006)
<i>Fusarium</i> sp.	Bromophenol blue	714 mg g ⁻¹	Zeroual et al. (2006)
<i>Geotrichum</i> sp.	Bromophenol blue	588 mg g ⁻¹	Zeroual et al. (2006)
<i>Aspergillus fumigatus</i>	Bromophenol blue	526 mg g ⁻¹	Zeroual et al. (2006)
<i>K. marxianus</i>	Remazol blue	161 mg g ⁻¹	Aksu and Dönmez (2003)
<i>Khuyveromyces waltiiq</i>	Reactive blue 19	14 mg g ⁻¹	Polman and Breckenridge (1996)
<i>C. lipolytica</i>	Remazol blue	250 mg g ⁻¹	Aksu and Dönmez (2003)
<i>Aspergillus fumigatus</i>	Methylene blue	93.5%	Kabbout and Taha (2014)
<i>Ochrobactrium</i> sp.			
<i>Salmonella enterica</i>			
<i>Pseudomonas aeruginosa</i>	Reactive black B	59.3 mg g ⁻¹	Kılıç et al. (2007)

(continued)

Table 3 (continued)

Organisms	Dye	Adsorbed mg g ⁻¹ /removal %	References
<i>Bacillus subtilis</i>	Congo red	92.8%	Sarim et al. (2019)
<i>Aeromonas</i> sp.	Red G	27.41 mg g ⁻¹	Hu (1992)
<i>Aureispira</i> sp.	Congo red	88.1%	Hasyimah et al. (2020)

Table 4 Modification of chitin of adsorption of dyes

Modification system	Dye sorbed	References
Sodium hypochlorite	Reactive red 141	Dolphen et al. (2007)
CaBr ₂ ·xH ₂ O/CH ₃ OH	Methylene blue	Cao et al. (2018)
Ultrasonic modified	Methylene blue	Yazidi et al. (2020)
Ultrasound-modified	Indium(III)	Li et al. (2019)
Ultrasonic processor	Methylene blue	Franco et al. (2015)
Ultrasonic processor	Methylene blue	Sellaoui et al. (2017)
HCl modified	Helactine, polactine and remazol	Klimiuk et al. (2003)
HCl and KOH modified	Helactine, polactine and remazol	Klimiuk et al. (2003)
Chitinase	Congo red	Hou et al. (2021)
Sonoenzymolysis	Congo red	Hou et al. (2021)
Maleic anhydride	Indigo carmine	Akkaya et al. (2009)
Maleic anhydride	Trypan blue	Akkaya et al. (2009)
1,2,4-benzenetricarboxylic anhydride	Indigo carmine	Akkaya et al. (2009)
1,2,4-benzenetricarboxylic anhydride	Trypan blue	Akkaya et al. (2009)
Acid treatment + ultrasonication	Methylene blue	Ablouh et al. (2020)
Polystyrene-modified	Methyl orange	Umar (2020)
Poly (acrylic acid)	Malachite green	Huang et al. (2012)
Poly (acrylic acid)	Methyl violet	Huang et al. (2012)
Poly (acrylic acid)	Paraquat	Huang et al. (2012)

Table 5 Adsorption of some dyes, heavy metals, pharmaceuticals and pesticides and adsorption capacity of chitosan and modified chitosan

Adsorbate	Adsorption capacity	Isotherm	References
Reactive red 222	250–420 μm	Langmuir	Juang et al. (1997)
Reactive yellow 145	380 μm	Langmuir	Juang et al. (1997)
Reactive blue 222	179 μm	Langmuir	Juang et al. (1997)
Copper(II) ions	110 mg/L	–	Mende et al. (2016)
Iron(II) ions	80 mg/L	–	Mende et al. (2016)
Nickel (II) ions	80 mg/L	–	Mende et al. (2016)
Reactive red 222	1106 mg g^{-1}	Langmuir	Wu et al. (2000)
Reactive red 189	950 mg g^{-1}	Langmuir	Chiou and Li (2003)
Reactive black 5	201.90 mg g^{-1}	Langmuir	Chatterjee et al. (2011)
Reactive black 5	4.83 mg g^{-1}	Langmuir and BET	Ong and Seou (2013)
Congo red	93 mg g^{-1}	Langmuir	Chatterjee et al. (2007)
Congo red	178.32 mg g^{-1}	Sips	Chatterjee et al. (2009)
Methylene blue	99.01 mg g^{-1}	–	Chatterjee et al. (2012)
Reactive yellow	334 mg g^{-1}	Langmuir	Kyzas and Lazaridis (2009)
Pb(II)	431.7 mg g^{-1}	Langmuir	Zhang et al. (2019)
Cd(II)	370.37 mg g^{-1}	Langmuir	Zhang et al. (2019)
Cr(VI)	374.4 mg g^{-1}	Langmuir	Guo et al. (2018)
Cr(VI)	166.98 mg g^{-1}	Langmuir	Ali (2018)
Ni (II)	100%	Langmuir	Abou El-Reash (2018)
Mn(II)	100%	Langmuir	Abou El-Reash (2018)
Co(II)	916.6 mg g^{-1}	Redlich-Peterson	Bahmani et al. (2019)
Hg(II)	204.1 mg g^{-1}	Langmuir	Liu et al. (2019)
Cefotaxime	1003.64 mg g^{-1}	Freundlich	Li et al. (2021)
Amoxicillin	8.71 mg g^{-1}	Langmuir	Adriano et al. (2005)
Clindamycin	238.24 mg g^{-1}	Langmuir	Gupta et al. (2017)
Tetracycline	388.52 mg g^{-1}	–	Li et al. (2020)
Cefotaxime	309.26 mg g^{-1}	–	Li et al. (2020)
Ciprofloxacin	267.7 mg g^{-1}	–	Wang et al. (2019)
Enrofloxacin	387.7 mg g^{-1}	–	Wang et al. (2019)
Cefazolin	1250 mg g^{-1}	Langmuir	Ahmadzadeh et al. (2017)
Gemifloxacin	84%	Langmuir	Mala and Dutta (2021)
Methyl parathion	86%	Langmuir	Yoshizuka et al. (2000)
Permethrin	99%	–	Dehaghi et al. (2014)
2,4-D	6.2 mg g^{-1}	Freundlich	Harmoudi et al. (2014)
Pentachlorophenol	94%	Langmuir	Shankar et al. (2020)
Malathion	322.6 mg g^{-1}	Langmuir	Jaiswal et al. (2012)

Table 6 Chitosan composite beads for adsorption of dyes, heavy metals etc.

Chitosan Composite with	Adsorbate	Reference
Magadite	Cationinc, anionic dyes	Mokhtar et al. (2020)
Nano ZnO	RB5	Çınar et al. (2017)
Carbon nanotube	Bilirubin	Ouyang et al. (2015)
Sodium alginate	Bisphenol A	Luo et al. (2019)
Oil palm ash	Reactive blue 19	Hasan et al. (2008)
Clay	Ni(II) and Cd(II)	Tirtom et al. (2012)
Magnetite	Ni(II) and Pb(II)	Tran et al. (2010)
Alginate	Cu(II)	Huang et al. (2018)
Bamboo charcoal	Silver(I)	Nitayaphat and Jintakosol (2015)
Graphene oxide-magnetite	Reactive blue 19	Le et al. (2019)
Activated clay	Tannic acid, humic acid	Chang and Juang (2004)
Activated clay	Methylene blue, reactive dye RR222	Chang and Juang (2004)
Montmorillonite	Silver(I)	Jintakosol and Nitayaphat (2016)
Palygorskite	Pb(II)	Rusmin et al. (2015)
Rice husk	Cr(VI)	Sugashini and Sheriffa (2013)
Alginate	Cr(VI)	Zhang et al. (2019)
Montmorillonite	Reactive red 120	Kittinaovarat et al. (2010)
Halloysite	Methylene blue	Peng et al. (2015)
Fe ₃ O ₄	Cu(II)	Chen et al. (2012)
Carbon nano tube	Hg(II)	Shawky et al. (2012)
Zirconium	Cr(VI)	Zhang et al. (2013)
Activated carbon carrier	Cu(II)	Li et al. (2017)
Fe ⁰ + carboxymethyl β-cyclodextrin	Arsenic(III) and (V)	Sikder et al. (2014)
Tea activated carbon	Methylene blue and acid blue 29	Auta and Hameed (2013)
β-cyclodextrin + hexamethylenetetramine	Anionic dye	Wang et al. (2019)
Nano-magnetite + heulandite	Methyl orange	Cho et al. (2015)
Sodium alginate	Acid black 172	Zhao et al. (2021)
Cellulose	Congo red	Vega-Negron et al. (2018)
Fe(OH) ₃	Congo red, methyl orange	Li et al. (2018)
Poly(ethylene glycol) and acrylamide monomer	Acid red 18	Zhao et al. (2012)
Montmorillonite	Remazol blue	Pereira et al. (2017)

(continued)

Table 6 (continued)

Chitosan Composite with	Adsorbate	Reference
Carbon clay	Azo acid blue 29	Marrakchi et al. (2020)
Coffee residue	Reactive red 152	Nitayaphat (2017)
Magnetic graphene oxide nanoparticle + isophthaloyl chloride	EBT	Jamali and Akbari et al. (2021)
Activated oil palm ash and zeolite	Acid blue 29	Khanday et al. (2017)
Alginate-bentonite	Congo red	Oussalah et al. (2019)
Kaolin-nanosized γ -Fe ₂ O ₃	Methyl orange	Zhu et al. (2010)
Zeolite	Reactive red 120	Jawad et al. (2020)
Bamboo charcoal	Reactive red 152	Nitayaphat (2014)
TiO ₂ nanoparticles-polyacrylamide matrix	Sirius yellow K-CF dye	Binaeian et al. (2020)
Calcium chloride	Methyl orange	Tay et al. (2020)
Maghemite	Methyl orange	Obeid et al. (2013)